Synthesis and Reactions of Titanium-Nitrogen Multiple Bonds

Laura R. Groom



Thesis submitted to the University of Oxford for the degree of
Doctor of Philosophy, January 2014.

The work described in this Thesis was carried out in the Chemistry Research Laboratory, University of Oxford from October 2010 to January 2014 under the supervision of Professor Philip Mountford. All work is my own unless stated to the contrary, and has not previously been submitted for any degree at this or any other university.

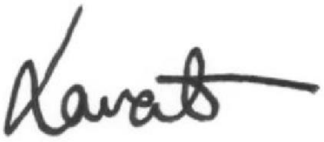

Laura R. Groom

January 2014

Abstract

Laura R. Groom Michaelmas 2013

Brasenose College D.Phil. Thesis

This Thesis reports the synthesis and reactions of new hydrazide, alkoxyimide and benzimidamide complexes (L)Ti=NX (X = NAr_2, NO^tBu or $C(Ar)NO^tBu$; L = dianionic supporting ligand or ligand set). The work is supported by DFT calculations which are used to rationalise the reaction outcomes observed and, in one case, the bonding in alkoxyimide complexes.

Chapter One provides a background to hydrazide complexes, starting with their relevance to nitrogen fixation. In addition, Group 4 imide, alkylidene hydrazide and alkoxyimide complexes are also reviewed. The Chapter focuses in particular on the synthesis, structure, and stoichiometric and catalytic reactions of these complexes with unsaturated substrates.

Chapter Two describes the development of the virtually unexplored 1,2-diamination reaction. The substrate scope and isolation of the vinylamine products are discussed. The protonation of the vinylimide complex $Ti(N_2N^{Me})\{NC(Ph)C(Me)NPh_2\}(py)$ and the overall diamination reaction itself is then explored through an in-depth experimental and computational study.

Chapter Three details the synthesis of cyclopentadienyl-amidinate supported alkoxyimide complexes. The first detailed reactivity study, supported by structural and computational studies, of any alkoxyimide complex is reported. Novel reactivity at $Ti=N_\alpha$ and, in one instance, $N_\alpha–O_\beta$ reductive bond cleavage is observed.

Chapter Four describes the reactivity of the benzimidamide complex $Cp^*Ti\{PhC(N^iPr)_2\}\{NC(Ar^{F_5})NO^tBu\}$ with a range of substrates including heterocumulenes, aldehydes, isonitriles and $B(Ar^{F_5})_3$. Novel reactivity at $Ti=N_\alpha$, and 3-component coupling is presented, and the experimental results supported by structural and computational studies.

Chapter Five presents full experimental procedures and characterising data for the new complexes reported.

CD Appendix contains CIF files for all new crystallographically characterised complexes.

Contents

	Declaration	i
	Abstract	ii
	Contents	iii
	Acknowledgements	vi
	Abbreviations	vii
	Notes	xii
Chapter One: Introduction		1
1.1	General introduction	2
1.2	Nitrogen fixation	3
1.3	Metal hydrazido(2-) complexes	4
1.3.1	Group 6 hydrazide complexes	7
1.3.2	Group 5 hydrazide complexes	11
1.4	Group 4 imide and hydrazide complexes	13
1.4.1	Group 4 imide complexes	13
1.4.2	Group 4 hydrazide complexes	25
1.5	Group 4 alkylidene hydrazide complexes	45
1.6	Group 4 alkoxyimide complexes	49
1.7	Summary and objectives	54
1.8	References	55
Chapter Two: 1,2- Diamination of internal alkynes		63
2.1	Overview	64
2.1.1	Background	65
2.2	Diamination catalysis	68
2.3	The scope of 1,2-diamination catalysis	73
2.4	Combined DFT and experimental investigation of the reaction of $Ti(N_2N^{Me})\{NC(Ph)C(Me)NPh_2\}(py)$ (**2.2**) with Ph_2NNH_2	76
2.5	Diamination *vs* hydrohydrazination	83
2.6	Combined DFT and experimental investigation of the catalytic 1,2-diamination reaction of $Ti(N_2N^{Me})(NNPh_2)(py)$ (**2.1**) with PhCCMe and Ph_2NNH_2	86
2.7	Catalyst resting state	90
2.8	Catalyst decomposition	94

2.9	Substrate effect on catalyst performance	96
2.9.1	Initial rates	96
2.9.2	Turnover numbers	100
2.10	Conclusions	103
2.11	References	106

Chapter Three: Synthesis and reactions of a cyclopentadienyl-amidinate titanium *tert*-butoxyimido compound 108

3.1	Introduction	109
3.2	Synthesis and bonding analysis of cyclopentadienyl-amidinate alkoxyimido compounds	112
3.3	Reactions with heterocumulenes	119
3.4	Reactions with aldehydes and ketones	128
3.5	Reactions with nitriles	136
3.6	Reactions with alkynes	144
3.7	Alkylation, protonation and related reactions	147
3.8	Conclusions	155
3.9	References	156

Chapter Four: Reactions of a cyclopentadienyl-amidinate titanium benzimidamido complex 166

4.1	Introduction	167
4.2	Reactions with heterocumulenes	169
4.3	Reactions with benzaldehydes and dimethyl formamide	175
4.3.1	Reactions with aldehydes	175
4.3.2	Reactions with ketones and dimethyl formamide	188
4.3.3	Selectivity	193
4.4	Reactions with nitriles	195
4.5	Reaction with $B(Ar^{F5})_3$	202
4.6	Conclusions	205
4.7	References	206

Chapter Five: Experimental details and characterising data 213

5.1 General methods and instrumentation 214
5.2 Literature preparations 214
5.3 Experimental details and characterising data for Chapter Two 216
5.4 Experimental details and characterising data for Chapter Three 224
5.5 Experimental details and characterising data for Chapter Four 240
5.6 X-ray data collection and processing parameters for Chapter Three 263
5.7 X-ray data collection and processing parameters for Chapter Four 266
5.8 References 268

Appendix 270

A.1 Isosurfaces and energies of the HOMO, HOMO-1 and HOMO-2 of $CpTi\{MeC(NMe)_2\}(NR)$ 271
A.2 Isosurfaces and energies of the HOMOs and LUMOs of $(4\text{-}C_6H_4X)C\{NC(Ar^{F_5})NO^tBu\}H$ (**23a-f**) 273
A.3 References 275

CD Appendix

Acknowledgements

Firstly, I would like to thank Prof. Philip Mountford for the last nearly 8(!) years at Oxford. Over the last 3 and a half years I am particularly thankful for his ideas, his motivation and, most noticeably, for listening. I have found my project very interesting and, in some cases, very challenging and I am thankful to Phil for his support during these particular times!

I have thoroughly enjoyed being part of the Mountford Group. Thanks must go to Dr Andrey Protchenko, Dr Andrew D. Schwarz, Dr Pei Jen Tiong, Dr Daniel Schofield, Dr Matt Blake, Liban Saleh, Junjuda Unruangsri, Adam Russell, Bryony Core, Laura Stevenson, Helen Yin, Richard Collins, Hiromasa Tanahashi, Lee Collins, Chee Onn and Jessica Rosenqvist. Everyone, past and present, has been great to talk too, great to work with and, most importantly, really good fun to be around. I would also like to thank Dr Andrew D. Schwarz and Dr Pei Jen Tiong, in particular, for their supervision and invaluable advice. For proof-reading this Thesis, Dr Andrew D. Schwarz, Dr Matt Blake, Adam Russell, Laura Stevenson, Richard Collins and Junjuda Unruangsri deserve a special mention. Special mention must also go to Junjuda Unruangsri who has been a great friend over the last few years, always someone I could talk to, laugh with and, most importantly, confide in. Indeed, I would like to thank all of my friends for their friendship and support during my time at Oxford.

Thanks must also go to our collaborators, Dr Ainara Nova and Dr Eric Clot of Université Montpellier, France and to Adam Russell (Oxford University) for the DFT calculations. I am also grateful to Dr Nick Rees, Colin Sparrow and Stephen Boyer for their help with NMR and mass spectroscopy and elemental analysis and Dr Andrew D. Schwarz for the collection of X-ray crystallographic data and for solution of molecular structures. I would also like to mention the other support staff in the department, in particular, Andy White, Alan Roper, Jude Nettleton and Dr Chris Blackwell who have provided much appreciated support to the lab.

Last but by no means least, I would like thank my mum, dad, sisters, Alice and Hannah, and brother, Jack, who have put up with me being "a student" for a further four years. Their endless support, motivation and cups of tea have been essential. Without it this Thesis would never have been written.

Abbreviations

General

Å	Ångstrom
Atm	atmosphere(s)
Avg	average
ca.	*circa*, about
calcd.	calculated
cf.	*confer*, compared to
Cp_{cent}	computed cyclopentadienyl ring carbon centroid
CSD	Cambridge Structural Database
°	degrees
°C	degrees Celsius
d	day(s)
fac	facially coordinating
g	grams
h	hour(s)
K	kelvin
kcal mol^{-1}	kilocalorie(s) per mole
mbar	millibar(s)
min	minute(s)
mL	millilitre(s)
mmol	millimole(s)
RT	room temperature
s	second(s)
μ	bridging
vs	versus

Chemical

acac	acetylacetonate
$AlNp_3$	trineopentylaluminum
Ar	aryl group
Ar'	2,6-$C_6H_3{}^iPr_2$
Ar^{F_2}	2,6-$C_6H_3F_2$
Ar^{F_5}	C_6F_5

$B(Ar^{F_5})_3$	$B(C_6F_5)_3$
bipy	2,2´-bipyridine
Bu	*n*-butyl
Bu^tpy	di-*tert*-butyl pyridine
Cp	C_5H_5
Cp*	C_5Me_5
DMAP	4-dimethylaminopyridine
dme	1,2-dimethoxyethane
dpma	*N*,*N*-di(pyrrolyl-α-methyl)-*N*-methylamine
dppe	$Ph_2PCH_2CH_2PPh_2$
E	generic chalcogen atom
Et	Ethyl
H_2Me_4taa	tetramethyl dibenzotetraaza[14]annulene
$H_2N_2^{PFP}N_{py}$	$MeC(2\text{-}C_5H_4N)(CH_2NHC_6F_5)_2$
$HC(Me_2pz)_3$	tris(3,5-dimethylpyrazolyl)methane
HIPT	$3,5\text{-}(2,4,6\text{-}C_6H_2{}^iPr_3)_2C_6H_3$
Hpypyr	2-(2′-pyridyl)-3,5-dimethylpyrrole
^{i}Pr	*iso*-propyl
KIE	kinetic isotope effect(s)
L	a supporting ligand (set)
LiHMDS	lithium hexamethyldisilazide
Me	methyl
Me_2pz	3,5-dimethylpyrazolyl
Me_2Calix	dianion of 1,3-dimethyl ether of *tert*-butyl calix[4]arene
Me_3[6]ane	1,3,5-trimethyltriazacyclohexane
Me_3[9]ane	1,4,7-trimethyltriazacyclononane
Mes	$2,4,6\text{-}C_6H_2Me_3$
MOCVD	metal organic chemical vapour deposition
N_2N^R	generic diamidoamine ligand
N_2N^{py}	$MeC(2\text{-}C_5H_4N)(CH_2NHSiMe_3)_2$
N_2N^{Me}	$MeN(CH_2CH_2NSiMe_3)_2$
$N_2N^{SiMe_3}$	$Me_3SiN(CH_2CH_2NSiMe_3)_2$
$N_2{}^{iPr}N$	$(MeN(CH_2CH_2N^iPr)_2$
$N_2{}^{Mes}N^{py}$	$MeC(2\text{-}C_5H_4N)\{CH_2N(Mes)\}_2$
$N_2{}^{SiH_3}N^{Me}$	$MeN(CH_2CH_2NSiH_3)_2$

$N_2^{TBS}N^{py}$	$MeC(2\text{-}C_5H_4N)\{CH_2N(Si^tBuMe_2)\}_2$
$N_2^{TFAP}N_{py}$	$MeC(2\text{-}C_5H_4N)\{CH_2NH(2\text{-}C_6F_4NMe_2)\}_2$
$(N^{Xyl})_2N_{py}$	$MeC(2\text{-}C_5H_4N)\{CH_2N(Xyl)\}_2$
$N^{Xyl}N$	2-(3,5-dimethylphenylamino)pyrrolinato
N_2O	$(O\text{-}(CH_2CH_2NSiMe_3)_2$
$N_2^{Ar}O$	$(O(2\text{-}C_6H_4NSiMe_3)_2$
OTf	$CF_3SO_3^-$
Ph	phenyl
py	pyridine
py′	4-pyrrolidinopyridine
pz	pyrazolyl
R	generic aryl or alkyl
^{t}Bu	*tert*-butyl
THF	tetrahydrofuran
TMEDA	N,N,N,N-tetramethylethylenediamine
tmtaa	tetramethyl dibenzotetraaza[14lannulene
Tol	$4\text{-}C_6H_4Me$
TTP	*meso*-tetra-*p*-tolylporphyrinato dianion
X	generic anionic ligand
Xyl	$2,6\text{-}C_6H_3Me_2$

Calculations

BDEs	bond dissociation energies
DFT	density functional theory
HOMO	highest occupied molecular orbital
LP	lone pair
LUMO	lowest unoccupied molecular orbital
MO	molecular orbital
NBO	natural bond orbital
TS	transition state(s)

Mass Spectrometry

EI	electron impact
ES	electrospay
FI	field ionisation

HR	high-resolution
m/z	mass to charge ratio
MS	mass spectrometry

Nuclear Magnetic Resonance Spectroscopy

$^{1}H\{^{19}F\}$	fluorine-decoupled ^{1}H
$^{13}C\{^{1}H\}$	proton-decoupled ^{13}C
$^{13}C\{^{19}F\}$	fluorine-decoupled ^{13}C
$^{11}B\{^{1}H\}$	proton-decoupled ^{11}B
$^{19}F\{^{1}H\}$	proton-decoupled ^{19}F
app.	apparent
br	broad
COSY	correlation spectrocopy
d	doublet
δ	chemical shift in ppm
HMBC	heteronuclear multiple bond correlation
HMQC	heteronuclear single quantum correlation
Hz	Hertz
i	*ipso*
J	coupling constant
m	*meta*
m	multiplet
MHz	Megahertz
NMR	nuclear magnetic resonance
NOE	nuclear Overhauser effect
o	*ortho*
p	*para*
ppm	parts per million
q	quartet
ROESY	rotating-frame nuclear Overhauser Effect spectroscopy
s	singlet
sept	septet
t	triplet
VT	variable temperature

Infrared Spectroscopy

br	broad
FT-IR	fourier transform infrared red
IR	infrared red
cm^{-1}	wavenumber
m	medium
s	strong
w	weak
ν	frequency

Notes

Literature compounds described in Chapters One, Three and Four of this Thesis are numbered **1.x**, **3.x**, **4.x** according to the Chapter in which they occur. The new compounds described in this Thesis are numbered **1** – **xx** or as **#**$^{+}$ if the cation alone is being referred to. In Chapter Two of this Thesis all literature and new compounds are numbered **2.x** for consistency and ease of reading. Model systems used in calculations are denoted by **#Q**. Density functional theory (DFT) calculated compounds are clearly stated in the text.

X-ray crystallography (for compounds **6**, **9c**, **10**, **15-BPh$_4$**, **17**, **23e** and **25**) was performed and molecular structures solved by Dr Andrew D. Schwarz.

DFT calculations were performed in collaboration with Dr Ainara Nova and Dr Eric Clot of Université Montpellier, France (to support experimental work discussed in Chapters Two and Three) and by Adam Russell of Oxford University (to support experimental work discussed in Chapter Four).

Chapter One

Introduction

1.1 General introduction

Over the past four decades, largely because of their relevance to the catalytic reduction of dinitrogen to ammonia, research into metal-nitrogen multiple bonds has flourished. Intermediates proposed in the fixation of dinitrogen and of particular relevance to this Thesis are imido and hydrazido complexes, (L)M=NR and (L)M=NNR$_2$ (R = alkyl or aryl), respectively. To date many practical applications of both ligands have been reported, either as spectator ligands (in the case of imide complexes) or as reactive sites themselves. These include the stoichiometric and catalytic reduction of dinitrogen,[1-6] carbodiimide metathesis,[7] olefin polymerisation,[8-12] MOCVD (Metal-Organic Chemical Vapour Deposition)[9, 13, 14] and new C–N bond forming reactions including hydroamination and hydrohydrazination (N-H bond addition across the C≡C bonds of alkenes, alkynes, allenes and carbodiimides).[15-27]

This Thesis describes the development of a new type of catalytic C–N bond forming reaction, namely 1,2-diamination (N-N bond addition across the C≡C bonds of alkynes) using titanium hydrazido(2-) complexes, Ti(N_2N^{Me})($NNAr_2$)(py) (N_2N^{Me} = $MeN(CH_2CH_2NSiMe_3)_2$, Ar = Ph, 4-$C_6H_4{}^tBu$ and 4-C_6H_4OMe). The synthesis of alkoxyimido and benzimidamido complexes, Cp*Ti{$PhC(N^iPr)_2$}(NO^tBu) and Cp*Ti{$PhC(N^iPr)_2$}{$NC(Ar^{F_5})NO^tBu$} (Ar^{F_5} = C_6F_5) is reported and their reactivity with small molecules, including isocyanates, carbonyl compounds and $B(Ar^{F_5})_3$, explored. Parts of this work have been published.[28, 29] Monomeric hydrazido(2-) complexes form the focus of this Chapter with a particular emphasis on Group 4 metals. The Chapter begins by describing their relevance to nitrogen fixation before discussing the synthesis, bonding and reactions of Groups 4, 5 and 6 hydrazido(2-) complexes. As further background, Group 4 imido compounds are also described. Finally, the current literature on the much less well-established Group 4 alkylidene hydrazido, (L)M=NNCRR′ (M = Ti or Zr; R, R′ = alkyl or aryl), and alkoxyimido, (L)Ti=NO^tBu, complexes is reported.

1.2 Nitrogen fixation

Nitrogen-containing compounds are found in fertilisers, drugs and explosives and as such are fundamental to mankind. However, the inherent stability of N_2, which otherwise would be a rich natural source of nitrogen, makes fixation to the more synthetically useful nitrogen-containing molecules, such as ammonia, more challenging. As a result, current industrial processes require very high temperatures and pressures, even in the presence of metal catalysts.[30-33] These include the well-renowned Haber Bosch process which requires temperatures of 400 °C, 200 atm pressure and a Fe-based catalyst to convert N_2 into NH_3. The alternative Frank-Caro cyanamide process converts N_2 into cyanamide using calcium carbide, CaC_2, and requires temperatures of 1000 °C.[34] In contrast, nitrogen fixation by nitrogenase enzymes is carried out at ambient temperatures and pressures. In 1992, the structure of the nitrogenase enzyme present in bacterium *Azotobacter vinelandii* was determined and the core of the active site shown to consist of an iron-molybdenum-sulfur cluster (FeMo-cofactor), Fig. 1.1.[35] However, despite significant research since then,[32, 36, 37] the mode of N_2 binding as well as the mechanism for nitrogen fixation is still unclear.[38]

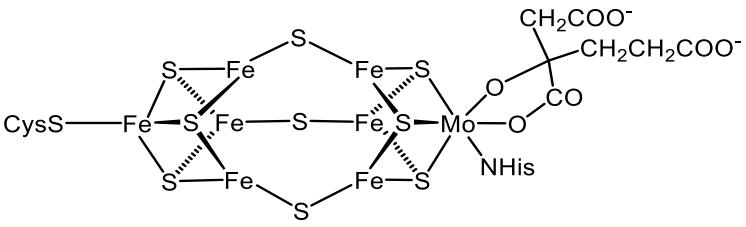

Figure 1.1. FeMo cofactor of FeMo nitrogenase.[35]

The presence of molybdenum and iron in the active site of a nitrogenase enzyme inspired work on the synthesis of other late transition metal complexes capable of reducing dinitrogen. During this time two significant systems were reported, $(P)_4M(N_2)L$ (**1.1**, Scheme 1.1, M = Mo or W, P = phosphine ligand, L = a monodentate ligand including N_2) synthesised by Chatt[1, 2] and $Mo(HIPTN_3N)$ (**1.2**; HIPT = 3,5-(2,4,6-$C_6H_2{}^iPr_3)_2C_6H_3$) synthesised by Schrock.[3-6] In the presence of a proton and electron source both systems were capable of reducing dinitrogen to ammonia, Scheme 1.1 gives the proposed mechanism using **1.1**.[1, 2] Although it is drawn as a cycle and indeed most of the intermediates proposed were isolated, catalytic activity was never achieved. On the other hand, Schrock's system using **1.2** was capable, *via* a similar cycle as proposed by Chatt (Scheme 1.1), in the first example of catalytic reduction of

dinitrogen to ammonia (4 cycles, $[2,6\text{-}HNC_5H_3Me_2][BAr_4]$ (Ar = 3,5-$C_6H_3(CF_3)_2$) and decamethylchromocene were used as sources of protons and electrons, respectively).[3-6]

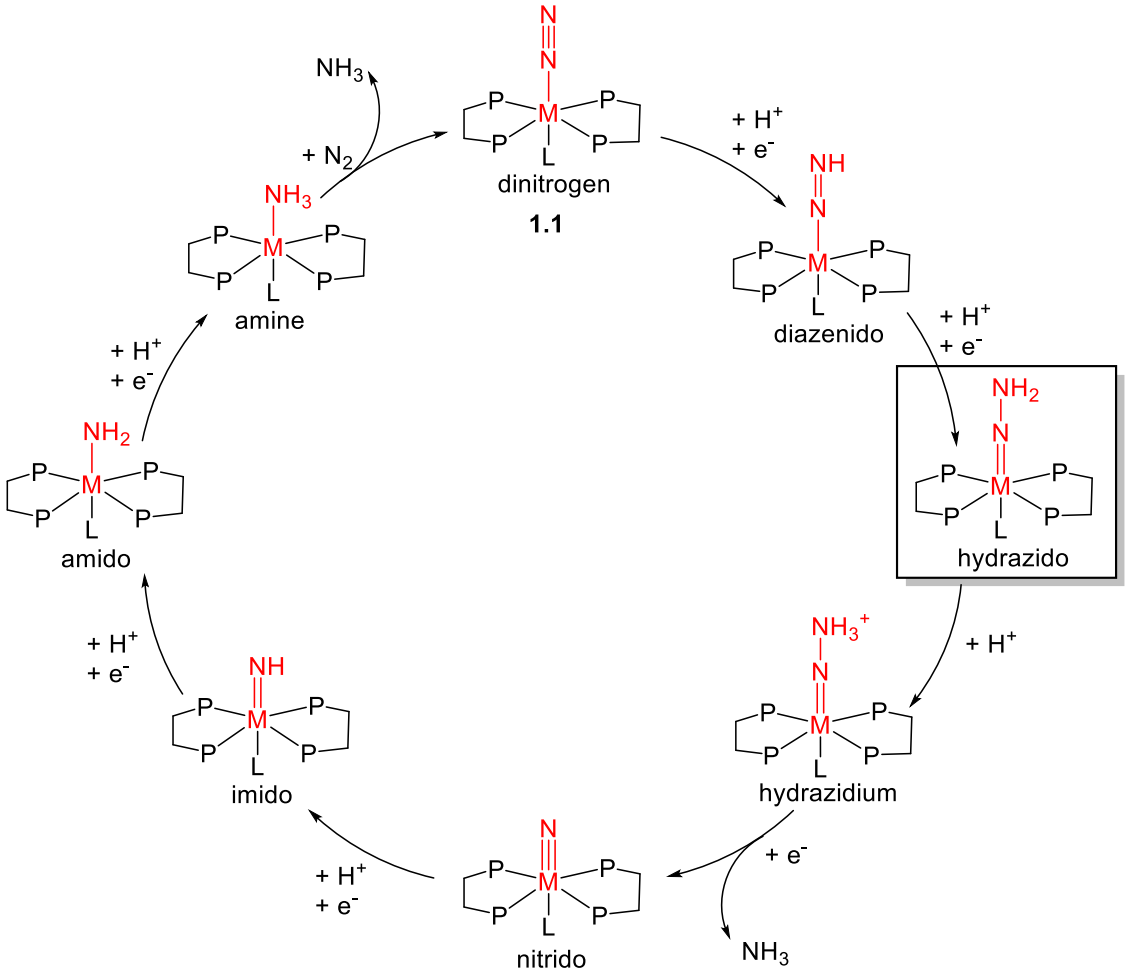

Scheme 1.1. The Chatt cycle (M = Mo or W).[1, 2]

1.3 Metal hydrazido(2-) complexes

Structural Features

As shown in Scheme 1.1 a hydrazido complex (denoted (L)M=$N_\alpha N_\beta RR'$) is a key intermediate in the reduction of dinitrogen to ammonia. Though the ligand is bound "end-on" in the complex given in Scheme 1.1, the presence of an $N_\beta RR'$ moiety enables these ligands to bond in various modes when coordinating to a metal, Fig. 1.2.[19] As presented in Figure 1.2, the formal charge on the hydrazido ligand (either -1 or -2) is dictated by the substituents bound to N_α. Hydrazido(2-) ligands can also coordinate through N_α to either one or two (μ) metals and, in both hydrazido(1-) and hydrazido(2-) complexes, with (η^2) or without (η^1) additional coordination of N_β. Monomeric, "end-

on" bound, η^1-hydrazido(2-) complexes will form the focus of this Thesis, since these are proposed to possess the most reactive hydrazido ligand.

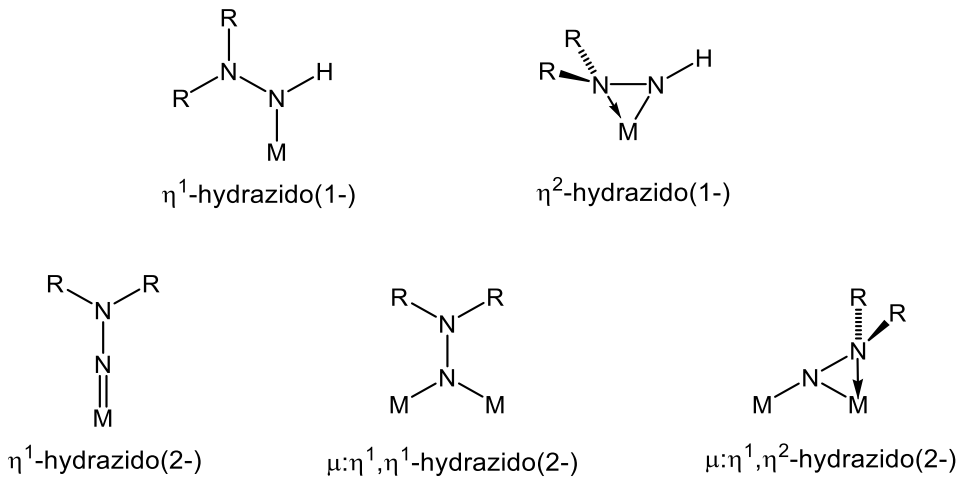

Figure 1.2. Bonding modes of hydrazide ligands.[19]

Although the valence bond description of the η^1-hydrazido(2-) bonding mode (Fig. 1.2) is drawn with M=N_α multiple and N_α–N_β single bonds, an alternative resonance form, known as the isodiazene resonance form, can exist, Fig. 1.3.[19] This resonance form arises from weak π-bond interactions between the ligand and the metal resulting in a dative M←N_α bond and N_α=N_β double bond. The relative contributions of the two resonance forms to a particular complex is identified through the relevant geometric parameters (M–N_α and N_α–N_β bond lengths and angles subtended at N_β) and, as illustrated in this Chapter, can significantly impact reactivity.

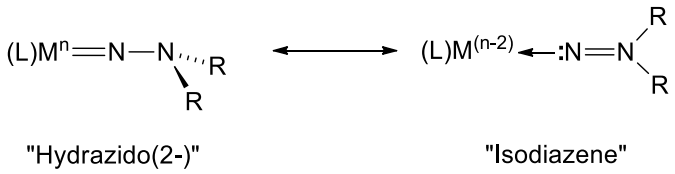

Figure 1.3. The hydrazido(2-) and neutral isodiazene resonance forms.[19]

Since the later transition metals are less reducing, η^1-hydrazido complexes of these metals (Group 6 metals and later) tend to show a larger contribution from the isodiazene resonance structure. The nominally dative M–N_α bond significantly reduces reactivity at this site and as such all reactivity is observed at N_β, *vide infra*. The early transition metals (in particular Group 4 metals), however, are much more reducing leading to significant π overlap between the metal and hydrazido ligand forming a metal-nitrogen multiple bond (formally a triple $\sigma^2\pi^4$ bond in most instances, though for ease of

representation the Ti−NX (X = R, NR_2, OR) moieties in this Thesis are all drawn as "Ti=N"). These complexes are said to have formally hydrazido(2-) ligands.

In general, this is consistent with Group 6 hydrazide complexes showing relatively long and short M–N_α and N_α–N_β bonds, respectively and exclusively planar geometry at N_β. Group 4 complexes, on the other hand, show significantly shorter and longer M–N_α and N_α–N_β bonds, respectively and, in the case of dialkyl hydrazide complexes, a pyramidal geometry at N_β (aryl substituents show planar geometry at N_β due to delocalisation of the N_β lone pair into the phenyl rings). Group 5 hydrazide complexes show intermediate behaviour and therefore both planar and pyramidal geometry at N_β has been observed. The hydrazido(2-) and isodiazene structures are often compared to Schrock and Fischer carbenes,[19, 39-41] respectively (Fig. 1.4).[42, 43] The former are found with early transition metals in high oxidation states, and the carbene, otherwise known as an alkylidene, is a dianionic 4-electron donor, much like the hydrazido(2-) ligand.[44] On the other hand, Fisher carbenes are bound to the less reducing later transition metals, and in general, are less reactive then their Schrock counterparts.

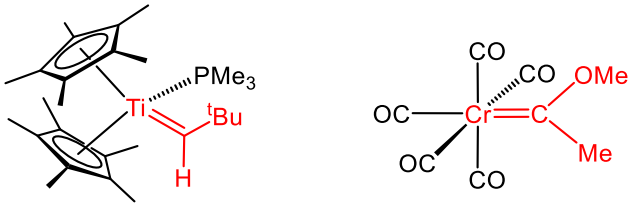

Schrock alkylidene Fischer carbene

Figure 1.4. Examples of Schrock and Fischer carbenes.[42, 43]

1.3.1 Group 6 hydrazide complexes

Synthetic entry points for Group 6 hydrazide complexes

The relevance of Group 6 hydrazide complexes to nitrogen reduction, as shown in Scheme 1.1, inspired further research on the synthesis and reactions of these ligands on the later transition metals. A significant contributor to this area of chemistry was Hidai and co-workers who synthesised a range of molybdenum and tungsten hydrazide complexes. For example, in 1976 the η^1-hydrazide complex $[Mo(N_2H_2)(F)(dppe)_2][BF_4]$ (**1.3**, Fig. 1.5, dppe = $Ph_2PCH_2CH_2PPh_2$) was synthesised from the corresponding dinitrogen complex $Mo(N_2)_2(dppe)_2$ with HBF_4,[45] followed two years later by the tungsten congener $[W(N_2H_2)(F)(dppe)_2][BF_4]$ (**1.4**).[46] In 1998, Field reported the triflate analogue, $[W(N_2H_2)(OTf)(dppe)_2][OTf]$ (OTf = $CF_3SO_3^-$) using the same synthetic methodology.[47] The triflate ligand could be easily displaced by MeCN forming the MeCN analogue $[W(N_2H_2)(NCMe)(dppe)_2][OTf]$ (**1.5**).

In 1996 Niemoth-Anderson *et al.* synthesised a range of alkyl and aryl hydrazide complexes by reaction of WCl_6 or $(MoCl_5)_2$ with the desired hydrazine or hydrazine hydrochloride salt forming $WCl_4(NNRR')$ and $MoCl_3(NNRR')$ (R = R′ = Me or Ph; R = Ph, R′ = H or Me).[48] The complexes were subsequently reduced in the presence of phosphine-based ligands forming $MCl_2(NNR_2)(PMe_2Ph)_3$ and $MCl_3(NNR_2)(dppe)$, for example $WCl_2(NNR_2)(PMe_2Ph)_3$ (R = Me (**1.6**) or Ph (**1.7**), Fig. 1.5) confirmed by structural analysis.[48] As expected the structural parameters vary between the two complexes **1.6** and **1.7**, for instance the W=N_α distance is shorter in **1.7** compared to the dialkyl complex **1.6** (1.761(8) *vs* 1.851(5) Å), *vide infra*. A further example of a diaryl η^1-hydrazido(2-) tungsten complex, namely $W(NNPh_2)(L)$ (**1.8**, Fig. 1.5, L = *tert*-butylcalix[4]arene) supported by a *tert*-butylcalix[4]arene ligand set, was successfully synthesised from $W(NNPh_2)(O^tBu)_4$ using a simple protonolysis methodology.[49] The complex is isolated as an isonitrile adduct following recrystallisation in MeCN. Interestingly, the same methodology targeting the molybdenum analogue resulted in formation of a dimeric structure, $[Mo(NNPh_2)(L)]_2$ containing two "end-on" bound hydrazide ligands.

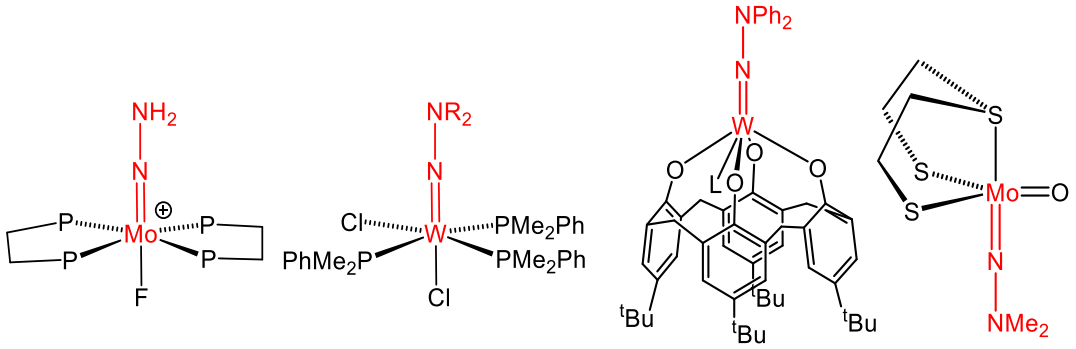

1.3 R = Me (**1.6**) or Ph (**1.7**) **1.8** (L = MeCN) **1.9**

Figure 1.5. Examples of structurally characterised molybdenum and tungsten η^1-hydrazido(2-) complexes.

In 2003, Sobota *et al.* found that the thiolate supported molybdenum oxide complexes $Mo\{X(CH_2CH_2S)_2\}(O)_2$ (X = O or S) were able to support terminal hydrazido(2-) ligands following reaction with the required hydrazine, for example $Mo\{S(CH_2CH_2S)_2\}(NNMe_2)(O)$ (**1.9**, Fig. 1.5).[50] The remaining oxide could be displaced by two chloride ligands using Me_3SiCl which, in the case of $Mo\{O(CH_2CH_2S)_2\}(NNMe_2)Cl_2$, forms a bis(hydrazido(2-)) complex on reaction with a further equiv of Me_2NNH_2.[50] A second example of a bis(hydrazido(2-)) molydenum complex, in this case structrally characterised, is $Mo(S_2CNMe_2)_2(NNPh_2)_2$.[51] Both ligands show linear Mo-N_α–N_β bond angles (169.9(8) °) and Mo-N_α and N_α–N_β bond lengths of 1.790(8) and 1.31(1) Å, respectively indicating a large isodiazene contribution. Reaction of $Mo(S_2CNMe_2)_2(NNMePh)_2$ with Me_3SiCl in methanol generated the mixed η^2-hydrazido(1-)/η^1-hydrazido(2-) complex $[Mo(S_2CNMe_2)_2(NHNMePh)(NNMePh)]$-$[BPh_4]$ (**1.10**, Fig. 1.6).[52] Compound **1.10** was structurally characterised and, as expected, shows two different Mo-N bond lengths in the η^2-hydrazido(1-) ligand (2.069(8) *vs* 2.175(9) Å). Moreover, both these distances and the N_α–N_β bond length (1.388(12) Å) are significantly longer than in the hydrazido(2-) ligand (1.75(1) and 1.285(14) Å, respectively).

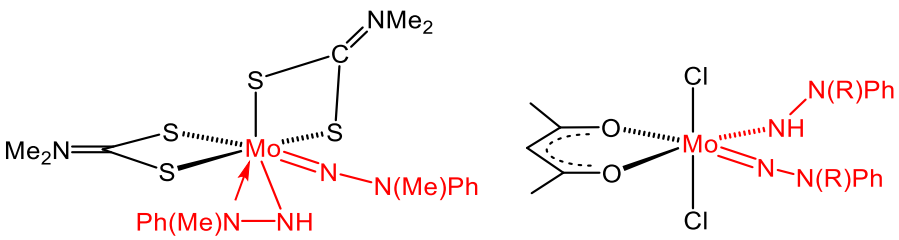

1.10 R = Me (**1.11a**) or Ph (**1.11b**)

Figure 1.6. Examples of structurally characterised mixed η^1-hydrazido(2-)/ hydrazido(1-) complexes.

In 1994 Carrillo and Gouzerh reported the mixed η^1-hydrazido(1-)/hydrazido(2-) complexes Mo(NHNRR′)(NNRR′)(acac)X_2 (R = R′ = Ph (**1.11a**), R = Ph, R′ = Me (**1.11b**); X = Cl, Br or I; acac = acetylacetonate, Fig 1.6) formed following reaction of the corresponding molybdenum oxide with the desired hydrazine.[53] Both **1.11a** and **1.11b** (X = Cl) were structurally characterised and show "end-on" coordination of both hydrazide ligands, compared to "end-on/side-on" bonding normally observed, *vide supra*. However, the structural parameters are very different between the two ligands. The Mo-N_α–N_β angles are near linear in the hydrazido(2-) ligand whereas in the hydrazido(1-) ligand the angles are significantly bent (171.9(4) and 173.8(2) *vs* 140.5(4) and 142.9(2) ° respectively). The Mo-N_α and N_α–N_β bond lengths are also significantly longer in the hydrazido(1-) ligands, as expected. The corresponding bis(hydrazido(2-)) complexes were easily accessible in both cases by reaction with various phosphorus reagents.[53] Examples of chromium hydrazides are much more limited compared to their heavier congeners, presumably due to their lower relevance to nitrogen fixation. However, one example is $[CpCrNN(SiMe_3)_2]_2$ (**1.12**) synthesised by Wiberg in 1978 from Cp_2Cr and $Me_3SiNNSiMe_3$.[54] Although not crystallographically characterised the structure is thought to be dimeric.

Stoichometric reactions

As part of the work by Hidai *et al.* both $[M(N_2H_2)(F)(dppe)_2][BF_4]$ (M = Mo (**1.3**) and W (**1.4**)) formed diazoalkane complexes, namely $[M(NNCRR')(F)(dppe)_2][BF_4]$ (M = Mo (**1.13**) or W (**1.14**), R = alkyl, aryl or allyl, Eq 1.1), following condensation with a range of aldehydes and ketones.[46] The bromide analogue $[M(N_2H_2)(Br)(dppe)_2][Br]$ gave $[M(Br)\{NN(H)C(O)NHPh\}(dppe)_2][Br]$ (**1.15**, M = Mo or W) when reacted with phenyl isocyanate.[55] Compound **1.15** could then be deprotonated with Et_3N to form a diazenido complex, (L)M=NNC(O)NHPh. The protons attached to N_β could also be removed on addition of a base such as KO^tBu, Et_3N or $NaBH_4$/EtOH as shown in the reaction of $[W(N_2H_2)(NCMe)(dppe)_2][OTf]$ (**1.5**) which resulted in double deprotonation of N_β forming the dinitrogen complex $W(N_2)(NCMe)(dppe)_2$.[47]

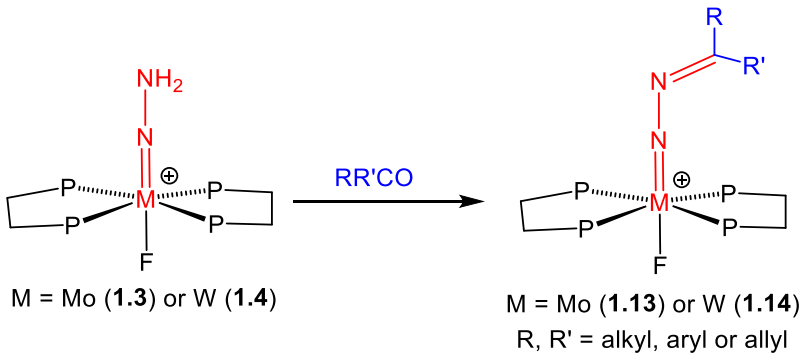

M = Mo (**1.3**) or W (**1.4**)

M = Mo (**1.13**) or W (**1.14**)
R, R' = alkyl, aryl or allyl

Equation 1.1

As mentioned in Section 1.3 and described here, the reactions of these later transition metal hydrazides are, in general, limited to nucleophilic attack by N_β. Therefore, on addition of oxygen based heterocycles such as furans and substituted cyclic acetals the N_β of (L)M=NNH_2 complexes effectively displaces the oxygen. This results in a range of nitrogen heterocycles such as lactams and pyrroles, respectively, for example [M(NNC_4H_4)(F)($dppe)_2$][BF_4] (M = Mo (**1.16**) and W(**1.17**), Eq 1.2).[2, 37] Cleavage of the N_α–N_β bond, as shown in Scheme 1.1, requires much more forcing reagents such as $LiAlH_4$ or concentrated acid.[56]

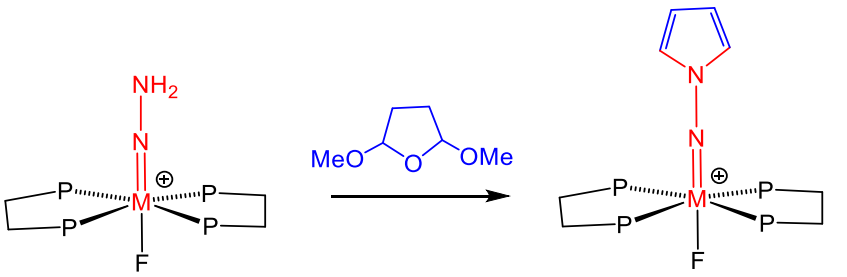

M = Mo (**1.3**) or W (**1.4**)

M = Mo (**1.16**) or W (**1.17**)

Equation 1.2

1.3.2 Group 5 hydrazide complexes

Alongside FeMo nitrogenases, Fe only [57, 58] and FeV nitrogenases[59, 60] have also been studied. However, Group 5 hydrazides are much less well-established than their Group 6 counterparts. As discussed in Section 1.3, the structures of these complexes are expected to show both isodiazene and hydrazido(2-) resonance forms.

Synthetic entry points for Group 5 hydrazide complexes

The first reported vanadium hydrazide complex was $Cp_2V\{NN(SiMe_3)_2\}$ (**1.18**, Fig. 1.7), synthesised by Wiberg in 1976 using the same synthetic route used to access the chromium analogue **1.12**.[61] The X-ray structure shows a linear V-N_α–N_β bond angle of 180 ° and short and long V=N_α and N_α–N_β bond lengths (1.666(6) and 1.369(9) Å, respectively) consistent with a hydrazido(2-) complex.[62] (L)V($NNMe_2$) (**1.19**, L = $N(CH_2CH_2S)_3$) supported by a tridentate sulfur ligand with an apical nitrogen donor was synthesised from the corresponding oxo species (L)V(O) and $Me_3SiNHNMe_2$.[63] The V=N_α and N_α–N_β distances are longer and shorter, respectively than in **1.18** (1.681(3) and 1.305(5) Å, respectively) indicating a higher contribution from the isodiazene resonance form. $V(OAr')_3(NNMe_2)$ could also be used to synthesise **1.19**, itself synthesised from reaction of $(NH_2Me_2)_2[\{VCl_3\}_2(\mu\text{-}NNMe_2)_3]$ with Li(OAr′) (Ar′ = 2,6-$C_6H_3{}^iPr_2$).[64] In 2000, Sanders *et al*. expanded the range of these complexes to include (L)V(NNRR′) (R = R′ = Ph (**1.19a**) or Me (**1.19b**); R = Ph, R′ = Me (**1.19c**)).[65] Other examples of structurally characterised vanadium η^1-hydrazide complexes include $[VCl_2(NH_2NMePh)_2(NNMePh)]Cl$, formed from reaction of $VC1_3(MeCN)_3$ with $Ph(Me)NNH_2$,[66] and $(C_9H_{18}NN)_2(OSiMe_3)_2V(\mu\text{-}O)V(O)(OSiMe_3)_2$ synthesised from H_4NVO_3.[67] Like **1.18**, both complexes possess short N_α–N_β bond distances (N_α–N_β = 1.295(17), 1.285(3) and 1.245(4) Å, respectively) along with long V=N_α bond lengths (1.696(24), 1.725(2) and 1.781(3) Å, respectively) consistent with isodiazene ligands.

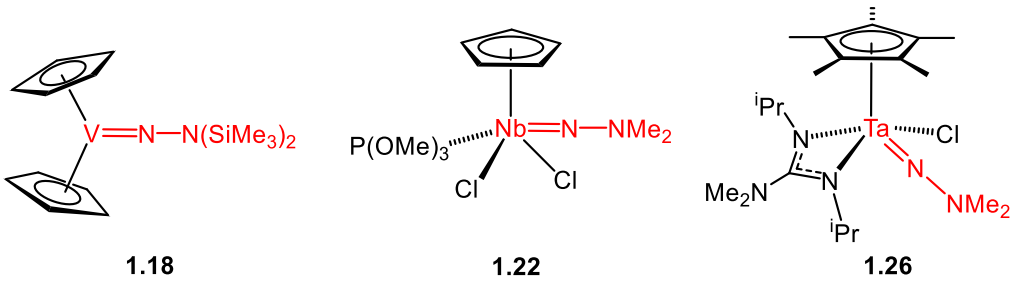

1.18 **1.22** **1.26**

Figure 1.7. Examples of Group 5 η^1-hydrazide complexes.

A route to half-sandwich niobium η^1-hydrazide compounds was reported by Green *et al.* in 1997.[68] This used the tetrachloride niobium complex $CpNbCl_4$ with Me_2NNH_2 and 2 equivs of NEt_3 to generate $CpNb(NNMe_2)Cl_2$ (**1.20**); both $(C_5H_4Me)Nb(NNMe_2)Cl_2$ (**1.21**) and $(C_5H_5)Nb(NNMePh)Cl_2$ were also synthesised in an analogous fashion. The structure of **1.20** is dimeric with one hydrazide ligand binding "end-on" to a single metal center in an η^1-fashion, the second ligand bridging in an η^2-fashion, denoted μ:η^1,η^2-hydrazido(2-) in Fig. 1.2. The η^1-hydrazide ligand is thought to act as a 4-electron donor, resulting in a short Nb=N_α bond distance of 1.67(2) Å. Accordingly the N_α–N_β distance is long (1.38(2) Å) consistent with a N_α–N_β single bond. The chlorides in these complexes are easily replaced by a range of other ligands including ^{t}BuO- and Me_2N-.[68] Addition of $P(OMe)_3$ resulted in formation of the monomeric species $CpNb(NNMe_2)Cl_2\{P(OMe)_3\}$ (**1.22**, Fig. 1.7). In this structure the Nb-N_α and N_α–N_β bond distances lengths are significantly longer and shorter, respectively than the terminal hydrazide ligand in **1.20**. This suggests that, in the case of **1.22**, the isodiazene resonance form is more dominant. Addition of $Li[C_5H_4R]$ (R = H or Me) to **1.20** and **1.21** generated $Cp_2Nb(NNMe_2)Cl$ and $(C_5H_4Me)_2Nb(NNMe_2)Cl$ (**1.23**), respectively.[69] Like **1.22**, compound **1.23** shows relatively long and short Nb-N_α and N_α–N_β bond lengths (1.794(2) and 1.340(3) Å, respectively) consistent with a bond order of less than 3 and greater than 1.

Examples of η^1-tantalum hydrazides in the literature include $[Ta\{NN(2,6\text{-}C_5H_6Me_2)\}_2Cl_4](Et_3NH)$ (**1.24**) synthesised, alongside the Nb analogue, from MCl_5.[67] In **1.24** the two hydrazido ligands are terminally bound to a single metal centre. The Ta-N_α and N_α–N_β bond lengths are consistent with an isodiazene representation, supported by a planar geometry at N_β. The pentachloride synthon was also used to synthesise the diphenyl hydrazide complexes $M(dme)Cl_3(NNPh_2)$ (M = Ta (**1.25**) or Nb, dme = 1,2-dimethoxyethane).[70, 71] The complex was structurally characterised in the case of **1.25** showing geometric parameters consistent with a hydrazido(2-) ligand.

Very recent work by Sita *et al*. reported the cyclopentadienyl-guanidinate supported dimethyl hydrazide complex $Cp^*Ta\{(Me_2N)C(N^iPr)_2\}(NNMe_2)(Cl)$ (**1.26**, Fig. 1.7) and, through reduction with KC_8, $Cp^*Ta\{(Me_2N)C(N^iPr)_2\}(NNMe_2)$.[72] The geometric parameters for both complexes suggest that, on reduction, the contribution from the hydrazide(2-) resonance form increases. This is observed by a decrease in the Ta=N_α bond distance and an increase in the N_α–N_β bond length; there is also a decrease in

planarity at N_β (176.54(13) *vs* 171.2(3) °). Both complexes undergo alkylation at N_β on reaction with MeOTf forming [Cp*Ta{$(Me_2N)C(N^iPr)_2$}$(NNMe_3)$(Cl)]OTf and [Cp*Ta{$(Me_2N)C(N^iPr)_2$}$(NNMe_3)$]OTf (**1.27**). Compound **1.27** is unstable in solution and on reaction with Na/Hg undergoes reductive N_α–N_β bond cleavage forming either [Cp*Ta{$(Me_2N)C(N^iPr)_2$}$(\mu\text{-}N)]_2$ or Cp*Ta{$(Me_2N)C(N^iPr)_2$}-(NH)(OTf) depending on the reaction conditions.[72]

1.4 Group 4 imide and hydrazide complexes

As a result of the limited reactivity involving M=N_α and/or N_α–N_β bonds in Group 6 hydrazide complexes (due to the large contribution from the isodiazene resonance form) research into Group 4 hydrazide complexes has rapidly expanded over the last 20 years. It was hoped that the more reducing metals would support the highly reduced hydrazido(2-) ligands which possess the more reactive M=N_α multiple bond. Previously, a significant amount of work had been carried out on the related imido compounds ((L)M=NR, R = alkyl or aryl), their practical applications in olefin polymerisation, hydroamination and MOCVD leading to these ligands being well-established on Group 4 metals. Comparisons between imides and hydrazides are regularly reported, and therefore the synthesis, bonding and reactions of Group 4 imide compounds will be discussed first.

1.4.1 Group 4 imide complexes

Synthetic entry points for titanium imide complexes

In 1990, Roesky *et al.* synthesised the first titanium imido complex, Ti{$NP(S)Ph_2$}$Cl_2(py)_3$, by reaction of $TiCl_4$ with $Ph_2P(S)N(SiMe_3)_2$.[73] In the same year, work by Rothwell *et al.* showed that thermolysis of Ti(Ar′O)$_2$(py′)$_2${η^2-N(Ph)N(Ph)} (py′ = 4-pyrrolidinopyridine) or through addition of py′ and H_2NPh to Ti(Ar′O)$_2${η^2-N(^{t}Bu)C(CH_2Ph)$_2$}(py′) yielded the imido complex Ti(Ar′O)$_2$(py′)$_2$(NPh) (**1.28**).[74] In both cases the imide complexes were fully characterised including X-ray structural analysis. Soon afterwards the titanium congener of one of the early zirconium imides, *vide infra*, Ti($NHSi^tBu_3$)$_2$(NSi^tBu_3) (**1.29**), also only a transient species, was synthesised from Ti($NHSi^tBu_3$)$_3$Cl and MeLi.[75] Other routes to monomeric imido complexes include the oxidation of Ti(II) species and reaction of (L)$TiCl_2$ complexes with 2 equivs of MNHR (M = Li or K).[7]

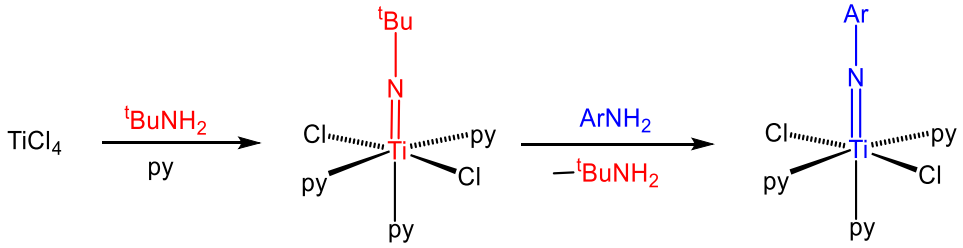

1.30 **1.40**

Scheme 1.2. Synthesis of $Ti(NR)Cl_2(py)_3$ (R = alkyl (**1.30**) or aryl (**1.41**)).[76]

Synthesis of $Ti(N^tBu)Cl_2(py)_3$ (**1.30**, Scheme 1.2)[76] and $Ti(N^tBu)Cl_2(Bu^tpy)_2$[77] revolutionised research into imide chemistry. Easily synthesised from $TiCl_4$, $^tBuNH_2$ and pyridine or 4-*tert*-butylpyridine, respectively in multigram quantities these complexes became a versatile entry point into a wide range of *tert*-butyl imide complexes through further reaction with a range of lithiated ligands, Scheme 1.3.[7, 78-80] For instance, in 1998, work from Mountford *et al.* reported a range of tetraaza macrocycle-supported imide complexes.[81] Once isolated, the *tert*-butylimide complex $Ti(N^tBu)(Me_4taa)$ (**1.31**) was used to synthesise the corresponding arylimido complexes Ti(NAr)(Me_4taa) (Ar = Ph (**1.32a**), Tol (**1.32b**), Xyl (2,6-$C_6H_3Me_2$, **1.32c**), 4-$C_6H_4NO_2$ (**1.32d**) and 4-$C_6H_4NMe_2$ (**1.32e**), H_2Me_4taa = tetramethyl dibenzotetraaza[14]annulene) using an imide/arylamine exchange reaction.[81, 82] Other examples include reaction of **1.30** with sodiated or lithiated Cp-based ligands such as $M[C_5R_5]$ (M = Li or Na, R = H or Me) to give the sandwich and half-sandwich titanium imido complexes, $Cp^RTi(N^tBu)(4\text{-}NC_5H_4R')(L)$ (L = Cl (**1.33**) or Cp^R (**1.34**); R = H, Me or Mes ($C_9H_4Me_3$); R′ = H or ^{t}Bu, Scheme 1.3).[83]

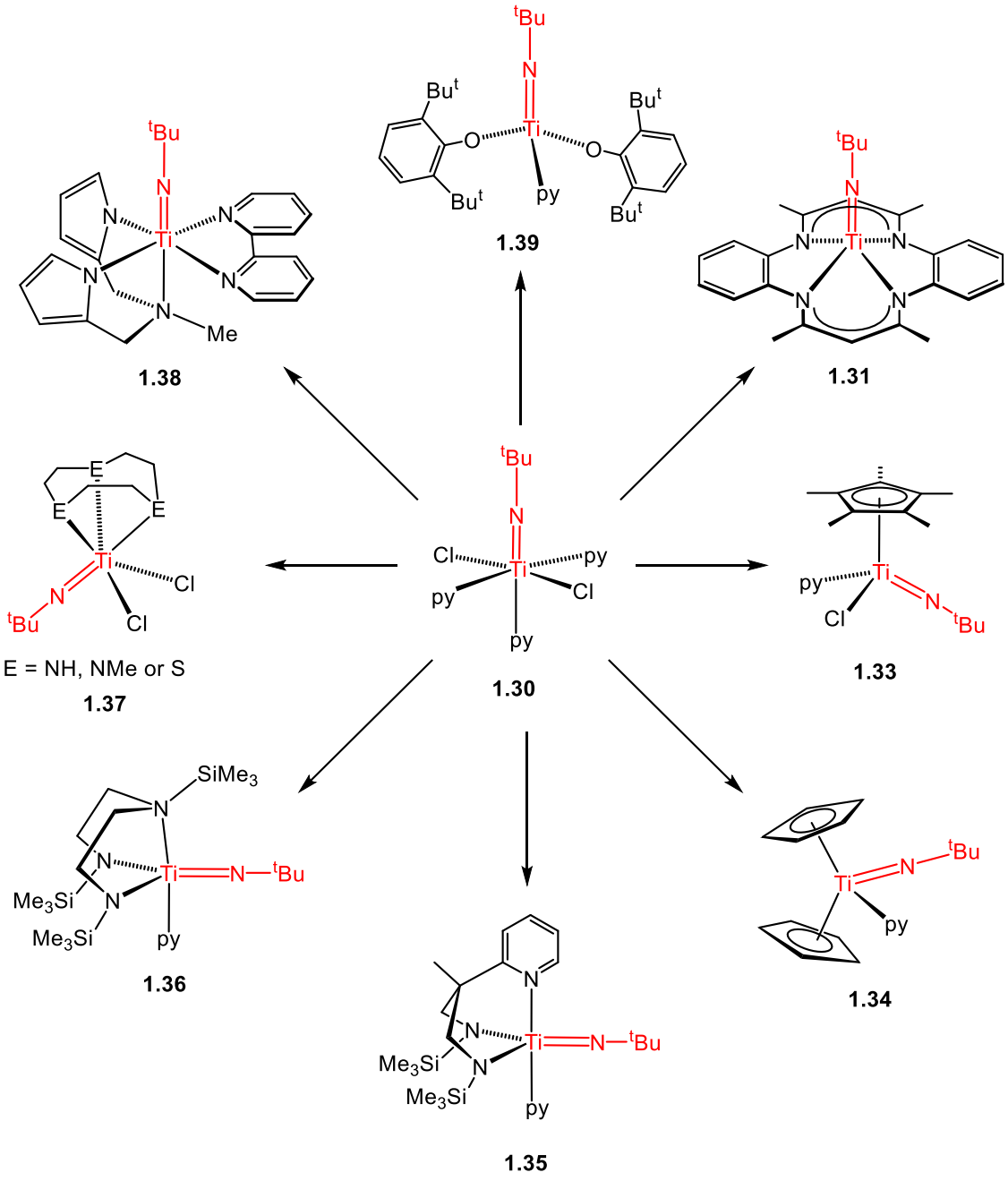

Scheme 1.3. Examples of various titanium *tert*-butylimido complexes synthesised from $Ti(N^tBu)Cl_2(py)_3$ (**1.30**).

Although the analogous reaction with $TiCl_4$, pyridine and $ArNH_2$ was unsuccessful, reaction of **1.30** with aryl amines did yield the corresponding aryl imido complexes $Ti(NAr)Cl_2(py)_3$ (**1.40**),[76-79] Scheme 1.2. Addition of lithiated ligands such as the tridentate nitrogen donor ligands $Li_2N_2N^{Me}$ or $Li_2N_2N^{py}$ (N_2N^{py} = $MeC(2\text{-}C_5H_4N)(CH_2NSiMe_3)_2$) then yielded the desired arylimide complexes.[79]

Another useful synthon for the synthesis of imido complexes is $Ti(NMe_2)_2Cl_2$ (**1.41**), synthesised from $Ti(NMe_2)_4$ and $TiCl_4$.[84] Protonolysis with the required amine, RNH_2

(R = alkyl or aryl), generated both alkyl and aryl imido complexes, $Ti(NR)Cl_2(NHMe_2)_2$ (R = alkyl (**1.42**) or aryl (**1.43**), Scheme 1.4).[84] Addition of the ligand *via* a second protonolysis reaction would then yield the desired complex, such as $Ti(NR)(Me_3[9]aneN_3)Cl_2$ (R = alkyl (**1.44**) or aryl (**1.45**), $Me_3[9]aneN_3$ = 1,4,7-trimethyltriazacyclononane).[8] In some cases compound **1.30** or **1.40** could be synthesised *via* **1.42** or **1.43**, respectively following heating in neat pyridine at 80 °C. Indeed, this procedure was used to synthesise a series of chiral imide complexes such as $Ti[N\{(S)\text{-}(-)\text{-}CH(Me)Ph\}]Cl_2(py)_3$ (**1.46**).[85] The *trans* pyridine in complexes such as **1.30**, **1.40** and **1.46** is relatively labile (due to the *trans* effect of the imide ligand, *vide infra*) and under vacuum is removed to form the chloride-bridged dimers $Ti_2(NR)_2Cl_2(\mu\text{-}Cl)_2(py)_4$ (R = ^{t}Bu (**1.47**) or aryl (**1.48**)).

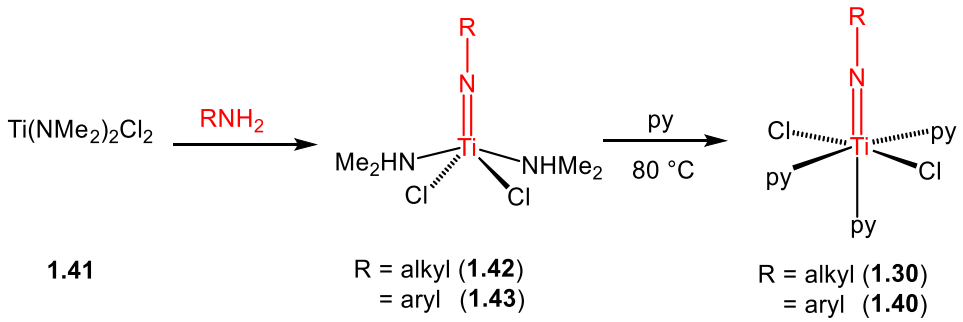

Scheme 1.4. Synthesis of $Ti(NR)Cl_2(NHMe_2)_2$ (R = alkyl (**1.42**) or aryl (**1.43**)).[84]

Synthetic entry points for zirconium and hafnium imide complexes

The larger radius of zirconium and hafnium compared to titanium can sometimes hinder synthesis of monomeric, terminal η^1-imido complexes. For example, limited steric protection on the aryl substituent of $Cp_2Zr(NHAr)(Me)$ leads to formation of nitrogen-bridged dimers, $[Cp_2ZrNAr]_2$, instead of the desired monomeric complexes.[86] In 1988, Bergman targeted the metallocene-supported zirconocene imido complexes $Cp_2Zr(NR)$ (R = alkyl or aryl) in an attempt to access a more reactive Zr=N multiple bond.[87] Attempts to synthesise these complexes from $Cp_2Zr(NHR)(CH_3)$ (**1.49**), itself synthesised from $Cp_2Zr(CH_3)Cl$ and LiNHR, only served to give reaction products *via* a proposed transient monomeric imide species $[Cp_2Zr(NR)]$ (R = ^{t}Bu (**1.50**) or Xyl (**1.51**), Fig. 1.8). However, thermolysis of **1.49** in THF did yield isolable imide complexes, namely $Cp_2Zr(NR)(THF)$ (R = ^{t}Bu (**1.52**) or Xyl (**1.53**)) which was subsequently characterised by X-ray crystallography in the case of **1.52**.[87, 88] Other Cp-

supported complexes were synthesised a few years later following a similar synthetic methodology, for example **1.54**, Fig. 1.8.[89]

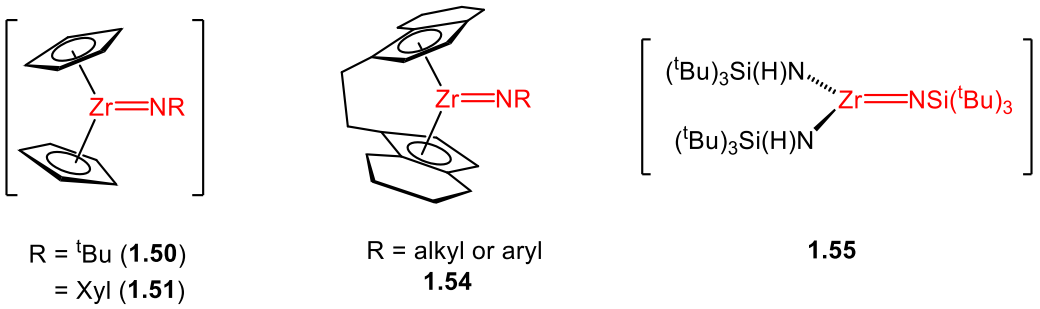

Figure 1.8. Examples of early zirconium imido complexes. Brackets indicate a transient species.

Furthermore, Wolczanski and co-workers synthesised the transient imide $[Zr\{N(H)Si^tBu_3\}_2(NSi^tBu_3)]$ (**1.55**, Fig. 1.8) from thermolysis of $Zr\{N(H)Si^tBu_3\}_3(CH_3)$. Again, subsequent trapping with THF yielded the isolable complex $Zr\{N(H)Si^tBu_3\}_2(NSi^tBu_3)(THF)$.[90] In 1992, Wigley *et al*. synthesised the zirconium analogue of $Ti(NAr)Cl_2(py)_3$, namely $Zr(NAr')Cl_2(py)_3$ (**1.56**, Ar′ = 2,6-$C_6H_3{}^iPr_2$), from reaction of $ZrCl_4(THF)_2$ with LiNHAr′, Me_3SiCl and pyridine.[91] In the absence of pyridine $Zr(NAr')Cl_2(THF)_2$ (**1.57**) was formed instead, as found with hafnium yielding $Hf(NAr')Cl_2(THF)_2$ (**1.58**). The cyclooctatetraenyl-supported complexes, which are isolated as nitrogen-bridged dimers $[(\eta^8\text{-}C_8H_8)M(NAr')]_2$ (M = Zr or Hf), could then be produced following reaction of **1.57** or **1.58** with $K_2[C_8H_8]$. A similar synthetic route to $Cp^*Zr(NAr')(py)_2Cl$ was also identified, starting from Cp^*ZrCl_3.[91]

Compound **1.56** was subsequently used to synthesis the first macrocycle-supported imido complex, Zr(tmtaa)(NAr′)(py) (tmtaa = tetramethyl dibenzotetraaza[14lannulene) *via* salt metathesis with Li_2[tmtaa],[92] as well as $Zr(N_2N^{py})(NAr')(py)$ supported by the chelating, dianionic N_3-donor ligand.[79] Other examples of macrocycle-supported complexes have also been synthesised by reaction of $(TTP)MCl_2$ (M = Zr or Hf, TTP = *meso*-tetra-*p*-tolylporphyrinato dianion) with 2 equivs of LiNHAr′ yielding (TTP)M=N(Ar′) (M = Zr (**1.59**) or Hf).[93] Once synthesised, these imide compounds reacted with excess amines to yield bis(amide) complexes in a facile protonation reaction.[93]

Structural features

A number of experimental and computational studies on the geometric and electronic structures of titanium imido complexes have been reported in the literature. In the cases discussed here, namely $Ti(NR)Cl_2(py)_3$ (R = alkyl (**1.30**) or aryl (**1.40**)), $Ti(NR)Cl_2(NHMe_2)_2$ (R = alkyl (**1.42**) or aryl (**1.43**)) and $Ti(NR)(Me_3[9]aneN_3)Cl_2$ (R = alkyl (**1.44**) or aryl (**1.45**)),[76, 84, 94, 95] the complexes are monomeric with multiple titanium nitrogen bonds (formally a triple $\sigma^2\pi^4$ bond) as shown by short Ti=N bond lengths (range 1.672(2) – 1.7420(13) Å) and linear Ti=N-R bond angles (range 164.46(17) – 180 °). In general, the alkyl imide complexes had shorter Ti=N bond lengths than their arylimide counterparts (avg. Ti=NR bond length, R = alkyl (1.690(1) Å), R = aryl (1.7183(7) Å)). For example, in the series of complexes $Ti(NR)Cl_2(NHMe_2)_2$ (R = ^{i}Pr (**1.42a**), Ph (**1.43a**), C_6F_5 (**1.43b**), 2,3,5,6-C_6HCl_4 (**1.43c**), 2-$C_6H_4CF_3$ (**1.43d**) and 2-$C_6H_4{}^t$Bu (**1.43e**))[84] and $Ti(NR)(Me_3[9]ane)Cl_2$ (R = ^{t}Bu (**1.44a**), Xyl (**1.45a**), Ar′ (**1.45b**), Ph (**1.45c**) and C_6F_5 (**1.45d**))[94] the Ti=N bond lengths were found to increase in the order Ti=N-R, R = alkyl < aryl < electron-withdrawing aryl. The increased Ti=NR bond length with electron-withdrawing aryl substituents was also identified in the series of complexes, $Ti(NR)Cl_2(py)_3$ (R = ^{t}Bu, (**1.30**), 4-C_6H_4Me (**1.40a**) and 4-$C_6H_4NO_2$ (**1.40b**)), where the Ti=N bond distance in **1.40b** is significantly longer than either **1.30** or **1.40a** (1.722(3) *vs* 1.705(3) and 1.705(4) Å, respectively).[76] In general, these complexes (**1.30** and **1.40**) showed longer Ti=N bonds than those observed in $Ti(NR)Cl_2(NHMe_2)_2$ (**1.42** and **1.43**) due to the increased coordination number around the metal and the *trans* influence of the pyridine ligand in $Ti(NR)Cl_2(py)_3$.

In 2011, DFT calculations were used to understand the structure and bonding of cyclopentadienyl-amidinate supported imide and hydrazide complexes using the model systems $CpTi\{MeC(NMe)_2\}(NR)$ (R = alkyl, aryl and NR_2).[96] In the case of the imide complexes, R = Me (**1_Me**) and Ph (**1_Ph**), the Ti=N bond length was found to be significantly shorter for **1_Me** compared to **1_Ph** (1.688 *vs* 1.709 Å) consistent with the experimental findings discussed above. This is a consequence of the π-acceptor nature of the phenyl group, resulting in donation from the Ti=N π orbital into the phenyl π* orbital, combined with donation from the π orbital on the phenyl ring into the Ti=N π* orbital, leading to a longer Ti=N bond.

One study into the structure of $Ti(NR)Cl_2(py)_3$ (**1.30**, **1.40a** and **1.40b**) focussed on the *trans* influence of the imido ligand[97] which, in some instances, can result in loss of the *trans*-pyridine under vacuum forming chloride-bridged dimers, $Ti_2(NR)_2Cl_2(\mu\text{-}Cl)_2(py)_4$ (R = ^{t}Bu (**1.47**) or aryl (**1.48**)).[98] However, although the Ti-py(*trans*) bonds in these complexes are significantly longer than the Ti-py(*cis*) distances, the *trans* influence (on σ donors such as pyridine) does not appear to be affected by the different imide substituents, since the difference in length between the Ti-py(*cis*) and Ti-py(*trans*) bonds is the same in all three complexes (0.193(4), 0.201(4) and 0.200(4) Å, respectively).

Stoichiometric reactions

With the exception of C-H activation, much of Group 4 imide chemistry with unsaturated substrates is dominated by [2+2] cycloaddition reactions at the M=N bond. For example, reaction of $Cp_2Zr(N^tBu)(THF)$ (**1.52**) with carbonyl compounds and carbodiimides gives $Cp_2Zr\{N(^tBu)C(R)(R)O\}$ (**1.60**) and $Cp_2Zr\{N(^tBu)C(NR)N(R)\}$ (**1.61**), respectively, Scheme 1.5. Other examples include reactions with alkenes, alkynes and allenes which, in some cases, can lead to hydroamination of the substrate, *vide infra*. For instance, $Cp_2Zr(NR)(THF)$ (R = ^{t}Bu (**1.52**) or Xyl (**1.53**)) gave [2+2] cycloaddition products with both internal and terminal alkynes, R′CCR″ (R′, R″ = H, Me or Ar), namely $Cp_2Zr\{N(R)C(R')C(R'')\}$ (R = ^{t}Bu (**1.62**, Scheme 1.5) or Xyl (**1.63**)).[88] In the case of $Cp_2Zr\{N(Xyl)C(Ph)C(Ph)\}$ (**1.63a**) the reaction is reversible under certain conditions (85 – 110 °C) and on addition of TolCCTol is shown to form an equilibrium mixture of **1.63a** and the corresponding tolyl cycloaddition product $Cp_2Zr\{N(Xyl)C(Tol)C(Tol)\}$.[88] The alkyl imido compound **1.52** also gave cycloaddition products with alkenes, such as acetylene (**1.64**, Scheme 1.5**)** and norbornene, in equilibrium with the starting material.[88]

Reaction of the cyclopentadienyl-amidinate supported aryl imido complexes $Cp^*Ti(N^{Xyl}N)(NAr)$ (Ar = Xyl (**1.65a**) or Mes (**1.65b**), $N^{Xyl}N$ = 2-(3,5-dimethylphenylamino)pyrrolinato) with terminal alkynes also produced azatitanacyclobutene products. In contrast, the alkyl imide $Cp^*Ti(N^{Xyl}N)(N^tBu)(NH_2{}^tBu)$ (**1.66**) was found to undergo C-H activation of ArC<u>CH</u> giving $Cp^*Ti(N^{Xyl}N)(NH^tBu)(CCAr)$ instead.[99] Compounds $[M\{N(H)Si^tBu_3\}_2(NSi^tBu_3)]$[75, 90] (M = Ti (**1.29**), or Zr (**1.55**)) and $Cp_2Zr(N^tBu)(THF)$

(**1.52**)[87] were also found to activate C-H bonds, in this case of benzene, whereas no reaction was observed for the aryl imide complex $Cp_2Zr(NXyl)(THF)$ (**1.53**) or the aryloxide-supported alkyl and aryl imide compounds $Ti(Ar'O)_2(py')_2(NR)$ (R = ^{t}Bu or Ph (**1.28**)) with 3-hexyne, even at 110 °C.[74] Indeed, compound **1.52** was found to activate a range of sp^2 C-H bonds including cyclopentene (**1.67**, Scheme 1.5), norbornene (above 45 °C) and the Cp ring of various Cp-supported transition metal complexes.[86]

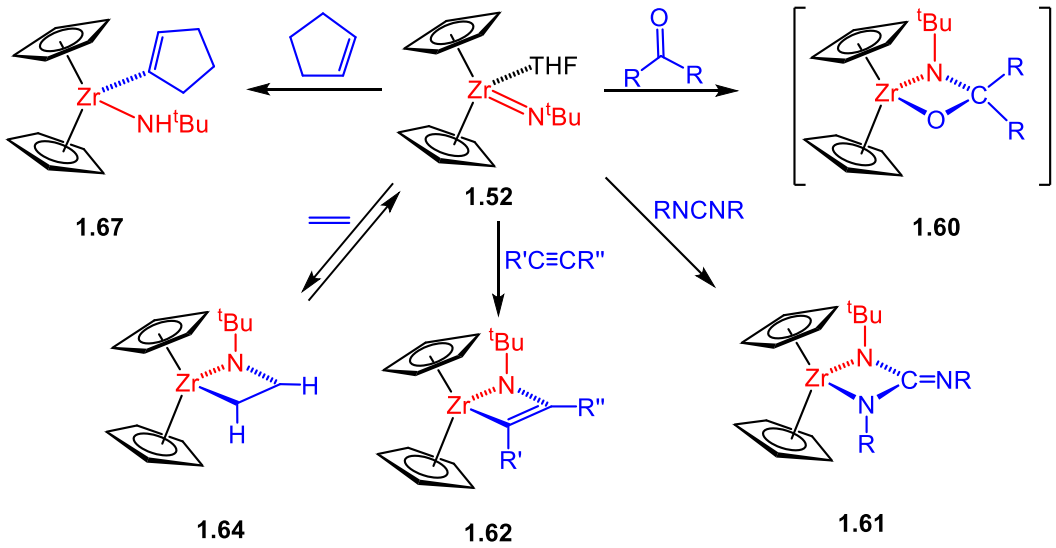

Scheme 1.5. Reactions of $Cp_2Zr(N^tBu)(THF)$ (**1.52**).

Reactions of titanium and zirconium imides with isocyanates are well-established affording azametallacycle products in all cases, for example (TTP)Zr{N(Ar′)C(N^{t}Bu)O} following reaction of (TTP)Zr(NAr′) (**1.59**) with ^{t}BuNCO. These cycloaddition complexes have been found to isomerise at room temperature over time, and in the case of **1.59** the final product is the κ^2*N*,*O*-bound ureate complex (TTP)Zr{N(^{t}Bu)C(NAr′)O}. On heating, both isomers are seen to undergo extrusion generating the carbodiimide, ^{t}BuNCNAr′.[93] Interestingly, reaction of Ti(NAr)(Me_4taa) (**1.32a**-**1.32e**) with Ar″NCO (Ar″ = Ph or Tol) gave the alternative κ^2*N*,*N*-bound ureate complexes Ti{N(Ar)C(O)N(Ar″)}(Me_4taa) (Ar = Ar″ = Ph (**1.68a**); Ar = Ph, Ar″ = Tol (**1.68b**), Eq 1.3).[82] Unlike the zirconium complexes, these complexes are stable to extrusion, though addition of pinacol to **1.68a** did generate Ti{OC(Me)$_2$C(Me)$_2$O}(Me_4taa) and the urea side product PhN(H)C(O)N(H)Ph (attempts with anilines in order to regenerate **1.32a** were not successful). As discussed with alkynes, these [2+2] cycloaddition reactions on Group 4 metals can sometimes be

reversible, and in this instance Ti{N(Ph)C(O)N(Tol)}(Me_4taa) (**1.68b**) was found to form **1.68a** in the presence of PhNCO. In this case an associative reaction pathway (forming a biureate species) is proposed, although previous studies into the reversible addition of isocyanates have also invoked dissociative mechanisms *via* ureate/imide complexes.[82] The titanium complex (TTP)Ti(N^iPr) did not appear to undergo cycloaddition reactions with carbodiimides and ketones. However, on addition of nitroso compound PhNO the corresponding diazene complex $PhNN^iPr$ was observed alongside the expected titanium oxo-species.[100] The alkyl zirconium imide complex **1.52** also gave imine or ketenimine side-products following cycloaddition-extrusion reactions with carbonyl compounds and carbodiimides.[86]

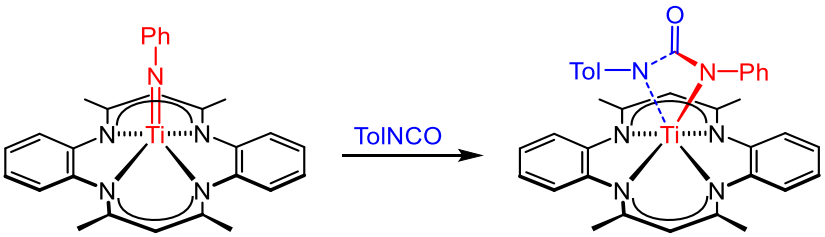

1.32a **1.68a**

Equation 1.3

A study in 2006 highlighted the effect of different N_α substituents, alkyl or aryl, on the products formed from reaction of imide complexes with heterocumulenes and carbonyl compounds.[95, 101] Reactions with alkyl imides generally resulted in formation of the sulfido or oxygen-bridged dimers following retrocyclisation from the inherently unstable [2+2] cycloaddition intermediates. Aryl substituents generally increased the stability of these intermediates allowing isolation of these compounds in several instances. For example the *N*,*O*-bound ureate complex Cp*Ti{MeC(N^iPr)$_2$}{OC(NXyl)N(R)}, formed from reaction of Cp*Ti{MeC(N^iPr)$_2$}(NR) (R = ^{t}Bu (**1.69**) or Xyl (**1.70**)) with XylNCO was stable for weeks in solution in the case of **1.70**, whereas extrusion to give the μ-oxo dimer and corresponding carbodiimide were the only products isolated in the reaction with **1.69**. This study also identified the possibility of multiple coupling of substrates such as CO_2 and TolNCO in which the second substrate normally inserts into the single Ti-N bond of the cycloaddition intermediate.

Scheme 1.6 shows the reaction of Ti(N_2N^{py})(N^tBu)(py) (**1.35**) with both MeCN and ^{t}BuCP which forms [2+2] cycloaddition products, **1.71** and **1.72**, respectively, in both instances.[102] In both complexes, the pyridyl nitrogen is released from the titanium metal reducing the coordination of the supporting ligand from tridentate to bidentate, presumably to reduce steric crowding. The regiochemistry was confirmed by X-ray diffraction in the case of **1.72** with the phosphorus atom bound to nitrogen, as expected, to allow formation of a more favourable Ti-C bond. Reaction with MeCN yielded a dimeric complex [Ti(N_2N^{py}){μ-η^2-NC(Me)N^{t}Bu}]$_2$ (**1.71**) which loses MeCN under vacuum generating a pyridine free analogue of **1.35**.

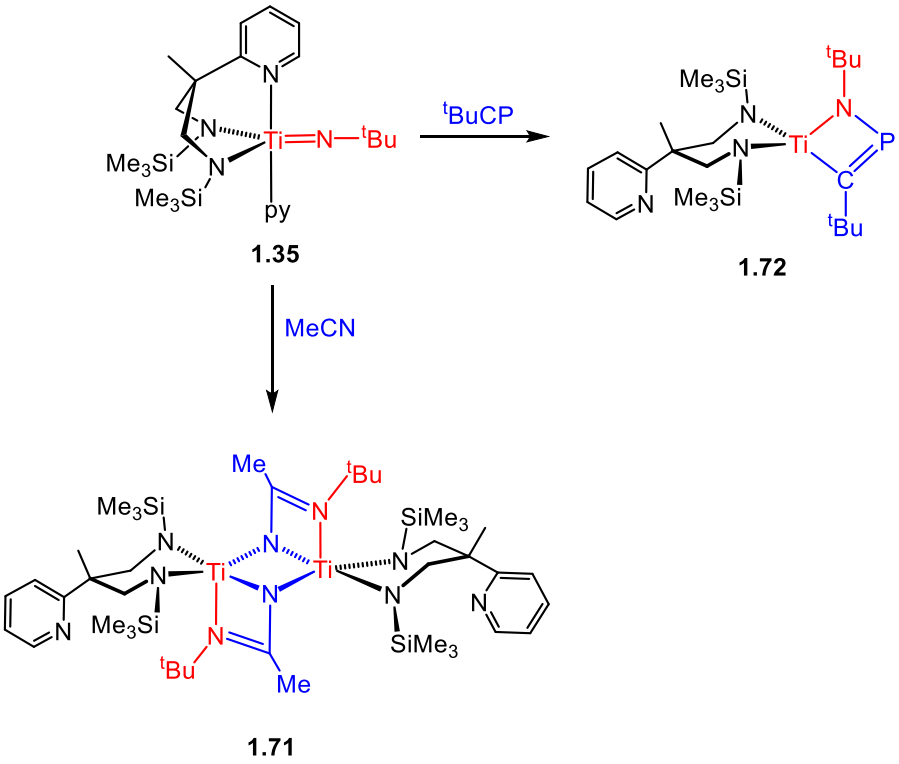

1.35 **1.72** **1.71**

Scheme 1.6. Reaction of Ti(N_2N^{py})(N^tBu)(py) (**1.35**) with MeCN and ^{t}BuCP.[102]

Catalytic hydroamination

Since 2000, imido ligands have found applications as spectator ligands on titanium catalysts in the polymerisation of ethylene, for instance Ti(NR)(TMEDA)Cl_2 (R = ^{t}Bu, 2-$C_6H_4{}^t$Bu or 2-C_6H_4Ph, TMEDA = N,N,N,N-tetramethylethylenediamine).[7, 103] Ti(NR)(Me_3[9]aneN_3)Cl_2 (**1.44** and **1.45**)[8] and cationic complexes [Ti(N^tBu)(Me_3[9]aneN_3)R]$^+$(R = Me or CH_2SiMe_3)[7, 104] have also proved effective. Alongside ethylene polymerisation, Group 4 imide complexes have also found applications in the catalytic hydroamination of alkynes (addition of N–H bonds across

the C≡C bond of alkynes) generating imines, Scheme 1.7.[7] For example, Cp_2TiMe_2 acts as an effective catalyst precursor (0.5 – 3.0 mol%) for the hydroamination of a range of terminal and internal alkynes as well as alkenes and allenes.[20, 105, 106] The active catalyst is thought to be the titanium imido species, $L^1L^2Ti(NR)$ (L^1L^2 = Cp or NHR), produced *via* the bis(amide) complex $L^1L^2Ti(NHR)_2$ following protonolysis of the methyl substituents. The imide complex then reacts with alkyne to generate a [2+2] cycloaddition species which is then protonated by amine, Scheme 1.7. The amine-alkene product then tautomerises to the more stable imine isomer, $R^1CH_2C(NR)R^2$.[106]

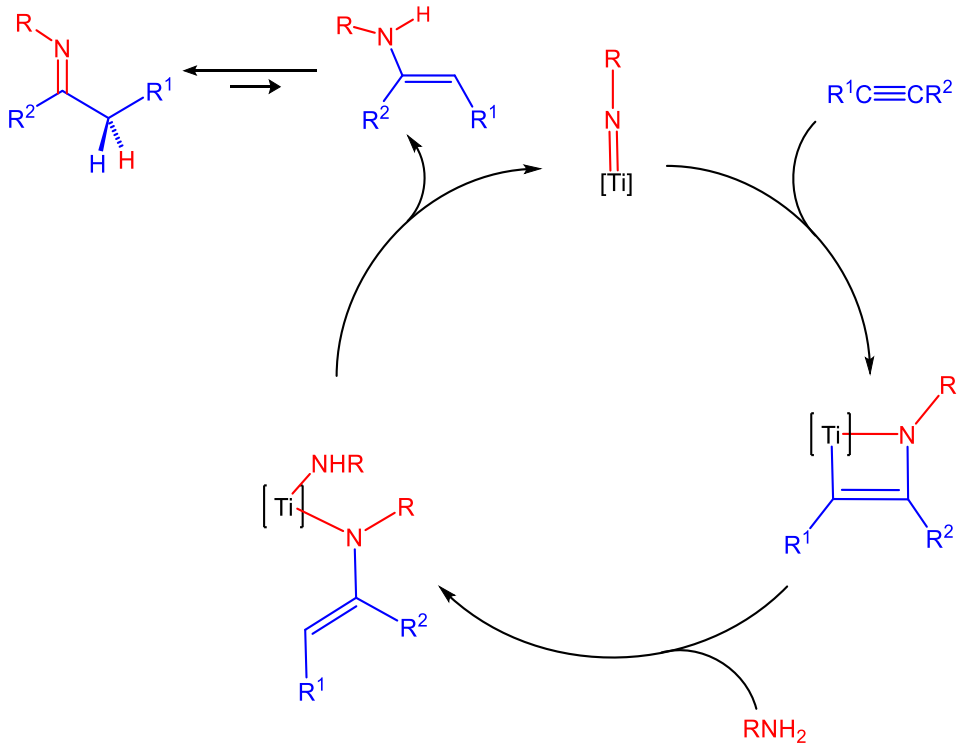

Scheme 1.7. General catalytic cycle for hydroamination (R = alkyl or aryl), hydrohydrazination ($R = NR_2$) or hydrooximination (R = OR) reactions.

The titanium complexes, $Cp^*Ti(N^{Xyl}N)(NR)(L)_n$ (R = aryl (**1.65**) or ^{t}Bu (**1.66**); L = $^t BuNH_2$ or py; *n* = 1 or 0),[99] catalyse the hydroamination of both terminal and internal alkynes over a period of 24 h at 5 mol% loading, although high temperatures of 105 °C were required and mixtures of linear and branched amines were isolated. Accordingly, a more general catalyst, $Cp^*Ti(N^{Xyl}N)Me_2$ (**1.73**), which has been shown to form imides on reaction with amines, was also found to be an effective hydroamination catalyst.[99] Moreover, both **1.66** and **1.73** were shown to be effective catalysts for intramolecular hydroamination reactions as well.[99] Other active catalysts reported in the literature include $Cp_2Ti(\eta^2\text{-}Me_3SiC_2SiMe_3)$,[107] $Ti(NMe_2)_2(dpma)$ (**1.74**, dpma =

N,*N*-di(pyrrolyl-α-methyl)-*N*-methylamine, Fig. 1.13)[19] and $Ti(NMe_2)_4$[108], with the proposed catalytic cycles proceeding *via* imide intermediates in all cases.

Bergman *et al.* have pioneered the research into zirconium catalysts for the hydroamination of alkynes, alkenes and allenes. In 1992, the bis(amide) complex $Cp_2Zr(NHXyl)_2$ was shown to catalyse the coupling of diphenylacetylene, 2-butyne and allene with $XylNH_2$. As mentioned, these bis(amide) zirconium catalysts require the R group to be at least as sterically bulky as 2,6-dimethylphenyl in order to prevent the formation of unreactive dimers.[109] More recently, $Zr(NMe_2)_4$ (**1.75**), $Cp_2Zr(NMe_2)_2$ and sulphonamide-supported zirconium complexes were also shown to be effective hydroamination catalysts of allenes, including tri-substituted allenes.[108] There are few reports, published only recently, on the use of Hafnium complexes as hydroamination catalysts.[110-112] These include the NHC-supported diiodide complex $(CCC^{tBu})Hf(NMe_2)I_2$ (**1.76**),[111] which is able to catalyse the intramolecular hydroamination/cyclisation of a range of aminoalkene substrates, alongside pyridyl-amido supported complexes,[110] although in both cases the hafnium catalysts were much slower than their zirconium congeners.

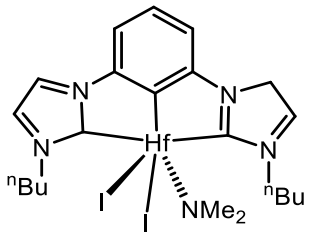

1.76

1.4.2 Group 4 hydrazide complexes

Synthetic entry points for titanium hydrazide complexes

Although the first monomeric η^1-titanium hydrazide complex, $Cp_2Ti\{NN(SiMe_3)_2\}$, was synthesised by Wiberg in 1978, from Cp_2TiCl_2 and two equivalents of 1,2-bis(trimethylsilyl)diazene ($Me_3SiN{=}NSiMe_3$),[54] it was not until 2004 when a Group 4 hydrazide was structurally characterised, namely $Ti(NNMe_2)(Bu^tpy)(dpma)$, by Odom *et al*.[19] In 2005, the diphenyl hydrazide analogues of the *tert*-butylimide synthons **1.30** and **1.44**, $Ti(NNPh_2)Cl_2(py)_3$ (**1.77**) and $Ti(NNPh_2)Cl_2(NHMe_2)_2$ (**1.78**), were reported. This allowed access to a wide range of hydrazide complexes (**1.79** – **1.90**, Schemes 1.8 and 1.9) following reaction with the desired lithiated or protonated ligand, respectively.[39] Compound **1.77** was synthesised from $Ti(N^tBu)Cl_2(py)_3$ and Ph_2NNH_2, in a *tert*-butylimide/hydrazine exchange methodology, much like the synthesis of arylimides from **1.30**,[78, 79] and **1.78** from $Ti(NMe_2)_2Cl_2$ (**1.41**) and Ph_2NNH_2.[84] Examples of various supporting ligand sets used to synthesise η^1-hydrazido(2-) complexes are given in Schemes 1.8 and 1.9.[39, 113-118] Attempts to synthesise an equivalent dimethyl hydrazide synthon from **1.30** or **1.41** with Me_2NNH_2 were unsuccessful, yielding dimers containing μ-η^1:η^2-hydrazido(2-) ligands in both cases (as found for the analogous reaction with *N*-aminopiperidine).[39]

As shown in Schemes 1.8 and 1.9, particularly successful supporting ligand sets are the dianionic tridentate nitrogen or oxygen donor ligands, as found in $(L)Ti(NNPh_2)(py)_n$ (L = N_2O ($N_2O = O(CH_2CH_2NSiMe_3)_2$, **1.80**), $N_2{}^{i\mathrm{Pr}}N$ ($N_2{}^{i\mathrm{Pr}}N = MeN(CH_2CH_2N^iPr)_2$, **1.82**), $N_2{}^{\mathrm{Ar}}O$ ($N_2{}^{\mathrm{Ar}}O = O(2\text{-}C_6H_4NSiMe_3)_2$, **1.83**), N_2N^{py} (**1.84**) and N_2N^{Me} (**1.86**); n = 1 or 2). These supporting ligands are capable of coordinating in both *fac* and *mer* fashions. However, when the apical donor is nitrogen, like in **1.86**, the complexes isolated only show *fac* coordination of the ligand.[113] On the other hand, when the apical donor is oxygen, as found in **1.80** and **1.83**, the ligand is more flexible, binding in a κ^3-*mer*-fashion in the pyridine complexes, but switching to *fac* coordination on addition of 2,2′-bipyridine.[117] The hydrazide ligand in these complexes can then coordinate *trans* to either the apical donor atom or the amide NR_2 ligands, for instance **1.82** *vs* **1.86**. DFT calculations have shown that hydrazide ligands bound *trans* to NMe are electronically favoured however, steric demands can make an equatorial position more favourable, consistent with experimental findings.[119]

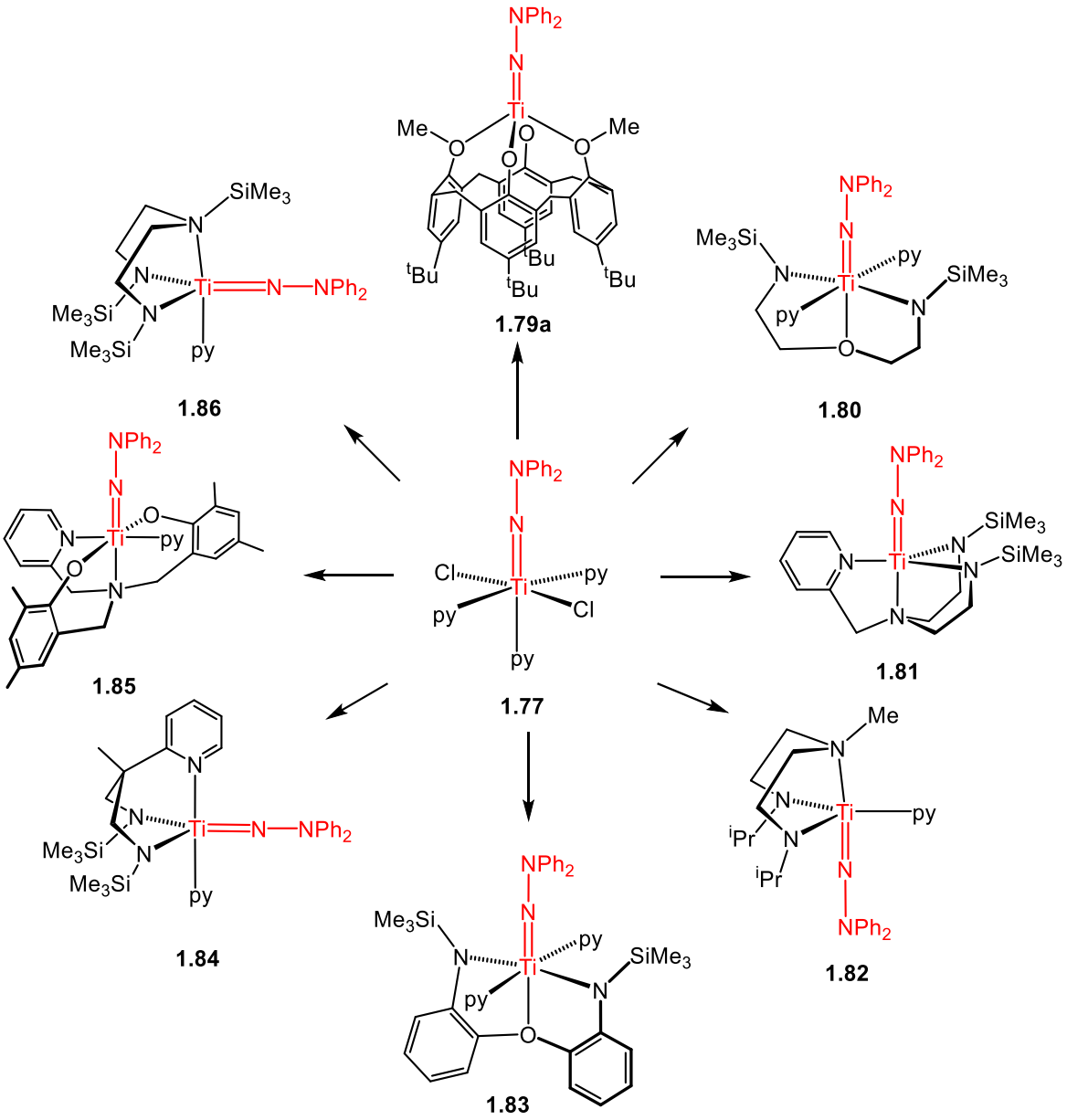

Scheme 1.8. Examples of various titanium diphenyl hydrazide complexes synthesised from $Ti(NNPh_2)Cl_2(py)_3$ (**1.77**).

In many cases, in particular with regards to catalytic C–N bond forming reactions such as hydrohydrazination, the hydrazide complex is synthesised *in situ*. For example, $Ti(NMe_2)_2$(dpma) (**1.74**, Fig. 1.13) is an effective catalyst for both hydroamination and hydrohydrazination where both the imide and hydrazide complexes $Ti(NR)(NHMe_2)_2$(dpma) (R = R or NR_2) are proposed as the active species.[19] Other examples are given in Figure 1.13.

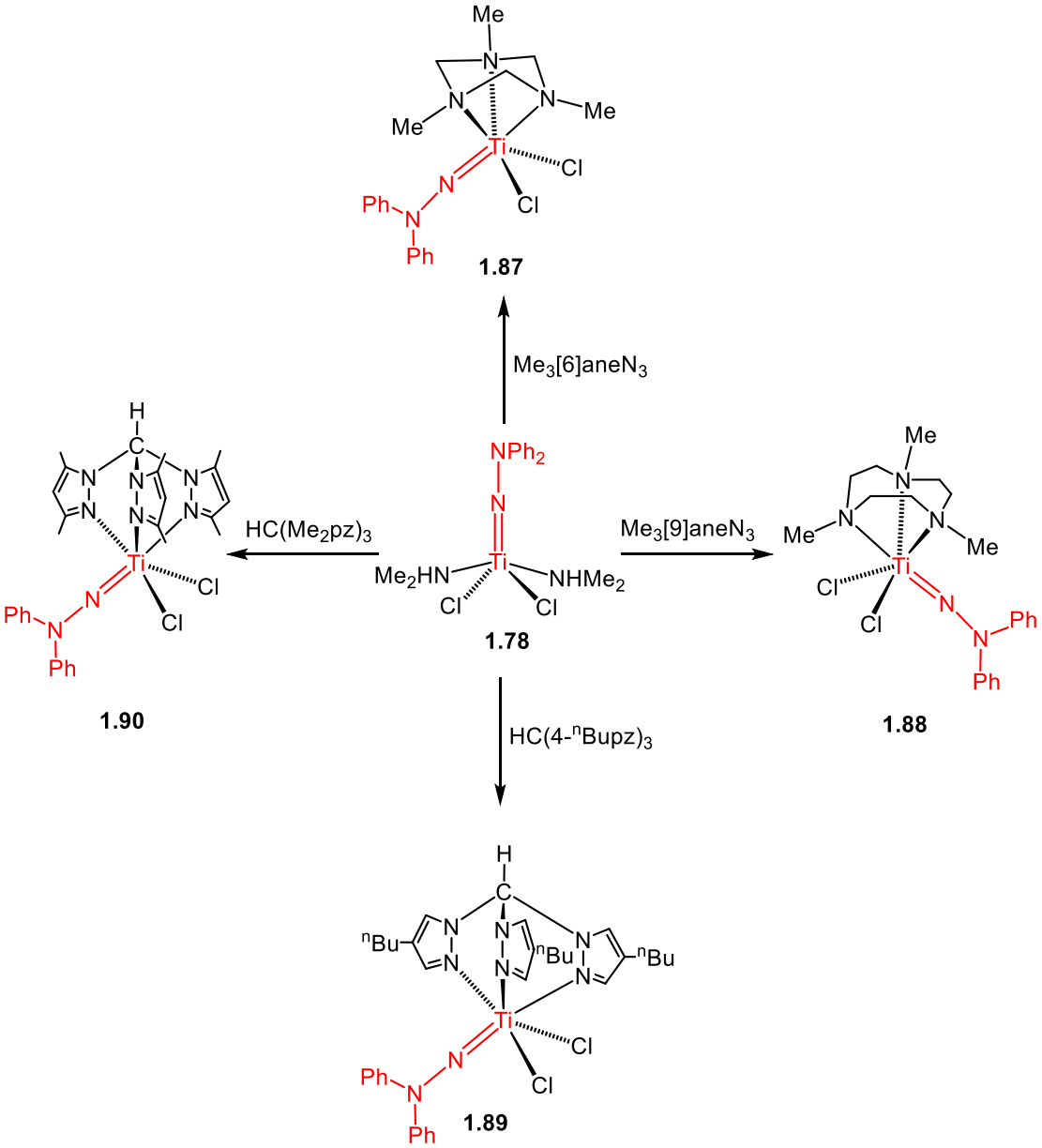

Scheme 1.9. Synthesis of various titanium diphenyl hydrazide complexes from $Ti(NNPh_2)Cl_2(NHMe_2)_2$ (**1.78**).[39]

As discussed, the cyclopentadienyl-amidinate supported complexes, $Cp^*Ti\{MeC(N^iPr)_2\}(NR)$ (R = ^{t}Bu (**1.69**), aryl (**1.70**)), have proved to be very successful for studying the reactivity of imide complexes with unsaturated substrates.[95, 96, 101, 120-124] In contrast to $Cp^*Ti(N^{Xyl}N)(NNRR')(L)$ (R = R′ = Ph (**1.91a**) or Me (**1.91b**); R = Ph, R′ = Me (**1.91c**); L = py or DMAP), synthesised from $Cp^*Ti(N^{Xyl}N)(N^tBu)(NH_2{}^tBu)$ (**1.66**) and $RR'NNH_2$,[26] the hydrazide analogues of **1.69** and **1.70** are unreactive towards alkyne substrates, presumably due to a less open metal

center. Despite this, $Cp^{*}Ti\{MeC(N^{i}Pr)_2\}$ has provided a robust ligand platform for comparing the reactions of imides with their hydrazide counterparts, *vide infra*. The sterically encumbered ligand set has also allowed access to terminal dimethyl hydrazide complexes which are otherwise prone to dimerisation forming unreactive dimers. For instance, the dimethyl hydrazide **1.91b** was only accessible in the presence of DMAP, attempts to synthesis the pyridine analogue only resulted in mixtures of both $Cp^{*}Ti(N^{Xyl}N)(NNMe_2)(py)$ and $[Cp^{*}Ti(N^{Xyl}N)(NNMe_2)]_2$.[26] However, the base-free diphenyl analogue could be synthesised, namely $Cp^{*}Ti(N^{Xyl}N)(NNPh_2)$ (**1.91a′**), either through addition of $B(Ar^{F5})_3$ to **1.91a** or following heat and reduced pressure.[26] The hydrazide complexes $Cp^{*}Ti\{MeC(N^{i}Pr_2)_2\}(NNRR')$ (R = R′ = Ph (**1.92a**) or Me (**1.92b**); R = Ph, R′ = Me (**1.92c**)) were synthesised from $Cp^{*}Ti\{MeC(N^{i}Pr)_2\}(N^{t}Bu)$ (**1.69**) and hydrazine in an analogous methodology to **1.91a** – **1.91c**.[96, 123] Other examples of Cp-supported titanium hydrazide complexes, $Cp_2Ti(NNPh_2)(py)$ (**1.93**) and $CpTi(NNPh_2)(py)(Cl)$ (**1.94**), are given in Scheme 1.10, all synthesised from the parent imide complex using a *tert*-butyl imide/hydrazine exchange reaction.

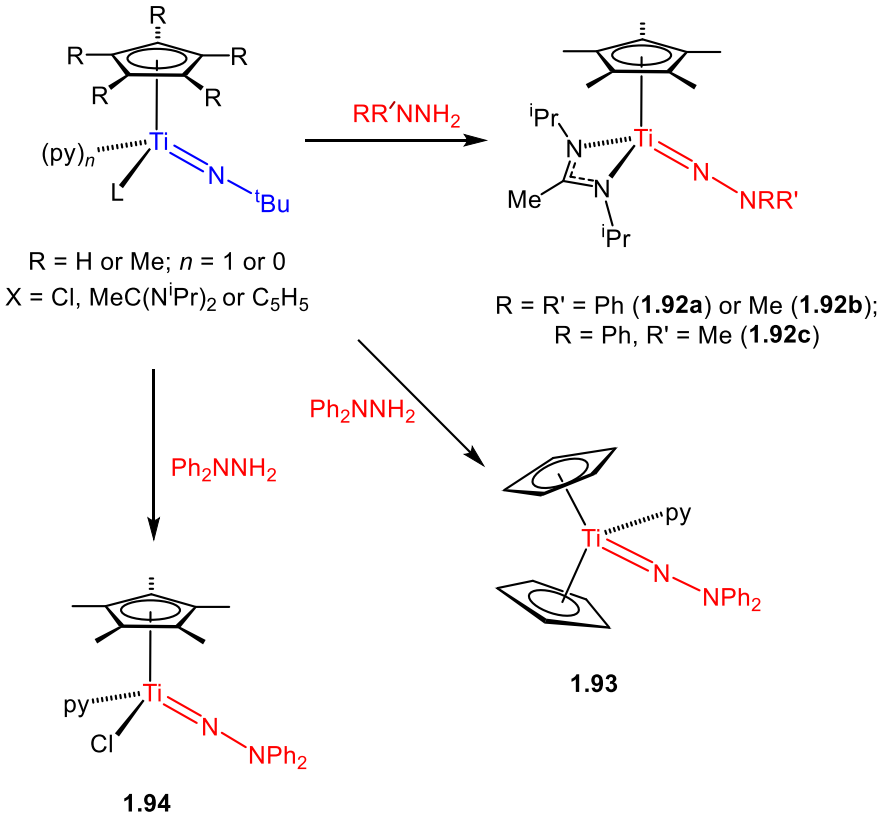

Scheme 1.10. Synthesis of various cyclopentadienyl-supported titanium hydrazide complexes from $Cp^{R}Ti(N^{t}Bu)(X)(py)_n$.

Synthetic entry points for zirconium and hafnium hydrazide complexes

The first monomeric η^1-zirconium hydrazide complex, $Cp_2Zr(NNPh_2)$ (**1.95**, Fig. 1.9), was synthesised in 1991 by Bergman *et al.* from thermolysis of $Cp_2Zr(NHNPh_2)(CH_2CH_2{}^tBu)$, itself formed from $Cp_2Zr(CH_2CH_2{}^tBu)Cl$ and $LiNHNPh_2$.[125] In the absence of a stabilising donor ligand such as DMAP, forming $Cp_2Zr(NNPh_2)(DMAP)$ (**1.96**, Fig, 1.9), this species quickly dimerises to the bridging μ-η^1:η^2-hydrazido(2-) complex.[125] In 2007 Gade *et al.* synthesised the second example of a zirconium hydrazide, $Zr(N_2{}^{TBS}N_{py})(NNPh_2)(py)$ (**1.97**, Fig. 1.9, $N_2{}^{TBS}N_{py}$ = MeC(2-C_5H_4N)($CH_2NSiMe_2{}^tBu)_2$), using $Zr(N_2{}^{TBS}N_{py})Cl_2$ and $LiNHNPh_2$ followed by addition of LiHMDS (LiHMDS = lithium hexamethyldisilazide).[126] An analogous method was used to synthesise the first hafnium hydrazide $Hf(N_2{}^{TBS}N_{py})(NNPh_2)(py)$ (**1.98**, Fig. 1.9) in 2008.[127] However, attempts to use the same synthetic route to generate calixarene-supported zirconium hydrazide complexes, $Zr(NNR_2)(Me_2Calix)$ (R = Me or Ph, Me_2Calix = dianion of 1,3-dimethyl ether of *tert*-butyl calix[4]arene), only generated the bis(hydrazido(1-)) complexes $Zr(NHNR_2)_2(Me_2Calix)$.[116]

A useful synthon for zirconium hydrazide synthesis, in particular for synthesising complexes supported by tridentate nitrogen-based ligands, is $Zr(NMe_2)_4$ (**1.75**). For instance, $Zr\{(N^{Xyl})_2N_{py}\}(NNR)(DMAP)_2$ (R = C_9H_{10} (**1.99**) or $C_{12}H_8$, Fig. 1.9, $(N^{Xyl})_2N_{py}$ = MeC(2-C_5H_4N)($CH_2NXyl)_2$) is synthesised *via* reaction of **1.75** with the neutral ligand $(HN^{Xyl})_2N_{py}$ followed by a second protonolysis reaction with the desired hydrazine.[128] Interestingly, attempts to synthesise hydrazide complexes with electron-withdrawing aryl substituents bound to the amide nitrogens of the supporting ligand, namely $H_2N_2{}^{PFP}N_{py}$ ($H_2N_2{}^{PFP}N_{py}$ = MeC(2-C_5H_4N)($CH_2N(H)C_6F_5)_2$), yielded $Zr(N_2{}^{TFAP}N_{py})F_2$ (**1.100**, $N_2{}^{TFAP}N_{py}$ = MeC(2-C_5H_4N){CH_2N(2-$C_6F_4NMe_2$)}$_2$) following reaction with **1.75**. Reaction of **1.100** with $LiNHNPh_2$ and LiHMDS however, did yield the monomeric hydrazido(2-) complex $Zr(N_2{}^{TFAP}N_{py})(NNPh_2)$ (**1.101**, Fig. 1.9).[129] Furthermore, as discussed previously, in catalytic C–N bond forming reactions the active species, in this case a zirconium hydrazide, is often synthesised *in situ* from the corresponding diamide complex, for example $Zr\{(N^{Xyl})_2N_{py}\}(NMe_2)_2$ (**1.102**).[130]

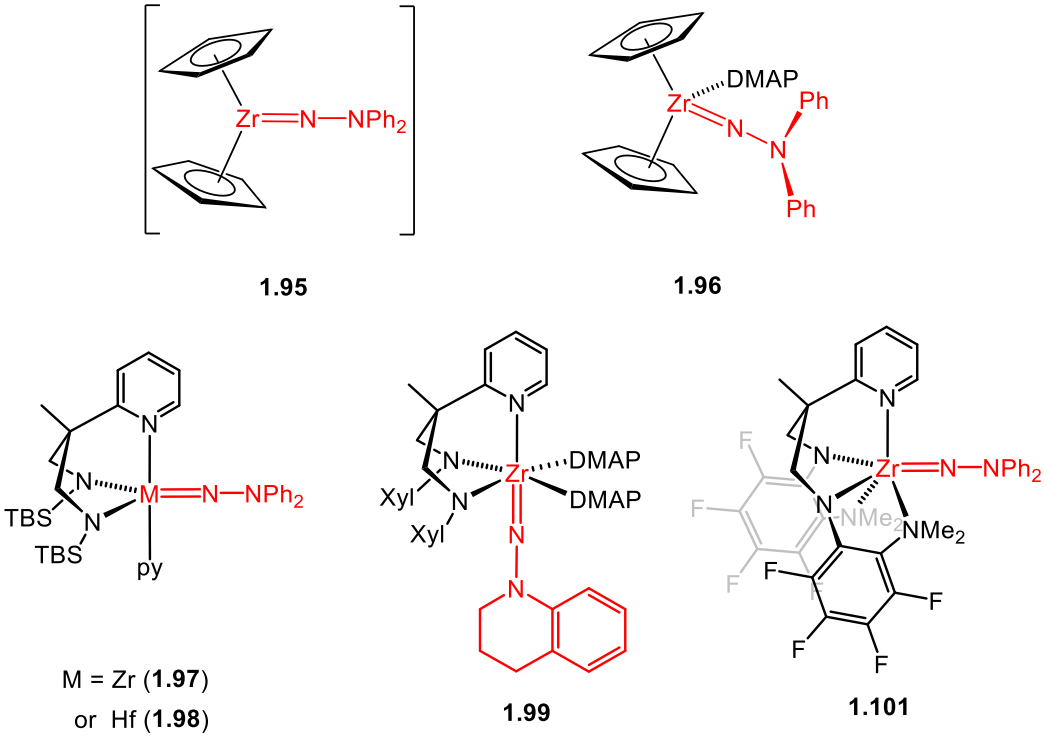

Figure 1.9. Examples of zirconium η^1-hydrazido(2-) complexes.

Structural features

To date there have been four comprehensive studies into the effect of N_β substituents on the geometry of titanium hydrazide complexes.[26, 40, 96, 116] In one case, using Cp*Ti($N^{Xyl}N$)(NNR$_1$R$_2$)(L) (**1.91a** – **1.91c**),[26] the ligand (L) was varied between the different complexes preventing detailed structural comparisons. However, in the cyclopentadienyl-amidinate supported hydrazide complexes, Cp*Ti{MeC(N^iPr)$_2$}(NNR$_1$R$_2$) (**1.92a** – **1.92c**),[96] the N_β substituents were varied from dialkyl to diaryl (R$_1$ = R$_2$ = Ph (**1.92a**) or Me (**1.92b**); R$_1$ = Me, R$_2$ = Ph (**1.92c**)) and all three compounds structurally characterised. In all cases, the respective short and long Ti=N_α (1.723(2) – 1.734(2) Å) and N_α–N_β (1.369(2) – 1.386(2) Å) bond lengths and linear Ti–N_α–N_β bond angles (159.5(1) – 166.3(2) °) are all consistent with formally Ti≡N triple bonds and N–N single bonds. The ligands are therefore formal η^1-hydrazido(2-) ligands, as given in Fig. 1.3. However, with aryl substituents the N_β appears planar, consistent with *sp*^{2} hybridisation, from lone pair delocalisation into at least one phenyl ring (the dimethyl hydrazido complex, **1.92b**, possesses a pyramidal N_β as expected). In all three cases there is donation of the N_β lone pair into the Ti=N_α π^* antibonding orbital, resulting in a longer Ti=N_α bond. On moving from a pyramidal to a more planar geometry the donation from the N_β lone pair into the Ti=N_α π^* orbital

is increased, consistent with the experimental observations, the Ti=N bond length increases in the order **1.92b** (NMe_2) < **1.92c** (NMePh) ≈ **1.92a** (NPh_2). Accordingly, DFT calculations showed that on forcing N_β to be planar in the case of **1.92b** the Ti=N_α bond lengthened by 0.011 Å. The DFT calculated Ti=N_α–R bond lengths were therefore found to increase in the order R = NPh_2 < NMePh < NMe_2 (planar N_β) in line with increasing basicity of N_β. The relative bond lengths of Ti=N_α and N_α–N_β are also related, with the shortest Ti=N_α bond found with the longest N_α–N_β bond, and *vice versa*.

Compared to imido complexes, the structure and bonding of which was described in Section 1.4.1, hydrazide complexes, in general, show longer Ti=N_α bonds than alkyl imide complexes, as expected based on N_βRR′ lone pair donation lengthening the Ti=N_α bond. On the other hand, the Ti=N_α bond lengths of aryl imide complexes lie in between dialkyl and diaryl hydrazide complexes. This is a consequence of the π accepting nature of the phenyl ring leading to Ti=N_α π orbital to phenyl π* orbital and phenyl π orbital to Ti=N_α π* orbital interactions as described above.[96, 131] To conclude, the Ti=N_α bond lengths of hydrazide and imide complexes supported by cyclopentadienyl-amidinate ligands are found to increase in the order Ti=N_α–R, R = Me < NMe_2 < Ph < NPh_2 ≈ NMePh < NMe_2 (planar N_β).

Stoichiometric reactions involving the M=N_α multiple bond

Like their imide counterparts, Group 4 hydrazides show a wide range of reactivity at the M=N_α multiple bond. Indeed, [2+2] cycloaddition reactions are proposed as the first step in almost all reactions with unsaturated substrates, in particular with heterocumulenes and alkynes, which are now well-established. Once formed, these cycloaddition products, which are isolable in some cases, can undergo further reaction. Those reactions not involving the N_α–N_β bond, include insertion of a second substrate into the, now single, M–N bond or extrusion of an organic fragment leaving behind a metal-oxo species.

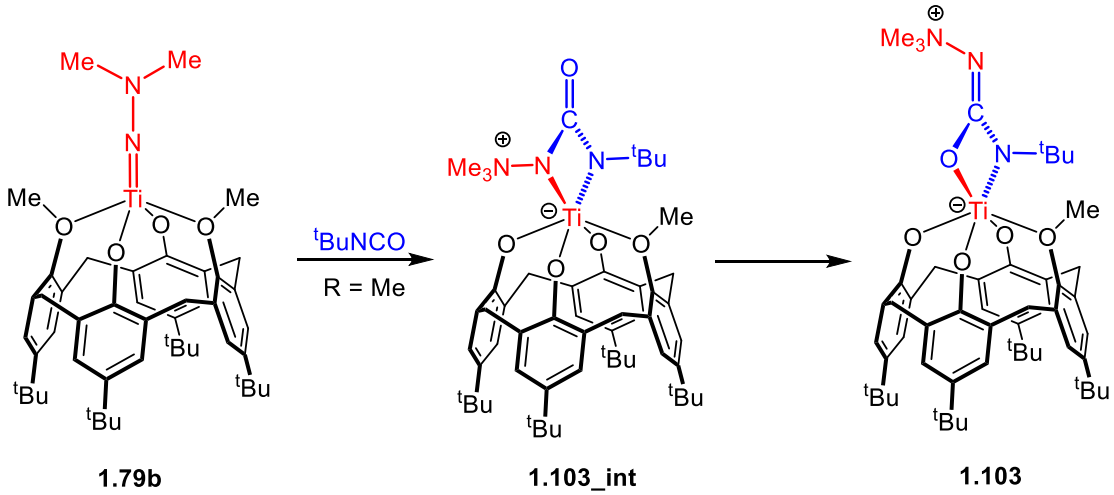

1.79b **1.103_int** **1.103**

Scheme 1.11. Reaction of Ti(NNMe$_2$)(Me$_2$Calix) (**1.79b**) with ^{t}BuNCO.[116]

In 2008, Ti(NNMe$_2$)(Me$_2$Calix) (**1.79b**) was shown to form Ti{N(^{t}Bu)C(NNMe$_3$)O}(MeCalix) (**1.103**) on reaction with ^{t}BuNCO, Scheme 1.11.[116] The proposed intermediate is the zwitterionic κ^2*N,N*′-bound ureate complex Ti{N(NMe$_3$)C(O)N(^{t}Bu)}(MeCalix) (**1.103_int**) following [2+2] cycloaddition of ^{t}BuNCO to Ti=N$_\alpha$ and abstraction of a methyl from the supporting ligand. Although the range of Ti(NNRR′)(Me$_2$Calix) complexes (R = R′ = Ph (**1.79a**) or Me (**1.79b**); R = Me, R′ = Ph (**1.79c**)) were tested with a range of substrates, only two other types of reaction with **1.79b** were successful, namely reaction with alkylating agents, resulting in alkylation at N$_\beta$, and reaction with PhC(O)H to give [Ti(μ-O)(Me$_2$Calix)]$_2$ and PhC(NNMe$_2$)H presumably following extrusion from the [2+2] cycloaddition intermediate Ti{N(NMe$_2$)C(Ph)(H)O}(Me$_2$Calix).[116]

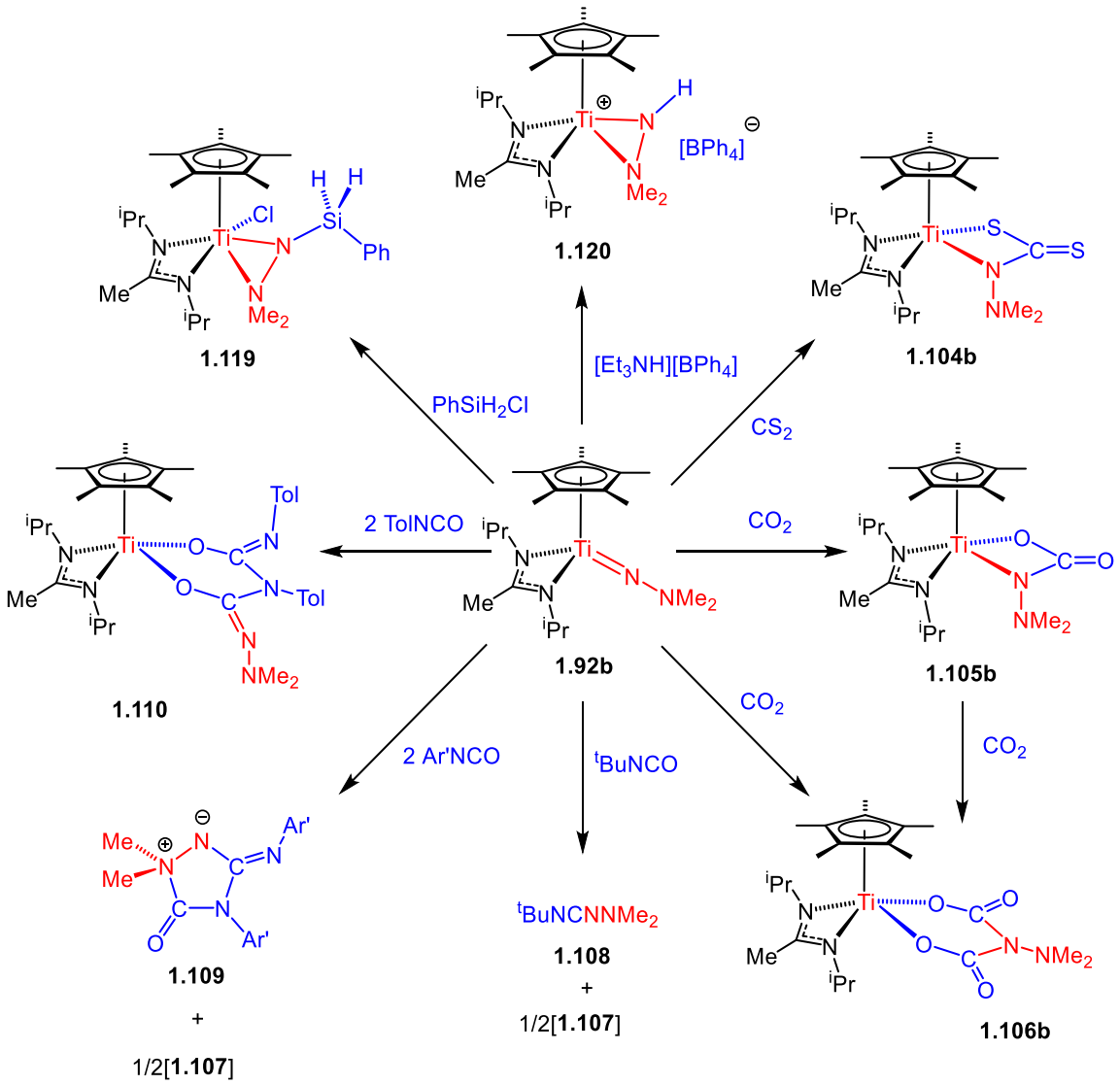

Scheme 1.12. Reaction of Cp*Ti{MeC(N^{i}Pr)$_2$}(NNMe$_2$) (**1.92b**) with (un)saturated substrates.[96]

As mentioned, a wide range of reactions at Ti=N$_\alpha$ were observed using cyclopentadienyl-amidinate supported hydrazide complexes Cp*Ti{MeC(N^{i}Pr)$_2$}(NNR$_2$) (R = Ph (**1.92a**) or Me (**1.92b**)).[96] Reaction of **1.92a** or **1.92b** with CO$_2$ and CS$_2$ gave [2+2] cycloaddition products, Cp*Ti{MeC(N^{i}Pr)$_2$}{N(NR$_2$)C(X)X} (R = Ph or Me, X = S (**1.104a** and **1.104b**) or O (**1.105a** and **1.105b**), Scheme 1.12). With CO$_2$ both complexes, **1.105a** and **1.105b**, proceeded to insert a second CO$_2$ molecule into the newly formed Ti–N bond generating the "double insertion" complexes Cp*Ti{MeC(N^{i}Pr)$_2$}-{OC(O)N(NR$_2$)C(O)O} (R = Ph (**1.106a**) or Me (**1.106b**), Scheme 1.12). Reaction of **1.92a** and **1.92b** with isocyanates gave different reaction products depending on the identity of the N$_\beta$

substituents. With **1.92a** the [2+2] cycloaddition products formed with Ar′NCO, TolNCO and ^{t}BuNCO were stable and isolable in all cases, reminiscent of Ti(N_2N^{Me})($NNPh_2$)(py) (**1.86**) with ArNCE (E = O, S or Se). Conversely, reaction of **1.92b** with ^{t}BuNCO and Ar′NCO gave only the titanium μ-oxo dimer [Cp*Ti{MeC($N^{i}Pr$)$_2$}(O)]$_2$ (**1.107**) and the organic fragments, ^{t}BuNCNNMe$_2$ (**1.108**, Scheme 1.12), and N(Me)$_2$NC(NAr´)N(Ar´)C(O) (**1.109**, Scheme 1.12), respectively following extrusion from the inherently unstable cycloaddition intermediates. Reaction of **1.92b** with 2 equivs of TolNCO gave Cp*Ti{MeC($N^{i}Pr$)$_2$}{OC($NNMe_2$)N(Tol)C(NTol)O} (**1.110**, Scheme 1.12) following the same cycloaddition-extrusion pathway as with RNCO (R = Ar′ or ^{t}Bu). In this case rapid cycloaddition of the extruded organic fragment to (L)Ti=O formed Cp*Ti{MeC($N^{i}Pr$)$_2$}{N(Tol)C($NNMe_2$)O} (not observed) which then reacts with a second equivalent of TolNCO to give **1.110**.

A single isomer is formed in all cycloaddition reactions between **1.92** and isocyanates. From structural characterisation and IR and ROESY NMR spectroscopic data the ureate ligand is thought to coordinate in a κ^2*N,O*-fashion in all cases, in contrast to that observed with Ti($NNMe_2$)(Me_2Calix) (**1.79b**).[116] On the other hand, reaction of Cp*Ti(N^{Xyl}N)(NNRR′)(L) (R = Ph, R′ = Ph (**1.91a**) or Me (**1.91c**)) with PhNCS and PhNCO gave a mixture of both κ^2*N,E* (E = O or S) and κ^2*N,N′* isomers.[132] Subsequent DFT calculations indicate that κ^2*NN′* isomers are favoured electronically, but that steric constraints can make it more energetically favourable to have a κ^2*NE* arrangement.[95, 96, 133]

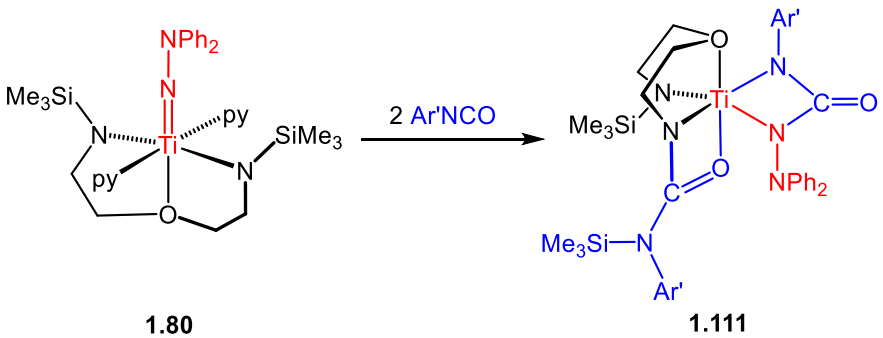

1.80 **1.111**

Equation 1.4

Although the reaction of Ti(N_2O)($NNPh_2$)(py)$_2$ (**1.80**) with Ar′NCS gave the expected cycloaddition product, Ti(N_2O){N(NPh_2)C(NAr′)S}(py),[117] as observed with Ti(N_2N^{Me})($NNPh_2$)(py) (**1.86**),[133] reaction with Ar′NCO required two equivs to reach

completion. Subsequent structural analysis showed formation of Ti{O($CH_2CH_2NSiMe_3$)($CH_2CH_2NC(O)N(SiMe_3)Ar'$)}{$N(NPh_2)C(O)N(Ar')$} (**1.111**, Eq 1.4), whereby one equiv of Ar′NCO has undergone the expected [2+2] cycloaddition reaction to Ti=N_α to form a κ^2*NN*-ureate ligand. However, a further equiv of Ar′NCO has also reacted with one of the Ti–N_{amide} bonds which, following a 1,3-$SiMe_3$ sigmatropic shift, generates the observed product, **1.111**.[117]

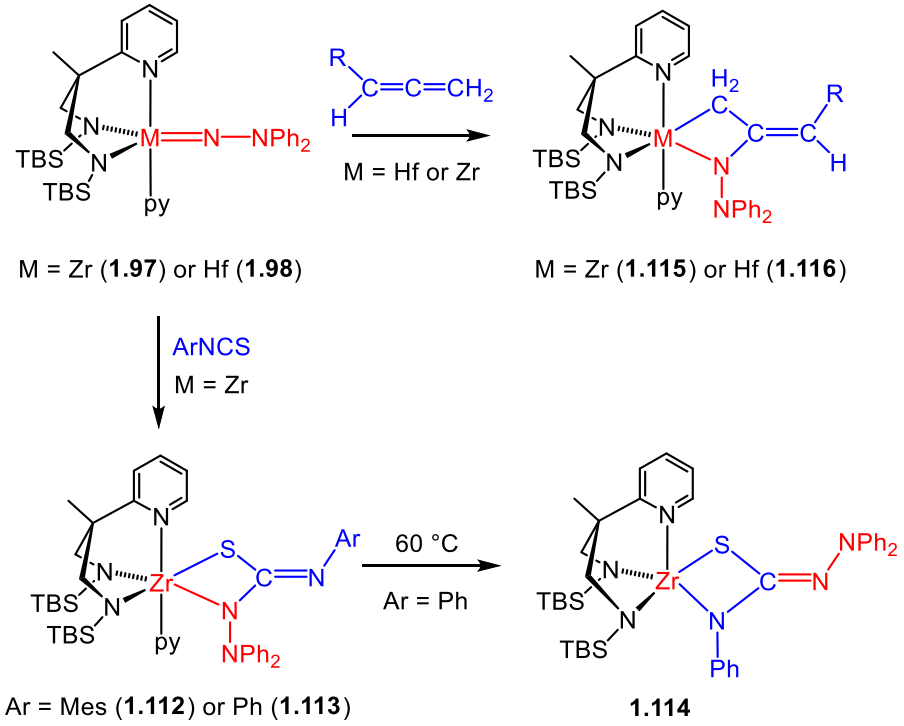

Scheme 1.13. Reaction of ($N_2^{TBS}N_{py}$)($NNPh_2$)(py) (M = Zr (**1.97**) or Hf (**1.98**)) with allenes and ArNCS.[134]

Reactions of isocyanates and isothiocyanates with zirconium hydrazides are much less well-developed. However, recent work by Gade *et al.* has shown that reaction of Zr($N_2^{TBS}N_{py}$)($NNPh_2$)(py) (**1.97**) with MesNCS and PhNCS also give isolable cycloaddition products, namely Zr($N_2^{TBS}N_{py}$){$N(NPh_2)C(NAr)S$}(py) (Ar = Mes (**1.112**) or Ph (**1.113**), Scheme 1.13), binding to zirconium in a κ^2*N*,*S*-fashion.[134] On heating, **1.113** isomerises to form Zr($N_2^{TBS}N_{py}$){$N(Ph)C(NNPh_2)S$} (**1.114**, Scheme 1.13). Reaction of zirconium and hafnium hydrazide complexes **1.97** and **1.98** also gave cycloaddition products with a range of alkyl and aryl allenes, $R(H)CCCH_2$, namely M($N_2^{TBS}N_{py}$){$N(NPh_2)C(C\{H\}R)CH_2$}(py) (M = Zr (**1.115**) and Hf (**1.116**), Scheme 1.13) with Markovnikov regioselectivity in both cases.[134] Although stable at room temperature these complexes undergo further reaction at high temperature, *vide infra*.

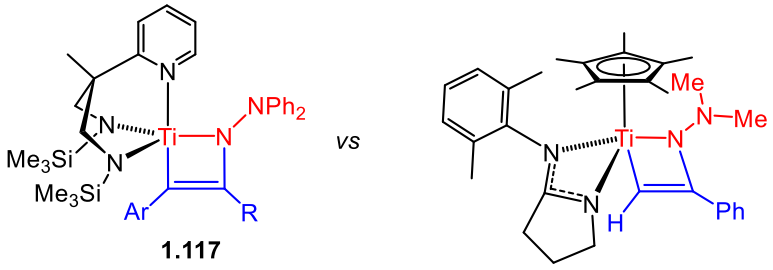

1.117

R = Me, Ar = Ph, 4-$C_6H_4CF_3$ or C_6F_5
R = H, Ar = Ph, Tol, 3-C_6H_4F, 4-$C_6H_4CF_3$ or C_6F_5

1.118

Figure 1.10. Ti(N_2N^{py}){N(NPh$_2$)C(R)C(Ar)}(py) (**1.117**)[135] and Cp*Ti(N^{Xyl}N){N(NMe$_2$)C(Ph)C(H)} (**1.118**).[26]

In 2011, work by Mountford *et al.* reported the reactions of Ti(N_2N^{py})(NNPh$_2$)(py) (**1.84**) with both terminal and internal alkynes which gave isolable [2+2] cycloaddition products of the type Ti(N_2N^{py}){N(NPh$_2$)C(R)C(Ar)}(py) (**1.117**, Ar = phenyl or substituted phenyl; R = H or Me, Fig. 1.10).[135] These reactions were seen to form a single regioisomer, with the CAr carbon bound directly to titanium. This is in contrast to the isomer formed in the reaction of Cp*Ti(N^{Xyl}N)(NNMe$_2$) (**1.91b**) with PhCCH, giving Cp*Ti(N^{Xyl}N){N(NMe$_2$)C(Ph)C(H)} (**1.118**), in which the C(H) carbon is bound to titanium, Fig. 1.10.[26] The former is calculated to be electronically favoured, since this stabilises the HOMO which lies predominately on the carbon bound to titanium and N_α, see Chapter 2 for further details.[135] The larger steric requirement of the Cp*-amidinate ligand in **1.91b** prevents the alkyne from approaching the titanium metal center with the CAr carbon orientated towards the metal and so, in this case, the regiochemistry is sterically favoured.[99]

A recent investigation into the reactions of Cp*Ti{MeC(N^{i}Pr)$_2$}(NNMe$_2$) (**1.92b**) with silanes have reported 1,2-addition of Si–H and Si–X bonds across Ti=N_α, affording complexes of the type Cp*Ti{MeC(N^{i}Pr)$_2$}(X){N(NMe$_2$)SiH$_2$Ph} (e.g. X = Cl (**1.119**), Scheme 1.12).[122, 124] Coordination of N_β to titanium is also seen on reaction with [Et$_3$NH][BPh$_4$], forming [Cp*Ti{MeC(N^{i}Pr)$_2$}{η^2-N(H)NMe$_2$}][BPh$_4$] (**1.120**, Scheme 1.12), confirmed by structural analysis.[122] Though reaction with the triethylammonium salt gave protonation at N_α, reaction with alkylating agents MeI, CH$_2$PhBr and EtBr resulted in alkylation at N_β, much like Ti(NNMe$_2$)(Me$_2$Calix) (**1.79b**), yielding [Cp*Ti{MeC(N^{i}Pr)$_2$}(NNRMe$_2$)][X] (R = Me, X = I; R = CH$_2$Ph or Et, X = Br).[116]

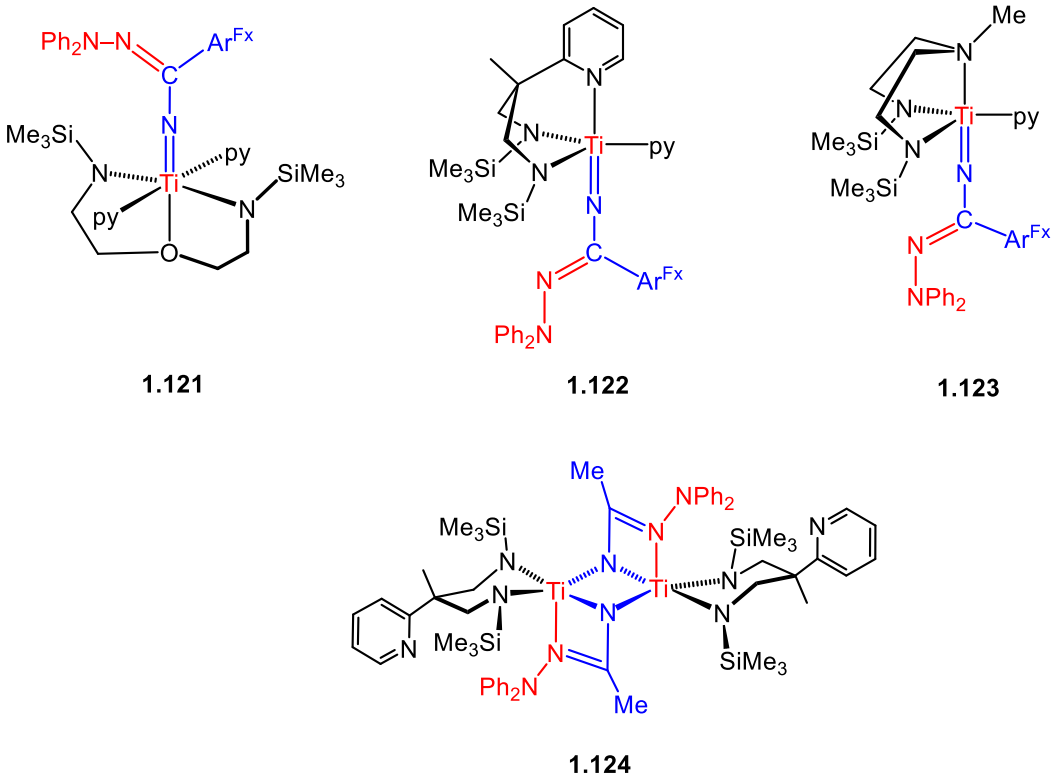

Figure 1.11. Reaction products of titanium diphenyl hydrazide complexes with organic nitriles.

Reaction of hydrazide complexes with isonitriles can result in N_α–N_β bond cleavage, *vide infra*, however, compounds **1.92b** and Ti($N_2^{Ar}O$)($NNPh_2$)(py) (**1.83**) gave adducts on reaction with ^{t}BuNC and XylNC, respectively yielding Cp*Ti{MeC(N^iPr)$_2$}($NNMe_2$)(CN^tBu)[136] and Ti($N_2^{Ar}O$)($NNPh_2$)(CNXyl)(py).[117] Reactions of Group 4 hydrazides with organic nitriles have only recently appeared in the literature and in all cases result in insertion of the nitrile into the Ti=N_α bond. For example the diamide-amine and diamide-ether supported titanium hydrazide complexes (L)Ti($NNPh_2$)(py)$_n$ react with $Ar^{Fx}CN$ (Ar^{Fx} = Ar^{F5} or 2,6-$C_6H_3F_2$) to give (L)Ti{NC(Ar^{Fx})$NNPh_2$}(py)$_n$ (L = N_2O (**1.121**), N_2N^{py} (**1.122**) and N_2N^{Me} (**1.123**); n = 1 or 2, Fig. 1.11).[117, 133] The electron-withdrawing nature of the nitrile substituent appears vital in producing stable and isolable monomeric complexes. For instance, reaction of Ti(N_2O)($NNPh_2$)(py) (**1.80**) and Ti($N_2^{Ar}O$)($NNPh_2$)(py) (**1.83**) with PhCN resulted in complicated mixtures,[117] and reaction of Ti(N_2N^{py})($NNPh_2$)(py) (**1.84**) produced a dimeric structure with MeCN, namely [Ti(N_2N^{py}){μ-η^2-NC(Me)$NNPh_2$}]$_2$ (**1.124**), reminiscent of [Ti(N_2N^{py}){μ-η^2-NC(Me)N^{t}Bu}]$_2$ (**1.71**).[133] Cycloaddition intermediates are proposed in all cases.

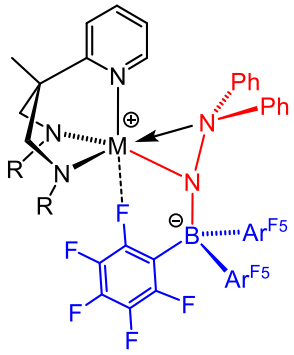

M = Zr (**1.125**) or Ti (**1.126**); R = $SiMe_3$ or $SiMe_2{}^tBu$

Finally, as previously mentioned $B(Ar^{F5})_3$ can be used to remove coordinated pyridine and, in at least one case, generate base-free terminal hydrazide(2-) complexes.[26] In other examples, more than one equiv of borane is required. As expected one equiv removes the pyridine as a py·$B(Ar^{F5})_3$ adduct whereas the second equiv coordinates to N_α whilst N_β coordinates to the metal forming a η^2–hydrazido(1-) complex. A stabilising M···F interaction (from one of aryl groups on $B(Ar^{F5})_3$) is also present in both $M(N_2N^R)\{\eta^2\text{-}N(B\{Ar^{F5}\}_3)NPh_2\}$ (M = Zr, N_2N^R = $N_2{}^{TBS}N_{py}$ (**1.125**) and M = Ti, N_2N^R = N_2N^{Me} (**1.126**)).[133,127]

Stoichiometric reactions involving the N_α–N_β bond

The relatively weak N_α–N_β bond in Group 4 hydrazide complexes (a N_α–N_β single bond in the case of early transition metals) is what differentiates their reactivity from their imido counterparts. Reductive N_α–N_β bond cleavage can be induced by reaction with oxidisable substrates such as CO (e.g. **1.127**, Fig. 1.12), isonitriles (for example, reaction of $Ti(N_2N^{Me})(NNPh_2)(py)$ (**1.86**) with XylNC forming $Ti(N_2N^{Me})(NPh_2)(NCNXyl)(py))$[133] and alkynes, Fig. 1.12. Heat can also be used, as seen in the cycloaddition complexes $M(N_2{}^{TBS}N_{py})\{N(NPh_2)C(C\{H\}Cy)CH_2\}(py)$ (M = Zr or Hf) which form **1.128** or **1.129**, respectively (Fig. 1.12) on heating to 80 °C in toluene.[134]

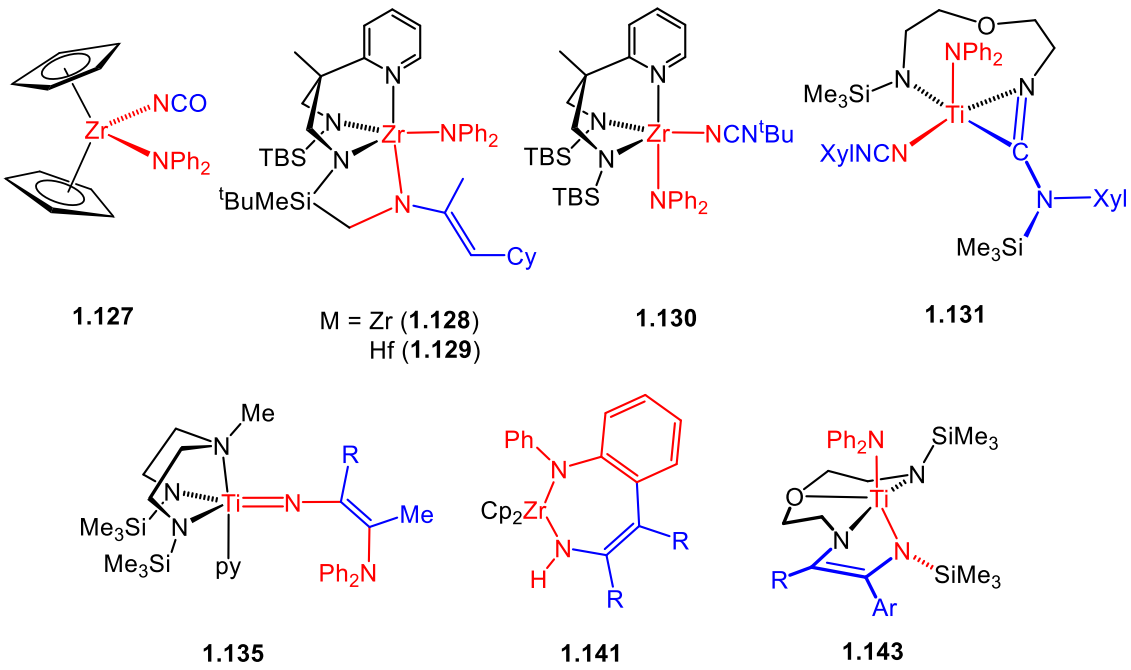

Figure 1.12. Reaction products of titanium diphenyl hydrazide complexes following reductive N_α–N_β bond cleavage. R = alkyl or aryl.

The DFT calculated mechanism for MeNC insertion into the N_α–N_β bond of $Ti(N_2^{SiH_3}N^{Me})(NNPh_2)(py)$ (**A1**, $N_2^{SiH_3}N^{Me}$ = $MeN(CH_2CH_2NSiH_3)_2$), a model for **1.86**, is shown in Scheme 1.14.[133] Loss of pyridine followed by coordination of MeNC forms $Ti(N_2^{SiH_3}N^{Me})(NNPh_2)(CNMe)$ (**A3**). These adducts have been discussed previously with $Cp^*Ti\{MeC(N^iPr)_2\}(NNMe_2)$ (**1.92b**) and $Ti(N_2^{Ar}O)(NNPh_2)(py)$ (**1.83**) and RNC (R = ^{t}Bu or Xyl).[117, 136] Coordination of N_β to titanium in the three-membered cycloaddition intermediate **A5** helps to induce N_α–N_β bond cleavage, forming the final product $Ti(N_2^{SiH_3}N^{Me})(NPh_2)(NCNMe)$ (**A6**). This reaction pathway is also observed for $Zr(N_2^{TBS}N_{py})(NNPh_2)$ (**1.97**) and $Ti(N_2O)(NNPh_2)(py)$ (**1.80**),[117] also with ^{t}BuNC, forming (L)M(NPh)(NCN^tBu) (M = Ti, L = N_2N^{py}; M = Zr, L = $N_2^{TBS}N_{py}$ (**1.130**, Fig. 1.12)).

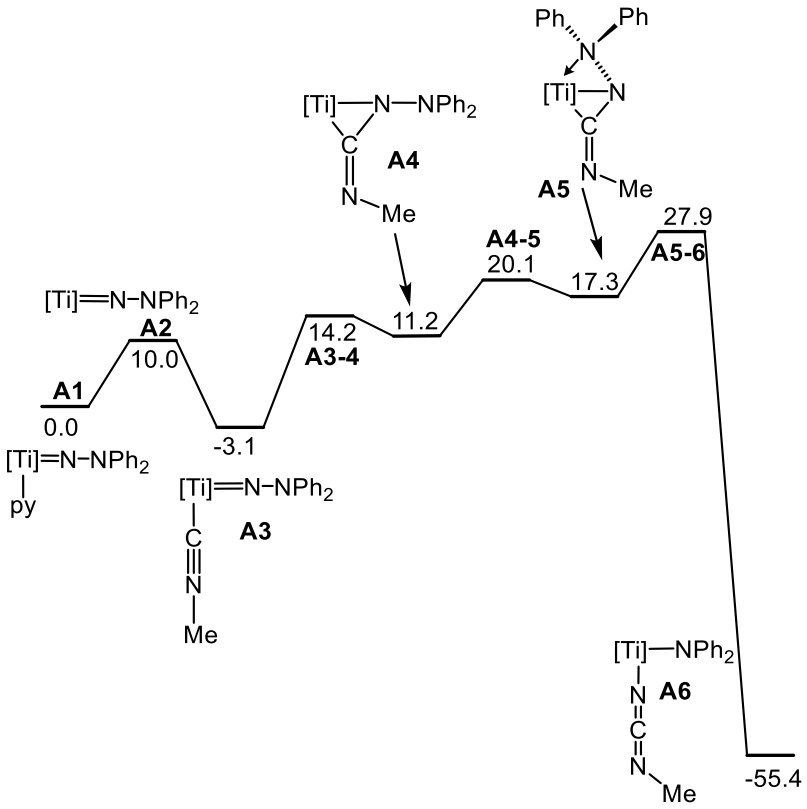

Scheme 1.14. Gibbs free energy (kcal mol^{-1}) profile for MeNC insertion into the N_α–N_β bond of Ti($N_2^{SiH_3}N^{Me}$)($NNPh_2$)(py) (**A1**).[133]

Reaction of **1.80** with XylNC required 2 equivs to reach completion yielding a product (**1.131**, Fig. 1.12) reminiscent of that observed with ArʹNCO, *vide supra* (**1.111**, Eq 1.4). In this case, one equiv of XylNC has cleaved the N_α–N_β bond, as detailed above, and the second equiv has reacted with one of the N–$SiMe_3$ bonds forming **1.131**, Fig 1.12. N_α–N_β bond cleavage is also observed with Zr($N_2^{TBS}N_{py}$)($NNPh_2$) (**1.97**) and 0.5 equivs of Ph_3PSe or propylene sulfide giving the dimeric structures Zr($N_2^{TBS}N_{py}$)(NPh_2)}$_2$(μ-N_2E) (E = S (**1.132**) or Se (**1.133**)).[126] In 2013, reaction of Zr($N_2^{TBS}N_{py}$)($NNPh_2$) (**1.97**) with excess I_2 was reported to release tetraphenyl hydrazine and N_2.[137] On addition of 0.5 equiv of iodine, only the release of N_2 was observed leaving behind the amide complex Zr($N_2^{TBS}N_{py}$)(NPh)(I). Addition of 0.5 equiv of PhEEPh (E = S or Se) to **1.97** also resulted in loss of dinitrogen alongside formation of Zr($N_2^{TBS}N_{py}$)(NPh)(EPh). A radical mechanism is proposed in both cases.

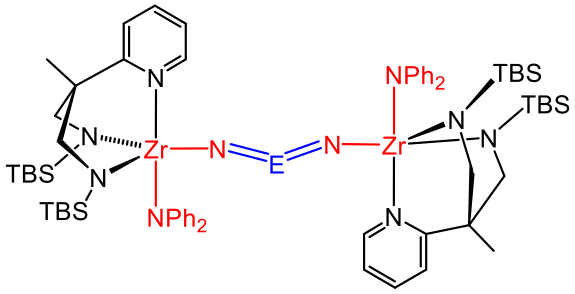

E = S (**1.132**) or Se (**1.133**)

Over a period of 3 d Ti(N_2N^{py}){N(NPh_2)C(Me)C(Ph)}(py) (**1.117**, formed from Ti(N_2N^{py})($NNPh_2$)(py) (**1.84**) and PhCCMe, *vide supra*) underwent further reaction forming the vinylimido complex Ti(N_2N^{py}){NC(Ph)C(Me)NPh_2}(py) (**1.134**, Eq 1.5).[135] Replacing the supporting ligand with the diamide-amine ligand set, N_2N^{Me}, dramatically reduced the reaction time, indeed in this case the cycloaddition intermediates were not observed, generating a range of vinylimido complexes Ti(N_2N^{Me}){NC(R)C(Me)NPh_2}(py) (**1.135**, R = alkyl or aryl, Fig. 1.12, see Chapter Two for further details).[114, 135]

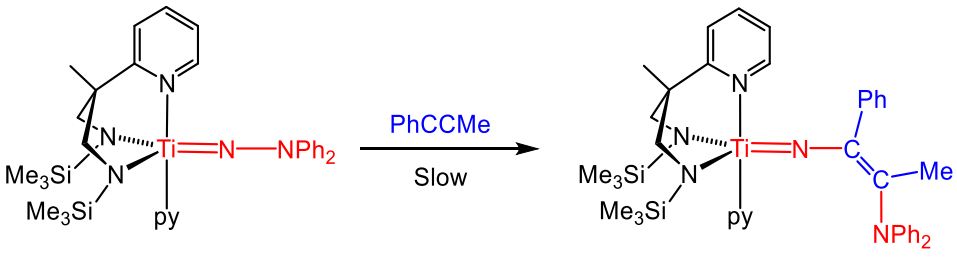

1.84 **1.134**

Equation 1.5.

Reaction of **1.86** and diaryl alkynes, ArCCAr, also gave the N_α–N_β insertion compounds Ti(N_2N^{Me}){NC(Ar)C(Ar)NPh_2}(py) (Ar = Ph (**1.136**), 4-C_6H_4OMe (**1.137**) and 4-$C_6H_4CF_3$ (**1.138**)).[138] However, in the case of **1.136** and **1.137** these compounds are formed alongside Ti{MeN($CH_2CH_2NSiMe_3$)(CH_2CH_2NH)}{N($SiMe_3$)C(Ar)C(Ar)-1,2-C_6H_4N(Ph)} (Ar = Ph (**1.139**) and 4-C_6H_4OMe (**1.140**), Eq 1.6). This is reminiscent of work by Bergman and Gade *et al*. on the reactions of $Cp_2Zr(NNPh_2)$ (**1.95**)[125] and Zr($N_2^{TBS}N_{py}$)($NNPh_2$)(py) (**1.97**)[130, 139] with a range of internal alkynes giving Cp_2Zr{N(Ph)C_6H_4C(R)C(R)N(H)} (**1.141**, R = alkyl or aryl, Fig. 1.12) and Zr($N_2^{TBS}N_{py}$){N(Ph)C_6H_4C(R)C(R)N(H)} (**1.142**, R = alkyl or aryl), respectively. The resulting indole can be accessed, for instance by acid hydrolysis of

1.141[140] or, in the case of **1.142**, by protonolysis using hydrazine, indeed $Zr\{(N^{Xyl})_2N_{py}\}(NMe_2)_2$ (**1.102**) is an effective catalyst for indole formation, *vide infra*.[139] The proposed mechanism for formation of **1.142** starting from the vinylimide complex $Zr(N_2{}^{TBS}N_{py})\{NC(R^1)C(R^2)NPh_2\}(py)$ is similar to formation of the vinylimide itself. Coordination of $N_\beta Ph_2$ to zirconium induces Ph_2N–C bond breaking and formation of a three membered $-N_\alpha\{C(R^1)C(R^2)\}$ ligand. In this case, nucleophilic attack by one of the *ortho* phenyl carbons onto $\underline{C}R^2$, followed by hydrogen transfer to N_α generates the 7-membered ring. The mechanism is presumed to be analogous for **1.139** and **1.140**, except in these cases the final step is a 1,3-$SiMe_3$ sigmatropic shift.

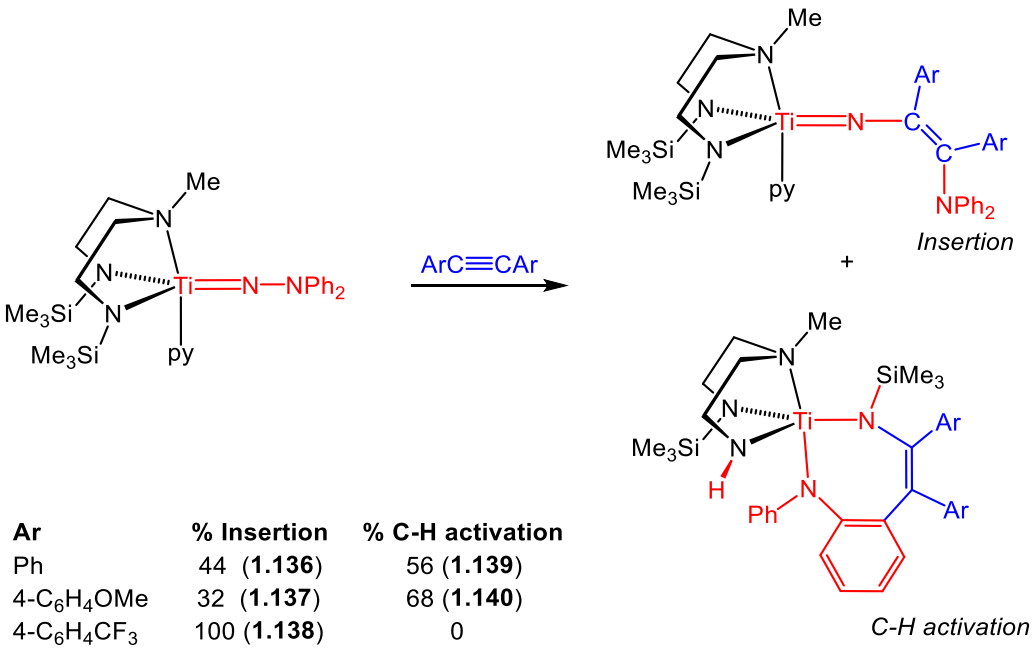

Ar	% Insertion	% C-H activation
Ph	44 (**1.136**)	56 (**1.139**)
4-C_6H_4OMe	32 (**1.137**)	68 (**1.140**)
4-$C_6H_4CF_3$	100 (**1.138**)	0

Equation 1.6.

Titanium hydrazide, $Ti(N_2O)(NNPh_2)(py)$ (**1.80**) reacts with ArCCR (Ar = Ph or substituted phenyl, R = H or Me) to yield **1.143**, Fig. 1.12.[117] The proposed mechanism is analogous to formation of the vinylimide complex **1.135** from **1.86**, except in this case one of the $\underline{N}(SiMe_3)$ groups on the supporting ligand acts as the nucleophile causing overall net insertion of PhCCMe into one of the Ti–$N(SiMe_3)$ bonds.

Catalytic reactions

Since titanium imido complexes proved effective catalysts for the hydroamination of alkynes forming imines, one focus of research on titanium hydrazides was on their ability to catalyse the corresponding transformation, namely hydrohydrazination (N-H bond addition across the C≡C bonds of alkynes) to form hydrazones, Scheme 1.7.

Figure 1.13 gives some examples of titanium hydrohydrazination catalysts (**1.74, 1.144 – 1.148**).[19, 23, 24, 26] The reaction conditions usually involve high temperatures (>75 °C) and long reaction times (2 – 75 h) with harsher conditions usually required for internal alkynes (RCCMe) compared to RCCH.[26] However, recent work by Gade *et al*. showed hydrazide complexes Cp*Ti(N^{Xyl}N)(NNRR′)(L) (**1.91a** – **1.91c**) were capable of catalysing the hydrohydrazination of a range of terminal alkynes at ambient temperatures with quantitative conversion (5 mol% catalyst loading) reached within 1 h.[26] Within these reactions only one regioisomer is formed, with Markovnikov selectivity, consistent with the stereochemistry defined by the [2+2] cycloaddition intermediate, *vide supra*. Although hydrazones are the products produced from the various hydrohydrazination reactions, further reaction to produce indoles,[19, 21, 22, 107, 141] pyrroles,[141] and tryptamines[23] for example, have also been described. In some cases an external Lewis acid such as $ZnCl_2$ is required,[19, 21, 107, 141] although "one-pot" procedures have also been reported.[22]

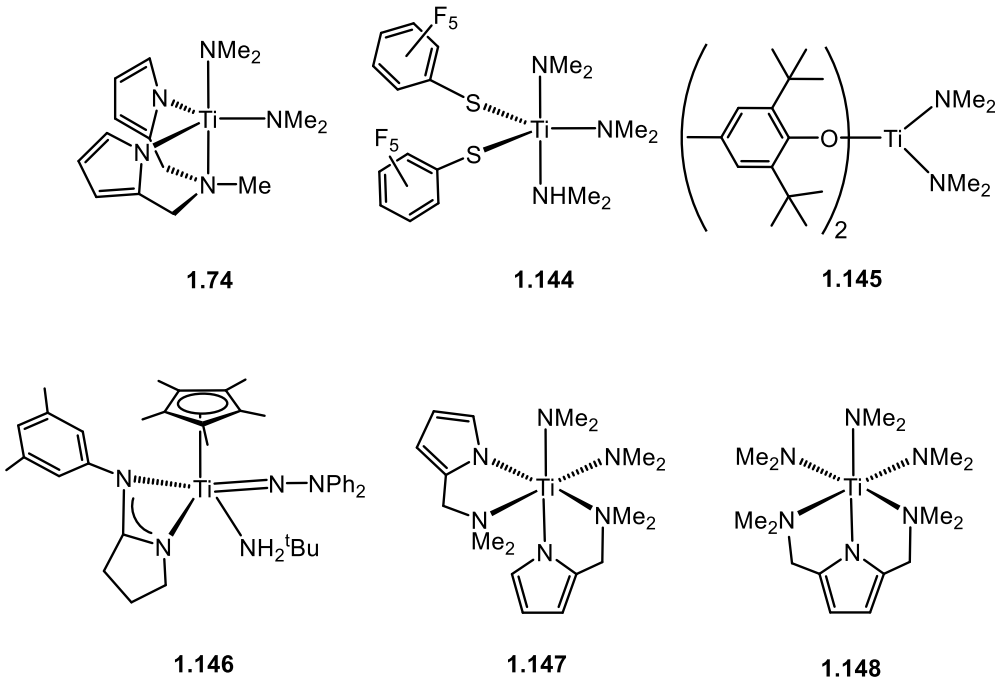

Figure 1.13. Examples of titanium hydrohydrazination catalysts. Compounds **1.147** and **1.148** are also catalysts for iminohydrohydrazination.

The proposed mechanism for hydrohydrazination is shown in Scheme 1.7. As mentioned, compounds **1.74**, **1.144**, **1.45**, **1.147** and **1.148** are pre-catalysts in these types of reactions, the active species, namely the hydrazide complex, is then made *in situ* on reaction with hydrazine. Compounds **1.147** and **1.148** are also catalysts for

iminohydrohydrazination, the mechanism of which is given in Scheme 1.15.[24] Odom also reported the use of $Ti(NMe_2)_2(pypyr)_2$ (Hpypyr = 2-(2′-pyridyl)-3,5-dimethylpyrrole)) in the formation of pyrazoles *via* catalytic iminohydrohydrazination reactions coupling terminal alkynes, isonitriles and mono-substituted hydrazines which cyclise without the need for an external Lewis acid.[142] As discussed, a different reaction pathway is found for zirconium hydrazides, in particular $Zr\{(N^{Xyl})_2N_{py}\}(NMe_2)_2$ (**1.102**), and alkynes which, on addition of hydrazine, can generate indoles catalytically (10 mol% catalyst loading).

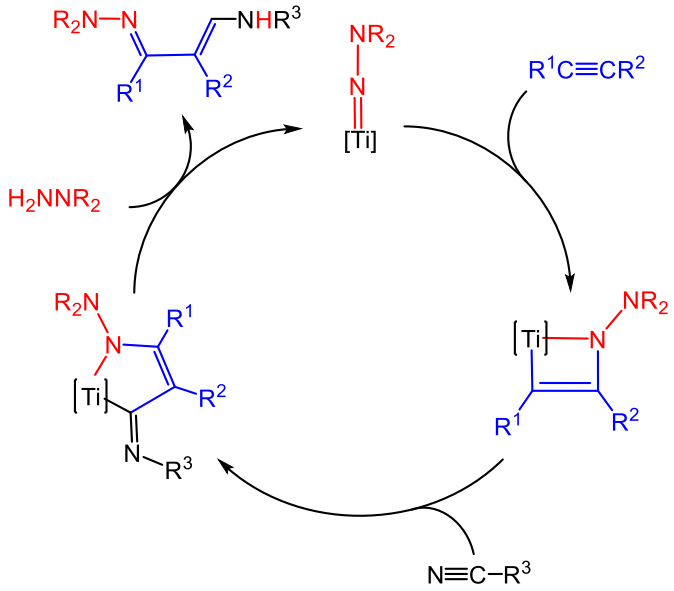

Scheme 1.15. General catalytic cycle for iminohydrohydrazination.[24]

The diamide-amine supported titanium complex $Ti(N_2N^{Me})(NNPh_2)(py)$ (**1.86**) undergoes N_α–N_β insertion with a range of internal alkynes, *vide supra*. The resulting vinylimide complex, **1.135**, then undergoes protonolysis with hydrazine releasing the vinylamine $H_2NC(Ph)C(Me)NPh_2$ (**1.149**), regenerating **1.86**.[114] This new type of catalysis, termed 1,2-diamination (N-N bond addition across the C≡C bonds of alkynes) will be covered in Chapter 2 of this Thesis. Very recently, work undertaken by Mountford *et al.* found that substitution of the -N$\underline{SiMe_3}$ groups on the supporting ligand of **1.86** with sterically less demanding isopropyl substituents, generating the diphenyl hydrazide complex **1.82** (Scheme 1.8), leads to a dramatic change in catalyst behaviour, switching the catalysis from 1,2–diamination of internal alkynes to hydrohydrazination of terminal alkynes.[118] Studies into this system also provided insight into a new vinyl-acetylide intermediate, $Ti(N_2^{iPr}N)(CCR)\{N(NPh_2)C(H)C(H)R\}$ (**1.150**, R = $SiMe_3$ or

substituted phenyl, Scheme 1.16) formed from Ti(N_2^{iPr}N)($NNPh_2$)(py) (**1.82**) and 2 equivs of alkyne. This is an unprecedented catalyst resting state in the already well-established hydrohydrazination reaction. The proposed mechanism, starting from a pyridine free intermediate, Ti(N_2^{iPr}N)($NNPh_2$) (**1.82′**), is given in Scheme 1.16.[115, 118]

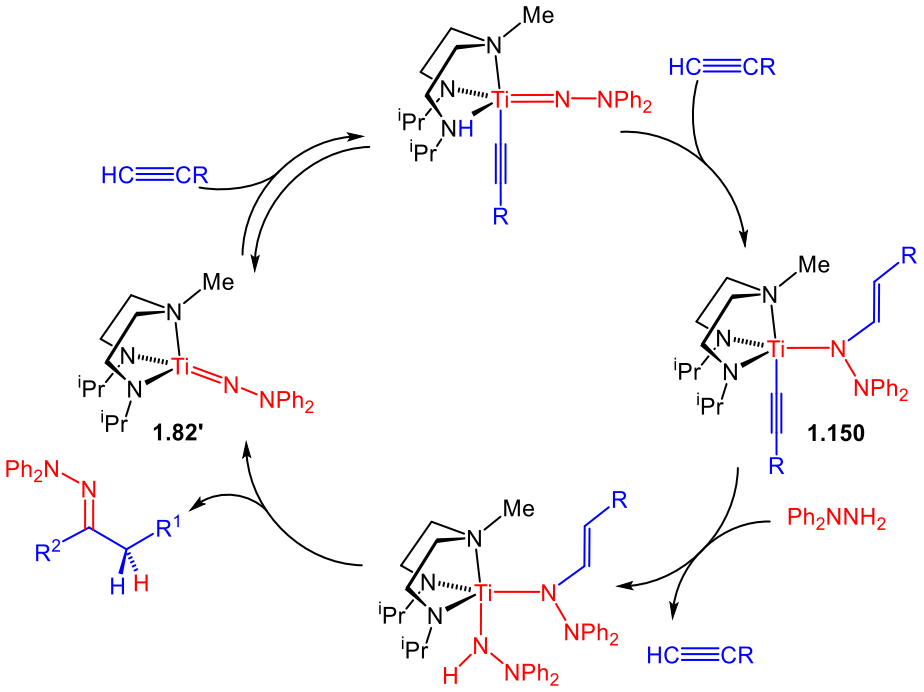

Scheme 1.16. Proposed mechanism for catalytic hydrohydrazination using Ti(N_2^{iPr}N)($NNPh_2$)(py) (**1.82**).[115]

1.5 Group 4 alkylidene hydrazide complexes

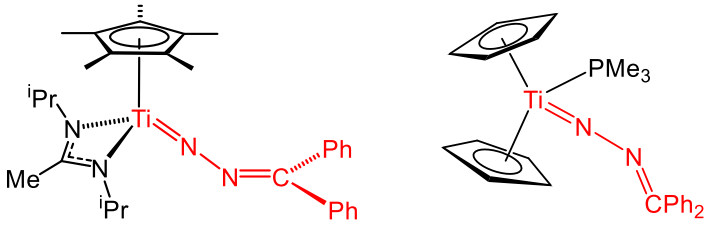

Figure 1.14. Structurally characterised titanium η^1-alkylidene hydrazido(2-) complexes.

Although Group 4 imide and hydrazide complexes are now well-established in the literature other derivatives such as alkylidene hydrazido complexes, otherwise known as diazoalkane or hydrazonido complexes, which possess $N_\alpha N_\beta CR_2$ ligands, are significantly less well-developed. Synthesis of these complexes normally involves the

use of potentially explosive diazoalkanes, although azines, dinitrogen and hydrazones have also been used.[143] Indeed, recent work by Mountford *et al.* used a *tert*-butylimide/hydrazone exchange methodology to synthesis Cp*Ti{MeC(N^{i}Pr)$_2$}(NNCPh$_2$) (**1.151**, Fig. 1.14).[121]

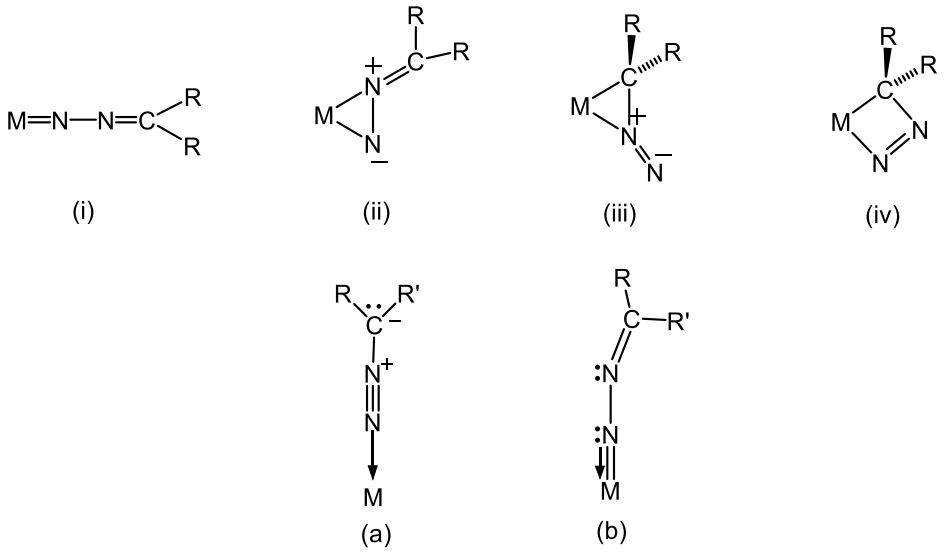

Figure 1.15. *(Top)* Possible bonding modes for an alkylidene hydrazido ligand coordinated to a metal. *(Bottom)* Various resonance forms for an alkylidene hydrazido ligand coordinated in a monomeric η^1-fashion.[144]

Like hydrazides, the addition of an $N_\beta CR_2$ moiety enables these ligands to coordinate through more than one binding mode, as depicted in Fig. 1.15. Within the monomeric η^1 bonding mode ((i), Fig. 1.15) there are two possible resonance forms, (a) and (b) (Fig. 1.15), with the % contribution of each identified through the M–N_α, N_α–N_β and N_β–C_α bond distances and M–N_α–N_β and N_α–N_β–C_α bond angles.[144] To date there have only been two structurally characterised titanium η^1-alkylidene hydrazido(2-) complexes, **1.151** and Cp$_2$Ti(NNCPh$_2$)(PMe$_3$) (**1.152**),[145] Fig 1.14. The bond lengths and angles of **1.151** are consistent with resonance form (b), Fig. 1.15, with relatively short Ti=N_α and N_β–C bond lengths (1.751(16) and 1.304(2) Å, respectively) and a long N_α–N_β bond distance of 1.329(2) Å. Accordingly, the N_α–N_β–C angle is also bent (120.22(16) °). Like the analogous hydrazide complexes, DFT analysis of the bonding in **1.151** showed destabilisation of the Ti=N_α π_v orbital by the N_β lone pair. Although both **1.151** and the dimethyl hydrazide complex **1.92b** are stabilised by the pyramidal geometry around N_β, the extent of N_β lone pair donation is found to be much less significant in the case of **1.151**, consistent with the Ti=N_α–R bond length increasing in the order R = Me < Ph < NCPh$_2$ < NMe$_2$. Compared to **1.151**, the alkylidene hydrazido

ligand in **1.152** is significantly less reduced, with a longer Ti=N_α distance (1.751(16) *vs* 1.829(11) Å) and shorter N_α–N_β bond length (1.329(2) *vs* 1.262(15) Å). This is supported by previous work on titanium complexes which suggest that *bis*-Cp supporting ligand sets help to stabilise the Ti(II) rather than Ti(IV) oxidation state.[146]

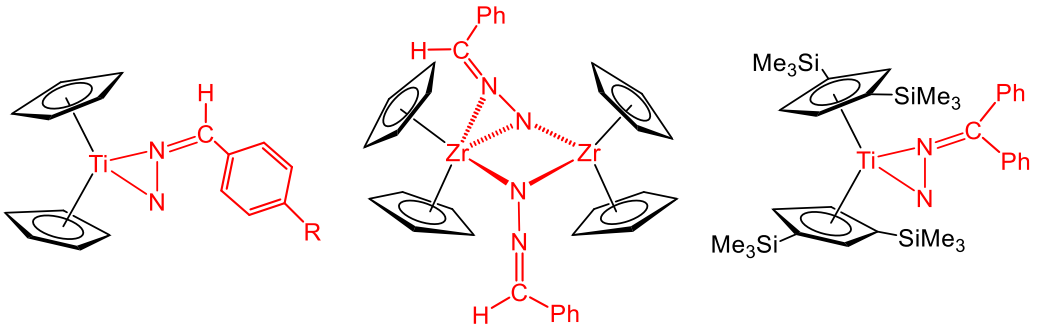

1.153 **1.154** **1.156**

Figure 1.16. Examples of Group 4 alkylidene hydrazido complexes.

Although η^1-alkylidene hydrazido ligands on titanium are rare, complexes which possess side-on bonding ligands, as shown in (ii), Fig. 1.15, are more common. These include $Cp^*_2Ti\{\eta^2\text{-}NNC(H)SiMe_3\}$ and $Cp^*_2Ti\{\eta^2\text{-}NNC(H)Ar\}$ (**1.153**, Ar = Ph (**1.153a**), Tol (**1.153b**), 4-$C_6H_4CF_3$, 4-C_6H_4Cl and 4-$C_6H_4NMe_2$, Fig. 1.16) synthesised by Bergman *et al.*[147, 148] and $Cp^*CpTiCl\{N(H)NCPh_2\}$ and $Ti\{\eta^5\text{-}C_5H_4(SiMe_2\text{-}\eta^1\text{-}NNCPh_2)\}Cl_2$ synthesised by Cuenca *et al.*[149] Dimeric structures containing alkylidene hydrazide ligands, bonding in a similar fashion to μ- η^1:η^2-hydrazido(2-) ligands, have also been observed, for example reaction of Cp_2ZrCl_2 with $Li_2NNC(H)Ph$ produced the zirconium dimer, $[Cp_2Zr]_2(\mu\text{-}\eta^1\text{:}\eta^1\text{-}NNCHPh)(\mu\text{-}\eta^1\text{:}\eta^2\text{-}NNCHPh)$ (**1.154**, Fig. 1.16).[150]

To date only a few studies on the reactivity of these complexes have been reported. In 1998 Bergman reported the reaction of **1.153b** with CO which resulted in N_α–N_β bond cleavage forming $Cp^*_2Ti\{NC(H)Tol\}(NCO)$ (**1.155**, Fig, 1.17),[147, 148] reminiscent of $Cp_2Zr(NNPh_2)(DMAP)$ (**1.96**).[125] In contrast reaction of $\{\eta^5\text{-}1,3\text{-}C_5H_3(SiMe_3)_2\}_2Ti(\eta^2\text{-}NNCPh_2)$ (**1.156**, Fig. 1.16) with CO yields the adduct $\{\eta^5\text{-}1,3\text{-}C_5H_3(SiMe_3)_2\}_2Ti(NNCPh_2)(CO)$ (**1.157**, Fig. 1.17).[151] Adducts were also observed on addition of ^{t}BuNC and DMAP to **1.156** and **1.153a** yielding the η^1-alkylidene hydrazide complexes $Cp^*_2Ti\{NNC(H)Ph\}(^t\text{BuNC})$ and $\{\eta^5\text{-}1,3\text{-}C_5H_3(SiMe_3)_2\}_2Ti(NNCPh_2)(DMAP)$, respectively.[147, 151] Reaction of primary silanes with $Cp^*Ti\{MeC(N^iPr)_2\}(NNCPh_2)$ (**1.151**) formed $Cp^*Ti\{MeC(N^iPr)_2\}\text{-}\{N(RSiH_2)N(CHPh_2)\}$[121] presumably *via* $Cp^*Ti\{MeC(N^iPr)_2\}\text{-}$

{N(RSiH$_2$)N(CPh$_2$)}(H) since reaction of **1.153b** with Ph$_2$SiH$_2$ or PhSiH$_3$ gave Cp*Ti{N(PhSiRH)NC(H)Tol}(H) (R = H or Ph (**1.158**), Fig. 1.17) following Si-H bond addition across Ti-N.[137] Moreover, a comprehensive study into the reactivity of **1.151** highlighted similar behaviour to the imide and hydrazide compounds **1.69**, **1.92a** and **1.92b** forming cycloaddition and "double insertion" products with heterocumulenes and alkynes. For example, Cp*Ti{MeC(N^{i}Pr)$_2$}{SC(NNCPh$_2$)N(Tol)C(NTol)O} (**1.159**) Cp*Ti{MeC(N^{i}Pr)$_2$}{N(NCPh$_2$)C(Ar^{F5})C(H)} (**1.160**) and Cp*Ti{MeC(N^{i}Pr)$_2$}{N(NCPh$_2$)C(Ar^{F5})NC(Ar^{F5})N} (**1.161**) following reaction with TolNCS and TolNCO, Ar^{F5}CCH and Ar^{F5}CN, respectively, Fig. 1.17.[121]

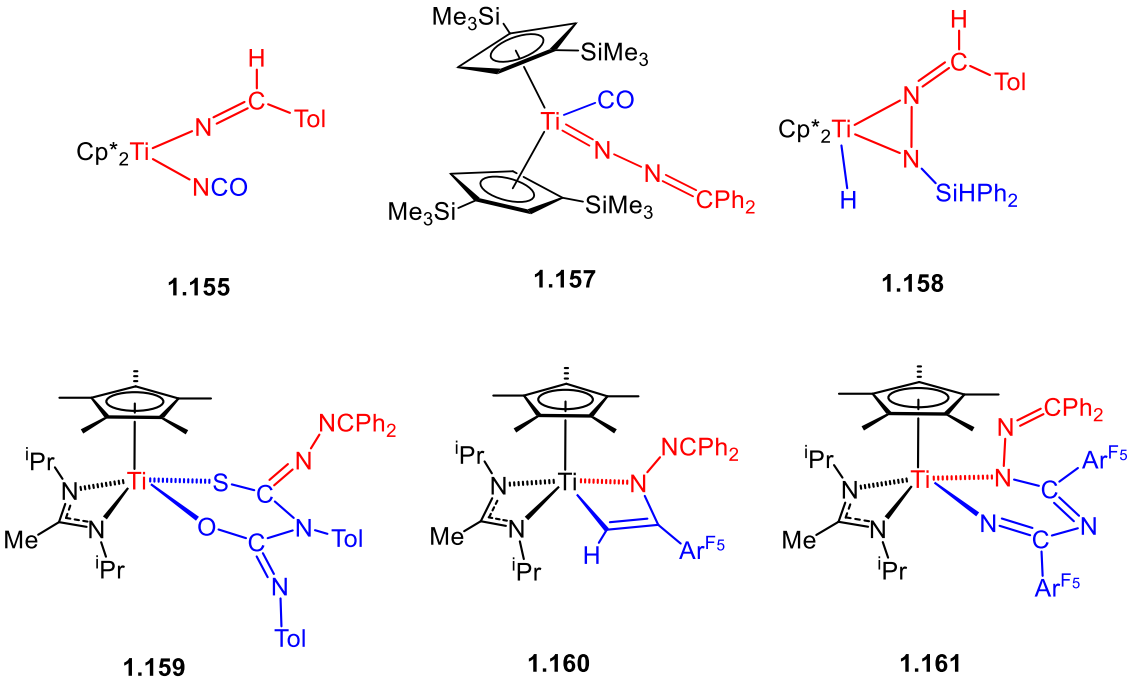

Figure 1.17. Reaction products from titanium alkylidene hydrazide complexes with small substrates.

1.6 Group 4 alkoxyimide complexes

The interesting range of reactivity, in particular the catalytic C–N bond forming reactions shown by the Group 4 (L)Ti=N–X systems (X = R and NR_2) prompted work in our group, in collaboration with Dr Eric Clot and Dr Ainara Nova at Université Montpellier, on the synthesis of complexes with other heteroatoms bound to N_α, for instance phosphorus, oxygen or sulfur. The reaction mechanism, calculated by DFT, for the insertion of MeCCMe into the N_α–N_β bond of hydrazide complex $Ti(N_2^{SiH_3}N^{Me})(NNMe_2)(py)$ (**B1**) (used as a model for **1.86**) is detailed in Fig. 1.18. As an initial study into alternative catalytic systems, the substituents bound to N_α were varied from NMe_2 (**B1**) to either OMe (**C1**) or PMe_2 (**D1**) and the energies of the corresponding intermediates calculated, Fig. 1.18. Phosphorus was found not to coordinate to titanium inhibiting formation of **D3** and so was not investigated further. However, as shown by Fig. 1.18 insertion of MeCCMe into the N_α–O_β bond of $Ti(N_2^{SiH_3}N^{Me})(NOMe)(py)$ (**C1**) is energetically favourable. The transition state for N_α–O_β bond cleavage, which is the rate-determining step in the analogous reaction with hydrazides ($\Delta G^{\ddagger}$ = 22 kcal mol^{-1}),[135] lies at only 0.5 kcal mol^{-1} above the starting material, **C1**.

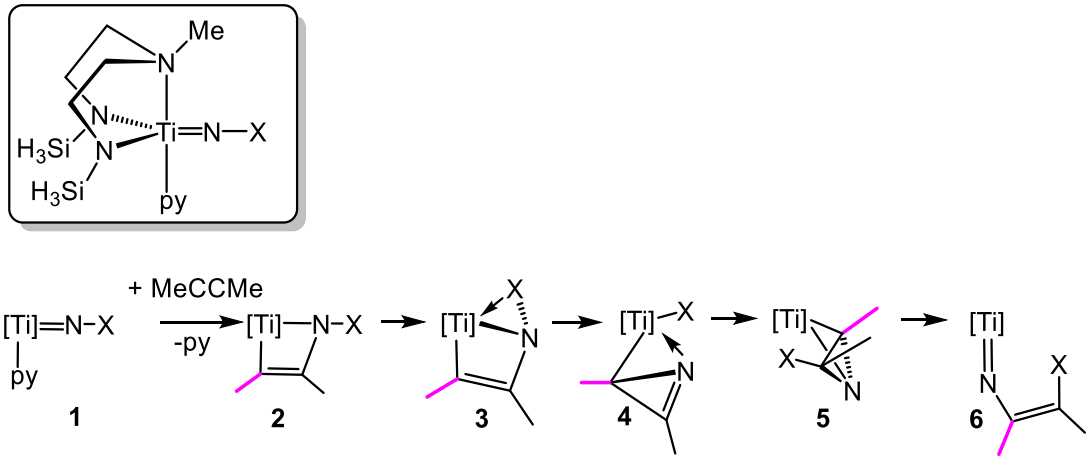

Compound	X	2	3	TS3-4	4	5	TS5-6	6
B1	NMe_2	1.9	4.2	22.0	4.2	3.1	10.6	-31.6
C1	OMe	-4,6	0.7	0.5	-33.1	-22.7	-2.5	-43.9
D1	PMe_2	1,7	*	*	*	*	*	*

*PMe_2 does not coordinate Ti to form **3**.

Figure 1.18. DFT calculated energies (kcal mol^{-1}) for the insertion of MeCCMe into the N_α–X_β bond of $Ti(N_2^{SiH_3}N^{Me})(NX)(py)$ (X = NMe_2 (**B1**), OMe (**C1**) and PMe_2 (**D1**)).

In 2011, the first Group 4 alkoxyimides were reported by Mountford *et al.*, Schemes 1.17 and 1.18.[131, 152] $Ti(NO^tBu)Cl_2(NHMe_2)_2$ (**1.162**) was successfully formed in an analogous fashion to the corresponding imide and hydrazide compounds, from $Ti(NMe_2)_2Cl_2$ (**1.41**) and $^tBuONH_2$. Further reaction with the desired protonated ligand generated a range of dichloride complexes, $(L)TiCl_2$, (L = $Me_3[9]aneN_3$ (**1.163**), $HC(Me_2pz)_3$ ($HC(Me_2pz)_3$ = tris(3,5-dimethylpyrazolyl)methane, **1.164**) and $Me_3[6]aneN_3$ ($Me_3[6]aneN_3$ = trimethyl-1,3,5-triazacyclohexane, **1.165**)), Scheme 1.17. Unfortunately *tert*-butylimide/alkoxyamine exchange with $Ti(N^tBu)Cl_2(py)_3$ (**1.30**) (analogous to the synthetic route used to generate aryl hydrazide $Ti(NNPh_2)Cl_2(py)_3$ (**1.77**)) was not successful in yielding $Ti(NO^tBu)Cl_2(py)_3$ (**1.166**). However, compound **1.166** was accessible following the addition of excess pyridine to $Ti(Me_3[6]aneN_3)(NO^tBu)Cl_2$ (**1.165**), as shown in Scheme 1.17.

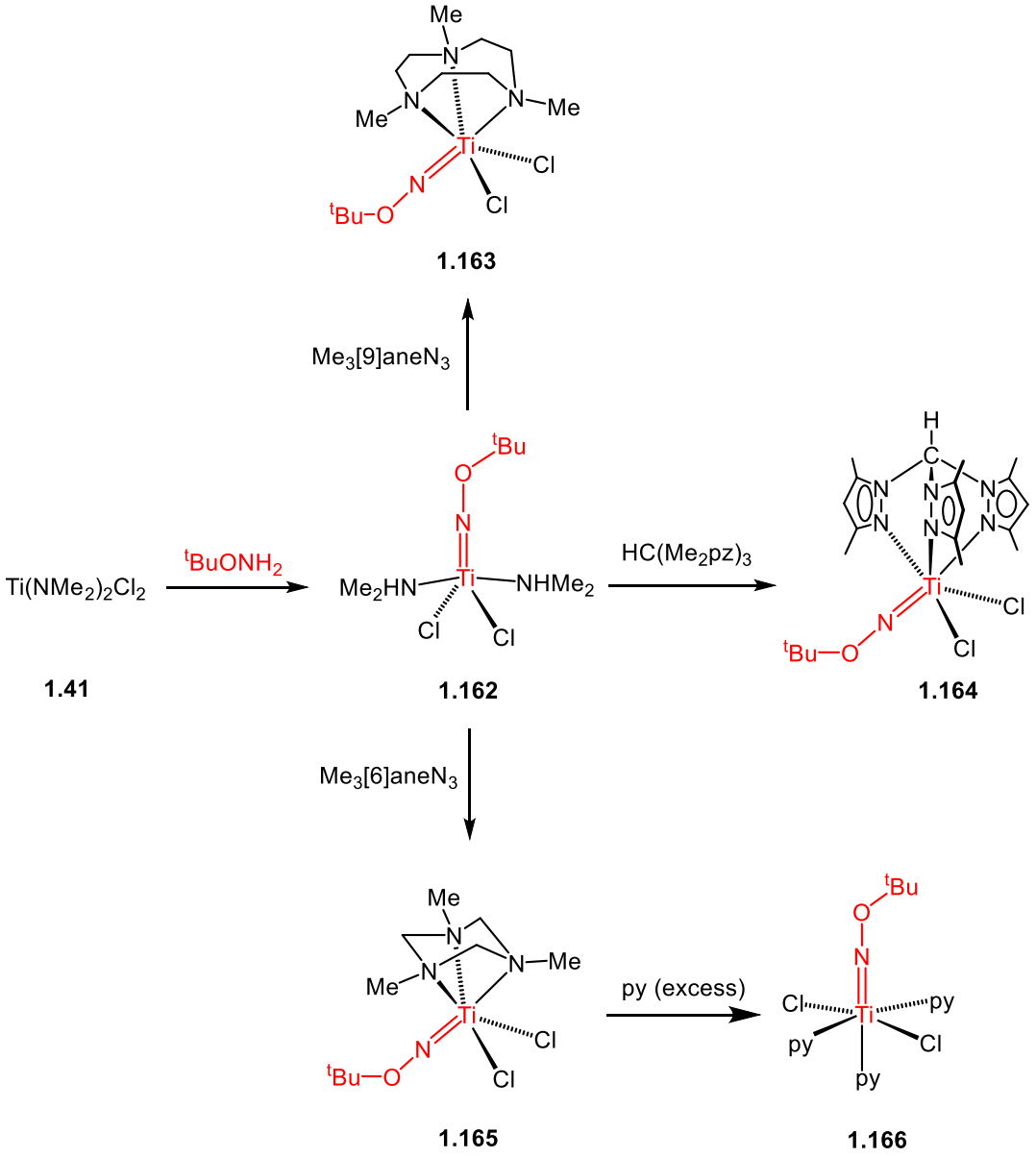

Scheme 1.17. Synthesis of various titanium *tert*-butoxyimido complexes from $Ti(NO^tBu)Cl_2(NHMe_2)$(**1.162**).[131]

Once formed $Ti(NO^tBu)Cl_2(py)_3$ (**1.166**) yielded a range of alkoxyimido complexes *via* salt metathesis reactions with various lithiated ligands, for example $Li_2N_2N^{Me}$ and $Li_2N_2N^{py}$ to form the corresponding complexes $Ti(N_2N^{Me})(NO^tBu)(py)$ (**1.167**) and $Ti(N_2N^{py})(NO^tBu)(py)$ (**1.168**), respectively, Scheme 1.18.[131] Compound **1.167** was isolated as a mixture of two geometric isomers, based on the relative position of the NO^tBu ligand to the NSiMe$_3$ amide nitrogens (**1.167a** and **1.167b**, Scheme 1.18). DFT calculations carried out on the full systems determined the axial position to be electronically favoured by *ca.* 1.2 kcal mol^{-1}.[131] This is also the case for the analogous hydrazide complexes, *vide supra*, and is a consequence of the steric interactions

between N_2N^R and NR as well as the π-donor characteristics of the relevant ligands. Addition of 2,2´-bipyridine to the mixture of **1.167** resulted in a single product, namely Ti(N_2N^{Me})(NO^{t}Bu)(bipy) (**1.169**, Scheme 1.18).

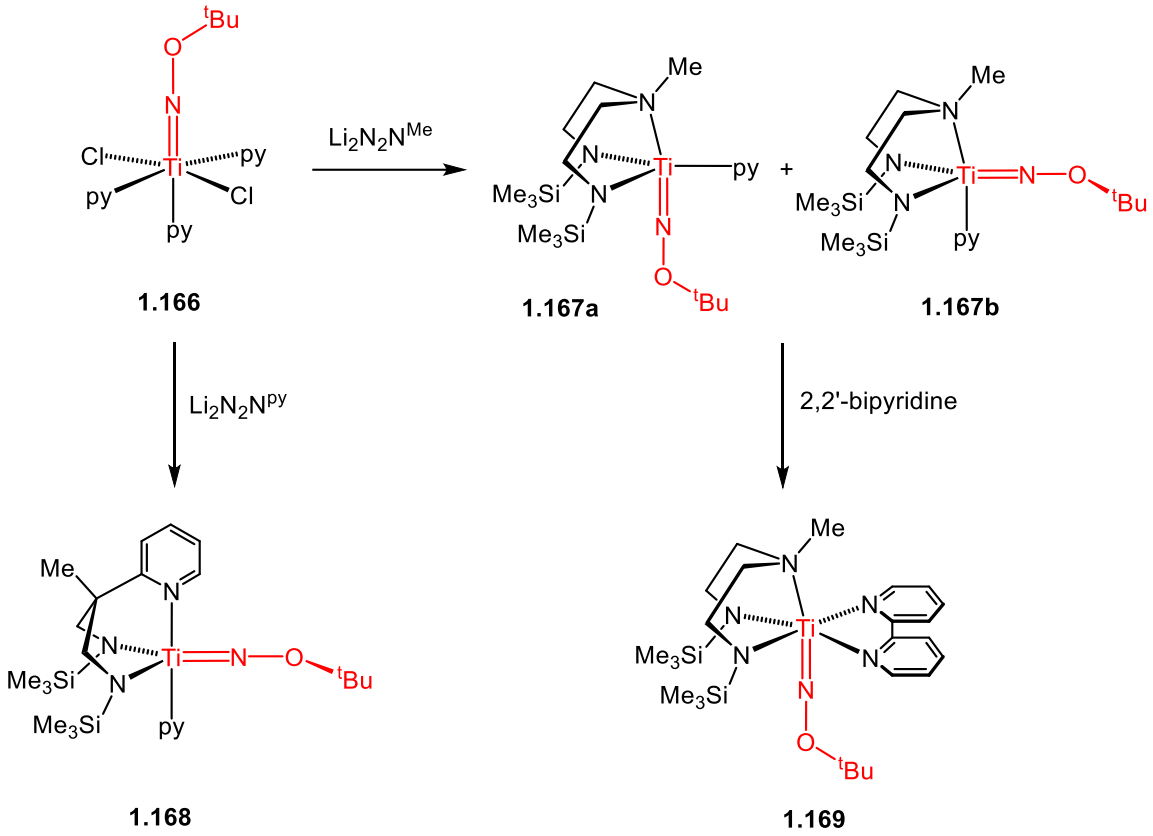

Scheme 1.18. Synthesis of various titanium *tert*-butoxyimido complexes from Ti(NO^{t}Bu)$Cl_2(py)_3$ (**1.166**).[131]

To date there has only been one DFT investigation into the bonding of alkoxyimido complexes compared to their hydrazide and imide analogues.[131] In this study DFT calculations were carried out on Ti(NOMe)$Cl_2(NHMe_2)$ (**2_OMe**), a model for **1.162**, and compared to the DFT computed imide and hydrazide analogues Ti(NR)$Cl_2(NHMe_2)$ (R = Me (**2_Me**), Ph (**2_Ph**) and NMe_2 (**2_NMe2**, used as model for R = NPh_2, and therefore N_β is planar)). In all cases the short Ti=N_α bonds (range 1.667 – 1.699 Å) and near linear Ti=N_α–X_β bond angles were consistent with formally triple Ti≡N_α bonds. Donation of the lone pair on N_β of **2_NMe2** or, to a lesser extent, the filled π orbital in **2_Ph** into the Ti=N_α π* orbital (a secondary π interaction, Ti=N_α π donation into the phenyl π* ring is also present in **2_Ph**, *vide supra*) leads to a lengthening of the Ti=N_α bond compared to **2_Me**. Lone pair donation from the –OR group of the alkoxyimido ligand into the Ti=N_α π* orbital is also present in **2_OMe**,

although due to the increased electronegativity of oxygen and therefore more contracted 2p atomic orbitals the interaction is less significant than in **2_Ph** and **2_NMe$_2$**. The DFT calculations therefore support the experimental trend in Ti=N$_\alpha$ bond lengths increasing in the order **2_Me** < **2_OMe** < **2_Ph** < **2_NMe$_2$**.

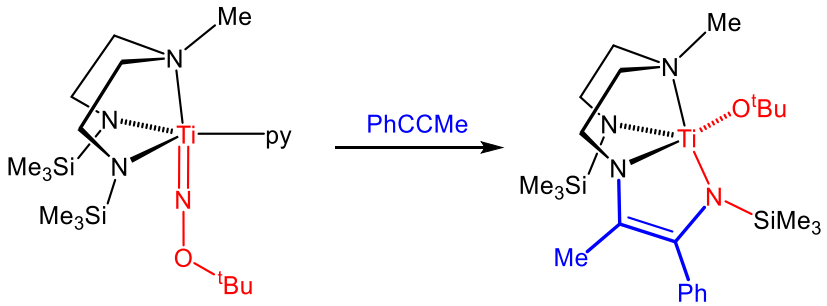

1.167 **1.170**

Equation 1.7

Reaction of **1.167** with PhCCMe resulted in net insertion of the alkyne into one of the Ti–NSiMe$_3$ bonds forming MeN(CH$_2$CH$_2$NSiMe$_3$)(CH$_2$CH$_2$NC(Me)=C(Ph)-NSiMe$_3$)Ti(O^{t}Bu) (**1.170**, Eq 1.7) instead of the desired complex, Ti(N$_2$N^{Me}){NC(Ph)C(Me)O^{t}Bu}(py). [152] This is reminiscent of **1.143** (Fig. 1.12), formed from reaction of Ti(N$_2$O)(NNPh$_2$)(py) (**1.80**) with ArCCR, *vide supra*, and is the first and only reaction product reported for a Group 4 alkoxyimide complex.

1.7 Summary and objectives

This Chapter described the synthesis and reactions of Groups 4-6 hydrazido and Group 4 imido complexes. As mentioned in Section 1.4.2, the hydrazide complex Ti(N_2N^{Me})($NNPh_2$)(py) (**1.86**) is an effective catalyst for the diamination of PhCCMe and Ph_2NNH_2 yielding the vinylamine $H_2NC(Ph)C(Me)NPh_2$ (**1.149**).[114] A combined DFT and experimental analysis has already been carried out on the first step of the reaction, namely the insertion of alkynes into the N_α–N_β bond of **1.86** yielding Ti(N_2N^{Me}){$NC(Ph)C(Me)NPh_2$}(py) (**1.135**).[135] However, so far limited work has been undertaken on either the protonation of the vinylimide ligand or on the overall catalytic cycle. One aim of this Thesis is therefore to examine both of these, including exploring the scope of the catalysis, carrying out a detailed kinetic investigation, supported by DFT calculations, and investigating catalyst stability.

This Chapter also described the synthesis of the first Group 4 alkoxyimide complexes, (L)Ti=NOR, using a protonolysis route with $Ti(NMe_2)_2Cl_2$ (**1.41**) and $^tBuONH_2$.[152] The reaction of Ti(N_2N^{Me})(NO^tBu)(py) (**1.167**) with PhCCMe was also described in the only example of a reaction of a Group 4 alkoxyimide. The second aim of this Thesis is therefore to use a novel *tert*-butylimide/alkoxyamine exchange methodology to synthesise a cyclopentadienyl-amidinate supported alkoxyimido complex and investigate its reactivity with a wide range of substrates. As discussed, similar methodologies have successfully been used to synthesise a range of hydrazide and imide complexes. The cyclopentadienyl-amidinate supported ligand set will be used since it has provided a robust ligand platform for studying the reactions of imide, hydrazide and alkylidene hydrazide complexes. It will therefore also allow comparisons to be drawn between the structure and reactivity of the alkoxyimido functional group with other (L)Ti=N–X complexes described above.

The third aim of this thesis is to investigate the reactions of the benzimidamide complex, Cp*Ti{$PhC(N^iPr)_2$}{$NC(Ar^{F5})NO^tBu$} formed from reaction of alkoxyimido Cp*Ti{$PhC(N^iPr)_2$}(NO^tBu) with $Ar^{F5}CN$. This is a novel functional group on titanium, and it is proposed that the electron-withdrawing nature of the Ar^{F5} group will help to stabilise intermediates which are otherwise not observed or isolable with other (L)Ti=N–X systems.

1.8 References

1. J. Chatt, A. J. Pearman and R. L. Richards, *J. Chem. Soc., Dalton Trans.*, 1977, 1852.
2. M. Hidai, *Coord. Chem. Rev.*, 1999, **185-186**, 99.
3. R. R. Schrock, *Angew. Chem. Int. Ed.*, 2008, **47**, 5512.
4. R. R. Schrock, *Acc. Chem. Res.*, 2005, **38**, 955.
5. W. W. Weare, X. Dai, M. J. Byrnes, J. M. Chin, R. R. Schrock and P. Mueller, *Proc. Natl. Acad. Sci.*, 2006, **103**, 17099.
6. D. V. Yandulov and R. R. Schrock, *Inorg. Chem.*, 2005, **44**, 1103.
7. N. Hazari and P. Mountford, *Acc. Chem. Res.*, 2005, **38**, 839.
8. N. Adams, H. J. Arts, P. D. Bolton, D. Cowell, S. R. Dubberley, N. Friederichs, C. Grant, M. Kranenburg, A. J. Sealey, B. Wang, P. J. Wilson, A. R. Cowley, P. Mountford and M. Schröder, *Chem. Commun.*, 2004, 434.
9. P. D. Bolton and P. Mountford, *Adv. Synth. Catal.*, 2005, **347**, 355.
10. H. R. Bigmore, S. R. Dubberley, M. Kranenburg, S. C. Lawrence, A. J. Sealey, J. D. Selby, M. Zuideveld, A. R. Cowley and P. Mountford, *Chem.Commun.*, 2006, 436.
11. H. R. Bigmore, M. Zuideveld, R. M. Kowalczyk, A. R. Cowley, M. Kranenbrug, E. J. L. McInnes and P. Mountford, *Inorg. Chem.*, 2006, **45**, 6411.
12. P. J. Wilson, A. J. Blake, P. Mountford and M. Schröder, *Chem. Commun.*, 1998, 1007.
13. C. H. Winter, P. H. Sheridan, T. S. Lewkebandara, M. J. Heeg and J. W. Proscia, *J. Am. Chem. Soc.*, 1992, **114**, 1095.
14. T. S. Lewkebandra, P. H. Sheridan, M. J. Heeg, A. L. Rheingold and C. H. Winter, *Inorg. Chem.*, 1994, **33**, 5879.
15. I. Bytschkov and S. Doye, *Eur. J. Org. Chem.*, 2003, 935.
16. S. Doye, *Synlett*, 2004, 1653.
17. L. L. Schafer and A. V. Lee, *Eur. J. Inorg. Chem.*, 2007, 2243.
18. T. E. Müller, K. C. Hultzsch, M. Yus, F. Foubelo and M. Tada, *Chem. Rev.*, 2008, **108**, 3795.
19. Y. Li, Y. Shi and A. L. Odom, *J. Am. Chem. Soc.*, 2004, **126**, 1794.
20. J. S. Johnson and R. G. Bergman, *J. Am. Chem. Soc.*, 2001, **123**, 2923.
21. C. Cao, Y. Shi and A. L. Odom, *Org. Lett.*, 2002, **4**, 2853.

22. L. Ackermann and R. Born, *Tet. Letts.*, 2004, **45**, 9541.
23. V. Khedkar, A. Tillack, M. Michalik and M. Beller, *Tet. Letts.*, 2004, **45**, 3123.
24. S. Banerjee, Y. Shi, C. Cao and A. L. Odom, *J. Organomet. Chem.*, 2005, **690**, 5066.
25. S. Banerjee, E. Barnea and A. L. Odom, *Organometallics*, 2008, **27**, 1005.
26. K. Weitershaus, H. Wadepohl and L. H. Gade, *Organometallics*, 2009, **28**, 3381.
27. P. D. Schweitzer, H. Wadepohl and L. H. Gade, *Organometallics*, 2013, **32**, 3697.
28. L. R. Groom, A. D. Schwarz, A. Nova, E. Clot and P. Mountford, *Organometallics*, 2013, **32**, 7520.
29. L. R. Groom, A. F. Russell, A. D. Schwarz and P. Mountford, *Organometallics*, 2014, **33**, 1002.
30. M. Hidai, *Chem. Rev.*, 1995, **95**, 1115.
31. F. A. Cotton, G. Wilkinson, C. A. Murillo and M. Bochmann, *Advanced Inorganic Chemistry*, 6th edn., Wiley-Interscience, New York, 1999.
32. M. D. Fryzuk and S. A. Johnson, *Coord. Chem. Rev.*, 2000, **200-202**, 379.
33. V. Smil, *Enriching the Earth: Fritz Haber, Carl Bosch and the Transformation of World Food Production* MIT Press, Cambridge, 2004.
34. G. Ertl, *Angew. Chem. Int. Ed.*, 2008, **47**, 3524.
35. J. Kim and D. C. Rees, *Science* 1992, **257**, 1677.
36. B. A. MacKay and M. D. Fryzuk, *Chem. Rev.*, 2004, **104**, 385.
37. M. Hidai and Y. Mizobe, *Chem. Rev.*, 1995, **95**, 1115.
38. L. C. Seefeldt, I. G. Dance and D. R. Dean, *Biochemistry*, 2004, **43**, 1401.
39. T. B. Parsons, N. Hazari, A. R. Cowley, J. C. Green and P. Mountford, *Inorg. Chem.*, 2005, **44**, 8442.
40. J. D. Selby, M. Feliz, A. D. Schwarz, E. Clot and P. Mountford, *Organometallics*, 2011, **30**, 2295.
41. S. Kahlal, J.-Y. Saillard, J.-R. Hamon, C. Manzur and D. Carrillo, *J. Chem. Soc., Dalton Trans.*, 1998, 1229.
42. R. Aumann and E. O. Fischer, *Angew. Chem. Int. Ed.*, 1967, **6**, 879.
43. R. R. Schrock, *Chem. Rev.* , 2002, **102**, 145.
44. C. Elschenbroich and A. Salzer, *Organometallics: a concise introduction*, 2nd edn., VCH, Weinheim, 1992.

45. M. Hidai, T. Kodama, M. Sato, M. Harakawa and Y. Uchida, *Inorg. Chem.*, 1976, **15**, 2694.
46. M. Hidai, Y. Mizobe, M. Sato, T. Kodama and Y. Uchida, *J. Am. Chem. Soc.*, 1978, **100**, 5740.
47. L. D. Field, N. G. Jones and P. Turner, *Organometallics*, 1998, **17**, 2394.
48. J. D. Niemoth-Anderson, J. R. D. Debord, T. A. George, C. R. Ross, II and J. J. Stezowski, *Polyhedron*, 1996, **15**, 4031.
49. C. Redshaw and M. R. Elsegood, *Inorg. Chem.*, 2000, **39**, 5164.
50. Z. Janas, L. B. Jerzykiewicz, R. L. Richards and P. Sobota, *Inorg. Chim. Acta*, 2003, **350**, 379.
51. J. Chatt, B. A. L. Crichton, J. R. Dilworth, P. Dahlstrom, R. Gutkoska and J. A. Zubieta, *Transition Met. Chem.*, 1979, **4**, 271.
52. J. Chatt, J. R. Dilworth, P. L. Dahlstrom and J. Zubieta, *J. Chem. Soc., Chem. Commun.*, 1980, 786.
53. C. Bustos, C. Manzur, D. Carrillo, F. Robert and P. Gouzerh, *Inorg. Chem.*, 1994, **33**, 1427.
54. N. Wiberg, H.-W. Haring, G. Huttner and P. Friedrich, *Chem. Ber.*, 1978, **111**, 2708.
55. K. Iwanami, Y. Mizobe, T. Takahashi, T. Kodama, Y. Uchida and M. Hidai, *Bull. Chem. Soc. Jpn.*, 1981, **54**, 1773.
56. P. C. Bevan, J. Chatt, G. J. Leigh and E. G. Leelamani, *J. Organomet. Chem.*, 1977, **139**, C59.
57. E. Krahn, B. J. R. Weiss, M. Krockel, J. Groppe, G. Henkel, S. P. Cramer, A. X. Trautwein, K. Schneider and A. Muller, *J. Biol. Inorg. Chem.*, 2002, **7**, 37.
58. S. Siemann, K. Schneider, M. Dröttboom and A. Müller, *Eur. J. Biochem.*, 2002, **269**, 1650.
59. D. Rehder, *Coord. Chem. Rev.*, 1999, **182**, 297.
60. R. R. Eady, *Coord. Chem. Rev.*, 2003, **237**, 23.
61. N. Wiberg, H. W. Häring and O. Schieda, *Angew. Chem. Int. Ed.*, 1976, **15**, 386.
62. M. Veith, *Angew. Chem. Int. Ed.*, 1976, **15**, 387.
63. S. C. Davies, D. L. Hughes, Z. Janas, L. Jerzykiewicz, R. L. Richards, J. R. Sanders and P. Sobota, *Chem. Commun.*, 1997, 1261.
64. R. A. Henderson, Z. Janas, L. B. Jerzykiewicz, R. L. Richards and P. Sobota, *Inorg. Chim. Acta*, 1999, **285**, 178.

65. S. C. Davies, D. L. Hughes, Z. Janas, L. B. Jerzykiewicz, R. L. Richards, J. R. Sanders, J. E. Silverston and P. Sobota, *Inorg. Chem.*, 2000, **39**, 3485.
66. J. Bultitude, L. F. Larkworthy, D. C. Povey, G. W. Smith, J. R. Dilworth and G. J. Leigh, *J. Chem. Soc., Chem. Commun.*, 1986, 1748.
67. A. A. Danopoulos, R. S. Hay-Motherwell, G. Wilkinson, T. K. N. Sweet and M. B. Hursthouse, *Polyhedron*, 1997, **16**, 1081.
68. M. L. H. Green, J. T. James, J. F. Saunders and J. Souter, *J. Chem. Soc., Dalton Trans.*, 1997, 1281.
69. M. L. H. Green, J. T. James and A. N. Chernega, *J. Chem. Soc., Dalton Trans.*, 1997, 1719.
70. I. A. Tonks and J. E. Bercaw, *Inorg. Chem.*, 2010, **49**, 4648.
71. I. A. Tonks, A. C. Durrell, H. B. Gray and J. E. Bercaw, *J. Am. Chem. Soc.*, 2012, **134**, 7301.
72. A. J. Keane, P. Y. Zavalij and L. R. Sita, *J. Am. Chem. Soc.*, 2013, **135**, 9580.
73. H. W. Roesky, H. Voelker, M. Witt and M. Noltemeyer, *Angew. Chem. Int. Ed.*, 1990, **29**, 669.
74. J. E. Hill, R. D. Profilet, P. E. Fanwick and I. P. Rothwell, *Angew. Chem. Int. Ed.*, 1990, **29**, 664.
75. C. C. Cummins, C. P. Schaller, G. D. Van Duyne, P. T. Wolczanski, A. W. E. Chan and R. Hoffmann, *J. Am. Chem. Soc.*, 1991, **113**, 2985.
76. A. J. Blake, P. E. Collier, S. C. Dunn, W.-S. Li, P. Mountford and O. V. Shishkin., *J. Chem. Soc., Dalton Trans.*, 1997, 1549.
77. S. C. Dunn, A. S. Batsanov and P. Mountford, *J. Chem. Soc., Chem. Commun.*, 1994, 2007.
78. P. Mountford, *Chem. Commun.*, 1997, 2127.
79. L. H. Gade and P. Mountford, *Coord. Chem. Rev.*, 2001, **216-217**, 65.
80. E. Mueller, J. Mueller, F. Olbrich, W. Brueser, W. Knapp, D. Abeln and F. T. Edelmann, *Eur. J. Inorg. Chem.*, 1998, 87.
81. D. Swallow, J. M. McInnes and P. Mountford, *J. Chem. Soc., Dalton Trans.*, 1998, 2253.
82. A. J. Blake, J. M. McInnes, P. Mountford, G. I. Nikonov, D. Swallow and D. J. Watkin, *J. Chem. Soc., Dalton Trans.*, 1999, 379.
83. S. C. Dunn, P. Mountford and D. A. Robson, *J. Chem. Soc., Dalton Trans.*, 1997, 293.

84. N. Adams, H. R. Bigmore, T. L. Blundell, C. L. Boyd, S. R. Dubberley, A. J. Sealey, A. R. Cowley, M. E. G. Skinner and P. Mountford, *Inorg. Chem.*, 2005, **44**, 2882.
85. C. Lorber, R. Choukroun and L. Vendier, *Eur. J. Inorg. Chem.*, 2006, 4503.
86. A. P. Duncan and R. G. Bergman, *The Chemical Record*, 2002, **2**, 431.
87. P. J. Walsh, F. J. Hollander and R. G. Bergman, *J. Am. Chem. Soc.*, 1988, **110**, 8729.
88. P. J. Walsh, F. J. Hollander and R. G. Bergman, *Organometallics*, 1993, **12**, 3705.
89. R. L. Zuckerman, S. W. Krska and R. G. Bergman, *J. Am. Chem. Soc.*, 2000, **122**, 751.
90. C. C. Cummins, S. M. Baxter and P. T. Wolczanski, *J. Am. Chem. Soc.*, 1988, **110**, 8731.
91. D. J. Arney, M. A. Bruck, S. R. Huber and D. E. Wigley, *Inorg. Chem.*, 1992, **31**, 3749.
92. A. J. Blake, P. Mountford, G. I. Nikonov and D. Swallow, *Chem. Commun.*, 1996, 1835.
93. J. L. Thorman, I. A. Guzei, V. G. Young, Jr. and L. K. Woo, *Inorg. Chem.*, 1999, **38**, 3814.
94. N. Adams, H. J. Arts, P. D. Bolton, D. Cowell, S. R. Dubberley, N. Friederichs, C. M. Grant, M. Kranenburg, A. J. Sealey, B. Wang, P. J. Wilson, M. A. Zuideveld, A. J. Blake, M. Schröder and P. Mountford, *Organometallics*, 2006, **25**, 3888.
95. A. E. Guiducci, C. L. Boyd and P. Mountford, *Organometallics*, 2006, **25**, 1167.
96. P. J. Tiong, A. Nova, L. R. Groom, A. D. Schwarz, J. D. Selby, A. D. Schofield, E. Clot and P. Mountford, *Organometallics*, 2011, **30**, 1182.
97. N. Kaltsoyannis and P. Mountford, *J. Chem. Soc., Dalton Trans.*, 1999, 781.
98. N. Hazari, A. R. Cowley and P. Mountford, *Acta Crystallogr.*, 2004, **E60**, m1844.
99. K. Weitershaus, B. D. Ward, R. Kubiak, C. Muller, H. Wadepohl, S. Doye and L. H. Gade, *Dalton Trans.*, 2009, 4586.
100. J. L. Thorman and L. K. Woo, *Inorg. Chem.*, 2000, **39**, 1301.
101. A. E. Guiducci, C. L. Boyd, E. Clot and P. Mountford, *Dalton Trans.*, 2009, 5960.

102. S. M. Pugh, D. J. M. Trösch, D. J. Wilson, A. Bashall, F. G. N. Cloke, L. H. Gade, P. B. Hitchcock, M. McPartlin, J. F. Nixon and P. Mountford, *Organometallics*, 2000, **19**, 3205.
103. A. J. Nielson, M. W. Glenny and C. E. F. Rickard, *J.Chem. Soc., Dalton Trans.*, 2001, 232.
104. P. D. Bolton, E. Clot, A. R. Cowley and P. Mountford, *Chem. Commun.*, 2005, 3313.
105. B. F. Straub and R. G. Bergman, *Angew. Chem. Int. Ed.*, 2001, **40**, 4632.
106. E. Haak, I. Bytschkov and S. Doye, *Angew. Chem., Int. Ed.*, 1999, **38**, 3389.
107. A. Tillack, H. Jiao, I. Garcia Castro, C. G. Hartung and M. Beller, *Chem. Eur. J.*, 2004, **10**, 2409.
108. L. Ackermann, R. G. Bergman and R. N. Loy, *J. Am. Chem. Soc.*, 2003, **125**, 11956.
109. P. J. Walsh, A. M. Baranger and R. G. Bergman, *J. Am. Chem. Soc.*, 1992, **114**, 1708.
110. L. Luconi, A. Rossin, G. Tuci, S. Germain, E. Schulz, J. Hannedouche and G. Giambastiani, *Chem. Cat. Chem.*, 2013, **5**, 1142.
111. J. Cho, T. K. Hollis, E. J. Valente and J. M. Trate, *J. Organomet. Chem.*, 2010, **696**, 373.
112. K. Manna, W. C. Everett, G. Schoendorff, A. Ellern, T. L. Windus and A. D. Sadow, *J. Am. Chem. Soc.*, 2013, **135**, 7235.
113. J. D. Selby, C. D. Manley, A. D. Schwarz, E. Clot and P. Mountford, *Organometallics*, 2008, **27**, 6479.
114. J. D. Selby, C. D. Manley, M. Feliz, A. D. Schwarz, E. Clot and P. Mountford, *Chem. Commun.*, 2007, 4937.
115. L. C. Stevenson and P. Mountford, *Unpublished results*, 2013.
116. A. J. Clulow, J. D. Selby, M. G. Cushion, A. D. Schwarz and P. Mountford, *Inorg. Chem.*, 2008, **47**, 12049.
117. J. Unruangsri, H. Morgan, A. D. Schwartz, A. D. Schofield and P. Mountford, *Organometallics*, 2013, **32**, 3091.
118. A. D. Schwarz, C. S. Onn and P. Mountford, *Angew. Chem. Int. Ed.*, 2012, **51**, 12298.
119. B. D. Ward, G. Orde, E. Clot, A. R. Cowley, L. H. Gade and P. Mountford, *Organometallics*, 2004, **23**, 4444.

120. A. E. Guiducci, A. R. Cowley, M. E. G. Skinner and P. Mountford, *J. Chem. Soc., Dalton Trans.*, 2001, 1392.
121. P. J. Tiong, L. R. Groom, E. Clot and P. Mountford, *Chem. Eur. J.*, 2013, **19**, 4198.
122. P. J. Tiong, A. Nova, A. D. Schwarz, J. D. Selby, E. Clot and P. Mountford, *Dalton Trans.*, 2012, **41**, 2277.
123. P. J. Tiong, A. D. Schofield, J. D. Selby, A. Nova, E. Clot and P. Mountford, *Chem. Commun.*, 2010, **46**, 85.
124. P. J. Tiong, A. Nova, E. Clot and P. Mountford, *Chem. Commun.*, 2011, **47**, 3147.
125. P. J. Walsh, M. J. Carney and R. G. Bergman, *J. Am. Chem. Soc.*, 1991, **113**, 6343.
126. H. Herrmann, J. L. Fillol, H. Wadepohl and L. H. Gade, *Angew. Chem. Int. Ed.*, 2007, **46**, 8426.
127. H. Herrmann, J. L. Fillol, T. Gehrmann, M. Enders, H. Wadepohl and L. H. Gade, *Chem. Eur. J.*, 2008, **14**, 8131.
128. S. A. Scholl, H. Wadepohl and L. H. Gade, *Organometallics*, 2013, **32**, 937.
129. S. A. Scholl, G. T. Plundrich, H. Wadepohl and L. H. Gade, *Inorg. Chem.*, 2013, **52**, 10158.
130. T. Gehrmann, S. A. Scholl, J. L. Fillol, H. Wadepohl and L. H. Gade, *Chem. Eur. J.*, 2012, **18**, 3925.
131. A. D. Schwarz, A. Nova, E. Clot and P. Mountford, *Inorg. Chem.*, 2011, **50**, 12155.
132. K. Weitershaus, J. L. Fillol, H. Wadepohl and L. H. Gade, *Organometallics*, 2009, **28**, 4747.
133. A. D. Schofield, A. Nova, J. D. Selby, A. D. Schwarz, E. Clot and P. Mountford, *Chem. Eur. J.*, 2011, **17**, 265.
134. T. Gehrmann, G. T. Plundrich, H. Wadepohl and L. H. Gade, *Organometallics*, 2012, **31**, 3346.
135. A. D. Schofield, A. Nova, J. D. Selby, C. D. Manley, A. D. Schwarz, E. Clot and P. Mountford, *J. Am. Chem. Soc.*, 2010, **132**, 10484.
136. P. J. Tiong, D.Phil. Thesis, University of Oxford, 2012.
137. T. Gehrmann, J. Lloret-Fillol, H. Herrmann, H. Wadepohl and L. H. Gade, *Organometallics*, 2013, **32**, 3877.

138. A. D. Schofield, D.Phil. Thesis, University of Oxford, 2012.
139. T. Gehrmann, J. L. Fillol, S. A. Scholl, H. Wadepohl and L. H. Gade, *Angew. Chem. Int. Ed.*, 2011, **50**, 5757.
140. P. J. Walsh, F. J. Hollander and R. G. Bergman, *J. Am. Chem. Soc.*, 1990, **112**, 894.
141. A. L. Odom, *Dalton Trans.*, 2005, 225.
142. A. A. Dissanayake and A. L. Odom, *Chem. Commun.*, 2012, **48**, 440.
143. Y. Mizobe, Y. Ishii and M. Hidai, *Coord. Chem. Rev.*, 1995, **139**, 281.
144. M. Dartiguenave, M. Joëlle Menu, E. Deydier, D. Yves and H. Siebald, *Coord. Chem. Rev.*, 1998, **178-180**, 623.
145. L. B. Kool, M. D. Rausch, H. G. Alt, M. Herberhold, A. F. Hill, U. Thewalt and B. Wolf, *J. Chem. Soc., Chem. Commun.*, 1986, 408.
146. P. D. Bolton, E. Clot, N. Adams, S. R. Dubberley, A. R. Cowley and P. Mountford, *Organometallics*, 2006, **25**, 2806.
147. J. L. Polse, A. W. Kaplan, R. A. Andersen and R. G. Bergman, *J. Am. Chem. Soc.*, 1998, **120**, 6316.
148. A. W. Kaplan, J. L. Polse, G. E. Ball, R. A. Andersen and R. G. Bergman, *J. Am. Chem. Soc.*, 1998, **120**, 11649.
149. V. Tabernero, T. Cuenca and E. Herdtweck, *J. Organomet. Chem.*, 2002, **663**, 173.
150. G. M. Arvanitis, J. Schwartz and D. Van Engen, *Organometallics*, 1986, **5**, 2157.
151. T. E. Hanna, I. Keresztes, E. Lobkovsky, W. H. Bernskoetter and P. J. Chirik, *Organometallics*, 2004, **23**, 3448.
152. A. D. Schwarz, A. Nova, E. Clot and P. Mountford, *Chem. Commun.*, 2011, **47**, 4926.

Chapter Two

1,2 – Diamination of internal alkynes

2.1 Overview

As discussed in Chapter One of this Thesis, one particular area of interest is in the application of Group 4 hydrazide complexes in catalytic C–N bond forming reactions; in particular hydrohydrazination and iminohydrohydrazination reactions. Alongside, the virtually unexplored 1,2-diamination of alkynes to vinylamines was also mentioned. To date, only one reaction has been reported, namely the diamination of PhCCMe with Ph_2NNH_2 to form $H_2NC(Ph)C(Me)NPh_2$ (**2.1a**) using $Ti(N_2N^{Me})(NNPh_2)(py)$ (**2.1**, N_2N^{Me} = $MeN(CH_2CH_2NSiMe_3)_2$), Eq 2.1.[1] Vinylamine compounds of the type $H_2NC(R)C(R')NAr_2$ (R, R′ = alkyl or aryl, Ar = phenyl or substituted phenyl) are potential precursors to the more synthetically useful 1,2-diamino alkanes. In 2010, a combined experimental and computational study was carried out on the insertion of alkynes into the N_α–N_β of **2.1** forming the vinylimide complex $Ti(N_2N^{Me})\{NC(Ph)C(Me)NPh_2\}(py)$ (**2.2**, Eq 2.1).[2] This work will be summarised in Section 2.1.1 below.

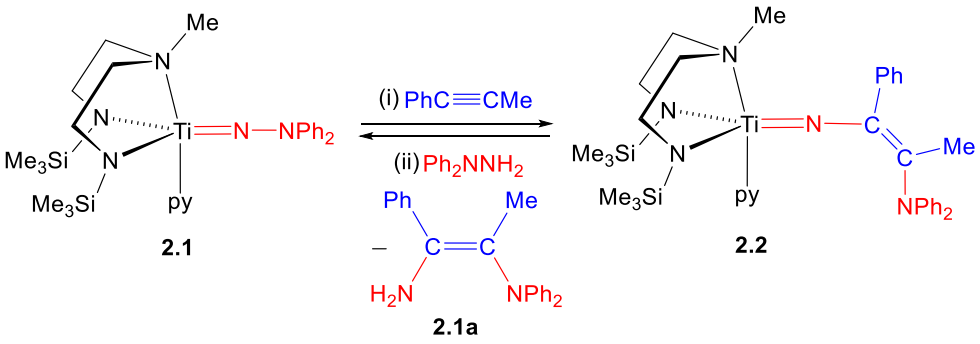

Equation 2.1

This Chapter describes the development of the diamination reaction including substrate scope, reaction rates and a kinetic investigation into the protonolysis of the vinylimide intermediate **2.2** with hydrazine, as well as the overall catalytic cycle. The decomposition reactions of the hydrazide catalyst by hydrazine and vinylamine will also be described. Part of this work, clearly stated in the text, has been carried out by a final year Oxford MChem student, Lee Collins, and a visiting summer research student (3-month placement), Hiromasa Tanahashi (Osaka University), under my direct supervision. The work is supported by DFT calculations which were performed by our collaborators, Dr Eric Clot and Dr Ainara Nova, at Université Montpellier.

2.1.1 Background

As mentioned, Section 1.4.2 of Chapter One described the reaction of Ti(N_2N^{Me})($NNPh_2$)(py) (**2.1**) with RCCMe (R = Me, Ph or substituted phenyl) which gave N_α–N_β insertion products of the type Ti(N_2N^{Me}){NC(R)C(Me)NPh_2}(py) (Eq 2.2, R = Ph (**2.2**), Me (**2.3**), Tol, (**2.4**), 4-$C_6H_4{}^tBu$ (**2.5**), 4-C_6H_4OMe (**2.6**), 4-$C_6H_4CF_3$ (**2.7**) or C_6F_5 (**2.8**)).[2] No intermediates were observed when the reactions were followed by ^1H NMR spectroscopy at room temperature. This is in contrast to the reaction of Ti(N_2N^{py})($NNPh_2$)(py) (**2.9**, N_2N^{py} = (2-NC_5H_4)CMe(CH_2NSiMe_3)$_2$) with PhCCMe which initially forms the [2+2] cycloaddition product Ti(N_2N^{py}){N(NPh_2)C(Me)C(Ph)}(py), albeit in equilibrium with the starting complex (*ca.* 45:55 ratio, respectively), before ultimately yielding the vinylimido complex Ti(N_2N^{py}){NC(Ph)C(Me)NPh_2}(py).[2]

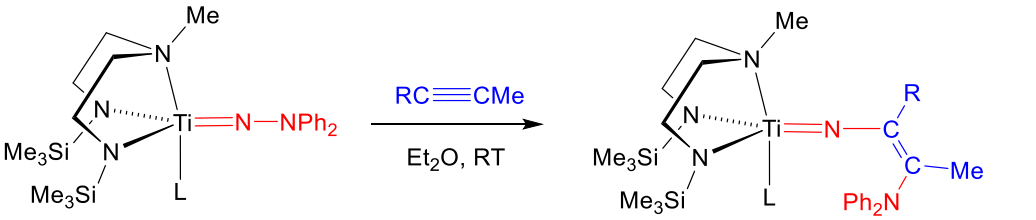

L = py (**2.1**) or DMAP (**2.10**)

L = py, R = Ph (**2.2**), Me (**2.3**), Tol (**2.4**), 4-$C_6H_4{}^tBu$ (**2.5**), 4-C_6H_4OMe (**2.6**), 4-$C_6H_4CF_3$ (**2.7**) or C_6F_5 (**2.8**). L = DMAP, R = Ph (**2.16**)

Equation 2.2

Compound **2.9** formed [2+2] cycloaddition products with a range of terminal and internal alkynes including TolCCH, (4-$C_6H_4CF_3$)CCH, PhCCMe and C_6F_5CCMe, Figure 2.1.[2] In all cases the reaction produced a single regioisomer, confirmed by X-ray diffraction studies in the cases of C_6F_5CCMe and (3-C_6H_4F)CCH, with the C(Ar) alkyne carbon bound to titanium (C_{Ti}). This is a consequence of the increased electron-withdrawing nature of Ar *vs* H or Me which reduces the destabilising electron-electron repulsion between the full π_{cc} orbital and the lone pair on N_α (LP_α) which, combined with the π^*_{cc} MO, make up the HOMO (largely based on N_α and C_{Ti}). Electron-withdrawing aryl groups bound to C_{Ti} help to lower the energy of both π_{cc} and π^*_{cc} orbitals reducing the unfavourable overlap between LP_α and π_{cc} whilst increasing the favourable overlap between the empty π^*_{cc} orbital and LP_α. Consequently, electron-withdrawing substituents on ArCCR also yield more thermodynamically stable

cycloaddition complexes, as observed experimentally. For instance, at low temperature (between -40 and -30 °C), the reactions of Ti(N_2N^{Me})($NNPh_2$)(py) (**2.1**) with ArCCMe (Ar = 4-$C_6H_4CF_3$ and C_6F_5) gave equilibrium mixtures of products including the [2+2] cycloaddition compounds Ti(N_2N^{Me}){N(NPh)C(Me)C(Ar)}(py) (Ar = 4-$C_6H_4CF_3$ (**2.7_int**) or C_6F_5 (**2.8_int**)). On warming, the mixtures proceeded to form the N_α–N_β insertion compounds, **2.7** and **2.8**, in quantitative yield by ^{1}H NMR spectroscopy. In contrast, no intermediates were observed in the reaction of **2.1** with PhCCMe, under otherwise identical conditions.

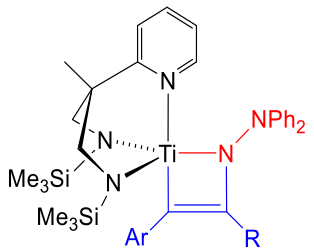

R = Me; Ar = Ph, 4-$C_6H_4CF_3$ or C_6F_5.
R = H; Ar = Ph, Tol, 3-C_6H_4F, 4-$C_6H_4CF_3$ or C_6F_5

Figure 2.1. Ti(N_2N^{py}){N(NPh_2)C(R)C(Ar)}(py)

On the other hand, electron-donating aryl groups on ArCCMe were seen to promote the N_α–N_β insertion reaction. The Hammett analysis of the overall reaction, as detailed in Eq 2.2, with a range of internal alkynes (4-C_6H_4X)CCMe (X = H, Me, OMe and ^{t}Bu) showed an increase in the observed rate constant, k_{obs}, in the order X = H < Me < ^{t}Bu < OMe. This gave a reaction constant, ρ, of -0.74(5) indicative of a build-up of positive charge at the Ar<u>C</u> alkyne carbon during the rate-determining step. An in-depth DFT analysis carried out on Ti($N_2^{SiH_3}N^{Me}$)($NNMe_2$)(py) ($N_2^{SiH_3}N^{Me}$ = $MeN(CH_2CH_2NSiH_3)_2$, **A1**), used as a model for **2.1**, proposed a mechanism as detailed in Scheme 2.1.[2] First, pyridine dissociation allows coordination of the alkyne to the metal which is then followed by a [2+2] cycloaddition reaction between the alkyne and Ti=N_α. Subsequent coordination of N_β to titanium brings about a conformational change in the 4-membered ring facilitating nucleophilic attack of the π density located on C_{Ti} into the N_α–N_β σ*orbital inducing N_α–N_β bond cleavage and C_{Ti}–N_α bond formation. This is the rate-determining step ($\Delta G^{\ddagger}$ = 17.8 kcal mol^{-1}) and therefore electron-donating aryl groups, which increase the nucleophilic nature of C_{Ti}, lower the energy of this transition state leading to an overall increase in k_{obs}. Nucleophilic attack

by N_β on C_{Me} followed by C–C bond formation ultimately yields the vinylimide complex.

Scheme 2.1. Gibbs free energy (kcal mol^{-1}) profile for MeCCMe insertion into the N_α–N_β bond of Ti($N_2^{SiH_3}N^{Me}$)($NNMe_2$)(py) (**A1**). The bond shown in blue for the alkyne is to help the reader trace the fate of the Ti-bound CMe group in **A4**. [Ti] = Ti($N_2^{SiH_3}N^{Me}$).[2]

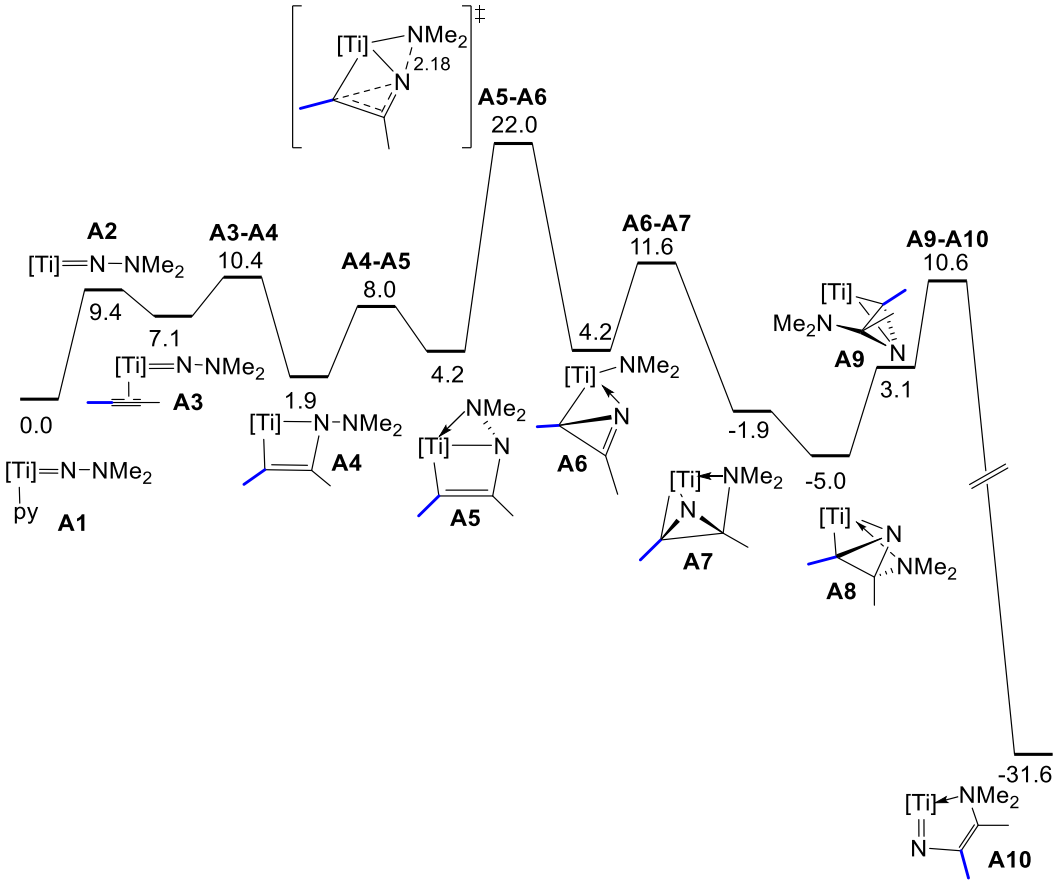

Like the azatitanacyclobutene products, Ti(N_2N^{py}){N(NPh_2)C(R)C(Ar)}(py), described above (Fig. 2.1) only one regioisomer is formed, with the C(Ar) and C(Me) alkyne carbons ending up bound to N_α and $N_\beta Ph_2$, respectively. According to DFT (Scheme 2.1, C–Me bond shown in blue) the stereochemistry is dictated by the orientation of the unsymmetrical alkyne in the [2+2] cycloaddition intermediate. As mentioned, the carbon attached to the more electron-withdrawing aryl group (as compared to Me) ends up bound to titanium, C_{Ti}. This carbon then acts as the nucleophile in step **A5-A6** ultimately forming a bond with N_α, consistent with the regioisomer observed.

An experimental study of the reaction of **2.1** with PhCCMe (in excess) gave pseudo first order kinetics with respect to **2.1**, in agreement with the rate equation given in Eq

2.3.[2] Interestingly, increasing the number of equivs of PhCCMe from 10 to 50 gave a non-linear plot of k_{obs} *vs* [PhCCMe], flattening out at high concentrations of alkyne indicative of saturation kinetics. Since the double reciprocal plot gave a linear correlation the rate law could be explained by Equations 2.4 and 2.5. These are derived from a reaction mechanism which involves an initial equilibrium between **2.1** and a more reactive pyridine-free intermediate. This occurs before the rate-determining step, consistent with the mechanism proposed by DFT in Scheme 2.1. Accordingly, reaction with the DMAP analogue of **2.1**, namely Ti(N_2N^{Me})($NNPh_2$)(DMAP) (**2.10**) or **2.1** in the presence of 1 or 2 equivs of pyridine significantly reduced the rate of reaction. A bis(pyridine) adduct is also formed in the presence of excess pyridine which could also contribute to the reduced rate.

$$\text{Rate} = k_{obs}[\mathbf{2.1}] \tag{2.3}$$

$$k_{obs} = \frac{k_1 k_2[\text{PhCCMe}]}{k_2[\text{PhCCMe}] + k_{-1}[\text{py}]} \tag{2.4}$$

$$\frac{1}{k_{obs}} = \frac{1}{k_1} + \frac{k_{-1}[\text{py}]}{k_1 k_2} \times \frac{1}{[\text{PhCCMe}]} \tag{2.5}$$

2.2 Diamination catalysis

As mentioned, the vinylimide ligand in Ti(N_2N^{Me}){N(Ph)C(Me)NPh_2}(py) (**2.2**) is released as the vinylamine, H_2NC(Ph)C(Me)NPh_2 (**2.1a**), following protonation with Ph_2NNH_2, regenerating the diphenyl hydrazide complex, **2.1**, Eq 2.1. Indeed, initial experiments showed that 10 mol% of **2.1**, on the NMR tube scale, could catalyse the 1,2-diamination of PhCCMe and Ph_2NNH_2 in quantitative yield at room temperature ($t_{1/2}$ *ca.* 1 h by ^{1}H NMR spectroscopy).[1] Further work carried out by a Part II student, Lee Collins, under my direct supervision, showed that the reaction could be carried out on a preparative scale in benzene (catalyst loading of 10 mol%) yielding **2.1a** in 74% isolated yield.[3] The diaminoalkene product was isolated following the addition of water to the reaction mixture effectively separating the organometallic species from the organic product **2.1a**. Separation of the layers followed by extraction and subsequent removal of the volatiles under reduced pressure gave **2.1a** as a pale orange powder.

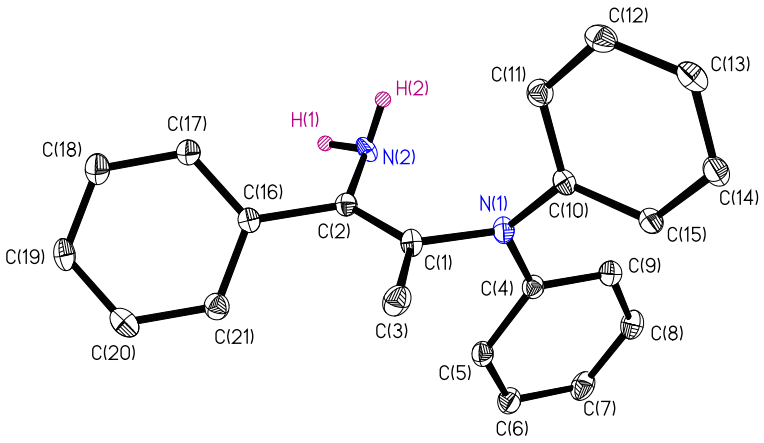

Figure 2.2: Displacement ellipsoid plot (20 % probability) of $H_2NC(Ph)C(Me)NPh_2$ (**2.1a**). C-bound H atoms omitted for clarity. Selected experimental bond lengths with corresponding distances determined by DFT in parentheses (Å): C(1)-C(2) 1.344(4) (1.362), C(1)-N(1) 1.470(3) (1.435), C(1)-C(3) 1.503(8) (1.503), C(2)-N(2) 1.384(5) (1.395), C(2)-C(16) 1.494(4) (1.483).[3]

Compound **2.1a** was subsequently characterised by X-ray diffraction, the molecular structure is given in Fig. 2.2. However, two overlapping orientations of the molecule were present in the crystals preventing accurate bond distance and angle determination. Therefore, to support the geometric parameters determined by X-ray diffraction, the bond lengths and angles of **2.1a**, along with ^{13}C NMR shifts, were calculated by DFT (Figures 2.2 and 2.3). The DFT calculated structure indicates delocalisation of the NPh_2 lone pair, which lies orthogonal to the C=C π system, into the N–C_{ipso} bonds. Accordingly, the sum of the angles at NPh_2 is 359.9 °, indicative of sp^2 hybridisation. In contrast, the NH_2 nitrogen appears intermediate between sp^2 and sp^3 hybridisation with a sum of 339.9 ° for the subtended angles. This is consistent with a partially developed 2p orbital which lies 25 ° out of the N–C=C–N plane. However, partial delocalisation of the lone pair into the H_2N–C bond does result in a shorter distance compared to Ph_2N–C (1.395 *vs* 1.435 Å, respectively). Finally, the C=C bond length is short, 1.362 Å, as expected for a C=C double bond. These conclusions are in good agreement with the geometric parameters determined by X-ray diffraction (selected experimental bond lengths are given in Fig. 2.2). The predicted NMR data are also in agreement with the ^{13}C NMR shifts obtained for **2.1a** in C_6D_6 (Fig. 2.3). The two alkene carbons, C(1) and C(2), are found at δ 139.2 and 111.9 ppm, respectively compared to δ 149.9 and 120.5 ppm determined by DFT. The methyl and C_{ipso} carbons C(3) and C(16), respectively are observed at δ 16.3 ppm and δ 140.0 ppm (compared to δ 17.2

and 146.1 ppm determined by DFT). Taken together these observations confirm the addition of $Ph_2N–NH_2$ across the C≡C bond of PhCCMe in a *cis* fashion forming $H_2NC(Ph)C(Me)NPh_2$ (**2.1a**) as depicted by the valence bond representation in Eq 2.1.

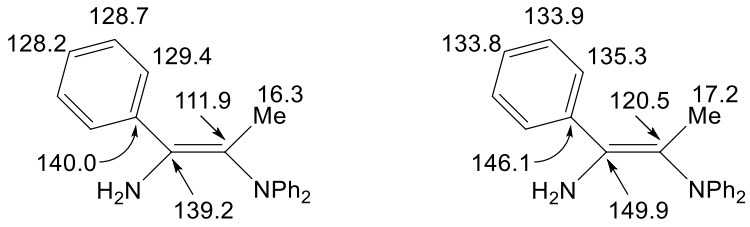

Figure 2.3. Left: experimental ^{13}C NMR shifts (ppm) for $H_2NC(Ph)C(Me)NPh_2$ (**2.1a**).[1] Right: corresponding ^{13}C NMR shifts (ppm) predicted by DFT.

As part of our investigation into the diamination of alkynes DFT calculations were carried out on various isomers of **2.1a**, Fig. 2.4. First, the calculations show that the alternative regioisomer of **2.1a**, namely $Ph_2NC(Ph)C(Me)NH_2$ (**2.1a′**), is slightly more thermodynamically stable by 1.0 kcal mol^{-1}. In both computed molecules the tautomer used is consistent with the bond distances and angles given by the molecular structure in Figure 2.2. Indeed, the diaminoalkene was found to be more thermodynamically favourable compared to the alternative imine tautomer (**2.1a_taut**) by 6.3 kcal mol^{-1} suggesting that once formed, compound **2.1a** does not tautomerise in solution. The 1,2-diamine product is also more thermodynamically stable than $Ph_2NNC(R)C(R')H_2$ (R = Ph, R′ = Me (**2.11**) or R = Me, R′ = Ph (**2.11′**)) formed by the more well-established hydrohydrazination reaction. In contrast to **2.1a**, the imine tautomer of the hydrohydrazination product is more thermodynamically stable by 1.2 and 3.4 kcal mol^{-1}, respectively, though both are still significantly higher in energy than **2.1a**. For completeness, the energy of the *trans* isomer of **2.1a** was determined (**2.1a_trans**) and found to be energetically less stable by 2.7 kcal mol^{-1}.

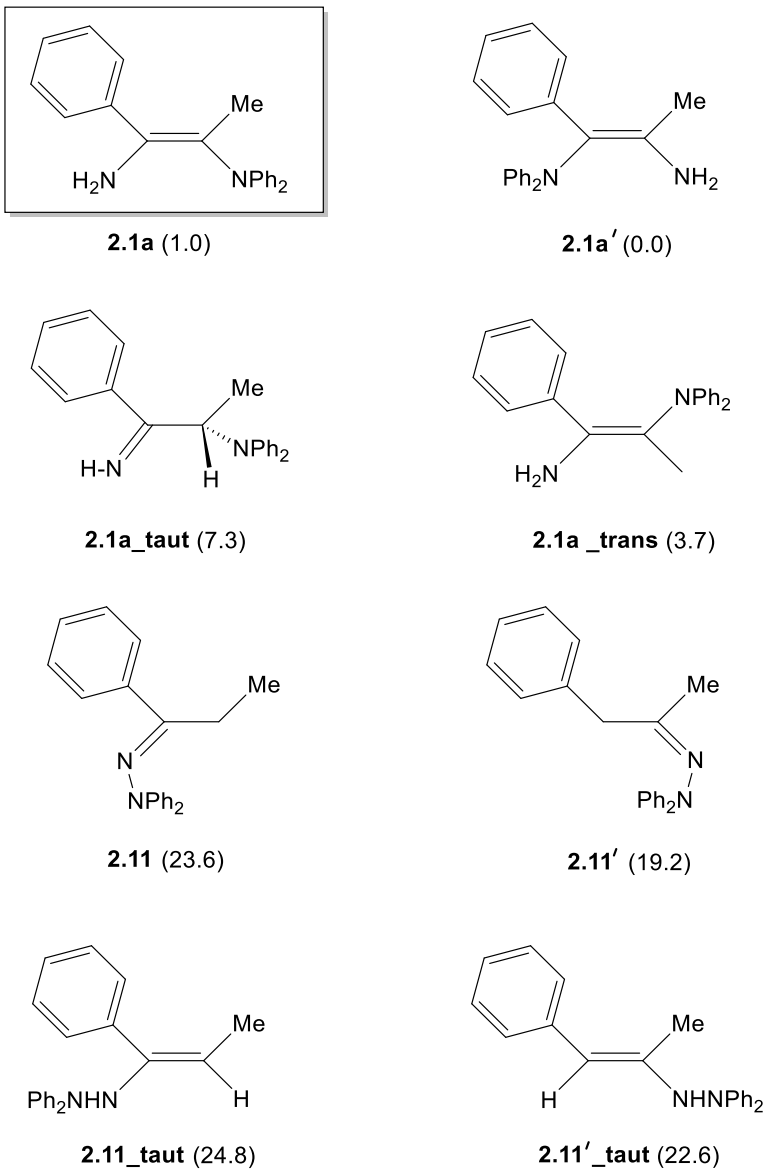

Figure 2.4. Isomers of $H_2NC(Ph)C(Me)NPh_2$ (**2.1a**) modelled by DFT with associated electronic energies in parentheses (kcal mol^{-1}).

As part of the Part II project, the hydrazide complex, $Ti(N_2N^{Me})(NNPh_2)(py)$ (**2.1**), was tested under catalytic conditions (5 mol% catalyst loading) with RCCMe (R = Me, 4-$C_6H_4{}^tBu$ and 4-C_6H_4OMe), alkynes which were previously shown to form the corresponding vinylimide complexes $Ti(N_2N^{Me})\{NC(R)C(Me)NPh_2\}(py)$ (R = Me (**2.3**), 4-$C_6H_4{}^tBu$ (**2.5**) and 4-C_6H_4OMe (**2.6**)) in quantitative yield by ^1H NMR spectroscopy (Eq 2.2).[2] The reactions with ArCCMe appeared to behave in an analogous fashion to PhCCMe yielding $H_2NC(Ar)C(Me)NPh_2$ (Ar = 4-$C_6H_4{}^tBu$ (**2.1b**) and 4-C_6H_4OMe (**2.1c**)) in quantitative yield by ^1H NMR spectroscopy ($t_{1/2}$ ~ 1 and 3 h, respectively). On scale up compounds **2.1b** and **2.1c** were isolated in 59 and 98%

yields, respectively, although a higher catalyst loading of 25 mol% was required in the case of Ar = 4-C_6H_4OMe, *vide infra*. The catalysis with MeCCMe was significantly slower, reaching only 30% conversion after 48 h at room temperature. Nonetheless, $H_2NC(Me)C(Me)NPh_2$ (**2.1d**) was successfully isolated on a preparative scale although, as expected, a high catalyst loading was required and it was unfortunately not possible to separate the product completely from unreacted Ph_2NNH_2.

In the hope of expanding the scope of this novel catalytic reaction, two new hydrazido complexes were synthesised, namely $Ti(N_2N^{Me})(NNAr_2)(py)$ (Ar = 4-$C_6H_4{}^tBu$ (**2.12**) and 4-C_6H_4OMe (**2.13**)) using the well-established imide/hydrazine exchange reactions of $Ti(N^tBu)Cl_2(py)_3$ with Ar_2NNH_2 followed by reaction with $Li_2N_2N^{Me}$ (Eq 2.6).[1, 3-5] On reaction with PhCCMe both complexes were found to react in an analogous manner to **2.1** producing the vinylimido complexes $Ti(N_2N^{Me})\{NC(Ph)C(Me)NAr_2\}(py)$ (Ar = 4-$C_6H_4{}^tBu$ (**2.14**) and 4-C_6H_4OMe (**2.15**)) in quantitative yield on the NMR tube scale (isolated yields of 84 and 89%, respectively). Both **2.12** and **2.13** were catalytically active yielding the corresponding vinylamine products $H_2NC(Ph)C(Me)NAr_2$ (Ar = 4-$C_6H_4{}^tBu$ (**2.12a**) and 4-C_6H_4OMe (**2.13a**)) in quantitative yields within 24 h on the NMR tube scale (5 mol% catalyst loading). Compounds **2.12a** and **2.13a** were subsequently isolated on a preparative scale in 71 and 88% yield, respectively.[3]

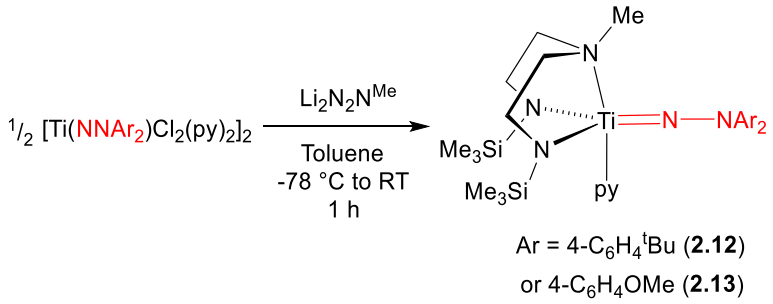

Equation 2.6

2.3 The scope of 1,2-diamination catalysis

Hydrazide catalysts **2.1**, **2.12** and **2.13** were tested for catalytic activity with a wide range of internal alkynes and aryl hydrazines, as detailed in Scheme 2.2, on the NMR tube scale in C_6D_6 at 5 mol% catalyst loading. Reactions which yielded vinylamine products were then carried out on a preparative scale and isolated in 30 – 98% yield, as shown in Figure 2.5. This work, with the exception of electron-withdrawing alkynes *vide infra*, was carried out by Hiromasa Tanahashi and Lee Collins, under my direct supervision. The catalytic loading was *ca.* 10 mol% unless otherwise stated.

Scheme 2.2. Catalytic cycle for the 1,2-diamination of various internal alkynes with aryl hydrazines using Ti(N_2N^{Me})($NNAr_2$)(py) (Ar = Ph (**2.1**), 4-$C_6H_4{}^tBu$ (**2.12**) or C_6H_4OMe (**2.13**)).

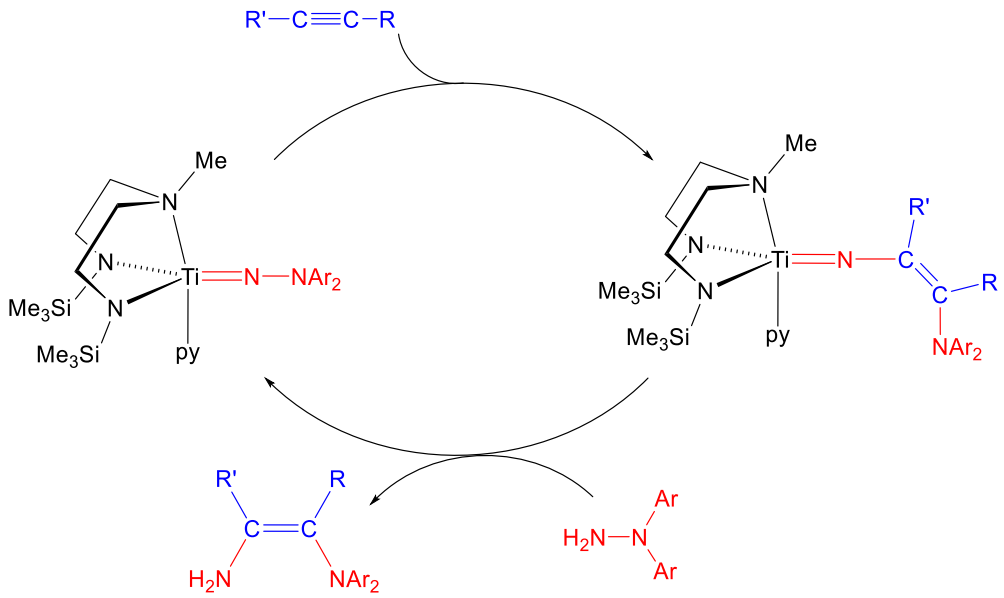

R = Me, R' = Ph, 4-C_6H_4OMe, 4-$C_6H_4{}^tBu$, 4-$C_6H_4CF_3$ or Me; R = R' = 4-$C_6H_4CF_3$
Ar = Ph, 4-C_6H_4OMe or 4-$C_6H_4{}^tBu$;

Reaction of **2.12** and **2.13** with MeCCMe and Ar_2NNH_2 (Ar = 4-C_6H_4OMe or 4-$C_6H_4{}^tBu$) gave no detectable amount of $H_2NC(Me)C(Me)NAr_2$ when followed by ^1H NMR spectroscopy, either at room temperature or on heating to 60 °C for 4 d, *vide infra*. The vinylamine products, once isolated, were unstable in air and/or light producing a mixture of unidentified compounds within a few h at room temperature. Their unstable nature significantly hindered any further purification, in particular separating the product from any remaining hydrazine. A slight excess of alkyne (1.1 or

1.2 equivs) was therefore used when possible, depending on the volatility of the substrate, to ensure complete consumption of the hydrazine.

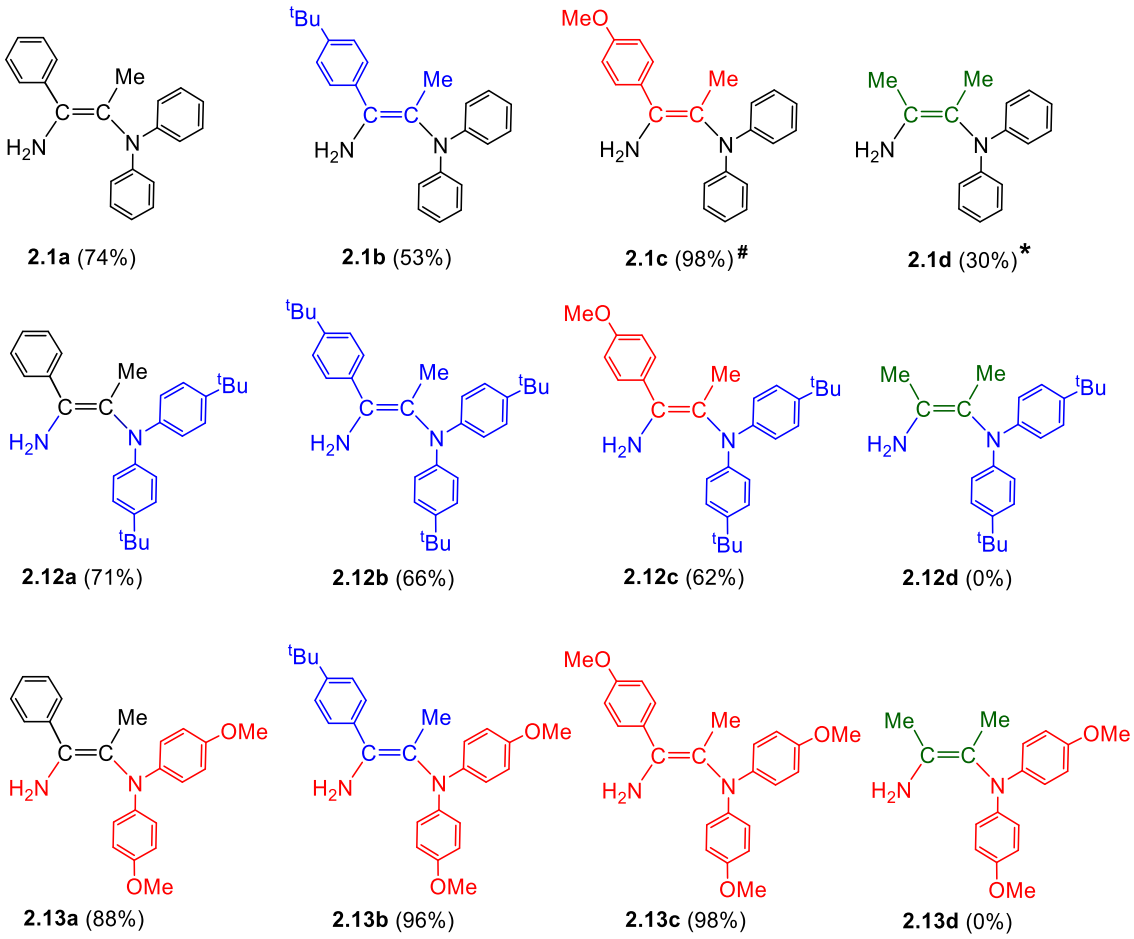

Figure 2.5. Vinylamine compounds, $Ar_2NC(Me)C(R)NH_2$ (Ar = Ph, 4-$C_6H_4{}^tBu$ or 4-C_6H_4OMe; R = Me, Ph, 4-$C_6H_4{}^tBu$ or 4-C_6H_4OMe). Isolated yields are given in parentheses underneath. Reaction conditions: room temperature with *ca.* 10 mol% catalyst loading unless otherwise stated. Reaction times 22 h to 4 d. # 25 mol%, * *ca.* 20 mol% catalyst loading.

The stoichiometric reactions of **2.1** with electron-withdrawing aryl alkynes, ArCCMe (Ar = 4-$C_6H_4CF_3$ and C_6F_5), were found to follow a different kinetic regime due to the increased stability of the cycloaddition intermediates **2.7_int** and **2.8_int**, *vide supra*.[2] However, since the reactions ultimately gave the vinylimide compounds $Ti(N_2N^{Me})\{NC(Ar)C(Me)NPh_2\}(py)$ (Ar = $C_6H_4CF_3$ (**2.7**) or C_6F_5 (**2.8**)) in quantitative yield by ^1H NMR spectroscopy, Ph_2NNH_2 was added to both and the reactions monitored by NMR spectroscopy. Within 30 min at room temperature, resonances consistent with formation of $H_2NC(Ar)C(Me)NPh_2$ and **2.1** were observed in both

reactions. (4-$C_6H_4CF_3$)CCMe was subsequently tested under catalytic conditions (5 mol% loading of **2.1**) giving H_2NC(4-$C_6H_4CF_3$)C(Me)NPh_2 (**2.1e**) in 93% yield after 48 h by ^{1}H NMR spectroscopy. The reaction was then carried out with **2.12** and **2.13**, under otherwise identical conditions, producing similar results (97 and 86% conversion, respectively after 48 h). All three reactions were carried out on a preparative scale, with 10 mol% catalyst loading and 48 h reaction time, and the vinylamine products isolated in 60 – 73% yield, Figure 2.6.

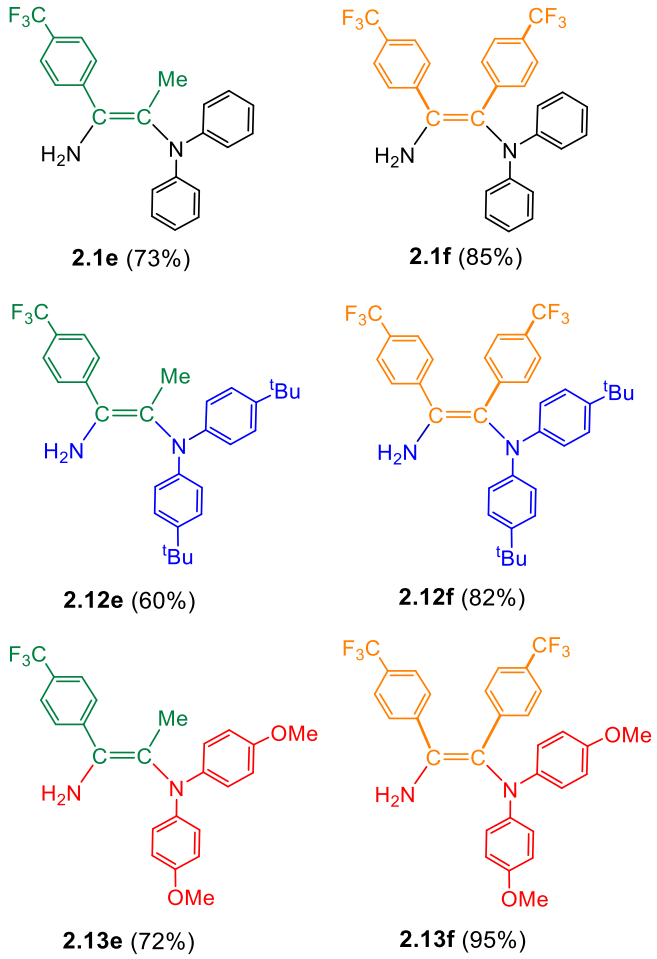

Figure 2.6. Vinylamine compounds, $H_2NC(R)C(4\text{-}C_6H_4CF_3)NAr_2$ (Ar = Ph, $C_6H_4{}^tBu$ or C_6H_4OMe; R = Me or 4-$C_6H_4CF_3$). Isolated yields are given in parentheses underneath. All reactions carried out at room temperature with 10 mol% (R = Me) or 25 mol% (R = 4-$C_6H_4CF_3$) catalyst loading. Reaction times 48 h (R = Me) or 4 d (R = 4-$C_6H_4CF_3$).

As discussed in Chapter One, reaction of **2.1** with diaryl alkynes, ArCCAr (Ar = Ph, 4-C_6H_4OMe and 4-$C_6H_4CF_3$) produced varied results depending on the electronic properties of the *para*-X substituent on the aryl group of the alkyne.[6] When X is more

electron-donating, as in the case of Ar = 4-C_6H_4OMe (σ_p = -0.27), formation of Ti{MeN($CH_2CH_2NSiMe_3$)(CH_2CH_2NH)}{N($SiMe_3$)C(Ar)C(Ar)-1,2-C_6H_4N(Ph)} was favoured over the vinylimide complex (68:32 ratio). Therefore, since in the proposed mechanism the 1,2-diamination reaction relies on formation of the N_α–N_β insertion complex only the electron-withdrawing diaryl alkyne (4-$C_6H_4CF_3$)CC(4-$C_6H_4CF_3$) was tested under catalytic conditions (5 mol% catalyst loading). The NMR tube scale reactions with hydrazide catalysts, **2.1**, **2.12** and **2.13**, were successful yielding $H_2NC(Ar)C(Ar)NAr'_2$ (Ar = 4-$C_6H_4CF_3$, Ar′ = Ph (**2.1f**), 4-$C_6H_4{}^tBu$ (**2.12f**) or 4-C_6H_4OMe (**2.13f**)) albeit in only 33 – 45% conversion after 48 h, as judged by ^{19}F NMR spectroscopy. However, all three reactions were carried out on preparative scale (25 % catalyst loading) and the products isolated in 82 – 95% yield, Fig 2.6.

2.4 Combined DFT and experimental investigation of the reaction of Ti(N_2N^{Me}){NC(Ph)C(Me)NPh_2}(py) (2.2) with Ph_2NNH_2

To further our understanding of the catalytic reaction, a combined DFT and experimental investigation into the protonation of the vinylimide complex, **2.2**, with Ph_2NNH_2 was carried out, Eq 2.7. For computational efficiency Ti($N_2{}^{SiH_3}N^{Me}$){NC(Me)C(Me)NMe_2}(py) (**B1**) was used as a model for **2.2**, and Me_2NNH_2 as a model for the hydrazine substrate. This also allowed direct comparison with the DFT calculations previously performed on the insertion of MeCCMe into the N_α–N_β bond of Ti($N_2{}^{SiH_3}N^{Me}$)($NNMe_2$)(py) (**A1**), Scheme 2.1. All DFT calculations discussed in this Chapter refer to Gibbs free energies in the gas phase at 298 K. The proposed reaction pathway is given in Scheme 2.3.

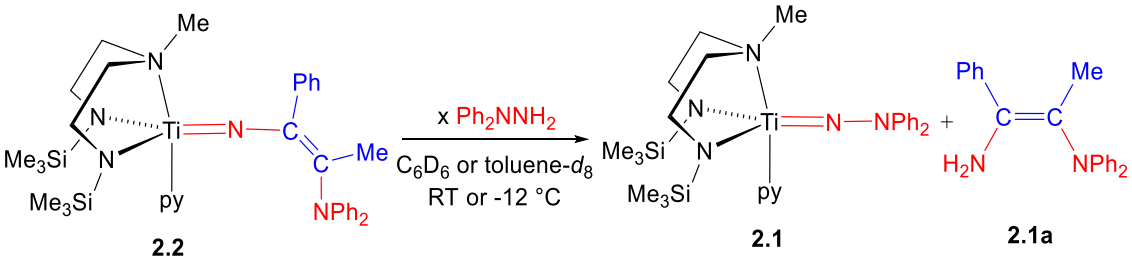

Equation 2.7

Scheme 2.3. Gibbs Free Energy (kcal mol^{-1}) Profile for the protonation reaction of Ti{MeN($CH_2CH_2NSiH_3$)$_2$}{NC(Me)C(Me)NMe_2}(py) (**B1**) with Me_2NNH_2. Values in brackets are the calculated energy barriers.

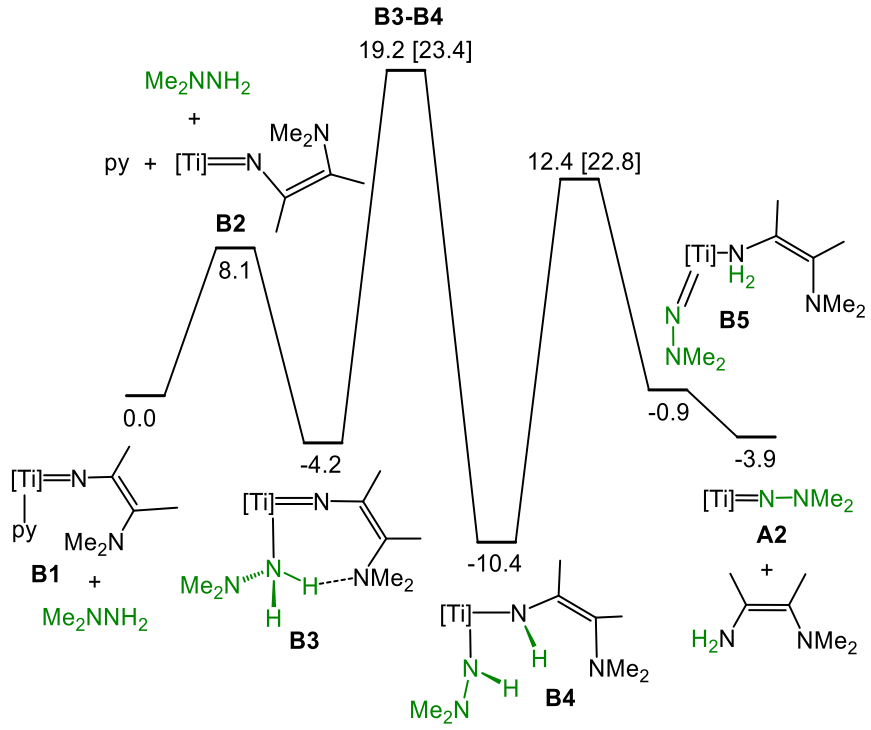

The initial steps involve replacement of pyridine by hydrazine, *via* a base-free intermediate **B2**, forming **B3** in an overall energetically favourable process (ΔG = -4.2 kcal mol^{-1}). The increased stability of the hydrazine adduct **B3** is assumed to be a consequence of a hydrogen bonding interaction (N···H distance = 2.01 Å) which is not possible in the pyridine adduct **B1**. Following formation of **B3** two successive hydrogen transfers from Me_2NNH_2 to the vinylimide ligand forms a mixed hydrazide-vinylamine complex, **B5** which lies at -0.9 kcal mol^{-1} lower in energy than the starting complex. Like *tert*-butylimide/hydrazine exchange reactions which are used to synthesis hydrazides, the basicity of the vinylimide ligand is an important factor in whether the protonation reaction takes place. Electron-withdrawing substituents on ArCCMe would therefore slow down or even prevent the protonolysis reaction from happening. The energy barriers for protonation are similar, $\Delta G^{\ddagger}$ = 23.4 and 22.8 kcal mol^{-1}, respectively and make up the rate-limiting steps in the reaction. Once **B5** is formed, the vinylamine ligand is released in an energetically favoured process to form **A2** (*cf.* Scheme 2.1) which can either be trapped by pyridine or hydrazine, or react further with alkyne.

The reaction between Ti(N_2N^{Me}){NC(Ph)C(Me)NPh_2}(py) (**2.2**) and Ph_2NNH_2 (1:1 ratio, Eq 2.7) in C_6D_6 at room temperature was monitored by ^{1}H NMR spectroscopy and the evolution of H_2NC(Ph)C(Me)NPh_2 (**2.1a**) (and decay of the vinylimide complex **2.2**) measured by integration over a period of ~ 3 h. The reaction was fast, reaching 66% conversion in 3 min, preventing a full kinetic study under these conditions. Reducing the reaction temperature to -12 °C provided a more suitable time frame for monitoring the reaction (~10 h), Fig. 2.7. Under both stoichiometric and pseudo first order conditions (10 equivs Ph_2NNH_2) the reaction did not follow the expected second or pseudo first order kinetics with respect to **2.2**. The non-linear correlations indicated a general decrease in k_{obs} over the course of reaction which is a consequence of side reactions and compound decomposition discussed in Section 2.8 below. To assess the true rate of the reaction, without needing to take into account these other non-productive side reactions, the initial rates method was used to effectively calculate the rate, d[**2.1a**]/d*t*, at time = 0, t_0. Previous work in our group has successfully used this method to analyse the rate of alkyne cycloaddition to amide-supported titanium imido compounds.[7] The graph of [**2.1a**] *vs* time for the stoichiometric reaction at -12 °C gave the expected non-linear plot, Fig. 2.7. The equation of the curve takes the form as given in Eq 2.8, differentiation of the curve at t_0, as detailed in Eq 2.9, ultimately gives the rate of reaction (mol dm^{-3} s^{-1}).

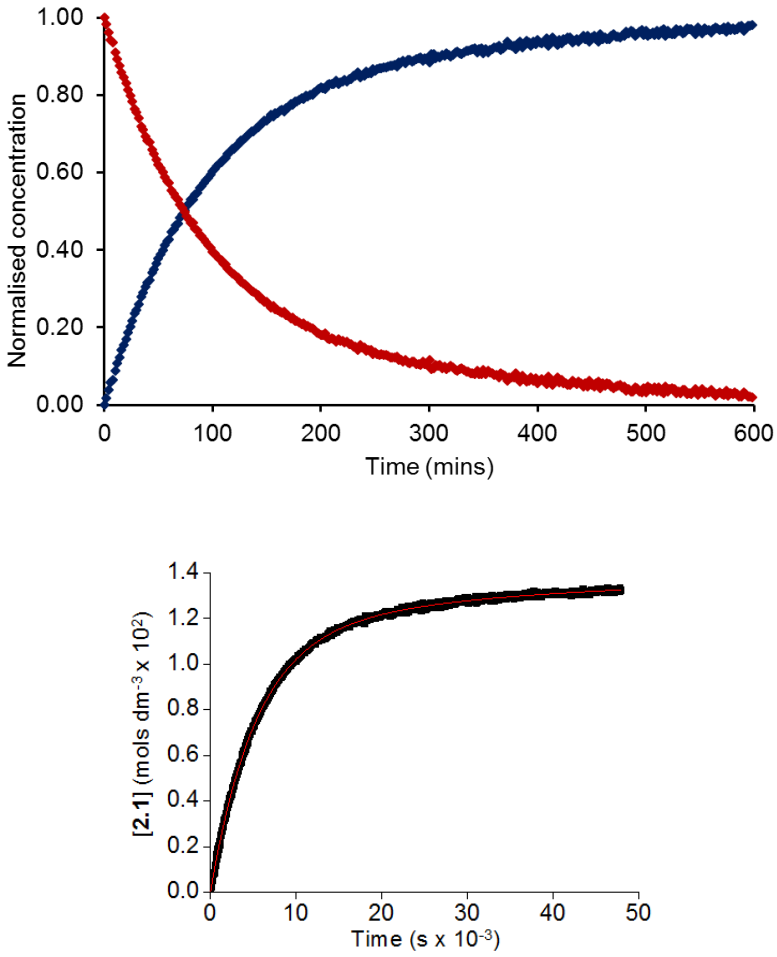

Figure 2.7. Top: decay of Ti(N_2N^{Me}){NC(Ph)C(Me)NPh_2}(py) (**2.2**, red diamonds) and growth of H_2NC(Ph)C(Me)NPh_2 (**2.1a**, blue diamonds) with time for the reaction between **2.2** and Ph_2NNH_2 (1:1 ratio) at -12 °C, $[Ti]_0$ = 0.02 mol dm^{-3}. Bottom: the corresponding plot of [H_2NC(Ph)C(Me)NPh_2] (**2.1a**) *vs* time plotted in Origin. The best-fit line (r^2 = 1.000) shown gave A_1 = -0.01113(16), B_1 = 5232(66), A_2 = -0.00272(8) and B_2 = 28389(3475) giving an initial rate of 0.222(4) x 10^{-5} mol dm^{-3} s^{-1}.

$$y = y_0 + A_1 e^{x/B_1} + A_2 e^{x/B_2} \tag{2.8}$$

$$\frac{dy_0}{dx_0} = \frac{A_1}{B_1} + \frac{A_2}{B_2} \tag{2.9}$$

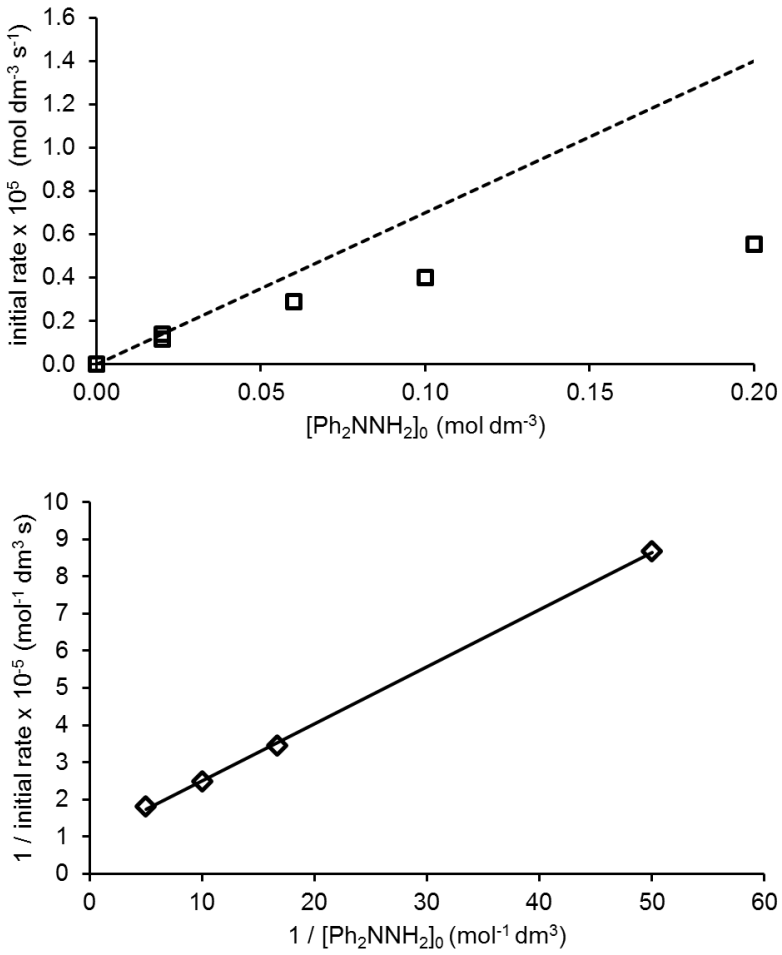

Figure 2.8. Top: plot of initial rate *vs* $[Ph_2NNH_2]_0$ for the reaction of $Ti(N_2N^{Me})\{NC(Ph)C(Me)NPh_2\}(py)$ (**2.2**) with Ph_2NNH_2; the dotted line is that expected for a linear relationship between initial rate and $[Ph_2NNH_2]_0$ based on extrapolation from the first data point (0.140(5) x 10^{-5} mol dm^{-3} s^{-1}), $[Ti]_0$ = 0.02 mol dm^{-3}. Bottom: the corresponding double-reciprocal plot. The linear fit (r^2 = 1.000) gives an intercept of 1/initial rate = 0.97(6) x 10^5 mol^{-1} dm^3 s.

When the reaction between **2.2** and Ph_2NNH_2 (1 – 10 equivs, 0.02 – 0.20 mol dm^{-3}) was monitored at -12 °C in toluene-d_8 the evolution of **2.1a** followed similar behaviour as detailed above and therefore initial rates in each case were obtained using the initial rates method. As shown in Figure 2.8, the initial rate does not scale linearly with initial concentration of Ph_2NNH_2, the reaction clearly showing the onset of saturation kinetics from as low as 0.06 mol dm^{-3} of hydrazine (3 equivs). On the other hand, the double reciprocal plot shown in Figure 2.8 gives a good linear fit (r^2 = 1.000) over the range of concentration of hydrazine used. These observations can be explained by the mechanism and associated rate law detailed in Scheme 2.4 and Eqs 2.10 and 2.11. The

loss of pyridine forming a reactive pyridine-free intermediate (**2.2′**) in the first step of the reaction is supported by the DFT analysis which puts this intermediate at 8.1 kcal mol^{-1} higher in energy than the starting complex. This is followed by a series of reaction steps, denoted *"k_2"* in Scheme 2.4, including the rate-limiting step(s) which, from DFT analysis, is proposed as the first proton transfer step ($\Delta G^{\ddagger}$ = 23.4 kcal mol^{-1}). This is somewhat reminiscent of the reaction of **2.1** with PhCCMe, which also showed saturation kinetics at high concentrations of alkyne, in which a similar mechanism to that shown in Scheme 2.4 was proposed.[2] Indeed, the extracted values for k_1 are similar in both instances, 5.2(3) x 10^{-4} and 8.7(6) x 10^{-4} s^{-1}, respectively.

Scheme 2.4. Experimentally implicated steps in the formation of **2.1** and **2.1a** from **2.2** and Ph_2NNH_2.

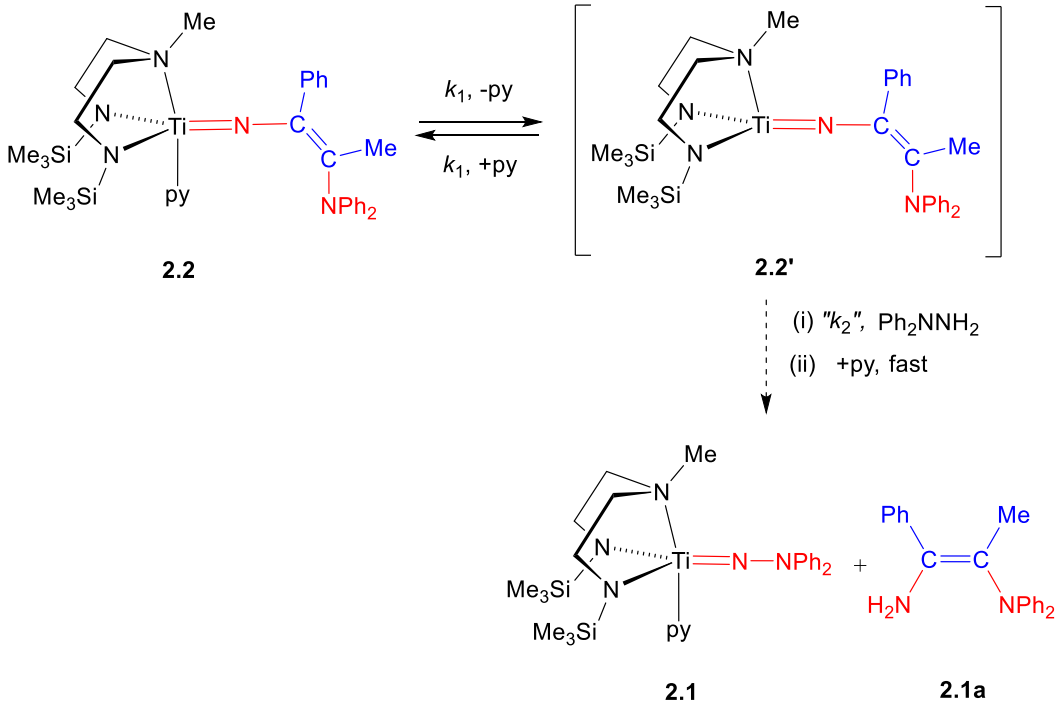

$$\text{Intial Rate} = \frac{k_1 k_2[Ph_2NNH_2][Ti]}{k_2[Ph_2NNH_2] + k_{-1}[py]} \qquad (2.10)$$

$$\frac{1}{\text{Inital rate}} = \frac{1}{k_1[Ti]} + \frac{k_{-1}[py]}{k_1 k_2[Ti]} \times \frac{1}{[Ph_2NNH_2]} \qquad (2.11)$$

As a test of Eq 2.10 the DMAP analogue of **2.1** namely $Ti(N_2N^{Me})\{NC(Ph)C(Me)NPh_2\}(DMAP)$ (**2.16**, Eq 2.2) was used instead of **2.2** under otherwise identical reaction conditions. According to Eq 2.10 and Scheme 2.4, the

stronger σ donor properties of DMAP compared to pyridine should result in a slower rate of ligand dissociation, k_1, leading to an overall decrease in the rate of reaction. Accordingly, on monitoring the reaction by ^{1}H NMR spectroscopy compound **2.16** was found to react significantly more slowly with Ph_2NNH_2 than **2.2** (initial rate = 0.008(7) *vs* 0.222(4) x 10^{-5} mol dm^{-3} s^{-1}; 1.5 *vs* 16% conversion within 30 min) to produce the DMAP analogue of compound **2.1**, namely Ti(N_2N^{Me})($NNPh_2$)(DMAP) (**2.10**, Eq 2.2).

Reaction of Ti(N_2N^{Me}){NC(Ph)C(Me)NPh_2}(py) (**2.2**) with Ph_2NND_2 (1:1 ratio) was carried out at -12 °C. At this temperature the reaction was too slow to accurately record the initial rate. After 12 h the reaction had reached *ca.* 20% conversion compared with 65% conversion in the equivalent reaction with Ph_2NNH_2 giving an approximate kinetic isotope effect, k_H/k_D of 3. This is consistent with related systems involving N–H bond cleavage in the rate-determining step.[8] Increasing the number of equivs of Ph_2NND_2 to 5 only provided a slight increase in the rate, as expected based on the saturation kinetics shown by Fig. 2.8, the reaction only reaching *ca.* 45% conversion after 10 h (compared to 50 min in the equivalent reaction with Ph_2NNH_2). The reaction was carried out at room temperature and the percentage conversion compared to the equivalent reaction with Ph_2NNH_2, which as discussed above was too fast to determine the initial rate, giving an analogous kinetic isotope effect k_H/k_D of 3 (25% *vs* 80% conversion in 7 min). The significant decrease in reaction time on using Ph_2NND_2 compared to Ph_2NNH_2 is in agreement with the rate-determining steps involving N–H/D bond breaking as presented in the DFT proposed mechanism.

As discussed, formation of **2.2** by the insertion of PhCCMe into the N_α–N_β bond of Ti(N_2N^{Me})($NNPh_2$)(py) (**2.1**) was modelled using Ti($N_2{}^{SiH_3}N^{Me}$)($NNMe_2$)(py) (**A1**) and MeCCMe (Scheme 2.1). The energy of activation is similar to that calculated for the vinylimide protonation reaction, $\Delta G^‡$ = 22.0 *vs* 19.2 or 23.4 kcal mol^{-1} (highest energy barrier (step **B3**-**B4**) calculated for protonation) suggesting similar rates of reaction. The reaction of **2.1** with PhCCMe was carried out at -12 °C using 1 and 5 equivs of alkyne under otherwise identical conditions to the vinylimide protonation reaction. The reaction with 5 equivs of PhCCMe was fast, essentially reaching completion on mixing at -35 °C, preventing analysis of the rate. However, in the 1:1 reaction the rate for alkyne insertion was found to be *ca.* 3 times faster than the corresponding protonation reaction (initial rate = 0.56(7) *vs* 0.178(5) x 10^{-5} mol dm^{-3} s^{-1}). This equates to a difference in $\Delta G^‡$ of less than 1 kcal mol^{-1} consistent with the DFT calculations. When

applying to the catalytic systems, *vide infra*, it is worth noting that these are the initial rates measured for the independent reactions and that under catalytic conditions the relative rates may be affected by the other reagents in the system.

2.5 Diamination *vs* hydrohydrazination

N–H bond addition across the C≡C bond of alkynes in catalytic hydrohydrazination reactions is significantly more developed than N–N bond addition,[9-16] which so far has only been established in the case of **2.1**.[1] Experimental and DFT calculations propose a similar mechanism in both cases, up to formation of a common [2+2] cycloaddition intermediate.[2, 9, 14, 16, 17] The next series of reaction steps, either direct protonation of the azametallacycle or insertion of the alkyne into the N_α–N_β bond, determine the type of catalysis.

To understand the two different reaction pathways in the case of **2.1**, further DFT analysis was carried out on the model system **A1** with MeCCMe and Me_2NNH_2, Scheme 2.5. As described, the first step in both hydrohydrazination and 1,2-diamination is [2+2] cycloaddition, forming **A4**. From **A4** N_α–N_β insertion or protonation are both feasible reaction pathways with similar Gibbs free energies (ΔG = -31.9 and -29.1 kcal mol^{-1}, respectively) requiring further analysis of the individual reaction steps. Two possible mechanisms were identified for protonation of the cycloaddition intermediate **A4** and are given in Scheme 2.6, the initial steps in the insertion mechanism, including the rate-determining step were already given in Scheme 2.1. The rate-determining step for the insertion reaction (N_α–N_β bond cleavage) was significantly lower than the rate-limiting steps for either of the two proposed mechanisms for protonation ($\Delta G^{\ddagger}$ = 20.1 *vs* 28.9/27.8 kcal mol^{-1}, respectively) consistent with **2.1** undergoing 1,2-diamination rather than hydrohydrazination.

Scheme 2.5. Gibbs Free Energy (kcal mol^{-1}) Profile for the hydrohydrazination and 1,2-diamination reaction between Ti($N_2^{SiH_3}N^{Me}$)($NNMe_2$)(py) (**A1**) or CpTi($N^{Xyl}N$)$NNMe_2$(py) (**C1**) and MeCCMe and Me_2NNH_2.

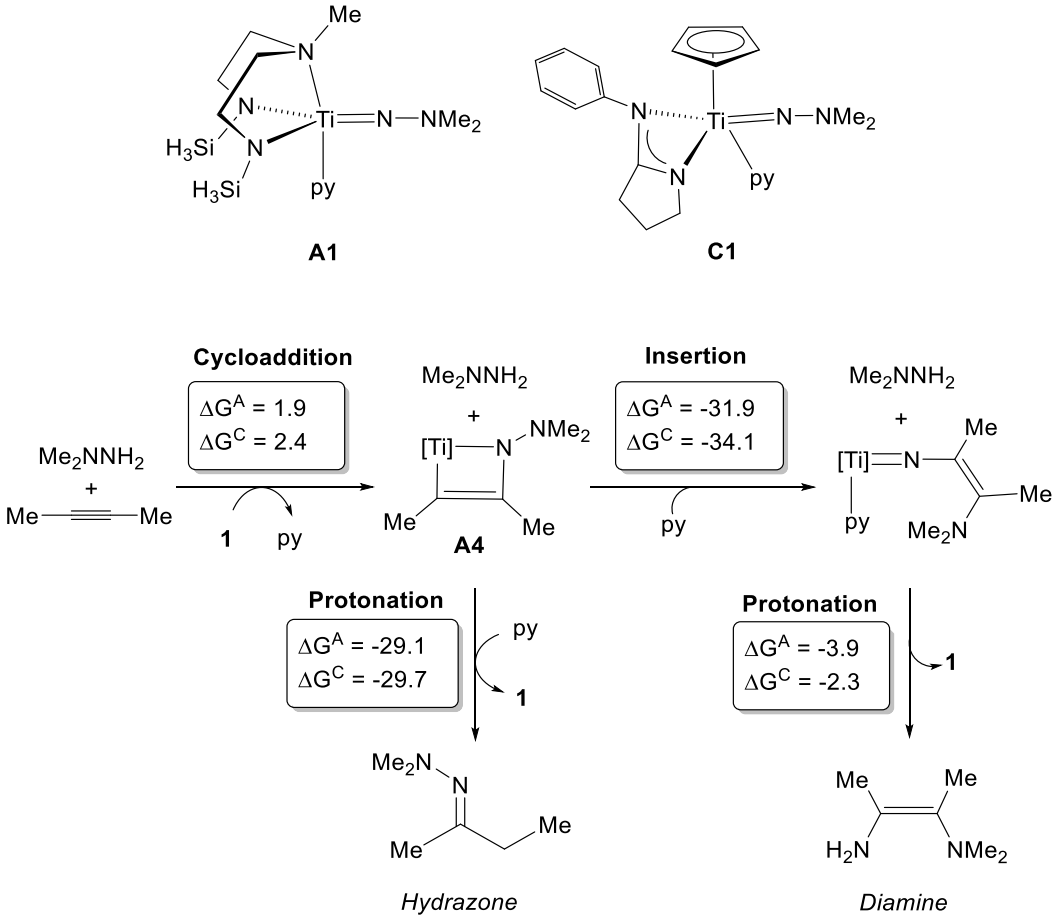

A DFT analysis was then carried out on CpTi($N^{Xyl}N$)($NNMe_2$)(py) (**C1**), a model for Cp*Ti($N^{Xyl}N$)($NNPh_2$)($^tBuNH_2$) synthesised by Gade *et al*[16] ($N^{Xyl}N$ = 2-aminopyrrolinato, pyridine was used in place of $^tBuNH_2$ in order to make a more direct comparison between the two systems), with MeCCMe and Me_2NNH_2 to understand why, in this case, hydrohydrazination is the preferred reaction pathway. Due to the unsymmetrical nature of the aminopyrrolinato ligand two separate reaction pathways are found depending on the relative position of the organic substrate with respect to this ligand. From the cycloaddition intermediate, which lies at 2.4 or 5.7 kcal mol^{-1} higher than **C1** the overall Gibbs free energies are slightly more favourable for the N_α–N_β insertion reaction rather than direct protonation, ΔG = -34.1 *vs* -29.7 kcal mol^{-1}, respectively. However, on attempts to gain insights into the relative energies of the individual reaction steps, the rate-determining step for the N_α–N_β insertion reaction was found to be substantially higher than the relevant rate-limiting step in the most

favourable mechanism (as with **A4** more than one possible mechanism for protonation was identified) found for the protonation reaction ($\Delta G^{\ddagger}$ = 32.8 *vs* 18.5 kcal mol^{-1}, respectively) explaining the switch from 1,2-diamination to hydrohydrazination.

Scheme 2.6. Gibbs Free Energy (kcal mol^{-1}) Profile for two reaction pathways accessible for the hydrohydrazination (**H**) reaction between Ti($N_2^{SiH_3}N^{Me}$)($NNMe_2$)(py) (**A1**) and MeCCMe and Me_2NNH_2 starting from the cycloaddition intermediate Ti($N_2^{SiH_3}N^{Me}$){NC(Me)C(Me)NMe_2} (**A4**).

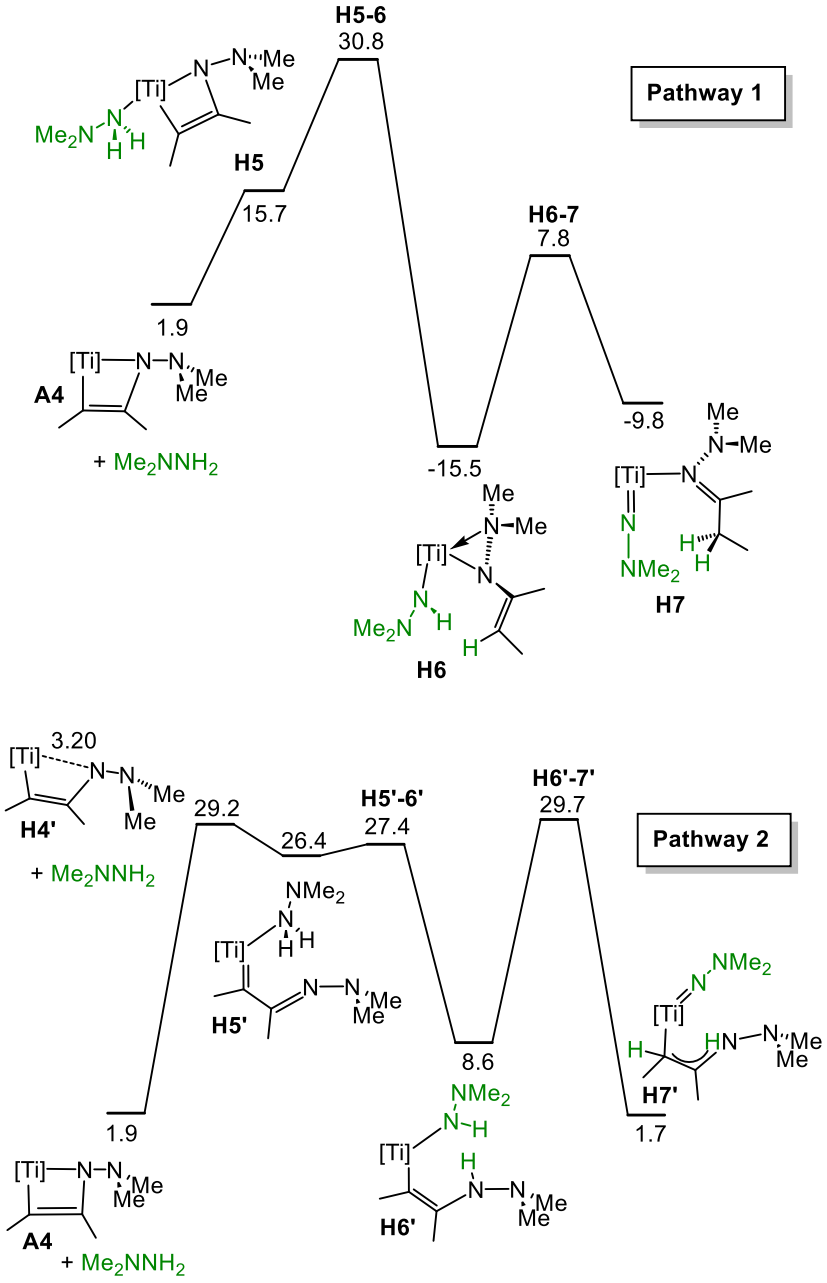

2.6 Combined DFT and experimental investigation of the catalytic 1,2-diamination reaction of Ti(N_2N^{Me})($NNPh_2$)(py) (2.1) with PhCCMe and Ph_2NNH_2

As expected, when the reaction of **2.1** (5 – 25 mol%) with Ph_2NNH_2 and PhCCMe (0.20 mol dm^{-3}) was monitored at room temperature in C_6D_6 the evolution of **2.1a** did not follow well-behaved first or second order kinetics due to catalyst decomposition. Rate constants in each case were therefore obtained using the initial rates method. The resulting plot of initial rate *vs* mol% catalyst loading gave a linear fit (r^2 = 0.978, intercept = -0.4(7)) as shown in Figure 2.9. The corresponding double-log plot (Fig. 2.9, r^2 = 0.964) gives a gradient of 0.97(8) consistent with a 1st order dependence on metal, which in turn, is consistent with the rate law given in Eq 2.12 (x = 1); the linear double-log plot is explained by Eq 2.13.

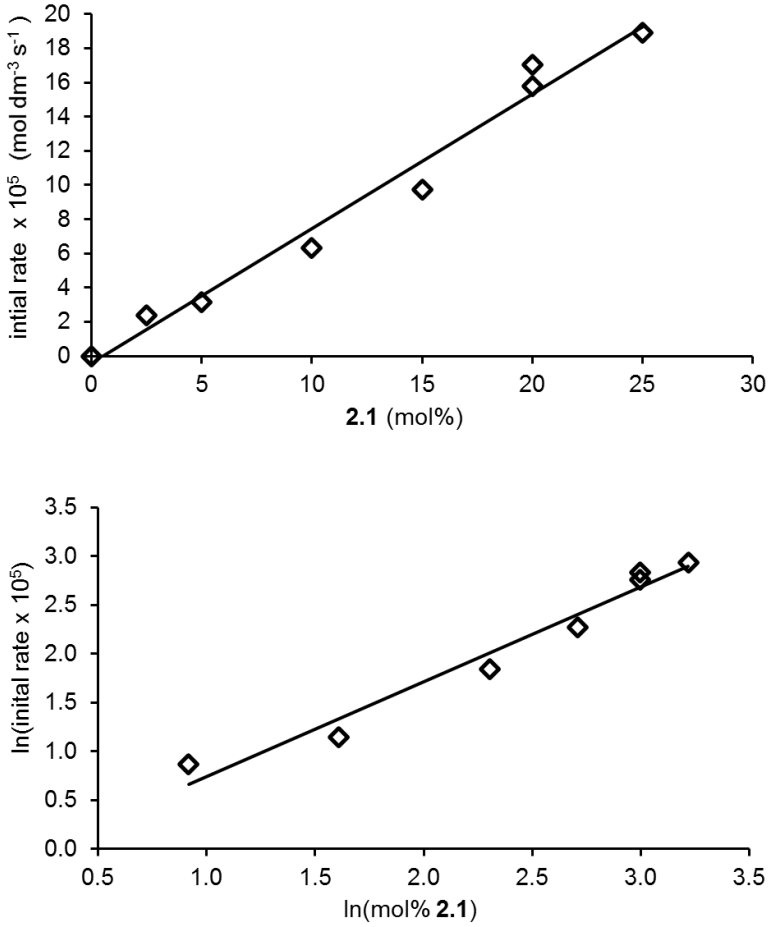

Figure 2.9. Top: plot of initial rate *vs* mol% of Ti(N_2N^{Me})($NNPh_2$)(py) (**2.1**) for the reaction of **2.1** with PhCCMe and Ph_2NNH_2. The best-fit line shown had r^2 = 0.978. Bottom: the corresponding double-log plot. The linear fit (r^2 = 0.964) gives a gradient of 0.97(8).

$$\text{Initial rate} = k_{obs}\,[\mathbf{2.1}]^{x} \qquad (2.12)$$

$$\ln(\text{initial rate}) = \ln(k_{obs}) + x\ln([\mathbf{2.1}]) \qquad (2.13)$$

The catalytic reaction with 5 mol% catalyst loading (**2.1**) was carried out in the presence of excess PhCCMe (0.40 mol dm^{-3}, 40 equivs) compared to Ph_2NNH_2 (20 equivs) under otherwise identical reaction conditions. The initial rate remained unchanged compared to the reaction with 20 equivs of PhCCMe (initial rate = 6.8(3) *vs* 7.1(6) x 10^{-5} mol dm^{-3} s^{-1}, respectively) suggesting a 0th order dependence on alkyne concentration. To confirm, **2.1** was added to pre-mixed solutions of Ph_2NNH_2 and PhCCMe in 1:3:x ratios, where x (number of equivs of alkyne) was varied between 3 and 11 equivs, Eq 2.14, and the reactions followed by ^{1}H NMR spectroscopy at room temperature. The results are given in Figure 2.10 and clearly show a non-linear relationship between initial rate and number of equivs of PhCCMe used. Indeed, compared to the linear fit shown for the expected values, presuming a 1st order dependence on PhCCMe, the initial rate appears to reach saturation above 3 equivs of PhCCMe (0.06 mol dm^{-3}). This is consistent with the relative rates of the alkyne insertion and vinylimide protonation reactions determined separately, *vide supra*, which indicate that in the catalytic cycle the protonation step is turnover-limiting.

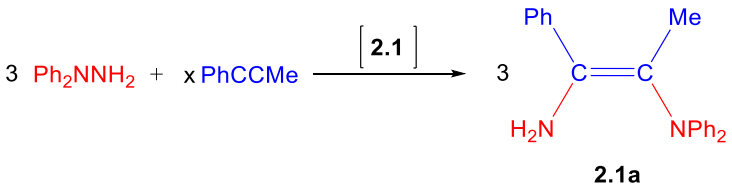

Equation 2.14

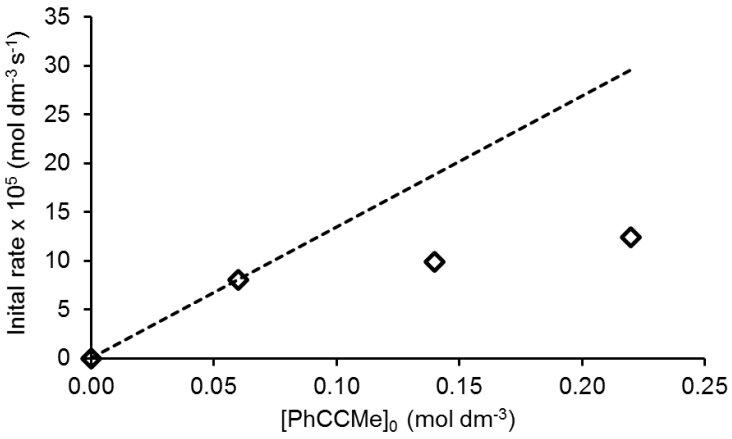

Figure 2.10. Plot of $[PhCCMe]_0$ *vs* initial rate for the reaction of $Ti(N_2N^{Me})(NNPh_2)(py)$ (**2.1**) with 3 equivs of Ph_2NNH_2 and x equivs of PhCCMe (x = 3, 7 and 11), $[Ti]_0$ = 0.02 mol dm^{-3}. The dotted line is that expected for a linear relationship between [PhCCMe] and initial rate based on extrapolation from the first data point (8.07(9) x 10^{-5} mol dm^{-3} s^{-1}).

However, similar results were obtained in experiments which vary the concentration of hydrazine. The reactions were carried out under analogous conditions to that described above except in this case the concentration of alkyne was kept constant at 0.06 mol dm^{-3} (3 equivs) and the hydrazine concentration varied between 0.02 – 0.22 mol dm^{-3} (1 – 11 equivs), Eq 2.15. The results are given in Fig. 2.11 alongside the linear fit predicted for a 1st order dependence on initial hydrazine concentration. As shown in Fig. 2.11, the initial rate is significantly slower than expected above concentrations of 0.02 mol dm^{-3} of Ph_2NNH_2. This is reminiscent of the stoichiometric vinylimide protonation reaction, in which both reactions show saturation kinetics above a certain concentration of Ph_2NNH_2.

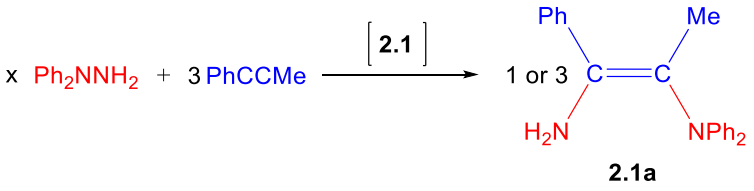

Equation 2.15

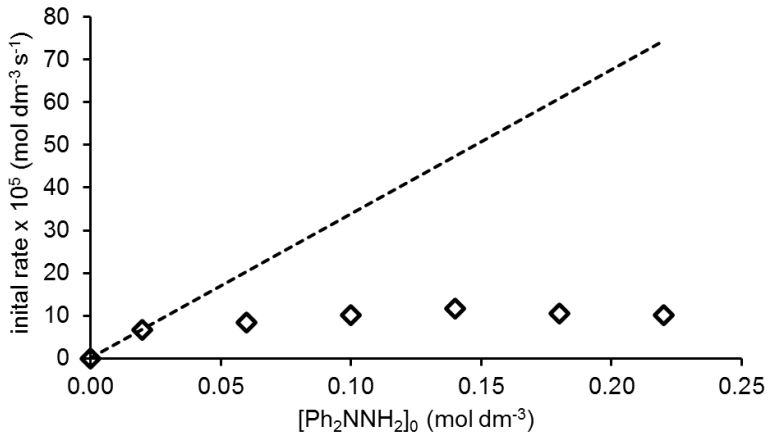

Figure 2.11. Plot of $[Ph_2NNH_2]_0$ *vs* initial rate for the reaction of $Ti(N_2N^{Me})(NNPh_2)(py)$ (**2.1**) with 3 equivs of PhCCMe and x equivs of Ph_2NNH_2 (x = 1 – 11), $[Ti]_0$ = 0.02 mol dm^{-3}. The dotted line is that expected for a linear relationship between $[Ph_2NNH_2]_0$ and initial rate based on extrapolation from the first data point (7(2) x 10^{-5} mol dm^{-3} s^{-1}).

In both experimental and DFT investigations into the reaction mechanisms of both the alkyne insertion and vinylimide protonation reactions, dissociation of pyridine (or perhaps hydrazine in the presence of an excess) is proposed as the first step (as part of a pre-equilibrium). To test the existence of an initial equilibrium involving the loss of pyridine in the catalytic reaction, which would explain the saturation kinetics observed in Fig. 2.11, the reaction of **2.1** with PhCCMe and Ph_2NNH_2 (10 mol% of **2.1**) was carried out in the presence of 5 equivs (extra added) of pyridine. When followed at room temperature in C_6D_6 the reaction rate was significantly reduced, taking nearly 12 h to reach 85% conversion, compared to ~ 7 h for the analogous reaction without excess pyridine. Indeed, on calculation of the initial rate, the reaction was found to be almost 3 times slower (initial rate = 2.15(6) *vs* 6.3(1) mol dm^{-3} s^{-1}, respectively).

To test for the expected presence of a kinetic isotope effect under catalytic conditions the reaction of **2.1** with 3 equivs of PhCCMe and Ph_2NND_2 was carried out under otherwise identical conditions. The rate of reaction was significantly reduced, highlighted by the initial rate which was *ca.* 3.6 times slower than the corresponding reaction with Ph_2NNH_2 (initial rate = 2.23(8) *vs* 8.07(9) mol dm^{-3} s^{-1}, respectively). This kinetic isotope effect is similar to that observed in the stoichiometric reactions (*ca.* 3) which is consistent with protonation of the vinylimide complex being turnover-limiting, compared to alkyne insertion, with proton transfer being the rate-determining step.

2.7 Catalyst resting state

The combined experimental and DFT study into the stoichiometric and catalytic reactions indicate at least two effective resting states during catalysis, namely the hydrazide and vinylimide complexes **2.1** and **2.2**. When the reaction of **2.1** with 3 equivs of Ph_2NNH_2 and PhCCMe was followed by ^1H NMR spectroscopy at room temperature in C_6D_6 both **2.1** and **2.2** were identified in the reaction mixture within 5 min, alongside a third unknown species. The unidentified complex was thought to be a side product formed between either **2.1** or **2.2** and Ph_2NNH_2 or $H_2NC(Ph)C(Me)NPh_2$ (**2.1a**). As a test, control NMR tube scale experiments were set up between compounds **2.1** and **2.2**, and Ph_2NNH_2 and **2.1a** (each experiment in a 1:1 ratio). When followed by ^1H NMR spectroscopy the reaction between **2.2** and **2.1a** formed an *ca.* 52:48 equilibrium mixture of the insertion complex **2.2** and a new bis(vinylamide) complex, $Ti(N_2N^{Me})\{N(H)C(Ph)C(Me)NPh_2\}_2$ (**2.17**) alongside resonances attributed to free pyridine, Eq 2.16. The signals associated with **2.17** were identical to those assigned to the unknown third species in the 1:3:3 reaction described above. Accordingly, the equilibrium was shifted in favour of **2.17** on removal of pyridine under reduced pressure and redissolving in C_6D_6. Although bis(vinylamide) complexes on titanium are not known, recent work in our group has shown that addition of $XylNH_2$ to imide complex $Ti(N_2N^{iPr})(NXyl)(py)$ (N_2N^{iPr} = $MeN(CH_2CH_2N^iPr)_2$) generates equilibrium mixtures of starting materials and $Ti(N_2N^{iPr})\{N(H)Xyl\}_2(py)$, confirmed in this case by X-ray crystallography.[18] Proton transfers from free amines or hydrazines to bound amide ligands is also a common synthetic route to both imide and hydrazide complexes, for instance reaction of $Ti(NMe_2)_2Cl_2$ with $^tBuNH_2$ to generate $Ti(N^tBu)Cl_2(NHMe_2)_2$.[4, 19, 20]

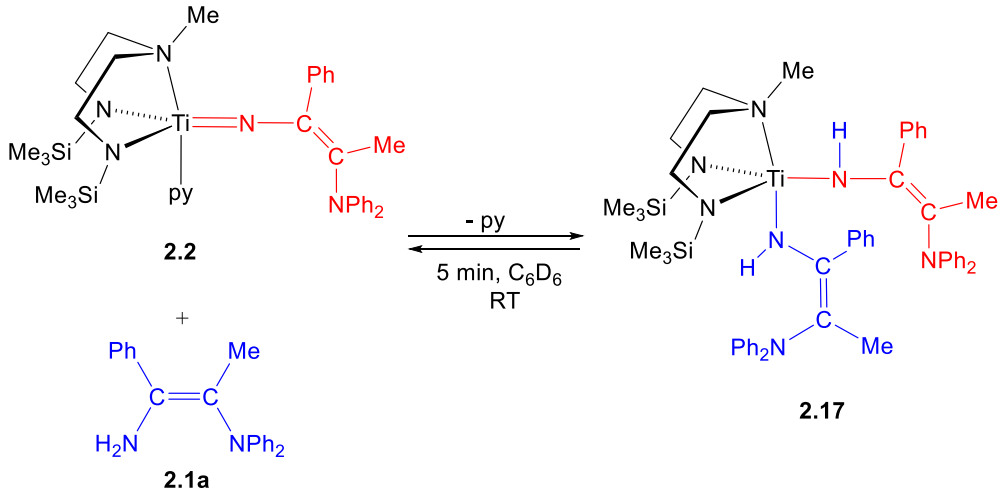

Equation 2.16

At room temperature the bis(vinylamide) complex **2.17** shows fluxional behaviour with broad resonances observed in the ^{1}H NMR spectrum. At low temperature (-40 °C) two new C<u>Me</u> resonances are seen at δ 2.07 and 1.57 ppm alongside a new N<u>Me</u> signal at δ 1.83 ppm. The CH_2 groups on the diamide-amine ligand appear as four multiplets consistent with a C_1 symmetric structure, alongside two characteristic N–H signals at δ 9.45 and 9.19 ppm. To confirm these protons originate from the NH_2 group of **2.1a** the deuterated analogue, **2.1a-*d*$_2$**, was synthesised *in situ* by reaction of **2.2** with Ph_2NND_2. To the mixture of **2.1** and $D_2NC(Ph)C(Me)NPh_2$ (**2.1a-*d*$_2$**) was added 1 equiv of PhCCMe reforming **2.2**, Scheme 2.7. The 1:1 mixture of **2.1a-*d*$_2$** and **2.2** was cooled to -40 °C and analysed by ^{1}H and ^{2}H NMR spectroscopy. As expected, the ^{1}H NMR spectrum is essentially identical to the corresponding reaction with protio-**2.17** and therefore the spectrum shows formation of an equivalent bis(vinylamide) complex, **2.17-*d*$_2$,** with the exception of the N–H resonances, previously observed at δ 9.45 and 9.19 ppm, which are now reduced to 0.1 of their expected integration in the ^{1}H NMR spectrum. Accordingly, in the ^{2}H spectrum recorded at the same temperature a new broad resonance is observed at δ 9.2 ppm, in the region expected for N–D groups bound to titanium. Compound **2.17** was characterised *in situ* by ^{1}H and ^{13}C NMR spectroscopy.

Scheme 2.7. Reaction of $D_2NC(Ph)C(Me)NPh_2$ (**2.1a-*d*$_2$**) with $Ti(N_2N^{Me})\{NC(Ph)C(Me)NPh_2\}(py)$ (**2.2**) formed following reaction of $Ti(N_2N^{Me})\{NC(Ph)C(Me)NPh_2\}(py)$ (**2.2**) with Ph_2NND_2 and PhCCMe (1:1:1 ratio).

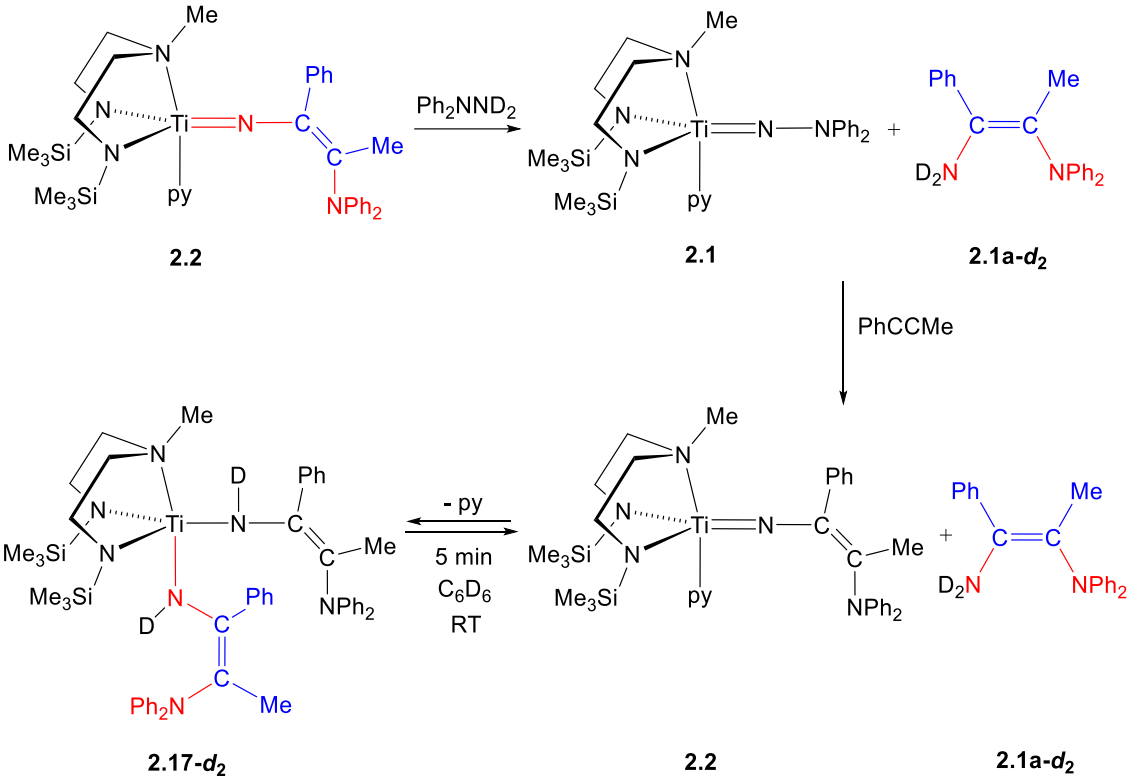

To investigate the behaviour of complexes **2.14** and **2.15**, formed from insertion of PhCCMe into the N_α–N_β bond of $Ti(N_2N^{Me})(NNAr_2)(py)$ (Ar = 4-$C_6H_4{}^tBu$ (**2.12**) and 4-C_6H_4OMe (**2.13**)), with the corresponding vinylamine products, **2.12a** and **2.13a**, 1:1 reactions were set up *via in situ* generation of **2.12a** and **2.13a** using the same method as detailed in Scheme 2.7. The reactions were followed by ^1H NMR spectroscopy at room temperature in C_6D_6. As expected, both reaction mixtures immediately give an equilibrium mixture of starting materials and $Ti(N_2N^{Me})\{N(H)C(Ph)C(Me)NAr_2\}_2$ (Ar = 4-$C_6H_4{}^tBu$ (**2.18**) and 4-C_6H_4OMe (**2.19**)). Like **2.17**, the resonances attributed to **2.18** and **2.19** are broad at room temperature consistent with exchange between free and bound vinylamine. However, in both ^1H NMR spectra, broad singlets are observed above δ 9.0 ppm (δ 9.32 ppm, **2.18**; δ 9.54 and 9.35 ppm, **2.19**) characteristic of N–H signals. Indeed, the spectra are very similar to the ^1H NMR spectra recorded for the equivalent reaction with Ar = Ph. As expected, the position of equilibrium varies between the three vinylimide compounds, lying furthest to the right, as defined by Eq 2.16, in the case of Ar = 4-C_6H_4OMe presumably due to the stronger σ donor properties

of –OMe substituents compared to H (% conversion to the bis(vinylamide) complex; **2.17** (48%) ~ **2.18** (52%) < **2.19** (60%)).

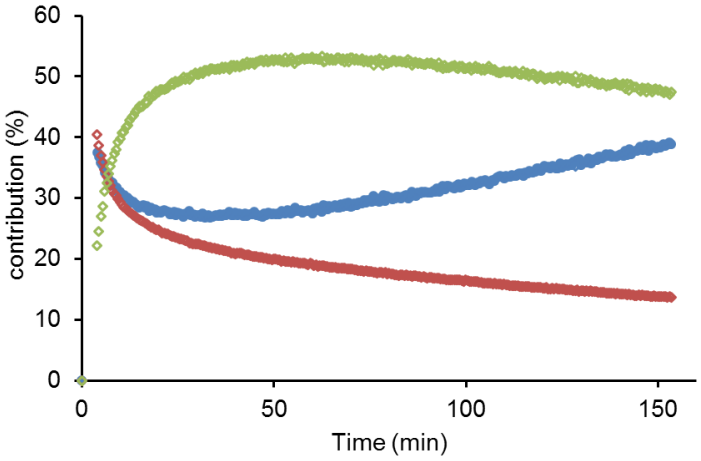

Figure 2.12. Plot of % contribution *vs* time for the reaction of $Ti(N_2N^{Me})(NNPh_2)(py)$ (**2.1**) with 3 equivs of PhCCMe and Ph_2NNH_2 at room temperature, $[Ti]_0$ = 0.02 mol dm^{-3}. $Ti(N_2N^{Me})(NNPh_2)(py)$ (**2.1**) is shown in blue diamonds, $Ti(N_2N^{Me})\{NC(Ph)C(Me)NPh_2\}(py)$ (**2.2**) is shown in red diamonds and $Ti(N_2N^{Me})\{N(H)C(Ph)C(Me)NPh_2\}_2$ (**2.17**) is shown in green diamonds.

Figure 2.12 shows the % contribution of compounds **2.1**, **2.2** and **2.17** to the total titanium species present in the reaction of **2.1** with 3 equivs of $PhNNH_2$ and PhCCMe. At the start of the reaction alkyne and hydrazine are in excess. Since the vinylimide protonation reaction appears to reach saturation more quickly than the alkyne insertion reaction the relative increase in rate is significantly greater for the insertion reaction. This increases the proportion of the catalyst which is present as the vinylimide compound (**2.2**), which in turn increases the amount of bis(vinylamide) complex (**2.17**). The proportion of bis(vinylamide) complex present also increases as the amount of vinylamine product is produced, reaching a maximum after *ca.* 50 min reaction time (53%). After this point, the alkyne concentration has reduced decreasing the rate of alkyne insertion compared to protonation of the vinylimide. This allows the two processes to become competitive increasing the proportion of hydrazide complex present in the reaction mixture, which in turn reduces the amount of **2.17**. Accordingly, in the reactions described above where alkyne concentration was increased relative to hydrazine concentration, the proportion of the vinylimide and bis(vinylamide) complexes is increased compared to the hydrazide complex. In turn, on increasing the

hydrazine concentration relative to alkyne, the catalyst resting state is largely the hydrazide complex.

Catalyst testing starting with 5 mol% of vinylimide complex **2.2** with PhCCMe and Ph_2NNH_2 showed similar behaviour to hydrazide catalyst **2.1**, giving the same initial rate (initial rate = 1 x 10^{-4} mol dm^{-3} s^{-1}). To test whether complex **2.17** has a significant effect on the rate of catalysis a 1:1 mixture of **2.2** and **2.1a** was used to generate **2.17** *in situ*. This mixture was then tested for catalytic activity (5 mol% titanium) under analogous conditions and the evolution of **2.1a** monitored by ^{1}H NMR spectroscopy. The testing gave similar results, initial rate = 1.0(2) x 10^{-4} mol s^{-1} demonstrating that the bis(vinylamide) complex **2.17** can readily re-enter the cycle by re-forming **2.2**. This is supported by the 1:3:3 reactions which show hydrazide compound **2.1** as the only titanium species remaining once the reaction has reached completion.

2.8 Catalyst decomposition

As described in Sections 2.4 and 2.6 the observed rate constant, k_{obs}, for either the vinylimide protonation reaction, as detailed in Eq 2.7, or the overall catalytic reaction, as given in Scheme 2.2, appears to decrease over time, requiring the use of the initial rates method to calculate the rate of the reaction. This is ascribed to loss of titanium complex, either hydrazide or vinylimide complexes **2.1** and **2.2**, through decomposition and/or non-productive side reactions with the other substrates present in the reaction mixture. One possible side reaction has already been discussed in the formation of a bis(vinylamide) complex between **2.2** and vinylamine product **2.1a**, namely $Ti(N_2N^{Me})\{N(H)C(Ph)C(Me)NPh_2\}_2$ (**2.17**), although this did not appear to impede the initial rate of catalysis. However, reaction of hydrazide catalyst, **2.1**, with either $H_2NC(Ph)C(Me)NPh_2$ (**2.1a**) or Ph_2NNH_2 resulted in the formation of protio-ligand, $MeN\{CH_2CH_2N(H)SiMe_3\}_2$, alongside other unidentified compounds at room temperature, Eq 2.17. This is not unexpected since protonation of these supporting amide ligands has been observed in the reactions of $Ti(N_2N^{SiMe_3})(N^tBu)(py)$ ($N_2N^{SiMe_3}$ = $Me_3SiN(CH_2CH_2NSiMe_3)_2$) and other similar *tert*-butyl imides with Ph_2NNH_2 as well as in reactions with $Ti(N_2N^{py})(NMe_2)_2$.[5] It is assumed that since the supporting ligand is displaced all resulting compounds from this reaction are not catalytically active and therefore result in overall loss of catalyst activity, referred to hereafter as ″catalyst decomposition″. The rate of decomposition is similar in the presence of 1 equiv of either

2.1a or Ph_2NNH_2. For instance, after 16 h at room temperature, in the presence of 1 equiv of **2.1a**, 13% of the catalyst has decomposed compared to 11% in the equivalent experiment with hydrazine. However, in both cases the substrates are detrimental. For instance, in the presence of 20 equivs of Ph_2NNH_2, 32% of **2.1** has been destroyed after 30 min and, after 24 h, could no longer be detected by ^1H NMR spectroscopy. Interestingly, the rate of decomposition is increased on addition of 20 equivs of **2.1a**, which appears to destroy the catalyst within 30 min.

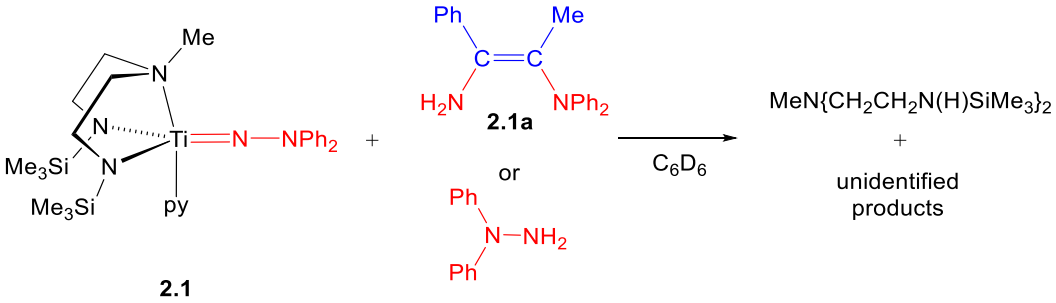

Equation 2.17

Concurrent work carried out in our group on ligand modification has found replacing the $SiMe_3$ groups on the N_2N^{Me} ligand with substituted phenyl groups, bearing a wide range of substituents from electron-withdrawing fluorines to alkyl groups, have also provided successful catalysts; though the reactions require heating at 70 °C to achieve appreciable conversion.[21] For example, $Ti\{MeN(CH_2CH_2NC_6F_5)_2\}(NNPh_2)(py)$ (**2.20**) (with PhCCMe and Ph_2NNH_2) reached quantitative conversion within 16 h ($t_{1/2}$ = 1 h). However, in these series of complexes both *cis* and *trans* isomers of **2.1a** are produced (in a ratio of 90:10 in the case of **2.20**) and in some cases the hydrazone $MeC(NNPh_2)CH_2Ph$, from competing hydrohydrazination reactions, and $HNPh_2$ following an, as yet, unidentified mechanism are also observed. In an attempt to improve the performance of catalyst **2.1** either in terms of rate and/or turnover number, the catalytic reaction (5 mol% loading of **2.1** with PhCCMe and Ph_2NNH_2) was followed by ^1H NMR spectroscopy at 76 °C in C_6D_6. Within 5 min the catalysis had reached 55% conversion (turnover number = 11/20) after which time no further conversion was observed. Consequently, although the increase in temperature did lead to a significant increase in rate, at room temperature the equivalent reaction had reached 10% conversion, the various reaction pathways leading to catalyst degradation were also increased resulting in rapid catalyst death and ultimately a poorer turnover number.

2.9 Substrate effect on catalyst performance

2.9.1 Initial rates

Work discussed in this section was carried out by the author, Hiromasa Tanahashi and Lee Collins. As discussed in Section 2.1, since the rate-determining step in the alkyne insertion reaction involves nucleophilic attack of C_{Ti} on N_α, the rate of alkyne insertion into the N_α–N_β bond of **2.1** increases with electron-rich substituents on the aryl group of ArCCMe.[2] The observed rate constant, k_{obs} was determined in the cases of (4-C_6H_4X)CCMe (X = H, OMe and ^{t}Bu) and found to increase in line with their associated Hammett substituent constants, σ_p, in other words k_{obs} increases in the order H < ^{t}Bu < OMe. The observed rate constant could not be determined for X = CF_3 as the electron-withdrawing nature of the substituent stabilised the cycloaddition intermediate, **2.7_int**, affecting the overall kinetic regime. In order to determine the effect of the substrate on diamination catalysis, the initial rate was calculated for the various catalytic reactions described in Scheme 2.2. The results are summarised in Table 2.1. In all cases, the reactions were monitored by ^{1}H NMR spectroscopy over a period of 48 – 72 h (unless quantitative conversion had already been reached) at 5 mol% catalyst loading in C_6D_6 at room temperature.

Table 2.1. Initial rates (x 10^5 mol dm^{-3} s^{-1}) for the diamination reaction of internal alkynes with diaryl hydrazines using Ti(N_2N^{Me}){NN(4-$C_6H_4X)_2$}(py) (5 mol%; X = H (**2.1**), ^{t}Bu (**2.12**) and OMe (**2.13**)).

(4-$C_6H_4X)_2NNH_2$,	(4-C_6H_4X)CCMe, X =				RCCR, R =	
X =	H	OMe	^{t}Bu	CF_3	4-$C_6H_4CF_3$	Me
H	6.8(9)	5(1)	15(3)	3.9(6)	1.1(1)	0.16(2)
OMe	6(2)	5(2)	8(1)	5.0(3)	2.1(2)	0
^{t}Bu	9.3(1)	9(2)	10(1)	5.4(7)	2.9(6)	0

Reactions carried out at room temperature with 5 mol% catalyst loading, [Ti] = 0.01 mol dm^{-3} in C_6D_6 (0.6 mL).

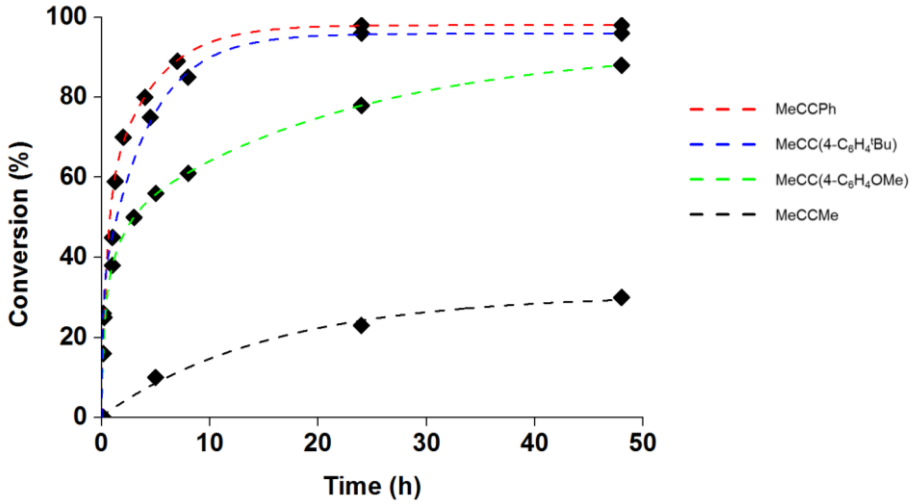

Figure 2.13. Plot of % conversion *vs* time for the diamination reaction of internal alkynes with Ph_2NNH_2 using $Ti(N_2N^{Me})(NNPh_2)(py)$ (**2.1**, 5 mol%), [Ti] = 0.01 mol dm^{-3} in C_6D_6 (0.6 mL). The best-fit lines are drawn to help guide the eye.

In terms of the effect of alkyne substituents on the rate of diamination, Table 2.1 and Figure 2.13 clearly show the slowest initial rates for butyne and the more sterically hindering diaryl alkyne ArCCAr (Ar = 4-$C_6H_4CF_3$) with electron-withdrawing CF_3 groups. This is consistent with a slow rate of alkyne insertion,[2, 6] non-quantitative protonation reaction, *vide infra*, and electron-withdrawing groups reducing the basicity of the vinylimide ligands as discussed in Section 2.4. The negative effect of electron-withdrawing substituents on the rate of catalysis is also observed in the relative initial rates for ArCCMe (Ar = 4-$C_6H_4CF_3$) compared to the more electron-rich aryl alkynes (avg. initial rate = 4.8(3) *vs* 8.2(6) mol dm^{-3} s^{-1}). The fastest initial rate is observed with (4-$C_6H_4{}^tBu$)CCMe and Ph_2NNH_2 (initial rate = 15(3) mol dm^{-3} s^{-1}). The remaining results are similar, with average initial rates of 7.4(7) *vs* 6(1) mol dm^{-3} s^{-1} for PhCCMe and (4-C_6H_4OMe)CCMe, respectively, compared to 11(1) mol dm^{-3} s^{-1} for (4-$C_6H_4{}^tBu$)CCMe. Therefore in contrast to the N_α–N_β bond insertion reaction, the average initial rate for diamination increases in the order (4-C_6H_4X)CCMe, X = CF_3 < OMe ~ H < ^{t}Bu with average k_{rel} values given as 1.0 < 1.3 < 1.5 < 2.3, respectively.

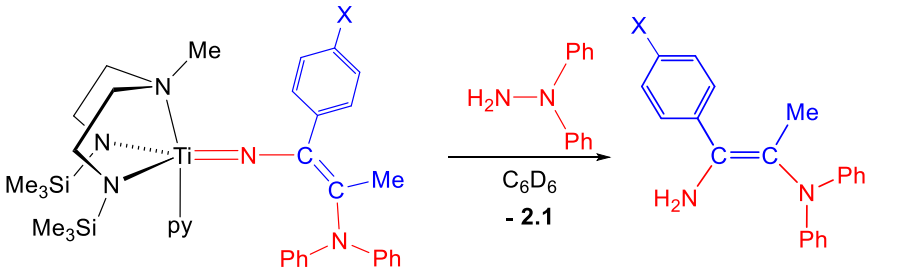

X = H (**2.2**), ^{t}Bu (**2.5**), OMe (**2.6**) or CF_3 (**2.7**)

X = H (**2.1a**), ^{t}Bu (**2.1b**), OMe (**2.1c**) or CF_3 (**2.1e**)

	k_{CF3}	<	k_{OMe}	<	k_H	<	k_{tBu}	
k_{rel}	1.0	:	1.3	:	1.6	:	2.2	

Equation 2.18

To gain a better understanding of the alkyne dependence, the relative rates of vinylimide protonation were determined through reaction of 1 equiv of Ph_2NNH_2 with a pre-mixed solution of Ti(N_2N^{Me}){NC(Ph)C(Me)NPh_2}(py) (**2.1**) and Ti(N_2N^{Me}){NC(Ar)C(Me)NPh_2}(py) (Ar = 4-$C_6H_4{}^{t}$Bu (**2.5**), 4-C_6H_4OMe (**2.6**), or 4-$C_6H_4CF_3$ (**2.7**), 1:1 ratio), Eq 2.18. The proportions of starting material and/or products were calculated by ^{1}H NMR spectroscopy giving the relative rates of protonation. Once combined the results showed a relative increase in the rate of vinylimide protonation in the order (4-C_6H_4X)CCMe, X(k_{rel}) = CF_3 (1.0) < OMe (1.3) < H (1.6) < ^{t}Bu (2.2) in line with the alkyne dependence shown by the catalytic reaction. This supports the hypothesis that the turnover-limiting step lies within the vinylimide protonation reaction rather than the alkyne insertion step of the catalysis.

To identify whether alkyne insertion is faster than protonation of the vinylimide in the cases of the symmetrical alkynes, ArCCAr (Ar = 4-$C_6H_4CF_3$) and MeCCMe, the initial rates of the individual reactions with **2.1** were determined. The insertion reactions proceeded smoothly at room temperature reaching full conversion within 50 and 90 min, respectively. However, due to the complicated mixture of products produced on addition of Ph_2NNH_2 it was not possible to accurately measure initial rates for the protonation reactions. In particular, with regard to MeCCMe, although it was possible to identify signals characteristic of the vinylamine product in both the ^{1}H and ^{13}C spectra soon after addition, the various other products produced provides an explanation for the poor catalyst performance in the case of **2.1** and no apparent catalytic reaction with **2.12** and **2.13**.

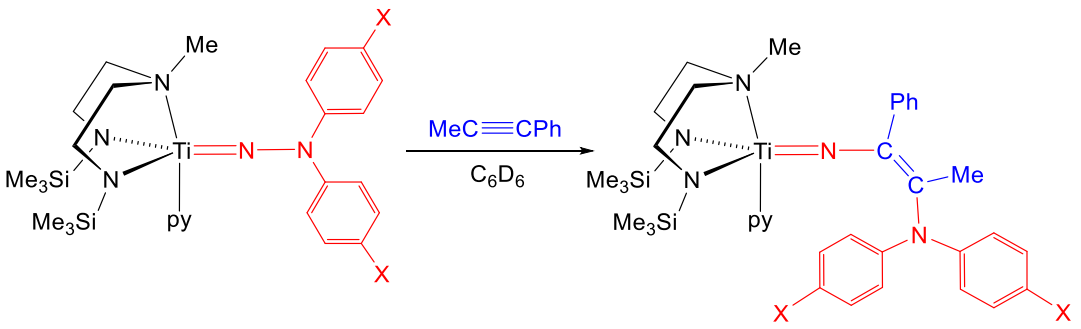

X = H (**2.1**), ^{t}Bu (**2.12**) or OMe (**2.13**)

X = H (**2.2**), ^{t}Bu (**2.14**) or OMe (**2.15**)

$k_H \sim k_{tBu} < k_{OMe}$
k_{rel} 1.0 : 1.0 : 1.3

Equation 2.19

The effect of the *para*-X substituent on the hydrazine substrate was then determined, starting with the effect on the rate of alkyne insertion. Through equivalent competition reactions, whereby 1 equiv of PhCCMe was added to a pre-mixed solution of Ti(N_2N^{Me})($NNAr_2$)(py) (Ar = 4-C_6H_4OMe (**2.12**) or $C_6H_4{}^{t}$Bu (**2.13**)) and **2.1** (1:1 ratio, Eq 2.19), the relative rates of alkyne insertion were shown to increase in the order Ar = 4-C_6H_4X, X(k_{rel}) = H(1.0) ~ ^{t}Bu (1.0) < OMe (1.3). This is in contrast to the relative rates of diamination which show, with PhCCMe, an increase in the order Ar = 4-C_6H_4X, X = OMe < H < ^{t}Bu with k_{rel} = 1.0 < 1.1 < 1.6, Table 2.1 and Fig. 2.14, again supporting the proposal that the turnover-limiting step of catalysis lies in protonation of the vinylimide.

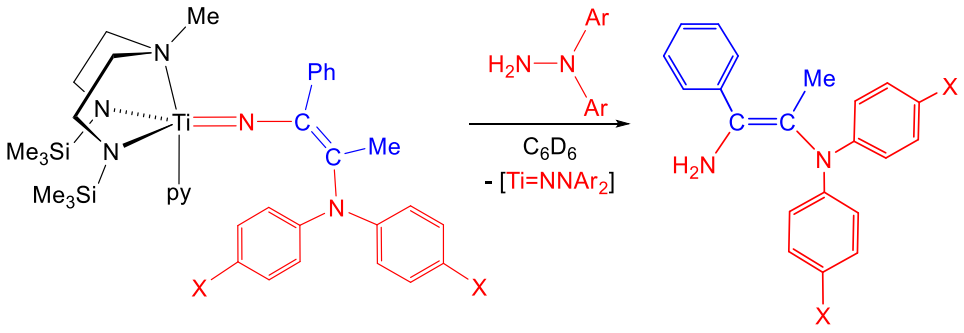

X = H (**2.2**), ^{t}Bu (**2.14**) or OMe (**2.15**)

X = H (**2.1a**), ^{t}Bu (**2.12a**) or OMe (**2.13a**)

$k_{OMe} \sim k_H < k_{tBu}$

Equation 2.20

As a further test, the reactions of Ti(N_2N^{Me}){NC(Ph)C(Me)NAr_2}(py) (Ar = Ph (**2.2**), 4-$C_6H_4{}^{t}$Bu (**2.14**) or C_6H_4OMe (**2.15**)) with Ar_2NNH_2 (1:1 ratio, Eq 2.20) were

monitored by ^{1}H NMR spectroscopy at room temperature and the relative rates of reaction shown to increase in the order Ar = 4-C_6H_4X, X = OMe ~ H < ^{t}Bu. The reaction with (4-$C_6H_4{}^{t}Bu)_2NNH_2$ was complete within ~ 10 min. At such time the reactions with (4-$C_6H_4OMe)_2NNH_2$ and Ph_2NNH_2 had reached 74 and 85% conversion, respectively. This correlation is analogous to that shown in the catalytic diamination reaction, supporting prior arguments that the vinylimide protonation reaction is rate-determining. Conversely, in the case of electron-withdrawing alkynes, ArCCR (Ar = $C_6H_4CF_3$, R = $C_6H_4CF_3$ or Me), the rate of diamination is shown to increase in the order (4-$C_6H_4X)_2NNH_2$, X = H < OMe < ^{t}Bu with avg. k_{rel} = 1.0 < 1.4 < 1.7. This could be due to a combination of factors, which at the present time are not understood.

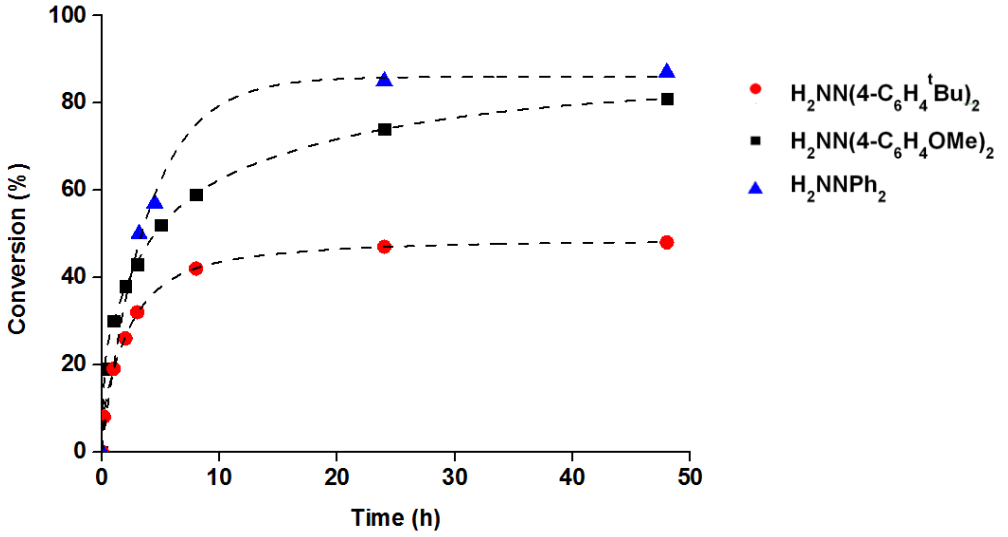

Figure 2.14. Plot of % conversion *vs* time for the diamination reaction of PhCCMe with diaryl hydrazines using Ti(N_2N^{Me}){NN(4-$C_6H_4X)_2$}(py) (2.5 mol%; X = H (**2.1**), ^{t}Bu (**2.12**) and OMe (**2.13**)), [Ti] = 0.005 mol dm^{-3} in C_6D_6 (0.6 mL). The best-fit lines are drawn to help guide the eye.

2.9.2 Turnover numbers

In order to determine the overall merits of the different catalyst systems, the maximum turnover numbers were also obtained for each reaction, Table 2.2 and Fig. 2.13, on the NMR tube scale. To differentiate between reactions which reached over 90% conversion within 24 h, the catalyst loading was reduced to 2.5 mol% and the reactions repeated, these results are given in Table 2.3 (and Fig. 2.14). The lowest turnover numbers are found for RCCR (R = Me or 4-$C_6H_4CF_3$) consistent with the lowest initial rates. This is supported by the complicated mixture of products produced on protonation

of the vinylimide complexes, *vide supra*, ultimately reducing the amount of active catalyst. Interestingly, although the initial rates are similar for Ph and 4-C_6H_4OMe aryl groups on either the alkyne or hydrazine substrate, systems using either (4-$C_6H_4OMe)_2NNH_2$ or (4-C_6H_4OMe)CCMe appear more susceptible to catalyst decomposition resulting in a lower turnover at both 5 and 2.5 mol% catalyst loading. Indeed, when analysing only turnover numbers the phenyl group on either the alkyne or hydrazine appears to give the most robust catalyst system showing the highest turnover numbers, although the differences are rather small. More significantly, although (4-$C_6H_4CF_3$)CCMe gave the lowest initial rates relative to other ArCCMe alkynes, the average turnover number at 5 mol% catalyst loading is comparable to (4-$C_6H_4{}^tBu$)CCMe (19 *vs* 18, respectively).

Table 2.2. Maximum turnover numbers for the diamination reaction of internal alkynes with diaryl hydrazines using Ti(N_2N^{Me}){NN(4-$C_6H_4X)_2$}(py) (5 mol%; X = H (**2.1**), ^{t}Bu (**2.12**) and OMe (**2.13**).

(4-$C_6H_4X)_2NNH_2$, X =	(4-C_6H_4X)CCMe, X =				RCCR, R =	
	H	OMe	^{t}Bu	CF_3	4-$C_6H_4CF_3$	Me
H	20	18	19	19	7	8
OMe	20	16	18	18	7	0
^{t}Bu	20	16	18	19	10	0

Reactions carried out at room temperature with 5 mol% catalyst loading, [Ti] = 0.01 mol dm^{-3}, in C_6D_6 (0.6 mL).

Table 2.3. Maximum turnover numbers for the diamination reaction of internal alkynes with diaryl hydrazines using Ti(N_2N^{Me}){NN(4-$C_6H_4X)_2$}(py) (2.5 mol%; X = H (**2.1**), ^{t}Bu (**2.12**) and OMe (**2.13**).

(4-$C_6H_4X)_2NNH_2$, X =	(4-C_6H_4X)CCMe, X = H	^{t}Bu	CF_3
H	36	32	33
OMe	20		
^{t}Bu	33	21	12

Reactions carried out at room temperature with 2.5 mol% catalyst loading, [Ti] = 0.005 mol dm^{-3} in C_6D_6 (0.6 mL).

As discussed, catalyst decomposition arises from protonation of the supporting ligand of the hydrazide catalyst by either the hydrazine substrate or the vinylamine product. To investigate alkyne and hydrazine substituent effects on the rate of catalyst decomposition 1 equiv of hydrazide catalyst Ti(N_2N^{Me})($NNAr_2$)(py) (Ar = Ph (**2.1**), 4-$C_6H_4{}^t$Bu (**2.12**) or C_6H_4OMe (**2.13**)) was mixed with 3 equivs of hydrazine, Ar_2NNH_2, or vinylamine product, $H_2NC(Ar)C(Me)NAr_2$, Scheme 2.8. As described in Section 2.8, at high concentrations, the vinylamine product, **2.1a**, is more poisonous than H_2NNPh_2 with respect to the rate of catalyst decomposition. This is also observed in reactions with **2.12** and **2.13**, for example when Ar = 4-C_6H_4OMe addition of 3 equivs of hydrazine results in *ca.* 53% catalyst decomposition after 24 h. However, in the presence of H_2NC(4-C_6H_4OMe)C(Me)N(4-C_6H_4OMe)$_2$ (**2.13b**) 100% of the catalyst has decomposed within the same time frame. This results in an increase in the rate of catalyst decomposition as the reaction progresses since [vinylamine] *vs* [hydrazine] increases over time.

With respect to the effect of alkyne and hydrazine substituents on the rate of decomposition, it appears that the *p*-C_6H_4OMe substituent is the most damaging, resulting in the maximum amount of catalyst decomposition within 24 h, Scheme 2.8. As a consequence the turnover numbers for reactions with either (4-C_6H_4OMe)CCMe or (4-C_6H_4OMe)$_2NNH_2$ would be reduced compared to 4-$C_6H_4{}^t$Bu and Ph analogues, as observed experimentally, *vide supra*. On average the rate of decomposition appears to increase in the order 4-C_6H_4X, X = H < ^{t}Bu << OMe, also explaining the slightly

lower turnover numbers achieved in reactions with ^{t}Bu substituents compared to the Ph analogues, despite the higher initial rate.

Scheme 2.8. Top: reaction of Ti(N_2N^{Me})($NNAr_2$)(py) (Ar = Ph (**2.1**), 4-$C_6H_4{}^{t}$Bu (**2.12**) or C_6H_4OMe (**2.13**)) with 3 equivs of Ar_2NNH_2. Bottom: reaction of Ti(N_2N^{Me})($NNAr_2$)(py) (Ar = Ph (**2.1**), 4-$C_6H_4{}^{t}$Bu (**2.12**) or C_6H_4OMe (**2.13**)) with 3 equivs of $H_2NC(Ar)C(Me)NAr_2$.

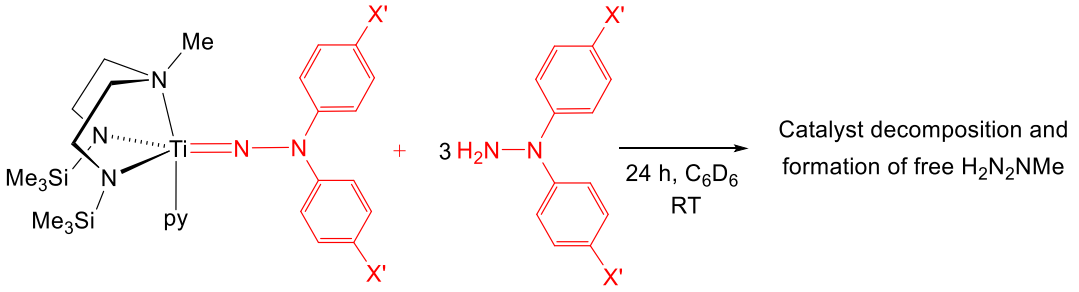

X' = OMe (52%) >> ^{t}Bu (30%) > H (25%)

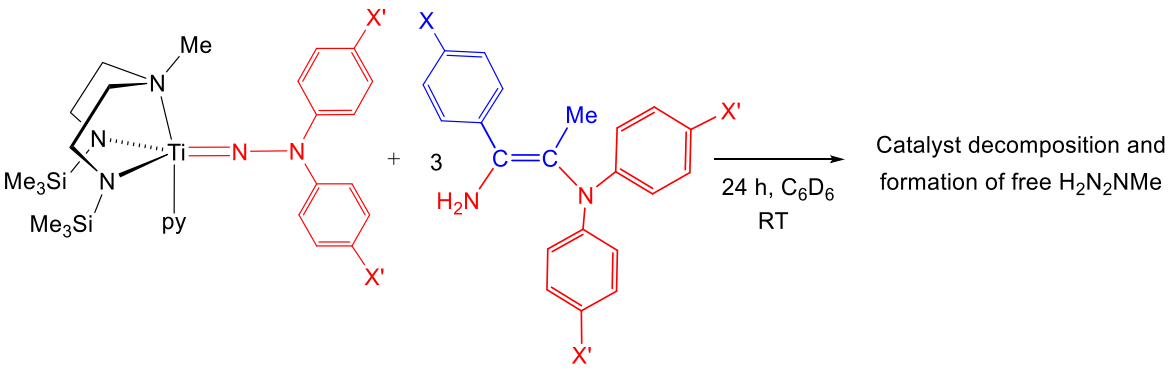

X', X = OMe (100%) >> ^{t}Bu (34%) > H (20%)

2.10 Conclusions

This Chapter has detailed the development of a novel 1,2-diamination reaction between hydrazines and alkynes generating vinylamine products. Three hydrazide complexes, namely Ti(N_2N^{Me})($NNAr_2$)(py) (Ar = Ph (**2.1**), 4-$C_6H_4{}^{t}$Bu (**2.12**) or 4-C_6H_4OMe (**2.13**)) were tested for catalytic activity with a series of alkynes. Unfortunately, under catalytic conditions reaction with MeCCMe only gave the corresponding diamine product, $H_2NC(Me)C(Me)NPh_2$ (**2.1d**), in the case of **2.1**. No significant catalytic reaction was observed between MeCCMe, Ar_2NNH_2 (Ar = 4-$C_6H_4{}^{t}$Bu or 4-C_6H_4OMe) and **2.12** or **2.13** at 5 mol% catalyst loading presumably due to the relatively slow rate of alkyne insertion, a complex protonation reaction and significant catalyst decomposition. The

remaining vinylamine products were isolated in 53 – 98% yields using, on average, 10 mol% catalyst loading.

In order to understand the catalytic cycle it was divided into two separate reactions, insertion of an alkyne into the N_α–N_β bond of the hydrazide complex Ti(N_2N^{Me})($NNAr_2$)(py) giving Ti(N_2N^{Me}){NC(R)C(R)NAr_2}(py) followed by protonolysis of the vinylimide complex by hydrazine producing the vinylamine product. Kinetic studies undertaken on the protonation reaction, as discussed in this Chapter, propose a similar rate law to the one previously reported for the alkyne insertion reaction. The mechanism for protonation of the vinylimide complex Ti(N_2N^{Me}){NC(Ph)C(Me)NPh_2}(py) (**2.2**) therefore follows initial loss of pyridine forming a reactive pyridine-free intermediate, Ti(N_2N^{Me}){NC(Ph)C(Me)NPh_2} (**2.2′**), before the rate-determining step(s) of the reaction. This is consistent with the significantly slower rate observed for Ti(N_2N^{Me}){NC(Ph)C(Me)NPh_2}(DMAP) (**2.10**), the DMAP analogue of **2.2**. The proposed rate law was supported by DFT calculations carried out on the reaction of Ti($N_2{}^{SiH_3}N^{Me}$){NC(Me)C(Me)NMe_2}(py) (**B1**) with Me_2NNH_2. In these calculations proton transfer from the hydrazine to the vinylimide ligand was found to be rate-determining with a calculated energy barrier of 23.4 kcal mol^{-1} to the transition state which lies 19.2 kcal mol^{-1} higher than the starting complex **B1**. This was consistent with the significantly slower reactions with Ph_2NND_2. The calculated activation barrier is similar to that determined for the rate-limiting step in the alkyne insertion reaction ($\Delta G^{\ddagger}$ = 23.4 *vs* 22.0 kcal mol^{-1}) corresponding to N_α–N_β bond cleavage. This agrees with the experimentally determined initial rates of reaction, and with both vinylimide and hydrazide complexes being observed during the catalysis, as effective catalyst resting states. A third effective resting state was found to be a bis(vinylamide) complex, namely Ti(N_2N^{Me}){N(H)C(Ph)C(Me)NPh_2}$_2$ (**2.17**) formed between the vinylimide complex (**2.2**) and the vinylamine product (**2.1a**).

The mechanism for diamination was modelled by DFT using Ti($N_2{}^{SiH_3}N^{Me}$)($NNMe_2$)(py) (**A1**) and compared to the more commonly observed hydrohydrazination reaction pathway. Unlike Cp*Ti($N^{Xyl}N$)($NNPh_2$)(py), modelled by CpTi($N^{Xyl}N$)($NNMe_2$)(py) (**C1**), the activation barrier for protonation of the cycloaddition intermediate Ti(N_2N^{Me}){N(NPh_2)C(Me)C(Ph)}(py) (**A4**) was significantly higher than the activation barrier to N_α–N_β cleavage in the alternative

insertion reaction ($\Delta G^{\ddagger}$ = 20.1 *vs* 28.9/27.8 kcal mol^{-1}), providing an explanation for why, in this case, diamination is favoured over hydrohydrazination.

The rate of catalysis was found to have a 0th order dependence on alkyne and hydrazine but a 1st order dependence on Ti(N_2N^{Me})($NNPh_2$)(py) (**2.1**). Saturation kinetics were indicative of loss of pyridine being the first step in both reactions, which was supported by a significant decrease in the initial rate of catalysis in the presence of 5 (extra added) equivs of pyridine. The kinetic isotope effect of *ca.* 3.6 was in agreement with the stoichiometric reaction and with proton-transfer being the rate-limiting step.

Decomposition of the hydrazide catalyst by hydrazine and vinylamine required the use of the initial rates method to analyse the rate of the various catalyst systems described. The symmetrical alkynes MeCCMe and ArCCAr were the most poorly performing. The electron-withdrawing nature of ArCCMe (Ar = 4-$C_6H_4CF_3$) also gave low initial rates. The dependence on electron-rich aryl alkynes, ArCCMe, Ar = Ph, 4-$C_6H_4{}^tBu$ and 4-C_6H_4OMe was found to increase in the order OMe < H < ^{t}Bu, in contrast to that determined for the alkyne insertion reaction, but consistent with the relative rates of vinylimide protonation. The effect of the different hydrazine substituents, 4-C_6H_4X (X = H, ^{t}Bu and OMe), was divided into two studies. The effect on the rate of insertion of PhCCMe was found to increase in the order H~ ^{t}Bu < OMe, in contrast to the dependence shown by the catalysis. The effect on the rate of protonation however, did model that seen for the catalysis increasing in the order OMe ~ H < ^{t}Bu. This supports the hypothesis that protonation of the vinylimide, compared to alkyne insertion, is turnover-limiting.

The turnover numbers were then analysed. Although ^{t}Bu substituents gave the highest initial rates, they did not give the highest turnover numbers. Indeed, Ph substituents were found to give the most robust catalyst systems. Interestingly, although ArCCMe (Ar = 4-$C_6H_4CF_3$) gave low initial rates of reactions, the turnover numbers were high consistent with electron-withdrawing groups slowing down the rate of ligand protonolysis. The relative rates of catalyst decomposition were then explored with control experiments and found to support these findings.

Further work in this area is primarily focussed on catalyst development, as mentioned briefly in Section 2.8. Currently, work is being carried out on varying the substituents bound to the amide nitrogens on the N_2N^{Me} ligand, primarily in an attempt to reduce or

prevent decomposition of the active catalyst. Interestingly, replacement of $SiMe_3$ with *iso*-propyl substituents led to a dramatic switch in catalyst behaviour from 1,2-diamination of internal alkynes to hydrohydrazination of terminal alkynes, as discussed in Section 1.4.2 of this Thesis.

2.11 References

1. J. D. Selby, C. D. Manley, M. Feliz, A. D. Schwarz, E. Clot and P. Mountford, *Chem. Commun.*, 2007, 4937.
2. A. D. Schofield, A. Nova, J. D. Selby, C. D. Manley, A. D. Schwarz, E. Clot and P. Mountford, *J. Am. Chem. Soc.*, 2010, **132**, 10484.
3. L. R. Collins, Part II Thesis (Honour School of Natural Science), University of Oxford, 2012.
4. T. B. Parsons, N. Hazari, A. R. Cowley, J. C. Green and P. Mountford, *Inorg. Chem.*, 2005, **44**, 8442.
5. J. D. Selby, C. D. Manley, A. D. Schwarz, E. Clot and P. Mountford, *Organometallics*, 2008, **27**, 6479.
6. A. D. Schofield, D.Phil. Thesis, University of Oxford, 2012.
7. N. Vujkovic, B. D. Ward, A. Maisse-Francois, H. Wadepohl, P. Mountford and L. H. Gade, *Organometallics*, 2007, **26**, 5522.
8. A. D. Schwarz, C. S. Onn and P. Mountford, *Angew. Chem. Int. Ed.*, 2012, **51**, 12298.
9. Y. Li, Y. Shi and A. L. Odom, *J. Am. Chem. Soc.*, 2004, **126**, 1794.
10. J. S. Johnson and R. G. Bergman, *J. Am. Chem. Soc.*, 2001, **123**, 2923.
11. C. Cao, Y. Shi and A. L. Odom, *Org. Lett.*, 2002, **4**, 2853.
12. L. Ackermann and R. Born, *Tet. Letts.*, 2004, **45**, 9541.
13. V. Khedkar, A. Tillack, M. Michalik and M. Beller, *Tet. Letts.*, 2004, **45**, 3123.
14. S. Banerjee, Y. Shi, C. Cao and A. L. Odom, *J. Organomet. Chem.*, 2005, **690**, 5066.
15. S. Banerjee, E. Barnea and A. L. Odom, *Organometallics*, 2008, **27**, 1005.
16. K. Weitershaus, H. Wadepohl and L. H. Gade, *Organometallics*, 2009, **28**, 3381.
17. J. D. Selby, C. Schulten, A. D. Schwarz, A. Stasch, E. Clot, C. Jones and P. Mountford, *Chem.Commun.*, 2008, 5101.
18. L. C. Stevenson and P. Mountford, *Unpublished results*, 2013.

19. N. Adams, H. R. Bigmore, T. L. Blundell, C. L. Boyd, S. R. Dubberley, A. J. Sealey, A. R. Cowley, M. E. G. Skinner and P. Mountford, *Inorg. Chem.*, 2005, **44**, 2882.
20. N. Adams, A. R. Cowley, S. R. Dubberley, A. J. Sealey, M. E. G. Skinner and P. Mountford, *Chem. Commun.*, 2001, 2738.
21. A. D. Schwarz, O. Masataka and P. Mountford, *Unpublished results*, 2013.

Chapter Three

Synthesis and reactions of a cyclopentadienyl-amidinate titanium *tert*-butoxyimido compound

3.1 Introduction

As discussed in Chapter One, Group 4 alkyl and aryl imido complexes (L)M=NR (M = Group 4 metal, R = alkyl or aryl) have been studied in considerable depth over the past 20 years.[1-7] Much of this work has centered on the wide range of stoichiometric reactions that the polar M=N multiple bond (formally a $\sigma^2\pi^4$ triple bond in most instances[5, 8-14,15]) undergoes with both saturated and unsaturated substrates. Catalytic applications of these complexes usually involve the imido group as the reactive site, most notably in alkene, allene and alkyne hydroamination.[16-19] Alongside this chemistry, and building on initial reports by Wiberg[20] and Bergman,[21] the related terminal dialkyl or diaryl hydrazido(2-) complexes (L)M=N–NR_2 (R = alkyl or aryl) have increasingly been studied in terms of synthesis and reactivity for M = Ti[22-45] and Zr[46-60] in particular. Terminal alkylidene hydrazido complexes of titanium, (L)Ti=NNCRR′ (R, R′ = hydrocarbyl or H) – which can alternatively be viewed as highly reduced diazoalkane species – have also been reported and studied for their reactions with H_2, silanes and unsaturated polar and non-polar substrates.[61-66] Investigations of the bonding in Group 4 dialkyl, diaryl and alkylidene hydrazido complexes have accompanied the synthetic, structural and reactivity studies.[26, 28, 32, 40, 47, 67] Like their imido analogues, Group 4 hydrazido complexes undergo a range of reactions at the M=N_α bond, undergoing cycloaddition, cycloaddition-insertion, cycloaddition-elimination and NNR_2 group transfer with unsaturated substrates,[22, 27, 29, 33-35, 37-39, 42, 43, 51, 53] and also 1,2-addition of Si–H or Si–Cl bonds.[41, 44] In addition, both N_α–N_β bond reductive cleavage or insertion reactions with oxidisable substrates such as CO,[21] isonitriles[39, 46] and alkynes (as illustrated in Chapter Two)[29, 37, 58, 68] are also becoming established for these complexes (in contrast to the situation for their Group 5 or 6 analogues which show no such reactivity with unsaturated substrates).[69-72]

As described in Section 1.6, this unusual and interesting chemistry prompted work in our group on developing synthetic methodologies for the hitherto unknown titanium alkoxyimido complexes, (L)Ti=NOR,[73, 74] with the hope of accessing both new Ti=N_α multiple bond chemistry as well as N_α–O_β bond reactivity. For example, the mechanism[37, 54, 58] of alkyne insertion into the N_α–N_β of certain titanium and zirconium hydrazides is related to that for (reductive) cleavage of the peroxide ligand O_α–O_β bond in $Cp^*_2Hf(R)(OO^tBu)$ to form $Cp^*_2Hf(OR)(O^tBu)$ (R = H or alkyl).[75] However,

although transition metal imido and hydrazido compounds have been extensively studied across the transition metal series, the corresponding alkoxyimides remain poorly explored, both in terms of synthesis and bonding, and also with respect to the reactivity of such complexes.

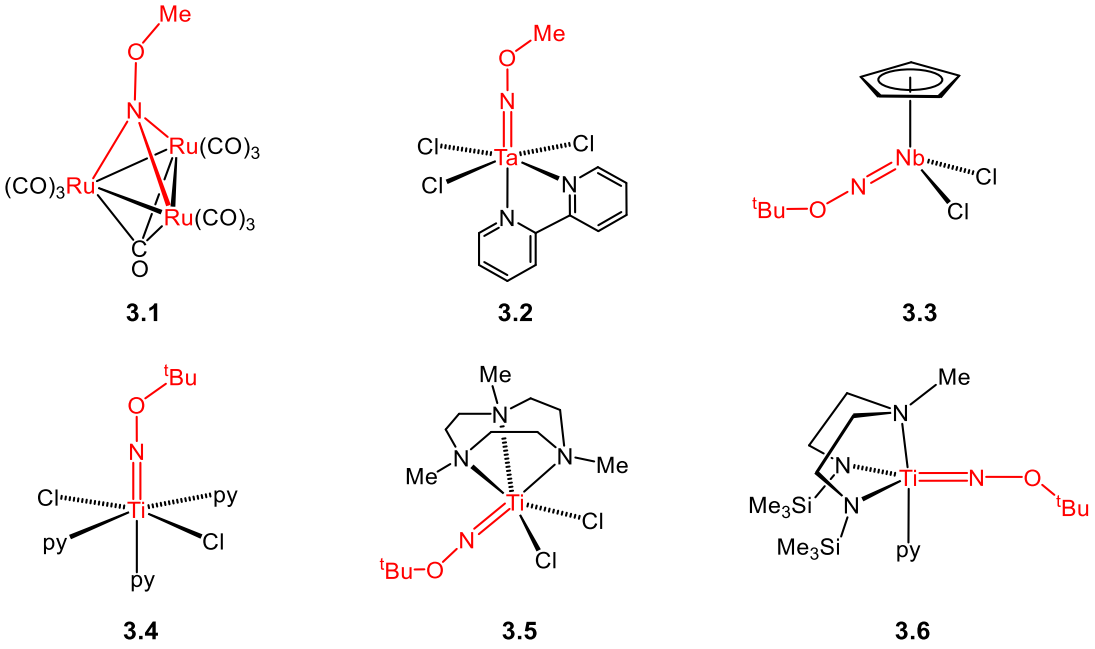

Figure 3.1. Selected examples of transition metal alkoxyimido complexes.[73, 74, 76-78]

The first alkoxyimido complex was reported in the early 1980s, namely the trimetallic ruthenium structure $Ru_3(CO)_{10}(NOMe)$ (**3.1**, Fig. 3.1),[76] followed a few years later by the monomeric $Ta(NOMe)Cl_3(bipy)$ (**3.2**, Fig. 3.1)[77] and half-sandwich Group 5 (e.g. **3.3**, Fig. 3.1) and 6 complexes.[77-81] Our group, as detailed in Chapter One of this Thesis, recently reported the syntheses and electronic structures of the first Group 4 alkoxyimido complexes (e.g. **3.4** – **3.6**, Fig. 3.1) along with a preliminary example of their reactivity with alkynes (*vide infra*).[73, 74] Rational synthetic routes to terminal alkoxyimido complexes have so far included methylation of metal nitroso compounds,[76, 82] de-hydrohalogenation of metal chloride compounds[77, 78] or protonolysis of metal amide compounds.[73, 74] Crystallographic studies and DFT calculations suggest that like hydrazides and imides, the alkoxyimido ligand is a 4-electron donor with a formal charge of -2, capable of bonding to transition metals through one σ- and two π-bonds.[73, 74]

To date, the reactivity of alkoxyimido complexes is very limited. Reaction of **3.1** with certain alkynes formed $Ru_3(CO)_9(\mu_3\text{-NOMe})(\mu_3\text{-}\eta^2\text{-RCCPh})$ (R = H or Ph),[83] whilst

heating at 90 °C in toluene resulted in N–O bond cleavage giving the corresponding nitrene $Ru_3(CO)_9(OMe)(N)$.[84] Hydrogenation of **3.1** in the presence of $Ru_3(CO)_{12}$ generated a mixture of species including $Ru_5(\mu\text{-}H)_3(CO)_{13}(\mu_4\text{-}NH)(\mu_3\text{-}OMe)$ also following reductive N–O bond cleavage.[84] Furthermore, transmetallation of **3.1** using $CpMo(CO)_3H$ led to the mixed Ru/Mo trimetallic structures $Ru_2Mo(\mu\text{-}H)(CO)_8(Cp)(\mu_3\text{-}NOMe)$ and $Ru_2Mo(\mu\text{-}H)(CO)_8(Cp)(\mu_3\text{-}NH)$.[81]

Reaction of $Ti(NO^tBu)Cl_2(NHMe_2)_2$ or $Ti(NO^tBu)Cl_2(py)_3$ (**3.4**, Fig. 3.1) with neutral tridentate or lithiated anionic nitrogen based ligand sets yielded a range of Group 4 alkoxyimido complexes, for instance $Ti(NO^tBu)(Me_3[9]aneN_3)Cl_2$ (**3.5**, Fig. 3.1, $Me_3[9]aneN_3$ = trimethyl-1,4,7-triazacyclononane) and $Ti(N_2N^{Me})(NO^tBu)(py)$ (**3.6**, Fig. 3.1, N_2N^{Me} = $MeN(CH_2CH_2NSiMe_3)_2$).[73, 74] However, as yet only one reaction involving a titanium alkoxyimide ligand has been reported, namely the reaction of PhCCMe and **3.6** resulting in **3.7** (Fig. 3.2) *via* reductive cleavage of the N_α–O_β bond and formation of two new N–C bonds.[73] This is in contrast to the corresponding reaction of PhCCMe with the hydrazide analogue $Ti(N_2N^{Me})(NNPh_2)(py)$ (**3.8**), as explored in Chapter Two, which also gives initial Ti=N cycloaddition but ultimately yields the vinylimido product $Ti(N_2N^{Me})\{NC(Ph)C(Me)NPh_2\}(py)$ (**3.9**, Fig. 3.2).[29, 37]

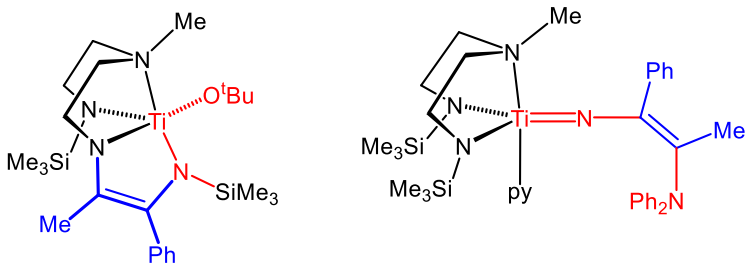

3.7 **3.9**

Figure 3.2. Reaction products following reaction of $Ti(N_2N^{Me})(NX)(py)$ (X = O^tBu (**3.6**) or NPh_2 (**3.8**)) with PhCCMe. [29, 37, 73] The fragments derived from the Ti=NX and alkyne moieties are shown in red and blue, respectively.

As illustrated in Sections 1.4 and 1.5, the cyclopentadienyl-amidinate supporting ligand set, together with related ones,[34, 35, 45, 85] has proved a robust and flexible platform for studying and comparing the reactivity of imido and dimethyl and diphenyl and alkylidene hydrazido compounds of the type $Cp^*Ti\{MeC(N^iPr)_2\}(N^tBu)$ (**3.10**), $Cp^*Ti\{MeC(N^iPr)_2\}(NAr)$ (Ar = Tol (**3.11a**) or Xyl (**3.11b**, Xyl = 2,6-$C_6H_3Me_2$)),[86-90] $Cp^*Ti\{MeC(N^iPr)_2\}(NNR_2)$ (R = Ph (**3.12**) or Me (**3.13**))[29, 38, 41, 42, 44] and

Cp*Ti{MeC(N^{i}Pr)$_2$}(NNCPh$_2$) (**3.14**).[66] This Chapter will report the first imide/alkoxyamine exchange strategy for the synthesis of a cyclopentadienyl-amidinate supported terminal alkoxyimido complex and report on its reactivity with (un)saturated molecules including CS_2, isocyanates, aldehydes, ketones, nitriles, Ar^{F5}CCH and B(Ar^{F5})$_3$. DFT calculations described in this Chapter were performed by our collaborators (Dr Eric Clot and Dr Ainara Nova) at Université Montpellier. The work has been published in full.[91]

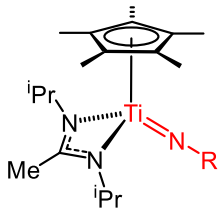

R = ^{t}Bu (**3.10**) or Ar (**3.11**)

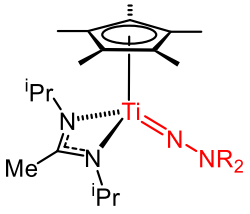

R = Ph (**3.12**) or Me (**3.13**)

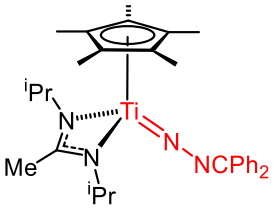

3.14

3.2 Synthesis and bonding analysis of cyclopentadienyl-amidinate alkoxyimido compounds

Previously, it was found that stable monomeric titanium alkoxyimido compounds were only accessible using the bulky *tert*-butoxy group.[74] Therefore, the work described in this Chapter has focussed exclusively on this substituent. The cyclopentadienyl-amidinate supported complexes Cp*Ti{MeC(N^{i}Pr)$_2$}(NAr) (**3.11**),[89] Cp*Ti{MeC(N^{i}Pr)$_2$}(NNR$_2$) (R = Ph (**3.12**) or Me (**3.13**))[42] and Cp*Ti{MeC(N^{i}Pr)$_2$}(NNCPh$_2$) (**3.14**)[66] can be synthesised from the readily-prepared Cp*Ti{MeC(N^{i}Pr)$_2$}(N^{t}Bu) (**3.10**)[89] *via tert*-butylimide-arylamine/hydrazine exchange reactions. Consequently, this strategy was also employed to make the corresponding alkoxyimido complex Cp*Ti{MeC(N^{i}Pr)$_2$}(NO^{t}Bu) (**1**) from **3.10** and ^{t}BuONH$_2$, itself conveniently prepared in multigram quantities.[92] Compound **1** was isolated as a dark green viscous oil in effectively quantitative yield (Eq 3.1).

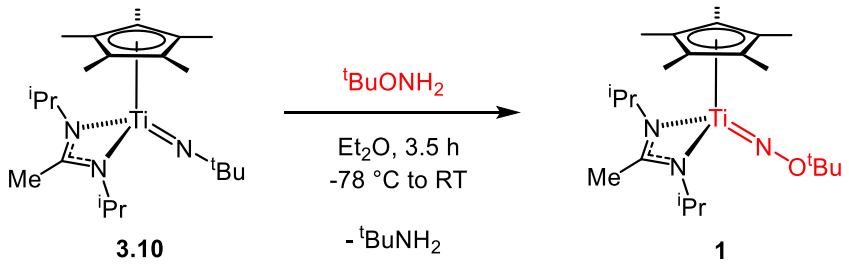

Equation 3.1

Although **1** could be obtained in analytically pure form, difficulty in handling prompted us to develop a more crystalline derivative. Alternative amidinate ligand precursors, Li[PhC(N^{i}Pr)$_2$] (**3.15**),[93] Li[MeC(NTol)$_2$][94] and Li[^{t}BuC(N^{i}Pr)$_2$][94] were prepared by nucleophilic addition to the corresponding carbodiimide and subsequently reacted with Cp*Ti(N^{t}Bu)Cl(py) (**3.16**)[95] by analogy with the synthesis of **3.10**[89] and certain analogues.[88, 89] The reactions with Li[MeC(NTol)$_2$] and Li[^{t}BuC(N^{i}Pr)$_2$] proved unsuccessful, the latter being consistent with previous results regarding the synthesis of aluminium amidinate complexes where steric constraints prevented ligand complexation.[94] However, in the case of **3.15**, heating at 60 °C for 18 h in benzene afforded Cp*Ti{PhC(N^{i}Pr)$_2$}(N^{t}Bu) (**2**, Scheme 3.1) as a dark red oil in near-quantitative yield. Subsequent *tert*-butylimide/*tert*-butoxyamine exchange between **2** and ^{t}BuONH$_2$ yielded Cp*Ti{PhC(N^{i}Pr)$_2$}(NO^{t}Bu) (**3**, Scheme 3.1), again in quantitative yield when followed by ^{1}H NMR spectroscopy. Larger scale reactions afforded **3** as a fine green powder in multigram quantities and 70% isolated yield. This is the first example of an alkoxyimide synthesis utilising an alkylimide/alkoxyamine ligand exchange methodology.

Scheme 3.1. Synthesis of Cp*Ti{PhC(N^{i}Pr)$_2$}(NO^{t}Bu) (**3**) starting from Li[PhC(N^{i}Pr)$_2$] (**3.15**) and Cp*Ti(N^{t}Bu)Cl(py) (**3.16**).

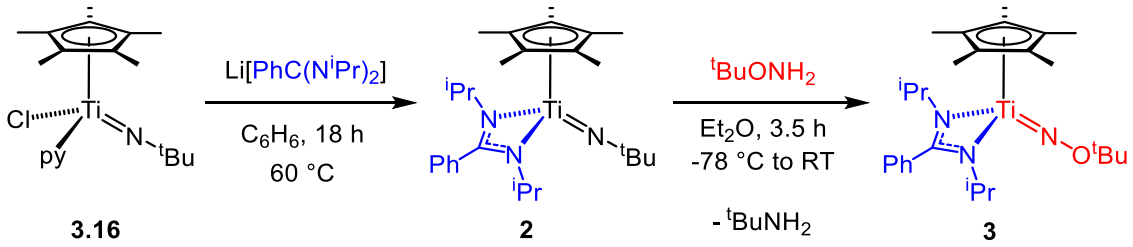

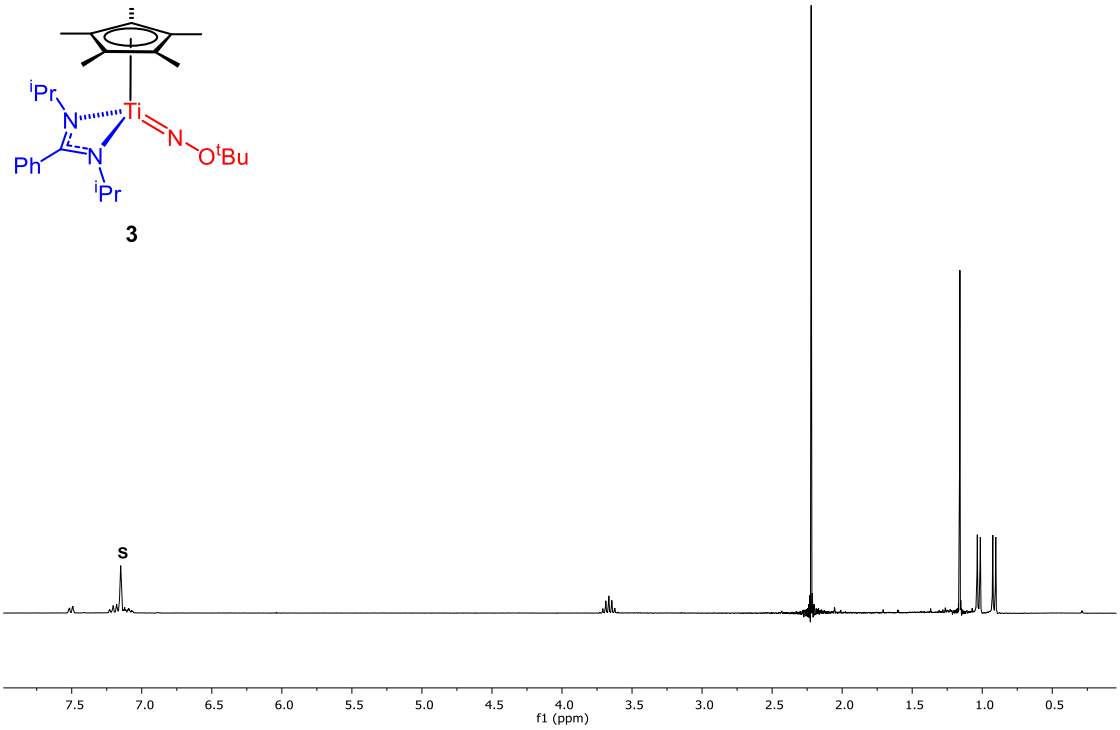

Figure 3.3. ^{1}H NMR spectrum (299.9 MHz, 293 K) of Cp*Ti{PhC(N^{i}Pr)$_2$}(NO^{t}Bu) (**3**) in C_6D_6 ("s" denotes residual protio-solvent).

The ^{1}H NMR spectrum of **3**, given in Fig. 3.3, is consistent with a C_s symmetric species. Alongside Cp* and *tert*-butyl signals, the resonances assigned to the *iso*-propyl substituents are observed as a single septet and one pair of doublets. The molecular structure of **3**, determined by X-ray crystallography, is shown in Fig. 3.4 and selected bond lengths and angles are listed in Table 3.1. Compound **3** possesses a 3-legged piano stool geometry around titanium with η^5-C_5Me_5, κ^2*N*,*N*′-PhC(N^{i}Pr)$_2$ and η^1-NO^{t}Bu ligands. The bond lengths and angles associated with the Cp*Ti{PhC(N^{i}Pr)$_2$} fragment are similar to those found for the xylylimido and hydrazido homologues **3.11b**,[89] **3.12**, **3.13**[42] and **3.14**[66] and for cyclopentadienyl and amidinate complexes of titanium(+4) in general.[96] The metric parameters associated with the Ti=NO^{t}Bu group are similar to those for the previously reported titanium *tert*-butoxyimides.[73, 74] The short average Ti(1)-N(1) distance of 1.713(2) Å lies within the expected range for titanium *tert*-butoxyimides (range 1.686(2) – 1.734(2) Å) and, together with the near linear Ti=N–O average angle of 162.9(2) °, indicates substantial Ti=N$_\alpha$ multiple bond character as expected. The Ti(1)–N(1) bond distance is comparable within error to that of the dimethylhydrazide **3.13** (1.723(2) Å) but significantly shorter than for the xylylimido and diphenyl and alkylidene hydrazido compounds **3.11b**, **3.12** and **3.14** (1.738(2), 1.734(2) and 1.751(2) Å, respectively). The average N(1)–O(1) bond distance (1.379(3)

Å) is indicative of a single bond,[97] and the average N(1)–O(1)–C(1) angle of 112.8(2) ° is consistent with the bent geometry found for (L)M=N–OR linkages in general.[96] In the previous studies[73, 74] of *tert*-butoxyimido compounds the Ti=N$_\alpha$ distances were generally intermediate between those in the homologous alkylimido and phenylimido analogues, and shorter than in the diphenylhydrazido counterparts. Although a crystallographically characterised alkylimido analogue is not available for comparison, the experimental data for **3** in comparison with **3.11b**, **3.12**, **3.13** and **3.14** appears consistent with these trends.

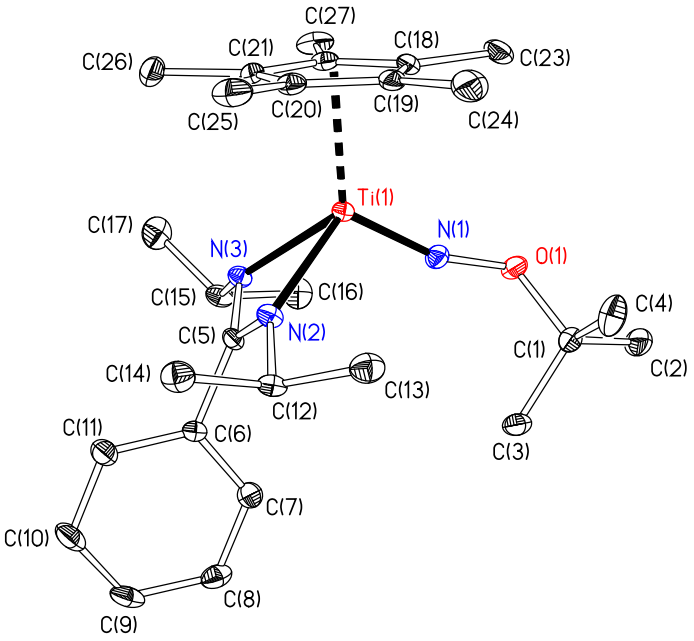

Figure 3.4. Displacement ellipsoid plot (20% probability) of Cp*Ti{PhC(N^{i}Pr)$_2$}(NO^{t}Bu) (**3**). H atoms omitted for clarity.

Table 3.1. Selected bond lengths (Å) and angles (˚) for Cp*Ti{PhC(N^iPr)$_2$}(NO^tBu) (**3**). Cp_{cent} is the computed centroid for the Cp* ring carbons. Values in brackets are for the other crystallographically independent molecule.

Ti(1)-Cp_{cent}	2.054 [2.048]	Cp_{cent}-Ti(1)-N(1)	122.02 [120.97]
Ti(1)-N(1)	1.709(3) [1.716(3)]	Cp_{cent}-Ti(1)-N(2)	122.46 [122.26]
Ti(1)-N(2)	2.114(3) [2.131(3)]	Cp_{cent}-Ti(1)-N(3)	120.85 [120.95]
Ti(1)-N(3)	2.121(3) [2.119(3)]	N(2)-Ti(1)-N(3)	64.02(12) [63.99(12)]
N(1)-O(1)	1.381(4) [1.377(4)]	Ti(1)-N(1)-O(2)	163.8(3) [161.9(3)]
O(1)-C(1)	1.460(5) [1.456(5)]	N(1)-O(1)-C(1)	113.1(3) [112.4(3)]

A number of computational studies into the bonding of Group 4 imido and hydrazido complexes have previously been carried out, and the electronic structure of the M=NR and M=NNR_2 (R = alkyl or aryl) moieties is well understood.[8-14, 26, 28, 32, 40, 47, 67] So far, however, there has been only one computational study of any alkoxyimido complex (mentioned in Section 1.6, Chapter One). This focussed on the model compound Ti(NOMe)Cl_2($NHMe_2$)$_2$ (an analogue of the real compound possessing a Ti=NO^tBu group), in comparison with the imido and hydrazido systems Ti(NR)Cl_2($NHMe_2$)$_2$ (R = Me, Ph, NMe_2).[74] To gain further understanding into the bonding of alkoxyimido complexes, DFT calculations were carried out on the model system CpTi{MeC($NMe)_2$}(NOMe) (**1Q_OMe**) using the B3PW91 functional. The geometry, key orbital representations and associated energies are shown in Figure 3.5. Comparative DFT calculations have previously been carried out on the imido and hydrazido homologues CpTi{MeC($NMe)_2$}(NR) (R = Me (**1Q_Me**), Ph (**1Q_Ph**), NMe_2 (**1Q_NMe_2**, pyramidal N_β) and NPh_2 (**1Q_NPh_2**, planar N_β).[42] Additional details for these model complexes can be found in the Appendix (Fig. A1a,b). The DFT calculations predict Ti=NR bond lengths in the order Ti=N–Me (1.688 Å) < Ti=N–OMe (1.698 Å) < Ti=N–NMe_2 (1.705 Å) < Ti=N–Ph (1.709 Å) < Ti=N–NPh_2 (1.713 Å) consistent with the experimental and previous computational results described above.[74]

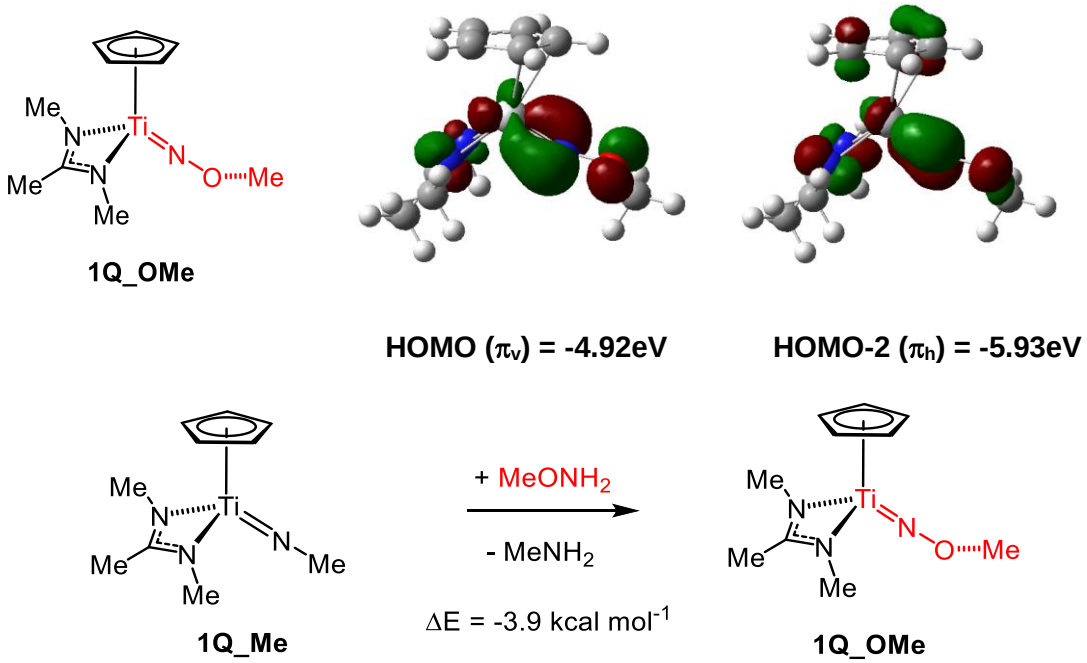

Figure 3.5. Top: DFT model compound CpTi{MeC(NMe)$_2$}(NOMe) (**1Q_OMe**) and associated isosurfaces and energies of the HOMO (π_v) and HOMO-2 (π_h). Bottom: DFT computed isodesmic reaction between **1Q_Me** and MeONH$_2$ (electronic energy).

All of the complexes have formal Ti≡N$_\alpha$ triple bonds containing two orthogonal 3d$_\pi$-2p$_\pi$ interactions (denoted π_v and π_h) with a predominantly ligand-based, out-of-phase 2p AO combination from the nitrogen atoms of the amidinate ligand being either the HOMO-1 or HOMO (for **1Q_Me**). This latter MO can mix with π_h under the approximate *C*$_s$ symmetry of CpTi{MeC(NMe)$_2$}(NR). Because of this mixing effect and the orientation of the –Ph,–NMe$_2$ and –NPh$_2$ substituents (*vide infra*) the energy of π_h is relatively insensitive to the N$_\alpha$ substituents and varies non-systematically between the complexes. However, the energy of π_v is very dependent on the N$_\alpha$ substituent. As described previously,[42] in the case of the –NR$_2$ groups (**1Q_NMe2** and **1Q_NPh2**) the N$_\beta$ lone pair (LP) destabilises π_v through an antibonding interaction (the energy of π_v in these complexes is -4.30 and -4.24 eV, respectively, *cf*. -5.47 eV in the benchmark model **1Q_Me**). Likewise, in **1Q_Ph**, interaction of one of the filled –Ph ring π-MOs with π_v is also destabilising (energy of π_v = -4.98eV). As can be seen in Fig 3.5, the –OMe substituent of **1Q_OMe** possesses an approximately pure 2p lone pair due to the formal *sp*^{2} hybridisation at O. This LP is oriented (dihedral angle Cp$_{cent}$-Ti···O-R = 130.0 ^{o} in **1Q_OMe** *cf*. 125.2 in the real compound **3**) such that it can interact, in an antibonding way, with both π_h and π_v which results in a π_v energy of -4.92 eV. The

destabilising effect is thus comparable to that found in **1Q_Ph**, but less than in the hydrazido analogues **1Q_NR$_2$**. This trend is analogous to that found in the model compounds Ti(NR)Cl$_2$(NHMe$_2$)$_2$ (R = OMe, Me, Ph, NMe$_2$).[74]

The trends in experimental and computed Ti=NR bond distances can also be accounted for by the nature of the R-substituent. As noted previously,[42] a second-order NBO (natural bond orbital) perturbation analysis[98] of **1Q_NR$_2$** (R = Me (pyramidal N$_\beta$) or Ph (planar N$_\beta$)) found significant donation (19.2 and 26.1 kcal mol^{-1}, respectively) from the –NR$_2$ LP into the Ti=N$_\alpha$ π^*_v NBO, thus lengthening the Ti=N$_\alpha$ bond. In the case of **1Q_Ph** a smaller interaction between a filled ring π orbital and π^*_v (12.1 kcal mol^{-1}) was accompanied by competition from a Ph ring π^* acceptor orbital for the –NPh 2p AO (as indicated by an interaction energy of 26.2 kcal mol^{-1} between π_v and a Ph ring π^* NBO). This combination of "push-pull" effects accounts for the longer M=NR bonds found in general for arylimido compounds compared to their alkylimido counterparts.[96, 99] In **1Q_OMe** the NBO analysis found donation from the oxygen LP into both π^*_v and π^*_h (interaction energy 8.7 and 9.7 kcal mol^{-1}, respectively) as a consequence of the orientation of the –OMe group. The net interaction energy of 18.4 kcal mol^{-1} is comparable to that for **1Q_NMe$_2$** for the Ti=N$_\alpha$ π^* orbital alone, and consistent with the experimental and computational similarity of the (L)Ti=NOR and (L)Ti=NNMe$_2$ bond distances, and the lengthening of the (L)Ti=NOR bond compared to (L)Ti=NR (R = ^{t}Bu or Me) in both cases.

Figure 3.5 also shows the DFT computed reaction of **1Q_Me** and MeONH$_2$ forming **1Q_OMe** and MeNH$_2$. The ΔE value of -3.9 kcal mol^{-1} is comparable to those for the corresponding processes for PhNH$_2$, Ph$_2$NNH$_2$ and Me$_2$NNH$_2$ (ΔE = -2.5, -5.1, -4.0 kcal mol^{-1}, respectively),[42] consistent with experiment where the *tert*-butylimido/amine or hydrazine exchange reactions of Cp*Ti{RC(N^{i}Pr)$_2$}(N^{t}Bu) (R = Me (**3.10**) or Ph (**2**)) are all quantitative.

3.3 Reactions with heterocumulenes

As mentioned, the reaction chemistry of alkoxyimido compounds in general is virtually unexplored and so one aim of this Thesis is to develop their reactions with a range of unsaturated substrates. Group 4 imido and hydrazido complexes typically undergo [2+2] cycloaddition reactions with heterocumulenes such as CO_2, isocyanates and their heavier congeners. Further reactions such as retro-cyclisation and extrusion of a new organic species, or insertion of a second molecule of substrate into the first-formed metallacycles have all been observed.[1-6, 22, 27, 29, 33-35, 37-39, 42, 43, 51, 53] The most relevant systems for comparison with **3** are clearly the homologous cyclopentadienyl-amidinate systems Cp*Ti{MeC(N^{i}Pr)$_2$}(NR) (R = ^{t}Bu (**3.10**), aryl (**3.11**), NPh_2 (**3.12**), NMe_2 (**3.13**) and $NCPh_2$ (**3.14**)) which have been studied in considerable detail previously.[29, 38, 41, 42, 44, 66, 86-90]

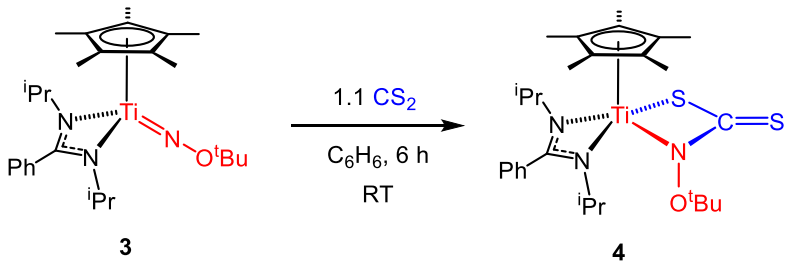

3 **4**

Equation 3.2

When the reaction of **3** with CO_2 (*ca.* 1.1 atm. pressure) was followed by ^{1}H NMR spectroscopy in C_6D_6 at room temperature, mixtures from which no single products could be identified were observed. In contrast, addition of 1 or more equivs of CS_2 to a benzene solution of **3** resulted in a single apparently C_s symmetric product **4** according to ^{1}H NMR spectroscopy at room temperature. However, on cooling a sample to -50 °C in toluene-d_8 the PhC(N^{i}Pr)$_2$ ligand *iso*-propyl resonances decoalesced into 4 doublets (diastereotopic CH$\underline{\text{Me}}_2$) and two overlapping septets (C$\underline{\text{H}}$Me$_2$), Fig. 3.6, consistent with the C_1 symmetric thiocarbamate-type [2+2] cycloaddition product Cp*Ti{PhC(N^{i}Pr)$_2$}{SC(S)N(O^{t}Bu)} (**4**, Eq 3.2, Fig. 3.6).

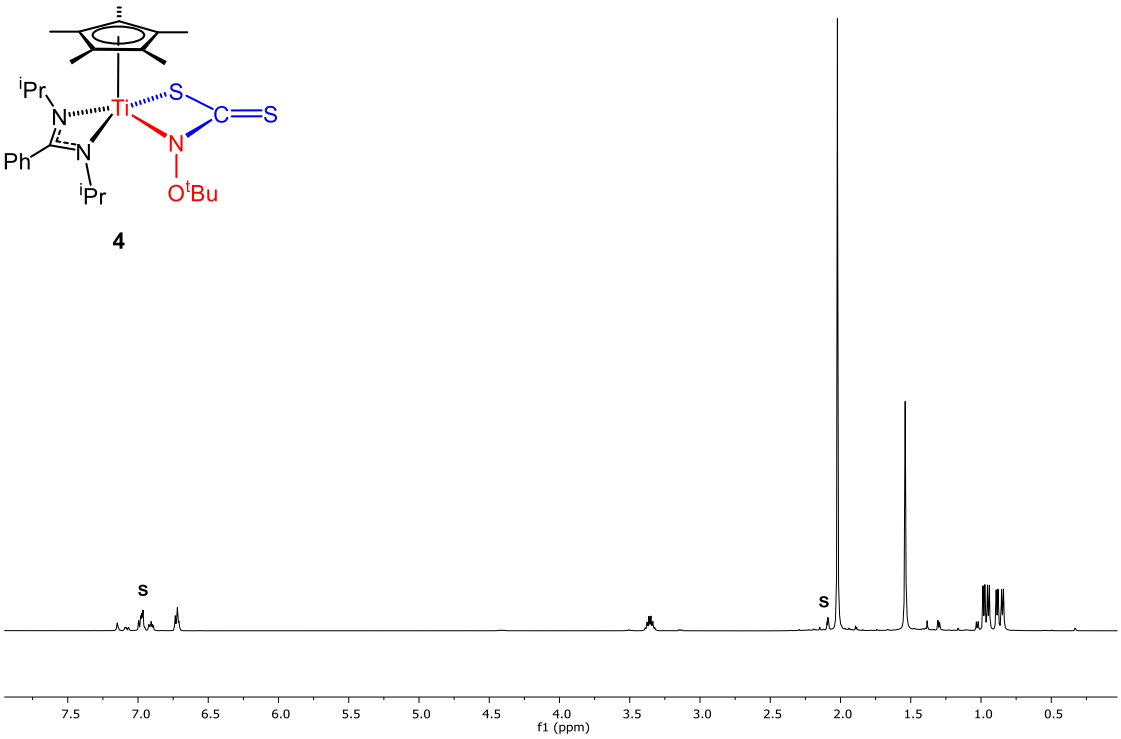

Figure 3.6. ^{1}H NMR spectrum (499.9 MHz, 223 K) of Cp*Ti{PhC(N^{i}Pr)$_2$}{SC(S)N(O^{t}Bu)} (**4**) in toluene-d_8 ("s" denotes residual protio-solvent).

The ^{13}C NMR spectrum at -50 °C revealed a SCS resonance at δ 148.1 ppm, analogous to the hydrazido cycloaddition products Cp*Ti{MeC(N^{i}Pr)$_2$}{N(R)C(S)S} (R = NMe$_2$, NPh$_2$ or NNCPh$_2$, *ca.* δ 150 – 160 ppm).[42, 66] Compound **4** was isolated in 65% yield and characterised by elemental analysis, ^{1}H and ^{13}C NMR and IR spectroscopy. No further reaction with CS$_2$ was observed at room temperature. Like the hydrazide-derived products, **4** is stable in solution for days although heating at 70 °C for up to a week generated unknown mixtures. This is in contrast to the arylimido counterparts Cp*Ti{MeC(N^{i}Pr)$_2$}{N(Ar)C(S)S} (Ar = Xyl or Tol) which extrude the corresponding isothiocyanate, ArNCS, forming the sulfido-bridged dimer [Cp*Ti{MeC(N^{i}Pr)$_2$}(μ-S)]$_2$.[89]

The reactions of **3** with the representative isocyanates Ar′NCO, TolNCO and ^{t}BuNCO (Ar′ = 2,6-C$_6$H$_3$^{i}Pr$_2$) are summarised in Scheme 3.2 and discussed below. No reaction was observed between **3** and the isothiocyanate Ar′NCS at room temperature, while heating at 60 °C gave complex mixtures. Reaction with TolNCS (1 or 2 equivs) also resulted in unknown mixtures and so reactions with isothiocyanates were not pursued further.

Scheme 3.2. Reactions of Cp*Ti{PhC(N^{i}Pr)$_2$}(NO^{t}Bu) (**3**) with isocyanates (Ar′ = 2,6-C$_6$H$_3$^{i}Pr$_2$).

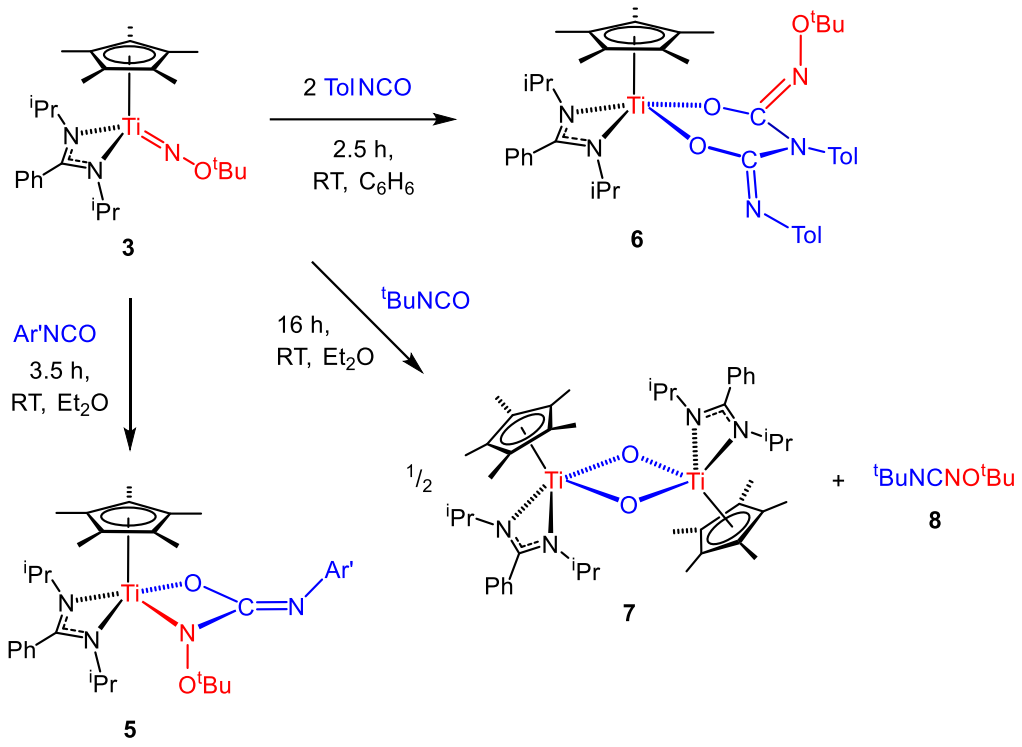

Reaction with the bulkier Ar′NCO formed the cycloaddition product Cp*Ti{PhC(N^{i}Pr)$_2$}{OC(NAr′)N(O^{t}Bu)} (**5**) within 90 min at room temperature. The compound was isolated in 40% yield and no further reaction was observed. Although **5** could not be structurally authenticated, the ^{1}H NMR spectrum of **5** in toluene-d_8 at -30 °C is indicative of C_1 symmetry and a ROESY NMR experiment was consistent with the κ^2*N*,*O*-coordination mode shown in Scheme 3.2. The IR spectrum shows a *ν*(C=N) band at 1631 cm^{-1} which compares well with a number of imido and hydrazido derived analogues of the type Cp*Ti{MeC(N^{i}Pr)$_2$}{N(R)C(NAr′)O} (R = aryl, NPh$_2$, NCPh$_2$) (*ν*(C=N) in the range 1609 – 1622 cm^{-1}).[42, 66, 89] Like these previous arylimido and hydrazido products, **5** was stable to carbodiimide (Ar′NCNO^{t}Bu) elimination, although unknown decomposition species were observed by ^{1}H NMR spectroscopy over 2 d in C$_6$D$_6$.

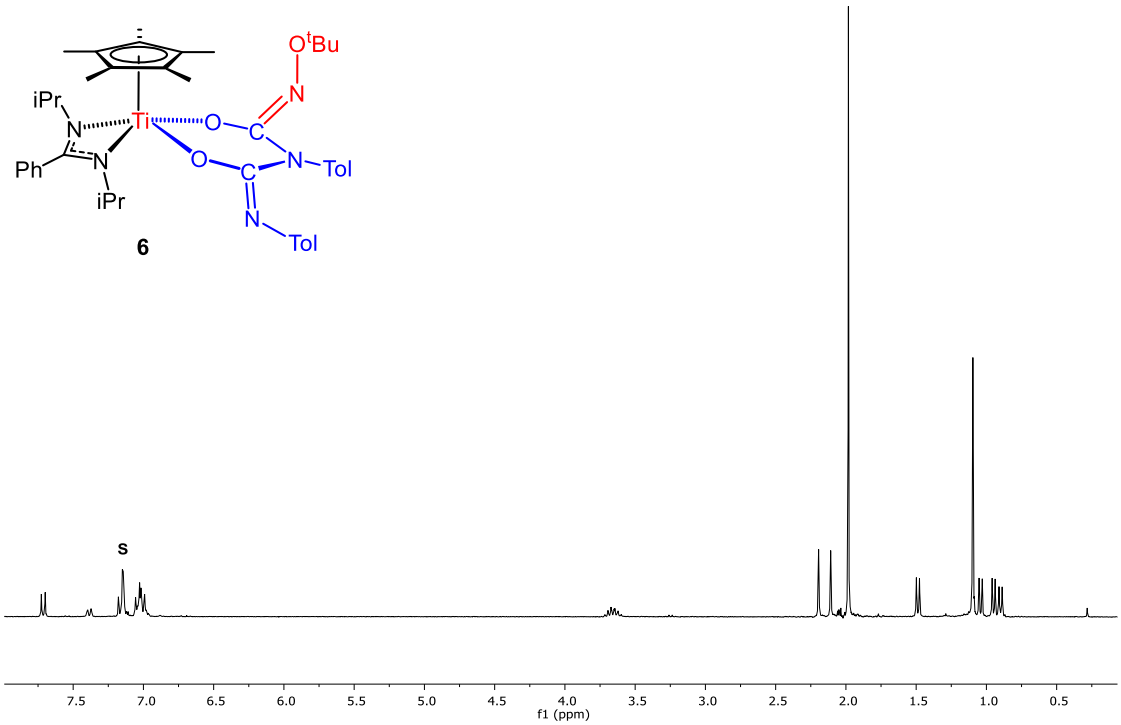

Figure 3.7. ^{1}H NMR spectrum (299.9 MHz, 293 K) of Cp*Ti{PhC(N^{i}Pr)$_2$}-{OC(NTol)N(Tol)C(NO^{t}Bu)O} (**6**) in C_6D_6 ("s" denotes residual protio-solvent).

When followed on the NMR tube scale, the reaction between **3** and 1 equiv of TolNCO gave unknown mixtures. However, upon reaction with 2 equivs TolNCO, one major product (**6**) was formed within 30 min, which was isolated in 60% yield on scale up. Compound **6** was identified by NMR spectroscopy and X-ray crystallography as the "double-insertion" compound Cp*Ti{PhC(N^{i}Pr)$_2$}-{OC(NTol)N(Tol)C(NO^{t}Bu)O}. The solution ^{1}H and ^{13}C NMR spectra, Fig. 3.7, are consistent with the solid state structure shown in Fig. 3.8 with selected bond length and angles listed in Table 3.2, in particular confirming the C_1 symmetry of the compound and the presence of two inequivalent tolyl groups derived from the TolNCO.

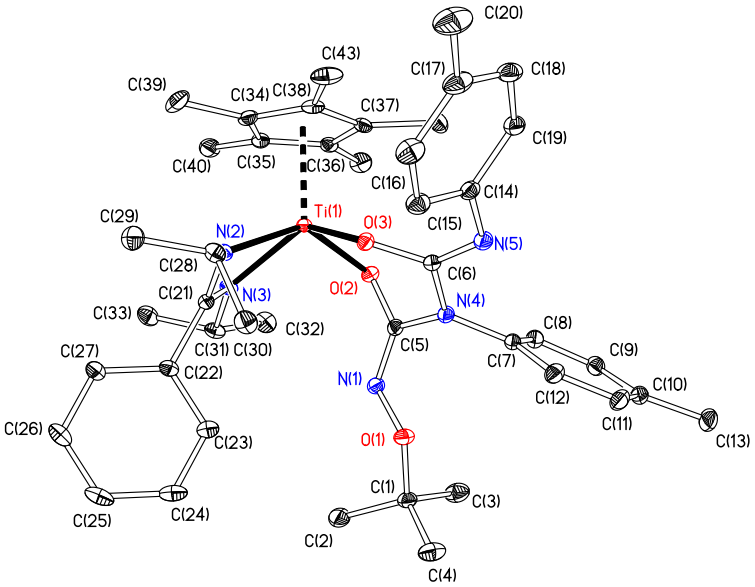

Figure 3.8. Displacement ellipsoid plot (20% probability) of Cp*Ti{PhC(N^{i}Pr)$_2$}-{OC(NTol)N(Tol)C(NO^{t}Bu)O} (**6**). H atoms omitted for clarity.

Table 3.2. Selected bond lengths (Å) and angles (°) for Cp*Ti{PhC(N^{i}Pr)$_2$}{OC(NTol)N(Tol)C(NO^{t}Bu)O} (**6**). Cp$_{cent}$ is the computed centroid for the Cp* ring carbons.

Ti-Cp$_{cent}$	2.049	Cp$_{cent}$-Ti(1)-N(2)	114.88
Ti(1)-N(2)	2.0726(10)	Cp$_{cent}$-Ti(1)-N(3)	116.67
Ti(1)-N(3)	2.0979(10)	Cp$_{cent}$-Ti(1)-O(2)	110.36
Ti(1)-O(2)	1.9197(9)	Cp$_{cent}$-Ti(1)-O(3)	113.45
Ti(1)-O(3)	1.9527(9)	N(2)-Ti(1)-N(3)	63.73(4)
N(1)-C(5)	1.2851(17)	Ti(1)-O(2)-C(5)	113.21(7)
N(1)-O(1)	1.4242(14)	Ti(1)-O(3)-C(6)	131.78(8)
N(4)-C(5)	1.4141(16)	O(2)-Ti(1)-O(3)	84.63(4)
N(4)-C(6)	1.4024(15)	O(2)-C(5)-N(4)	115.65(10)
N(4)-C(7)	1.4267(16)	C(5)-N(1)-O(1)	109.93(10)
N(5)-C(6)	1.2822(17)	N(1)-O(1)-C(1)	110.71(9)
O(1)-C(1)	1.4539(15)	C(5)-N(4)-C(6)	117.85(10)
O(2)-C(5)	1.3337(15)	N(4)-C(6)-O(3)	113.47(10)
O(3)-C(6)	1.3184(15)	N(4)-C(6)-N(5)	119.30(11)

The molecular structure shows a five-coordinate titanium center in a four-legged piano stool geometry. In addition to the η^5-C_5Me_5 and κ^2*N*,*N*′-PhC(N^{i}Pr)$_2$ supporting ligands, two new Ti–O bonds make up part of the newly formed six-membered ring derived from the two TolNCO moieties and the original NO^{t}Bu fragment of **3**. The N(4)–C(5), N(4)–C(6) and N(4)–C(7) bonds are consistent with C–N single bonds whereas N(1)–C(5) and N(5)–C(6) are significantly shorter, consistent with the double bond representation shown in Scheme 3.2. The structure is reminiscent of the previously reported Cp*Ti{MeC(N^{i}Pr)$_2$}{OC(NR)N(Tol)C(NTol)O} (R = NMe_2 or $NCPh_2$), formed by reaction of **3.13** or **3.14** with 2 equivs TolNCO,[42, 66] although in **6** the six-membered ring has a significantly more non-planar arrangement. The IR spectrum of **6** shows two *ν*(C=N) bands at 1623 and 1587 cm^{-1} which are comparable to those seen in the previous cases (1623 and 1604; 1619 and 1599 cm^{-1} for **3.13** and **3.14**, respectively). Although the unsymmetrical structure found for **6** has the aforementioned precedents in the hydrazide literature, this type of "double insertion" product is relatively unusual, with C_s symmetric products of the type Cp*Ti{MeC(N^{i}Pr)$_2$}{OC(E)N(R)C(E)O} (R = Tol or NPh_2; E = O or NTol) usually being formed in case of reactions of CO_2 or TolNCO with Cp*Ti{MeC(N^{i}Pr)$_2$}(NR) (R = Tol (**3.11a**) or NPh_2 (**3.12**, for CO_2 only)), and these reactions have been studied in detail both experimentally and computationally.[42, 86, 89, 90]

Scheme 3.3 shows the proposed mechanism for formation of **6** which is analogous to that determined by DFT calculations for **3.13** and consistent with the reactions of **3** with Ar′NCO and ^{t}BuNCO (*vide infra*).[42] Thus [2+2] cycloaddition of TolNCO to **3** forms the intermediate **6_int1** which is the analogue of the fully characterised **5**. Species **6_int1** is not observed and undergoes extrusion (retro-cyclisation) of the *tert*-butoxy carbodiimide ^{t}BuONCNTol forming a transient titanium oxo species Cp*Ti{PhC(N^{i}Pr)$_2$}(O). Although such species can easily dimerise, they are also able to undergo cycloaddition reactions with carbodiimides or other unsaturated species.[22, 100, 101] In this case, cycloaddition of the extruded ^{t}BuONCNTol to the transient oxo species is rapid compared with dimerisation, either reforming **6_int1** or the isomeric **6_int2** containing a Ti–N(Tol) single bond. As shown previously,[89] such ureato species are able to insert isocyanates, in this case forming **6**. Interestingly, although Scheme 3.3 proposes **6_int1** as a likely intermediate, this compound apparently does not undergo insertion of TolNCO into the Ti–N(O^{t}Bu) in preference to rearrangement to **6_int2**.

This is attributed to either the electron-withdrawing nature of the –O^{t}Bu group decreasing the nucleophilicity of the Ti–N(O^{t}Bu) nitrogen in comparison to Ti–N(Tol), or/and the steric bulk of the *tert*-butyl substituent.

Scheme 3.3. Proposed mechanism for the reaction of Cp*Ti{PhC(N^{i}Pr)$_2$}(NO^{t}Bu) (**3**) with TolNCO leading to Cp*Ti{PhC(N^{i}Pr)$_2$}{OC(NTol)N(Tol)C(NO^{t}Bu)O} (**6**).

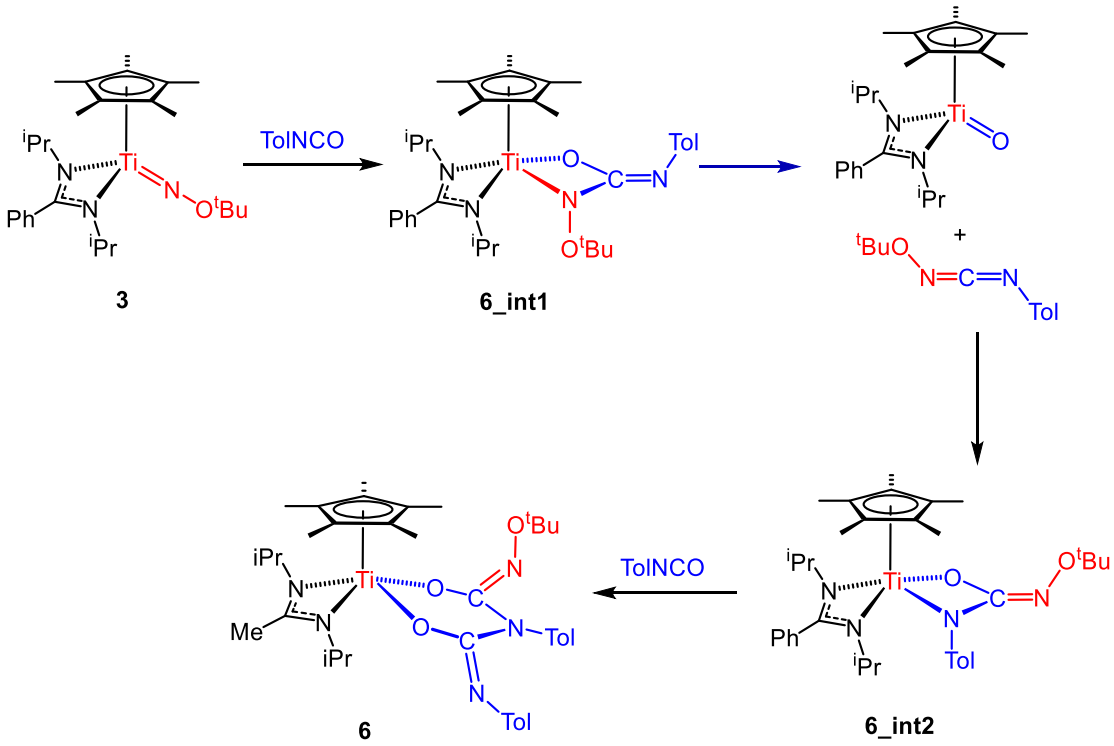

As shown in Scheme 3.2, reaction of **3** with ^{t}BuNCO over a period of 16 h resulted in a gradual colour change from green to yellow alongside formation of a yellow precipitate, identified as the oxo-bridged dimer [Cp*Ti{PhC(N^{i}Pr)$_2$}(μ-O)]$_2$ (**7**). A number of analogues of **7** have been reported previously from reactions of this type.[86, 88, 89] The molecular structure and selected bond length and angles for **7**, which lie within the expected ranges,[96] are presented in Fig. 3.9 and Table 3.3. Careful evaporation of the filtrate gave the alkoxycarbodiimide by-product ^{t}BuNCNO^{t}Bu (**8**) as a colourless oil which was characterised by NMR and IR spectroscopy and high resolution FI mass spectrometry. The IR spectrum showed ν(C=N) bands at 2257 and 2065 cm^{-1} in the expected range.[102-105] Unfortunately, due to its relatively high volatility, **8** could only be isolated as a pure sample in *ca.* 10% yield (sufficient to enable full characterisation). However, since the reaction of **3** with ^{t}BuNCO is quantitative (as judged by ^{1}H NMR monitoring in C_6D_6 (no intermediates analogous to **5** were observed)) **8** could be isolated as diethyl ether solutions in high yield. No examples of alkoxycarbodiimides

have previously been reported although amino-carbodiimides have been reported previously by others[106, 107] and also by our group *via* a similar cycloaddition-elimination protocol to that forming **8**.[42, 66] The cycloaddition-extrusion reaction leading to **7** and **8** is analogous to that found previously for reactions of Cp*Ti{MeC(N^{i}Pr)$_2$}(NR) (R = ^{t}Bu (**3.10**) or Ar (**3.11**)) and Cp*Ti{MeC(N^{i}Pr)$_2$}(NNMe$_2$) (**3.13**) with ^{t}BuNCO. With **3.11** unstable cycloaddition intermediates could be observed, but ultimately in all cases carbodiimides were formed along with the corresponding oxo-bridged dimer.

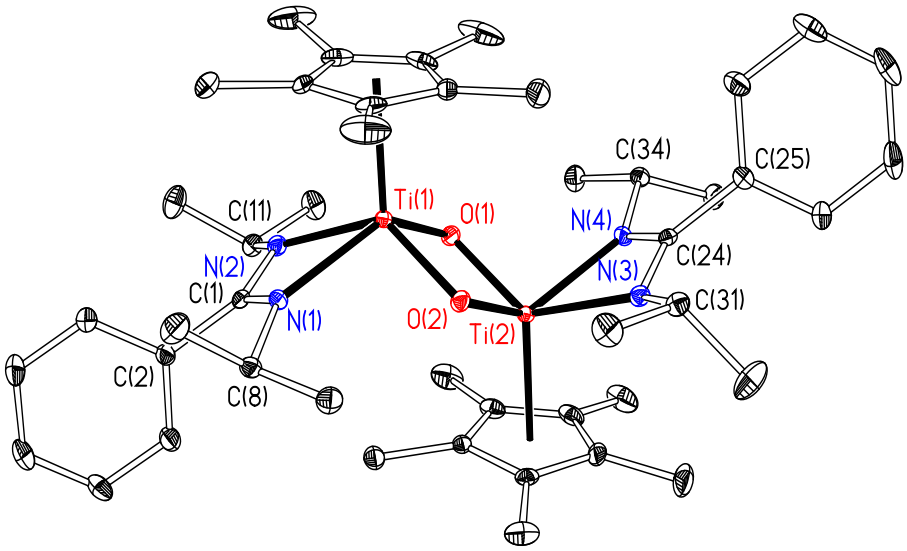

Figure 3.9. Displacement ellipsoid plot (20 % probability) of [Cp*Ti{PhC(N^{i}Pr)$_2$}(μ-O)]$_2$ (**7**). H atoms omitted for clarity.

Table 3.3. Selected bond lengths (Å) and angles (°) for [Cp*Ti{PhC(N^{i}Pr)$_2$}(μ-O)]$_2$ (**7**). Cp$_{cent(1)}$ and Cp$_{cent(2)}$ are the computed centroids for the Cp* ring carbons.

Ti(1)-Cp$_{cent(1)}$	2.138	Cp$_{cent(1)}$-Ti(1)-N(1)	107.92
Ti(2)-Cp$_{cent(2)}$	2.143	Cp$_{cent(1)}$-Ti(1)-N(2)	108.69
Ti(1)-N(1)	2.1954(19)	Cp$_{cent(2)}$-Ti(2)-N(3)	109.45
Ti(1)-N(2)	2.195(2)	Cp$_{cent(2)}$-Ti(2)-N(4)	108.00
Ti(2)-N(3)	2.215(2)	Cp$_{cent(1)}$-Ti(1)-O(1)	115.88
Ti(2)-N(4)	2.168(2)	Cp$_{cent(1)}$-Ti(1)-O(2)	118.75
Ti(1)-O(1)	1.8670(17)	Cp$_{cent(2)}$-Ti(2)-O(1)	116.00
Ti(1)-O(2)	1.8572(18)	Cp$_{cent(2)}$-Ti(2)-O(2)	118.78
Ti(2)-O(1)	1.8599(18)	N(1)-Ti(1)-N(2)	60.60(8)
Ti(2)-O(2)	1.8614(17)	N(3)-Ti(2)-N(4)	60.61(8)
		O(1)-Ti(1)-O(2)	81.17(8)
		O(1)-Ti(2)-O(2)	81.25(7)
		Ti(1)-O(1)-Ti(2)	98.64(8)
		Ti(1)-O(2)-Ti(2)	98.94(9)

3.4 Reactions with aldehydes and ketones

The metathesis reactions between transition metal imido compounds and organic carbonyls to form ketimines or aldimines *via* cycloaddition-elimination reactions is well-established.[2, 3, 5, 23, 65, 70, 108-115] In particular, both Cp*Ti{MeC(N^{i}Pr)$_2$}(N^{t}Bu) (**3.10**) and Cp*Ti{MeC(N^{i}Pr)$_2$}(NTol) (**3.11a**) undergo ketone and aldehyde C=O/Ti=NR bond metathesis reactions with MeC(O)Me, PhC(O)Ph, PhC(O)H and PhCOMe, and in some instances [2+2] cycloaddition intermediates were observed.[89] By analogy, it was reasoned that reaction of **3** with aldehydes or ketones should give access to oxime ethers (i.e. compounds of the general type RC(NOR′)R″).[116]

Scheme 3.4. Reaction of Cp*Ti{PhC(N^{i}Pr)$_2$}(NO^{t}Bu) (**3**) with PhC(O)H, PhC(O)Me and PhC(O)Ph.

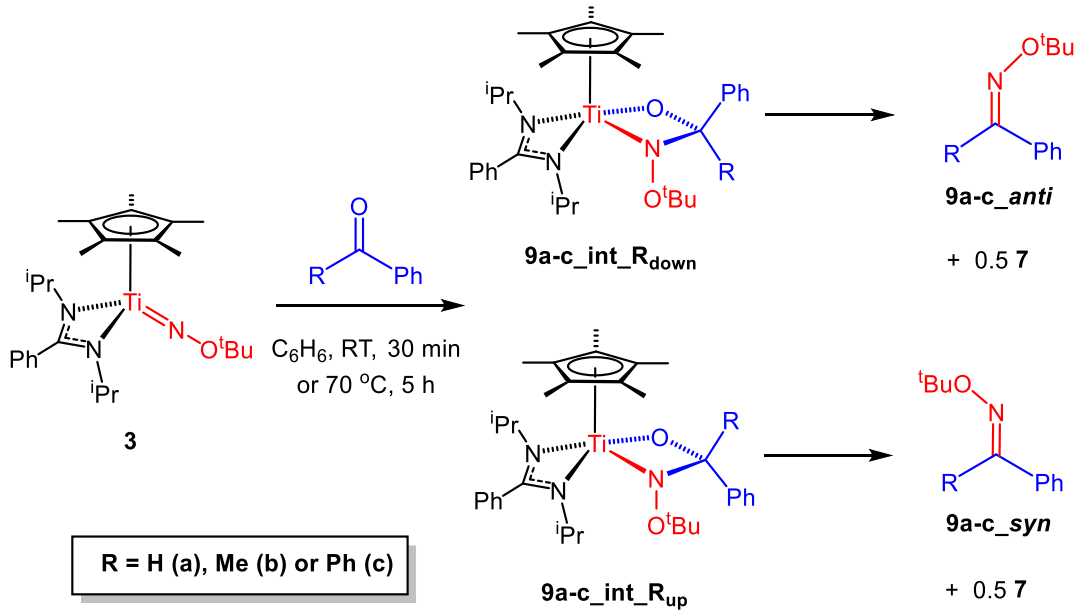

The main synthetic routes to oxime ethers are reaction of an oxime with carbon electrophiles, such as alkyl halides, epoxides and activated olefins, or reaction of an aldehyde or ketone with the HCl salt of the alkoxyamine.[92, 116-121] Oxime ethers are formed as one of two isomers, *syn* or *anti*, where *anti* is defined as a Z arrangement of the nitrogen- and highest molecular weight carbon-bound substituents.[118] As discussed above, reaction of **3** with ^{t}BuNCO demonstrated the potential for NO^{t}Bu transfer to another fragment (in that case ^{t}BuNC, forming ^{t}BuNCNO^{t}Bu (**8**)). To explore the scope of the NO^{t}Bu group transfer processes further, reactions with selected aldehydes and ketones were carried out. Scheme 3.4 summarises the reactions of **3** with PhC(O)H, PhC(O)Me and PhC(O)Ph, along with the proposed likely intermediates.

Reaction of **3** with PhC(O)H in C_6D_6 at room temperature gave quantitative formation of the oxo-bridged dimer $[Cp^*Ti\{PhC(N^iPr)_2\}(\mu\text{-}O)]_2$ (**7**) and oxime ether PhC(NO^{t}Bu)H, (**9a**) in a *ca.* 4:1 ratio of geometric isomers. Scale up and distillation (80-110 °C, 8 x 10^{-2} mbar) gave **9a** as a colourless oil in 70% yield. Based on the ^{1}H and ^{13}C NMR spectra (*vide infra*), the two isomers are assigned as *anti* (major) and *syn* (minor), denoted **9a_*anti*** and **9a_*syn*** in Scheme 3.4. Following their formation, no significant interconversion between the two isomers was observed in solution or upon distillation. This is consistent with previous studies which found that, unlike imines, it is only under harsh thermal or photochemical conditions that *syn-anti* isomerisation of oxime ethers is observed.[122-124]

Comparison with literature data established the minor isomer as **9a_*syn*** which gives a diagnostic ^{1}H NMR singlet for *syn*-PhC(NO^{t}Bu)H at δ 8.03 ppm.[120] Literature data for **9a_*anti*** are more limited, but the presence of the *anti*-PhC(NO^{t}Bu)H singlet at δ 7.27 ppm is consistent with other NMR studies on the geometric isomerism of oxime ethers.[119, 125] The *o*-C_6H_5 hydrogens for **9a_*anti*** are found at δ 7.85 ppm, consistent with the aryl ring being *cis* to the O^{t}Bu group.[118] The assignments were confirmed by comparison of the experimental ^{13}C NMR data with the corresponding ^{13}C isotropic magnetic shielding tensors calculated by DFT (Fig. 3.10). Interestingly, the DFT calculations (Fig. 3.10) showed that the *minor* isomer **9a_*syn*** is 1.9 kcal mol^{-1} *more* thermodynamically stable than **9a_*anti*** at 298 K. This suggests that the overall reaction is governed by kinetic/mechanistic constraints, given that **9a_*syn*** and **9a_*anti*** do not interconvert once formed.

Reaction of **3** with PhC(O)Me at room temperature afforded PhC(NO^{t}Bu)Me[121] (**9b**, Scheme 3.4), which again was readily separated from **7** by distillation in very good yield (75%). The known compound PhC(NO^{t}Bu)Me also exists as a mixture of *syn*- and *anti*-isomers, **9b_*syn*** and **9b_*anti***, and the assignments were confirmed by comparison with literature NMR values[121] and DFT calculated isotropic ^{13}C magnetic shielding tensors. However, in this case it is now the *syn* isomer which is the major species, formed in *ca.* 9:1 ratio with respect to the *anti* counterpart. As was also the case for **9a**, DFT calculations (Fig. 3.10) found that **9b_*syn*** is more thermodynamically stable than **9b_*anti*** by 5.6 kcal mol^{-1} at 298 K.

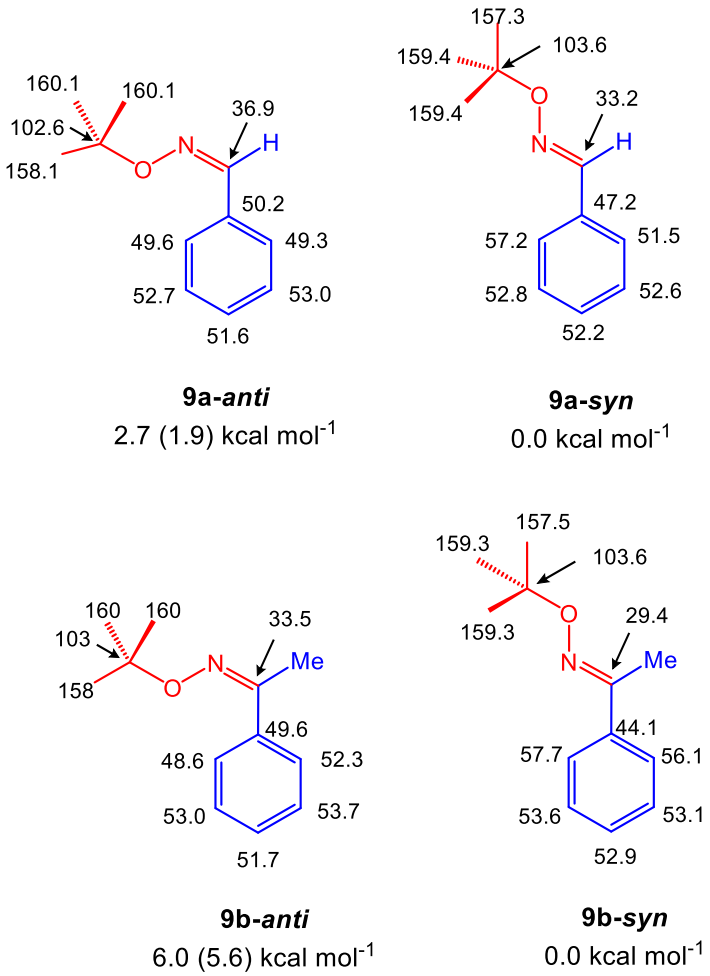

Figure 3.10. Computed isotropic magnetic shielding tensors and pairwise relative Gibbs free energies at 298 K (the values in parentheses include a dispersion correction) for the *anti* and *syn* isomers of PhC(NO^{t}Bu)R (R = H (**9a**) or Me (**9b**)).

Based on DFT studies discussed below, Scheme 3.4 shows the two likely metallacycle intermediates, denoted **9_int_R$_{down}$** and **9_int_R$_{up}$**, (R = H or Me) formed *en route* to the *anti* and *syn* isomers of **9a** and **9b**, respectively. Metallacycles of this type have been explicitly observed by us previously in the reactions of Cp*Ti{MeC(N^{i}Pr)$_2$}(NTol) (**3.11a**) with PhC(O)R (R = H, Me or Ph) which ultimately give the corresponding imines PhC(NTol)R and the μ-oxo dimer [Cp*Ti{MeC(N^{i}Pr)$_2$}(μ-O)]$_2$.[89] The metallacycles **9_int_R$_{up/down}$** differ in the orientation of the substrate-derived R- and Ph-substituents, each diastereomer leading specifically to one isomer of PhC(NO^{t}Bu)R as illustrated.

Although no intermediates were observed at room temperature in the reactions of **3**, when PhC(O)H was added to a pre-cooled toluene-d_8 solution of **3** at -50 °C two products were observed in the ^{1}H NMR spectrum within 5 min. The spectra were

consistent with formation of the cycloaddition intermediates Cp*Ti{PhC(N^{i}Pr)$_2$}{N(O^{t}Bu)C(Ph)(H)O} (**9a_int**), present as a major and minor isomer in *ca.* 7:3 ratio. Warming to -10 °C gave complete consumption of the minor isomer to form **7** and **9a_*syn***. The major isomer extruded **9a_*anti*** only slowly at this temperature, but on warming to 0 °C the reaction reached completion within 30 min. The major and minor isomers are tentatively assigned as the metallacycles **9a_int_H$_{up}$** and **9a_int_H$_{down}$**, respectively, but due to the numerous overlapping resonances in the ^{1}H NMR spectrum it was not possible to assign the data completely. In a similar way, when the reaction of **3** with PhC(O)Me was carried out under analogous conditions, no reaction was observed until -30 °C, and at this point one major cycloaddition intermediate, tentatively assigned as the cycloaddition product **9b_int_Me$_{up}$**, was observed. This started to undergo extrusion at -10 °C, and upon warming to 0 °C the reaction reached completion within 25 min. Note that although only one cycloaddition intermediate was unambiguously identified at low temperature (because of the low proportion of **3** converting to the other diastereomer), two isomers of the oxime ether (**9b_*syn*** and **9b_*anti***, 9:1 ratio) were formed on warming, as in the room temperature experiment.

In an additional attempted crossover-type experiment, PhC(O)H was added to a solution of **3** in toluene-d_8 at -50°C, at which temperature both the cycloaddition products **9a_int_H$_{up}$** and **9a_int_H$_{down}$** were formed as above and were stable to extrusion. Subsequently, 1 equiv of TolC(O)H was added and, following a further 10 min at -50 °C, the solution allowed to warm to room temperature at which point extrusion took place effectively immediately. The ^{1}H NMR spectrum showed no detectable consumption of the TolC(O)H, showing that extrusion of PhC(NO^{t}Bu)H from **9a_int_H$_{up}$** and **9a_int_H$_{down}$** is much faster than loss of PhC(O)H to reform **3** (which could then react with either PhC(O)H or TolC(O)H). For comparison, when the reaction of **3** with TolC(O)H was carried out in a separate NMR tube scale reaction, TolC(NO^{t}Bu)H (**9d**) was formed immediately as a mixture of *anti* and *syn* isomers in a 7:3 ratio, respectively. These were characterised by ^{1}H and ^{13}C NMR spectroscopy and high resolution mass spectroscopy. In a further NMR tube scale experiment, the reaction of a 1:1 mixture of PhC(O)H and TolC(O)H with 1 equiv of **3** formed a 1:1 mixture of **9a** and **9d**, confirming that the two aldehydes can compete effectively when both are available prior to metallacycle formation.

Finally, as mentioned, the tolylimide **3.11a** reacts with PhC(O)Ph to give the ketimine PhC(NTol)Ph although this reaction took 9 d to reach completion at room temperature.[89] The synthesis of the corresponding oxime ether, PhC(NO^{t}Bu)Ph (**9c**), has been previously attempted by Rad and Khalafi-Nezhad *et al.* during their studies of the use of alcohols and oximes, in the presence of DBU, PPh_3, CCl_4 and $^tBu_4NI$, to prepare such species.[116] Addition of PhC(O)Ph to **3** in C_6D_6 quantitatively formed **9c** (Scheme 3.4), albeit at a much slower rate (2 d at room temperature) than for PhC(O)R (R = H or Me). At 70 °C, the reaction was *ca.* 90% complete within 2 h and reached quantitative conversion within 17 h. On scale up, **9c** was isolated by sublimation as a cream solid in 93% yield. The structure was confirmed by X-ray crystallography, the molecular structure is given in Fig. 3.11 with selected distances and angles in Table 3.4. The geometric parameters all lie within the expected parameters, the N(1)–C(5) distance is short (1.2888(12) Å), consistent with a C=N double bond, and both phenyl rings are significantly twisted out of the {C(12)C(5)N(1)C(6)} plane in order to minimise steric repulsions.

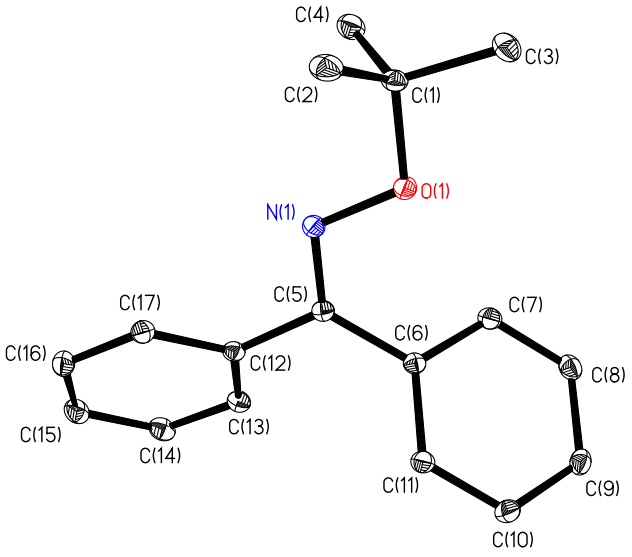

Figure 3.11. Displacement ellipsoid plot (20% probability) of PhC(NO^{t}Bu)Ph (**9c**). H atoms omitted for clarity.

Table 3.4. Selected bond lengths (Å) and angles (°) for PhC(NO^{t}Bu)Ph (**9c**).

C(1)-O(1)	1.4631(11)	N(1)-O(1)-C(1)	110.50(7)
N(1)-O(1)	1.3980(9)	C(5)-N(1)-O(1)	112.30(7)
N(1)-C(5)	1.2888(12)	C(6)-C(5)-N(1)	125.68(8)
C(5)-C(12)	1.4886(12)	C(12)-C(5)-N(1)	114.77(8)
C(5)-C(6)	1.4910(12)		

Fig. 3.12 shows the DFT computed reaction profile for the reaction of **3** with PhC(O)R (R = H, Me). The actual experimental molecules have been considered in the calculations. Gibbs free energy values are given at 298 and 253 K, and the calculations include D3 corrections for dispersion. Two pathways were found, shown in blue (Path 1) and red (Path 2), leading to *anti*- and *syn*- PhC(NO^{t}Bu)R, respectively (R = H or Me). In both cases (R = H or Me) the reaction proceeds *via* an entropically disfavoured [2+2] cycloaddition of the substrate C=O group to Ti=NO^{t}Bu *via* TS1, forming intermediate metallacycles **9_int_R$_{down}$** (Path 1) or **9_int_R$_{up}$** (Path 2). These species differ in the orientation of the R-group with respect to the Cp* ligand and are predicted to be observable at low temperature in each case (less unfavourable TΔS contribution to the ΔG for **3** + PhC(O)R → **9_int_R$_{up/down}$,** see ΔG values at 253 K in Fig. 3.12). For R = Me, steric interactions destabilise both metallacycles in comparison with those formed from PhC(O)H, but **9b_int_Me$_{down}$** is destabilised more (with respect to **9a_int_H$_{down}$**) than **9b_int_Me$_{up}$**. All of the **9_int_R$_{up/down}$** species are unstable with respect to extrusion of the oxime ether and Cp*Ti{PhC(N^{i}Pr)$_2$}(O) (the dimerisation energy for this to form **7** was not calculated, but is known experimentally to be exergonic).

Two important points should be noted regarding possible extrusion processes from **9_int_R$_{up/down}$**. First, although elimination from **9_int_R$_{up/down}$** of the starting PhC(O)R is predicted to be feasible *via* transition state TS1 ($\Delta G^{\ddagger}$ = 17.1 – 19.7 kcal mol^{-1}), loss of the product PhC(NO^{t}Bu)R is more kinetically favourable (*via* TS2, $\Delta G^{\ddagger}$ = 8.6 – 14.5 kcal mol^{-1}). Second, elimination of PhC(NO^{t}Bu)R from **9_int_R$_{down}$** gives exclusively the *anti*-isomer while elimination from **9_int_R$_{up}$** gives exclusively the *syn*-isomer.

The relative energies of TS1, TS2 and **9_int_R$_{up/down}$** account qualitatively for the experimental observations and product isomer selectivity for R = H and Me. In the case

of PhC(O)H, formation of **9a_int_H$_{down}$** (Path 1) *via* TS1 is kinetically favoured by $\Delta\Delta G^{\ddagger}$ = 2.2 kcal mol^{-1}. Once formed, extrusion of the thermodynamically less stable product **9a_*anti*** *via* TS2 is predicted to be slower than extrusion of **9a_*syn*** from the minor isomer **9a_int_H$_{up}$**. In the case of PhC(O)Me, however, the relative energies of TS1 for Path 1 and Path 2 (and the relative energies of **9b_int_Me$_{up/down}$** *cf.* **9a_int_H$_{up/down}$**) swap over due to the influence of the substrate –Me group. There is therefore a higher kinetic preference for the **9b_int_Me$_{up}$** metallacycle and, in turn, the more stable product **9b_*syn***, in accord with experiment.

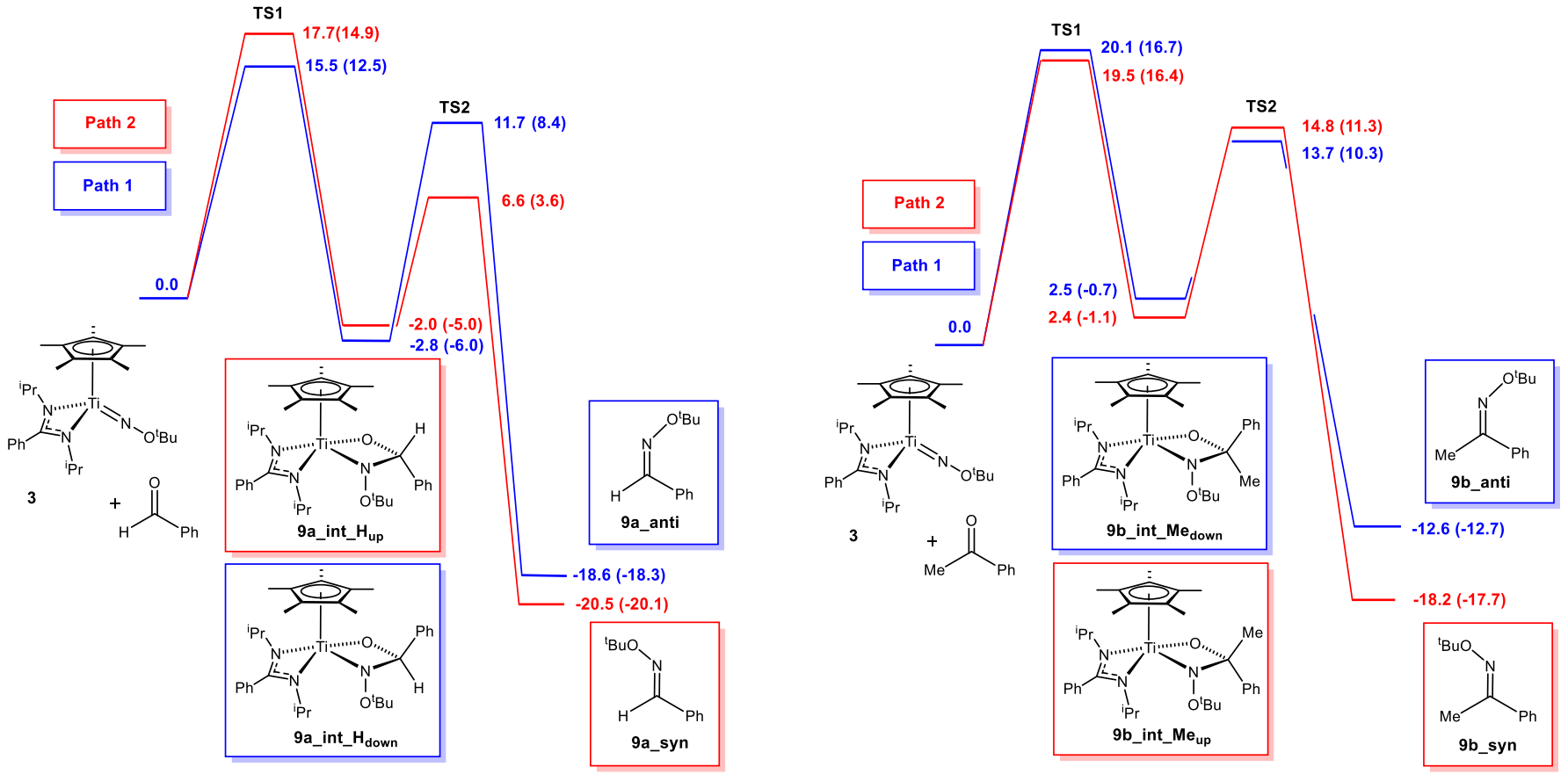

Figure 3.12. Gibbs free energy diagram (kcal mol^{-1}) at 298 K for the cycloaddition-extrusion reactions of Cp*Ti{PhC(N^iPr)$_2$}(NO^tBu) (**3**) with PhC(O)H (left) and Ph(CO)Me (right). Values in parentheses are the Gibbs free energies at 253 K. The Cp*Ti{PhC(N^iPr)$_2$}(O) side-product is not shown.

3.5 Reactions with nitriles

Although the reactions of nitriles with transition metal nitrides,[126, 127] alkylidenes[128-132] and alkylidynes[133-138] are very well established, the corresponding reactions with transition metal imides are almost unknown. As mentioned in Chapter One, the first example was for Ti(N_2N^{py})(N^tBu)(py) (N_2N^{py} = (2-NC_5H_4)CMe(CH_2NSiMe_3)$_2$) with MeCN and gave rise to the dimeric complex Ti$_2$(N_2N^{py})$_2${μ-NC(Me)(N^tBu)}$_2$.[139] More recently, reactions of fluorinated benzonitriles $Ar^{Fx}CN$ (Ar^{Fx} = Ar^{F2} (2,6-$C_6H_3F_2$) or Ar^{F5} (C_6F_5)) with diamido-amine- or diamido-ether-supported hydrazides (L)Ti($NNPh_2$)(py)$_n$ (L = N_2N^{Me}, N_2N^{py}, O($CH_2CH_2NSiMe_3$)$_2$; n = 1 or 2) gave net Ti=N_α insertion products of the type (L)Ti{NC(Ar^{Fx})$NNPh_2$}(py)$_n$ containing a new class of hydrazonamide ligand.[37, 39, 68] These reactions are reminiscent of the Zr=P insertion reaction of Cp_2Zr(PMes*)(PMe_3) (Mes* = 2,4,6-$C_6H_2{}^tBu_3$) with PhCN.[140] More recently, the alkylidene hydrazide Cp*Ti{MeC(N^iPr)$_2$}($NNCPh_2$) (**3.14**) was found to undergo head-to-tail coupling of two molecules of ArCN (Ar = Ph or Ar^{F5}) across the Ti=N_α bond to form Cp*Ti{MeC(N^iPr)$_2$}{N($NCPh_2$)C(Ar)NC(Ar)N} containing a six-membered metallacycle.[66] Although hydrazonamide-type intermediates were proposed, none were observed experimentally. In contrast, none of the imido analogues of **3.14**, namely **3.10** or **3.11**, showed any reactivity towards nitriles. The double nitrile addition reactions of **3.14** were the first of their kind for any hydrazido or related complex, although multiple coupling of two alkynes[141, 142] or of an alkyne and a nitrile[39] across (L)Ti=NR (R = hydrocarbyl or NPh_2) bonds are known. The only related example of a double addition of nitriles was reported for the transient oxo and sulfido complexes Cp*$_2$Zr(E) (E = O or S).[143]

Scheme 3.5 shows the reactions of **3** with various benzonitriles ArCN (Ar = Ph, Ar^{F2} or Ar^{F5}) varying the extent of fluorination of the phenyl ring. When monitored on the NMR tube scale in C_6D_6, the reaction with $Ar^{F5}CN$ was complete within 5 min to give Cp*Ti{PhC(N^iPr)$_2$}{NC(Ar^{F5})O^{t}Bu} (**10**) as established by X-ray diffraction (*vide infra*). The corresponding reaction with $Ar^{F2}CN$ was slightly slower (80% and 100% conversion to **11** after 5 min and 1 h, respectively), whereas with PhCN the reaction only reached completion, forming **12**, after 19 h (70% after 1 h). The NMR spectra for **10** – **12** were very similar, consistent with the formation of a new *tert*-butoxybenzimidamide complex Cp*Ti{PhC(N^iPr)$_2$}{NC(Ar)O^{t}Bu} in each case. Compounds **11** and **10** were isolated on the preparative scale as a green oil or solid in

97% and 33% yield, respectively, and characterised by ^{1}H, ^{13}C and ^{19}F NMR, mass and IR spectroscopy and elemental analysis. The low yield for **10** is attributed to its high solubility. Attempted scale up of the reaction with PhCN was unsuccessful producing unknown mixtures. Similarly disappointing results were obtained using MeCN.

Scheme 3.5. Reaction of Cp*Ti{PhC(N^{i}Pr)$_2$}(NO^{t}Bu) (**3**) with benzonitriles. Inset: likely metallacycle intermediate (not observed).

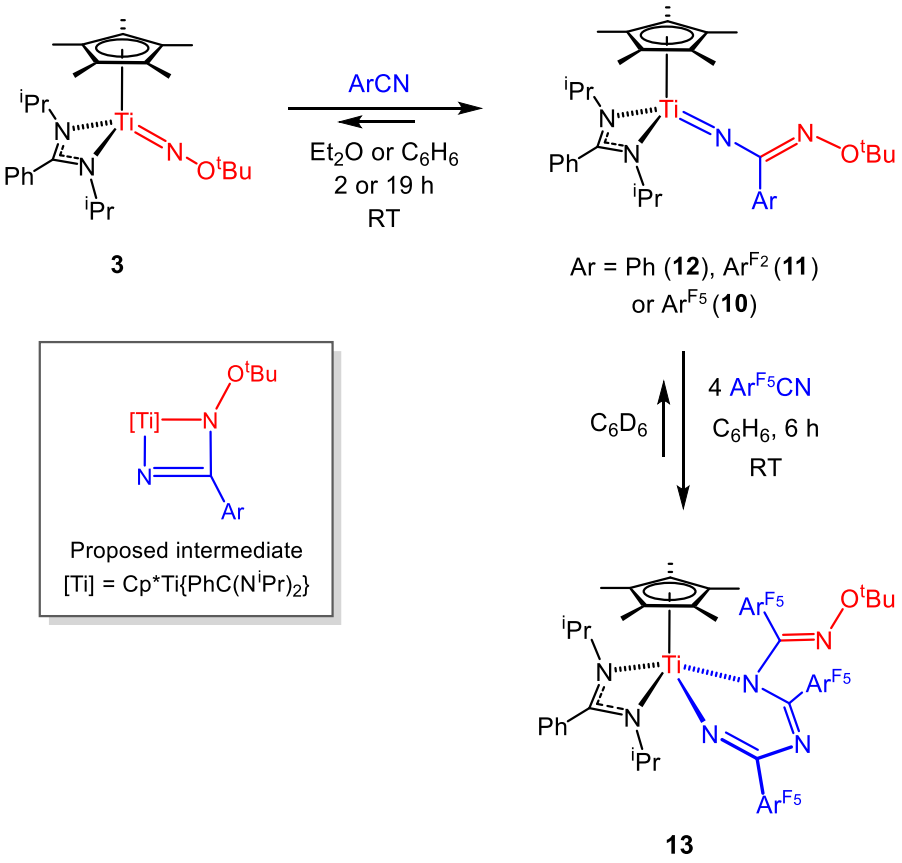

The slower rates of reaction with Ar^{F_2}CN and PhCN compared with Ar^{F_5}CN are consistent with previous studies of benzonitriles with Ti(N$_2$N^{Me})(NNPh$_2$)(py) (**3.8**). DFT calculations showed that increased fluorination of the nitrile substrate both lowered the activation barrier to the intermediate metallacycles Ti(N$_2$N^{Me}){N(NPh$_2$)C(Ar)N} and increased the thermodynamic stability of the final products Ti(N$_2$N^{Me}){NC(Ar^{Fx})NNPh$_2$}(py) by stabilising the electron-rich Ti=NC(Ar)NPh$_2$ group.[39] An analogous intermediate (see inset to Scheme 3.5) is likely in the reactions reported here (although not observed), and the inability to isolate **12** attributed to its likely lower stability. To further test these hypotheses, competition experiments were carried out. Reaction of **11** with Ar^{F_5}CN (1 equiv) resulted in immediate formation of **10** and free Ar^{F_2}CN, consistent with the more electron deficient

nitrile yielding the more thermodynamically stable insertion product. This reaction also highlighted the reversibility of these insertion reactions which previously had not been observed. Likewise, addition of $Ar^{F5}CN$ to *in situ* generated **12** also led to immediate formation of **10** and free PhCN.

Analogues of *tert*-butoxypentafluorobenzimidamide, $H_2NC(Ar^{F5})NO^tBu$, such as O-alkyl-benzamidoximes, $H_2NC(C_6H_4Br)NOR$, have been shown to be useful in the synthesis of O-alkoxyamidine compounds which show antimicrobial activity.[144] Synthesis of the O-alkyl-benzamidoxime compounds is non-trivial requiring multiple steps and toxic stannyl reagents.[144] With this in mind $^tBuONH_2$ was added to both **10** and **11** with the hope of effecting benzimidamide/alkoxyamine exchange generating **3** and $H_2NC(Ar)NO^tBu$ (Ar = Ar^{F5} and Ar^{F2}). However, upon addition of $^tBuONH_2$ complicated mixtures were observed in the ^1H and ^{19}F NMR spectra from which no products could be identified.

Diffraction-quality crystals of **10** were grown from a saturated hexane solution at -80 °C. The molecular structure is shown in Fig. 3.13 and selected bond lengths and angles are listed in Table 3.5. Compound **10** is a four-coordinate titanium complex with a 3-legged piano stool geometry around the metal and η^5-C_5Me_5, κ^2*N*,*N*′ amidinate and η^1-*tert*-butoxypentafluorobenzimidamide ligands. The Ti(1)–N(1) and N(2)–C(1) bond lengths (1.747(4) Å and 1.285(6) Å, respectively) indicate a multiple Ti=N bond and C=N double bond, whereas the N(1)–C(1) and N(2)–O(1) bond lengths (1.362(5) and 1.429(5) Å, respectively) are more consistent with single bonds indicating limited delocalisation across the $Ti=NC(Ar^{F5})NO^tBu$ fragment. Compared to **3** the Ti(1)–N(1) bond is significantly longer (1.747(4) *vs* 1.713(2) (avg.) Å) but still consistent with a $Ti{\equiv}N_\alpha$ triple bond. Related molecular structures of hydrazonamides $(L)Ti\{NC(Ar^{Fx})NNPh_2\}(py)_n$ (n = 1 or 2) also show longer $Ti=N_\alpha$ bond lengths when compared to the parent hydrazido compounds $(L)Ti(NNPh_2)(py)_n$ which is explained by the fluorinated aryl ring withdrawing electron density away from N_α.[39, 68]

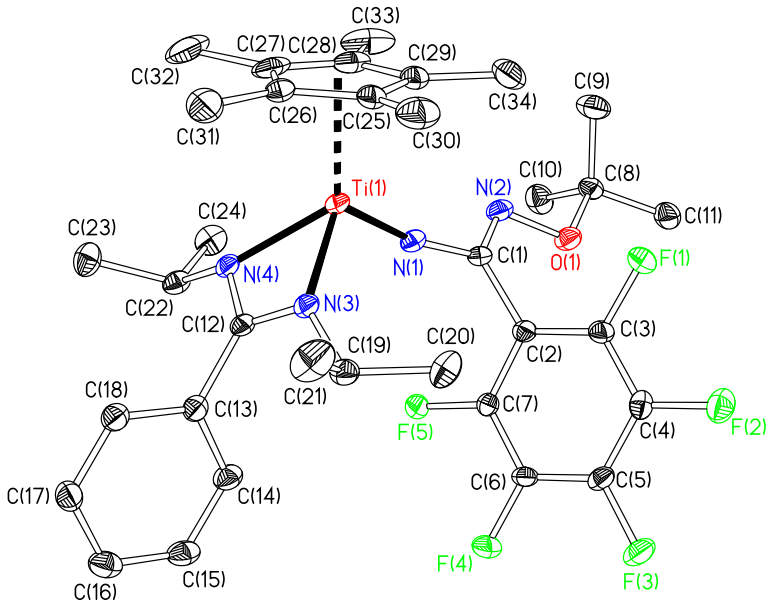

Figure 3.13. Displacement ellipsoid plot (20% probability) of Cp*Ti{PhC(N^{i}Pr)$_2$}{NC(Ar^{F5})NO^{t}Bu} (**10**). H atoms omitted for clarity.

Table 3.5. Selected bond lengths (Å) and angles (°) for Cp*Ti{PhC(N^{i}Pr)$_2$}{NC(Ar^{F5})NO^{t}Bu} (**10**). Cp$_{cent}$ is the computed centroid for the Cp* ring carbons.

Ti-Cp$_{cent}$	2.046	Cp$_{cent}$-Ti(1)-N(1)	121.78
Ti(1)-N(1)	1.747(4)	Cp$_{cent}$-Ti(1)-N(3)	120.38
Ti(1)-N(3)	2.080(4)	Cp$_{cent}$-Ti(1)-N(4)	121.87
Ti(1)-N(4)	2.074(4)	N(3)-Ti(1)-N(4)	64.97(15)
N(1)-C(1)	1.362(5)	Ti(1)-N(1)-C(1)	167.0(3)
N(2)-C(1)	1.285(6)	N(1)-C(1)-N(2)	121.7(4)
N(2)-O(1)	1.429(5)	C(1)-N(2)-O(1)	109.5(3)
O(1)-C(8)	1.448(5)	N(2)-O(1)-C(8)	110.6(3)

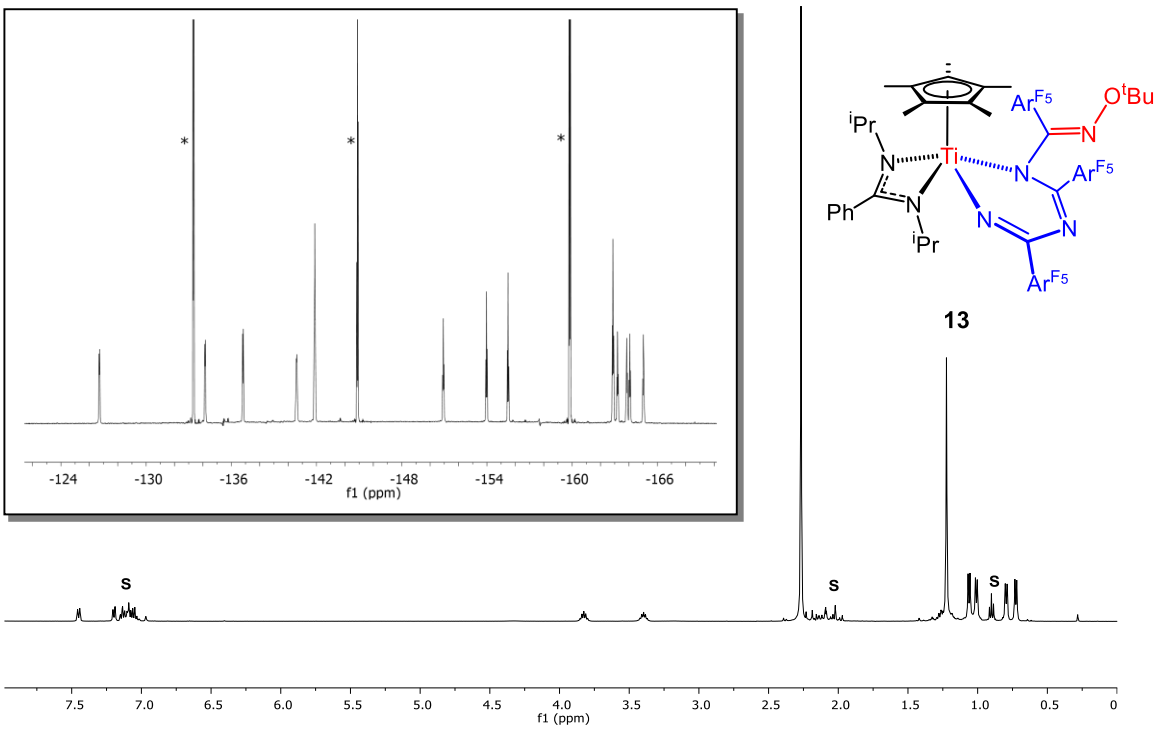

Figure 3.14. ^{1}H NMR spectrum (499.9 MHz, 263 K) of Cp*Ti{PhC(N^{i}Pr)$_2$}{N(C{Ar^{F5}}NO^{t}Bu)C(Ar^{F5})NC(Ar^{F5})N} (**13**) in toluene-d_8 ("s" denotes residual protio-solvent). Inset: corresponding ^{19}F NMR spectrum (282.1 MHz, 263 K, resonances marked with * correspond to excess Ar^{F5}CN).

Addition of 2 equivs of Ar^{F5}CN to **3** in C_6D_6 afforded an approximately statistical mixture of **10** and a new product identified by NMR spectroscopy and X-ray crystallography as Cp*Ti{PhC(N^{i}Pr)$_2$}{N(C{Ar^{F5}}NO^{t}Bu)C(Ar^{F5})NC(Ar^{F5})N} (**13**, Scheme 3.5) after 5 h at room temperature. The compounds **10** (and Ar^{F5}CN) and **13** are in equilibrium and warming the NMR tube solution to 60 °C favoured **10**, as expected based on entropic considerations. Addition of 5 equivs of Ar^{F5}CN to **3** led to sole formation of **13** within 45 min. On scale up using 5 equivs Ar^{F5}CN, **13** was isolated as an orange solid in 49% yield. When pure **13** is dissolved in C_6D_6 an equilibrium mixture of it and **10** and Ar^{F5}CN is formed (ratio of **10** : **13** *ca* 50:50; K_{eq} = 1.4 x 10^{-4} M^2 after 23 h at room temperature). The ^{1}H NMR spectrum of **13** in toluene-d_8 at -10 °C, given in Fig. 3.14, showed the formation of a C_1 symmetric product with characteristic inequivalent *iso*-propyl groups on the PhC(N^{i}Pr)$_2$ ligand. Restricted rotation on the NMR timescale for two of the fluorinated rings resulted in 5 separate ^{19}F resonances per ring in the ^{19}F NMR spectrum (see inset to Fig. 3.14), together with

three further resonances for the third ring. Based on the solid state structure (Fig. 3.15), the two constrained rings are assigned to those containing C(9) and C(16).

In contrast to the reaction with $Ar^{F5}CN$, addition of an excess of $Ar^{F2}CN$ to **3** gave only the insertion product, **11**. This difference between $Ar^{F2}CN$ and $Ar^{F5}CN$ is reminiscent of the reactions of **3.14** with PhCN and $Ar^{F5}CN$ to form Cp*Ti{MeC(N^{i}Pr)$_2$}{N(NCPh$_2$)C(Ar)NC(Ar)N}. While the product with Ar = Ar^{F5} was stable in solution at room temperature, that with Ar = Ph was much more labile and when treated with 2 equivs $Ar^{F5}CN$ underwent exchange of one PhCN unit to give a mixed-nitrile metallacycle.[66]

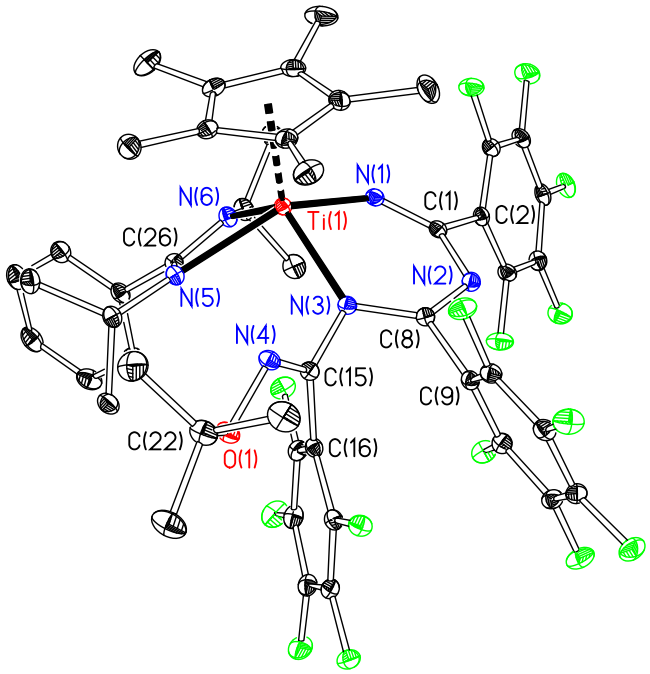

Figure 3.15. Displacement ellipsoid plot (20% probability) of Cp*Ti{PhC(N^{i}Pr)$_2$}{N(C{Ar^{F5}}NO^{t}Bu)C(Ar^{F5})NC(Ar^{F5})N} (**13**). H atoms omitted for clarity.

Table 3.6. Selected bond lengths (Å) and angles (°) for Cp*Ti{PhC(N^{i}Pr)$_2$}{N(C{Ar^{F5}}NO^{t}Bu)C(Ar^{F5})NC(Ar^{F5})N} (**13**). Cp$_{cent}$ is the computed centroid for the Cp* ring carbons.

Ti(1)-Cp$_{cent}$	2.089	Cp$_{cent}$-Ti(1)-N(1)	107.87
Ti(1)-N(1)	1.8756(12)	Cp$_{cent}$-Ti(1)-N(3)	118.69
Ti(1)-N(3)	2.1820(11)	Cp$_{cent}$-Ti(1)-N(5)	110.92
Ti(1)-N(5)	2.2267(11)	Cp$_{cent}$-Ti(1)-N(6)	120.15
Ti(1)-N(6)	2.0829(12)	N(5)-Ti(1)-N(6)	61.60(4)
N(1)-C(1)	1.2673(18)	N(1)-Ti(1)-N(3)	79.92(5)
N(2)-C(1)	1.3850(17)	Ti(1)-N(1)-C(1)	140.68(10)
N(2)-C(8)	1.3139(18)	C(1)-N(2)-C(8)	117.07(11)
N(3)-C(8)	1.3634(18)	N(3)-C(15)-N(4)	118.49(12)
N(3)-C(15)	1.4280(17)	C(15)-N(4)-O(1)	111.19(11)
N(4)-C(15)	1.2808(18)	N(4)-O(1)-C(22)	111.07(10)
N(4)-O(1)	1.4058(15)		
O(1)-C(22)	1.4700(16)		
C(1)-C(2)	1.5085(18)		
C(8)-C(9)	1.5118(18)		

Addition of pentane to an Et$_2$O solution of **13** and Ar^{F5}CN followed by slow cooling to 4 °C resulted in diffraction-quality orange crystals. The molecular structure is shown in Fig. 3.15 and selected bond lengths and angles are given in Table 3.6. Like Cp*Ti{PhC(N^{i}Pr)$_2$}{OC(NTol)N(Tol)C(NO^{t}Bu)O} (**6**), compound **13** is a half-sandwich titanium complex with a 4-legged piano stool geometry around the metal and η^5-C$_5$Me$_5$ and κ^2*N*,*N*′ amidinate ligands. The solid state structure confirms coupling of a further two molecules of Ar^{F5}CN across the Ti=N$_\alpha$ bond of **10** in a head-to-tail manner, consistent with the NMR data. Of particular interest is the approximately planar, six-membered metallacycle. The N(1)–C(1) and N(2)–C(1) bond lengths are significantly different (1.2673(18) *vs* 1.3850(17), $\Delta_{N\text{-}C}$ = 0.118(3) Å) and consistent with N=C and N–C double and single bonds, respectively.[97] Although their N(3)–C(8) and N(2)–C(8) counterparts are also different (1.3634(18) *vs* 1.3139(18) Å) and consistent with single and double bond character, the difference ($\Delta_{N\text{-}C}$ = 0.050(3) Å) is somewhat smaller. These data, together with the rather different Ti(1)–N(1) and Ti(1)–N(3) distances ($\Delta_{Ti\text{-}}$

$_N$ = 0.306(2) Å) suggest (*cf.* Fig. 3.16) contributions from both **A′** and **A″** resonance forms to the bonding in **13** leading to the net description **A**. Likewise, the bond distances to the amidinate ligand, Ti(1)–N(5) and Ti(1)–N(6), are also unequal (2.2267(11) and 2.0829(12) Å, respectively) with the longer Ti(1)–N(5) bond being *trans* to the shorter Ti(1)–N(1) bond. With specific reference to the NC(Ar^{F5})NO^{t}Bu fragment that remains intact during the reaction, the N(3)–C(15) bond distance is significantly longer than that found in **10** (1.4280(17) *vs* 1.362(5) Å, respectively) which is attributed to the change in nitrogen hybridisation from *sp* in **10** to *sp*^{2} in **13** and a loss of conjugation between N(3) and C(15). Otherwise, the other geometric parameters are similar to those seen in **10**. The structural parameters for the six-membered metallacycle in **13** are similar to those in the corresponding fragment of Cp*Ti{MeC(N^{i}Pr)$_2$}{N(NCPh$_2$)C(Ar^{F5})NC(Ar^{F5})N} except in that case the contribution from the resonance form corresponding to **A″** in Fig. 3.16 seemed to be slightly larger ($\Delta_{N\text{-}C}$ = 0.080(7) and 0.014(7) Å in comparison with the values mentioned above) while the difference in Ti–N$_{metallacycle}$ distances (1.868(4) and 2.147(3) Å) was comparable with **13**.[66]

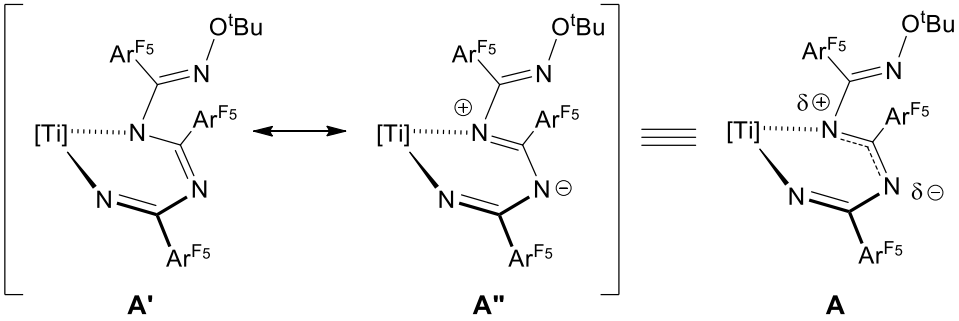

Figure 3.16. Resonance contributions to the bonding in Cp*Ti{PhC(N^{i}Pr)$_2$}{N(C{Ar^{F5}}NO^{t}Bu)C(Ar^{F5})NC(Ar^{F5})N} (**13**). [Ti] = Cp*Ti{PhC(N^{i}Pr)$_2$}.

Scheme 3.6 illustrates two alternative routes for the formation of **13** from **10**. Both begin by the [2+2] cycloaddition of Ar^{F5}CN to Ti=N$_\alpha$ of **10** to form an azametallacyclobutene intermediate **13_int1** as found in both titanium imido and hydrazido chemistry.[39, 139] Insertion of another equiv of Ar^{F5}CN into the new Ti–NC(Ar^{F5}) bond would lead directly to **13**. On the other hand, ring-opening *via* **13_int2** and [2+2] cycloaddition (to form **13_int3**), followed by isomerisation would also afford **13**. An analogous mechanism was proposed for the formation of

Cp*Ti{MeC(N^{i}Pr)$_2$}{N(NCPh$_2$)C(Ar^{F5})NC(Ar^{F5})N} from **3.14**. However, when the reaction was followed by ^{1}H NMR spectroscopy no intermediates were seen prior to **13** and therefore which of the two pathways is operative cannot be identified.

Scheme 3.6. Potential pathways for the formation of Cp*Ti{PhC(N^{i}Pr)$_2$}{N(C{Ar^{F5}}NO^{t}Bu)C(Ar^{F5})NC(Ar^{F5})N} (**13**). [Ti] = CpTi{PhC(N^{i}Pr)$_2$}; Ar^{F5} = C$_6$F$_5$.

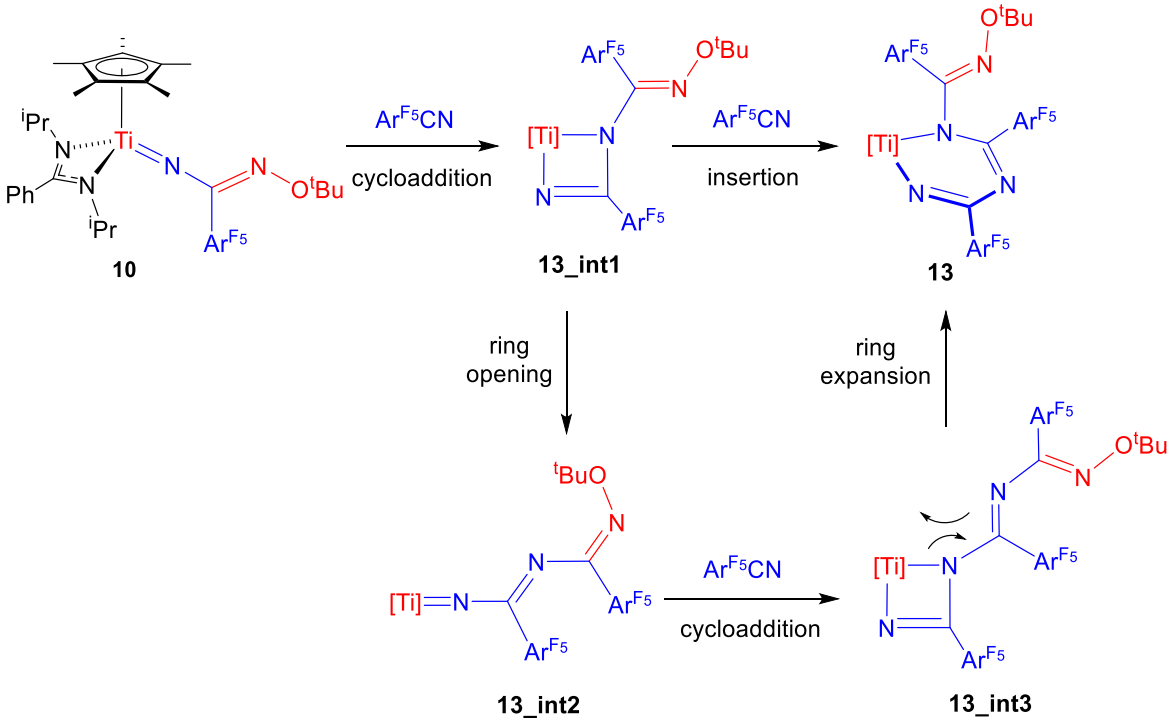

3.6 Reactions with alkynes

As mentioned in Section 1.4 of this Thesis, reactions of Group 4 imides and hydrazides with alkynes has been a topic of continuing interest for over 20 years, producing a range of new C–N bond forming reactions, some of which are catalytic.[1-6, 16-19, 2, 5, 21, 24, 25, 27, 29, 30, 33, 35, 37, 43, 54, 58, 60, 115, 132, 145-157] In the case of terminal alkynes, there is also the possibility of competitive 1,2-C–H bond activation across the M=NR bond.[64, 85, 148, 158] Of particular relevance are the N$_\alpha$–N$_\beta$ bond reductive cleavage reactions[29, 37, 58, 68] available for hydrazides. As mentioned, the only previously reported reaction of a Group 4 alkoxyimido complex with alkynes is that of Ti(N$_2$N^{Me})(NO^{t}Bu)(py) (**3.6**) with PhCCMe forming **3.7** (Fig. 3.2) *via* N–O bond cleavage.[73]

Disappointingly, no reactions were observed between Cp*Ti{MeC(N^{i}Pr)$_2$}(NO^{t}Bu) (**1**) and alkynes such as PhCCMe and Ar^{CF3}CCMe (Ar^{CF3} = 4-C$_6$H$_4$CF$_3$). NMR tube scale

reactions of $Ar^{CF_3}CCH$ and **3** gave complicated mixtures. In contrast, reaction of $Ar^{F_5}CCH$ with **3** in C_6D_6 resulted in a purple solution and a single product, Cp*Ti(O^{t}Bu){NC(Ar^{F_5})C(H)N(^{i}Pr)C(Ph)N(^{i}Pr)} (**14**), after 16 h at room temperature (Scheme 3.7). Compound **14** was isolated in 80% yield upon scale up.

Scheme 3.7. Reaction of Cp*Ti{PhC(N^{i}Pr)$_2$}(NO^{t}Bu) (**3**) with $Ar^{F_5}CCH$ and proposed mechanism of formation for Cp*Ti(O^{t}Bu){NC(Ar^{F_5})C(H)-N(^{i}Pr)C(Ph)N(^{i}Pr)} (**14**).

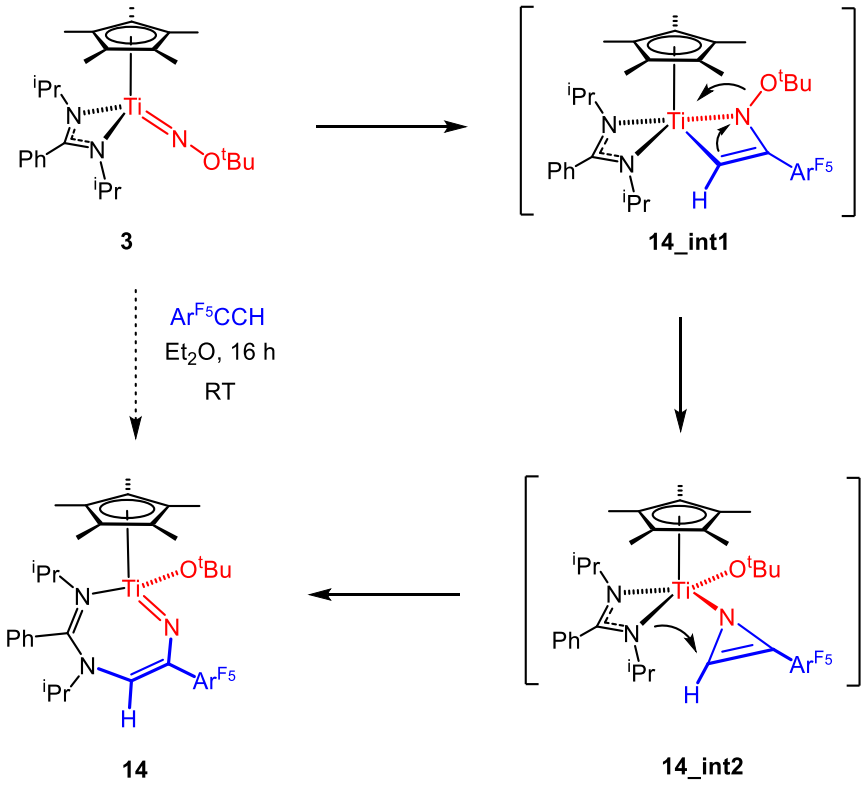

The ^{1}H, ^{13}C and ^{19}F NMR spectra for **14** revealed a C_1 symmetric species with two inequivalent ^{i}Pr groups, resonances attributable to Ph, Cp* and C_6F_5 groups (with five inequivalent F environments at 223 K due to restricted rotation), and a singlet at δ 6.86 ppm of relative intensity 1H in the ^{1}H NMR spectrum assigned to the incorporated alkyne moiety. At first sight the NMR data appear to indicate formation of the [2+2] cycloaddition product **14_int1** (or its isomer with CAr^{F_5} bound to Ti) depicted in Scheme 3.7, analogous to Cp*Ti{PhC(N^{i}Pr)$_2$}{SC(S)N(O^{t}Bu)} (**4**), Cp*Ti{PhC(N^{i}Pr)$_2$}{OC(NAr′)N(O^{t}Bu)} (**5**), and to the metallacyclobutene species formed between $Ar^{F_5}CCH$ and **3.14**, Cp*Ti{MeC(N^{i}Pr)$_2$}{N(NCPh$_2$)C(Ar^{F_5})C(H)} (**3.17**).[66]

However, the shift of δ 6.86 ppm for the alkyne-derived CC$\underline{H}$ is at much higher field than is usually found for such [2+2] cycloaddition products (for example δ 9.19 ppm in

the case of **3.17**).[37, 39, 85, 141, 149, 159] In addition, the ^{13}C resonances for the HCCAr^{F5} residue (δ 138.9 and 108.8 ppm, respectively) are also inconsistent with the formation of a cycloaddition product (δ 167.8 and 140.3 ppm for **3.17** by way of example). Most importantly, a ^{1}H-^{13}C HMBC experiment (Fig. 3.17) revealed coupling of the HCCAr^{F5}-derived hydrogen with one of the *iso*-propyl group NC(H)MeMe carbons and also between NC(H)MeMe and HCCAr^{F5}. A ^{1}H ROESY NMR experiment also showed through space interactions between one NC(H)MeMe and HCCAr^{F5}. Considering these NMR data the product is assigned as Cp*Ti(O^{t}Bu){NC(Ar^{F5})C(H)N(^{i}Pr)C(Ph)N(^{i}Pr)} (**14**, Scheme 3.7).

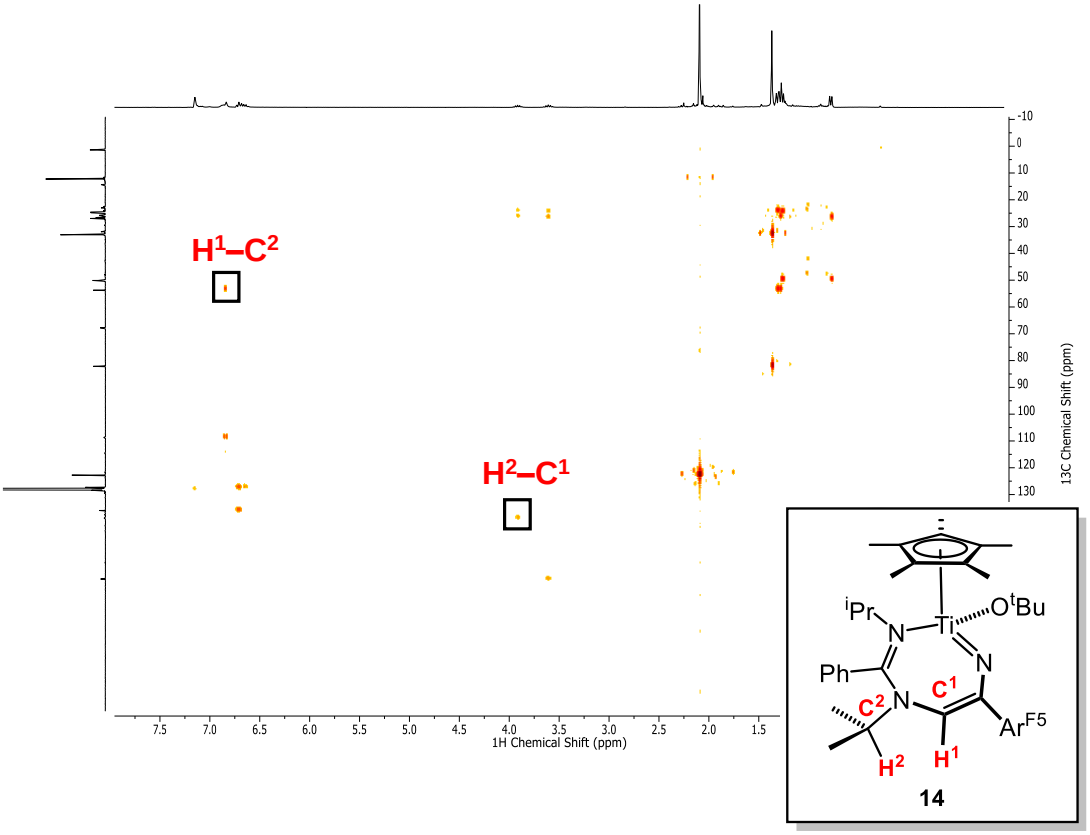

Figure 3.17. Gradient selective ^{1}H-^{13}C Heteronuclear Multiple-Bond Correlation (HMBC) NMR spectrum for Cp*Ti(O^{t}Bu){NC(Ar^{F5})C(H)N(^{i}Pr)C(Ph)N(^{i}Pr)} (**14**).

The mechanism of formation of **14**, given in Scheme 3.7, is probably similar to that previously described for formation of **3.7** and **3.9** (Fig. 3.2) and recent hydrazide reactions involving azirinyl intermediates.[37, 54, 58, 68, 73] Thus initial cycloaddition (**14_int1**) precedes N_{α}–O_{β} bond cleavage and formation of an azirinyl intermediate (**14_int2**). This in turn undergoes nucleophilic attack by one of the amidinate nitrogens. Non-innocent behaviour of an amidinate ligand in these types of complexes is not unprecedented, having previously been observed in the reaction of

Cp*Ti{MeC(N^{i}Pr)$_2$}(N^{t}Bu) (**3.10**) with CS_2 which involves insertion of CS_2 into a Ti–$N_{amidinate}$ bond generating crystallographically authenticated [Cp*Ti{N(^{i}Pr)C(Me)N(^{i}Pr)C(S)S}(μ-S)]$_2$ (**3.18**).[89]

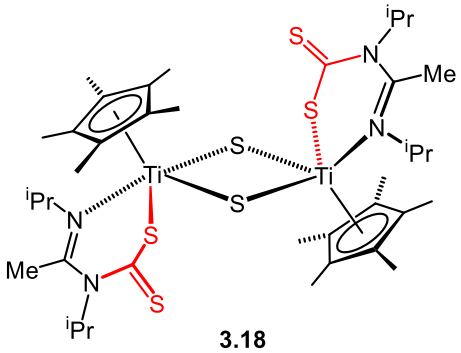

3.18

Unfortunately, while the reaction of **3** shows that reductive cleavage of the alkoxyimido N_α–O_β bond is possible with the appropriate alkyne, treatment with CO or the isonitriles XylNC or ^{t}BuNC (reagents that are known to induce N_α–N_β bond cleavage in a number of hydrazido compounds[21, 39, 46]) led to the formation of complex and unknown mixtures and these reactions were not investigated further.

3.7 Alkylation, protonation and related reactions

Since the discovery that Group 6 hydrazide compounds were found to be possible intermediates in the reduction of dinitrogen to ammonia[160] reactions of these complexes with proton sources and alkylating agents have been intensely explored.[71, 72, 161] Reactions with alkyl halides resulted in alkylation at N_β whereas protonation reactions resulted in reaction at either N_α or N_β. Although analogous reactions with Group 4 hydrazides are much more limited,[24, 31] a recent detailed study from our group showed that reaction of Cp*Ti{MeC(N^{i}Pr)$_2$}(NNMe$_2$) (**3.13**) with alkyl halides (MeI, EtBr and PhCH$_2$Br) resulted exclusively in alkylation at N_β whereas protonation with [Et$_3$NH][BPh$_4$] gave exclusively protonation of N_α.[41, 44] So as to understand better the nature of the Group 4 M=NO^{t}Bu group, reactions of **3** with a number of potential Brønsted and Lewis acids were carried out.

Reactions of **3** with the alkylating agents MeI, [Me$_3$O][BF$_4$] and Me$_2$SO$_4$ were disappointing, ultimately resulting in unknown mixtures. Reaction with [HNEt$_3$][BPh$_4$] in THF-d_8 required 2 equivs to reach completion, yielding a new set of resonances in the ^{1}H NMR spectrum consistent with NEt$_3$ and apparently a new titanium complex. Removal of the THF-d_8 and NEt$_3$ by-product and re-dissolving the remaining solid in

C_6D_5Br resulted in diffraction-quality colourless crystals. Single crystal X-ray diffraction showed these to be $[PhC(N^iPrH)_2][BPh_4]$ (**15-BPh$_4$**, Eq 3.3).

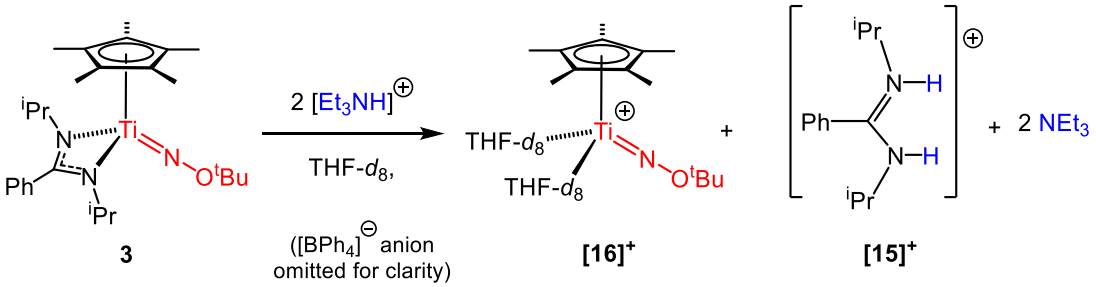

Equation 3.3

The molecular structure and selected bond lengths and angles are given in Fig. 3.18 and Table 3.7 and the metric data are within the expected ranges. Compound **15-BPh$_4$** was independently synthesised *via* anion exchange between $[PhC(N^iPrH)_2]Cl$ and $Na[BPh_4]$ and isolated in 63% yield. $[Cp^*Ti(NO^tBu)(THF)_2][BPh_4]$ (**16-BPh$_4$**, Eq 3.3) is formed alongside **15-BPh$_4$**. Attempts to isolate **16-BPh$_4$** on scale up either as the THF or bipy adduct (to form a less labile species) were unsuccessful. However, direct evidence for **16**$^+$ was found using positive ion electrospray mass spectrometry for a solution of **15** and **16** generated *in situ* in THF-d_8. Complexes with both one and two coordinated THF molecules were identified in the mass spectrum with the correct isotope distribution (*m/z* = 343 and 415, respectively).

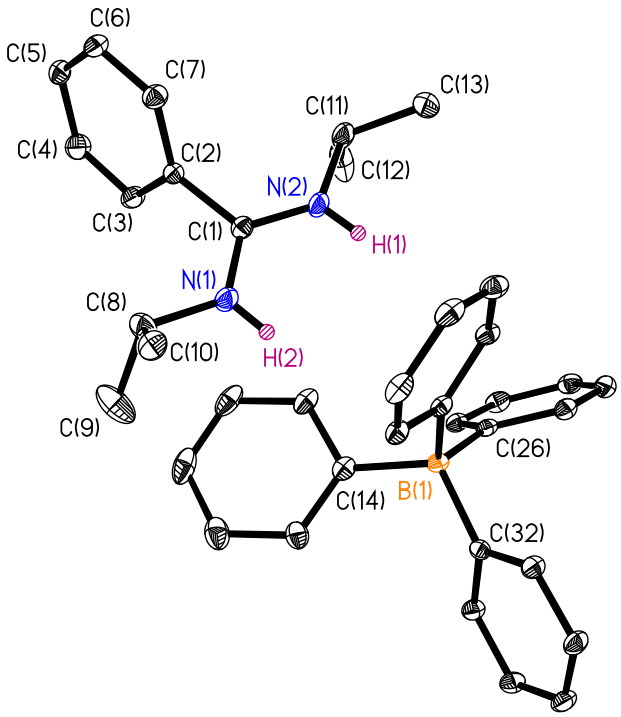

Figure 3.18. Displacement ellipsoid plot (20 % probability) of $[PhC(N^iPrH)_2][BPh_4]$ (**15-BPh$_4$**). C-bound H atoms omitted for clarity.

Table 3.7. Selected bond lengths (Å) and angles (°) for $[PhC(N^iPrH)_2][BPh_4]$ (**15-BPh$_4$**).

N(1)-C(1)	1.3061(17)	N(1)-C(1)-N(2)	120.16(12)
N(1)-C(8)	1.4847(17)	H(2)-N(1)-C(1)	118.4(11)
N(2)-C(1)	1.3159(17)	H(1)-N(2)-C(1)	120.1(11)
N(2)-C(11)	1.4809(18)		
C(1)-C(2)	1.4901(18)		

Group 4 hydrazides $M(N_2^RN^{py})(NNPh_2)(py)$ are known to readily form zwitterionic N_α-adducts of the type $M(N_2^RN^{py})\{\eta^2\text{-}N(NPh_2)B(Ar^{F5})_3\}$ (**3.19**; $N_2^RN^{py}$ = (2-NC_5H_4)$CMe(CH_2NR)_2$; M = Ti, R = $SiMe_3$ (**a**); M = Zr (**b**) or Hf (**c**), R = $SiMe_2{}^tBu$)) with $B(Ar^{F5})_3$.[39, 47] On the other hand, although **3.13** showed no apparent reactivity towards $B(Ar^{F5})_3$,[44] it was hoped that the corresponding reaction of **3** with $B(Ar^{F5})_3$ might nevertheless provide additional insight into the chemistry of the alkoxyimido functional group.

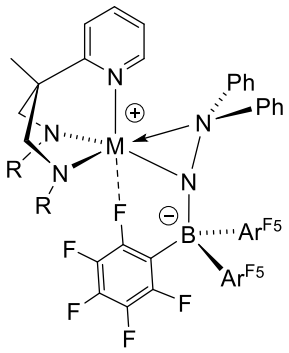

3.19

Compound **3** reacted very slowly with 1 equiv of $B(Ar^{F5})_3$ in C_6D_6 at room temperature, giving less than 10% conversion to a new compound, $Cp^*Ti\{PhC(N^iPr)_2\}\{\eta^2\text{-}ON(H)B(Ar^{F5})_3\}$ (**17**), after 24 h. Heating for 5 d at 70 °C drove the reaction to *ca*. 70% completion, and use of an excess of borane also effected complete conversion at room temperature after 2 d (after which time the excess borane remained unreacted). When monitored by ^{1}H NMR, *iso*-butene was also formed (either at room temperature or at 70 °C) alongside **17** as judged by multiplet and triplet (^4J = 1.2 Hz) resonances at δ 4.74 (2 H) and 1.58 (6 H) ppm (Fig. 3.20).[162, 163] The reaction was scaled up in benzene at 70 °C for 16 h to give **17** as an orange crystalline solid whose identity was confirmed by single crystal X-ray diffraction. The molecular structure is shown in Fig. 3.19 and selected bond lengths and angles in Table 3.8.

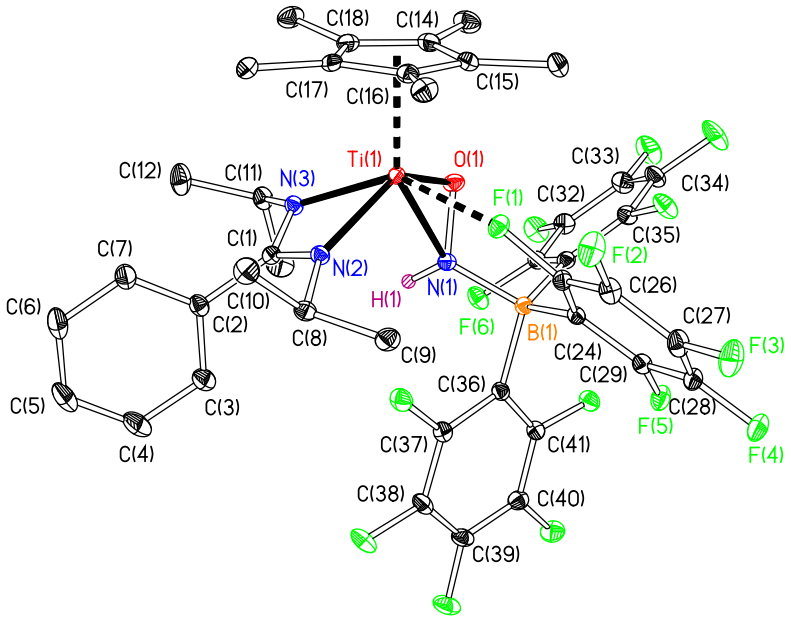

Figure 3.19. Displacement ellipsoid plot (20% probability) of Cp*Ti{PhC(N^{i}Pr)$_2$}{η^2-ON(H)B(Ar^{F_5})$_3$} (**17**). C-bound H atoms omitted for clarity.

Table 3.8. Selected bond lengths (Å) and angles (°) for Cp*Ti{PhC(N^{i}Pr)$_2$}{η^2-ON(H)B(Ar^{F_5})$_3$} (**17**). Cp$_{cent}$ is the computed centroid for the Cp* ring carbons.

Ti(1)-Cp$_{cent}$	2.063	Cp$_{cent}$-Ti(1)-N(1)	147.04
Ti(1)-N(1)	2.1242(12)	Cp$_{cent}$-Ti(1)-N(2)	116.16
Ti(1)-N(2)	2.1620(11	Cp$_{cent}$-Ti(1)-N(3)	110.77
Ti(1)-N(3)	2.0576(11)	Cp$_{cent}$-Ti(1)-O(1)	106.97
T(1)-O(1)	1.8549(10)	Cp$_{cent}$-Ti(1)-F(1)	101.30
Ti(1)-F(1)	2.2903(8)	N(2)-Ti(1)-N(3)	63.23(4)
N(1)-B(1)	1.5850(18)	N(1)-Ti(1)-O(1)	41.72(4)
N(1)-O(1)	1.4392(14)	Ti(1)-N(1)-O(1)	59.07(6)
C(25)-F(1)	1.3814(16)	Ti(1)-O(1)-N(1)	79.21(6)
		Ti(1)-N(1)-B(1)	139.51(9)

Compound **17** is a half-sandwich titanium complex with η^5-C_5Me_5, κ^2*N*,*N*′ amidinate, η^2-ON(H)B(Ar^{F_5})$_3$ ligands as well as a Ti···F interaction between the metal and an *o*-C_6F_5 fluorine atom. The distances and angles associated with the Cp*Ti{PhC(N^iPr)$_2$} fragment are unexceptional and so this discussion will focus on the ON(H)B(Ar^{F_5})$_3$ moiety which formally comprises a HNO (nitroxyl) ligand[164] additionally N-bound to B(Ar^{F_5})$_3$. Four structurally characterised complexes containing HNO as a ligand, either with η^2- (one example) or η^1- (three examples, all N-bound) coordination, and over 20 with N-substituted η^2-ON(H)R ligands (avg. N–O distance = 1.396 Å, range 1.371 – 1.498 Å) have been reported, all for transition metals in Groups 5 – 9.[96] With respect to titanium, seven Ti(+4) complexes with η^2-ON(R)R′ ligands (R, R′ = alkyl) have been structurally authenticated (avg. distances (range): N–O = 1.429 (1.402 – 1.446), Ti–O = 1.912 (1.872 –1.980), Ti–N = 2.128 (2.095 – 2.230) Å),[96] for example Ti(η^2-$ONMe_2$)$_4$ and Cp*$TiMe_2${η^2-ON(^{t}Bu)Me}.[165, 166] The Ti(1)–O(1), Ti(1)–N(1) and N(1)–O(1) distances for **17** lie near to or within these ranges. The N(1)–B(1) bond length of 1.5850(18) Å in **17** is comparable to those in M($N_2^RN^{py}$){η^2-N(NPh_2)B(Ar^{F_5})$_3$} (**3.19**, 1.562(3) – 1.598(3) Å)[39, 47] and also, for example, [B(Ar^{F_5})$_3$(N_3)]$^-$ (1.583(2) Å),[167] Ti(NEt_2)$_3${NH_2B(Ar^{F_5})$_3$} (1.595(3) Å) and CpTi(NMe_2)$_2${NH_2B(Ar^{F_5})$_3$} (1.598(2) Å).[168] The Ti(1)···F(1) interaction in **17** (2.2903(8) Å, which is less than the sum of the van der Waals radii of 3.92 Å[169]) is electrostatic in nature and presumably augmented by the formal positive charge on titanium. A similar Ti···F interaction was found in Ti($N_2^{SiMe_3}N^{py}$){η^2-N(NPh_2)B(Ar^{F_5})$_3$} (**3.19a**),[39] albeit with a slightly longer distance of 2.4840(15) Å. Also, as found in **3.19a**, there is a small but significant lengthening of the C(25)–F(1) bond (1.3814(16) Å) compared to the other aryl C–F bond lengths (range 1.3361(17) – 1.3565(16) Å). Taken together, these structural parameters are consistent with the zwitterionic representation of **17** shown in Scheme 3.8. Furthermore, **17** is therefore the first fully authenticated nitroxyl complex of a Group 4 metal, stabilised by borane coordination.

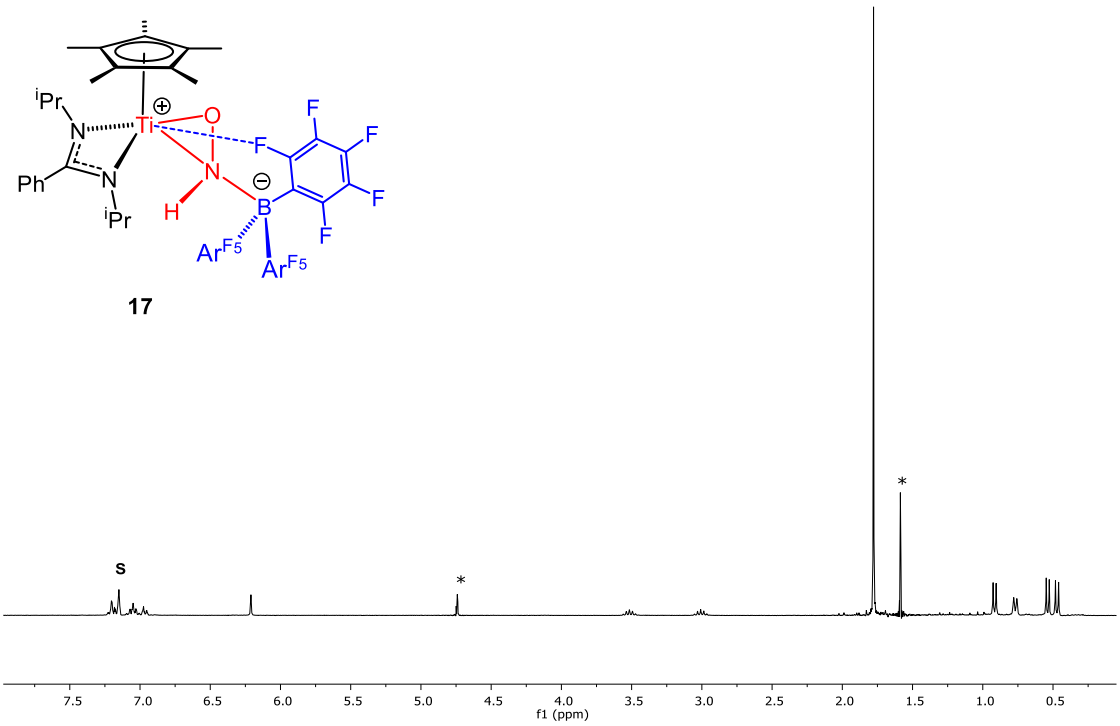

Figure 3.20. ^{1}H NMR spectrum (299.9 MHz, 293 K) of Cp*Ti{PhC(N^{i}Pr)$_2$}{η^2-ON(H)B(Ar^{F5})$_3$} (**17**) in C_6D_6 ("s" denotes residual protio-solvent, resonances marked with * correspond to *iso*-butene).

The spectroscopic data for **17** are consistent with the solid state structure. The ^{1}H and ^{13}C data, Fig. 3.20, are indicative of a C_1 symmetric complex containing Cp* and PhC(N^{i}Pr)$_2$ ligands, but no *tert*-butyl group, this being the source of the eliminated *iso*-butene. A signal at δ 6.05 ppm (in CD_2Cl_2) is assigned to the N-bound hydrogen, and the IR spectrum shows a ν(N-H) band at 3296 cm^{-1}. The ^{11}B NMR spectrum shows a resonance at δ -8 ppm, consistent with a tetra-coordinate boron.[170] Note that at room temperature no exchange between free and coordinated B(Ar^{F5})$_3$ is observed on the NMR timescale. The ^{19}F NMR spectrum of pure **17** is broad at room temperature, but on cooling to -20 °C shows 13 separate fluorine environments. Examination of the relative intensities and changes in appearance on warming to room temperature establishes that, at -20 °C, two of the C_6F_5 rings display restricted rotation on the NMR timescale whereas one is able to rotate relatively freely. From the appropriate coalescence points the activation free energies for exchange *within* and *between* the rings was found to be comparable within error ($\Delta G^{\ddagger}$ = 13.1(1) and 12.7(1) kcal mol^{-1} at 291 and 268 K, respectively) indicating a geared process as illustrated in Scheme 3.8.[171]

Scheme 3.8. Mechanism for Ar^{F5} ring exchange in Cp*Ti{PhC(N^{i}Pr)$_2$}-{η^2-ON(H)B(Ar^{F5})$_3$} (**17**)

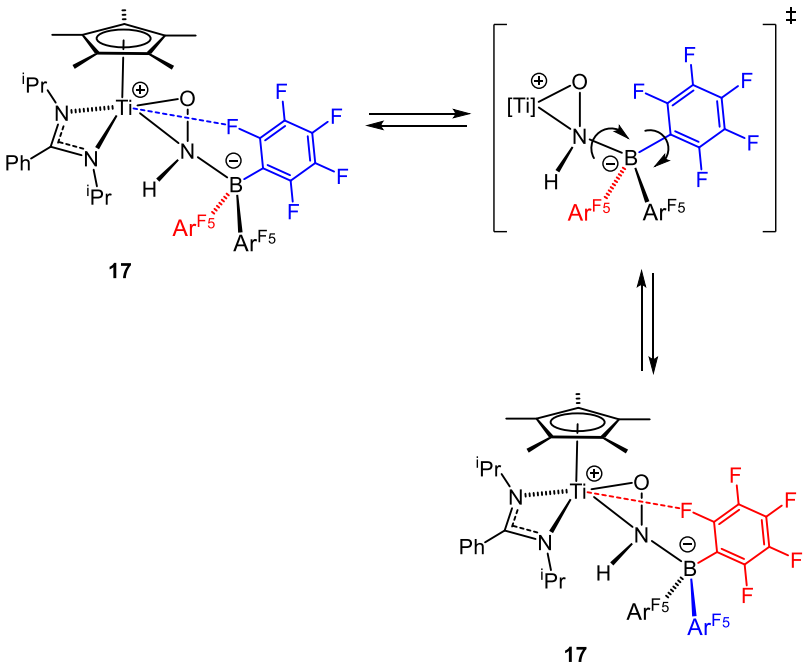

A proposed mechanism for formation of **17** is given in Scheme 3.9. Since **3** itself is thermally stable at 70 °C for several days in solution it is proposed that *iso*-butene elimination is preceded by borane coordination to the alkoxyimido nitrogen in an analogous manner to that in M($N_2^RN^{py}$){η^2-N(NPh_2)B(Ar^{F5})$_3$} (**3.19**). This generates a formally zwitterionic species, potentially with coordination of the O-*tert*-butyl group to the formally cationic metal center, depicted as **17_int**. Indeed, *iso*-butene elimination is not uncommon from cationic Group 4 complexes containing either *tert*-butoxy ligands[172] or ligands with –O^{t}Bu substituents such as Carpentier's cationic *tert*-butyl enolate systems.[162, 173] Subsequent intramolecular hydrogen transfer to nitrogen leads to alkene elimination and formation of the new borane-stabilised nitroxyl ligand. Finally it is noted that whereas $AlMe_3$ readily coordinates to the oxygen atom of Cp*$TiMe_2$(η^2-$ONEt_2$) to form Cp*$TiMe_2$\{η^2-O($AlMe_3$)NEt_2\},[174] excess B(Ar^{F5})$_3$ does not coordinate to the nitroxyl oxygen of **17**.

Scheme 3.9. Reaction of Cp*Ti{PhC(N^{i}Pr)$_2$}(NO^{t}Bu) (**3**) with B(Ar^{F5})$_3$ and proposed mechanism for formation of Cp*Ti{PhC(N^{i}Pr)$_2$}{η^2-ON(H)B(Ar^{F5})$_3$} (**17**).

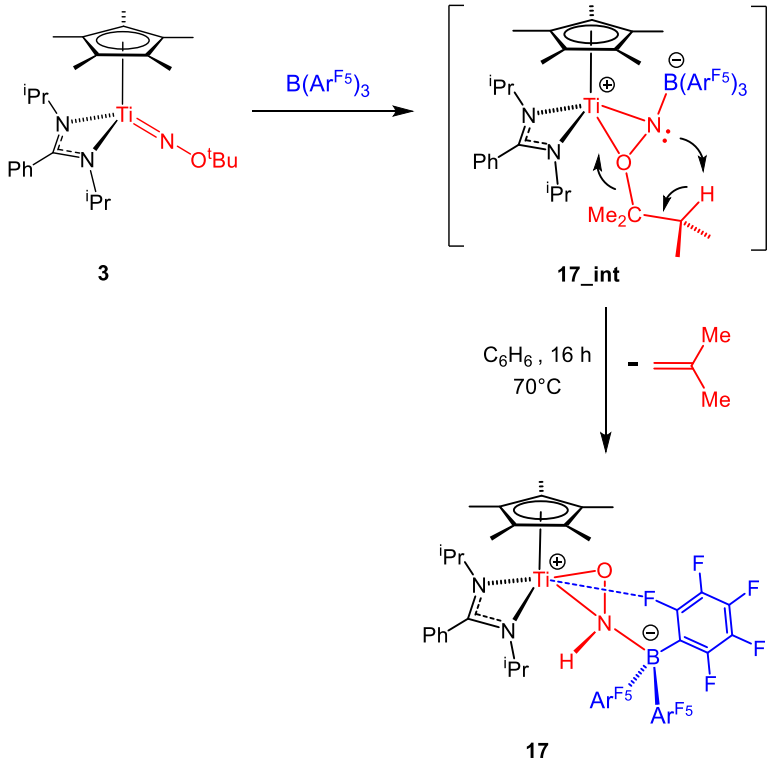

3.8 Conclusions

This Chapter has reported the first use of imide/alkoxyamine exchange to synthesise new alkoxyimido complexes, namely Cp*Ti{MeC(N^{i}Pr)$_2$}(NO^{t}Bu) (**1**) and Cp*Ti{PhC(N^{i}Pr)$_2$}(NO^{t}Bu) (**3**). Following this, the first thorough investigation into the reactions of alkoxyimido complexes with small molecules was undertaken. The reaction outcomes are reminiscent of those seen with imido, diphenyl and dimethyl and alkylidene hydrazido compounds. Although reaction with CO_2 produced complicated mixtures, addition of CS_2 gave the stable cycloaddition product Cp*Ti{PhC(N^{i}Pr)$_2$}{SC(S)N(O^{t}Bu)} (**4**). The reactions of **3** with isocyanates were dependent on the steric bulk of the isocyanate substituent. Thus with Ar′NCO the cycloaddition product Cp*Ti{PhC(N^{i}Pr)$_2$}{N(O^{t}Bu)C(NAr′)O} (**5**) was isolated, with TolNCO 2 equivs were needed to synthesise the "rearranged-double insertion" product Cp*Ti{PhC(N^{i}Pr)$_2$}{OC(NTol)N(Tol)C(NO^{t}Bu)O} (**6**), and finally with ^{t}BuNCO the carbodiimide derivative ^{t}BuONCN^{t}Bu (**8**) was formed following extrusion from the unstable cycloaddition intermediate. Cycloaddition-extrusion reaction pathways were also seen with aldehydes and ketones generating the oxo-dimer (**7**) and corresponding

oxime ethers PhC(NO^{t}Bu)H (**9a**) and PhC(NO^{t}Bu)Me (**9b**) as a mixture of geometric isomers. DFT calculations showed that the product distribution was attributed to the energy barrier to cycloaddition formation. The reaction also yielded the new oxime ether PhC(NO^{t}Bu)Ph (**9c**) in high yield, which was inaccessible following alternative routes. Reactions of **3** with $Ar^{F5}CN$ and $Ar^{F2}CN$ led to the net Ti=N_α insertion products Cp*Ti{PhC(N^{i}Pr)$_2$}{NC(Ar^{Fx})NO^{t}Bu} (Ar^{Fx} = Ar^{F5} (**10**) or Ar^{F2} (**11**)). With an excess of $Ar^{F5}CN$, the unusual insertion compound Cp*Ti{PhC(N^{i}Pr)$_2$}{N(C{Ar^{F5}}NO^{t}Bu)C(Ar^{F5})NC(Ar^{F5})N} (**13**) was formed. Reaction with both $Ar^{F5}CCH$ and [HNEt$_3$][BPh$_4$] led to reactions involving the amidinate supporting ligand, with reaction using $Ar^{F5}CCH$ inducing N_α–O_β bond cleavage and [HNEt$_3$][BPh$_4$] giving protonation of the amidinate ligand. Finally reaction with B(Ar^{F5})$_3$ resulted in loss of *iso*-butene to give Cp*Ti{PhC(N^{i}Pr)$_2$}{η^2-ON(H)B(Ar^{F5})$_3$} (**17**) the first example of a HNO (nitroxyl) adduct for a Group 4 metal (with B(Ar^{F5})$_3$ stabilisation).

Further work on alkoxyimide complexes currently involves supporting ligand development in order to provide a more suitable framework for alkyne insertion into the N_α–O_β bond, with the ultimate target of catalytic 1,2-oximination reactions. Synthesis of the first zirconium alkoxyimido complex or the investigation of other (L)Ti=N–X systems where X is boron, phosphorus or sulfur are also planned.

3.9 References

1. D. E. Wigley, *Prog. Inorg. Chem.*, 1994, **42**, 239.
2. A. P. Duncan and R. G. Bergman, *The Chemical Record*, 2002, **2**, 431.
3. P. Mountford, *Chem. Commun.*, 1997, 2127.
4. L. H. Gade and P. Mountford, *Coord. Chem. Rev.*, 2001, **216-217**, 65.
5. N. Hazari and P. Mountford, *Acc. Chem. Res.*, 2005, **38**, 839.
6. A. R. Fout, U. J. Kilgore and D. J. Mindiola, *Chem. Eur. J.*, 2007, **13**, 9428.
7. C. M. Kozak and P. Mountford, *Angew. Chem. Int. Ed.*, 2004, **43**, 1186
8. T. R. Cundari, *J. Am. Chem. Soc.*, 1992, **114**, 7879.
9. Z. Lin and M. B. Hall, *Coord. Chem. Rev.*, 1993, **123**, 149.
10. P. Mountford and D. Swallow, *J. Chem. Soc., Chem. Commun.*, 1995, 2357.
11. N. Kaltsoyannis and P. Mountford, *J. Chem. Soc., Dalton Trans.*, 1999, 781.
12. T. R. Cundari, *Chem. Rev.*, 2000, **100**, 807.

13. A. D. Schwarz, A. J. Nielson, N. Kaltsoyannis and P. Mountford, *Chem. Sci.*, 2012, **3**, 819.
14. S. C. Dunn, N. Hazari, N. M. Jones, A. G. Moody, A. J. Blake, A. R. Cowley, J. C. Green and P. Mountford, *Chem. Eur. J.*, 2005, **11**, 2111.
15. For ease of representation the Ti−NX (X = R, NR_2, OR) moieties are all drawn as "Ti=N", although in most cases the Ti−N linkage is best considered to be a triple bond.
16. I. Bytschkov and S. Doye, *Eur. J. Org. Chem.*, 2003, 935.
17. S. Doye, *Synlett*, 2004, 1653.
18. L. L. Schafer and A. V. Lee, *Eur. J. Inorg. Chem.*, 2007, 2243.
19. T. E. Müller, K. C. Hultzsch, M. Yus, F. Foubelo and M. Tada, *Chem. Rev.*, 2008, **108**, 3795.
20. N. Wiberg, H.-W. Haring, G. Huttner and P. Friedrich, *Chem. Ber.*, 1978, **111**, 2708.
21. P. J. Walsh, M. J. Carney and R. G. Bergman, *J. Am. Chem. Soc.*, 1991, **113**, 6343.
22. A. J. Blake, J. M. McInnes, P. Mountford, G. I. Nikonov, D. Swallow and D. J. Watkin, *J. Chem. Soc., Dalton Trans.*, 1999, 379.
23. J. L. Thorman and L. K. Woo, *Inorg. Chem.*, 2000, **39**, 1301.
24. Y. Li, Y. Shi and A. L. Odom, *J. Am. Chem. Soc.*, 2004, **126**, 1794.
25. S. Banerjee, Y. Shi, C. Cao and A. L. Odom, *J. Organomet. Chem.*, 2005, **690**, 5066.
26. T. B. Parsons, N. Hazari, A. R. Cowley, J. C. Green and P. Mountford, *Inorg. Chem.*, 2005, **44**, 8442.
27. S. Banerjee and A. L. Odom, *Organometallics*, 2006, **25**, 3099.
28. S. Patel, Y. Li and A. L. Odom, *Inorg. Chem.*, 2007, **46**, 6373.
29. J. D. Selby, C. D. Manley, M. Feliz, A. D. Schwarz, E. Clot and P. Mountford, *Chem. Commun.*, 2007, 4937.
30. S. Banerjee, E. Barnea and A. L. Odom, *Organometallics*, 2008, **27**, 1005.
31. A. J. Clulow, J. D. Selby, M. G. Cushion, A. D. Schwarz and P. Mountford, *Inorg. Chem.*, 2008, **47**, 12049.
32. J. D. Selby, C. D. Manley, A. D. Schwarz, E. Clot and P. Mountford, *Organometallics*, 2008, **27**, 6479.

33. J. D. Selby, C. Schulten, A. D. Schwarz, A. Stasch, E. Clot, C. Jones and P. Mountford, *Chem.Commun.*, 2008, 5101.
34. K. Weitershaus, J. L. Fillol, H. Wadepohl and L. H. Gade, *Organometallics*, 2009, **28**, 4747.
35. K. Weitershaus, H. Wadepohl and L. H. Gade, *Organometallics*, 2009, **28**, 3381.
36. T. Janssen, R. Severin, M. Diekmann, M. Friedemann, D. Haase, Saak, W., S. Doye and R. Beckhaus, *Organometallics*, 2010, **29**, 1806.
37. A. D. Schofield, A. Nova, J. D. Selby, C. D. Manley, A. D. Schwarz, E. Clot and P. Mountford, *J. Am. Chem. Soc.*, 2010, **132**, 10484.
38. P. J. Tiong, A. D. Schofield, J. D. Selby, A. Nova, E. Clot and P. Mountford, *Chem. Commun.*, 2010, **46**, 85.
39. A. D. Schofield, A. Nova, J. D. Selby, A. D. Schwarz, E. Clot and P. Mountford, *Chem. Eur. J.*, 2011, **17**, 265.
40. J. D. Selby, M. Feliz, A. D. Schwarz, E. Clot and P. Mountford, *Organometallics*, 2011, **30**, 2295.
41. P. J. Tiong, A. Nova, E. Clot and P. Mountford, *Chem. Commun.*, 2011, **47**, 3147.
42. P. J. Tiong, A. Nova, L. R. Groom, A. D. Schwarz, J. D. Selby, A. D. Schofield, E. Clot and P. Mountford, *Organometallics*, 2011, **30**, 1182.
43. A. D. Schwarz, C. S. Onn and P. Mountford, *Angew. Chem. Int. Ed.*, 2012, **51**, 12298.
44. P. J. Tiong, A. Nova, A. D. Schwarz, J. D. Selby, E. Clot and P. Mountford, *Dalton Trans.*, 2012, **41**, 2277.
45. P. D. Schweitzer, H. Wadepohl and L. H. Gade, *Organometallics*, 2013, **32**, 3697.
46. H. Herrmann, J. L. Fillol, H. Wadepohl and L. H. Gade, *Angew. Chem. Int. Ed.*, 2007, **46**, 8426.
47. H. Herrmann, J. L. Fillol, T. Gehrmann, M. Enders, H. Wadepohl and L. H. Gade, *Chem. Eur. J.*, 2008, **14**, 8131.
48. H. Herrmann, J. L. Fillol, H. Wadepohl and L. H. Gade, *Organometallics*, 2008, **27**, 172.
49. H. Herrmann, T. Gehrmann, H. Wadepohl and L. H. Gade, *Dalton Trans.*, 2008, 6231.

50. H. Herrmann, H. Wadepohl and L. H. Gade, *Dalton Trans.*, 2008, 2111.
51. T. Gehrmann, J. L. Fillol, H. Wadepohl and L. H. Gade, *Angew. Chem. Int. Ed.*, 2009, **48**, 2152.
52. R. F. Munha, L. F. Veiros, M. T. Duarte, M. D. Fryzuk and A. M. Martins, *Dalton Trans.*, 2009, 7494.
53. T. Gehrmann, J. L. Fillol, H. Wadepohl and L. H. Gade, *Organometallics*, 2010, **29**, 28.
54. T. Gehrmann, J. L. Fillol, S. A. Scholl, H. Wadepohl and L. H. Gade, *Angew. Chem. Int. Ed.*, 2011, **50**, 5757.
55. T. Gehrmann, J. L. Fillol, H. Wadepohl and L. H. Gade, *Organometallics*, 2012, **31**, 4504.
56. T. Gehrmann, M. Kruck, H. Wadepohl and L. H. Gade, *Chem. Commun.*, 2012, **48**, 2397.
57. T. Gehrmann, G. T. Plundrich, H. Wadepohl and L. H. Gade, *Organometallics*, 2012, **31**, 3346.
58. T. Gehrmann, S. A. Scholl, J. L. Fillol, H. Wadepohl and L. H. Gade, *Chem. Eur. J.*, 2012, **18**, 3925.
59. S. A. Scholl, G. T. Plundrich, H. Wadepohl and L. H. Gade, *Inorg. Chem.*, 2013, **52**, 10158.
60. S. A. Scholl, H. Wadepohl and L. H. Gade, *Organometallics*, 2013, **32**, 937.
61. L. B. Kool, M. D. Rausch, H. G. Alt, M. Herberhold, A. F. Hill, U. Thewalt and B. Wolf, *J. Chem. Soc., Chem. Commun.*, 1986, 408.
62. G. M. Arvanitis, J. Smegal, I. Meier, A. C. C. Wong, J. Schwartz and D. Van Engen, *Organometallics*, 1989, **8**, 2717.
63. A. W. Kaplan, J. L. Polse, G. E. Ball, R. A. Andersen and R. G. Bergman, *J. Am. Chem. Soc.*, 1998, **120**, 11649.
64. J. L. Polse, A. W. Kaplan, R. A. Andersen and R. G. Bergman, *J. Am. Chem. Soc.*, 1998, **120**, 6316.
65. T. E. Hanna, I. Keresztes, E. Lobkovsky, W. H. Bernskoetter and P. J. Chirik, *Organometallics*, 2004, **23**, 3448.
66. P. J. Tiong, L. R. Groom, E. Clot and P. Mountford, *Chem. Eur. J.*, 2013, **19**, 4198.
67. S. Kahlal, J.-Y. Saillard, J.-R. Hamon, C. Manzur and D. Carrillo, *J. Chem. Soc., Dalton Trans.*, 1998, 1229.

68. J. Unruangsri, H. Morgan, A. D. Schwarz, A. D. Schofield and P. Mountford, *Organometallics*, 2013, **32**, 3091.
69. B. F. G. Johnson, B. L. Haymore and J. D. Dilworth, in *Comprehensive Coordination Chemistry*, eds. G. Wilkinson, R. D. Gillard and J. A. McCleverty, Pergamon Press, Oxford, 1987, vol. 2, p. 100.
70. W. A. Nugent and J. M. Mayer, *Metal-Ligand Multiple Bonds*, Wiley-Interscience, New York, 1988.
71. R. R. Schrock, *Acc. Chem. Res.*, 2005, **38**, 955.
72. M. Hidai, *Coord. Chem. Rev.*, 1999, **185-186**, 99.
73. A. D. Schwarz, A. Nova, E. Clot and P. Mountford, *Chem. Commun.*, 2011, **47**, 4926.
74. A. D. Schwarz, A. Nova, E. Clot and P. Mountford, *Inorg. Chem.*, 2011, **50**, 12155.
75. A. van Asselt, B. D. Santarsiero and J. E. Bercaw, *J. Am. Chem. Soc.*, 1986, **108**, 8291.
76. R. E. Stevens and W. L. Gladfelter, *J. Am. Chem. Soc.*, 1982, **104**, 6454.
77. K. Haug, W. Hiller and J. Strähle, *Z. Anorg. Allg. Chem.*, 1986, **533**, 49.
78. M. L. H. Green, J. T. James and J. F. Sanders, *Chem. Commun.*, 1996, 1343.
79. W. B. Sharp, P. J. Daff, W. S. McNeil and P. Legzdins, *J. Am. Chem. Soc.*, 2001, **123**, 6272.
80. K. Arashiba, S. Matsukawa, S. Kuwata, Y. Tanabe, M. Iwasaki and Y. Ishii, *Organometallics*, 2006, **25**, 560.
81. K. K.-H. Lee and W. T. Wong, *J. Organomet. Chem.*, 1999, **577**, 323.
82. M. E. Barr, A. Bjarnason and L. F. Dahl, *Organometallics*, 1994, **13**, 1981.
83. E. N.-M. Ho and W.-T. Wong, *J. Chem. Soc., Dalton Trans.*, 1998, 4215.
84. K. K.-H. Lee and W.-T. Wong, *J. Chem. Soc., Dalton Trans.*, 1996, 1707.
85. K. Weitershaus, B. D. Ward, R. Kubiak, C. Muller, H. Wadepohl, S. Doye and L. H. Gade, *Dalton Trans.*, 2009, 4586.
86. A. E. Guiducci, A. R. Cowley, M. E. G. Skinner and P. Mountford, *J. Chem. Soc., Dalton Trans.*, 2001, 1392.
87. C. L. Boyd, A. E. Guiducci, S. R. Dubberley, B. R. Tyrrell and P. Mountford, *J. Chem. Soc., Dalton Trans.*, 2002, 4175.
88. C. L. Boyd, E. Clot, A. E. Guiducci and P. Mountford, *Organometallics*, 2005, **24**, 2347.

89. A. E. Guiducci, C. L. Boyd and P. Mountford, *Organometallics*, 2006, **25**, 1167.
90. A. E. Guiducci, C. L. Boyd, E. Clot and P. Mountford, *Dalton Trans.*, 2009, 5960.
91. L. R. Groom, A. D. Schwarz, A. Nova, E. Clot and P. Mountford, *Organometallics*, 2013, **32**, 7520.
92. S. G. Davies, C. J. Goodwin, D. Hepworth, P. M. Roberts and J. E. Thomson, *J. Org. Chem.*, 2010, **75**, 1214.
93. J. Richter, J. Feiling, H.-G. Schmidt, M. Noltemeyer, W. Brueser and F. T. Edelmann, *Z. Anorg. Allg. Chem.*, 2004, **630**, 1269.
94. M. P. Coles, D. C. Swenson, R. F. Jordan and V. G. Young, *Organometallics*, 1997, **16**, 5183.
95. S. C. Dunn, P. Mountford and D. A. Robson, *J. Chem. Soc., Dalton Trans.*, 1997, 293.
96. D. A. Fletcher, R. F. McMeeking and D. Parkin, *J. Chem. Inf. Comput. Sci.*, 1996, **36**, 746 (The UK Chemical Database Service: CSD version 5.34 updated May 2013).
97. F. H. Allen, O. Kennard, D. G. Watson, L. Brammer, A. G. Orpen and R. Taylor, *J. Chem. Soc., Perkin Trans. 2*, 1987, S1.
98. F. Weinhold and C. R. Landis, *Valency and Bonding: A Natural Bond Orbital Donor-Acceptor Perspective*, Cambridge University Press, Cambridge, 2005.
99. A. J. Blake, P. E. Collier, S. C. Dunn, W.-S. Li, P. Mountford and O. V. Shishkin., *J. Chem. Soc., Dalton Trans.*, 1997, 1549.
100. C. E. Housemekerides, D. L. Ramage, C. M. Kretz, J. T. Shontz, R. S. Pilato, G. L. Geoffroy, A. L. Rheingold and B. S. Haggerty, *Inorg. Chem.*, 1992, **31**, 4453.
101. J. L. Polse, R. A. Andersen and R. G. Bergman, *J. Am. Chem. Soc.*, 1995, **117**, 5393.
102. D. H. Williams and I. Fleming, *Spectroscopic Methods in Organic Chemistry*, 5th edn., McGraw-Hill, 1995.
103. S. Sakai, T. Fujinami, N. Otani and T. Aizawa, *Chem. Lett.*, 1976, 811.
104. T. Kiyoi, N. Seko, K. Yoshino and Y. Ito, *J. Org. Chem.*, 1993, **58**, 5118.
105. J. Tang, T. Mohan and J. G. Verkade, *J. Org. Chem.*, 1994, **59**, 4931.
106. J. H. Cooley, E. J. Evain, R. D. Willett and J. T. Blanchette, *J. Org. Chem.*, 1989, **54**, 1048.

107. S. Sarker, J. H. Cooley, R. D. Willett and A. L. Rheingold, *J. Org. Chem.*, 1995, **60**, 476.
108. W. A. Nugent, R. J. McKinney, R. V. Kasowski and F. A. Van-Catledge, *Inorg. Chim. Acta.*, 1982, **65**, L91.
109. S. Y. Lee and R. G. Bergman, *J. Am. Chem. Soc.*, 1996, **118**, 6396.
110. K. M. Doxsee and J. B. Farahi, *J. Chem. Soc., Chem. Commun.*, 1990, 1452.
111. H. W. Turner, J. D. Fellmann, S. M. Rocklage, R. R. Schrock, M. R. Churchill and H. J. Wasserman, *J. Am. Chem. Soc.*, 1980, **102**, 7809.
112. B. Moubaraki, K. S. Murray, P. J. Nichols, S. Thomson and B. O. West, *Polyhedron*, 1994, **13**, 485.
113. P. Royo and J. Sánchez-Nieves, *J. Organomet. Chem.*, 2000, **597**, 61.
114. P. J. Walsh, F. J. Hollander and R. G. Bergman, *Organometallics*, 1993, **12**, 3705.
115. H. Wang, H. Chan and Z. Xie, *Organometallics*, 2005, **24**, 3772.
116. M. N. S. Rad, A. Khalafi-Nezhad, F. Karimitabar and S. Behrouz, *Synthesis*, 2010, 1724.
117. G. W. Buchanan and B. A. Dawson, *Can. J. Chem.*, 1978, **56**, 2200.
118. E. Buehler, *J. Org. Chem.*, 1967, **32**, 261.
119. A. J. McCarroll and J. C. Walton, *Perkin 2*, 2000, 1868.
120. L. H. J. P. De, N. A. Rangel, M. A. Tetalman and C.-K. Tsai, *J. Org. Chem.*, 2007, **72**, 4126.
121. L. H. J. P. De and C.-K. Tsai, *J. Org. Chem.*, 2004, **69**, 3057.
122. A. Padwa and F. Albrecht, *J. Am. Chem. Soc.*, 1972, **94**, 1000.
123. E. J. Grubbs and J. A. Villarreal, *Tetrahedron Lett.*, 1969, 1841.
124. D. Y. Curtin, E. J. Grubbs and C. G. McCarty, *J. Am. Chem. Soc.*, 1966, **88**, 2775.
125. I. Pejkovic-Tadic, M. Hranisavljevic-Jakovljevic, S. Nesic, C. Pascual and W. Simon, *Helv. Chim. Acta*, 1965, **48**, 1157.
126. M. H. Chisholm, E. E. Delbridge, A. R. Kidwell and K. B. Quinlan, *Chem. Commun.*, 2003, 126.
127. R. L. Gdula, M. J. A. Johnson and N. W. Ockwig, *Inorg. Chem.*, 2005, **44**, 9140.
128. C. D. Wood, S. J. McLain and R. R. Schrock, *J. Am. Chem. Soc.*, 1979, **101**, 3210.
129. R. R. Schrock and J. D. Fellmann, *J. Am. Chem. Soc.*, 1978, **100**, 3359.

130. K. M. Doxsee, J. B. Farahi and H. Hope, *J. Am. Chem. Soc.*, 1991, **113**, 8889.
131. B. Hessen, J.-K. F. Buijink, A. Meetsma, J. Teuben, G. Helgesson, M. Hakansson, S. Jagner and A. L. Spek, *Organometallics*, 1993, **12**, 2268.
132. F. Basuli, H. Aneetha, J. C. Huffman and D. J. Mindiola, *J. Am. Chem. Soc.*, 2005, **127**, 17992.
133. M. L. Listemann and R. R. Schrock, *Organometallics*, 1985, **4**, 74.
134. J. H. Freudenberger and R. R. Schrock, *Organometallics*, 1986, **5**, 398.
135. M. H. Chisholm, K. Folting, M. L. Lynn, D. B. Tiedtke, F. Lemoigno and O. Eisenstein, *Chem. Eur. J.*, 1999, **5**, 2318.
136. A. M. Geyer, R. L. Gdula, E. S. Wiedner and M. J. A. Johnson, *J. Am. Chem. Soc.*, 2007, **129**, 3800.
137. B. C. Bailey, A. R. Fout, H. Fan, J. Tomaszewski, J. C. Huffman, J. B. Gary, M. J. A. Johnson and D. J. Mindiola, *J. Am. Chem. Soc.*, 2007, **129**, 2234.
138. A. M. Geyer, E. S. Wiedner, J. B. Gary, R. L. Gdula, N. C. Kuhlmann, M. J. A. Johnson, B. D. Dunietz and J. W. Kampf, *J. Am. Chem. Soc.*, 2008, **130**, 8984.
139. S. M. Pugh, D. J. M. Trösch, D. J. Wilson, A. Bashall, F. G. N. Cloke, L. H. Gade, P. B. Hitchcock, M. McPartlin, J. F. Nixon and P. Mountford, *Organometallics*, 2000, **19**, 3205.
140. T. L. Breen and D. W. Stephan, *J. Am. Chem. Soc.*, 1995, **117**, 11914.
141. N. Vujkovic, B. D. Ward, A. Maisse-Francois, H. Wadepohl, P. Mountford and L. H. Gade, *Organometallics*, 2007, **26**, 5522.
142. K. S. Lokare, J. T. Ciszewski and A. L. Odom, *Organometallics*, 2004, **23**, 5386.
143. M. J. Carney, P. J. Walsh, F. J. Hollander and R. G. Bergman, *Organometallics*, 1992, **11**, 761.
144. J. H. Ansede, M. Anbazhagan, R. Brun, J. D. Easterbrook, J. E. Hall and D. W. Boykin, *J. Med. Chem.*, 2004, **47**, 4335.
145. P. L. McGrane, M. Jensen and T. Livinghouse, *J. Am. Chem. Soc.*, 1992, **114**, 5459.
146. P. L. McGrane and T. Livinghouse, *J. Am. Chem. Soc.*, 1993, **115**, 11485.
147. J. L. Bennett and P. T. Wolczanski, *J. Am. Chem. Soc.*, 1997, **119**, 10696.
148. J. L. Polse, R. A. Andersen and R. G. Bergman, *J. Am. Chem. Soc.*, 1998, **120**, 13405.

149. B. D. Ward, A. Maisse-Francois, P. Mountford and L. H. Gade, *Chem. Commun.*, 2004, 704.
150. G. Zhao, F. Basuli, U. J. Kilgore, H. Fan, H. Aneetha, J. C. Huffman, G. Wu and D. J. Mindiola, *J. Am. Chem. Soc.*, 2006, **128**, 13575.
151. C. Cao, Y. Shi and A. L. Odom, *Org. Lett.*, 2002, **4**, 2853.
152. L. Ackermann and R. Born, *Tet. Letts.*, 2004, **45**, 9541.
153. V. Khedkar, A. Tillack, M. Michalik and M. Beller, *Tet. Letts.*, 2004, **45**, 3123.
154. A. Tillack, H. Jiao, I. Garcia Castro, C. G. Hartung and M. Beller, *Chem. Eur. J.*, 2004, **10**, 2409.
155. A. L. Odom, *Dalton Trans.*, 2005, 225.
156. A. A. Dissanayake and A. L. Odom, *Chem. Commun.*, 2012, **48**, 440.
157. C. D. Manley, Part II Thesis (Honour School of Natural Science), University of Oxford, 2007.
158. R. E. Blake, D. M. Antonelli, L. M. Henling, W. P. Schaefer, K. I. Hardcastle and J. E. Bercaw, *Organometallics*, 1998, **17**, 718.
159. P. D. Bolton, M. Feliz, A. H. Cowley, E. Clot and P. Mountford, *Organometallics*, 2008, **27**, 6096.
160. J. Chatt, A. J. Pearman and R. L. Richards, *Nature*, 1975, **253**, 39.
161. M. D. Fryzuk, *The Chemical Record*, 2003, **3**, 2.
162. B. Lian, L. Toupet and J.-F. Carpentier, *Chem. Eur. J.*, 2004, **10**, 4301.
163. P. D. Bolton, N. Adams, E. Clot, A. R. Cowley, P. J. Wilson, M. Schröder and P. Mountford, *Organometallics*, 2006, **25**, 5549.
164. N. N. Greenwood and A. Earnshaw, *Chemistry of the Elements*, 2nd edn., Butterworth–Heinemann, Oxford, 1997.
165. N. W. Mitzel, S. Parsons, A. J. Blake and D. W. H. Rankin, *J. Chem. Soc., Dalton Trans.*, 1996, 2089.
166. A. P. Dove, X. Xie and R. M. Waymouth, *Chem.Commun.*, 2005, 2152.
167. W. Fraenk, T. M. Klapötke, B. Krumm, H. Nöth, M. Suter, M. Vogt and M. Warchhold, *Can. J. Chem.*, 2002, **80**, 1444.
168. A. J. Mountford, W. Clegg, S. J. Coles, R. W. Harrington, P. N. Horton, S. M. Humphrey, M. B. Hursthouse, J. A. Wright and S. J. Lancaster, *Chem. Eur. J.*, 2007, **13**, 4535.
169. S. Alvarez, *Dalton Trans.*, 2013, **42**, 8617.
170. S. Hermanek, *Chem. Rev.*, 1992, **92**, 325.

171. R. B. Jordan, *Reaction Mechanisms of Inorganic and Organometallic Systems*, Oxford University Press, Oxford, 1998.

172. E. J. Stoebenau and R. F. Jordan, *J. Am. Chem. Soc.*, 2003, **128**, 8162.

173. B. Lian, C. W. Lehmann, C. Navarro and J.-F. Carpentier, *Organometallics*, 2005, **24**, 2466.

174. A. P. Dove, E. T. Kiesewetter, X. Ottenwaelder and R. M. Waymouth, *Organometallics*, 2009, **28**, 405.

Chapter Four

Reactions of a cyclopentadienyl-amidinate titanium benzimidamido complex

4.1 Introduction

Chapter Three of this Thesis described the synthesis and reactions of alkoxyimide Cp*Ti{PhC(N^{i}Pr)$_2$}(NO^{t}Bu) (**3**). This work was inspired by developments in Group 4 imide, (L)M=NR, and hydrazide, (L)M=NNR$_2$ (M = Ti[1-26] and Zr[27-42] in particular) chemistry. The unsaturated M=N multiple bonds (formally $\sigma^2\pi^4$ triple bonds in most instances[12, 20, 43-49]) normally act as the reactive site in imido and hydrazido complexes and undergo a wide range of addition reactions with saturated and, especially, unsaturated substrates. In some instances, imides act only as supporting or spectator ligands, for example in the context of olefin polymerisation.[50-54] In addition to M=N$_\alpha$ bond reactivity, it has been shown that Group 4 hydrazido complexes can also undergo reductive cleavage (e.g. with CO,[27] isonitriles[19, 26, 28]) or reductive insertion (with alkynes[9, 17, 26, 40]) reactions of the N$_\alpha$–N$_\beta$ bonds. The cylopentadienyl-amidinate ligand platform was chosen having been used very successfully in the past to study the reactivity of a range of imido,[55-59] hydrazido[9, 18, 21, 22, 24] and alkylidene hydrazido (i.e. (L)Ti=NNCRR′)[49] complexes, therefore allowing meaningful comparisons with these related functional groups.

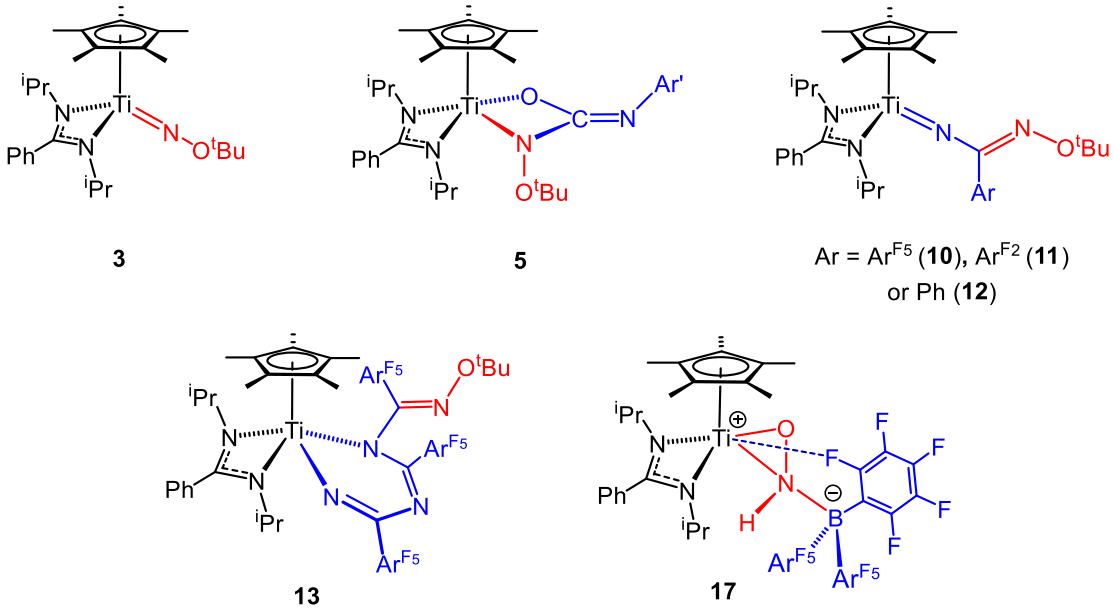

Figure 4.1. Cp*Ti{PhC(N^{i}Pr)$_2$}(NO^{t}Bu) (**3**) and its reaction products with Ar′NCO, B(Ar^{F5})$_3$ and benzonitriles. Atoms from the NO^{t}Bu ligand are shown in red and those from the organic substrates are shown in blue. Ar′ = 2,6-C$_6$H$_3$^{i}Pr$_2$, Ar^{F5} = C$_6$F$_5$.

The Ti=NO^{t}Bu moiety of **3** undergoes a number of new transformations for this type of functional group including: [2+2] cycloaddition reactions with CS_2 and Ar′NCO (forming **5**, Fig. 4.1; Ar′ = 2,6-$C_6H_3{}^iPr_2$); a double-addition reaction with TolNCO, coupling 2 equivs of substrate; net NO^{t}Bu group transfer with ^{t}BuNCO and PhC(O)R (R = H, Me, Ph) *via* C=O/Ti=N$_\alpha$ metathesis; reductive N$_\alpha$–O$_\beta$ bond cleavage with Ar^{F_5}CCH (Ar^{F_5} = C_6F_5); and formation of an unusual nitroxyl (HNO) complex upon reaction with B(Ar^{F_5})$_3$ with concomitant *iso*-butene elimination.[60] Of particular relevance to this Chapter are the reactions of **3** with benzonitriles to form the net Ti=N$_\alpha$ bond insertion products Cp*Ti{PhC(N^{i}Pr)$_2$}{NC(Ar)NO^{t}Bu} (Ar = Ar^{F_5} (**10**), $C_6H_3F_2$ (Ar^{F_2}, **11**) or Ph (**12**), Fig. 4.1) containing new benzimidamido functional groups, i.e. Ti=NC(Ar)NO^{t}Bu, also possessing a formal Ti≡N $\sigma^2\pi^4$ triple bond. The stability of these complexes increases in the order Ar = Ph (**12**) < Ar^{F_2} (**11**) < Ar^{F_5} (**10**) as the aryl groups become better able to stabilise the electron-rich multiple bond. Although the reactions of nitriles with transition metal nitrides,[61, 62] alkylidenes[63-67] and alkylidynes[68-73] are very well established, their reactions with transition metal imides and hydrazides are still relatively uncommon,[17, 19, 26, 49, 74] and the reaction chemistry of the benzimidamido ligand has therefore remained unexplored. Encouragingly in this regard, compound **10** reacted with an excess of Ar^{F_5}CN to form **13** (Fig. 4.1) containing two additional benzonitrile units. This was the first example of any reaction of an isolated benzimidamido complex, and only the second example of the double addition of nitriles across a M=NR bond. The first example was the very recently reported head-to-tail coupling of 2 equivs of ArCN across the Ti=NNCPh$_2$ bond of the alkylidene hydrazide Cp*Ti{MeC(N^{i}Pr)$_2$}(NNCPh$_2$) forming Cp*Ti{MeC(N^{i}Pr)$_2$}{N(NCPh$_2$)C(Ar)NC(Ar)N} (Ar = Ph or Ar^{F_5}).[49] The only related example of a similar double addition of nitriles was reported for the transient oxo and sulfido complexes Cp*$_2$Zr(E) (E = O or S).[75]

The reaction of **10** with further equivs of Ar^{F_5}CN prompted work on developing the compound's reaction chemistry with other substrates. This would also, in effect, result in multiple substrate/cross-coupling reactions of the Ti=NO^{t}Bu functional group of **3**. Interestingly, while multiple couplings of CO_2,[18, 22, 55, 58] isocyanates,[22, 49, 58] alkynes,[76] or of an alkyne and a nitrile[19] or isonitrile[5] across a number of Ti=N$_\alpha$R (R = hydrocarbyl, NR$_2$, NCPh$_2$ or NO^{t}Bu) bonds are known, these predominately involve insertion of the second substrate into the single Ti–X bond (X = N or C) of an initial [2+2] cycloaddition

intermediate (for example of the type **5** in Fig. 4.1). Multiple substrate coupling starting from **3** and nitriles would follow a different mechanistic paradigm with each stage involving substrate addition to a metal-nitrogen multiple bond (i.e. Ti=NO^{t}Bu followed by Ti=NC(Ar)NO^{t}Bu). This Chapter will therefore report the reactions of Cp*Ti{PhC(N^{i}Pr)$_2$}{NC(Ar^{F5})NO^{t}Bu} (**10**) with heterocumulenes, aldehydes, dimethyl formamide, isonitriles and B(Ar^{F5})$_3$. The work will be supported by DFT calculations carried out by Adam Russell at the University of Oxford. The majority of this work has been published.[77]

The benzimidamido compounds Cp*Ti{PhC(N^{i}Pr)$_2$}{NC(Ar)NO^{t}Bu} (Ar = Ar^{F5} (**10**) or Ar^{F2} (**11**)) are readily formed from Cp*Ti{PhC(N^{i}Pr)$_2$}(NO^{t}Bu) (**3**) and the corresponding nitrile, and when followed on the NMR tube scale the conversions are quantitative and effectively immediate in the case of **10**.[60] However, owing to its high solubility in aliphatic solvents, **10** could only be isolated in less than 35% yield on a preparative scale. Therefore, in the following chemistry **10** was generally generated *in situ* for reasons of efficiency. When reactions of formally isolated **10** were compared with those of the *in situ* generated system no differences were observed.

4.2 Reactions with heterocumulenes

The influence of N$_\alpha$ substituents, (L)Ti=N$_\alpha$–X, on the reactivity of titanium imido and hydrazido complexes with CO_2, CS_2 and isocyanates is well established[2, 11, 14, 22, 26, 49, 57-59, 78-80] and initial studies of alkoxyimido complexes have shown similar behavior to their hydrazido and imido counterparts.[49, 60] A [2+2] cycloaddition product is the key intermediate in all reactions with these substrates. However, there are relatively few examples where these intermediates are observed or (especially) isolated. Their unstable nature often leads to extrusion (*via* retro-cyclisation) of an organic fragment, leaving behind a titanium oxo species which, unless trapped, rapidly dimerises *via* μ-oxo bridge formation. It was therefore of interest to explore the reactions of Cp*Ti{PhC(N^{i}Pr)$_2$}{NC(Ar^{F5})NO^{t}Bu} (**10**) with heterocumulenes, in particular since the electron-withdrawing nature of the C_6F_5 substituent should help to stabilise these intermediates.

Scheme 4.1. Reaction of Cp*Ti{PhC(N^{i}Pr)$_2$}{NC(Ar^{F5})NO^{t}Bu} (**10**) with CO_2.

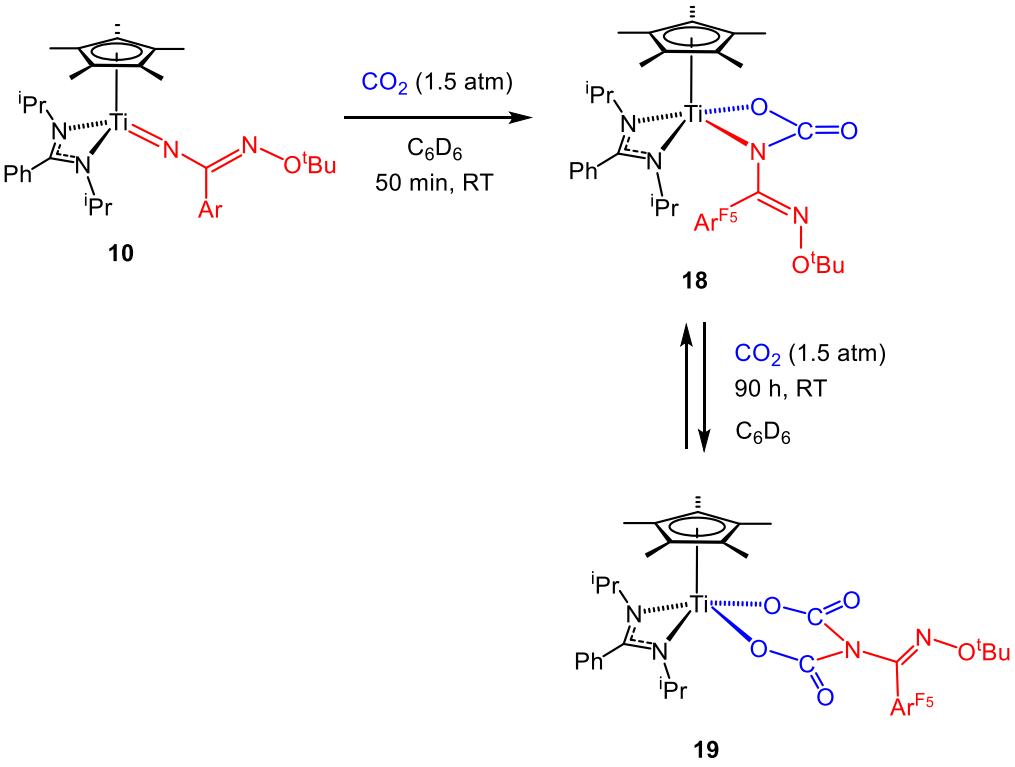

When the reaction of **10** with an excess of CO_2 (*ca.* 1.5 atm) was followed by NMR spectroscopy quantitative conversion to compound **18** was observed within 50 min at room temperature (Scheme 4.1). Compound **18** was isolated on the preparative scale in 66% yield and characterised by NMR and IR spectroscopy and elemental analysis. The NMR and other data are characteristic of the C_1 symmetric [2+2] cycloaddition product, Cp*Ti{PhC(N^{i}Pr)$_2$}{OC(O)N(C{Ar^{F5}}NO^{t}Bu)} (**18**), containing a *N*,*O*-bound carbamate-type ligand. For example, two apparent septets are observed in the ^{1}H NMR spectrum, given in Fig. 4.2, for the inequivalent *iso*-propyl groups, along with four doublets for the two pairs of diastereotopic methyl groups. The ^{19}F NMR spectrum, see inset to Fig. 4.2, shows 5 new resonances (range δ -137.7 to -164.9 ppm) which indicates restricted rotation about the C–C$_{ipso}$ bond to the C_6F_5 ring. The ^{13}C NMR C=O resonance at δ 155.8 ppm is similar to the corresponding values for Cp*Ti{MeC(N^{i}Pr)$_2$}{OC(O)N(NR$_2$)} (R = Ph, δ 160.6 ppm; R = Me, δ 158.1 ppm).[22] Finally, the IR spectra of **18** and Cp*Ti{MeC(N^{i}Pr)$_2$}{OC(O)N(NR$_2$)} all show strong ν(C=O) bands at 1690, 1684 and 1667 cm^{-1}, respectively, for the carbamate ligands.

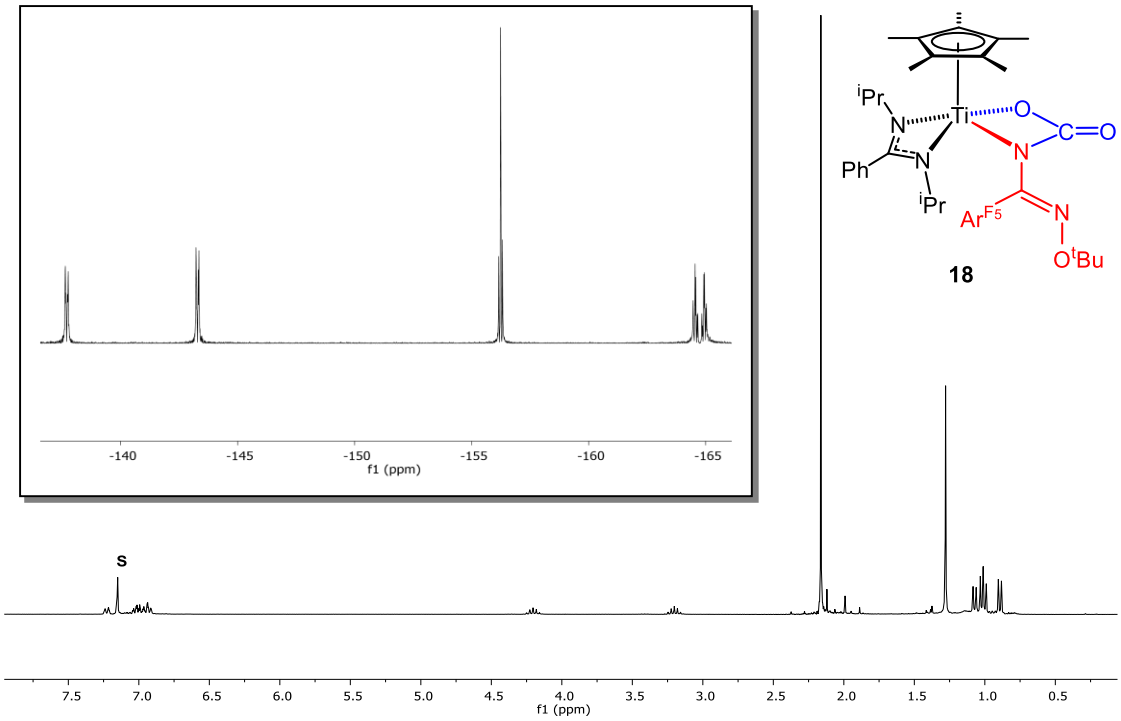

Figure 4.2. ^{1}H NMR spectrum (499.9 MHz, 293 K) of Cp*Ti{PhC(N^{i}Pr)$_2$}{OC(O)N(C{Ar^{F5}}NO^{t}Bu)} (**18**) in C_6D_6 ("s" denotes residual protio-solvent). Inset: corresponding ^{19}F NMR spectrum (282.1 MHz, 293 K).

Like its arylimido-[58] and hydrazido-[22] derived counterparts, compound **18** does not undergo retro-cyclisation to eliminate ^{t}BuONC(Ar^{F5})NCO, and is stable for many days in solution at room temperature. However, in the presence of an excess of CO_2, **18** eventually forms the C_s symmetric "double-insertion" compound Cp*Ti{PhC(N^{i}Pr)$_2$}{OC(O)N(C{Ar^{F5}}NO^{t}Bu)C(O)O} (**19**, Scheme 4.1). The reaction is slow, and when followed in C_6D_6 reaches only 70% conversion after *ca*. 90 h, at which stage no further reaction is observed. Upon heating the reaction mixture or attempted isolation, compound **19** eliminates CO_2 re-forming **18**. The reversible insertion of a heterocumulene into the Ti–N bond of a metallacyclic species such as **18** has been observed previously.[2] Compound **19** was characterised *in situ* by ^{1}H, ^{13}C and ^{19}F NMR spectroscopy. The ^{1}H NMR spectrum shows one septet corresponding to the equivalent *iso*-propyl methine hydrogens, and two doublets for the methyl groups of these substituents. The ^{13}C NMR spectrum shows a shift in the C=O and NC(Ar^{F5})N resonances from δ 155.8 to 152.8 ppm, and δ 146.2 to 137.3 ppm, respectively. Related compounds Cp*Ti{MeC(N^{i}Pr)$_2$}{OC(O)N(NR$_2$)C(O)O} (R = Me or Ph) show corresponding C=O resonances at δ 152.8 and 152.7 ppm, respectively, which are also shifted to higher field compared to their respective cycloaddition precursors.[22]

Scheme 4.2. Reaction of Cp*Ti{PhC(N^{i}Pr)$_2$}{NC(Ar^{F5})NO^{t}Bu} (**10**) with CS_2.

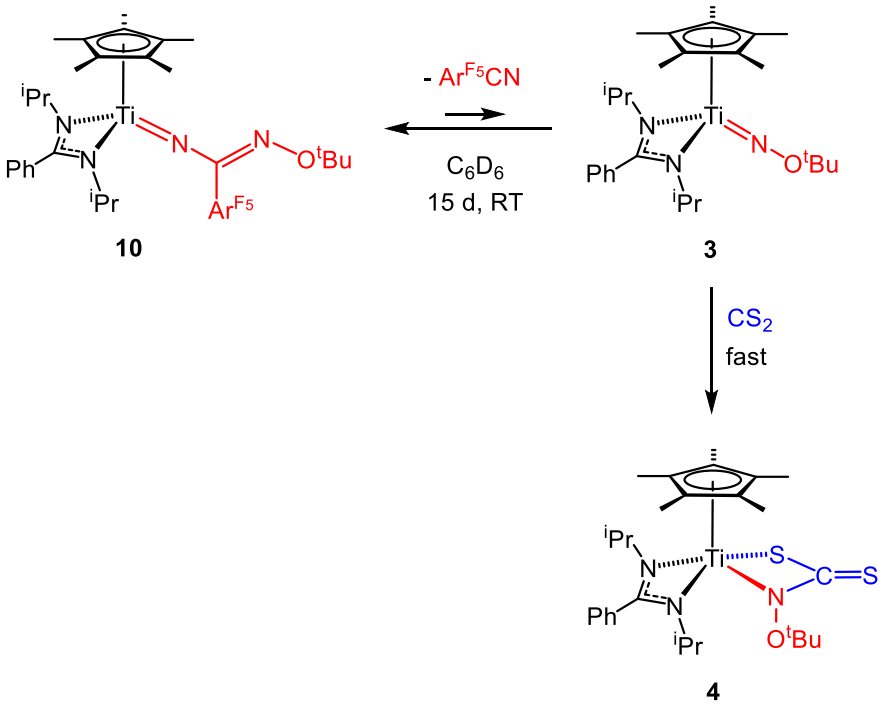

Reaction of **10** with a small excess of CS_2 in C_6D_6 resulted in the very slow formation of the previously reported[60] compound Cp*Ti{PhC(N^{i}Pr)$_2$}{SC(S)N(O^{t}Bu)} (**4**, Scheme 4.2, see Chapter Three for further details) and Ar^{F5}CN, and after 15 d at room temperature the reaction had still only reached *ca.* 65% conversion. At this stage significant amounts of unknown side-products were present in the ^{1}H NMR spectrum. The amount of these increased upon heating at 70 °C. The reaction probably proceeds *via* slow extrusion of Ar^{F5}CN from **10** yielding the alkoxyimido compound **3** (not observed) which, as previously reported, reacts relatively quickly with CS_2 to form the apparently more stable cycloaddition product **4**.[60] The extrusion of ArCN from benzimidamido complexes is precedented, having previously been observed in the reactions of insertion complexes **11** and **12** with Ar^{F5}CN, see Chapter Three for more details.[60] The corresponding reactions of the dimethyl, diphenyl and alkylidene hydrazido analogues of **10** all form stable [2+2] cycloaddition products with CS_2,[22, 49] whereas the imido-derived dithiocarbamates rapidly undergo retro-cyclisation and formation of isothiocyanates.[58]

Scheme 4.3. Reaction of Cp*Ti{PhC(N^{i}Pr)$_2$}{NC(Ar^{F5})NO^{t}Bu} (**10**) with ^{t}BuNCO.

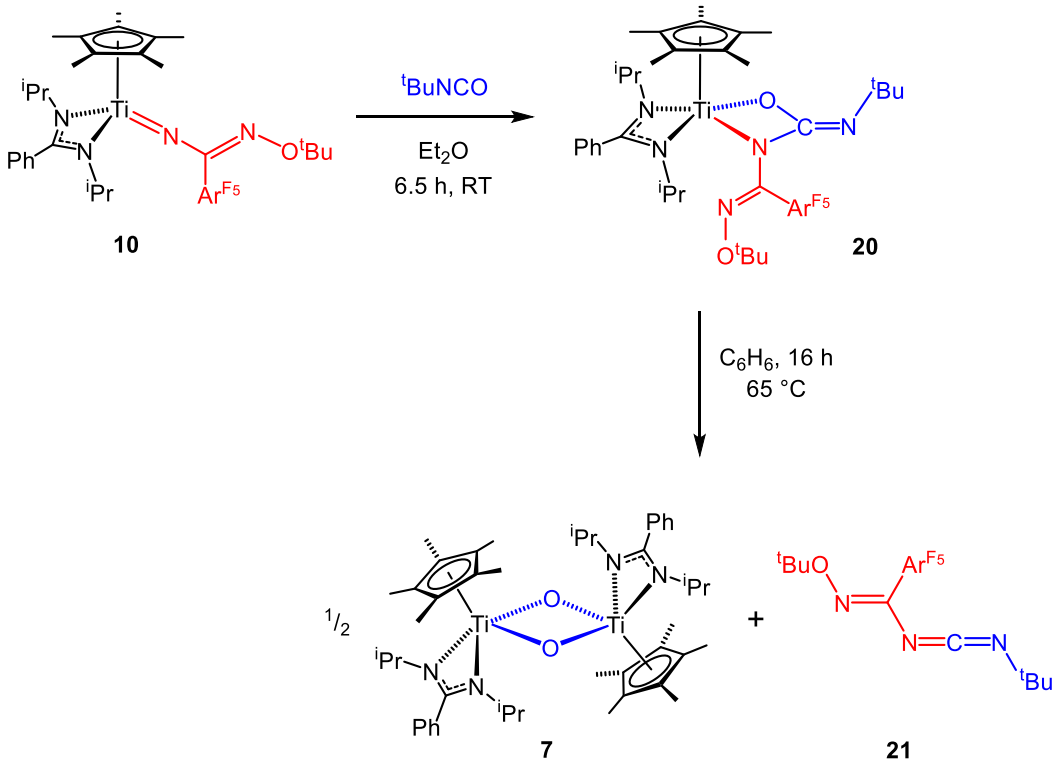

Reaction of **10** with 1 equiv of ^{t}BuNCO gave the *N,O*-bound ureate-type product Cp*Ti{PhC(N^{i}Pr)$_2$}{N(C{Ar^{F5}}NO^{t}Bu)C(N^{t}Bu)O} (**20**, Scheme 4.3), analogous to **18**, and isolated as a brown microcrystalline solid in 65% yield upon scale up. In contrast, reactions with aryl isocyanates (TolNCO and Ar′NCO (Ar′ = 2,6-C$_6$H$_3$^{i}Pr$_2$)) or isothiocyanates (^{t}BuNCS and TolNCS) produced complex mixtures and were not investigated further. The NMR data, given in Figure 4.3, for **20** are consistent with the proposed structure and the IR spectrum shows a strong band at 1631 cm^{-1} attributed to ν(C=N) of the ureate ligand, similar to that found for Cp*Ti{MeC(N^{i}Pr)$_2$}{N(NPh$_2$)C(N^{t}Bu)O}[22] and Cp*Ti{MeC(N^{i}Pr)$_2$}-{N(Xyl)C(N^{t}Bu)O}[58] (1653 and 1652 cm^{-1}, respectively). Compound **20** is relatively stable in solution at room temperature. Thus, after 16 h, solutions in C$_6$D$_6$ undergo less than 10% conversion to the μ-oxo dimer [Cp*Ti{PhC(N^{i}Pr)$_2$}(μ-O)]$_2$ (**7**)[60] and the new imidoylcarbodiimide ^{t}BuNCNC(Ar^{F5})NO^{t}Bu (**21**, Scheme 4.3), and even after 1 week only *ca*. 20% conversion occurs. As discussed in Chapter Three, under analogous conditions, the reaction of Cp*Ti{PhC(N^{i}Pr)$_2$}(NO^{t}Bu) (**3**) with ^{t}BuNCO slowly forms the carbodiimide ^{t}BuNCNO^{t}Bu and **7** following extrusion from the proposed intermediate Cp*Ti{PhC(N^{i}Pr)$_2$}{N(O^{t}Bu)C(N^{t}Bu)O} which was not observed in this case.[60] Therefore the benzimidamide functional group appears to help stabilise this type

of intermediate (i.e. **20**). The behaviour of **3** towards ^{t}BuNCO is comparable to that of its imido and dimethyl- and alkylidene-hydrazido homologues, whereas the diphenyl hydrazide Cp*Ti{MeC(N^{i}Pr)$_2$}(NNPh$_2$) forms a [2+2] cycloaddition product with ^{t}BuNCO without carbodiimide elimination. DFT studies have shown that both electronic and steric factors are important in such cycloaddition-elimination processes.[22, 58, 60]

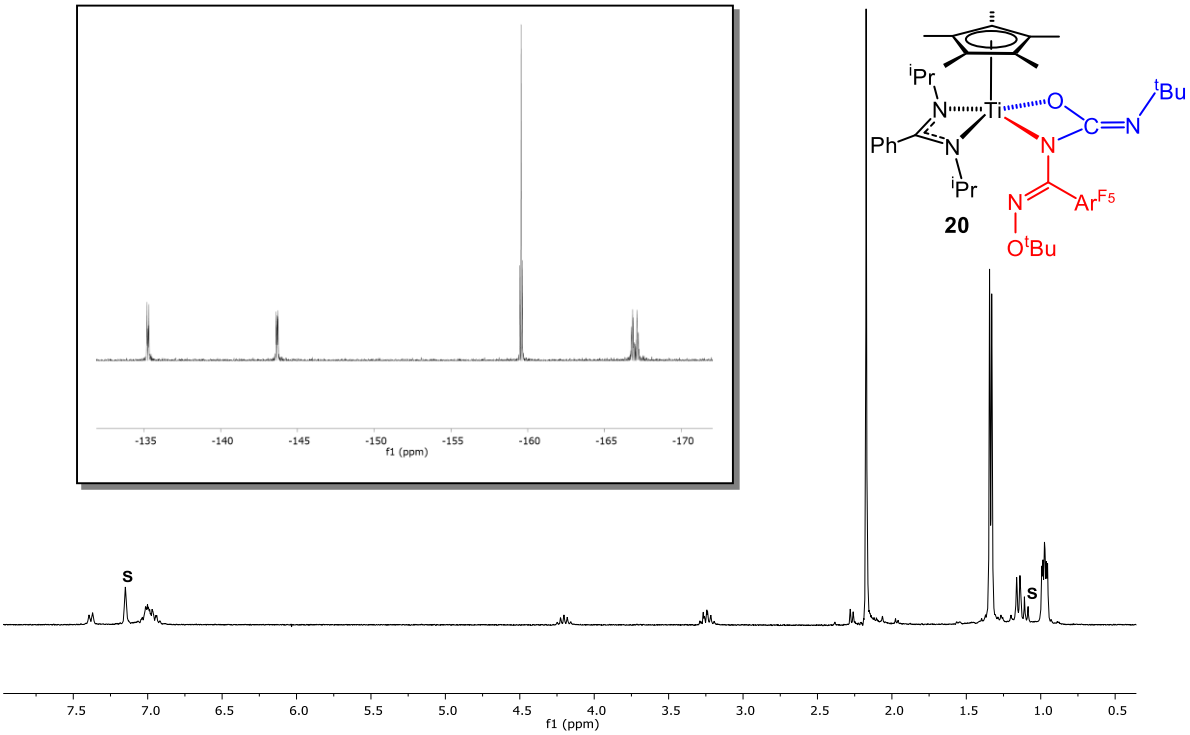

Figure 4.3. ^{1}H NMR spectrum (299.9 MHz, 293 K) of Cp*Ti{PhC(N^{i}Pr)$_2$}{N(C{Ar^{F5}}NO^{t}Bu)C(N^{t}Bu)O} (**20**) in C_6D_6 ("s" denotes residual protio-solvent). Inset: corresponding ^{19}F NMR spectrum (282.1 MHz, 293 K).

Heating a solution of **20** to 65 °C for 15 h nonetheless gave near-quantitative conversion to **21**, along with **7**. Compound **21** was isolated as an analytically pure, yellow oil in 71% yield by distillation (100 °C, 8 x 10^{-2} mbar). The ^{1}H, ^{13}C and ^{19}F NMR spectra indicate a single geometric isomer which, by analogy to **22a** (*vide infra*) and taking into account the steric constraints present in **20**, is assigned as having a *cis* arrangement of the –O^{t}Bu and –Ar^{F5} groups across (^{t}BuO)N=C(Ar^{F5}) and a *trans* arrangement of groups across N=C=N, as shown in Scheme 4.3. Imidoylcarbodiimides RNC(R^{1})NCNR^{2} can, in general, be synthesised from the corresponding imidoylthioureas, RNC(R^{1})N(H)C(S)NHR^{2}, and have been shown to undergo a rearrangement forming synthetically useful aminoquinazolines (R = Ph) or

dihydrotriazines (R = CHR′R″).[81] The transformation of **20** to **21** shown in Scheme 4.3 represents a new synthetic method for this type of compound, albeit rather limited in scope and presently without optimisation.

4.3 Reactions with benzaldehydes and dimethyl formamide

Previous reports of the reactions of Group 4 imides,[58, 59, 78-80, 82, 83] hydrazides,[11, 22, 49] and alkoxyimides[60] with aldehydes and ketones have shown their tendency to form unstable [2+2] cycloaddition products which rapidly extrude the corresponding imine, hydrazone or oxime ether, respectively. Given the relative stability of **20** it was hoped that reaction of **10** with aldehydes and related substrates would likewise form more stable cycloaddition products of the type Cp*Ti{PhC(N^{i}Pr)$_2$}{N(C{Ar^{F5}}NO^{t}Bu)C(R)(R′)O}.

4.3.1 Reactions with aldehydes

As shown in Eq 4.1, reaction of PhC(O)H with **10** rapidly formed the [2+2] cycloaddition product Cp*Ti{PhC(N^{i}Pr)$_2$}{N(C{Ar^{F5}}NO^{t}Bu)C(Ph)(H)O} (**22a**). Compound **22a** formed in quantitative yield on the NMR tube scale, and on scale up was isolated as a dark brown, microcrystalline solid in 82% yield. Only one set of signals were observed in the NMR spectra, given in Figure 4.4, consistent with formation of a single diastereomer (both the titanium and Ph<u>C</u>H carbon being stereogenic centers). A nuclear Overhauser effect (NOE) experiment showed a through-space interaction between the η-C$_5$Me$_5$ ligand and PhC<u>H</u> of the metallacycle, consistent with the structure shown in Eq 4.1, namely with the phenyl group orientated away from the η-C$_5$Me$_5$ ligand in the sterically least congested arrangement. This geometry was confirmed in the solid state by X-ray diffraction (*vide infra*). Interestingly, both the PhC<u>H</u> and Ph<u>C</u>H signals of **22a** appear as doublets (J = 2.1 and 1.4 Hz, respectively) due to C-H···F interactions. This is either a consequence of scalar coupling or cross-correlation interactions[84] between Ph<u>CH</u> and Ar^{F5}, as confirmed by a ^{1}H{^{19}F} NMR experiment in which the PhC<u>H</u> signal appeared as a singlet. The ^{19}F NMR spectrum, see inset to Fig. 4.4, showed 5 resonances at room temperature, consistent with restricted rotation about the C–C$_{ipso}$ bond to the C$_6$F$_5$ ring.

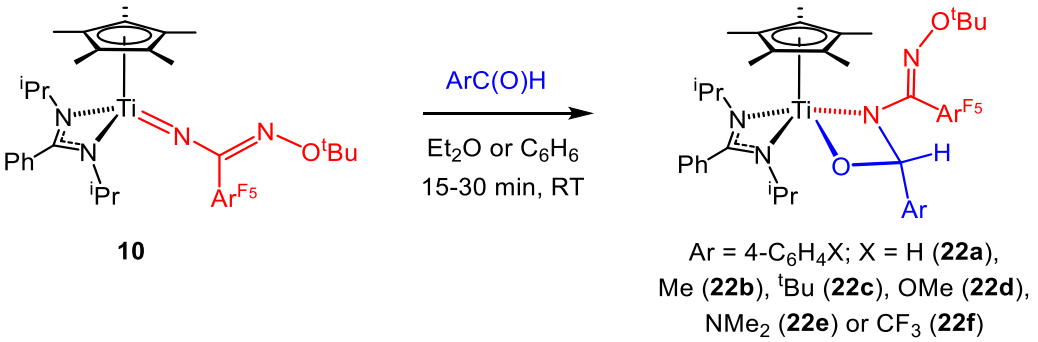

Equation 4.1

The PhC<u>H</u> "up" arrangement for **22a** is the same as that found in Cp*Ti{MeC(N^{i}Pr)$_2$}{N(^{t}Bu)C(Ph)(H)O}, formed from Cp*Ti{MeC(N^{i}Pr)$_2$}(N^{t}Bu) and PhC(O)H. In contrast, for the reaction of the homologous tolylimido compound and PhC(O)H both isomers were observed,[58] as was also the case for the reaction of Cp*Ti{PhC(N^{i}Pr)$_2$}(NO^{t}Bu) (**3**) with PhC(O)H and PhC(O)Me.[60] Interestingly, whereas **22a** is stable in solution for several hours, all of these previously reported metallacycles rapidly underwent extrusion of the corresponding imines or oximes below room temperature, thus preventing their isolation on a preparative scale. To take advantage of this opportunity to study further these types of metallacycles a series of homologues, namely Cp*Ti{PhC(N^{i}Pr)$_2$}{N(C{Ar^{F5}}NO^{t}Bu)C(Ar)(H)O} (Ar = 4-C$_6$H$_4$X; X = Me (**22b**), ^{t}Bu (**22c**), OMe (**22d**), NMe$_2$ (**22e**) or CF$_3$ (**22f**); Eq 4.1) were prepared. The new compounds were obtained in near-quantitative yields and their NMR and other data were analogous to those of **22a**, indicating the presence of a single ArC<u>H</u> "up" isomer in each case.

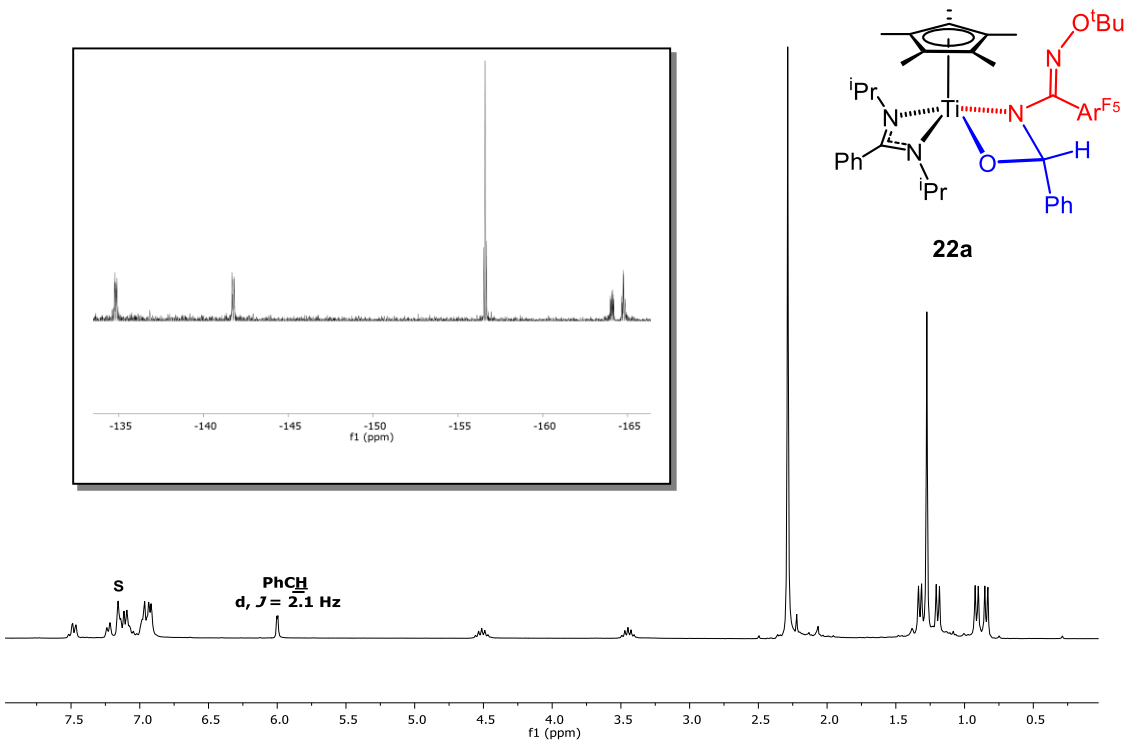

Figure 4.4. ^{1}H NMR spectrum (299.9 MHz, 293 K) of Cp*Ti{PhC(N^{i}Pr)$_2$}{N(C{Ar^{F5}}NO^{t}Bu)C(Ph)(H)O} (**22a**) in C_6D_6 ("s" denotes residual protio-solvent). Inset: corresponding ^{19}F NMR spectrum (282.1 MHz, 293 K).

Diffraction-quality crystals of **22a** were grown from a saturated *n*-hexanes solution at 4 °C. The molecular structure is shown in Fig. 4.5 and selected distances and angles are listed in Table 4.1. The structure confirms the incorporation of PhC(O)H to form a new N{C(Ar^{F5})NO^{t}Bu}C(H)(Ph)O ligand binding to titanium in a κ^2*N*,*O*-coordination mode. The stereochemistry around C(1) is consistent with the solution NOE measurements with H(1) directed towards the η-C_5Me_5 ligand. The metric parameters associated with both Cp*Ti{PhC(N^{i}Pr)$_2$} and NC(Ar^{F5})NO^{t}Bu fragments lie within the expected values.[85] The Ti(1)–N(1) bond length is increased relative to **10**, (2.0070(16) *vs* 1.747(4) Å) and is similar to the Ti–$N_{amidinate}$ single bonds (2.1160(18) and 2.0972(17) Å). The H(1)···F(1) distance of 2.59 Å is consistent with the observed doublet coupling in the ^{1}H NMR spectra of **22a**-**22f**. Despite the apparent close proximity of the Ph and Ar^{F5} rings, and the potential for mixed arene–perfluoroarene π-π interactions,[86] only two close interactions are observed, namely C(2)···C(9) = 3.054(3) Å and C(2)···C(14) = 3.346(3) Å.

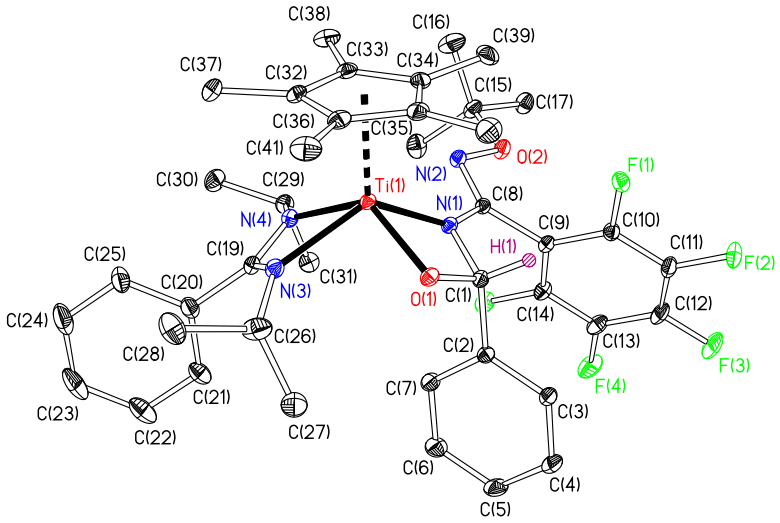

Figure 4.5. Displacement ellipsoid plot (20% probability) of Cp*Ti{PhC(N^{i}Pr)$_2$}{N(C{Ar^{F5}}NO^{t}Bu)C(Ph)(H)O} (**22a**). H(1) is drawn as a sphere of an arbitrary radius. All other H atoms omitted for clarity.

Table 4.1. Selected bond lengths (Å) and angles (°) for Cp*Ti{PhC(N^{i}Pr)$_2$}{N(C{Ar^{F5}}NO^{t}Bu)C(Ph)(H)O} (**22a**). Cp$_{cent}$ is the computed Cp* ring carbon centroid.

Ti(1)-Cp$_{cent}$	2.055	N(1)-C(1)	1.469(2)
Ti(1)-N(1)	2.0070(16)	N(1)-C(8)	1.358(2)
Ti(1)-N(3)	2.1160(18)	O(1)-C(1)	1.419(2)
Ti(1)-N(4)	2.0972(17)	C(1)-C(2)	1.519(3)
Ti(1)-O(1)	1.8980(14)		
Cp$_{cent}$-Ti(1)-N(1)	118.3	Cp$_{cent}$-Ti(1)-O(1)	118.9
Cp$_{cent}$-Ti(1)-N(3)	112.6	Cp$_{cent}$-Ti(1)-N(4)	113.7
N(3)-Ti(1)-N(4)	62.63(7)	O(1)-Ti(1)-N(1)	70.05(6)
Ti(1)-N(1)-C(1)	90.95(11)	Ti(1)-O(1)-C(1)	97.13(10)
O(1)-C(1)-N(1)	101.85(14)		

Although the ^{1}H NMR signals for **22a** are not broad at room temperature, spin saturation transfer measurements showed exchange on the NMR timescale between free (added) benzaldehyde and the PhC(O)H incorporated in **22a**. This is proposed to occur *via* a dissociative mechanism, transiently forming **10**, as has been observed previously for related imido compounds and carbonyl complexes.[58] As a test of this, bearing in mind the known irreversible reaction of **3** with PhC(O)H to form **7** and the oxime ether PhC(NO^{t}Bu)H (**9a**),[60] an NMR tube scale crossover experiment between **22a** and **3** in C_6D_6 was carried out which showed quantitative formation of the products shown in Eq 4.2.

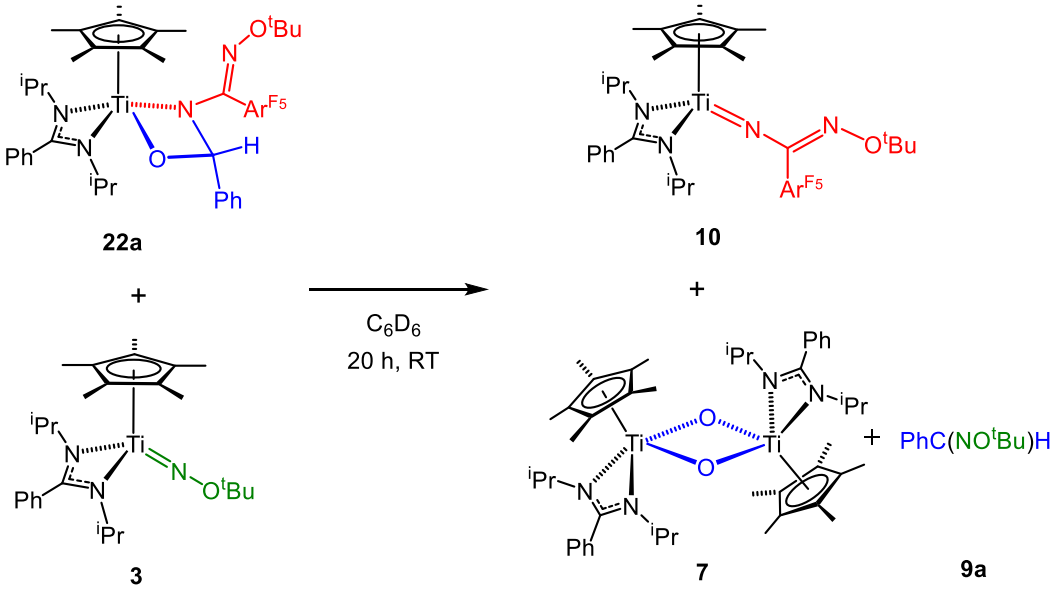

Equation 4.2

Previous studies have suggested that electron-withdrawing substituents can help to stabilise metallacyclic complexes formed from imides (and related systems) and unsaturated substrates.[17, 19] The relative stability of the complexes Cp*Ti{PhC(N^{i}Pr)$_2$}{N(C{Ar^{F5}}NO^{t}Bu)C(Ar)(H)O} (**22a-f**) and the reversible addition of PhC(O)H to the benzimidamido ligand of **10** prompted us to investigate this further. Thus *ca.* 1 equiv of each ArC(O)H (Ar = 4-C$_6$H$_4$X; X = Me, ^{t}Bu, OMe, NMe$_2$ or CF$_3$) was added to solutions of **22a** in C_6D_6 and the reactions monitored by ^{1}H NMR spectroscopy (Eq 4.3). Competition equilibria were established within 10 min.

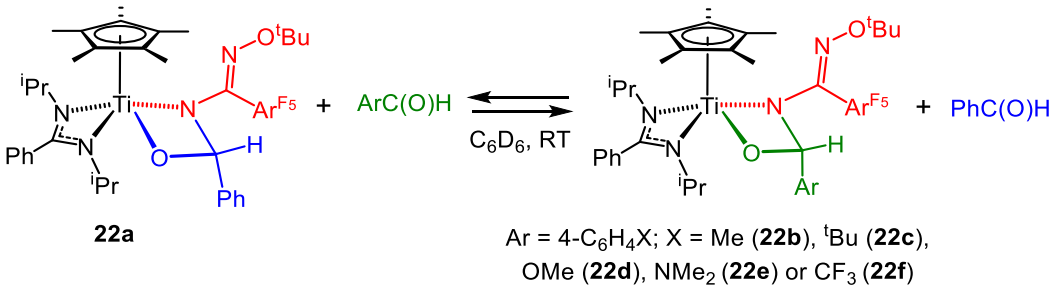

Equation 4.3

The equilibrium constants (K_{eq}) are listed in Table 4.2 below and are depicted graphically in semilogarithmic form in Fig. 4.6 against the corresponding Hammett substituent constants, σ_p.[87] The K_{eq} data clearly indicate a thermodynamic preference for cycloaddition products with electron-withdrawing *para*-substituents.

Table 4.2. Equilibrium constants (K_{eq}) for the reactions of Cp*Ti{PhC(N^{i}Pr)$_2$}{N(C{Ar^{F5}}NO^{t}Bu)C(Ph)(H)O} (**22a**) with ArC(O)H (Ar = 4-C$_6$H$_4$X; X = Me, ^{t}Bu, OMe, NMe$_2$ or CF$_3$) at 293 K in C$_6$D$_6$. σ_p is the Hammett substituent constant for X.

Ar	σ_p	K_{eq}
4-C$_6$H$_4$CF$_3$	0.54	8.28
4-C$_6$H$_4$Me	-0.17	0.42
4-C$_6$H$_4$^{t}Bu	-0.20	0.52
4-C$_6$H$_4$OMe	-0.27	0.12
4-C$_6$H$_4$NMe$_2$	-0.83	0.01

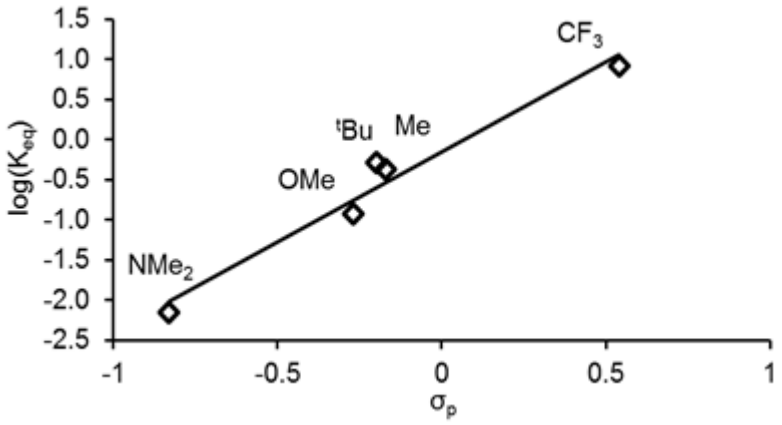

Figure 4.6. Plot of log(K_{eq}) *vs* σ_p for the reactions of Cp*Ti{PhC(N^{i}Pr)$_2$}{N(C{Ar^{F5}}NO^{t}Bu)C(Ph)(H)O} (**22a**) with ArC(O)H (Ar = 4-C_6H_4X; X = Me, ^{t}Bu, OMe, NMe_2 or CF_3) at 293 K in C_6D_6. The best-fit line shown has r^2 = 0.962.

Compound **22a** is not indefinitely stable in solution, and on heating a C_6D_6 solution at 70 °C, a colour change from brown to yellow, characteristic of the μ-oxo dimer **7**, is observed. The ^{1}H NMR spectrum showed quantitative formation of **7** and the 1,3-diazabutadiene derivative PhC{NC(Ar^{F5})NO^{t}Bu}H (**23a**, Eq 4.4). Analogous results were obtained for **22b-f** and the corresponding organic products **23a-f** were isolated by sublimation on scale up in 62 – 93% yield. Compounds **23a-f** exist predominantly as the single geometric isomer depicted in Eq 4.4 on the basis of the X-ray structure of **23e** and DFT calculations (*vide infra*). It is interesting to note the *trans* arrangement of the Ar– and –C(Ar^{F5})NO^{t}Bu groups with respect to the Ar(H)C=NC(Ar^{F5})NO^{t}Bu double bond. This is consistent with previous DFT studies of the cycloaddition-extrusion reactions of Cp*Ti{PhC(N^{i}Pr)$_2$}(NO^{t}Bu) (**3**) with PhC(O)R (R = H or Me) in which the metallacycle intermediates with the PhC<u>R</u> substituent oriented "up" towards Cp* gave rise to the product oxime ether PhC(NO^{t}Bu)R with a *trans* arrangement of the Ph– and –O^{t}Bu groups.[60]

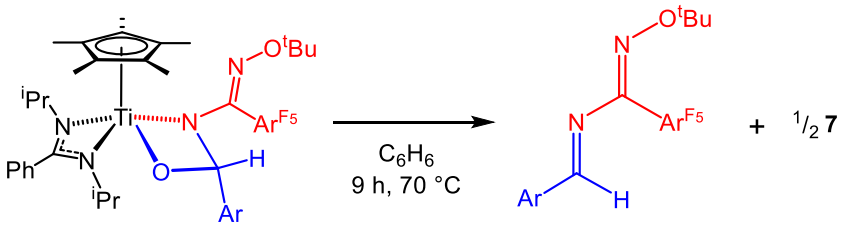

22a-f **23a-f**

Ar = 4-C_6H_4X; X = H (**a**), Me (**b**), ^{t}Bu (**c**),OMe (**d**), NMe_2 (**e**) or CF_3 (**f**)

Equation 4.4

The molecular structure of **23e** is shown in Fig. 4.10 and selected bond distances and angles can be found in Table 4.5 (*vide infra*). The structure establishes both the connectivity and the geometric isomer isolated. The metric parameters lie within the expected ranges and indicate discrete single and double bonds. The electronic and molecular structure of **23e** and its homologues are discussed in further detail below.[85]

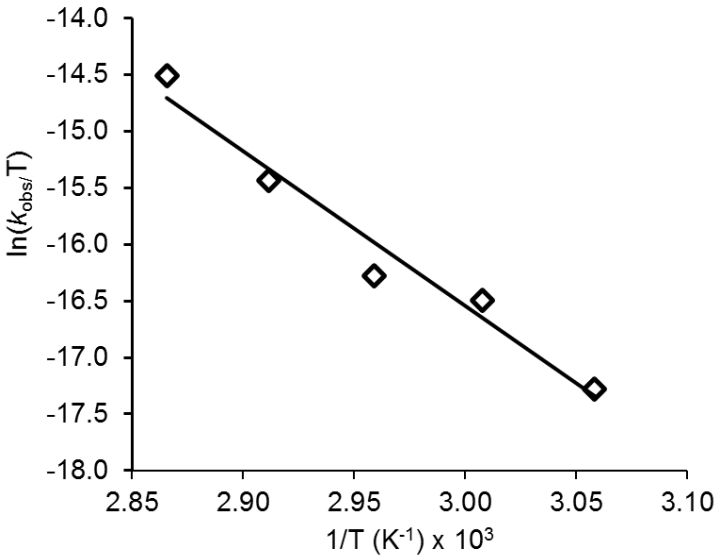

Figure 4.7. Eyring plot for the extrusion reaction of Cp*Ti{PhC(N^{i}Pr)$_2$}{N(C{Ar^{F5}}NO^{t}Bu)C(Ph)(H)O} (**22a**) in C_6D_6. Activation parameters derived from linear regression analysis (r^2 = 0.963): $\Delta H^{\ddagger}$ = 27(3) kcal mol^{-1}; $\Delta S^{\ddagger}$ = 1(9) cal mol^{-1} K^{-1}; $\Delta G_{343}^{\ddagger}$ = 27(4) kcal mol^{-1}.

The extrusion reaction of Cp*Ti{PhC(N^{i}Pr)$_2$}{N(C{Ar^{F5}}NO^{t}Bu)C(Ph)(H)O} (**22a**) in C_6D_6 was monitored in the temperature range 54 – 76 °C. The reactions followed first order kinetics as judged by linear semilogarithmic plots of ln([**22a**]$_t$/[**22a**]$_0$) *vs* time. An Eyring analysis of the rate constants, k_{obs}, was carried out (Fig. 4.7) giving the activation

parameters, $\Delta H^{\ddagger}$ = 27(3) kcal mol^{-1} and $\Delta S^{\ddagger}$ = 1(9) cal mol^{-1} K^{-1} ($\Delta G_{343}^{\ddagger}$ = 27(4) kcal mol^{-1}). The negligible value of $\Delta S^{\ddagger}$ is consistent with an early transition state for these dissociative reactions.[88]

Table 4.3. Rate constants (k_{obs}) for the extrusion reactions of Cp*Ti{PhC(N^{i}Pr)$_2$}{N(C{Ar^{F5}}NO^{t}Bu)C(Ar)(H)O} (Ar = 4-C$_6$H$_4$X; X = H (**22a**), Me (**22b**), ^{t}Bu (**22c**), OMe (**22d**), NMe$_2$ (**22e**) or CF$_3$ (**22f**)) at 70 °C in C$_6$D$_6$. σ_p is the Hammett substituent constant. The values in brackets are for T = 32 °C. Standard errors were obtained from linear regression analysis in each case.

Ar	σ_p	$k_{obs} \times 10^5$ (s^{-1})
Ph	0.00	6.79(3) [0.04][a]
4-C$_6$H$_4$Me	-0.17	8.09(3)
4-C$_6$H$_4$^{t}Bu	-0.20	10.11(3)
4-C$_6$H$_4$OMe	-0.27	11.80(8)
4-C$_6$H$_4$NMe$_2$	-0.83	[1.22(1)][c] 207 [d]
4-C$_6$H$_4$CF$_3$	0.54	16.4(1), 12.5(1)[b]

Notes: [a] calculated for 32 °C from the Erying plot for **22a** (see Fig. 4.7);[b] duplicate runs; [c] measured at 32 °C; [d] calculated assuming k_{obs}(70 °C)/ k_{obs}(32 °C) is the same for both **22a** and **22e**.

The corresponding first order rate constants (k_{obs}) were also determined for the extrusion reactions of Cp*Ti{PhC(N^{i}Pr)$_2$}{N(C{Ar^{F5}}NO^{t}Bu)C(4-C$_6$H$_4$X)(H)O} (X = Me (**22b**), ^{t}Bu (**22c**) or OMe (**22d**)) at 70 °C and are listed in Table 4.3. The increased k_{obs} values (range 8.09(3) – 11.80(8) x 10^{-5} s^{-1}) compared to that for **22a** at this temperature (6.79(3) x 10^{-5} s^{-1}) show that electron-releasing *para*-substituents stabilise the transition state to extrusion. Attempts to measure k_{obs} at 70 °C for **22e** possessing the most electron-releasing *para*-NMe$_2$ substituent were unsuccessful. The reaction reached greater than 50% completion within 5 min, and the broad ^{1}H resonances hindered accurate ^{1}H NMR integration. Therefore k_{obs} for **22e** was measured at 32 °C and the corresponding k_{obs} for **22a** at 32 °C was calculated from the Eyring plot in Fig.

4.7. Comparison of the k_{obs} values at 32 °C (1.22(1) x 10^{-5} s^{-1} for **22e** *vs* 0.04 x 10^{-5} s^{-1} for **22a**) shows that extrusion from **22e** is *ca*. 30 times faster than from **22a**. The k_{obs} for **22e** at 70 °C was estimated as 207 x 10^{-5} s^{-1}, assuming that k_{obs}(70 °C)/ k_{obs}(32 °C) is the same for both **22a** and **22e** (i.e. that $\Delta S^{\ddagger}$ is negligible in each case as found experimentally for **22a** and that the $\Delta G^{\ddagger}$ values for extrusion are primarily controlled by the $\Delta H^{\ddagger}$ terms).

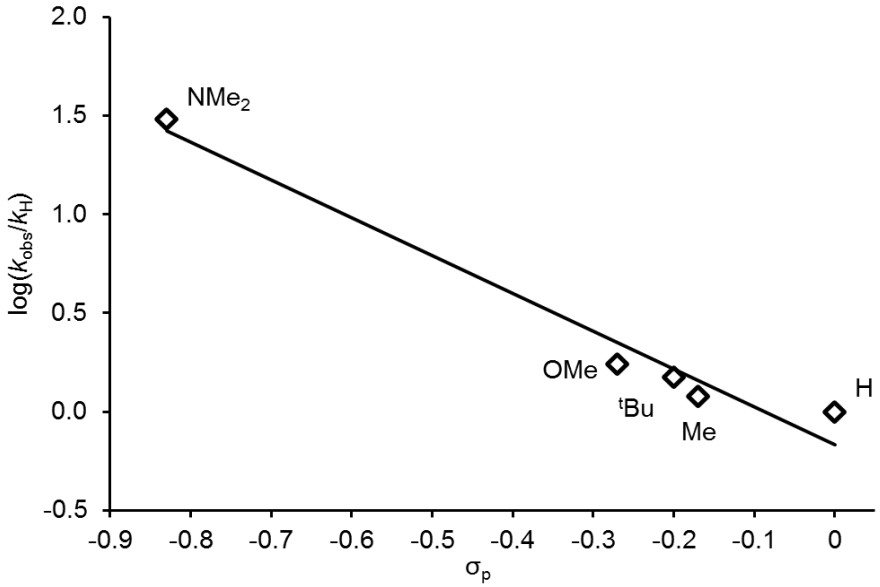

Figure 4.8. Plot of log(k_{obs}/k_H) *vs* σ_p for the extrusion reaction of Cp*Ti{PhC(N^iPr)$_2$}{N(C{Ar^{F5}}NO^tBu)C(4-C_6H_4X)(H)O} (**22a-e**) at 70 °C in C_6D_6. The best-fit line shown has r^2 = 0.965 giving ρ = -1.9(2). k_H is k_{obs} for X = H and k_{obs} for **22e** was estimated from data collected at 32 °C (see Table 4.3).

Fig 4.8 shows a plot of log(k_{obs}/k_H) *vs* σ_p for **22a-e** based on the experimental or estimated k_{obs} values ($k_H = k_{obs}$ for **22a**; σ_p is the Hammett substituent constant) which gave a reaction constant (ρ) of -1.9(2). This is consistent with a build-up of positive charge on the Ar<u>C</u>(H) carbon in the rate-determining step, indicating a transition state consisting more of C–O bond breaking than C–N bond forming character. Unexpectedly, the k_{obs} value of 14.5 x 10^{-5} s^{-1} (average of two independent experiments) for compound **22f** was significantly higher than that expected based on the Hammett plot (0.42 x 10^{-5} s^{-1}) and the data for **22a-e**. It is not possible to explain this difference, which may reflect a switch to a different mechanism for this most stable of the metallacycles (*cf.* the K_{eq} data in Table 4.2 and Fig. 4.6).

Figures 4.6 and 4.8 show that while PhC(O)H forms a more thermodynamically stable metallacycle (**22a**) than (4-$C_6H_4NMe_2$)C(O)H, the latter (**22e**) is significantly more reactive towards extrusion, forming **23e**. Scheme 4.4 summarises a competition experiment that illustrates this interplay. Addition of an equimolar solution of PhC(O)H and (4-$C_6H_4NMe_2$)C(O)H to **10** (1:1:1 initial ratio) in C_6D_6 at room temperature gave predominantly **22a** and unreacted (4-$C_6H_4NMe_2$)C(O)H (ratio **22a**:**22e** ≈ 10:1 in accordance with Fig. 4.6). After heating the mixture at 65 °C for 21 h the ^{1}H NMR spectrum showed formation of the organic products **23a** and **23e** in a *ca.* 2:1 ratio, in accordance with the Curtin–Hammett principle.[89]

Scheme 4.4. Reaction of Cp*Ti{PhC(N^{i}Pr)$_2$}{NC(Ar^{F5})NO^{t}Bu} (**10**) with PhC(O)H and ArC(O)H (Ar = 4-$C_6H_4NMe_2$; 1:1 ratio). **22a** and **22e** are formed in a 10:1 ratio and **23a** and **23e** in a 2:1 ratio.

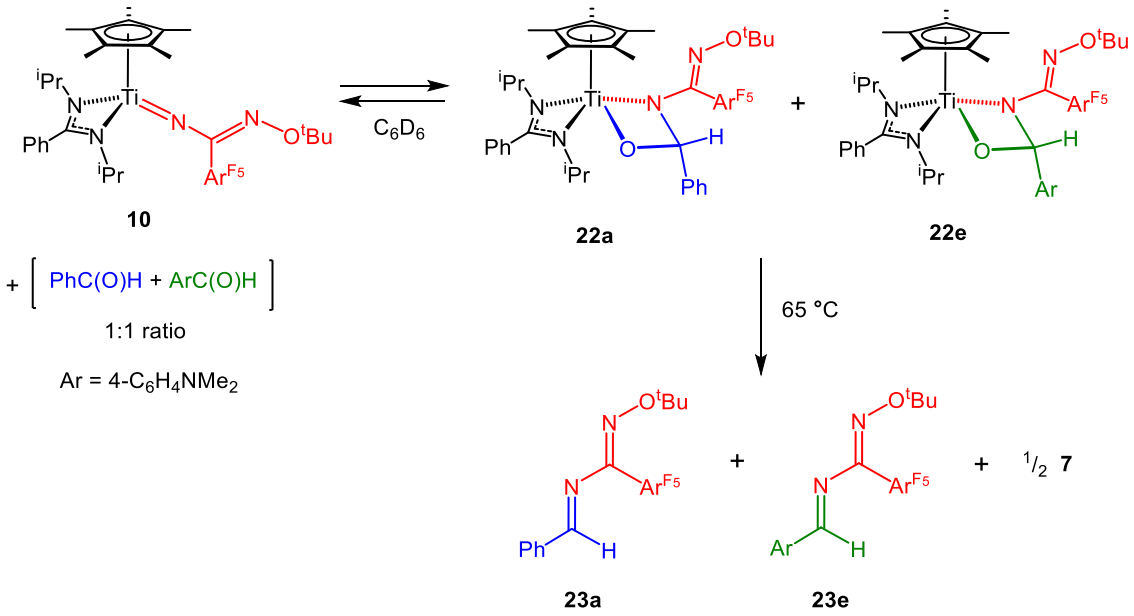

The organic products **23a-d** were isolated as white/cream solids, and **23f** was a pale yellow oil. In contrast, **23e** was obtained as an orange solid suggesting a significant effect of the *para*-NMe_2 group on the electronic structure. Table 4.4 lists the experimental λ_{max} values and absorption coefficients for the lowest energy bands in the UV-visible spectra of **23a-f** measured in *n*-hexanes. The absorption coefficients lie in the range 1.4 – 5.8 x 10^4 M^{-1} cm^{-1} and do not vary in a systematic manner. However, whereas the λ_{max} values for **23a-d** and **23f** appear between *ca.* 271 and 281 nm, that for **23e** is at 360 nm, tailing into the blue end of the visible spectrum, accounting for the orange colour. UV-visible spectra were also measured for **23a** and **23e** in MeOH, the

higher dielectric constant ($\varepsilon = 32.6$)[90] resulting in a small bathochromic shift in the λ_{max} in each case ($\Delta\lambda_{max}$ = 15 and 23 nm, respectively) but having no significant effect on the extinction coefficients.

Table 4.4. Experimental λ_{max} values (nm) and absorption coefficients (ε) for (4-C_6H_4X)C{NC(Ar^{F_5})NO^{t}Bu}H (**23a-f**), together with HOMO-LUMO gaps (eV) determined by DFT. The spectra were measured as *n*-hexanes solutions.

Compound	*para*-X	λ_{max} (nm)	ε x 10^{-4} (M^{-1} cm^{-1})	HOMO-LUMO separation (eV)
23a	H	271	3.0	2.64
23b	Me	275	5.4	2.60
23c	^{t}Bu	275	3.7	2.61
23d	OMe	281	5.8	2.53
23e	NMe_2	360	5.3	2.28
23f	CF_3	274	1.4	2.55

DFT calculations were carried out at the GGA:BP/TZP level on minimised geometries of compounds **23a-f** and, as expected, revealed generally similar electronic structures. Fig. 4.9 depicts isosurfaces for the HOMO and LUMO of **23a** and **23e**; further details for the other derivatives are given in the Appendix, Fig. A2a,b. The computed HOMO–LUMO separations are listed for all of the compounds in Table 4.4. For **23a-d** and **23f** the values fall in the range 2.53 – 2.64 eV. For **23e** the value is 2.28 eV and hence the trends in HOMO-LUMO separations qualitatively correspond well with the trends in λ_{max}.[91] The destabilising effect of the *para*-NMe_2 substituent on both the HOMO and LUMO of **23e** is evident from Figure 4.9 (bottom) which clearly shows the antibonding aryl(π)–$NMe_2(2p_\pi)$ interaction in each orbital. This is responsible for the general destabilisation of these frontier MOs relative to those of **23a** (Fig. 4.9, top). However, while the HOMO of **23e** is destabilised by 0.87 eV, the LUMO is only destabilised by 0.51 eV, explaining the decrease in HOMO–LUMO separation from **23a** to **23e**. Mulliken population analyses found that the $NMe_2(2p_\pi)$ atomic orbital contributions to the HOMO and LUMO of **23e** is 18% and 3.4%, respectively, consistent with the

different changes in energy. Similarly, the next smallest HOMO–LUMO separation (and next longest λ_{max}) was found for **23d** (*para*-OMe group) although the higher electronegativity of oxygen compared with nitrogen leads to an overall decrease in contribution of the OMe($2p_{\pi}$) lone pair to both the HOMO and LUMO (8.6% and 2.2% contributions, respectively).

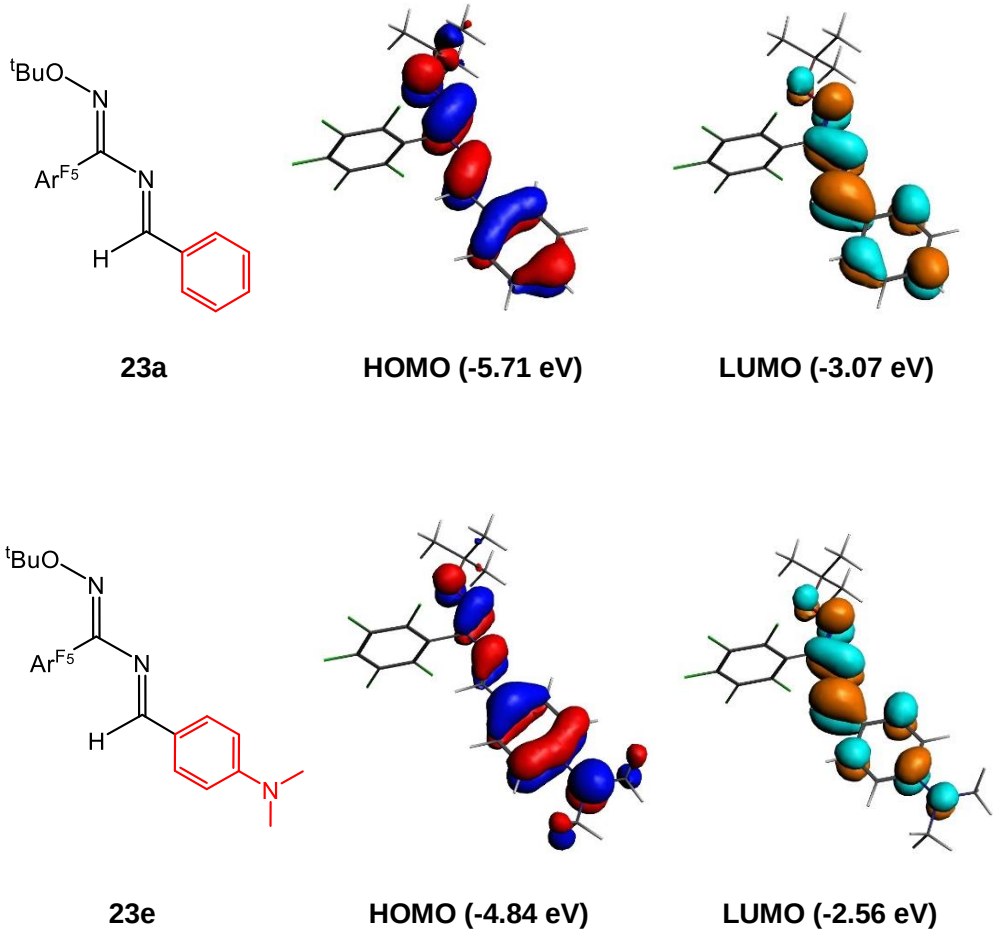

Figure 4.9. Isosurfaces and energies of the HOMO and LUMO of PhC{NC(Ar^{F5})NO^{t}Bu}H (**23a**, top) and (4-$C_6H_4NMe_2$)C{NC(Ar^{F5})NO^{t}Bu}H (**23e**, bottom).

4.3.2 Reactions with ketones and dimethyl formamide

Reaction of **10** with either PhC(O)Me or PhC(O)Ph gave disappointing results. The reaction with PhC(O)Me in C_6D_6 at room temperature generated a complex mixture of products within 15 min.[58] Analogous results were found for Cp*Ti{MeC(N^{i}Pr)$_2$}(NTol) with ketones of the type RC(O)Me and it was proposed that concomitant side-reactions stemming from the enol tautomers (RC(OH)CH$_2$) may be responsible.[92] Heating at 70 °C was required to effect a reaction between **10** and PhC(O)Ph, and even after 9 d it had only reached *ca.* 45% conversion. At this point the ^{1}H NMR spectrum also showed significant impurities and was not investigated further. In contrast, reaction between **10** and HC(O)NMe$_2$ in C_6D_6 formed the fluxional intermediate Cp*Ti{PhC(N^{i}Pr)$_2$}{NC(Ar^{F_5})NO^{t}Bu}{OC(NMe$_2$)H} (**24**) within 5 min. This, in turn, converted quantitatively to the μ-oxo dimer **7** and the 1,3-diazabutadiene Me$_2$N{NC(Ar^{F_5})NO^{t}Bu}H (**25**) after 1 h (Scheme 4.5; 10% conversion after 5 min). On scale up, **25** was isolated by sublimation as a white solid in 64% yield and its identity confirmed by X-ray diffraction (*vide infra*).

Compound **24** was too unstable to be isolated and the resonances of the Cp*, PhC(N^{i}Pr)$_2$ and HC(O)NMe$_2$ were only slightly shifted from those of **10** and the free formamide. Accordingly, by analogy to the crystallographically characterised σ-adduct Cp*Ti{PhC(N^{i}Pr)$_2$}{NC(Ar^{F_5})NO^{t}Bu}(CN^{t}Bu) (**28**, *vide infra*) it is assigned the structure shown in Scheme 4.5, existing in dynamic equilibrium on the NMR timescale with the enantiomer **24′** as implied by the apparent molecular C_s symmetry. Compound **25** is proposed to form by a similar cycloaddition-extrusion mechanism to that established for **23a-f**. The fast reaction and lack of observation of any intermediates (i.e. analogues of **22a-f**) is consistent with the strong π-donor ability of the –NMe$_2$ group which, by analogy with the results for the reactions with ArC(O)H, would both destabilise any intermediate metallacycle and accelerate the rate of extrusion of **25** from it.

Scheme 4.5. Reaction of Cp*Ti{PhC(N^{i}Pr)$_2$}{NC(Ar^{F5})NO^{t}Bu} (**10**) with HC(O)NMe$_2$.

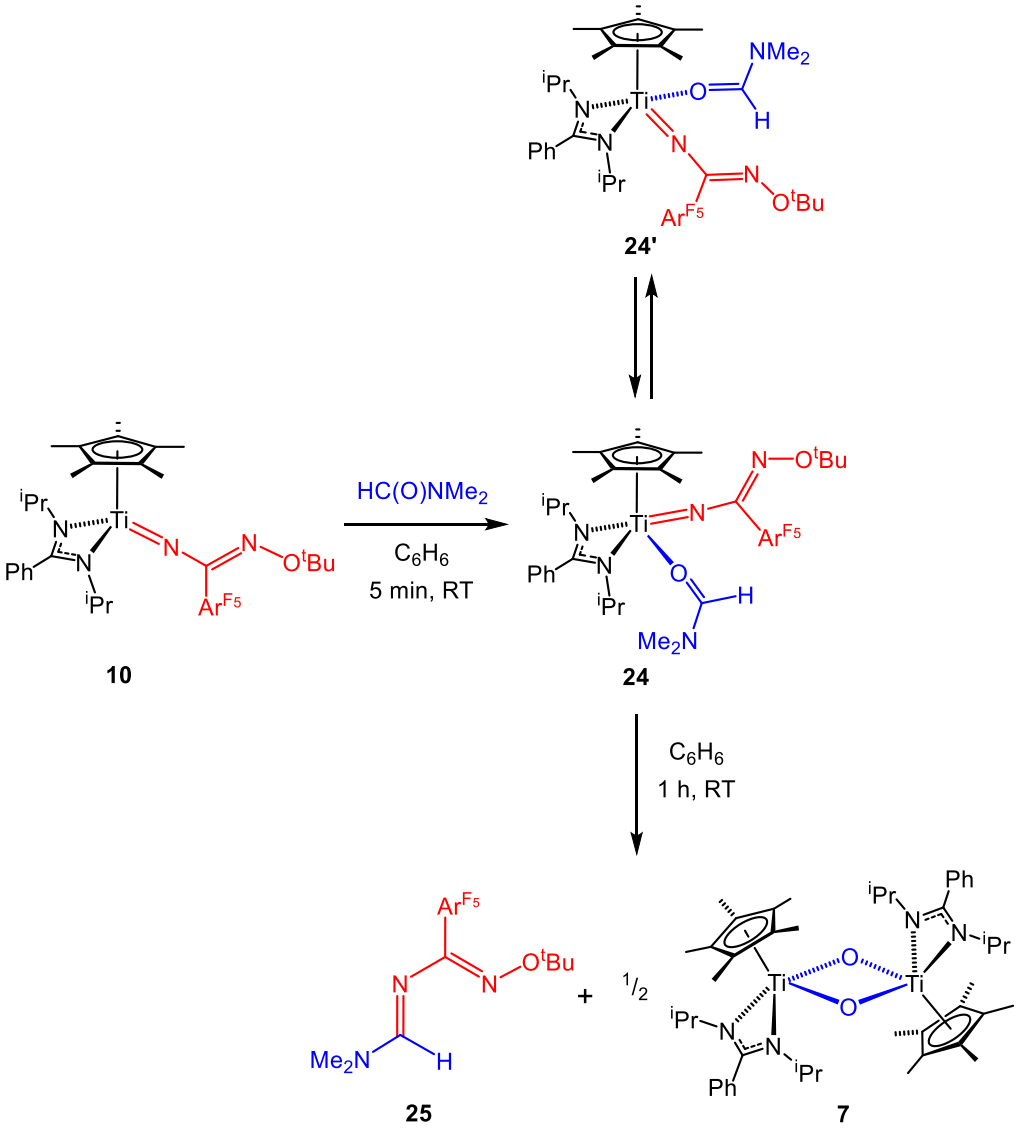

The solid state structures of (4-C$_6$H$_4$NMe$_2$)C{NC(Ar^{F5})NO^{t}Bu}H (**23e**) and **25** are shown in Fig. 4.10 and selected bond distances and angles are given in Table 4.5. In general terms the metric parameters lie within the expected ranges for the various bond types and functional groups.[85, 93] In particular, the N(1)–C(5) and N(2)–C(12) distances (range 1.281(5) – 1.2990(16) Å) and N(2)–C(5) distances (1.394(5) and 1.3826(15) Å) are consistent with double and single bonds and the 1,3-diazabutadiene structures shown in Eq 4.4 and Scheme 4.5. The Ar^{F5} ring is approximately orthogonal to the N(1)–C(5)–N(2) moiety in each compound (angles between the least-squares planes = 76.8 and 68.8°, respectively), whereas the –C$_6$H$_4$NMe$_2$ and –NMe$_2$ groups are approximately co-planar with the C(12)–N(2)–C(5) linkage as shown by the dihedral

angles N(2)–C(12)–C(13)–C(14,18) = 3.1 º (avg.) and N(2)–C(12)–N(3)–C(13,14) = 3.9 º (avg.). The most significant difference between **23e** and **25** is the geometry about the N(2)–C(5) bond. Compound **23e** adopts a *transoid* conformation of the C=N double bonds whereas **25** has a *cisoid* one (*cf.* Fig. 4.11) as quantified by the N(1)–C(5)–N(2)–C(12) dihedral angles of 174.8 and 35.3 º, respectively. For **23e** this dihedral angle is close to the ideal value of 180 º, whereas for **25** it deviates significantly from 0 º due to repulsion between H(1) and the N(1) lone pair. The relatively poor precision of the structure for **23e** (due to the poorly-diffracting nature of the crystals) prevents a more detailed comparison of its individual bond distances and angles with those of **25**, but analysis of the DFT computed structures for each compound confirmed the general structural features.

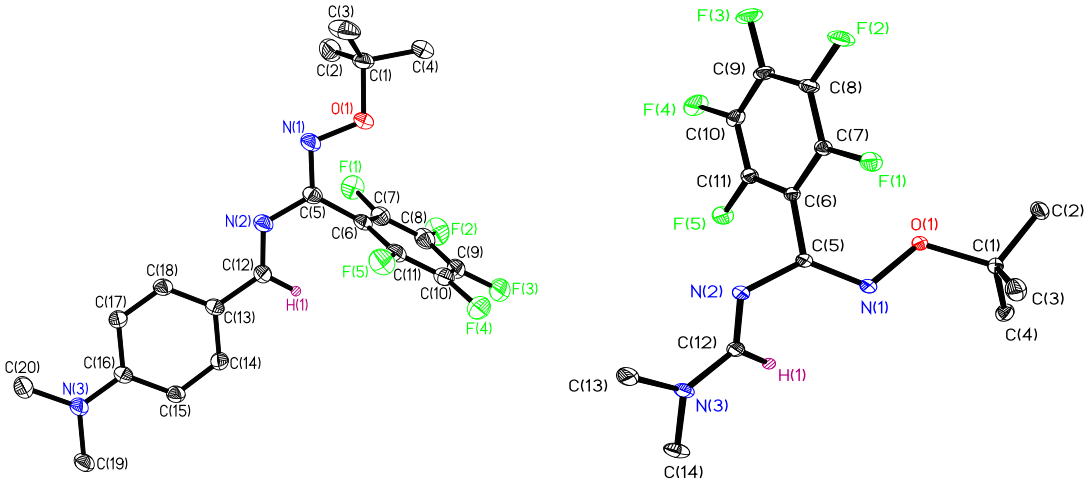

Figure 4.10. Displacement ellipsoid plots (20% probability) of (4-$C_6H_4NMe_2$)C{NC(Ar^{F_5})NO^{t}Bu}H (**23e**, left) and Me_2N{NC(Ar^{F_5})NO^{t}Bu}H (**25**, right). H(1) is drawn as a sphere of an arbitrary radius in each case and the other H atoms are omitted for clarity.

Table 4.5. Selected bond lengths (Å) and angles (°) for (4-$C_6H_4NMe_2$)C{NC(Ar^{F5})NO^{t}Bu}H (**23e**) and Me_2NC{NC(Ar^{F5})NO^{t}Bu}H (**25**).

Parameter	**23e**	**25**
N(1)-O(1)	1.408(4)	1.4199(13)
N(1)-C(5)	1.290(5)	1.2872(16)
N(2)-C(5)	1.394(5)	1.3826(15)
N(2)-C(12)	1.281(5)	1.2990(16)
N(3)-C(16)	1.371(5)	
N(3)-C(12)		1.3318(16)
C(1)-O(1)	1.464(5)	1.4605(14)
C(5)-C(6)	1.479(5)	1.4959(16)
C(12)-C(13)	1.443(5)	
N(1)-O(1)-C(1)	112.0(3)	110.61(8)
N(2)-C(5)-N(1)	116.3(4)	121.85(11)
N(3)-C(12)-N(2)		122.81(12)
C(5)-N(1)-O(1)	108.7(3)	109.91(9)
C(12)-N(2)-C(5)	118.8(3)	117.01(11)

To explore further these differences in apparent conformational preference, DFT calculations were carried out on PhC{NC(Ar^{F5})NO^{t}Bu}H (**23a**), **23e** and **25** in their *transoid* and *cisoid* conformations. Corresponding calculations were also carried out on the hypothetical HC{NC(Ar^{F5})NO^{t}Bu}H (**26**) with H in place of the 4-C_6H_4X or NMe_2 groups of **23a**,**e** and **25**. In each case the calculated geometries and metric parameters compared well with the experimental ones, namely a well-defined 1,3-diazabutadiene structure with an approximately co-planar –N(1)=C–N(2)=C– linkage in the *transoid* conformations, and a somewhat twisted arrangement for the *cisoid* ones. Since the calculations found no significant or systematic difference in entropy between each pair

of conformers (ΔS typically varied between *ca.* -0.5 and 1.5 cal mol^{-1} K^{-1}) the discussion will focus only on the differences in enthalpy (ΔH).[94]

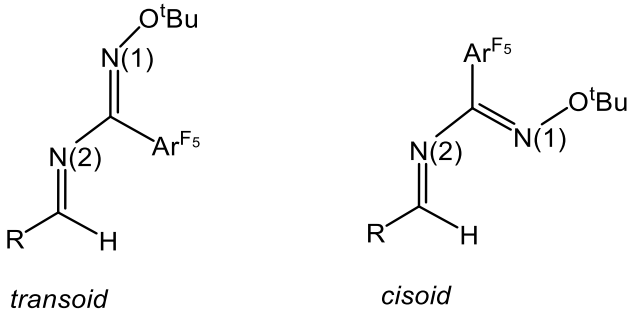

Figure 4.11. *Transoid* and *cisoid* isomers of RC{NC(Ar^{F5})NO^{t}Bu}H (R = 4-C_6H_4X (**23a-f**), NMe_2 (**25**) or H (**26**)).

In agreement with the experimental structures, the *transoid* isomer of **23e** was 0.67 kcal mol^{-1} more stable than the *cisoid* alternative, whereas for **25** the *cisoid* conformer was the more stable isomer by a similar amount (ΔH = 0.65 kcal mol^{-1}). The enthalpy difference (ΔH = 0.80 kcal mol^{-1}) in favour of the *transoid* form for **23a** was slightly larger than for **23e**, suggesting that the *para*-NMe_2 group in the latter slightly destabilises the *transoid* conformer relative to the *cisoid* one. For the hypothetical HC{NC(Ar^{F5})NO^{t}Bu}H (**26**), having only a H atom in place of 4-C_6H_4X or NMe_2, the *transoid* form was 1.23 kcal mol^{-1} more stable, showing that this is the intrinsically more stable conformer in this type of system, although the energy differences are all rather small. Examination of the Mulliken atomic charges (*q*) for N(2) revealed that changing the R-group in *transoid*-RC{NC(Ar^{F5})NO^{t}Bu}H from H to progressively better π-donor substituents gave a build up of charge on this atom: R = H, *q*(N(2)) = -0.2291; R = Ph, *q*(N(2)) = -0.2578; R = 4-$C_6H_4NMe_2$, *q*(N(2)) = -0.2751; R = NMe_2, *q*(N(2)) = -0.3286. Therefore it seems that increased lone pair repulsion between N(2) and N(1) in the *transoid* conformer with increasing R-group π-donation may be an important factor leading to a switch towards the *cisoid* alternative.

The small ΔH values suggest that both the *transoid* and *cisoid* forms of **23a-f** and **25** may exist in solution since ΔH values of *ca.* ±0.70 kcal mol^{-1} (assuming ΔS ≈ 0 as discussed) correspond to a *ca.* 1:±4 ratios of conformers. Although only one set of NMR resonances is seen experimentally in all cases, it was considered possible that both conformers could be present in solution but in fast dynamic equilibrium on the NMR timescale. To determine whether *cisoid* ↔ *transoid* interconversions might be

energetically feasible the corresponding transition states were determined by DFT for the *transoid* to *cisoid* isomerisation of **23a** and **23e** ($\Delta H^{\ddagger}$ = 4.71 and 4.36 kcal mol^{-1}, respectively) and for the *cisoid* to *transoid* isomerisation of **25** ($\Delta H^{\ddagger}$ = 3.78 kcal mol^{-1}). The computed $\Delta S^{\ddagger}$ values were small and in the range -3 to -5 cal mol^{-1} K^{-1}. Taken together, the DFT calculations estimate that the maximum $\Delta G^{\ddagger}$ for the *cisoid* ↔ *transoid* transformations is less than *ca.* 6.5 kcal mol^{-1} at 298 K. This readily accessible barrier is consistent with the observation of a single time-averaged set of NMR resonances in all cases.

4.3.3 Selectivity

In the presence of both PhC(O)H and ^{t}BuNCO (1:1 ratio) Cp*Ti{PhC($N^{i}Pr)_2$}($NO^{t}Bu$) (**3**) is found to react solely with PhC(O)H, forming PhC($NO^{t}Bu$)H and the oxo-bridged dimer (**7**), whilst leaving the ^{t}BuNCO unreacted, Scheme 4.6. This is not unexpected since the irreversible reaction of **3** with PhC(O)H is significantly faster than with ^{t}BuNCO, see Chapter Three for further details.[60] On the other hand, experiments discussed above have shown that the reaction of **10** with PhC(O)H to form Cp*Ti{PhC($N^{i}Pr)_2$}{N(C{Ar^{F5}}$NO^{t}Bu$)C(Ph)(H)O} (**22a**) is reversible which, unlike with **3**, could give further insights into the thermodynamic and kinetic preference of Ti=N multiple bonds for different carbonyl compounds. A series of competition experiments testing the selectivity of **10** for isocyanates, aldehydes and amides were therefore designed.

First, the equivalent competition reaction between **10** and a pre-mixed solution of PhC(O)H and ^{t}BuNCO (1:1 ratio) was carried out, Scheme 4.6. After 5 min only resonances attributed to Cp*Ti{PhC($N^{i}Pr)_2$}{N(C{Ar^{F5}}$NO^{t}Bu$)C(Ph)(H)O} (**22a**) and unreacted ^{t}BuNCO were identified in the ^{1}H NMR spectrum. Over time, as already discussed, **22a** undergoes an irreversible cycloaddition-extrusion process releasing PhC(NC{Ar^{F5}}$NO^{t}Bu$)H (**23a**). However, since the extrusion of PhC(O)H from **22a** to reform **10** is fast (as identified through spin saturation transfer measurements), faster than extrusion to form the oxo-bridged dimer **7** and **23a**, this implies both a kinetic and thermodynamic preference for cycloaddition reactions between Ti=NR bonds and aldehydes rather than with isocyanates. As a test, 1 equiv of PhC(O)H was added to pre-formed Cp*Ti{PhC($N^{i}Pr)_2$}-{N(C{Ar^{F5}}$NO^{t}Bu$)C($N^{t}Bu$)O} (**20**). Within 35 mins, a new (unidentified) non-symmetric species, **27**, was observed in both the ^{1}H and ^{19}F

NMR spectra. This suggests further reaction of **20** with PhC(O)H, rather than extrusion of ^{t}BuNCO to form **10** which, as shown, would react with PhC(O)H to form **22a**. This implies that if **20** had formed in the reaction of **10** with both PhC(O)H and ^{t}BuNCO, it would have reacted further with PhC(O)H forming **27**. Therefore since only **22a** and unreacted ^{t}BuNCO were observed in the ^{1}H NMR spectrum, **22a** is both kinetically and thermodynamically favoured.

Scheme 4.6. Reaction of Cp*Ti{PhC(N^{i}Pr)$_2$}(NO^{t}Bu) (**3**) with PhC(O)H and ^{t}BuNCO (1:1 ratio, top) and of Cp*Ti{PhC(N^{i}Pr)$_2$}{NC(Ar^{F5})NO^{t}Bu} (**10**) with PhC(O)H and ^{t}BuNCO (1:1 ratio, bottom).

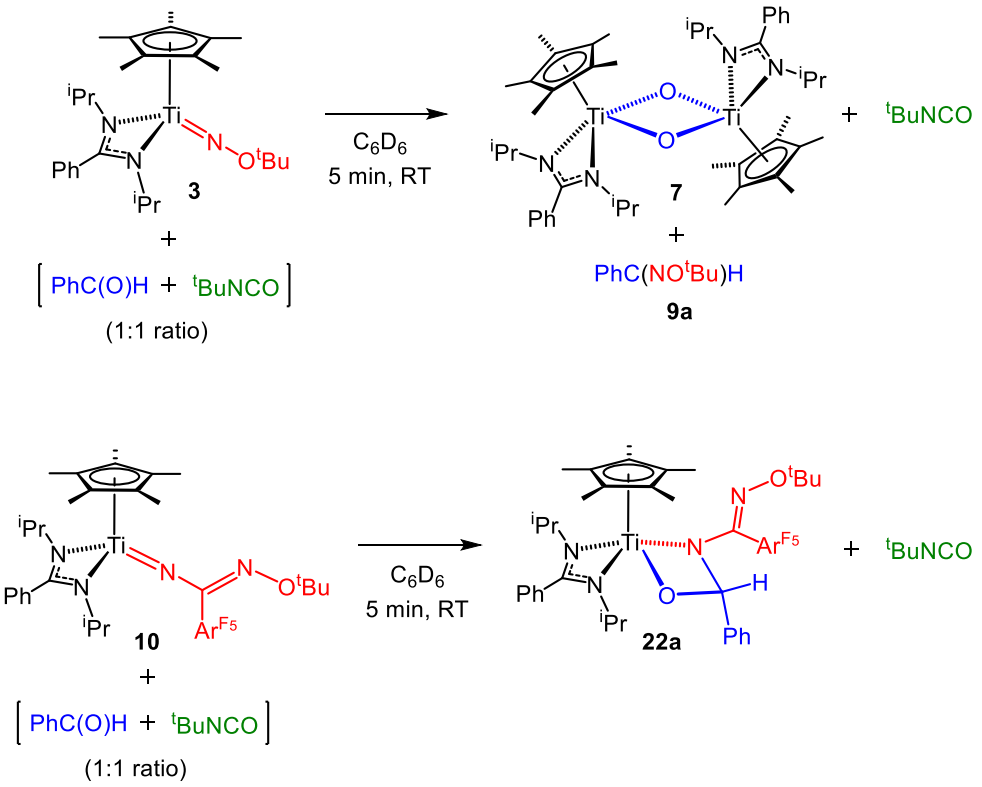

Scheme 4.7. Reaction of Cp*Ti{PhC(N^{i}Pr)$_2$}{NC(Ar^{F5})NO^{t}Bu} (**10**) with HC(O)NMe$_2$ and ^{t}BuNCO (1:1 ratio, top), and of Cp*Ti{PhC(N^{i}Pr)$_2$}{NC(Ar^{F5})NO^{t}Bu} (**10**) with HC(O)NMe$_2$ and PhC(O)H (1:1 ratio, bottom).

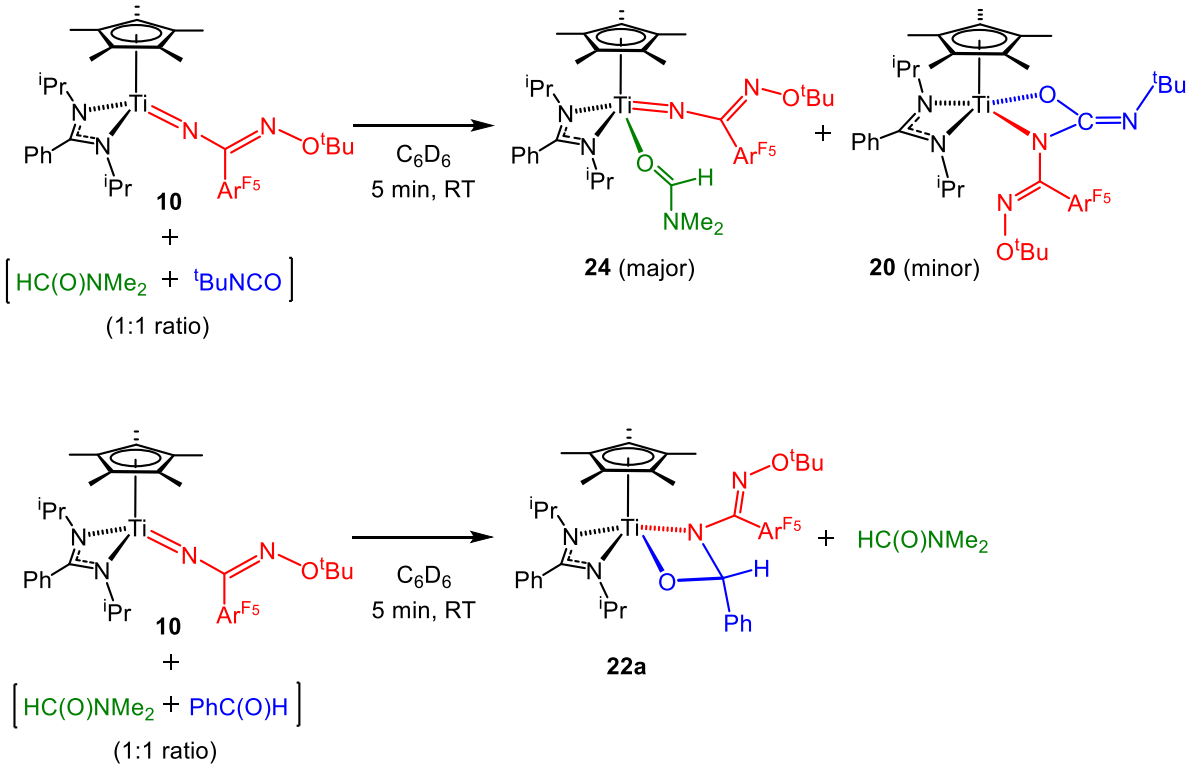

In a separate experiment, reaction of **10** with a pre-mixed solution of HC(O)NMe$_2$ and ^{t}BuNCO also resulted in limited reaction with the isocyanate (< 10%), instead preferring to form the adduct, **24**, Scheme 4.7, which over time undergoes cycloaddition-extrusion to form Me$_2$NC(NC{Ar^{F5}}NO^{t}Bu)H (**25**). This suggests that the Ti=N bond of **10** is selective for C=O bonds in the order ^{t}BuNCO < HC(O)NMe$_2$ < PhC(O)H. As a test, **10** was added to a pre-mixed solution of PhC(O)H and HC(O)NMe$_2$ (1:1 ratio, Scheme 4.7). Accordingly, only resonances attributed to **22a** and unreacted HC(O)NMe$_2$ were observed in the ^{1}H NMR spectrum.

4.4 Reactions with nitriles

There have been a number of reports of the reactions of transition metal imido and hydrazido complexes with organic isonitriles, with the commercially available ^{t}BuNC and XylNC derivatives being the most commonly studied.[79, 82, 95] [1+2] addition of RNC to the M=NR′ bond of imides or hydrazides forms η^2-carbodiimide complexes of the type (L)M(η^2-RNCNR′) which have been isolated in several cases for R′ =

hydrocarbyl.[76, 96] In other instances the first-formed carbodiimides are not observed but undergo further reactions. These include reactions with further equivalent(s) of isonitrile giving new heterocyclic complexes,[97-99] or in the case of certain Group 4 diphenyl hydrazido complexes, N_α–N_β bond cleavage resulting in mixed amide-metallated carbodiimide complexes (L)M(NPh_2)(NCNR).[19, 26, 28] In some instances, reaction with the M=NR′ bond does not occur and RNC σ-adducts can be isolated.[49, 100-102] Work from our group has previously reported on the reactions of Cp*Ti{RC(N^iPr)$_2$}(NR′) (R = Me or Ph; R′ = ^{t}Bu, aryl, NPh_2, NMe_2, $NNCPh_2$, O^tBu (**3**)) with isonitriles. In the case of the imido complexes no reaction was observed, whereas unknown mixtures were formed with the diphenyl hydrazido compound or **3**.[60, 102] The other complexes formed labile σ-adducts, one of which was structurally characterised.[49, 102]

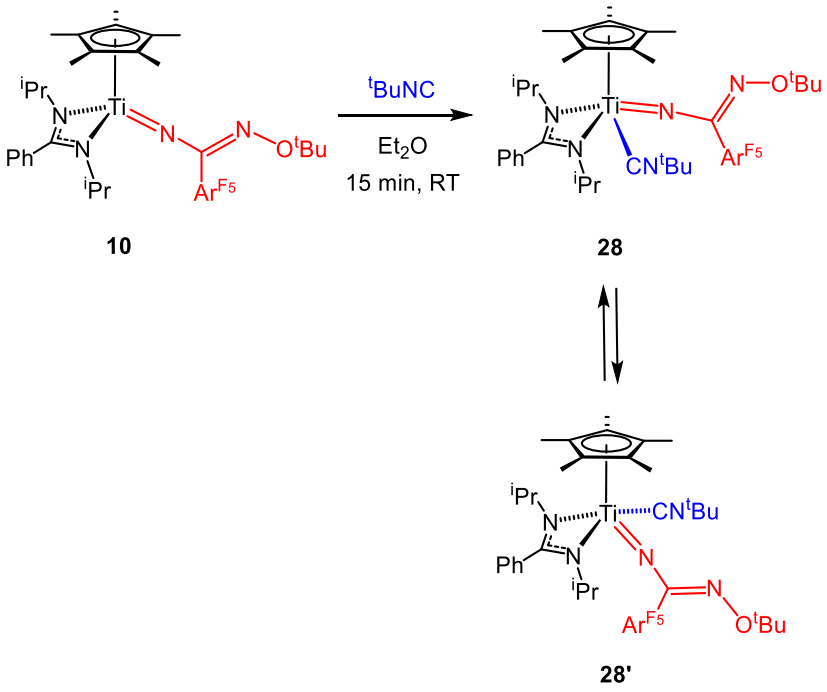

Equation 4.5

Reaction of **10** with ^{t}BuNC in Et_2O at room temperature formed the σ-adduct Cp*Ti{PhC(N^iPr)$_2$}{NC(Ar^{F5})NO^tBu}(CN^tBu) (**28**, Eq 4.5) which was isolated in 61% yield after crystallisation from pentane. When the reaction was followed on the NMR tube scale in C_6D_6 the conversion was quantitative. The NMR spectrum at room temperature indicated a C_s symmetric product on the NMR timescale. This is attributed to the rapid interconversion between the two enantiomers **28** and **28′** (Eq 4.5). Cooling a solution of **28** in toluene-d_8 showed the *iso*-propyl groups as two apparent septets and

four doublets, although the resonances remained broad, even at -80 °C. At this temperature the *o*-and *m*-C_6F_5 ^{19}F resonances were inequivalent, indicative of restricted rotation about the $N_2C–C_{ipso}$ bond of the benzimidamido ligand. The IR spectrum of **28** shows a strong ν(C≡N) band at 2186 cm^{-1}, at a higher frequency than that for free ^{t}BuNC (2138 cm^{-1}), consistent with coordination to the electron deficient titanium.[103-106] The ν(C≡N) band is at higher frequency than that for Cp*Ti{MeC(N^{i}Pr)$_2$}(NNCPh$_2$)(CN^{t}Bu) (2164 cm^{-1})[49] and the comparatively labile σ-adduct Cp*Ti{MeC(N^{i}Pr)$_2$}(NNMe$_2$)(CN^{t}Bu)[102] (2152 cm^{-1}). Other examples of titanium d^0 *tert*-butyl isocyanide adducts include (MPB)TiCl$_2$(CN^{t}Bu) (MPB^{2-} = 2,2′-methylenbis(6-*tert*-butyl-4-methylphenolate) dianion)[107] and TiCl$_4$(CN^{t}Bu)$_2$.[104]

Diffraction-quality crystals of **28** were grown from a saturated pentane solution at -30 °C. The molecular structure is shown in Fig. 4.12 and selected distances and angles are listed in Table 4.6. The structure confirms **28** as a half-sandwich complex with a 4-legged piano stool geometry around the metal with η^5-C_5Me_5 and κ^2*N*,*N*′-amidinate ligands, and is similar to that reported recently for Cp*Ti{MeC(N^{i}Pr)$_2$}(NNCPh$_2$)(CNXyl).[49, 102] The Ti(1)–C(12) bond distance of 2.191(2) Å in **28** is relatively short when compared to other titanium(+4) isonitrile adducts (2.232(2) – 2.256(6) Å), consistent with the relatively high frequency observed for ν(C≡N).[49, 104-106] The σ-only nature of the Ti–CN^{t}Bu bond is also indicated by the short C(12)–N(3) bond distance of 1.153(3) Å. The Ti(1)–N(1) bond is slightly longer than that in **10** (1.7739(17) in **28** *vs* 1.747(4) Å) which is attributed to the increased coordination number around titanium.

No further reaction was found for **28** at room temperature, and after 18 h at 70 °C in C_6D_6 only low intensity new resonances were observed. After 5 d complicated mixtures were formed and this reaction was not scaled up. The poor reactivity of **28** is probably due to the steric demands of the ^{t}BuNC ligand.

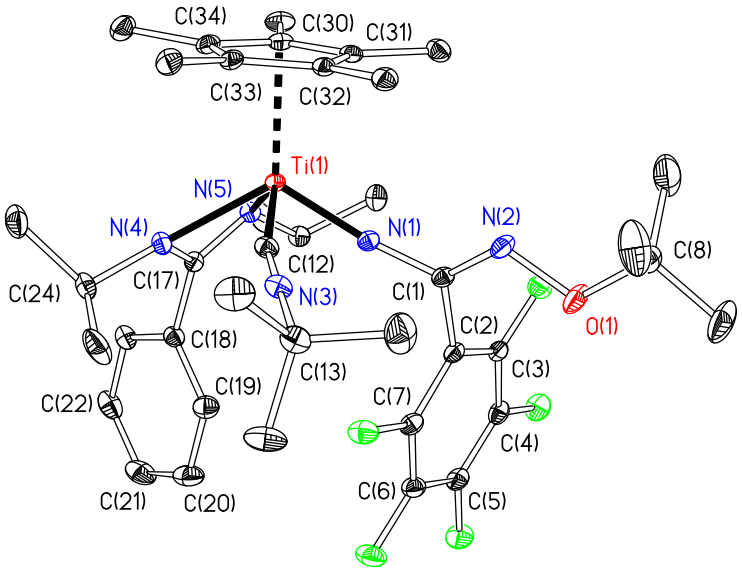

Figure 4.12. Displacement ellipsoid plot (20% probability) of Cp*Ti{PhC(N^{i}Pr)$_2$}{NC(Ar^{F5})NO^{t}Bu}(CN^{t}Bu) (**28**). H atoms omitted for clarity.

Table 4.6. Selected bond lengths (Å) and angles (°) for Cp*Ti{PhC(N^{i}Pr)$_2$}{NC(Ar^{F5})NO^{t}Bu}(CN^{t}Bu) (**28**). Cp$_{cent}$ is the computed Cp* ring carbon centroid.

Ti(1)-Cp$_{cent}$	2.091	Ti(1)-C(12)	2.191(2)
Ti(1)-N(1)	1.7739(17)	N(3)-C(12)	1.153(3)
Ti(1)-N(4)	2.1459(17)	N(3)-C(13)	1.462(3)
Ti(1)-N(5)	2.1957(17)		
Cp$_{cent}$-Ti(1)-N(1)	119.37	Cp$_{cent}$-Ti(1)-N(5)	115.62
Cp$_{cent}$-Ti(1)-N(4)	121.35	Cp$_{cent}$-Ti(1)-C(12)	104.69
N(4)-Ti(1)-N(5)	62.09(6)	Ti(1)-C(12)-N(3)	167.35(19)
Ti(1)-N(1)-C(1)	169.81(15)	C(12)-N(3)-C(13)	179.5(2)

Scheme 4.8. Reaction of Cp*Ti{PhC(N^{i}Pr)$_2$}{NC(Ar^{F5})NO^{t}Bu} (**10**) with XylNC.

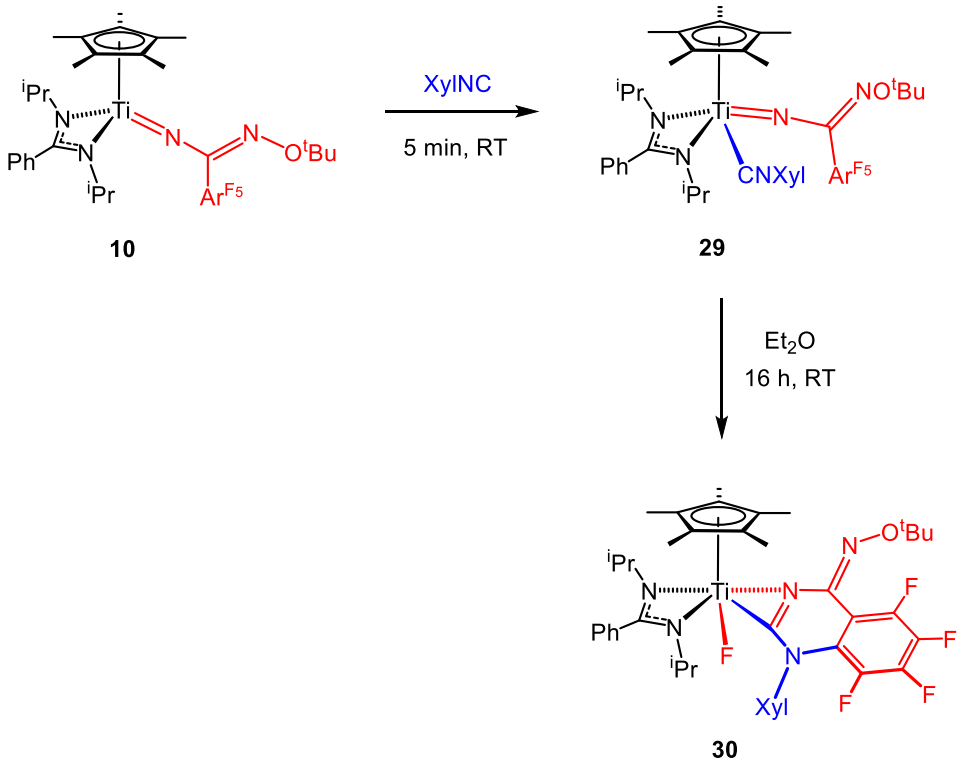

Reaction of **10** with XylNC on the NMR tube scale in C_6D_6 resulted in the immediate and quantitative formation of Cp*Ti{PhC(N^{i}Pr)$_2$}{NC(Ar^{F5})NO^{t}Bu}(CNXyl) (**29**, Scheme 4.8) which is unstable at room temperature and was characterised *in situ*. The dynamic NMR behavior is analogous to that for **28**: the room temperature NMR spectra indicate a C_s symmetric compound while at -70 °C the resonances are reminiscent of those for **28**. Over a period of *ca.* 16 h **29** converted quantitatively to a new compound, Cp*Ti{PhC(N^{i}Pr)$_2$}{NC(NO^{t}Bu)C$_6$F$_4$N(Xyl)C}(F) (**30**), which was isolated as an orange powder in 85% yield after scale up in diethyl ether. Diffraction-quality crystals were grown from *n*-hexane. The molecular structure is shown in Fig. 4.13 and selected bond distances and angles are listed in Table 4.7.

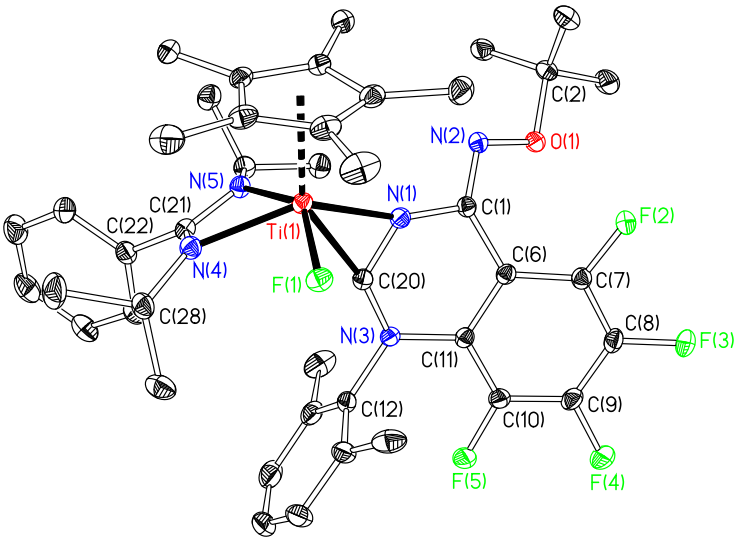

Figure 4.13. Displacement ellipsoid plot (20% probability) of Cp*Ti{PhC(N^{i}Pr)$_2$}-{NC(NO^{t}Bu)C$_6$F$_4$N(Xyl)C}(F) (**30**). H atoms omitted for clarity.

Table 4.7. Selected bond lengths (Å) and angles (°) for Cp*Ti{PhC(N^{i}Pr)$_2$}-{NC(NO^{t}Bu)C$_6$F$_4$N(Xyl)C}(F) (Xyl = 2,6-C$_6$H$_3$Me$_2$, **30**).

Ti(1)-Cp$_{cent}$	2.115	N(1)-C(1)	1.414(2)
Ti(1)-C(20)	2.1407(18)	N(2)-C(1)	1.283(2)
Ti(1)-N(1)	2.0773(16)	N(3)-C(11)	1.417(2)
Ti(1)-N(4)	2.1089(17)	N(3)-C(12)	1.456(2)
Ti(1)-N(5)	2.2471(16)	N(3)-C(20)	1.367(2)
Ti(1)-F(1)	1.8688(11)	C(6)-C(1)	1.472(3)
N(1)-C(20)	1.305(2)	C(11)-C(6)	1.416(3)
Cp$_{cent}$-Ti(1)-N(1)	113.3	Cp$_{cent}$-Ti(1)-N(5)	109.23
Cp$_{cent}$-Ti(1)-N(4)	110.17	Cp$_{cent}$-Ti(1)-C(20)	148.90
Cp$_{cent}$-Ti(1)-F(1)	101.81	N(4)-Ti(1)-N(5)	60.31(6)
Ti(1)-N(1)-C(20)	74.65(10)	Ti(1)-C(20)-N(1)	69.35(10)
C(1)-N(2)-O(1)	111.76(15)	N(1)-C(1)-N(2)	116.64(16)

Compound **30** is a half-sandwich complex with a 5-legged piano stool geometry. In addition to the expected η^5-C_5Me_5 and κ^2*N*,*N*′-amidinate ligands, the titanium is coordinated to a fluoride ligand and a new heterocyclic fragment derived from the XylNC (i.e. C(20), N(3) and the xylyl group) and benzimidamido ligands of **29**. The metric parameters for the Cp*Ti{PhC(N^{i}Pr)$_2$} fragment lie within the expected values and are similar to those for complexes supported by this ligand set. The Ti(1)–F(1) bond length of 1.8688(11) Å lies within the range reported for other cyclopentadienyl-supported titanium complexes reported in the literature (range 1.812 – 1.937 Å).[85] The heterocyclic fragment may be viewed as a 2-metallated 1-arylquinazolin-4(1*H*)-one oxime ether. The Ti(1)–N(1) and Ti(1)–C(20) bond distances of 2.0773(16) and 2.1407(18) Å, respectively, are consistent with this description. The C(20)–N(1) and C(1)–N(2) bond lengths are indicative of C=N double bonds (1.305(2) and 1.283(2) Å, respectively). The intermediate distances for N(3)–C(20) (1.367(2) Å) and N(1)–C(1) (1.414(2) Å) indicates slightly differing extents of delocalisation. The NMR data are consistent with this C_1 symmetric complex existing also in solution. In particular, one singlet and four multiplets were observed in the ^{19}F NMR spectrum at -20 ^{o}C, the singlet being at δ -101.8 ppm which suggested that it may no longer be bonded to carbon. A ^{19}F COSY NMR experiment showed scalar coupling between the other four ^{19}F atoms (range δ -118.7 to -162.7 ppm) but no apparent coupling to the singlet resonance. In the ^{13}C NMR spectrum the quaternary signal corresponding to the metal-bound C(20) was observed at δ 216.7 ppm.

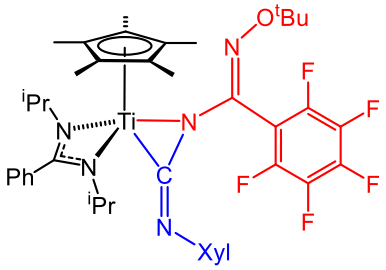

30_int

Following initial formation of **29**, the mechanism for formation of **30** is proposed to proceed *via* [1+2] addition of XylNC to Ti=NC(Ar^{F5})NO^{t}Bu forming **30_int** containing an η^2-carbodiimide ligand. Related compounds have been reported previously, for example in the reactions of Cp*Ir(N^{t}Bu)[76] and Cp$_2$Zr(N^{t}Bu)(THF)[96] with ^{t}BuNC. Subsequent nucleophilic attack by XylNC on the *ortho* position of the Ar^{F5} group displaces the fluorine which forms a new bond to titanium. Other examples of C–F

activation using d^0 Group 4 metal species have been reported[41, 108, 109] and titanium fluoride compounds are not uncommon.[41, 108-113] Quinazoline-type compounds have been used in the synthesis of many pharmaceutical agents including anti-fungal, anti-cancer and anti-HIV drugs.[114] Conventional synthetic routes to quinazolines include reaction of 2-aminobenzophenones and benzylic amines in the presence of I_2 and *tert*-butyl hydroperoxide,[115] using (2-bromophenyl)-methylamines with amides in the presence of air, CuI, K_2CO_3 and *i*-PrOH,[116] and from imidoylcarbodiimides.[81]

In an attempt to extend this reactivity, XylNC was added to a C_6D_6 solution of Cp*Ti{PhC(N^{i}Pr)$_2$}{NC(Ar^{F_2})NO^{t}Bu} (**11**) and the reaction monitored by ^{1}H and ^{19}F NMR spectroscopy. Within 5 min a σ-adduct, Cp*Ti{PhC(N^{i}Pr)$_2$}{NC(Ar^{F_2})NO^{t}Bu}(CNXyl) (**31**), analogous to **28** and **29** was formed and characterised by NMR *in situ*. After 16 h at room temperature a second set of signals were observed in the ^{1}H and ^{19}F NMR spectra, attributed to a new compound Cp*Ti{PhC(N^{i}Pr)$_2$}{NC(NO^{t}Bu)C$_6$FH$_3$N(Xyl)C}(F) (**32**), the analogue of **30**. However, the rate of the reaction was slow and after 5 d had only reached 70% completion. At this stage significant amounts of other (unknown) products had also formed and it was decided not to scale up this reaction. The slower rate of reaction of **31** compared to **29** is attributed to the decreased electrophilicity of the 2,6-$C_6H_3F_2$ ring in the former compared to C_6F_5.

4.5 Reaction with B(Ar^{F_5})$_3$

As mentioned, Group 4 hydrazides M(N$_2^R$N^{py})(NNPh$_2$)(py) readily form zwitterionic N$_\alpha$-adducts of the type M(N$_2^R$N^{py}){η^2-N(NPh$_2$)B(Ar^{F_5})$_3$} (**4.1**; M = Ti, Zr or Hf, R = SiMe$_3$ or SiMe$_2$^{t}Bu) with B(Ar^{F_5})$_3$.[19, 29] In an extension of this chemistry Chapter Three described the reaction of Cp*Ti{PhC(N^{i}Pr)$_2$}(NO^{t}Bu) (**3**) with an excess of B(Ar^{F_5})$_3$, but in this case the reaction is accompanied by *iso*-butene elimination from the O-*tert*-butyl group and formation of a HNO (nitroxyl) ligand with B(Ar^{F_5})$_3$ stabilisation (**17**).[60] *Iso*-butene elimination from cationic Group 4 complexes containing either *tert*-butoxy ligands[117] or ligands with -O^{t}Bu substituents such as Carpentier's cationic *tert*-butyl enolate systems is not uncommon.[118, 119] It was therefore interesting to examine the corresponding reaction of **10**.

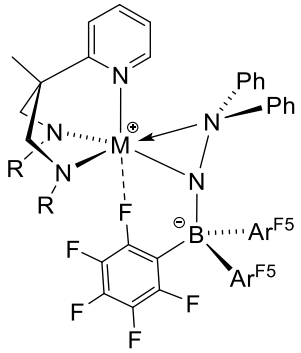

4.1

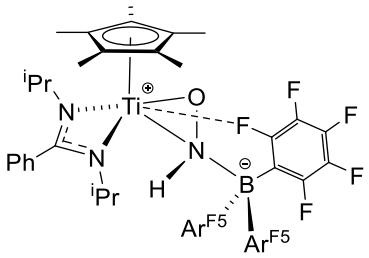

17

Addition of $B(Ar^{F_5})_3$ to **10** in C_6D_6 at room temperature led to consumption of *ca.* 1 equiv of borane after 7 h and formation of two new compounds, **33** (major, 86%) and **34** (minor, 14%), together with a small amount of *iso*-butene (Scheme 4.9). In addition to the expected new signals in the ^1H and ^{19}F NMR spectra for **33**, a new ^{11}B NMR resonance was observed at δ -7 ppm, indicative of four-coordinate boron[120] and N-coordination of $B(Ar^{F_5})_3$. Compound **33** is tentatively assigned as $Cp^*Ti\{PhC(N^iPr)_2\}\{N(B\{Ar^{F_5}\}_3)C(Ar^{F_5})N(O^tBu)\}$ as shown in Scheme 4.9 with a labile κ^2*N*,*N*′-borata-amidinate-type ligand, formed by addition of the borane to the N_α atom of **10** (*cf.* the corresponding N_α adducts **4.1** and **17** which have similar ^{11}B NMR shifts). Further characterisation and isolation of **33** was complicated by its instability towards elimination of *iso*-butene and emergence of $Cp^*Ti\{PhC(N^iPr)_2\}\{ON(B\{Ar^{F_5}\}_3)C(Ar^{F_5})N(H)(B\{Ar^{F_5}\}_3)\}$ (**34**). Formation of **34** was relatively slow at room temperature but the compound could nonetheless be isolated in analytically pure form, albeit only in 26% yield, after heating a mixture of **10** and 2 equivs of the borane in C_6H_6 for 4 d at 70 °C. It was not possible to obtain diffraction-quality crystals of **34** and the structure is assigned by analogy to those of **4.1** and **17** on the basis of the spectroscopic and other analytical data.

Scheme 4.9. Reaction of Cp*Ti{PhC(N^{i}Pr)$_2$}{NC(Ar^{F5})NO^{t}Bu} (**10**) with B(Ar^{F5})$_3$.

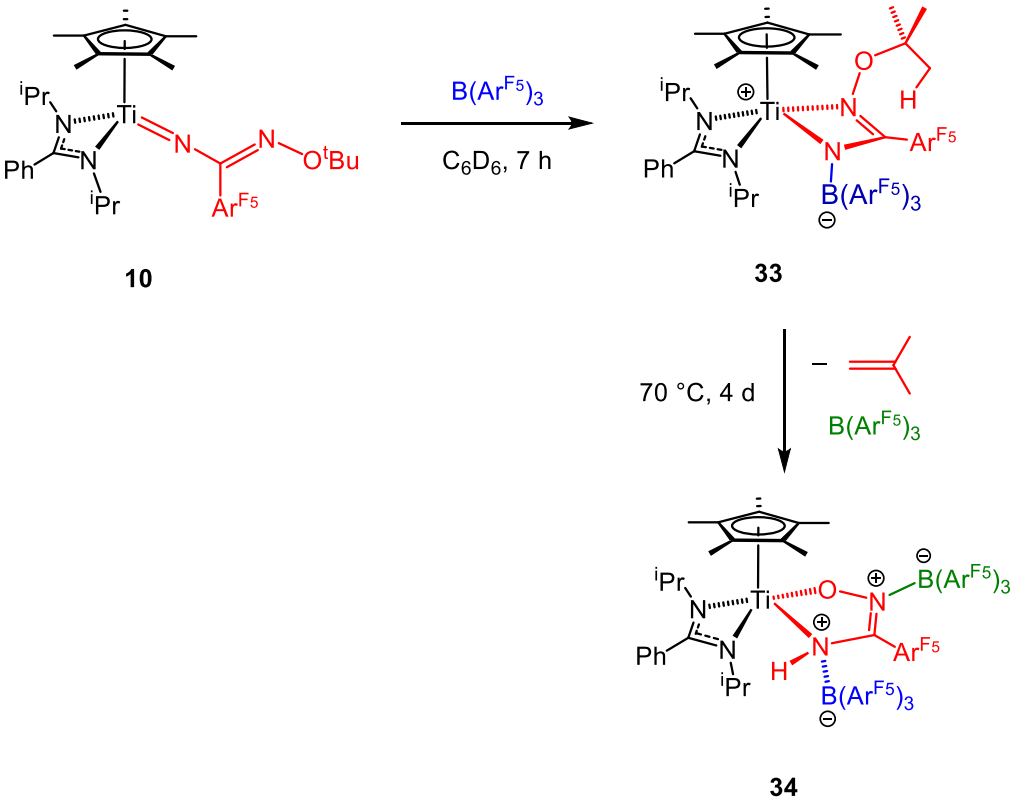

10 **33** **34**

The room temperature ^{1}H NMR spectrum of **34**, given in Figure 4.14, is consistent with a C_1 symmetric complex. In addition to resonances for the *iso*-propyl, Cp* and phenyl groups, a slightly broad singlet at δ 6.67 ppm (integral 1H), which couples to the C$_{ipso}$ of (H)NC<u>Ar</u>^{F5}NO and also to (H)N<u>C</u>Ar^{F5}N, was assigned to N<u>H</u> (the corresponding ν(N–H) is found at 3393 cm^{-1} in the IR spectrum). The room temperature ^{19}F NMR spectrum was very broad at room temperature, but on cooling to -60 ^{o}C the appearance of at least 22 multiplets (some overlapping) qualitatively confirmed the presence of 2 equivs of B(Ar^{F5})$_3$ in **34**. The room temperature ^{11}B NMR spectrum showed a single resonance δ -7 ppm which broadened into the baseline on cooling to -80 °C. Taken together, the ^{19}F and ^{11}B NMR variable temperature spectra suggest that at room temperature the two B(Ar^{F5})$_3$ groups are in dynamic exchange on the NMR timescale, but unfortunately low temperature limiting spectra could not be obtained. The loss of *iso*-butene from **33** to form **34** is reminiscent of the reactions of **3** to form **17**.

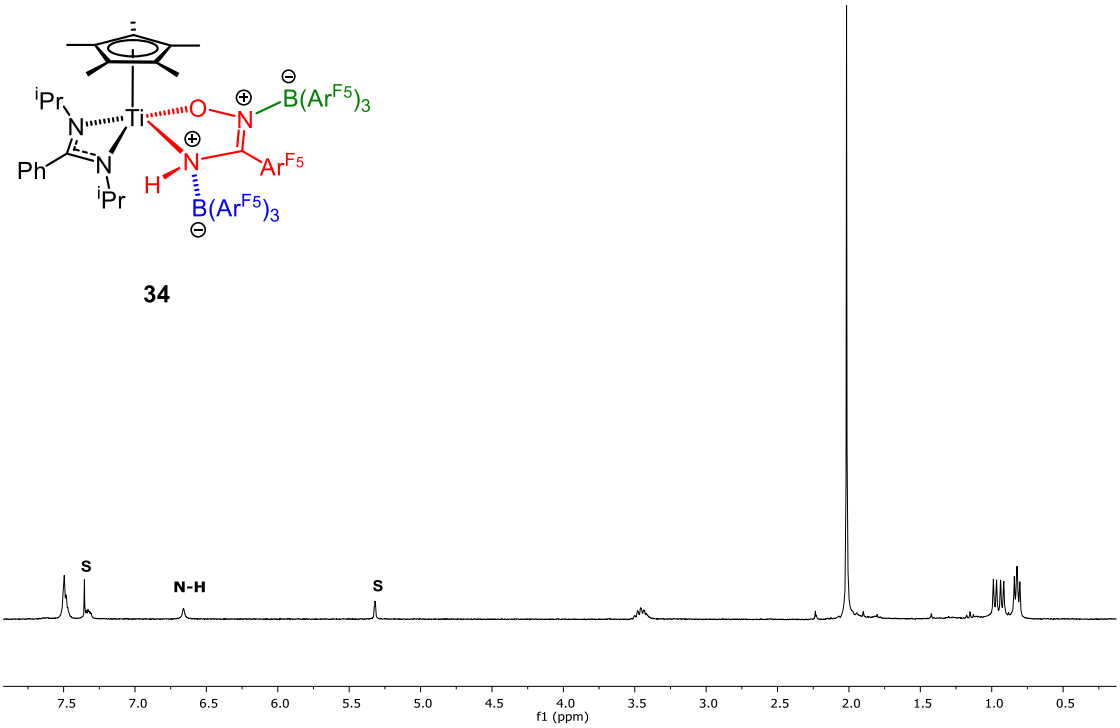

Figure 4.14. ^{1}H NMR spectrum (299.9 MHz, 293 K) of Cp*Ti{PhC(N^{i}Pr)$_2$}{ON(B{Ar^{F5}}$_3$)C(Ar^{F5})N(H)(B{Ar^{F5}}$_3$)} (**34**) in $CDCl_2$ ("S" denotes residual protio-solvent).

4.6 Conclusions

The first reactivity study of the benzimidamido ligand in Cp*Ti{PhC(N^{i}Pr)$_2$}{NC(Ar^{F5})NO^{t}Bu} (**10**) has allowed access to range of stable [2+2] cycloaddition intermediates which were isolated in good yields with CO_2 (forming **18**), isocyanates (forming **20**) and a series of aryl aldehydes (forming **22a-f**). The reactions with aryl aldehydes were reversible and allowed quantitative assessment of the relative stability of the corresponding metallacycles as a function of the ring-substituents. Upon heating, **20** and **22a-f** gave ^{t}BuNCNC(Ar^{F5})NO^{t}Bu (**21**) and (4-C$_6$H$_4$X)C{NC(Ar^{F5})NO^{t}Bu}H (**23a-f**), respectively *via* a stereospecific extrusion reaction. Reaction of **10** with HC(O)NMe$_2$ was more facile, yielding Me$_2$NC{NC(Ar^{F5})NO^{t}Bu}H (**25**) within 1 h at room temperature. DFT calculations on **23a-f** and **25** probed the electronic structure of these compounds and the relative energies of their conformers. Reaction of **10** with ^{t}BuNC and XylNC gave σ-adducts, Cp*Ti{PhC(N^{i}Pr)$_2$}{NC(Ar^{F5})NO^{t}Bu}(CNR) (R = ^{t}Bu (**28**) or Xyl (**29**)), and the latter underwent further reaction yielding Cp*Ti{PhC(N^{i}Pr)$_2$}{NC(NO^{t}Bu)C$_6$F$_4$N(Xyl)C}(F) (**30**) following a C–F activation

mechanism. Reaction of **10** with 2 equivs $B(Ar^{F_5})_3$ resulted in $Cp^*Ti\{PhC(N^iPr)_2\}\{ON(B\{Ar^{F_5}\}_3)C(Ar^{F_5})N(H)(B\{Ar^{F_5}\}_3)\}$ (**34**) following loss of *iso*-butene. In all of these reactions, the new organometallic or organic products contain the benzimidamide moiety, $NC(Ar^{F_5})NO^tBu$, derived initially from the *tert*-butoxyimido ligand of $Cp^*Ti\{PhC(N^iPr)_2\}(NO^tBu)$ (**3**) and $Ar^{F_5}CN$, and thus these represent new multicomponent coupling reactions.

4.7 References

1. N. Wiberg, H.-W. Haring, G. Huttner and P. Friedrich, *Chem. Ber.*, 1978, **111**, 2708.
2. A. J. Blake, J. M. McInnes, P. Mountford, G. I. Nikonov, D. Swallow and D. J. Watkin, *J. Chem. Soc., Dalton Trans.*, 1999, 379.
3. J. L. Thorman and L. K. Woo, *Inorg. Chem.*, 2000, **39**, 1301.
4. Y. Li, Y. Shi and A. L. Odom, *J. Am. Chem. Soc.*, 2004, **126**, 1794.
5. S. Banerjee, Y. Shi, C. Cao and A. L. Odom, *J. Organomet. Chem.*, 2005, **690**, 5066.
6. T. B. Parsons, N. Hazari, A. R. Cowley, J. C. Green and P. Mountford, *Inorg. Chem.*, 2005, **44**, 8442.
7. S. Banerjee and A. L. Odom, *Organometallics*, 2006, **25**, 3099.
8. S. Patel, Y. Li and A. L. Odom, *Inorg. Chem.*, 2007, **46**, 6373.
9. J. D. Selby, C. D. Manley, M. Feliz, A. D. Schwarz, E. Clot and P. Mountford, *Chem. Commun.*, 2007, 4937.
10. S. Banerjee, E. Barnea and A. L. Odom, *Organometallics*, 2008, **27**, 1005.
11. A. J. Clulow, J. D. Selby, M. G. Cushion, A. D. Schwarz and P. Mountford, *Inorg. Chem.*, 2008, **47**, 12049.
12. J. D. Selby, C. D. Manley, A. D. Schwarz, E. Clot and P. Mountford, *Organometallics*, 2008, **27**, 6479.
13. J. D. Selby, C. Schulten, A. D. Schwarz, A. Stasch, E. Clot, C. Jones and P. Mountford, *Chem.Commun.*, 2008, 5101.
14. K. Weitershaus, J. L. Fillol, H. Wadepohl and L. H. Gade, *Organometallics*, 2009, **28**, 4747.
15. K. Weitershaus, H. Wadepohl and L. H. Gade, *Organometallics*, 2009, **28**, 3381.

16. T. Janssen, R. Severin, M. Diekmann, M. Friedemann, D. Haase, Saak, W., S. Doye and R. Beckhaus, *Organometallics*, 2010, **29**, 1806.
17. A. D. Schofield, A. Nova, J. D. Selby, C. D. Manley, A. D. Schwarz, E. Clot and P. Mountford, *J. Am. Chem. Soc.*, 2010, **132**, 10484.
18. P. J. Tiong, A. D. Schofield, J. D. Selby, A. Nova, E. Clot and P. Mountford, *Chem. Commun.*, 2010, **46**, 85.
19. A. D. Schofield, A. Nova, J. D. Selby, A. D. Schwarz, E. Clot and P. Mountford, *Chem. Eur. J.*, 2011, **17**, 265.
20. J. D. Selby, M. Feliz, A. D. Schwarz, E. Clot and P. Mountford, *Organometallics*, 2011, **30**, 2295.
21. P. J. Tiong, A. Nova, E. Clot and P. Mountford, *Chem. Commun.*, 2011, **47**, 3147.
22. P. J. Tiong, A. Nova, L. R. Groom, A. D. Schwarz, J. D. Selby, A. D. Schofield, E. Clot and P. Mountford, *Organometallics*, 2011, **30**, 1182.
23. A. D. Schwarz, C. S. Onn and P. Mountford, *Angew. Chem. Int. Ed.*, 2012, **51**, 12298.
24. P. J. Tiong, A. Nova, A. D. Schwarz, J. D. Selby, E. Clot and P. Mountford, *Dalton Trans.*, 2012, **41**, 2277.
25. P. D. Schweitzer, H. Wadepohl and L. H. Gade, *Organometallics*, 2013, **32**, 3697.
26. J. Unruangsri, H. Morgan, A. D. Schwarz, A. D. Schofield and P. Mountford, *Organometallics*, 2013, **32**, 3091.
27. P. J. Walsh, M. J. Carney and R. G. Bergman, *J. Am. Chem. Soc.*, 1991, **113**, 6343.
28. H. Herrmann, J. L. Fillol, H. Wadepohl and L. H. Gade, *Angew. Chem. Int. Ed.*, 2007, **46**, 8426.
29. H. Herrmann, J. L. Fillol, T. Gehrmann, M. Enders, H. Wadepohl and L. H. Gade, *Chem. Eur. J.*, 2008, **14**, 8131.
30. H. Herrmann, J. L. Fillol, H. Wadepohl and L. H. Gade, *Organometallics*, 2008, **27**, 172.
31. H. Herrmann, T. Gehrmann, H. Wadepohl and L. H. Gade, *Dalton Trans.*, 2008, 6231.
32. H. Herrmann, H. Wadepohl and L. H. Gade, *Dalton Trans.*, 2008, 2111.

33. T. Gehrmann, J. L. Fillol, H. Wadepohl and L. H. Gade, *Angew. Chem. Int. Ed.*, 2009, **48**, 2152.
34. R. F. Munha, L. F. Veiros, M. T. Duarte, M. D. Fryzuk and A. M. Martins, *Dalton Trans.*, 2009, 7494.
35. T. Gehrmann, J. L. Fillol, H. Wadepohl and L. H. Gade, *Organometallics*, 2010, **29**, 28.
36. T. Gehrmann, J. L. Fillol, S. A. Scholl, H. Wadepohl and L. H. Gade, *Angew. Chem. Int. Ed.*, 2011, **50**, 5757.
37. T. Gehrmann, J. L. Fillol, H. Wadepohl and L. H. Gade, *Organometallics*, 2012, **31**, 4504.
38. T. Gehrmann, M. Kruck, H. Wadepohl and L. H. Gade, *Chem. Commun.*, 2012, **48**, 2397.
39. T. Gehrmann, G. T. Plundrich, H. Wadepohl and L. H. Gade, *Organometallics*, 2012, **31**, 3346.
40. T. Gehrmann, S. A. Scholl, J. L. Fillol, H. Wadepohl and L. H. Gade, *Chem. Eur. J.*, 2012, **18**, 3925.
41. S. A. Scholl, G. T. Plundrich, H. Wadepohl and L. H. Gade, *Inorg. Chem.*, 2013, **52**, 10158.
42. S. A. Scholl, H. Wadepohl and L. H. Gade, *Organometallics*, 2013, **32**, 937.
43. T. R. Cundari, *J. Am. Chem. Soc.*, 1992, **114**, 7879.
44. Z. Lin and M. B. Hall, *Coord. Chem. Rev.*, 1993, **123**, 149.
45. P. Mountford and D. Swallow, *J. Chem. Soc., Chem. Commun.*, 1995, 2357.
46. N. Kaltsoyannis and P. Mountford, *J. Chem. Soc., Dalton Trans.*, 1999, 781.
47. T. R. Cundari, *Chem. Rev.*, 2000, **100**, 807.
48. A. D. Schwarz, A. J. Nielson, N. Kaltsoyannis and P. Mountford, *Chem. Sci.*, 2012, **3**, 819.
49. P. J. Tiong, L. R. Groom, E. Clot and P. Mountford, *Chem. Eur. J.*, 2013, **19**, 4198.
50. N. Adams, H. J. Arts, P. D. Bolton, D. Cowell, S. R. Dubberley, N. Friederichs, C. Grant, M. Kranenburg, A. J. Sealey, B. Wang, P. J. Wilson, A. R. Cowley, P. Mountford and M. Schröder, *Chem. Commun.*, 2004, 434.
51. P. D. Bolton and P. Mountford, *Adv. Synth. Catal.*, 2005, **347**, 355.

52. H. R. Bigmore, S. R. Dubberley, M. Kranenburg, S. C. Lawrence, A. J. Sealey, J. D. Selby, M. Zuideveld, A. R. Cowley and P. Mountford, *Chem.Commun.*, 2006, 436.
53. H. R. Bigmore, M. Zuideveld, R. M. Kowalczyk, A. R. Cowley, M. Kranenbrug, E. J. L. McInnes and P. Mountford, *Inorg. Chem.*, 2006, **45**, 6411.
54. P. J. Wilson, A. J. Blake, P. Mountford and M. Schröder, *Chem. Commun.*, 1998, 1007.
55. A. E. Guiducci, A. R. Cowley, M. E. G. Skinner and P. Mountford, *J. Chem. Soc., Dalton Trans.*, 2001, 1392.
56. C. L. Boyd, A. E. Guiducci, S. R. Dubberley, B. R. Tyrrell and P. Mountford, *J. Chem. Soc., Dalton Trans.*, 2002, 4175.
57. C. L. Boyd, E. Clot, A. E. Guiducci and P. Mountford, *Organometallics*, 2005, **24**, 2347.
58. A. E. Guiducci, C. L. Boyd and P. Mountford, *Organometallics*, 2006, **25**, 1167.
59. A. E. Guiducci, C. L. Boyd, E. Clot and P. Mountford, *Dalton Trans.*, 2009, 5960.
60. L. R. Groom, A. D. Schwarz, A. Nova, E. Clot and P. Mountford, *Organometallics*, 2013, **32**, 7520.
61. M. H. Chisholm, E. E. Delbridge, A. R. Kidwell and K. B. Quinlan, *Chem. Commun.*, 2003, 126.
62. R. L. Gdula, M. J. A. Johnson and N. W. Ockwig, *Inorg. Chem.*, 2005, **44**, 9140.
63. C. D. Wood, S. J. McLain and R. R. Schrock, *J. Am. Chem. Soc.*, 1979, **101**, 3210.
64. R. R. Schrock and J. D. Fellmann, *J. Am. Chem. Soc.*, 1978, **100**, 3359.
65. K. M. Doxsee, J. B. Farahi and H. Hope, *J. Am. Chem. Soc.*, 1991, **113**, 8889.
66. B. Hessen, J.-K. F. Buijink, A. Meetsma, J. Teuben, G. Helgesson, M. Hakansson, S. Jagner and A. L. Spek, *Organometallics*, 1993, **12**, 2268.
67. F. Basuli, H. Aneetha, J. C. Huffman and D. J. Mindiola, *J. Am. Chem. Soc.*, 2005, **127**, 17992.
68. M. L. Listemann and R. R. Schrock, *Organometallics*, 1985, **4**, 74.
69. J. H. Freudenberger and R. R. Schrock, *Organometallics*, 1986, **5**, 398.
70. M. H. Chisholm, K. Folting, M. L. Lynn, D. B. Tiedtke, F. Lemoigno and O. Eisenstein, *Chem. Eur. J.*, 1999, **5**, 2318.

71. A. M. Geyer, R. L. Gdula, E. S. Wiedner and M. J. A. Johnson, *J. Am. Chem. Soc.*, 2007, **129**, 3800.
72. B. C. Bailey, A. R. Fout, H. Fan, J. Tomaszewski, J. C. Huffman, J. B. Gary, M. J. A. Johnson and D. J. Mindiola, *J. Am. Chem. Soc.*, 2007, **129**, 2234.
73. A. M. Geyer, E. S. Wiedner, J. B. Gary, R. L. Gdula, N. C. Kuhlmann, M. J. A. Johnson, B. D. Dunietz and J. W. Kampf, *J. Am. Chem. Soc.*, 2008, **130**, 8984.
74. S. M. Pugh, D. J. M. Trösch, D. J. Wilson, A. Bashall, F. G. N. Cloke, L. H. Gade, P. B. Hitchcock, M. McPartlin, J. F. Nixon and P. Mountford, *Organometallics*, 2000, **19**, 3205.
75. M. J. Carney, P. J. Walsh, F. J. Hollander and R. G. Bergman, *Organometallics*, 1992, **11**, 761.
76. D. S. Glueck, J. Wu, F. J. Hollander and R. G. Bergman, *J. Am. Chem. Soc.*, 1991, **113**, 2041.
77. L. R. Groom, A. F. Russell, A. D. Schwarz and P. Mountford, *Organometallics*, 2014, **33**, 1002.
78. L. H. Gade and P. Mountford, *Coord. Chem. Rev.*, 2001, **216-217**, 65.
79. N. Hazari and P. Mountford, *Acc. Chem. Res.*, 2005, **38**, 839.
80. P. Mountford, *Chem. Commun.*, 1997, 2127.
81. J. Goerdeler and W. Eggers, *Chem. Ber.*, 1986, **119**, 3737.
82. A. P. Duncan and R. G. Bergman, *The Chemical Record*, 2002, **2**, 431.
83. S. Y. Lee, *J. Am. Chem. Soc.*, 1996, **118**, 6396.
84. L.-C. So, C.-C. Liu, M. C. W. Chan, J. C. Y. Lo, K.-H. Sze and N. Zhu, *Chem. Eur. J.*, 2012, **18**, 565.
85. D. A. Fletcher, R. F. McMeeking and D. Parkin, *J. Chem. Inf. Comput. Sci.*, 1996, **36**, 746 (The UK Chemical Database Service: CSD version 5.34 updated May 2013).
86. For leading references see: N. Adams, A. R. Cowley, S. R. Dubberley, A. J. Sealey, M. E. G. Skinner, P. Mountford, *Chem. Commun.*, 2001, 2738.
87. C. Hansch, A. Leo and R. W. Taft, *Chem. Rev.*, 1991, **91**, 165.
88. R. B. Jordan, *Reaction Mechanisms of Inorganic and Organometallic Systems*, Oxford University Press, Oxford, 1998.
89. J. March, *Advanced Organic Chemistry*, 4th edn., Wiley-Interscience, New York, 1992.

90. A. J. Gordon and R. A. Ford, *The Chemist's Companion: A handbook of Practical Data, Techniques and References.*, Wiley, 1973.
91. Time-dependent DFT (TD-DFT) calculations for **14a** and **14e** confirmed that the first significant lowest energy bands correspond to the $1A_{(HOMO)} \rightarrow 1A_{(LUMO)}$ transitions.
92. S. Y. Lee and R. G. Bergman, *J. Am. Chem. Soc.*, 1996, **118**, 6396.
93. F. H. Allen, O. Kennard, D. G. Watson, L. Brammer, A. G. Orpen and R. Taylor, *J. Chem. Soc., Perkin Trans. 2*, 1987, S1.
94. Estimations of entropy using DFT can be subject to errors of at least 7 cal mol^{-1} K^{-1}, giving variations in $T\Delta S$ of ca. ± 2 kcal mol-1 at 298 K (P. Y. Ayala and H. B. Schlegel, *J. Chem. Phys.*, 1988, **108**, 2314, and references therein). This is comparable to the calculated differences in ΔH between the conformers under consideration and therefore we prefer to neglect the small differences in entropy between them in this case.
95. D. E. Wigley, *Prog. Inorg. Chem.*, 1994, **42**, 239.
96. P. J. Walsh, F. J. Hollander and R. G. Bergman, *Organometallics*, 1993, **12**, 3705.
97. A. D. Danopoulos, G. Wilkinson, T. K. N. Sweet and M. B. Hursthouse, *J. Chem. Soc., Dalton Trans.*, 1996, 271.
98. A. J. Blake, P. E. Collier, L. H. Gade, M. McPartlin, P. Mountford, M. Schubart and I. J. Scowen, *Chem. Commun.*, 1997, 1555.
99. A. Bashall, P. E. Collier, L. H. Gade, M. McPartlin, P. Mountford, S. M. Pugh, S. Radojevic, M. Schubart, I. J. Scowen and D. J. M. Trösch, *Organometallics*, 2000, **19**, 4784.
100. A. W. Kaplan, J. L. Polse, G. E. Ball, R. A. Andersen and R. G. Bergman, *J. Am. Chem. Soc.*, 1998, **120**, 11649.
101. S. C. Dunn, N. Hazari, A. R. Cowley, J. C. Green and P. Mountford, *Organometallics*, 2006, **25**, 1755.
102. P. J. Tiong, D.Phil. Thesis, University of Oxford, 2012.
103. A. Vogler, *Isonitrile Chemistry*, Academic Press, Inc., New York and London, 1971.
104. T. Carofiglio, C. Floriani, A. Chiesi-Villa and C. Guastini, *Inorg. Chem.*, 1989, **28**, 4417.

105. T. Carofiglio, P. G. Cozzi, C. Floriani, A. Chiesi-Villa and C. Rizzoli, *Organometallics*, 1993, **12**, 2726.
106. F. E. Hahn and T. Lügger, *J. Organomet. Chem.*, 1995, **501**, 341.
107. C. Floriani, F. Corazza, W. Lesueur, A. Chiesi-Villa and C. Guastini, *Angew. Chem. Int. Ed. Engl.*, 1989, **28**, 66.
108. J. L. Kiplinger, T. G. Richmond and C. E. Osterberg, *Chem. Rev.*, 1994, **94**, 373.
109. J. A. Bexrud, C. Li and L. L. Schafer, *Organometallics*, 2007, **26**, 6366.
110. M. Sotoodeh, I. Lechtweis, H. W. Roesky, M. Noltemeyer and H.-G. Schmidt, *Chem. Ber.*, 1993, **126**, 913.
111. C. H. Winter, X. X. Zhou and M. J. Heeg, *Inorg. Chem.*, 1992, **31**, 1808.
112. M. Klahn, P. Arndt, A. Spannenberg, A. Gansaeuer and U. Rosenthal, *Organometallics*, 2008, **27**, 5846.
113. R. Kickbusch and D. Lentz, *Chem. Commun.* , 2010, **46**, 2118.
114. Z. Wang, M. Wang, X. Yao, Y. Li, J. Tan, L. Wang, W. Qiao, Y. Geng, Y. Liu and Q. Wang, *Eur. J. Med. Chem.*, 2012, **53**, 275.
115. J. Zhang, D. Zhu, C. Yu, C. Wan and Z. Wang, *Org. Lett.*, 2010, **12**, 2841.
116. C. Wang, S. Li, H. Liu, Y. Jiang and H. Fu, *J. Org. Chem.*, 2010, **75**, 7936.
117. E. J. Stoebenau and R. F. Jordan, *J. Am. Chem. Soc.*, 2003, **128**, 8162.
118. B. Lian, L. Toupet and J.-F. Carpentier, *Chem. Eur. J.*, 2004, **10**, 4301.
119. B. Lian, C. W. Lehmann, C. Navarro and J.-F. Carpentier, *Organometallics*, 2005, **24**, 2466.
120. S. Hermanek, *Chem. Rev.*, 1992, **92**, 325.

Chapter Five

Experimental details and characterising data

5.1 General methods and instrumentation

All manipulations were carried out using standard Schlenk line or dry-box techniques under an atmosphere of argon or dinitrogen. Solvents were either degassed by sparging with dinitrogen and dried by passing through a column of the appropriate drying agent[1] or refluxed over sodium (toluene), potassium (THF) or Na/K alloy (Et_2O) and distilled. Deuterated solvents were dried over sodium (C_6D_6 and toluene-d_8), potassium (THF-d_8) or CaH_2 (C_6D_5Br) distilled under reduced pressure and stored under argon in Teflon valve ampoules. Unless otherwise stated NMR samples were prepared under dinitrogen in 5 mm Wilmad 507-PP tubes fitted with J. Young Teflon valves. ^{1}H, $^{1}H\{^{19}F\}$, $^{13}C\{^{1}H\}$, $^{13}C\{^{19}F\}$, ^{11}B and ^{19}F spectra were recorded on Varian Mercury-VX 300, Varian Unity Plus 500 or Bruker Avance III 500 spectrometers or on a Bruker AVC 500 spectrometer fitted with a ^{13}C cryoprobe. ^{1}H, $^{1}H\{^{19}F\}$, $^{13}C\{^{1}H\}$ and $^{13}C\{^{19}F\}$ spectra were referenced internally to residual protio-solvent (^{1}H) or solvent (^{13}C) resonances, and are reported relative to tetramethylsilane ($\delta = 0$ ppm). ^{19}F and ^{11}B were referenced externally to $CFCl_3$ or $Et_2O{\cdot}BF_3$, respectively. Assignments were confirmed as necessary with the use of two dimensional ^{1}H-^{1}H, ^{13}C-^{1}H, ^{19}F-^{19}F and ^{13}C-^{19}F NMR correlation experiments. IR spectra were recorded on a Perkin Elmer Paragon 1000 FTIR, a Nicolet Magna 560 E.S.P. FTIR or a Thermo Scientific Nicolet iS5 FTIR spectrometer and samples prepared in a dry-box using NaCl plates as a Nujol mull or as a thin film. UV-visible spectra were recorded on a T60U spectrometer at 298 K in 1 cm path length cuvettes with [**23**] = 5.17 μmol dm^{-3} in either *n*-hexanes or MeOH. Mass spectra were recorded by the mass spectrometry service of Oxford University's Department of Chemistry. Elemental analyses were carried out by Elemental Microanalysis Ltd, Devon or by the Elemental Analysis Service at the London Metropolitan University.

5.2 Literature preparations

$Ti(N_2N^{Me})(NNPh_2)(py)$ (**2.1**),[2] $Ti(N_2N^{Me})\{NC(Ph)C(Me)NPh_2\}(py)$ (**2.2**),[3] $Cp^*Ti\{MeC(N^iPr)_2\}(N^tBu)$ (**3.10**),[4] $Cp^*Ti(N^tBu)Cl(py)$ (**3.16**),[5] $^tBuONH_2$,[6] $Li[^tBuC(N^iPr_2)_2]$,[7] $MeCC(4\text{-}C_6H_4CF_3)$,[8] $Ar^{F_5}CCH$ ($Ar^{F_5} = C_6F_5$),[9, 10] $[Et_3NH][BPh_4]$[11] and $[PhC(NH^iPr)_2]Cl$[12, 13] were synthesised according to published procedures. $Ti(N_2N^{Me})\{NC(Ph)C(Me)NPh_2\}(DMAP)$ (**2.16**), $Ti(N_2N^{Me})\{NC(R)C(R')NPh_2\}(py)$, ($R = 4\text{-}C_6H_4{}^tBu$, $4\text{-}C_6H_4OMe$, $4\text{-}C_6H_4CF_3$ or Ar^{F_5}; $R' = Me$ or $4\text{-}C_6H_4CF_3$) and $(4\text{-}C_6H_4CF_3)CC(4\text{-}C_6H_4CF_3)$ were kindly provided by Dr Daniel Schofield.

$Ti(N_2N^{Me})(NNAr_2)(py)$ (Ar = Ph (**2.1**), 4-$C_6H_4{}^tBu$ (**2.12**) or 4-C_6H_4OMe (**2.13**)), $H_2NN(4\text{-}C_6H_4{}^tBu)_2$, $H_2NN(4\text{-}C_6H_4OMe)_2$ and $H_2NC(Ph)C(Me)NPh_2$ (**2.1a**) were prepared by Hiromasa Tanahashi and Lee Collins under my supervision, and $B(Ar^{F_5})_3$ by LANXESS Elastomers BV. 1,1-diphenylhydrazine was obtained from Sigma-Aldrich as the hydrogen chloride salt, from which the free hydrazine was obtained by basification, drying and removal of residual solvent, followed by distillation under inert atmospheric conditions. Deuteration of the hydrazine, forming Ph_2NND_2, was carried out as detailed below. All other reagents were purchased from commercial suppliers and (for liquid reagents) degassed before use, unless specified otherwise. $Ar^{F_5}CN$, Ar′NCO (Ar′ = 2,6-$C_6H_3{}^iPr_2$), PhCCMe and MeCCMe were dried over CaH_2 and distilled before use. $HC(O)NMe_2$ was degassed by sparging with dinitrogen and dried by passing through a column of activated alumina.[1] $Li[PhC(N^iPr)_2]$ (**3.15**)[14] and $Li[MeC(NTol)_2]$[7] were synthesised using modified published procedures given below.

$Li[PhC(N^iPr)_2]$ (3.15). To a stirred solution of $^iPrNCN^iPr$ (9.71 mL, 62.7 mmol) in ether (50 mL), cooled to 0 °C, was added PhLi (33.0 mL, 1.9M in $^nBu_2O$, 62.7 mmol) in dropwise aliquots immediately producing a light pink precipitate. After 5 h at RT the volatiles were removed under reduced pressure and hexane (50 mL) added. The mixture was cooled to -80 °C yielding **3.15** as a light pink crystalline solid which was isolated by filtration and dried *in vacuo*. Yield: 11.6 g (88%).

$Li[MeC(NTol)_2]$. To a stirred solution of TolNCNTol (1.33 g, 6.00 mmol) in ether (15 mL), cooled to 0 °C, was added MeLi (3.75 mL, 1.6 M in Et_2O, 6.00 mmol) in dropwise aliquots. A colour change to yellow was observed. After 17 h at RT the volatiles were removed under reduced pressure yielding $Li[MeC(NTol)_2]$ as a yellow solid which was washed with hexane (3 x 10 mL) before being dried *in vacuo*. Yield: 1.07 g (73%).

Procedure for deuteration of Ph_2NNH_2. Air sensitive techniques were used throughout. To a solution of Ph_2NNH_2 (0.500 g, 2.71 mmol) in benzene (5 mL) was added D_2O (5 mL) and NaOD (200 μL, 40% w/v in D_2O, 1.95 mmol) and the resulting mixture was stirred rapidly for 15 min. To this was added a solution of DCl (280 μL, 35% w/v in D_2O, 2.62 mmol) and the mixture stirred for a further 30 min. Afterwards, the mixture was extracted with benzene (2 x 5 mL) and the organic fractions combined before drying over $NaSO_4$. Once filtered the volatiles were removed under reduced pressure to give Ph_2NND_2 as a colourless oil which was dried *in vacuo*. Yield: 0.300 g (59%).

5.3 Experimental details and characterising data for Chapter Two

$H_2NC(4\text{-}C_6H_4CF_3)C(Me)NPh_2$ (2.1e). To a solution of $Ti(N_2N^{Me})(NNPh_2)(py)$ (**2.1**, 0.0455 g, 0.0800 mmol) in benzene (2 mL) was added a pre-mixed solution of (4-$C_6H_4CF_3$)CCMe (0.162 g, 0.880 mmol) and Ph_2NNH_2 (0.147 g, 0.800 mmol) in benzene (15 mL). An immediate colour change from green to red was observed. After 48 h H_2O (20 mL) was added and the solution vigorously stirred. The organic layer was removed and the aqueous layer extracted with benzene (2 x 10 mL) and the organic fractions combined. After drying over $MgSO_4$, the solution was filtered and the volatiles removed under reduced pressure to give **2.1e** as a dark yellow oil which was dried *in vacuo*. Yield: 0.237 g (73%). ^{1}H NMR (C_6D_6, 299.9 MHz, 293 K): δ 7.33-7.12, 6.90-6.85 (14 H, m, 4-$C_6H_4CF_3$ and 2 x C_6H_5), 2.89 (2 H, br. s, NH_2), 1.65 (3 H, s, CMe) ppm. $^{13}C\{^1H\}$ NMR (C_6D_6, 75.4 MHz, 293 K): δ 145.8 (*i*-C_6H_5), 142.3 (m, *i*-$C_6H_4CF_3$), 138.2 ((4-$C_6H_4CF_3$)C=CMe), 129.4 (app. q, ^1J = 32.4, 4-$C_6H_4CF_3$), 129.7 (*m*-C_6H_5), 129.4 (*o*-$C_6H_4CF_3$), 125.3 (q, ^4J = 3.8 Hz, *m*-$C_6H_4CF_3$), 122.0 (*p*-C_6H_5), 120.7 (*o*-C_6H_5), 113.1 ((4-$C_6H_4CF_3$)C=CMe), 15.9 (CMe) ppm. The resonance for *p*-$C_6H_4CF_3$ could not be observed. $^{19}F\{^1H\}$ NMR (C_6D_6, 282.1 MHz, 293 K): δ -62.2 (s, CF_3) ppm. IR (thin film, cm^{-1}): 3447 (br. w), 3358 (br. w), 3062 (br. w), 3035 (br. w), 2923 (br. w), 2853 (br. w), 1649 (w), 1617 (w), 1587 (m), 1490 (s), 1405 (w), 1382 (w), 1324 (s), 1293 (m), 1274 (w), 1256 (w), 1166 (m), 1125 (m), 1107 (m), 1067 (m), 1029 (w), 1017 (m), 849 (m), 751 (m), 734 (w), 694 (m). ESI^+-HRMS: *m/z* found (calcd. for $C_{22}H_{20}F_3N_2$, $[M + H]^+$) 369.1570 (369.1573).

$H_2NC(4\text{-}C_6H_4CF_3)C(Me)N(4\text{-}C_6H_4{}^tBu)_2$ (2.12e). To a solution of $Ti(N_2N^{Me})\{NN(4\text{-}C_6H_4{}^tBu)_2\}(py)$ (**2.12**, 0.0204g, 0.0300 mmol) in benzene (3 mL) was added a pre-mixed solution of (4-$C_6H_4CF_3$)CCMe (0.0608 g, 0.330 mmol) and $(4\text{-}C_6H_4{}^tBu)_2NNH_2$ (0.0890 g, 0.300 mmol) in benzene (9 mL). An immediate colour change from green to red was observed. After 48 h H_2O (15 mL) was added and the solution vigorously stirred. The organic layer was removed and the aqueous layer extracted with benzene (2 x 10 mL) and the organic fractions combined. After drying over $MgSO_4$, the solution was filtered and the volatiles removed under reduced pressure to give **2.12e** as a yellow solid which was dried *in vacuo*. Yield: 0.0950 g (60%). ^{1}H NMR (C_6D_6, 299.9 MHz, 293 K): δ 7.20-6.90 (12 H, m, 4-$C_6H_4CF_3$ and 4-$C_6H_4{}^tBu$), 2.98 (2 H, br. s, NH_2), 1.74 (3 H, s, CMe), 1.28 (18 H, s, CMe_3) ppm. $^{13}C\{^1H\}$ NMR (C_6D_6, 75.4 MHz, 293 K):

δ 144.3 (*p*-$C_6H_4{}^tBu$), 143.5 (*i*-$C_6H_4{}^tBu$), 142.5 (*i*-$C_6H_4CF_3$), 138.1 ((4-$C_6H_4CF_3$)C=CMe), 129.8 (app. q, ^1J = 32.6, 4-$C_6H_4CF_3$), 129.4 (*o*-$C_6H_4CF_3$) 126.5 (*o*-$C_6H_4{}^tBu$), 125.3 (q, ^4J = 3.8 Hz, *m*-$C_6H_4CF_3$), 120.4 (*m*-$C_6H_4{}^tBu$), 113.6 ((4-$C_6H_4CF_3$)C=CMe), 34.3 (CMe_3), 31.7 (CMe_3), 16.1 (CMe) ppm. The resonance for *p*-$C_6H_4CF_3$ could not be observed. $^{19}F\{^1H\}$ NMR (C_6D_6, 282.1 MHz, 293 K): δ -62.2 (s, CF_3) ppm. IR (NaCl plates, Nujol mull, cm^{-1}): 3449 (br. w), 3364 (br, w), 1656 (w), 1605 (w), 1510 (s), 1365 (m), 1324 (s), 1298 (m), 1266 (m), 1168 (m), 1130 (s), 1106 (m), 1067 (m), 1018 (w), 849 (w), 823 (w), 803 (w), 717 (w). ESI^+-HRMS: *m/z* found (calcd. for $C_{30}H_{35}F_3N_2Na$, $[M + Na]^+$) 503.2627 (503.2645).

$H_2NC(4\text{-}C_6H_4CF_3)C(Me)N(4\text{-}C_6H_4OMe)_2$ (2.13e). To a solution of Ti(N_2N^{Me}){$NN(4\text{-}C_6H_4OMe)_2$}(py) (**2.13**, 0.0500g, 0.0800 mmol) in benzene (6 mL) was added a pre-mixed solution of (4-$C_6H_4CF_3$)CCMe (0.160 g, 0.880 mmol) and (4-$C_6H_4OMe)_2NNH_2$ (0.200 g, 0.800 mmol) in benzene (15 mL). An immediate colour change from green to red was observed. After 48 h H_2O (30 mL) was added and the solution vigorously stirred. The organic layer was removed and the aqueous layer extracted with benzene (2 x 20 mL) and the organic fractions combined. After drying over $MgSO_4$, the solution was filtered and the volatiles removed under reduced pressure to give **2.13e** as a dark yellow oil which was dried *in vacuo*. Yield: 0.270 g (72%). ^1H NMR (C_6D_6, 299.9 MHz, 293 K): δ 7.35 (2 H, d, ^3J = 8.1 Hz, *m*-$C_6H_4CF_3$), 7.23 (2 H, d, ^3J = 8.4 Hz, *o*-$C_6H_4CF_3$), 7.14 (2 H, d, ^3J = 9.0 Hz, *m*-C_6H_4OMe), 6.84 (2 H, d, ^3J = 9.0 Hz, *o*-C_6H_4OMe), 3.37 (6 H, s, OMe), 3.01 (2 H, br. s, NH_2), 1.72 (3 H, s, CMe) ppm. $^{13}C\{^1H\}$ NMR (C_6D_6, 75.4 MHz, 293 K): δ 155.2 (*p*-C_6H_4OMe), 142.7 (m, *i*-$C_6H_4CF_3$), 139.9 (*i*-C_6H_4OMe), 137.3 ((4-$C_6H_4CF_3$)C=CMe), 129.7 (app. q, ^1J = 32.3, $C_6H_4CF_3$), 129.4 (*o*-$C_6H_4CF_3$), 125.3 (q, ^4J = 3.7 Hz, *m*-$C_6H_4CF_3$), 121.9 (*m*-C_6H_4OMe), 115.2 (*o*-C_6H_4OMe), 113.9 ((4-$C_6H_4CF_3$)C=CMe), 55.2 (OMe), 15.9 (CMe) ppm. The resonance for *p*-$C_6H_4CF_3$ could not be observed. $^{19}F\{^1H\}$ NMR (C_6D_6, 282.1 MHz, 293 K): δ -62.2 (s, CF_3) ppm. IR (thin film, cm^{-1}): 3440 (br. w), 3353 (br. w), 3038 (br. w), 2996 (br. w), 2949 (br. w), 2933 (br. w), 2909 (br. w), 2834 (w), 1650 (w), 1616 (m), 1588 (w), 1502 (s), 1464 (m), 1442 (m), 1406 (w), 1381 (w), 1324 (s), 1293 (m), 1239 (s), 1179 (m), 1166 (m), 1125 (s), 1106 (m), 1066 (m), 1037 (m), 1017 (m), 850 (m), 825 (m), 805 (w), 779 (w), 732 (w), 713 (w), 681 (w), 649 (w), 628 (w). ESI^+-HRMS: *m/z* found (calcd. for $C_{24}H_{24}F_3N_2O_2$, $[M + H]^+$) 429.1768 (429.1784).

$H_2NC(4\text{-}C_6H_4CF_3)C(4\text{-}C_6H_4CF_3)NPh_2$ (2.1f). To a solution of $Ti(N_2N^{Me})(NNPh_2)(py)$ (**2.1**, 0.0455g, 0.0800 mmol) in benzene (2 mL) was added a pre-mixed solution of $(4\text{-}C_6H_4CF_3)CC(4\text{-}C_6H_4CF_3)$ (0.101 g, 0.320 mmol) and Ph_2NNH_2 (0.0590 g, 0.320 mmol) in benzene (10 mL). An immediate colour change from green to red was observed. After 4 d H_2O (15 mL) was added and the solution vigorously stirred. The organic layer was removed and the aqueous layer extracted with benzene (2 x 10 mL) and the organic fractions combined. After drying over $MgSO_4$, the solution was filtered and the volatiles removed under reduced pressure to give **2.1f** as a dark yellow oil which was dried *in vacuo*. Yield: 0.136 g (85%). ^{1}H NMR (C_6D_6, 299.9 MHz, 293 K): δ 7.22-6.76 (18 H, m, 4-$C_6H_4CF_3$ and C_6H_5), 3.22 (2 H, br. s, NH_2) ppm. $^{13}C\{^1H\}$ NMR (C_6D_6, 75.4 MHz, 293 K): δ 145.6 (*i*-C_6H_5), 141.7 (m, *i*-$C_6H_4CF_3$), 141.6 (m, *i*-$C_6H_4CF_3$), 141.3 ($Ph_2N\underline{C}{=}CNH_2$), 130.6 (q, ^1J = 32.3, $C_6H_4\underline{C}F_3$), 129.8 (*o*-$C_6H_4CF_3$), 129.8 (*m*-NC_6H_5), 129.2 (*o*-$C_6H_4CF_3$), 129.2 (*p*-$C_6H_4CF_3$), 128.6 (*p*-$C_6H_4CF_3$), 127.4 (q, ^1J = 32.1, $C_6H_4\underline{C}F_3$), 125.8 (q, ^4J = 3.6 Hz, *m*-$C_6H_4CF_3$), 125.1 (q, ^4J = 3.8 Hz, *m*-$C_6H_4CF_3$), 122.5 (*p*-C_6H_5), 120.6 (*o*-C_6H_5), 117.3 ($Ph_2NC{=}\underline{C}NH_2$) ppm. $^{19}F\{^1H\}$ NMR (C_6D_6, 282.1 MHz, 293 K): δ -62.1 (3 F, s, CF_3), -62.4 (3 F, s, CF_3) ppm. IR (thin film, cm^{-1}): 3478 (br. w), 3379 (br. w), 3062 (br. w), 3036 (br. w), 2963 (w), 2928 (w), 1928 (br. w). 1605 (s), 1588 (m), 1492 (s), 1449 (w), 1410 (m), 1324 (s), 1295 (m), 1276 (m), 1262 (w), 1234 (w), 1165 (s), 1121 (s), 1108 (s), 1069 (s), 1016 (m), 884 (w), 845 (m), 802 (w), 750 (m), 695 (m), 628 (w). ESI^--HRMS: *m/z* found (calcd. for $C_{28}H_{19}F_6N_2$, $[M\text{-}H]^-$) 497.1463 (497.1458).

$H_2NC(4\text{-}C_6H_4CF_3)C(4\text{-}C_6H_4CF_3)N(4\text{-}C_6H_4{}^tBu)_2$ (2.12f). To a solution of $Ti(N_2N^{Me})\{NN(4\text{-}C_6H_4{}^tBu)_2\}(py)$ (**2.12**, 0.0545g, 0.0800 mmol) in benzene (3 mL) was added a pre-mixed solution of $(4\text{-}C_6H_4CF_3)CC(4\text{-}C_6H_4CF_3)$ (0.101 g, 0.320 mmol) and $(4\text{-}C_6H_4{}^tBu)_2NNH_2$ (0.0949 g, 0.320 mmol) in benzene (14 mL). An immediate colour change from green to red was observed. After 4 d H_2O (20 mL) was added and the solution vigorously stirred. The organic layer was removed and the aqueous layer extracted with benzene (2 x 10 mL) and the organic fractions combined. After drying over $MgSO_4$, the solution was filtered and the volatiles removed under reduced pressure to give **2.12f** as a yellow solid which was dried *in vacuo*. Yield: 0.160 g (82%). ^{1}H NMR (C_6D_6, 299.9 MHz, 293 K): δ 7.30-6.89 (16 H, m, 4-$C_6H_4CF_3$ and 4-$C_6H_4{}^tBu$), 3.33 (2 H, br. s, NH_2), 1.21 (18 H, s, CMe_3) ppm. $^{13}C\{^1H\}$ NMR (C_6D_6, 75.4 MHz, 293 K): δ 144.9 (*p*-$C_6H_4{}^tBu$), 143.3 (*i*-$C_6H_4{}^tBu$) 142.1 (m, *i*-$C_6H_4CF_3$), 141.9 (m, *i*-

$C_6H_4CF_3$), 141.2 ((4-$C_6H_4{}^tBu)_2N\underline{C}$=$CNH_2$), 130.5 (q, ^1J = 32.3, $C_6H_4\underline{C}F_3$), 129.9 (*o*-$C_6H_4CF_3$), 129.3 (*o*-$C_6H_4CF_3$), 127.4 (q, ^1J = 32.3, $C_6H_4\underline{C}F_3$), 126.6 (*m*-$C_6H_4{}^tBu$), 125.8 (q, ^4J =3.8 Hz, *m*-$C_6H_4CF_3$), 125.1 (q, ^4J =3.8 Hz, *m*-$C_6H_4CF_3$), 117.7 ((4-$C_6H_4{}^tBu)_2NC$=$\underline{C}NH_2$), 120.2 (*o*-$C_6H_4{}^tBu$), 34.3 ($C_6H_4\underline{C}Me_3$), 31.5 ($C_6H_4C\underline{Me}_3$) ppm. The resonance for *p*-$C_6H_4CF_3$ could not be observed. $^{19}F\{^1H\}$ NMR (C_6D_6, 282.1 MHz, 293 K): δ -62.1 (3 F, s, CF_3), -62.4 (3 F, s, CF_3) ppm. IR (thin film, cm^{-1}): 2962 (w), 1607 (w), 1510 (m), 1410 (w), 1364 (w), 1322 (s), 1298 (w), 1261 (m), 1189 (w), 1165 (m), 1107 (m), 1070 (m), 1016 (m), 847 (m), 799 (m). ESI^--HRMS: *m/z* found (calcd. for $C_{36}H_{35}F_6N_2$, $[M\text{-}H]^-$) 609.2733 (609.2710).

$H_2NC(4\text{-}C_6H_4CF_3)C(4\text{-}C_6H_4CF_3)N(4\text{-}C_6H_4OMe)_2$ (2.13f). To a solution of $Ti(N_2N^{Me})\{NN(4\text{-}C_6H_4OMe)_2\}(py)$ (**2.13**, 0.0503g, 0.0800 mmol) in benzene (2 mL) was added a pre-mixed solution of $(4\text{-}C_6H_4CF_3)CC(4\text{-}C_6H_4CF_3)$ (0.101 g, 0.320 mmol) and $(4\text{-}C_6H_4OMe)_2NNH_2$ (0.0782 g, 0.320 mmol) in benzene (15 mL). An immediate colour change from green to red was observed. After 4 d H_2O (20 mL) was added and the solution vigorously stirred. The organic layer was removed and the aqueous layer extracted with benzene (2 x 10 mL) and the organic fractions combined. After drying over $MgSO_4$, the solution was filtered and the volatiles removed under reduced pressure to give **2.13f** as a yellow solid which was dried *in vacuo*. Yield: 0.170 g (95%). ^1H NMR (C_6D_6, 299.9 MHz, 293 K): δ 7.20-7.02 (12 H, m, $C_6H_4CF_3$ and C_6H_4OMe), 6.74 (4 H, m, *o*-C_6H_4OMe), 3.35 (2 H, br. s, NH_2), 3.29 (6 H, s, OMe) ppm. $^{13}C\{^1H\}$ NMR (C_6D_6, 75.4 MHz, 293 K): δ 155.4 (*p*-C_6H_4OMe), 142.2 (m, *i*-$C_6H_4CF_3$), 142.0 (m, *i*-$C_6H_4CF_3$), 140.2 ((4-$C_6H_4OMe)_2N\underline{C}$=$CNH_2$), 139.4 (*i*-$C_6H_4OMe$), 130.4 (q, ^1J = 32.3, $C_6H_4\underline{C}F_3$), 129.9 (*o*-$C_6H_4CF_3$), 129.6 (*o*-$C_6H_4CF_3$), 127.5 (q, ^1J = 32.1, $C_6H_4\underline{C}F_3$), 125.7 (q, ^4J = 3.8 Hz, *m*-$C_6H_4CF_3$), 125.0 (q, ^4J = 3.8 Hz, *m*-$C_6H_4CF_3$), 121.7 (*m*-C_6H_4OMe), 118.3 ((4-$C_6H_4OMe)_2NC$=$\underline{C}NH_2$), 115.2 (*o*-C_6H_4OMe), 55.1 (OMe) ppm. The resonance for *p*-$C_6H_4CF_3$ could not be observed. $^{19}F\{^1H\}$ NMR (C_6D_6, 282.1 MHz, 293 K): δ -62.1 (3 F, s, CF_3), -62.4 (3 F, s, CF_3) ppm. IR (thin film, cm^{-1}): 2963 (w), 1614 (w). 1502 (m), 1410 (w), 1322 (m), 1260 (m), 1238 (m), 1167 (w), 1106 (m) 1091 (m), 1070 (s), 1016 (s), 848 (w), 797 (s), 683 (w). ESI^--HRMS: *m/z* found (calcd. for $C_{30}H_{23}F_6N_2O_2$, $[M\text{-}H]^-$) 557.1687 (557.1669).

Kinetic measurements for reaction of Ti(N_2N^{Me}){NC(Ph)C(Me)NPh_2}(py) (2.2) with Ph_2NNH_2 or Ph_2NND_2 at room temperature To a solution of Ph_2NNH_2 or Ph_2NND_2 (0.0120 mmol) in C_6D_6 (0.3 mL) was added Ti(N_2N^{Me}){NC(Ph)C(Me)NPh_2}(py) (**2.2**, 8.2 mg, 0.0120 mmol) in C_6D_6 (0.3 mL), all at RT, before being transferred to an NMR tube equipped with a J. Young Teflon valve. A colour change from red to green/yellow was observed. The reaction was monitored by ^{1}H NMR spectroscopy using an array which recorded spectra (nt = 4 scans) every 20 secs. The ratios of the species were calculated by measuring the integrals of the C<u>Me</u> groups.

Kinetic measurements for low temperature reactions. The general procedure is as follows. In a glove box, compound **2.1**, **2.2** or **2.16** (0.0120 mmol) was weighed into a vial and dissolved in toluene-d_8 (0.3 mL) and cooled to -45 °C. In a separate vial, PhCCMe, Ph_2NNH_2 or Ph_2NND_2 was weighed and dissolved in toluene-d_8 (0.3 mL) and also cooled to -45 °C. The two vials were placed on a pre-cooled tile and the solutions combined using a pre-cooled pipette, agitated quickly and transferred to a pre-cooled J. Young NMR tube. The NMR tube was taken out of the glovebox and placed in a dry ice/acetone cold bath. The NMR probe was cooled to -12 °C (other reaction temperatures were used as noted in Chapter 2) and a blank toluene-d_8 sample added before being locked and shimmed. The experimental sample then replaced the blank sample and allowed to thermally equilibrate, the shimming was then checked and an array set up recording a spectrum of 4 scans every 120 s. The ratios of the species were calculated by measuring the integrals of the C<u>Me</u> groups. Initial rate constants were obtained from plots of [**2.2**] or [**2.1a**] *vs* time.

Kinetic measurements for catalytic experiments using Ti(N_2N^{Me})($NNPh_2$)(py) (2.1). The general procedure is as follows. In a glove box, compound **2.1** was weighed into a vial and dissolved in C_6D_6 (0.3 mL). In a separate vial, Ph_2NNH_2 (or Ph_2NND_2) and PhCCMe (and pyridine (4.9 μL, 0.0600 mmol) where appropriate) were dissolved in C_6D_6 (0.3 mL) and the solutions combined, agitated quickly and transferred to a J. Young NMR tube. A blank C_6D_6 sample was added to the NMR probe before being locked and shimmed (and heated to 70 °C as noted in the text). The experimental sample then replaced the blank sample (and allowed to thermally equilibrate where necessary) the shimming checked and an array set up recording a spectrum of 4 scans every 30 or 120 secs. The ratios of the species were calculated by measuring the integrals of the

starting alkyne and product alkene CMe groups. Initial rate constants were obtained from plots of [**2.1a**] *vs* time.

NMR tube scale synthesis of Ti(N_2N^{Me}){N(H)C(Ph)C(Me)NPh_2}$_2$ (2.17). To a solution of Ti(N_2N^{Me}){NC(Ph)C(Me)NPh}(py) (**2.2**, 25.0 mg, 0.0365 mmol) in C_6D_6 (0.3 mL) in an NMR tube equipped with a J. Young Teflon valve was added H_2NC(Ph)C(Me)NPh_2 (**2.1a**, 11.0 mg, 0.0365 mmol) in C_6D_6 (0.3 mL) at RT. The reaction was monitored by ^{1}H NMR spectroscopy. After 20 min, the volatiles were removed under reduced pressure and the resultant mixture dried *in vacuo* before being redissolved in C_6D_6 (0.6 mL). This was repeated and the mixture dissolved in toluene-d_8 (0.6 mL) before being cooled to -40 °C at which point ^{1}H NMR spectroscopy showed Ti(N_2N^{Me}){N(H)C(Ph)C(Me)NPh_2}$_2$ (**2.17**) and **2.2** in 87:13 ratio. Compound **2.17** was subsequently characterised by ^{1}H and ^{13}C NMR spectroscopy at -40 °C. ^{1}H NMR (toluene-d_8, 299.9 MHz, 233 K): δ 9.45 (1H, br. s, NH_a), 9.19 (1 H, br. s, NH_b), 7.60 (4 H, d, ^3J = 7.2 Hz, *o*-C_6H_5), 7.50 (4 H, d, ^3J = 7.8 Hz, o_a-N(C_6H_5)$_2$)), 7.38 (4 H, d, ^3J = 8.4 Hz, o_b-N(C_6H_5)$_2$), 7.25 (8 H, t, ^3J = 7.5 Hz, *m*-N(C_6H_5)$_2$)), 7.17-6.77 (10 H, m, overlapping *p*-N(C_6H_5)$_2$), *m*-C_6H_5, *p*-C_6H_5), 3.05 (2H, br. m, CH_2NSiMe_3 - inner protons), 2.86 (2 H, br. m, CH_2NSiMe_3 - outer protons), 2.54 (2 H, br. m, CH_2NMe - inner protons), 2.07 (3 H, s, CMe_b), 1.83 (3 H, s, NMe), 1.57 (CMe_a), 1.51 (2 H, br. m, CH_2NMe - outer protons), 0.09 (18H, br. s, SiMe_3) ppm. ^{13}C{^{1}H} NMR (toluene-d_8, 75.4 MHz, 233 K): δ 151.2 (CCMe_a), 149.2 (CCMe_b), 147.1 (i_a-N(C_6H_5)$_2$), 146.2 (i_b-N(C_6H_5)$_2$), 141.2 (i_b-C_6H_5), 140.7 (i_a-C_6H_5), 131.1 (o_b-C_6H_5), 130.0 (o_a-C_6H_5), 129.5 (m_a-N(C_6H_5)$_2$), 129.2 (m_b-N(C_6H_5)$_2$), 126.7 (m_a-C_6H_5), 126.5 (m_b-C_6H_5), 122.5 (o_a-N(C_6H_5)$_2$), 121.8 (p_a-N(C_6H_5)$_2$), 121.6 (p_b-N(C_6H_5)$_2$), 121.3 (*p*-C_6H_5), 120.4 (o_b-N(C_6H_5)$_2$), 120.1 (*p*-C_6H_5), 109.1 (CMe_b), 108.5 (CMe_a), 57.4 (CH_2NMe), 50.9 (CH_2NSiMe_3). 45.4 (NMe), 17.1 (CMe_b), 15.6 (CMe_a), 2.76 (SiMe_3) ppm. Note: subscripts ″a″ and ″b″ refer to the two –N(H)C(Ph)C(Me)NPh_2 groups.

NMR tube scale synthesis of Ti(N_2N^{Me}){N(D)C(Ph)C(Me)NPh_2}$_2$ (2.17-d_2). To a solution of Ti(N_2N^{Me}){NC(Ph)C(Me)NPh}(py) (**2.2**, 30.0 mg, 0.0438 mmol) in C_6D_6 (0.3 mL) in an NMR tube equipped with a J. Young Teflon valve was added Ph_2NND_2 (8.2 mg, 0.0438 mmol) in C_6D_6 (0.3 mL) at RT forming Ti(N_2N^{Me})($NNPh_2$)(py) (**2.1**) and H_2NC(Ph)C(Me)NPh_2 (**2.1a-d_2**). After 13.5 h, PhCCMe (5.5 μL, 0.0438 mmol) was added to the solution and left to stand for 1.5 h, after which time the volatiles were removed under reduced pressure and the mixture re-dissolved in toluene-d_8 (0.6 mL)

and cooled to -40 °C. The reaction was monitored by ^{1}H and ^{2}H NMR spectroscopy which confirmed formation of Ti(N_2N^{Me}){N(D)C(Ph)C(Me)NPh_2}$_2$ (**2.17-*d*$_2$**) alongside **2.2** in 80:20 ratio. ^{1}H NMR spectrum as for **2.17** except for absence of resonances at δ 9.45 and 9.19 ppm. ^{2}H NMR (toluene-*d*$_8$, 75.4 MHz, 233 K): δ 9.2 (br. s, overlapping ND_a and ND_b) ppm.

NMR tube scale reaction of Ti(N_2N^{Me}){NC(Ph)C(Me)N(4-$C_6H_4{}^tBu)_2$}(py) (2.14) with H_2NC(Ph)C(Me)N(4-$C_6H_4{}^tBu)_2$ (2.12a). To a pre-mixed solution of (4-$C_6H_4{}^tBu)_2NNH_2$ (13.0 mg, 0.0438 mmol) and PhCCMe (5.5 μL, 0.0438 mmol) in C_6D_6 (0.3 mL) in an NMR tube equipped with a J. Young Teflon valve was added Ti(N_2N^{Me}){NC(Ph)C(Me)N(4-$C_6H_4{}^tBu)_2$}(py) (**2.14**, 34.9 mg, 0.0438 mmol) in C_6D_6 (0.3 mL) all at RT. The reaction was monitored by ^{1}H NMR spectroscopy which, after 50 min, showed formation of Ti(N_2N^{Me}){N(H)C(Ph)C(Me)N(4-$C_6H_4{}^tBu)_2$}$_2$ (**2.18**) alongside **2.14** in 52:48 ratio. Compound **2.18** was subsequently characterised by ^{1}H NMR spectroscopy. ^{1}H NMR (C_6D_6, 299.9 MHz, 293 K): δ 9.32 (1 H, br. s, NH_a), 7.79-6.66 (26 H, br. m, overlapping 2 x C_6H_5 and 4 x $C_6H_4{}^tBu$), 2.94 (4 H, br. m, 2 x C$\underline{H}_2$NSiMe_3), 2.50 (2 H, br. m, C$\underline{H}_2$NMe), 2.02 (3 H, s, CMe), 1.81 (3 H, s, NMe), 1.34 (18 H, br s, $C_6H_4{}^tBu$), 0.02 (18 H, br. s, SiMe_3) ppm. The remaining resonances could not be assigned.

NMR tube scale reaction of Ti(N_2N^{Me}){NC(Ph)C(Me)N(4-$C_6H_4OMe)_2$}(py) (2.15) with H_2NC(Ph)C(Me)N(4-$C_6H_4OMe)_2$ (2.13a). To a pre-mixed solution of (4-$C_6H_4OMe)_2NNH_2$ (10.7 mg, 0.0438 mmol) and PhCCMe (10.9 μL, 0.0874 mmol) in C_6D_6 (0.3 mL) in an NMR tube equipped with a J. Young Teflon valve was added Ti(N_2N^{Me}){NN(4-$C_6H_4OMe)_2$}(py) (**2.13**, 27.5 mg, 0.0438 mmol) in C_6D_6 (0.3 mL) all at RT. A gradual colour change from green to red was observed. The reaction was monitored by ^{1}H NMR spectroscopy which, after 2 h, showed formation of Ti(N_2N^{Me}){N(H)C(Ph)C(Me)N(4-$C_6H_4OMe)_2$}$_2$ (**2.19**) alongside **2.15** in 60:40 ratio. Compound **2.19** was subsequently characterised by ^{1}H NMR spectroscopy. ^{1}H NMR (C_6D_6, 299.9 MHz, 293 K): δ 9.54 (1 H, br. s, NH_a), 9.35 (1 H, br. s, NH_b), 7.71-6.66 (26 H, br. m, overlapping 2 x C_6H_5 and 4 x C_6H_4OMe), 3.41 (12 H, br s, $C_6H_4O\underline{Me}$), 3.06 (2H, br. m, C$\underline{H}_2$NSiMe_3), 2.94 (2 H, br. m, C$\underline{H}_2$NSiMe_3), 2.52 (2 H, br. m, C$\underline{H}_2$NMe), 2.04 (3 H, s, CMe), 1.84 (3 H, s, NMe), 1.60 (5 H, br. m, CMe and C$\underline{H}_2$NMe), 0.01 (18 H, br. s, SiMe_3) ppm.

Catalyst decomposition experiments. The general procedure is as follows. In a glove box, compound **2.1**, **2.12** or **2.13** (0.0120 mmol) was weighed into a vial and dissolved in C_6D_6 (0.3 mL). In a separate vial, Ar_2NNH_2 or $H_2NC(Ar)C(Me)NAr_2$ (Ar = Ph (**2.1a**), 4-$C_6H_4{}^tBu$ (**2.12b**) or 4-C_6H_4OMe (**2.13c**)) was dissolved in C_6D_6 (0.3 mL) and the solutions combined, agitated quickly and transferred to a J. Young NMR tube. The solutions were monitored by ^1H NMR spectroscopy over a period of 24 h and the ratios of species calculated by measuring the integrals of *o*-C_6H_4X (X = H (**2.1**), ^{t}Bu (**2.12**) or OMe (**2.13**)) and $MeN\{C\underline{H}_2CH_2N(H)SiMe_3\}_2$.

Kinetic measurements for general catalytic experiments. The general procedure is as follows. In a glove box, the desired catalyst (**2.1**, **2.12**, **2.13**, **2.2** or **2.2** and **2.1a**, 6.00 or 3.00 μmol) was weighed into a vial and dissolved in C_6D_6 (0.3 mL). In a separate vial, hydrazine (0.120 mmol) and alkyne (0.120 mmol) were dissolved in C_6D_6 (0.3 mL) and the solutions combined, agitated quickly and transferred to a J. Young NMR tube. The solutions were monitored by ^1H NMR spectroscopy over a period of 48-72 h and the ratios of the species calculated by measuring the integrals of the starting alkyne and product alkene C<u>Me</u> groups. Initial rate constants (and corresponding turnover numbers) were obtained from plots of $[H_2NC(R)C(Me)NAr_2]$ *vs* time.

NMR tube scale competition reaction of Ti(N_2N^{Me}){NC(Ph)C(Me)NPh_2}(py) (2.2) and Ti(N_2N^{Me}){NC(Ar)C(Me)NPh_2}(py) (Ar = 4-$C_6H_4{}^tBu$ (2.5), 4-C_6H_4OMe (2.6) or 4-$C_6H_4CF_3$ (2.7)) with Ph_2NNH_2. The general procedure is as follows. To a solution of Ti(N_2N^{Me}){NC(Ph)C(Me)NPh_2}(py) (**2.2**, 8.2 mg, 0.0120 mmol) in C_6D_6 (0.2 mL) was added a solution of Ti(N_2N^{Me}){NC(Ar)C(Me)NPh_2}(py) (Ar = 4-$C_6H_4{}^tBu$ (**2.5**), 4-C_6H_4OMe (**2.6**) or 4-$C_6H_4CF_3$ (**2.7**), 0.0120 mmol) in C_6D_6 (0.2 mL). After mixing, 1 equiv of Ph_2NNH_2 (2.2 mg, 0.0120 mmol) in C_6D_6 (0.2 mL) was added before being transferred to an NMR tube equipped with a J. Young Teflon valve. The reaction was monitored by ^1H NMR spectroscopy giving **2.1** alongside the corresponding vinylamine products, **2.1a** and **2.1b**, **2.1c** or **2.1e**, within 30 min.

NMR tube scale competition reaction of Ti(N_2N^{Me})($NNPh_2$)(py) (2.1) and Ti(N_2N^{Me})($NNAr_2$)(py) (2.12 or 2.13) with PhCCMe. The general procedure is as follows. To a solution of Ti(N_2N^{Me})($NNPh_2$)(py) (**2.1**, 8.2 mg, 0.0120 mmol) in C_6D_6 (0.2 mL) was added a solution of Ti(N_2N^{Me})($NNAr_2$)(py) (**2.12** or **2.13**, 0.0120 mmol) in C_6D_6 (0.2 mL). After mixing, 1 equiv of PhCCMe (1.5 μL, 0.0120 mmol) in C_6D_6 (0.2 mL) was added before being transferred to an NMR tube equipped with a J. Young Teflon valve. The reaction was monitored by ^{1}H NMR spectroscopy and the ratios of the species calculated by measuring the integrals of the CMe groups.

NMR tube scale reaction of Ti(N_2N^{Me}){NC(Ph)C(Me)NAr_2}(py) (Ar = Ph (2.2), 4-$C_6H_4{}^tBu$ (2.14) or 4-C_6H_4OMe (2.15)) with Ar_2NNH_2. The general procedure is as follows. To a solution of Ti(N_2N^{Me}){NC(Ph)C(Me)NAr_2}(py) (Ar = Ph (**2.2**), 4-$C_6H_4{}^tBu$ (**2.14**) or 4-$C_6H_4{}^tBu$ (**2.15**), 9.00 μmol) in C_6D_6 (0.3 mL) in an NMR tube equipped with a J. Young Teflon valve was added Ar_2NNH_2 (9.00 μmol) in C_6D_6 (0.3 mL) all at RT. A gradual colour change from red to green/yellow was observed. The reaction was monitored by ^{1}H NMR spectroscopy and the ratios of the species calculated by measuring the integrals of the CMe groups.

NMR tube scale reaction of Ti(N_2N^{Me})($NNPh_2$)(py) (2.1) with RCCR (R = Me or 4-$C_6H_4CF_3$). To a solution of Ti(N_2N^{Me})($NNPh_2$)(py) (**2.1**, 0.0400 or 0.0120 mmol, respectively) in C_6D_6 (0.3 mL) in an NMR tube equipped with a J. Young Teflon valve was added MeCCMe (2.2 mg, 0.0400 mmol) or (4-$C_6H_4CF_3$)CC(4-$C_6H_4CF_3$) (3.8 mg, 0.0120 mmol) in C_6D_6 (0.3 mL) all at RT. The ^{1}H NMR spectrum recorded after 90 and 50 min, respectively showed quantitative formation of Ti(N_2N^{Me}){NC(R)C(R)NPh_2}(py) (R = Me (**2.3**) or 4-$C_6H_4CF_3$ (**1.138**), consistent with the literature values.[3]

5.4 Experimental details and characterising data for Chapter Three

Cp*Ti{MeC(N^iPr)$_2$}(NO^tBu) (1). To a solution of Cp*Ti{MeC(N^iPr)$_2$}(N^tBu) (**3.10,** 0.932 g, 2.36 mmol) in toluene (10 mL), cooled to -78 °C, was added $^tBuONH_2$ in toluene (1.8 M, 1.70 mL, 3.06 mmol) dropwise over a period of 5 min and the solution slowly warmed to RT. A colour change from red to dark green/black was observed. After 3.5 h the volatiles were removed under reduced pressure to afford **1** as a dark green oil, which was dried *in vacuo*. Yield: 0.941 g (97%). ^{1}H NMR (C_6D_6, 299.9 MHz, 293 K): δ 3.72 (2 H, sept., ^3J = 6.3 Hz NCHMeMe), 2.16 (15 H, s, C_5Me_5), 1.81 (3 H,

s, $MeCN_2$), 1.09 (9 H, s, $NOCMe_3$), 1.05 (6 H, d, ^3J = 6.6 Hz, NCHMeMe), 1.03 (6 H, d, ^3J = 6.3 Hz, NCHMeMe) ppm. $^{13}C\{^1H\}$ NMR (C_6D_6, 75.4 MHz, 293 K): δ 162.1 ($MeCN_2$), 119.2 (C_5Me_5), 80.1 ($NOCMe_3$), 49.1 (NCHMeMe), 26.9 ($NOCMe_3$), 26.6 (NCHMeMe), 25.5 (NCHMeMe), 12.1 (C_5Me_5), 11.6 ($MeCN_2$) ppm. IR (NaCl plates, Nujol mull, cm^{-1}): 1485 (s, br), 1468 (s, sh), 1416 (s, sh), 1359 (s), 1338 (s), 1317 (m), 1214 (s), 1173 (s), 1149 (s), 1123 (m), 1017 (m), 848 (m), 810 (m), 794 (m), 752 (w), 705 (m), 634 (w), 552 (w). EI-HRMS: *m/z* found (calcd. for $C_{22}H_{41}N_3OTi$, $[M]^+$) 411.2735 (411.2729).

Cp*Ti{PhC(N^{i}Pr)$_2$}(N^{t}Bu) (2). To a solution of Cp*Ti(N^{t}Bu)Cl(py) (**3.16**, 0.500g, 1.36 mmol) in benzene (10 mL) was added a solution of Li[PhC(N^{i}Pr)$_2$] (**3.15**, 0.342 g, 1.63 mmol) in benzene (10 mL) and heated to 60 °C. After 18 h the volatiles were removed under reduced pressure to afford **2** as a red, waxy oil which was extracted into pentane (3 x 5 mL). The volatiles were removed under reduced pressure and the resultant dark red oil dried *in vacuo*. Yield: 0.608 g (98%). ^1H NMR (C_6D_6, 299.9 MHz, 293 K): δ 7.45 (1 H, m, o_a-C_6H_5), 7.19-7.05 (4 H, m, overlapping o_b-C_6H_5, *m*-C_6H_5, *p*-C_6H_5), 3.56 (2 H, sept., ^3J = 6.3 Hz, NCHMeMe), 2.22 (15 H, s, C_5Me_5), 1.22 (9 H, s, $NCMe_3$), 1.05 (6 H, d, ^3J = 6.3 Hz, NCHMeMe), 0.91 (6 H, d, ^3J = 6.3 Hz, NCHMeMe) ppm. $^{13}C\{^1H\}$ NMR (C_6D_6, 75.4 MHz, 293 K): δ 165.8 ($MeCN_2$), 134.9 (*i*-C_6H_5), 128.8, 128.6, 128.3, 128.2, (*p*-C_6H_5, m_a-C_6H_5, m_b-C_6H_5, o_b-C_6H_5), 127.5 (o_a-C_6H_5), 119.4 (C_5Me_5), 67.3 ($NCMe_3$), 49.6 (NCHMeMe), 33.0 ($NCMe_3$), 26.8 (NCHMeMe), 25.5 (NCHMeMe), 12.9 (C_5Me_5) ppm. IR (NaCl plates, Nujol mull, cm^{-1}): 1638 (w), 1602 (w), 1528 (w), 1359 (s), 1338 (s), 1243 (s), 1220 (s), 1168 (s), 1140 (m), 1120 (m), 1073 (m), 1016 (s), 952 (w), 801 (m), 780 (s), 738 (w), 703 (s), 583 (w), 539 (m), 506 (w). EI-HRMS: *m/z* found (calcd. for $C_{27}H_{43}N_3Ti$, $[M]^+$) 457.2932 (457.2936).

Cp*Ti{PhC(N^{i}Pr)$_2$}(NO^{t}Bu) (3). To a solution of Cp*Ti{PhC(N^{i}Pr)$_2$}(N^{t}Bu) (**2**, 7.67 g, 16.8 mmol) in Et_2O (15 mL), cooled to -78 °C, was added $^tBuONH_2$ in toluene (1.8 M, 13.0 mL, 23.5 mmol) and the solution slowly warmed to RT. A colour change from red to dark green/black was observed. After 3.5 h the volatiles were removed under reduced pressure to afford **3** as a dark green oil, which was triturated in hexane (25 mL) and filtered. The resultant green solid was then washed with cold hexane (3 x 15 mL) cooled to -78 °C, filtered and dried *in vacuo*. Yield: 5.56 g (70%). Diffraction-quality crystals were grown from a saturated hexane solution slowly cooled to -80 °C. ^1H NMR (C_6D_6, 299.9 MHz, 293 K): δ 7.51 (1 H, d, ^3J = 8.1 Hz, o_a-C_6H_5), 7.23-7.07 (4 H, m,

overlapping o_b-C_6H_5, m-C_6H_5 and p-C_6H_5), 3.66 (2 H, sept., ^3J = 6.3 Hz, NC<u>H</u>MeMe), 2.21 (15 H, s, C_5Me_5), 1.15 (9 H, s, NOCMe_3), 1.02 (6 H, d, ^3J = 6.3 Hz, NCH<u>Me</u>Me), 0.91 (6 H, d, ^3J = 6.3 Hz, NCHMe<u>Me</u>) ppm. $^{13}C\{^1H\}$ NMR (C_6D_6, 75.4 MHz, 293 K): δ 164.8 (Ph<u>C</u>N_2), 135.1 (*i*-C_6H_5), 128.9, 128.6, 128.3 (*p*-C_6H_5, *m*-C_6H_5, o_b-C_6H_5), 127.7 (o_a-C_6H_5), 119.5 (<u>C</u>$_5$Me$_5$), 80.4 (NO<u>C</u>Me_3), 49.9 (N<u>C</u>HMeMe), 27.0 (NOC<u>Me</u>$_3$), 26.8 (NCHMe<u>Me</u>), 25.6 (NCH<u>Me</u>Me), 12.1 (C_5<u>Me</u>$_5$) ppm. IR (NaCl plates, Nujol mull, cm^{-1}): 1642 (w), 1357 (s), 1336 (s), 1260 (m), 1222 (m), 1168 (m), 1142 (s), 1076 (w), 1017 (m), 845 (m), 783 (w), 750 (m), 737 (m), 707 (s). EI-MS: *m/z* = 473 $[M]^+$ (2%). Anal. found (calcd. for $C_{27}H_{43}N_3OTi$): C, 68.61 (68.49); H, 9.17 (9.15); N, 8.58 (8.87)%.

Cp*Ti{PhC(N^{i}Pr)$_2$}(SC(S)N(O^{t}Bu)) (4). To a solution of Cp*Ti{PhC(N^{i}Pr)$_2$}(NO^{t}Bu) (**3**, 0.250 g, 0.528 mmol) in benzene (5 mL) was added CS_2 (38.1 μL, 0.634 mmol) all at RT. A colour change from green to dark brown was observed. After 6 h the volatiles were removed under reduced pressure to afford **4** as a dark brown oily solid which was then triturated with pentane (5 mL), filtered and the resultant brown powder dried *in vacuo*. Yield: 0.190 g (65%). ^1H NMR (toluene-d_8, 499.9 MHz, 223 K): δ 6.97 (2 H, m, *o*-C_6H_5), 6.91 (1 H, m, *p*-C_6H_5), 6.72 (2 H, m, *m*-C_6H_5), 3.36 (2 H, m, overlapping NC<u>H$_a$</u>MeMe and NC<u>H$_b$</u>MeMe), 2.02 (15 H, s, C_5Me_5), 1.54 (9 H, s, NOCMe_3), 0.98 (3 H, d, ^3J = 6.5 Hz, NCH$_a$<u>Me</u>Me), 0.95 (3 H, d, ^3J = 6.5 Hz, NCH$_a$Me<u>Me</u>), 0.89 (3 H, d, ^3J = 6.5 Hz, NCH$_b$<u>Me</u>Me), 0.85 (3 H, d, ^3J = 6.5 Hz, NCH$_b$Me<u>Me</u>) ppm. $^{13}C\{^1H\}$ NMR (toluene-d_8, 125.7 MHz, 223 K): δ 167.3 (Ph<u>C</u>N_2), 148.1 (SC(S)N), 132.6 (*i*-C_6H_5), 131.2 (<u>C</u>$_5$Me$_5$), 129.6 (o_a-C_6H_5), 129.0 (*p*-C_6H_5), 128.7 (o_b-C_6H_5), 128.5 (m_a-C_6H_5), 128.1 (m_b-C_6H_5), 78.6 (NO<u>C</u>Me_3), 51.7 (N<u>C</u>H$_b$MeMe), 51.6 (N<u>C</u>H$_a$MeMe), 28.7 (NOC<u>Me</u>$_3$), 25.7 (NCH$_b$Me<u>Me</u>), 25.6 (NCH$_b$<u>Me</u>Me), 25.16, 25.17 (overlapping NCH$_a$<u>Me</u>Me and NCH$_a$Me<u>Me</u>), 14.5 (C_5<u>Me</u>$_5$) ppm. Note: subscripts ″a″ and ″b″ refer to the two inequivalent ^{i}Pr groups. IR (NaCl plates, Nujol mull, cm^{-1}): 1639 (w), 1359 (s), 1330 (s), 1217 (m), 1197 (s), 1170 (m), 1142 (m), 1120 (m), 1103 (m), 1075 (w), 1040 (w), 1019 (m), 987 (w), 928 (s), 910 (s), 860 (w), 781 (s), 711 (m). Anal. found (calcd. for $C_{28}H_{43}N_3OS_2Ti$): C, 61.37 (61.18); H, 7.74 (7.89); N, 7.82 (7.64)%.

Cp*Ti{PhC(N^{i}Pr)$_2$}{OC(NAr′)N(O^{t}Bu)} (5). To a solution of Cp*Ti{PhC(N^{i}Pr)$_2$}(NO^{t}Bu) (**3**, 0.320 g, 0.676 mmol) in Et$_2$O (5 mL) was added Ar′NCO (144 μL, 0.676 mmol) all at RT. An immediate colour change from green to red/brown was observed. After 3.5 h, the volatiles were removed under reduced pressure to afford **5** as a dark brown solid which was then triturated with hexane (5 mL) at -30 °C, filtered and the resultant brown powder dried *in vacuo*. Yield: 0.184 g (40%). ^{1}H NMR (toluene-*d*$_8$, 499.9 MHz, 243 K): δ 7.59 (1 H, d, ^{3}J = 7.5 Hz, *o*$_a$-C$_6$H$_5$), 7.31 (1 H, d, ^{3}J = 7.5 Hz, *o*$_b$-C$_6$H$_5$), 7.22-7.00 (5 H, m, *m*-C$_6$H$_5$, *m*-2,6-C$_6$H$_3$^{i}Pr$_2$, *p*-2,6-C$_6$H$_3$^{i}Pr$_2$), 6.88 (1 H, m, *p*-C$_6$H$_5$), 3.73 (1 H, sept., ^{3}J = 6.5 Hz, NC$\underline{H}_a$MeMe), 3.64 (1 H, br. sept., 2,6-C$_6$H$_3$(C$\underline{H}_a$MeMe)$_2$), 3.18 (1 H, br. sept., 2,6-C$_6$H$_3$(C$\underline{H}_b$MeMe)$_2$), 3.06 (1 H, sept., ^{3}J = 6.5 Hz, NC$\underline{H}_b$MeMe), 2.08 (15 H, s, C$_5$Me$_5$), 1.75 (3 H, br. d, 2,6-C$_6$H$_3$(CH$_a$$\underline{Me}$Me)$_2$), 1.64 (3 H, br. d, 2,6-C$_6$H$_3$(CH$_b$$\underline{Me}$Me)$_2$), 1.50 (9 H, s, NOCMe$_3$), 1.42 (3 H, br. d, 2,6-C$_6$H$_3$(CH$_a$Me$\underline{Me}$)$_2$), 1.27 (3 H, d, ^{3}J = 6.5 Hz, NCH$_a$$\underline{Me}$Me), 1.21 (3 H, br. d, 2,6-C$_6$H$_3$(CH$_b$Me$\underline{Me}$)$_2$), 0.93 (3 H, d, ^{3}J = 6.5 Hz, NCH$_a$Me$\underline{Me}$), 0.63 (6 H, d, ^{3}J = 6.5 Hz, NCH$_b$$\underline{MeMe}$) ppm. ^{13}C{^{1}H} NMR (toluene-*d*$_8$, 125.7 MHz, 243 K): δ 170.7 (Ph$\underline{C}$N$_2$), 154.4 (OCN), 145.7 (*i*-2,6-C$_6$H$_3$^{i}Pr$_2$), 140.0 (*o*$_a$-2,6-C$_6$H$_3$^{i}Pr$_2$), 139.5 (*o*$_b$-2,6-C$_6$H$_3$^{i}Pr$_2$), 132.9 (*i*-C$_6$H$_5$), 129.1, 128.2, 128.5, (*p*-2,6-C$_6$H$_3$^{i}Pr$_2$, *m*$_a$-C$_6$H$_5$ and *m*$_b$-C$_6$H$_5$), 128.8 (*o*$_a$-C$_6$H$_5$ overlapping with solvent), 128.6 ($\underline{C}_5$Me$_5$ overlapping with solvent), 127.5 (*p*-C$_6$H$_5$), 122.6 (*o*$_b$-C$_6$H$_5$), 121.6 (*m*$_b$-2,6-C$_6$H$_3$^{i}Pr$_2$), 121.3 (*m*$_a$-2,6-C$_6$H$_3$^{i}Pr$_2$), 80.8 (NO$\underline{C}$Me$_3$), 50.5 (N$\underline{C}$H$_a$MeMe), 50.3 (N$\underline{C}$H$_b$MeMe), 29.5 (2,6-C$_6$H$_3$(C$\underline{H}_a$MeMe)$_2$), 28.5 (overlapping NOC$\underline{Me}_3$ and 2,6-C$_6$H$_3$(C$\underline{H}_b$MeMe)$_2$), 27.5 (NCH$_b$$\underline{Me}$Me), 26.5 (NCH$_aMe\underline{Me}$), 26.2 (NCH$_a$$\underline{Me}$Me), 25.1 (2,6-C$_6H_3$(CH$_aMe\underline{Me}$)$_2$), 23.8 (2,6-C$_6H_3$(CH$_a$$\underline{Me}$Me)$_2$), 23.6 (2,6-C$_6H_3$(CH$_b$$\underline{Me}$Me)$_2$), 23.2 (NCH$_bMe\underline{Me}$), 21.5 (2,6-C$_6H_3$(CH$_bMe\underline{Me}$)$_2$), 12.9 (C$_5$$\underline{Me}_5$) ppm. Note: subscripts ″a″ and ″b″ refer to the inequivalent aryl environments and ^{i}Pr groups. IR (NaCl plates, Nujol mull, cm^{-1}): 1631 (s), 1583 (s), 1510 (m), 1394 (s), 1359 (s), 1335 (s), 1220 (m), 1188 (m), 1148 (m), 1119 (m), 1102 (w), 1066 (m), 1045 (m), 1022 (m), 973 (m), 936 (w), 858 (w), 832 (w), 790 (m), 782 (m), 753 (w), 730 (s), 705 (m), 681 (w), 555 (w). Anal. found (calcd. for C$_{40}$H$_{60}$N$_4$O$_2$Ti): C, 71.04 (70.99); H, 8.73 (8.94); N, 8.06 (8.28)%.

Cp*Ti{PhC(N^{i}Pr)$_2$}{OC(NTol)N(Tol)C(NO^{t}Bu)O} (6). To a solution of Cp*Ti{PhC(N^{i}Pr)$_2$}(NO^{t}Bu) (**3**, 0.250 g, 0.528 mmol) in benzene (10 mL) was added TolNCO (140 μL, 1.11 mmol) all at RT. An immediate colour change from green to brown/red was observed. After 2.5 h, the volatiles were removed under reduced

pressure to afford **6** as a light brown crystalline solid. Pentane (10 mL) was added and the solution concentrated by half before cooling to -80 °C. The resulting solid was then isolated by filtration and the red/brown powder dried *in vacuo*. Yield: 0.235 g (60%). Diffraction-quality crystals were grown from a saturated Et_2O solution at 4 °C. ^{1}H NMR (C_6D_6, 299.9 MHz, 293 K): δ 7.72 (2 H, d, ^3J = 8.1 Hz, o_a-C_6H_4Me), 7.39 (2 H, d, ^3J = 7.5 Hz, *o*-C_6H_5), 7.16 (2 H, m, o_b-C_6H_4Me), 7.06 - 7.00 (7 H, m, overlapping *m*-C_6H_5, *p*-C_6H_5, m_a-C_6H_4Me, m_b-C_6H_4Me), 3.67 (2 H, overlapping sept., NC$\underline{H}_a$MeMe and NC$\underline{H}_b$MeMe), 2.20 (3 H, s, p_b-$C_6H_4\underline{Me}$), 2.12 (3 H, s, p_a-$C_6H_4\underline{Me}$), 1.99 (15 H, s, C_5Me_5), 1.49 (3 H, d, ^3J = 6.6 Hz, NCH$_a\underline{Me}$Me), 1.10 (9 H, s, NOCMe_3), 1.05 (3 H, d, ^3J = 6.9 Hz, NCH$_b\underline{Me}$Me), 0.96 (3 H, d, ^3J = 6.6 Hz, NCH$_a$Me$\underline{Me}$), 0.91 (3 H, d, ^3J = 6.9 Hz, NCH$_b$Me$\underline{Me}$) ppm. ^{13}C{^{1}H} NMR (C_6D_6, 75.4 MHz, 293 K): δ 170.4 (Ph$\underline{C}N_2$), 156.4 (OC$_a$N), 153.9 (OC$_b$N), 148.5 (i_b-C_6H_4Me), 141.3 (i_a-C_6H_4Me), 134.4 (m_a-C_6H_4Me), 133.8 (*i*-C_6H_5), 130.3 ($\underline{C}_5Me_5$), 129.6, 129.0, 128.3 (*p*-C_6H_5, m_b-C_5H_4Me, *m*-C_6H_5), 129.2 (p_b-C_6H_4Me), 129.2 (*o*-C_6H_5), 128.6 (p_a-C_6H_4Me), 128.5 (o_a-C_6H_4Me), 124.5 (o_b-C_6H_4Me), 76.7 (NO$\underline{C}Me_3$), 51.2 (N$\underline{C}H_b$MeMe), 50.9 (N$\underline{C}H_a$MeMe), 27.6 (NOC$\underline{Me}_3$), 26.6 (NCH$_a$Me$\underline{Me}$) 25.4 (NCH$_b\underline{Me}$Me), 24.8 (NCH$_b$Me$\underline{Me}$), 24.0 (NCH$_a\underline{Me}$Me), 21.1 (p_a-$C_6H_4\underline{Me}$), 21.1 (p_b-$C_6H_4\underline{Me}$), 12.8 ($C_5\underline{Me}_5$) ppm. Note: subscripts ″a″ and ″b″ refer to the inequivalent aryl environments and ^{i}Pr groups. IR (NaCl plates, Nujol mull, cm^{-1}): 1623 (s), 1587 (s), 1575 (s), 1512 (m), 1506 (m), 1422 (m), 1356 (s) 1337 (s), 1279 (w), 1250 (m), 1217 (m), 1195 (m), 1142 (m), 1112 (m), 1103 (w), 1088 (m), 1043 (w), 1021 (m), 1001 (m), 955 (m), 932 (w), 916 (w), 869 (w), 826 (w), 814 (m), 807 (m), 788 (w), 780 (m), 734 (m), 726 (m), 713 (w), 707 (m), 678 (w), 646 (w), 619 (m). EI-MS: *m/z* = 353 [OC(NO^{t}Bu)N(Tol)C(NTol)O]$^+$ (60%). Anal. found (calcd. for $C_{43}H_{57}N_5O_3Ti$): C, 70.09 (69.81); H, 7.59 (7.77); N, 9.42 (9.47)%.

Reaction of Cp*Ti{PhC(N^{i}Pr)$_2$}(NO^{t}Bu) with ^{t}BuNCO: synthesis of [Cp*Ti{PhC(N^{i}Pr)$_2$}(μ-O)]$_2$ (7) and ^{t}BuNCNO^{t}Bu (8). To a solution of Cp*Ti{PhC(N^{i}Pr)$_2$}(NO^{t}Bu) (**3**, 0.500 g, 1.06 mmol) in Et_2O (5 mL) was added ^{t}BuNCO (121 μL, 1.06 mmol) all at RT. A colour change from green to yellow was observed. After 16 h the solution was filtered yielding **7** as a yellow solid which was dried *in vacuo.* Yield: 0.289 g (68%). Removal of the volatiles from the filtrate gave **8** as a colourless liquid. Yield: *ca.* 10% due to the volatility of **8** itself. Diffraction-quality crystals of **7** were grown from a saturated hexane solution at 4 °C.

*Data for [Cp*Ti{PhC(N^{i}Pr)$_2$}(μ-O)]$_2$ (**7**).* ^{1}H NMR (C_6D_6, 299.9 MHz, 293 K): δ 7.35 (2 H, m, *o*-C_6H_5), 7.15 (3 H, m, overlapping *m*-C_6H_5 and *p*-C_6H_5), 3.69 (2 H, sept., ^3J = 6.3 Hz, NC<u>H</u>MeMe), 2.28 (15 H, s, C_5Me_5), 1.28 (6 H, d, ^3J = 6.6 Hz, NCH<u>Me</u>Me), 1.09 (6 H, d, ^3J = 6.3 Hz, NCHMe<u>Me</u>) ppm. ^{13}C{^{1}H} NMR (C_6D_6, 75.4 MHz, 293 K): δ 172.0 (Ph<u>C</u>N$_2$), 137.0 (*i*-C_6H_5), 128.3, 128.2, 127.9 (overlapping with solvent *p*-C_6H_5, *m*-C_6H_5, *o*-C_6H_5), 122.7 (<u>C</u>$_5$Me$_5$), 48.4 (N<u>C</u>HMeMe), 26.2 (NCHMe<u>Me</u>), 25.6 (NCH<u>Me</u>Me), 13.7 (C$_5$<u>Me</u>$_5$) ppm. IR (NaCl plates, Nujol mull, cm^{-1}): 1419 (m), 1359 (m), 1323 (s), 1261 (w), 1210 (m), 1165 (m), 1141 (m), 1108 (w), 1014 (m), 938 (w), 799 (w), 780 (m), 738 (w), 707 (m), 637 (s), 597 (m). EI-MS: *m/z* = 669 [*M* - Cp*]$^+$ (2%), 402 [Cp*Ti{PhC(N^{i}Pr)$_2$}(O)]$^+$ (90%). Anal. found (calcd. for $C_{46}H_{68}N_4O_2Ti_2$): C, 68.78 (68.65); H, 8.87 (8.52); N, 6.81 (6.96)%.

*Data for ^{t}BuNCNO^{t}Bu (**8**).* ^{1}H NMR (C_6D_6, 299.9 MHz, 293 K): δ 1.25 (9 H, s, NOCMe$_3$), 1.05 (9 H, s, NCMe$_3$) ppm. ^{13}C{^{1}H} NMR (C_6D_6, 75.4 MHz, 293 K): δ 154.7 (NCN), 79.2 (NO<u>C</u>Me$_3$), 57.8 (N<u>C</u>Me$_3$), 30.4 (NC<u>Me</u>$_3$), 27.1 (NOC<u>Me</u>$_3$) ppm. Solution IR (NaCl plates, Et_2O, cm^{-1}): 2257 (m), 2065 (s). FI-HRMS: *m/z* found (calcd. for $C_9H_{18}N_2O$, [*M*]$^+$) 170.1421 (170.1419).

PhC(NO^{t}Bu)H (9a). To a solution of Cp*Ti{PhC(N^{i}Pr)$_2$}(NO^{t}Bu) (**3**, 0.250 g, 0.528 mmol) in C_6H_6 (5 mL) was added PhC(O)H (53.7 μL, 0.528 mmol) all at RT. An immediate colour change to yellow was observed. After 30 min the volatiles were removed under reduced pressure and the resulting solid distilled (80-110 °C, 8 x 10^{-2} mbar, 2 h) onto a dry ice/acetone cold finger yielding **9a** as a colourless oil at RT. Yield: 0.066 g (70%). The ^{1}H NMR spectrum indicated an approximately 20:80 mixture of the *syn* and *anti* isomers.

Major isomer (anti): ^{1}H NMR (C_6D_6, 299.9 MHz, 293 K): δ 7.85 (2 H, d, *o*-C_6H_5), 7.27 (1 H, s, PhC(<u>H</u>)), 7.15-7.00 (3 H, m, overlapping *m*-C_6H_5 and *p*-C_6H_5), 1.39 (9 H, s, CMe$_3$) ppm. ^{13}C{^{1}H} NMR (C_6D_6, 75.4 MHz, 293 K): δ 144.7 (Ph<u>C</u>(H)), 132.0 (*i*-C_6H_5), 131.2 (*o*-C_6H_5), 129.6 (*p*-C_6H_5), 128.5 (*m*-C_6H_5), 79.4 (<u>C</u>Me$_3$), 27.6 (C<u>Me</u>$_3$) ppm.

Minor isomer (syn): The ^{1}H NMR spectrum was consistent with the literature values.[15] ^{1}H NMR (C_6D_6, 299.9 MHz, 293 K): δ 8.03 (1 H, s, PhC(H)), 7.45 (2 H, d, *o*-C_6H_5), 7.15-7.00 (3 H, m, overlapping *m*-C_6H_5 and *p*-C_6H_5), 1.38 (9 H, s, CMe$_3$) ppm. ^{13}C{^{1}H}

NMR (C_6D_6, 75.4 MHz, 293 K): δ 147.4(Ph<u>C</u>(H)), 133.8 (*i*-C_6H_5), 129.4 (*p*-C_6H_5), 128.8 (*m*-C_6H_5), 127.1 (*o*-C_6H_5), 79.0 (<u>C</u>Me_3), 27.8 (C<u>Me</u>$_3$) ppm.

Common data: IR (thin film, cm^{-1}): 3095 (w), 3058 (w), 3026 (w), 2975 (br, s), 2929 (br, m), 2868 (w), 1636 (m), 1491 (m), 1472 (w), 1448 (m), 1387 (m), 1364 (s), 1318 (w), 1297 (w), 1262 (m), 1190 (m), 1183 (m), 1101 (w), 1078 (w), 1031 (w), 950 (s), 933 (m), 915 (m), 882 (w), 839 (w), 819 (w), 806 (w), 757 (m), 692 (s), 629 (m). FI-HRMS: *m/z* found (calcd. for $C_{11}H_{15}NO$, $[M]^+$) 177.1152 (177.1154).

PhC(NO^{t}Bu)Me (9b). To a solution of Cp*Ti{PhC(N^{i}Pr)$_2$}(NO^{t}Bu) (**3**, 0.200 g, 0.423 mmol) in C_6H_6 (5 mL) was added PhC(O)Me (49.3µL, 0.423 mmol) all at RT. A colour change from green to yellow was observed. After 30 min the volatiles were removed under reduced pressure and the resulting solid distilled (80-110 °C, 8 x 10^{-2} mbar, 2 h) onto a dry ice/acetone cold finger yielding **9b** as a yellow liquid at RT. Yield: 0.061 g (75%). The ^{1}H NMR spectrum indicated an approximately 9:1 mixture of the *syn* and *anti* isomers and was consistent with the literature values.[16]

Major isomer (syn): ^{1}H NMR ($CDCl_3$, 499.9 MHz, 293 K): δ 7.69 (2 H, d, ^3J = 8.0 Hz, *o*-C_6H_5), 7.38-7.33 (3 H, m, overlapping *m*-C_6H_5 and *p*-C_6H_5), 2.22 (Me), 1.37 (9 H, s, CMe_3) ppm. ^{13}C{^{1}H} NMR ($CDCl_3$, 125.7 MHz, 293 K): δ 152.5 (Ph<u>C</u>(Me)), 137.7 (*i*-C_6H_5), 128.7 (*p*-C_6H_5), 128.4 (*m*-C_6H_5), 126.0 (*o*-C_6H_5), 78.8 (<u>C</u>Me_3), 27.9 (C<u>Me</u>$_3$), 12.4 (Me) ppm.

Minor isomer (anti): ^{1}H NMR (C_6D_6, 299.9 MHz, 293 K): δ 7.59 (2 H, m, *o*-C_6H_5), 7.39-7.31 (3 H, m, overlapping *m*-C_6H_5 and *p*-C_6H_5), 2.21 (Me), 1.30 (9 H, s, CMe_3) ppm. ^{13}C{^{1}H} NMR ($CDCl_3$, 125.7 MHz, 293 K): δ 151.2 (Ph<u>C</u>(Me)), 135.0 (*i*-C_6H_5), 128.6 (*p*-C_6H_5), 128.5 (*o*-C_6H_5), 127.9 (*m*-C_6H_5), 78.2 (<u>C</u>Me_3), 27.6 (C<u>Me</u>$_3$), 21.9 (Me) ppm**.**

NMR tube scale synthesis of Cp*Ti{PhC(N^{i}Pr)$_2$}{N(O^{t}Bu)C(Ph)(H)O} (9a_int). To a solution of Cp*Ti{PhC(N^{i}Pr)$_2$}(NO^{t}Bu) (**3**, 10.4 mg, 0.0220 mmol) in toluene-d_8 (0.5 mL) pre-cooled to -78 °C in an NMR tube equipped with a J. Young Teflon valve was added PhC(O)H (2.23 µL, 0.0220 mmol). An immediate colour change from dark green to yellow was observed. The solution was allowed to warm to -30 °C at which temperature the ^{1}H NMR spectrum showed quantitative conversion to [Cp*Ti{PhC(N^{i}Pr)$_2$}(µ-O)]$_2$ (**23**) and **9a_int** as a mixture of stereoisomers, **9a_int_H$_{upp}$** and **9a_int_H$_{down}$**.

Major isomer: ^{1}H NMR (toluene-d_8, 299.9 MHz, 243 K): δ 7.84 (2 H, app. d, *o*-C_6H_5), 7.22 (1 H, s, PhC<u>H</u>), 6.89 – 7.44 (8 H, m, *o*-C_6H_5, *m*-C_6H_5, *p*-C_6H_5, *m*-C_6H_5, *p*-C_6H_5), 3.53 (2 H, br. sept., ^{3}J = 6.6 Hz, NC<u>H</u>MeMe), 2.23 (15 H, s, C_5Me_5), 1.42 (9 H, s, NOCMe_3), 1.38 (6 H, br. d, ^{3}J = 6.6 Hz, NCH<u>Me</u>Me), 1.12 (6 H, br. d, ^{3}J = 6.3 Hz, NCHMe<u>Me</u>) ppm.

Minor isomer: ^{1}H NMR (toluene-d_8, 299.9 MHz, 243 K): δ 7.95 (1 H, s, PhC<u>H</u>), 7.70 (2 H, app. d, *o*-C_6H_5), 6.89 – 7.44 (8 H, m, overlapping *o*-C_6H_5, *m*-C_6H_5, *p*-C_6H_5, *m*-C_6H_5, *p*-C_6H_5), 3.31 (2 H, br. sept., ^{3}J = 6.3 Hz, NC<u>H</u>MeMe), 2.17 (15 H, s, C_5Me_5), 1.42 (9 H, s, NOCMe_3), 1.22 (6 H, d, ^{3}J = 6.6 Hz, NCH<u>Me</u>Me), 0.98 (6 H, d, ^{3}J = 6.3 Hz, NCHMe<u>Me</u>) ppm.

NMR tube scale synthesis of Cp*Ti{PhC(N^{i}Pr)$_2$}{N(O^{t}Bu)C(Ph)(Me)O} (9b_int). To a solution of Cp*Ti{PhC(N^{i}Pr)$_2$}(NO^{t}Bu) (**19**, 11.0 mg, 0.0232 mmol) in toluene-d_8 (0.4 mL) pre-cooled to -78 °C in an NMR tube equipped with a J. Young Teflon valve was added PhC(O)Me (2.71 μL, 0.0232 mmol). The solution was allowed to warm to -10 °C at which temperature the ^{1}H NMR spectrum showed quantitative conversion to [Cp*Ti{PhC(N^{i}Pr)$_2$}(μ-O)]$_2$ (**7**) and **9b_int**. ^{1}H NMR (toluene-d_8, 299.9 MHz, 263 K): δ 6.98 – 7.71 (10 H, m, overlapping 2 x C_6H_5), 3.50 (2 H, br. sept. ^{3}J = 6.6 Hz, NC<u>H</u>MeMe), 2.22 (15 H, s, C_5Me_5), 2.05 (3 H, s, Me) 1.42 (9 H, s, NOCMe_3), 1.35 (6 H, br. d, ^{3}J = 6.6 Hz, NCH<u>Me</u>Me), 1.11 (6 H, br. d, ^{3}J = 6.3 Hz, NCHMe<u>Me</u>) ppm.

Low temperature NMR tube scale reaction of Cp*Ti{PhC(N^{i}Pr)$_2$}(NO^{t}Bu) (3) with PhC(O)H and TolC(O)H (1:1 ratio). To a solution of Cp*Ti{PhC(N^{i}Pr)$_2$}(NO^{t}Bu) (**3**, 10.0 mg, 0.0211 mmol) in toluene-d_8 (0.5 mL) pre-cooled to -50 °C in an NMR tube equipped with a J. Young Teflon valve was added PhC(O)H (2.15 μL, 0.0211 mmol). An immediate colour change to orange/yellow was observed. After 15 min at -50 °C TolC(O)H (2.49 μL, 0.0211 mmol) was added. Following a further 10 min at -50 °C the solution was left to warm to room temperature and a subtle colour change to yellow observed. The ^{1}H NMR spectrum recorded after 15 min showed quantitative conversion to [Cp*Ti{PhC(N^{i}Pr)$_2$}(μ-O)]$_2$ (**7**) and PhC(NO^{t}Bu)(H) (**9a**), alongside TolC(O)H.

NMR tube scale synthesis of TolC(NO^{t}Bu)H (9d). To a solution of Cp*Ti{PhC(N^{i}Pr)$_2$}(NO^{t}Bu) (**3**, 40.0 mg, 0.0845 mmol) in toluene-d_8 (0.5 mL) in an NMR tube equipped with a J. Young Teflon valve was added TolC(O)H (9.96 μL,

0.0845 mmol) all at RT. An immediate colour change to yellow was observed and ^{1}H NMR spectroscopy showed quantitative conversion to **9d** as a mixture of *anti* and *syn* isomers in the ratio 7:3.

Major isomer (anti): ^{1}H NMR (toluene-d_8, 299.9 MHz, 293 K): δ 7.82 (2 H, d, ^{3}J = 8.4 Hz, *o*-C_6H_4Me), 7.30 (1 H, s, TolC(H)), 6.95 (2 H, d, ^{3}J = 8.1 Hz, *m*-C_6H_4Me), 2.28 (3 H, s, C_6H_4Me), 1.41 (9 H, s, CMe_3) ppm. ^{13}C{^{1}H} NMR (toluene-d_8, 75.4 MHz, 293 K): δ 144.7 (TolC(H)), 139.6 (*p*-C_6H_4Me), 131.3 (*o*-C_6H_4Me), 129.5 (*i*-C_6H_4Me), 129.3 (*m*-C_6H_4Me), 78.8 (CMe_3), 27.7 (CMe_3), 21.3 (C_6H_4Me) ppm

Minor isomer (syn): ^{1}H NMR (toluene-d_8, 299.9 MHz, 293 K): δ 8.08 (1 H, s, TolC(H)), 7.43 (2 H, d, ^{3}J = 8.1 Hz, *o*-C_6H_5), 6.89 (2 H, d, ^{3}J = 8.1 Hz, *m*-C_6H_4Me), 2.01 (3 H, s, C_6H_4Me), 1.40 (9 H, s, CMe_3) ppm. ^{13}C{^{1}H} NMR (toluene-d_8, 75.4 MHz, 293 K): δ 147.5 (TolC(H)), 139.3 (*p*-C_6H_4Me), 131.3 (*i*-C_6H_4Me), 129.6 (*m*-C_6H_4Me), 127.2 (*o*-C_6H_4Me), 79.3 (CMe_3), 27.9 (CMe_3), 21.3 (C_6H_4Me) ppm.

Common data: FI-HRMS: *m/z* found (calcd. for $C_{12}H_{17}NO$, $[M]^+$) 191.1308 (191.1310).

NMR tube scale reaction of Cp*Ti{PhC(N^{i}Pr)$_2$}(NO^{t}Bu) (3) with PhC(O)H and TolC(O)H (1:1 ratio). To a solution of Cp*Ti{PhC(N^{i}Pr)$_2$}(NO^{t}Bu) (**3**, 15.0 mg, 0.0317 mmol) in C_6D_6 (0.3 mL) in an NMR tube equipped with a J. Young Teflon valve was added a pre-mixed solution of TolC(O)H (3.74 μL, 0.0317 mmol) and PhC(O)H (3.22 μL, 0.0317 mmol) in C_6D_6 (0.3 mL) all at RT. An immediate colour change from dark green to yellow was observed. The ^{1}H NMR spectrum recorded after 1 h showed quantitative conversion to PhC(NO^{t}Bu)(H) (**9a**) and TolC(NO^{t}Bu)H (**9d**) in a 1:1 ratio, alongside [Cp*Ti{PhC(N^{i}Pr)$_2$}(μ-O)]$_2$ (**7**).

PhC(NO^{t}Bu)Ph (9c). To a solution of Cp*Ti{PhC(N^{i}Pr)$_2$}(NO^{t}Bu) (**3**, 0.250 g, 0.528 mmol) in benzene (5 mL) was added a solution of PhC(O)Ph (0.962 g, 0.528 mmol) in benzene (5 mL) and heated to 70 °C. After 24 h the volatiles were removed under reduced pressure and the resulting solid sublimed (80-100 °C, 8 x 10^{-2} mbar, 5 h) onto a dry ice/acetone cold finger yielding **9c** a cream solid. Yield: 0.125 g (93%). ^{1}H NMR (C_6D_6, 499.9 MHz, 293 K): δ 7.67 (2 H, m, o_a-C_6H_5), 7.35 (2 H, m, o_b-C_6H_5), 7.13-7.07 (6 H, m, overlapping m_a-C_6H_5, m_b-C_6H_5 and p_a-C_6H_5, p_b-C_6H_5), 1.33 (9 H, s, $NOCMe_3$) ppm. ^{13}C{^{1}H} NMR (C_6D_6, 125.7 MHz, 293 K): δ 155.3 (PhC(N)Ph), 138.1 (*i*-C_6H_5), 134.5 (*i*-C_6H_5), 129.9 (o_b-C_6H_5), 129.0, 128.5, 128.4, 128.4, 128.2 (p_a-C_6H_5, p_b-C_6H_5, m_a-C_6H_5, m_b-C_6H_5, o_a-C_6H_5), 79.3 ($NOCMe_3$), 27.8 ($NOCMe_3$) ppm. Note: subscripts

″a″ and ″b″ refer to the two inequivalent Ph environments. IR (NaCl plates, Nujol mull, cm^{-1}): 1665 (w), 1639 (w), 1600 (w), 1493 (m), 1445 (s), 1365 (m), 1359 (m), 1325(w), 1276 (m), 1263 (m), 1240 (w), 1193 (m), 1167 (w), 1074 (w), 1039 (w), 1001 (w), 990 (w), 959 (s), 917 (m), 867 (w), 807 (w), 785 (w), 769 (m), 763 (m), 696 (s), 667 (w), 642 (w), 603 (w). ESI^+-HRMS: *m/z* found (calcd. for $C_{17}H_{19}NNaO$, $[M + Na]^+$) 276.1354 (276.1359).

Cp*Ti{PhC(N^{i}Pr)$_2$}{NC(Ar^{F5})NO^{t}Bu} (10). To a solution of Cp*Ti{PhC(N^{i}Pr)$_2$}(NO^{t}Bu) (**3**, 0.230 g, 0.486 mmol) in benzene (10 mL) was added Ar^{F5}CN (61.2 μL, 0.486 mmol) all at RT. An immediate colour change from green to lime green was observed. After 1 h, the volatiles were removed under reduced pressure to afford **10** as a green oily solid. Et_2O (5 mL) was added and the solution cooled to -80 °C. The resulting green crystalline solid was isolated by filtration and dried *in vacuo*. Yield: 0.118 g (33%). Diffraction-quality crystals were grown from a saturated hexane solution at -80 °C. ^{1}H NMR (C_6D_6, 499.9 MHz, 293 K): δ 7.35 (1 H, d, ^3J = 8.0 Hz, o_a-C_6H_5), 7.12-7.06 (2 H, m, *m*-C_6H_5), 7.00 (1 H, t, ^3J = 7.5 Hz, *p*-C_6H_5), 6.93 (1 H, d, ^3J = 7.5 Hz, o_b-C_6H_5), 3.40 (2 H, sept., ^3J = 6.5 Hz, NC<u>H</u>MeMe), 2.21 (15 H, s, C_5Me_5), 1.40 (9 H, s, NOCMe$_3$), 0.81 (6 H, d, ^3J = 6.0 Hz, NCH<u>Me</u>Me), 0.77 (6 H, d, ^3J = 6.5 Hz, NCHMe<u>Me</u>) ppm. ^{13}C{^{1}H} NMR (C_6D_6, 125.7 MHz, 293 K): δ 166.9 (Ph<u>C</u>N$_2$), 150.1 (N<u>C</u>(C_6F_5)N), 143.2 (2 C, d, $^1J_{C\text{-}F}$ = 244.9 Hz, *o*-C_6F_5), 140.4 (1 C, d, $^1J_{C\text{-}F}$ = 249.9 Hz, *p*-C_6F_5), 137.8 (2 C, d, $^1J_{C\text{-}F}$ = 249.1 Hz, *m*-C_6F_5), 133.1 (*i*-C_6H_5), 129.0 (*p*-C_6H_5), 128.9 (*m*-C_6H_5), 127.4 (o_a-C_6H_5), 127.2 (o_b-C_6H_5), 123.6 (<u>C</u>$_5$Me$_5$), 113.2 (1 C, t, $^2J_{C\text{-}F}$ = 22.4 Hz, *i*-C_6F_5) 78.0 (NO<u>C</u>Me$_3$), 50.9 (N<u>C</u>HMeMe), 27.9 (NOC<u>Me</u>$_3$), 26.4 (NCHMe<u>Me</u>), 24.2 (NCH<u>Me</u>Me), 12.4 (C_5<u>Me</u>$_5$) ppm. ^{19}F{^{1}H} NMR (C_6D_6, 282.1 MHz, 293 K): δ -140.6 (2 F, m, *o*-C_6F_5), -157.7 (1 F, t, ^3J = 20.6 Hz, *p*-C_6F_5), -163.9 (2 F, app. t, *m*-C_6F_5) ppm. Note: subscripts ″a″ and ″b″ refer to the inequivalent aryl environments. IR (NaCl plates, Nujol mull, cm^{-1}): 1651 (w), 1528 (m), 1512 (s), 1492 (s), 1364 (s), 1340 (s), 1294 (m), 1259 (m), 1221 (m), 1194 (m), 1169 (m), 1140 (m), 1108 (m), 1033 (m), 1019 (m), 989 (s), 943 (s), 892 (M), 817 (w), 793 (m), 780 (m), 740 (m), 725 (m), 707 (m), 669 (m), 612 (m), 577 (m). EI-MS: *m/z* = 666 $[M]^+$ (7%). Anal. found (calcd. for $C_{34}H_{43}N_4OF_5Ti$): C, 61.38 (61.26); H, 6.59 (6.50); N, 8.30 (8.40)%.

Cp*Ti{PhC(N^{i}Pr)$_2$}{NC(Ar^{F2})NO^{t}Bu} (11). To a solution of Cp*Ti{PhC(N^{i}Pr)$_2$}(NO^{t}Bu) (**3**, 0.300 g, 0.634 mmol) in Et_2O (5 mL) was added a

solution of $Ar^{F_2}CN$ (0.881 g, 0.634 mmol) in Et_2O (5 mL) all at RT. An immediate colour change from green to lime green was observed. After 2 h the volatiles were removed under reduced pressure to afford **11** as a green oil which was dried *in vacuo*. Yield: 0.375 g (97%). ^{1}H NMR (C_6D_6, 499.9 MHz, 293 K): δ 7.49 (1 H, d, ^3J = 7.5 Hz, o_a-C_6H_5), 7.17 (1 H, m, m_a-C_6H_5), 7.09 (1 H, t, ^3J = 7.5 Hz, m_b-C_6H_5), 7.04 (1 H, m, *p*-C_6H_5), 6.98 (1 H, d, ^3J = 7.5 Hz, o_b-C_6H_5), 6.58 (3 H, m, overlapping *m*-$C_6F_2H_3$ and *p*-$C_6F_2H_3$), 3.47 (2 H, sept., ^3J = 6.0 Hz, NC<u>H</u>MeMe), 2.27 (15 H, s, C_5Me_5), 1.42 (9 H, s, $NOCMe_3$), 0.88 (6 H, d, ^3J = 6.5 Hz, NCH<u>Me</u>Me), 0.86 (6 H, d, ^3J = 6.0 Hz, NCHMe<u>Me</u>) ppm. ^{13}C{^{1}H} NMR (C_6D_6, 125.7 MHz, 293 K): δ 166.9 (Ph<u>C</u>N_2), 159.7 (dd, $^1J_{C\text{-}F}$ = 246.0 Hz, $^3J_{C\text{-}F}$ = 9.4 Hz, *o*-$C_6F_2H_3$), 153.8 (N<u>C</u>($C_6F_2H_3$)N), 133.7 (*i*-$C_6F_2H_3$), 128.8 (m_a-C_6H_5), 128.8 (m_b-C_6H_5), 128.7 (*p*-C_6H_5), 128.4 (*p*-$C_6F_2H_3$), 127.6 (o_a-C_6H_5), 127.4 (o_b-C_6H_5), 123.1 (<u>C</u>$_5$Me$_5$), 115.8 (t, $^2J_{C\text{-}F}$ = 23.9 Hz, *i*-$C_6F_2H_3$), 110.9 (dd, $^2J_{C\text{-}F}$ = 20.4 Hz, $^4J_{C\text{-}F}$ = 5.3 Hz *m*-$C_6F_2H_3$), 77.3 (NO<u>C</u>Me_3), 50.9 (N<u>C</u>HMeMe), 28.0 (NOC<u>Me</u>$_3$), 26.6 (NCHMe<u>Me</u>), 24.4 (NCH<u>Me</u>Me), 12.5 (C_5<u>Me</u>$_5$) ppm. ^{19}F{^{1}H} NMR (C_6D_6, 282.1 MHz, 293 K): δ -112.1 (m, *o*-$C_6F_2H_3$) ppm. Note: subscripts ″a″ and ″b″ refer to the inequivalent aryl environments. IR (NaCl plates, Nujol mull, cm^{-1}): 1622 (m), 1586 (m), 1528 (m), 1430 (br, s), 1361 (s), 1346 (s), 1270 (w), 1259 (m), 1231 (m), 1217 (m), 1195 (m), 1180 (m), 1168 (m), 1160 (m), 1139 (m), 1075 (w), 1060 (w), 1032 (w), 1015 (m), 1003 (s), 955 (m), 939 (m), 915 (w), 777 (m), 746 (w), 739 (w), 705 (m), 678 (w), 654 (w), 571 (w). EI-MS: *m/z* = 612 $[M]^+$ (65%). Anal. found (calcd. for $C_{34}H_{46}F_2N_4OTi$): C, 66.80 (66.66); H, 7.68 (7.57); N, 9.03 (9.15)%.

NMR tube scale synthesis of Cp*Ti{PhC(N^{i}Pr)$_2$}{NC(Ph)NO^{t}Bu} (12). To Cp*Ti{PhC(N^{i}Pr)$_2$}(NO^{t}Bu) (**3**, 18.8 mg, 0.0397 mmol) in C_6D_6 (0.5 mL) in an NMR tube equipped with a J. Young Teflon valve was added PhCN (4.05 μL, 0.0397 mmol) all at RT. A colour change from green to dark green was observed. After 19 h ^{1}H NMR spectroscopy showed effectively quantitative conversion to **12**. ^{1}H NMR (C_6D_6, 499.9 MHz, 293 K): δ 7.90 (2 H, dd, ^3J = 8.0 Hz, *o*-C_6H_5 of nitrile), 7.23 (2 H, app. t, ^3J = 8.0 Hz, *m*-C_6H_5 of nitrile), 7.20 (1 H, app. d, o_a-C_6H_5), 7.12-7.00 (5 H, m, overlapping o_b-C_6H_5, *m*-C_6H_5, *p*-C_6H_5 and *p*-C_6H_5 of nitrile), 3.49 (2 H, sept., ^3J = 6.5 Hz, NC<u>H</u>MeMe), 2.24 (15 H, s, C_5Me_5), 1.45 (9 H, s, $NOCMe_3$), 0.99 (6 H, d, ^3J = 6.5 Hz, NCH<u>Me</u>Me), 0.87 (6 H, d, ^3J = 6.5 Hz, NCHMe<u>Me</u>) ppm. ^{13}C{^{1}H} NMR (C_6D_6, 125.7 MHz, 293 K): δ 166.6 (Ph<u>C</u>N_2), 162.7 (N<u>C</u>(C_6H_5)N), 136.4 (*i*-C_6H_5 of nitrile), 133.6 (*i*-C_6H_5), 129.5 (*o*-C_6H_5 of nitrile), 128.8, 128.8, 128.7, 127.7, 127.7, 127.4 (o_a-C_6H_5, o_b-C_6H_5, *m*-C_6H_5,

p-C_6H_5, *m*-C_6H_5 of nitrile, *p*-C_6H_5 of nitrile), 122.4 ($\underline{C}_5Me_5$), 77.0 (NO$\underline{C}Me_3$), 50.6 (N$\underline{C}$HMeMe), 28.2 (NOC$\underline{Me}_3$), 26.6 (NCHMe$\underline{Me}$), 25.0 (NCH$\underline{Me}$Me), 12.4 ($C_5\underline{Me}_5$) ppm. Note: subscripts ″a″ and ″b″ refer to the inequivalent aryl environments.

NMR tube scale reaction of Cp*Ti{PhC(N^{i}Pr)$_2$}{NC(Ar^{F2})NO^{t}Bu} (11) with Ar^{F5}CN. To a solution of Cp*Ti{PhC(N^{i}Pr)$_2$}{NC(Ar^{F2})NO^{t}Bu} (**11**, 12.9 mg, 0.0211 mmol) in C_6D_6 (0.5 mL) in an NMR tube equipped with a J. Young Teflon valve was added Ar^{F5}CN (2.66 μL, 0.0211 mmol) all at RT. After 5 min ^{1}H and ^{19}F NMR spectra showed quantitative conversion to Cp*Ti{PhC(N^{i}Pr)$_2$}{NC(Ar^{F5})NO^{t}Bu} (**10**) and Ar^{F2}CN.

NMR tube scale reaction of Cp*Ti{PhC(N^{i}Pr)$_2$}{NC(Ph)NO^{t}Bu} (12) with Ar^{F5}CN. To a solution of Cp*Ti{PhC(N^{i}Pr)$_2$}{NC(Ph)NO^{t}Bu} (**12**, 15.0 mg, 0.0260 mmol) in C_6D_6 (0.5 mL) in an NMR tube equipped with a J. Young Teflon valve was added Ar^{F5}CN (3.27 μL, 0.0260 mmol) all at RT. After 5 min ^{1}H and ^{19}F NMR spectra showed quantitative conversion to Cp*Ti{PhC(N^{i}Pr)$_2$}{NC(Ar^{F5})NO^{t}Bu} (**10**) and PhCN.

Cp*Ti{PhC(N^{i}Pr)$_2$}{N(C(Ar^{F5})NO^{t}Bu)C(Ar^{F5})NC(Ar^{F5})N} (13). To a solution of Cp*Ti{PhC(N^{i}Pr)$_2$}(NO^{t}Bu) (**3**, 0.250 g, 0.528 mmol) in benzene (5 mL) was added Ar^{F5}CN (0.333 mL, 2.64 mmol) all at RT. A colour change from dark green to lime green (**10**) to red was observed. After 6 h at RT, the volatiles were removed under reduced pressure leaving behind an orange oil. Pentane (5 mL) was added and then removed under reduced pressure to afford **13** as an orange powder which was dried *in vacuo*. Yield: 0.400 g (88%). An analytically pure sample was obtained by washing with pentane (5 mL) at RT and the resultant orange powder dried *in vacuo*. Yield: 0.222 g (49%). Diffraction-quality crystals were grown in the presence of Ar^{F5}CN from an Et_2O/pentane mixture at 4 °C. ^{1}H NMR (toluene-d_8, 499.9 MHz, 263 K): δ 7.45 (1 H, d, ^3J = 8.0 Hz, o_a-C_6H_5), 7.20 (1 H, d, ^3J = 7.5, o_b-C_6H_5), 7.12 (2 H, m, *m*-C_6H_5), 7.06 (1 H, m, *p*-C_6H_5), 3.83 (1 H, app. sept, ^3J = 6.5 Hz, NC$\underline{H}_a$MeMe), 3.40 (1 H, app. sept, ^3J = 6.5 Hz, NC$\underline{H}_b$MeMe), 2.27 (15 H, s, C_5Me_5), 1.22 (9 H, s, NOCMe_3), 1.06 (3 H, d, ^3J = 7.0 Hz, NCH$_a\underline{Me}$Me), 1.01 (3 H, d, ^3J = 6.5 Hz, NCH$_b\underline{Me}$Me), 0.80 (3 H, d, ^3J = 6.0 Hz, NCH$_b$Me$\underline{Me}$), 0.73 (3 H, d, ^3J = 6.5 Hz, NCH$_a$Me$\underline{Me}$) ppm. ^{13}C{^{1}H} NMR (toluene-d_8, 125.7 MHz, 263 K): δ 174.7 (Ph$\underline{C}N_2$), 155.7 (N$\underline{C}$N), 148.2 (N$\underline{C}$N), 146.9 (N$\underline{C}$N), 129.4 (o_b-C_6H_5), 129.1 (*p*-C_6H_5), 128.8 (o_a-C_6H_5 overlapping with solvent), 127.6 (*m*-C_6H_5), 127.2 ($\underline{C}_5Me_5$), 116.0 (1 C, m, *i*-C_6F_5), 114.2 (1 C, m, *i*-C_6F_5), 110.9

(1 C, m, *i*-C_6F_5), 280.2 (NO<u>C</u>Me_3), 51.5 (N<u>C</u>H_bMeMe), 46.2 (NCH_aMeMe), 27.3 (NOC<u>Me</u>$_3$), 27.1 (NCH_a<u>Me</u>Me), 25.5 (CH_aMe<u>Me</u>), 24.5 (NCH_b<u>MeMe</u>) 13.0 (C_5<u>Me</u>$_5$) ppm. $^{13}C\{^{19}F\}$ NMR (toluene-d_8, 75.4 MHz, 263 K): 145.4 (o_{2b}-C_6F_5), 144.6 (overlapping o_3-C_6F_5 and o_{1b}-C_6F_5), 144.3 (overlapping o_{1a}-C_6F_5 and o_{2a}-C_6F_5) 142.1 (p_1-C_6F_5), 141.8 (p_2-C_6F_5), 141.1 (p_3-C_6F_5), 138.4 (m_{1b}-C_6F_5), 137.8 (m_3-C_6F_5), 137.7 (m_{2a}-C_6F_5), 137.6 (m_{2b}-C_6F_5), 137.1 (m_{1a}-C_6F_5), $^{19}F\{^1H\}$ NMR (toluene-d_8, 470.4 MHz, 263 K): -126.7 (1 F, d, ^3J = 23.0 Hz, o_{1a}-C_6F_5), -134.16 (1 F, d, ^3J = 22.1 Hz, o_{1b}-C_6F_5), -137.0 (1F, d, ^3J = 23.5 Hz, o_{2a}-C_6F_5), - 140.6 (1 F, app. d, ^3J = 14.6 Hz, o_{2b}-C_6F_5), -141.9 (2 F, m, o_3-C_6F_5), -150.9 (1 F, t, ^3J = 20.7 Hz, p_1-C_6F_5), -154.0 (1 F, t, ^3J = 21.2 Hz, p_2-C_6F_5), 155.5 (1 F, t, ^3J = 21.6, p_3-C_6F_5), -162.9 (2 F, m, m_3-C_6F_5), -163.2 (2 F, t, ^3J = 22.1 Hz, m_{1b}-C_6F_5), -163.9 (2 F, t, m, m_{2a}-C_6F_5), -164.1 (2 F, m, m_{2b}-C_6F_5), 165.0 (2 F, m, m_{1a}-C_6F_5) ppm. Note: subscript letters and numbers refer to the inequivalent Ph and Ar^{F5} environments and the two ^{i}Pr groups. IR (NaCl plates, Nujol mull, cm^{-1}): 1651 (w), 1595 (s), 1522 (s), 1491 (s), 1408 (s), 1366 (m), 1341 (w), 1316 (m), 1226 (w), 1215 (m), 1195 (m), 1147 (w), 1130 (m), 1117 (m), 1104 (w), 1078 (w), 1020 (w), 997 (s), 936 (m), 901 (w), 880 (w), 822 (m), 787 (w), 776 (w), 727 (w), 711 (w), 696 (w), 603 (w), 577 (w). Anal. found (calcd. for $C_{48}H_{43}F_{15}N_6OTi$): C, 54.88 (54.76); H, 4.17 (4.12); N, 7.82 (7.98)%.

NMR tube scale reaction of Cp*Ti{PhC(N^{i}Pr)$_2$}{N(C(Ar^{F5})NO^{t}Bu)-C(Ar^{F5})NC(Ar^{F5})N} (13). A solution of Cp*Ti{PhC(N^{i}Pr)$_2$}-{N(C(Ar^{F5})NO^{t}Bu)C(Ar^{F5})NC(Ar^{F5})N} (**13**) (15.0 mg, 0.0142 mmol) in C_6D_6 (0.6 mL) was monitored over time. After 23 h, ^{1}H NMR spectroscopy showed a mixture of Cp*Ti{PhC(N^{i}Pr)$_2$}{NC(Ar^{F5})NO^{t}Bu} (**10**) and Cp*Ti{PhC(N^{i}Pr)$_2$}-{NC(Ar^{F5})NC(Ar^{F5})N(C{Ar^{F5}}NO^{t}Bu)} (**13**) in a 50:50 ratio.

Cp*Ti(O^{t}Bu){NC(Ar^{F5})C(H)N(^{i}Pr)C(Ph)N(^{i}Pr)} (14). To a stirring solution of Cp*Ti{PhC(N^{i}Pr)$_2$}(NO^{t}Bu) (**3**, 0.298 g, 0.629 mmol) in Et_2O (5 mL) was added a solution of Ar^{F5}CCH (0.121 g, 0.629 mmol) in Et_2O (5 mL) all at RT. A colour change from green to purple was observed. After 16 h, the volatiles were removed under reduced pressure and the resultant purple oily solid extracted into cold pentane (2 x 5 mL) cooled to -78 °C. The volatiles were removed under reduced pressure to afford **14** as a purple powder which was dried *in vacuo*. Yield: 0.290 g (69%). ^{1}H NMR (C_6D_6, 499.9 MHz, 293 K): δ 6.86 (3 H, m, overlapping *o*-C_6H_5 and NC(Ar^{F5})C(H)N), 6.70 (2 H, t, ^3J = 7.0 Hz, *m*-C_6H_5), 6.64 (1 H, m, *p*-C_6H_5), 3.91 (1 H, sept., ^3J = 6.5 Hz, N(C$\underline{H}_a$MeMe)C(H)), 3.61 (1 H, sept., ^3J = 6.5 Hz, NC$\underline{H}_b$MeMe), 2.09 (15 H, s, C_5Me_5), 1.37 (9 H, s, NOCMe$_3$), 1.32 (3 H, d, ^3J = 6.5 Hz, NCH$_a$$\underline{Me}$Me), 1.29 (3 H, d, ^3J = 6.5 Hz, NCH$_a$Me$\underline{Me}$), 1.27 (3 H, d, ^3J = 6.5 Hz, NCH$_b$$\underline{Me}$Me), 0.77 (3 H, d, ^3J = 6.5 Hz, NCH$_b$Me$\underline{Me}$) ppm. ^{13}C{^{1}H} NMR (C_6D_6, 125.7 MHz, 293 K): δ 161.6 (Ph$\underline{C}$N$_2$), 138.9 (NC(Ar^{F5})$\underline{C}$(H)N), 136.0 (*i*-C_6H_5), 128.5 (*p*-C_6H_5), 127.5 (*m*-C_6H_5), 127.4 (*o*-C_6H_5), 122.8 ($\underline{C}_5Me_5$), 114.6 (1 C, t of d, $^2J_{C\text{-}F}$ = 15.1 Hz, $^3J_{C\text{-}F}$ = 3.5 Hz, *i*-C_6F_5) 108.8 (N$\underline{C}$(Ar^{F5})C(H)N), 82.2 (NO$\underline{C}$Me$_3$), 53.8 (N$\underline{C}$H$_a$MeMe), 50.2 (N$\underline{C}$H$_b$MeMe), 33.1 (NOC$\underline{Me}_3$), 27.0 (NCH$_b$$\underline{Me}$Me), 26.7 (NCH$_a$$\underline{Me}$Me), 24.9 (NCH$_bMe\underline{Me}$), 24.6 (NCH$_aMe\underline{Me}$), 12.3 ($C_5\underline{Me}_5$) ppm. Note: ^{19}F{^{1}H} NMR is broad at 293 K and therefore ^{13}C{^{19}F} and ^{19}F{^{1}H} NMR spectra were recorded at 223 K - ^{13}C{^{19}F} NMR (toluene-*d*$_8$, 75.4 MHz, 223 K): 142.2 (*o*$_a$-C_6F_5), 141.2 (*o*$_b$-C_6F_5), 137.3 (*m*$_b$-C_6F_5), 137.0 (*m*$_a$-C_6F_5), 135.5 (*p*-C_6F_5) ppm. ^{19}F{^{1}H} NMR (toluene-*d*$_8$, 282.1 MHz, 223 K): δ -142.6 (1 H, d, ^3J = 21.7 Hz, *o*$_a$-C_6F_5), -144.5 (1 H, d, ^3J = 24.8 Hz, *o*$_b$-C_6F_5), -165.7 (1 H, t, ^3J = 23.7 Hz, *m*$_a$-C_6F_5), -166.2 (1 H, t, ^3J = 20.9 Hz, *m*$_b$-C_6F_5), -167.6 (1 H, t, ^3J = 21.7 Hz, *p*-C_6F_5) ppm. Note: subscripts ″a″ and ″b″ refer to the inequivalent Ar^{F5} environments and ^{i}Pr groups. IR (NaCl plates, Nujol mull, cm^{-1}): 1641 (w), 1603 (w), 1562 (w), 1544 (w), 1514 (s), 1484 (s), 1453 (s), 1342 (m), 1319 (w), 1260 (m), 1246 (m), 1211 (m), 1181 (m), 1092 (m), 1018 (m), 1002 (s), 980 (m), 910 (w), 803 (w), 748 (w), 715 (w), 702 (w). EI-MS: *m/z* = 665 [*M*]$^+$ (65%). Anal. found (calcd. for $C_{35}H_{44}F_5N_3OTi$): C, 63.27 (63.16); H, 6.72 (6.66); N, 6.24 (6.31)%.

NMR tube scale synthesis of [PhC(N^{i}PrH)$_2$][BPh$_4$] (15-BPh$_4$). To a solution of Cp*Ti{PhC(N^{i}Pr)$_2$}(NO^{t}Bu) (**3**, 10.0 mg, 0.0211 mmol) in THF-*d*$_8$ (0.25 mL) in an NMR tube equipped with a J. Young Teflon valve was added a solution of [Et$_3$NH][BPh$_4$] (17.8 mg, 0.0422 mmol) in THF-*d*$_8$ (0.25 mL) all at RT. An immediate colour change to brown was observed and ^{1}H NMR spectroscopy showed quantitative conversion to **15-BPh$_4$**. Diffraction-quality crystals were grown from a saturated bromobenzene solution at RT.

Alternative synthesis [PhC(N^{i}PrH)$_2$][BPh$_4$] (15-BPh$_4$). To a solution of Na[BPh$_4$] (0.573 g, 1.67 mmol) in CH_2Cl_2 (15 mL) was added a solution of [PhC(N^{i}PrH)$_2$]Cl (0.403 g, 1.67 mmol) in CH_2Cl_2 (10 mL) all at RT. After 48 h the solution was filtered and the volatiles removed under reduced pressure leaving behind a white solid which was extracted into CH_2Cl_2 (2 x 5 mL). The volatiles were removed under reduced pressure to afford **15-BPh$_4$** as a white solid which was dried *in vacuo*. Yield: 0.556 g (63%). An analytically pure sample was obtained by washing with $CHCl_3$ (2 x 5 mL) at RT and by cooling the filtrate to -30 °C yielding a white crystalline solid which was isolated by filtration and dried *in vacuo*. Yield: 0.193 g (23%). ^{1}H NMR (THF-*d*$_8$, 299.9 MHz, 248 K): δ 8.95 (1 H, br. d, N$_a$^{i}Pr<u>H</u>), 8.28 (1 H, br. d, N$_b$^{i}Pr<u>H</u>), 7.60-7.55 (1 H, m, *p*-C$_6$H$_5$), 7.51-7.39 (4 H, m, overlapping *o*-C$_6$H$_5$ and *m*-C$_6$H$_5$), 7.27 (8 H, br m, *o*-B(C$_6$H$_5$)$_4$), 6.86 (8 H, t, ^3J = 7.2 Hz, *m*-B(C$_6$H$_5$)$_4$), 6.73 (4 H, t, ^3J = 7.2 Hz, *p*-B(C$_6$H$_5$)$_4$), 3.86 (1 H, br. m, N$_a$C<u>H</u>Me$_2$), 3.50 (1 H, br. m, N$_b$C<u>H</u>Me$_2$), 1.27 (6 H, d, ^3J = 6.3 Hz, N$_a$CH<u>Me</u>$_2$), 1.16 (6 H, d, ^3J = 6.6 Hz, N$_b$CH<u>Me</u>$_2$) ppm. ^{13}C{^{1}H} NMR (THF-*d*$_8$, 75.4 MHz, 248 K): δ 165.0 (q, $^1J_{BC}$ = 49.3 Hz, *i*-B(C$_6$H$_5$)$_4$), 163.4 (Ph<u>C</u>N$_2$), 137.2 (*o*-B(C$_6$H$_5$)$_4$), 133.2 (*i*-C$_6$H$_5$), 130.5 (*o*-C$_6$H$_5$), 129.8 (*p*-C$_6$H$_5$), 128.3 (*m*-C$_6$H$_5$), 125.7 (q, $^3J_{BC}$ 2.7 Hz, *m*-B(C$_6$H$_5$)$_4$), 121.9 (*p*-B(C$_6$H$_5$)$_4$), 50.1 (N$_b$<u>C</u>HMe$_2$), 46.1 (N$_a$<u>C</u>HMe$_2$), 23.0 (N$_b$CH<u>Me</u>$_2$), 21.6 (N$_a$CH<u>Me</u>$_2$) ppm. ^{11}B{^{1}H} NMR (THF-*d*$_8$, 96.2 MHz, 248 K): δ -5 (BPh$_4$) ppm. Note: subscripts ″a″ and ″b″ refer to the inequivalent -N^{i}PrH groups. IR (NaCl plates, Nujol mull, cm^{-1}): 3277 (s), 3226 (m), 3049 (m), 1626 (s), 1577 (m), 1551 (w), 1478 (m), 1426 (m), 1305 (m), 1263 (w), 1171 (w), 1143 (m), 1130 (m), 1066 (w), 1033 (m), 847 (w), 782 (m), 744 (m), 732 (s), 706 (s), 665 (w), 625 (w), 612 (m), 607 (m). FI$^+$-MS: *m/z* = 204 [PhC(N^{i}PrH)(N^{i}Pr)]$^+$ (100%), 242 [BPh$_3$]$^+$ (82%). Anal. found (calcd. for C$_{37}$H$_{41}$BN$_2$): C, 84.60 (84.72); H, 7.72 (7.88); N, 5.39 (5.34)%.

NMR tube scale synthesis of [Cp*Ti(NO^{t}Bu)(THF-d_8)$_2$][BPh$_4$] (16-BPh$_4$). To a solution of Cp*Ti{PhC(N^{i}Pr)$_2$}(NO^{t}Bu) (**3**, 10.0 mg, 0.0211 mmol) in THF-d_8 (0.25 mL) in an NMR tube equipped with a J. Young Teflon valve was added a solution of [Et$_3$NH][BPh$_4$] (17.8 mg, 0.0422 mmol) in THF-d_8 (0.25 mL). An immediate colour change to brown was observed and ^{1}H NMR spectroscopy showed quantitative conversion to **16-BPh$_4$**. ^{1}H NMR (THF-d_8, 299.9 MHz, 248 K): δ 7.27 (8 H, br m, *o*-B(C$_6$H$_5$)$_4$), 6.87 (8 H, t, ^3J = 7.2 Hz, *m*-B(C$_6$H$_5$)$_4$), 6.74 (4 H, t, ^3J = 7.2 Hz, *p*-B(C$_6$H$_5$)$_4$), 1.95 (15 H, s, C$_5$Me$_5$), 0.98 (9 H, s, NOCMe$_3$) ppm. ^{13}C{^{1}H} NMR (THF-d_8, 75.4 MHz, 248 K): δ 165.0 (1 B, q, $^1J_{BC}$ = 49.3 Hz, *i*-B(C$_6$H$_5$)$_4$), 137.1 (*o*-B(C$_6$H$_5$)$_4$) , 125.9 (*m*-B(C$_6$H$_5$)$_4$), 122.0 (*p*-B(C$_6$H$_5$)$_4$), 121.8 (C$_5$Me$_5$), 83.7 (NOCMe$_3$), 26.4 (NOCMe$_3$), 10.9 (C$_5$Me$_5$) ppm. ^{11}B{^{1}H} NMR (THF-d_8, 96.2 MHz, 248 K): δ -7 (BPh$_4$) ppm. ES$^+$-MS: *m/z* = 415 [Cp*Ti(NO^{t}Bu)(THF)$_2$]$^+$ (83%), 343 [Cp*Ti(NO^{t}Bu)(THF)]$^+$ (45%). Note that since these ES$^+$-MS samples were prepared in non-deuterated THF, only cations containing C$_4$H$_8$O (as opposed to C$_4$D$_8$O) are observed.

Cp*Ti{PhC(N^{i}Pr)$_2$}{η^2-ON(H)B(Ar^{F5})$_3$} (17). To a solution of Cp*Ti{PhC(N^{i}Pr)$_2$}(NO^{t}Bu) (**3**, 0.127 g, 0.269 mmol) in benzene (5 mL) was added a solution of B(Ar^{F5})$_3$ (0.159 g, 0.538 mmol) in benzene (5 mL) and heated to 70 °C. A colour change from green to orange was observed. After 16 h the volatiles were removed under reduced pressure and the resulting orange solid washed with pentane (1 x 5 ml) at RT to afford **17** as an orange powder. Yield: 0.150 g (60%). An analytically pure sample was obtained from subsequent washing with benzene (2 x 5 mL) at RT and the orange powder dried *in vacuo*. Yield: 0.0671 mg (27%). Diffraction-quality crystals were grown from the slow cooling of a saturated benzene solution. ^{1}H NMR (CD$_2$Cl$_2$, 499.9 MHz, 293 K): δ 7.51-7.41 (3 H, m, overlapping *m*-C$_6$H$_5$ and *p*-C$_6$H$_5$), 7.34 (1 H, m, *o*$_a$-C$_6$H$_5$), 7.19 (1 H, m, *o*$_b$-C$_6$H$_5$), 6.05 (1 H, s, NH), 3.61 (1 H, sept., ^3J = 6.5 Hz, NCH$_a$MeMe), 3.22 (1 H, sept., ^3J = 6.5 Hz, NCH$_b$MeMe), 2.10 (15 H, s, C$_5$Me$_5$), 1.11 (3 H, d, ^3J = 6.5 Hz, NCH$_a$MeMe), 0.87 (3 H, d, ^3J = 6.5 Hz, NCH$_a$MeMe), 0.74 (3 H, d, ^3J = 6.5 Hz, NCH$_b$MeMe), 0.60 (3 H, d, ^3J = 6.5 Hz, NCH$_b$MeMe) ppm. ^{13}C{^{1}H} NMR (CD$_2$Cl$_2$, 125.7 MHz, 293 K): δ 170.3 (PhCN$_2$), 148.7 (6 C, br. d, $^1J_{C\text{-}F}$ = 237.1 Hz, *o*-C$_6$F$_5$), 139.8 (3 C, br. d, $^1J_{C\text{-}F}$ = 249.4 Hz, *p*-C$_6$F$_5$), 137.5 (6 C, br. d, $^1J_{C\text{-}F}$ = 249.7 Hz, *m*-C$_6$F$_5$), 133.1 (*i*-C$_6$H$_5$), 130.0 (C$_5$Me$_5$), 129.7, 129.1, 129.0, 128.8 (*o*$_a$-C$_6$H$_5$, *m*-C$_6$H$_5$ and *p*-C$_6$H$_5$), 127.9 (*o*$_b$-C$_6$H$_5$), 121.1 (3 C, br. s, *i*-C$_6$F$_5$), 51.1 (NCH$_a$MeMe), 50.3 (NCH$_b$MeMe), 26.8 (NCH$_a$MeMe), 26.2 (NCH$_b$MeMe), 24.0 (NCH$_b$MeMe), 23.6

(NCH_aMeMe), 12.5 (C_5Me_5) ppm. $^{11}B\{^1H\}$ NMR (CD_2Cl_2, 96.2 MHz, 298 K): δ -8 ($B(C_6F_5)_3$) ppm. Note: $^{19}F\{^1H\}$ NMR is broad at 298 K and therefore was recorded at 253 K - $^{19}F\{^1H\}$ NMR (CD_2Cl_2, 282.1 MHz, 253 K): δ -129.0 (1 F, br d., o_{1a}-C_6F_5), -130.5 (1 F, br d., o_{1b}-C_6F_5), -136.1 (2 F, br d., o_2-C_6F_5), -145.5 (v br s, 2 F, o_3-C_6F_5), -158.4 (1 F, br t., p_3-C_6F_5), -158.7 (1 F, br t., p_1-C_6F_5), -160.2 (1 F, br t., p_2-C_6F_5), -161.6 (2 F, br t., m_3-C_6F_5), -164.2 (1 F, br t., m_{1b}-C_6F_5), -165.2 (1 F, br t., m_{1a}-C_6F_5), -166.3 (2 F, br t., m_2-C_6F_5) ppm. Note: subscript letters and numbers refer to the inequivalent Ph and Ar^{F5} environments and ^{i}Pr groups. IR (NaCl plates, Nujol mull, cm^{-1}): 3296 (w), 1644 (m), 1517 (s), 1338 (m), 1281 (m), 1220 (w), 1147 (w), 1092 (s), 1043 (w), 1021 (m), 980 (m), 958 (m), 811 (w), 782 (w), 732 (w), 723 (w), 708 (m), 695 (m), 676 (m). EI-MS: *m/z* = 417 $[M\text{-}B(C_6F_5)_3]^+$, 512 $[B(C_6F_5)_3]^+$. Anal. found (calcd. for $C_{41}H_{35}BF_{15}N_3OTi$): C, 52.83 (52.99); H, 3.82 (3.80); N, 4.57 (4.52)%.

5.5 Experimental details and characterising data for Chapter Four

***In situ* synthesis of Cp*Ti{PhC(N^iPr)$_2$}{NC(Ar^{F5})NO^tBu} (10).** In all reactions Cp*Ti{PhC(N^iPr)$_2$}{NC(Ar^{F5})NO^tBu} (**10**) was synthesised *in situ* for convenience. An example method is as follows. To a stirring solution of Cp*Ti{PhC(N^iPr)$_2$}(NO^tBu) (**3**, 0.350 g, 0.739 mmol) in benzene (5 mL), was added $Ar^{F5}CN$ (93.2 μL, 0.739 mmol) all at RT. An immediate colour change from dark green to lime green was observed and the solution left to stir for 15 min quantitatively forming **10**.

Cp*Ti{PhC(N^iPr)$_2$}{OC(O)N(C{Ar^{F5}}NO^tBu)} (18). A solution of Cp*Ti{PhC(N^iPr)$_2$}{NC(Ar^{F5})NO^tBu} (**10**, 0.422 g, 0.634 mmol) in benzene (5 mL) was freeze-pump-thawed three times. The solution was then exposed to CO_2 at a pressure of *ca.* 1.5 atm at RT. After 1 h the volatiles were removed under reduced pressure to afford **18** as a dark green solid which was washed with cold pentane (3 x 5 mL) cooled to -78 °C, filtered, and dried *in vacuo*. Yield: 0.296 g (66%). ^1H NMR (C_6D_6, 499.9 MHz, 293 K): δ 7.23 (1 H, d, ^3J = 7.5 Hz, o_a-C_6H_5), 7.05 - 6.92 (4 H, m, o_b-C_6H_5, *m*-C_6H_5 and *p*-C_6H_5), 4.20 (1 H, app. sept., ^3J = 6.5 Hz, NCH_aMeMe), 3.20 (1 H, app. sept., ^3J = 6.5 Hz, NCH_bMeMe), 2.16 (15 H, s, C_5Me_5), 1.28 (9 H, s, $NOCMe_3$), 1.07 (3 H, d, ^3J = 6.5 Hz, NCH_aMeMe), 1.02 (3 H, d, ^3J = 6.5 Hz, NCH_bMeMe) 1.00 (3 H, d, ^3J = 7.0 Hz, NCH_aMeMe), 0.89 (3 H, d, ^3J = 6.5 Hz, NCH_bMeMe) ppm. $^{13}C\{^1H\}$ NMR (C_6D_6, 125.7 MHz, 293 K): δ 171.6 ($PhCN_2$), 155.8 (OC(O)N), 146.2 ($NC(C_6F_5)N$), 144.0 (1 C, d, $^1J_{C\text{-}F}$ = 246.2 Hz, o_a-C_6F_5), 143.5 (1 C, d, $^1J_{C\text{-}F}$ = 242.8 Hz, o_b-C_6F_5), 141.2 (1 C, d, $^1J_{C\text{-}F}$ = 251.4 Hz, *p*-C_6F_5), 138.0 (1 C, d,

$^{1}J_{C\text{-}F}$ = 248.8 Hz, *m*$_a$-C_6F_5), 137.8 (1 C, d, $^{1}J_{C\text{-}F}$ = 248.9 Hz, *m*$_b$-C_6F_5), 133.0 (*i*-C_6H_5), 132.2 ($\underline{C}_5Me_5$), 129.5 (*p*-C_6H_5), 128.6 (*o*$_b$-C_6H_5), 128.5 (*o*$_a$-C_6H_5), 128.1 (overlapping with solvent *m*-C_6H_5), 112.3 (1 C, app. t of t, $^{2}J_{C\text{-}F}$ = 19.8 Hz, $^{3}J_{C\text{-}F}$ = 3.8 Hz, *i*-C_6F_5), 78.0 (NO$\underline{C}$Me$_3$), 51.4 (N$\underline{C}$H$_b$MeMe), 50.5 (N$\underline{C}$H$_a$MeMe), 27.8 (NOC$\underline{Me}_3$), 25.3 (NCH$_a$Me$\underline{Me}$), 25.1 (NCH$_a\underline{Me}$Me), 24.8 (NCH$_b$Me$\underline{Me}$), 24.0 (NCH$_b\underline{Me}$Me), 13.0 ($C_5\underline{Me}_5$) ppm. $^{19}F\{^{1}H\}$ NMR (C_6D_6, 282.1 MHz, 293 K): δ -137.7 (1 F, app. d., ^{3}J = 23.1 Hz, *o*$_a$-C_6F_5), -143.3 (1 F, app. d., ^{3}J = 23.1 Hz, *o*$_b$-C_6F_5), -156.2 (1 F, t, ^{3}J = 21.4 Hz, *p*-C_6F_5), -164.6 (1 F, m, *m*$_a$-C_6F_5), -164.9 (1 F, m, *m*$_b$-C_6F_5) ppm. Note: subscripts ″a″ and ″b″ refer to the inequivalent Ph and Ar^{F_5} environments and ^{i}Pr groups. IR (NaCl plates, Nujol mull, cm^{-1}): 1690 (s), 1655 (w), 1578 (w), 1521 (m), 1496 (s), 1424 (m), 1362 (s), 1337 (m), 1293 (w), 1259 (w), 1218 (m), 1176 (m), 1143 (w), 1110 (m), 1070 (w), 1044 (w), 1023 (m), 990 (m), 954 (m), 921 (m), 901 (w), 786 (w), 707 (w). Anal. found (calcd. for $C_{35}H_{43}F_5N_4O_3Ti$): C, 58.89 (59.16); H, 6.29 (6.10); N, 7.76 (7.88) %.

NMR tube scale synthesis of Cp*Ti{PhC(N^{i}Pr)$_2$}{OC(O)N(C{Ar^{F_5}}-NO^{t}Bu)C(O)O} (19). A solution of Cp*Ti{PhC(N^{i}Pr)$_2$}{OC(O)N(C{Ar^{F_5}}NO^{t}Bu)} (**18**, 25.0 mg, 0.0351 mmol) in C_6D_6 (0.35 mL) in a 0.77 mm New Era NE-HP5-M NMR tube equipped with a controlled atmosphere valve was freeze-pump-thawed three times. The solution was then exposed to CO_2 at a pressure of *ca.* 1.5 atm at RT. The reaction was monitored by ^{1}H and ^{19}F NMR spectroscopy. The ^{1}H NMR spectrum recorded after 5 d at RT indicated the reaction had reached 63% conversion to **19**. **19** was characterised by ^{1}H, ^{13}C and ^{19}F NMR spectroscopy. ^{1}H NMR (C_6D_6, 499.9 MHz, 293 K): δ 7.03-6.92 (3 H, m, *m*-C_6H_5 and *p*-C_6H_5), 6.82 (1 H, m, *o*$_a$-C_6H_5), 6.65 (1 H, d, ^{3}J = 7.0 Hz, *o*$_b$-C_6H_5), 3.41 (2 H, app. sept., ^{3}J = 6.5 Hz, NC$\underline{H}$MeMe), 1.99 (15 H, s, C_5Me_5), 1.37 (9 H, s, NOCMe$_3$), 0.95 (6 H, d, ^{3}J = 6.5 Hz, NCH$\underline{Me}$Me), 0.93 (6 H, d, ^{3}J = 6.5 Hz, NCH$\underline{Me}$Me) ppm. $^{13}C\{^{1}H\}$ NMR (C_6D_6, 125.7 MHz, 293 K): δ 171.7 (Ph$\underline{C}$N$_2$), 152.8 (OC(O)N), 145.0 (2 C, d, $^{1}J_{C\text{-}F}$ = 249.5 Hz, *o*-C_6F_5), 141.9 (1 C, d, $^{1}J_{C\text{-}F}$ = 254.6 Hz, *p*-C_6F_5), 137.9 (2 C, d, $^{1}J_{C\text{-}F}$ = 250.8 Hz, *m*-C_6F_5), 137.3 (N$\underline{C}$(C_6F_5)N), 132.4 ($\underline{C}_5Me_5$), 132.3 (*i*-C_6H_5), 129.4 (*p*-C_6H_5), 128.1 (overlapping with solvent *o*$_b$-C_6H_5, *m*-C_6H_5), 127.7 (*o*$_a$-C_6H_5), 109.2 (1 C, app. t of t, $^{2}J_{C\text{-}F}$ = 17.6 Hz, $^{3}J_{C\text{-}F}$ = 3.3 Hz, *i*-C_6F_5), 81.5 (NO$\underline{C}$Me$_3$), 51.6 (N$\underline{C}$HMeMe), 27.7 (NOC$\underline{Me}_3$), 24.7, 24.6 (NCH$\underline{MeMe}$), 12.8 ($C_5\underline{Me}_5$) ppm. $^{19}F\{^{1}H\}$ NMR (C_6D_6, 282.1 MHz, 293 K): δ -134.1 (2 F, app. d., ^{3}J = 18.9 Hz, *o*-C_6F_5), -154.2 (1 F, app t of t, ^{3}J = 21.4 Hz, ^{4}J = 3.1 Hz, *p*-C_6F_5), -164.1 (2

F, m, *m*-C_6F_5) ppm. Note: subscripts ″a″ and ″b″ refer to the inequivalent Ph environments.

NMR tube scale reaction of Cp*Ti{PhC(N^{i}Pr)$_2$}{NC(Ar^{F_5})NO^{t}Bu} (10) with CS_2. To a solution of Cp*Ti{PhC(N^{i}Pr)$_2$}{NC(Ar^{F_5})NO^{t}Bu} (**10**, 14.4 mg, 0.0215 mmol) in C_6D_6 (0.5 mL) in an NMR tube equipped with a J. Young Teflon valve was added CS_2 (1.55 μL, 0.0258 mmol) at RT. The reaction was monitored by ^{1}H and ^{19}F NMR spectroscopy. After 15 d Cp*Ti{PhC(N^{i}Pr)$_2$}{N(O^{t}Bu)C(S)S} (**4**) and Ar^{F_5}CN were observed in 70% yield.

Cp*Ti{PhC(N^{i}Pr)$_2$}{N(C{Ar^{F_5}}NO^{t}Bu)C(N^{t}Bu)O} (20). To a solution of Cp*Ti{PhC(N^{i}Pr)$_2$}{NC(Ar^{F_5})NO^{t}Bu} (**10**, 0.352 g, 0.528 mmol) in diethyl ether (5 mL) was added ^{t}BuNCO (60.3 μL, 0.528 mmol) all at RT. A gradual colour change from lime green to dark yellow was observed and the solution left to stir for 6.5 h. Volatiles were then removed under reduced pressure to afford **20** as a brown powder which was dried *in vacuo*. Yield: 0.261 g (65%). ^{1}H NMR (C_6D_6, 499.9 MHz, 293 K): δ 7.37 (1 H, d, ^3J = 7.5 Hz, *o*$_a$-C_6H_5), 7.00 (4 H, m, overlapping *o*$_b$-C_6H_5, *m*-C_6H_5, and *p*-C_6H_5), 4.20 (1 H, app. sept., ^3J = 7.0 Hz, NC<u>H</u>$_a$MeMe), 3.24 (1 H, app. sept., ^3J = 6.5 Hz, NC<u>H</u>$_b$MeMe), 2.17 (15 H, s, C_5Me_5), 1.33 (9 H, s, NCMe$_3$), 1.33 (9 H, s, NOCMe$_3$), 1.15 (3 H, d, ^3J = 7.0 Hz, NCH$_a$<u>Me</u>Me), 0.97 (9 H, m, overlapping NCH$_a$Me<u>Me</u>, NCH$_b$<u>Me</u>Me, NCH$_b$Me<u>Me</u>) ppm. ^{13}C{^{1}H} NMR (C_6D_6, 125.7 MHz, 293 K): δ 170.6 (Ph<u>C</u>N$_2$), 148.2, 146.7 (OCN and N<u>C</u>(Ar^{F_5})N), 133.9 (*i*-C_6H_5), 130.3 (<u>C</u>$_5$Me$_5$), 129.3 (*m*-C_6H_5), 128.7 (*o*$_a$-C_6H_5), 128.7 (*o*$_b$-C_6H_5), 128.6 (*p*-C_6H_5) 113.9 (1 C, app. t, $^2J_{C\text{-}F}$ = 21.3 Hz, *i*-C_6F_5), 77.8 (NO<u>C</u>Me$_3$), 51.0 (N<u>C</u>Me$_3$), 50.8 (N<u>C</u>H$_b$MeMe), 50.1 (N<u>C</u>H$_a$MeMe), 32.2 (NC<u>Me</u>$_3$), 27.8 (NOC<u>Me</u>$_3$), 25.5 (NCH$_a$<u>Me</u>Me), 25.6, 24.6, 24.5 (NCH$_a$Me<u>Me</u>, <u>NCH$_b$MeMe</u>, NCH$_b$Me<u>Me</u>), 12.9 (C$_5$<u>Me</u>$_5$) ppm. ^{13}C NMR (HMQC ^{19}F-observed, C_6D_6, 282.1 MHz, 293 K): δ 144.2 (*o*$_a$-C_6F_5), 142.8 (*o*$_b$-C_6F_5), 140.6 (*p*-C_6F_5), 137.6 (*m*-C_6F_5), 137.3 (*m*-C_6F_5) ppm. ^{19}F{^{1}H} NMR (C_6D_6, 282.1 MHz, 293 K): δ -135.3 (1 H, m, *o*$_a$-C_6F_5), -143.6 (1 H, m, *o*$_b$-C_6F_5), -159.7 (1 H, m, *p*-C_6F_5), -166.9 (1 H, m, *m*$_a$-C_6F_5), -167.2 (1 H, m, *m*$_b$-C_6F_5) ppm. Note: subscripts ″a″ and ″b″ refer to the inequivalent Ph and Ar^{F_5} environments and ^{i}Pr groups. IR (NaCl plates, Nujol mull, cm^{-1}): 1631 (s), 1579 (m), 1516 (s), 1494 (s), 1483 (m), 1453 (s), 1423 (m), 1401 (m), 1360 (s), 1335 (m), 1289 (w), 1261 (m), 1221 (m), 1196 (w), 1174 (m), 1148 (w), 1101 (m), 1062 (m), 1020 (m), 990 (m), 967 (m), 943 (w), 899 (w), 861 (w), 797 (br. w), 732 (w),

704 (w). Anal. found (calcd. for $C_{39}H_{52}F_5N_5O_2Ti$): C, 60.99 (61.17); H, 6.72 (6.84); N, 8.98 (9.15) %.

^{t}BuNCNC(Ar^{F5})NO^{t}Bu (21). To a solution of Cp*Ti{PhC(N^{i}Pr)$_2$}{NC(Ar^{F5})NO^{t}Bu} (**10**, 0.493 g, 0.739 mmol) in benzene (5 mL) was added ^{t}BuNCO (84.4 μL, 0.739 mmol) all at RT. A gradual colour change from lime green to dark yellow was observed and the solution left to stir for 3 h before being heated to 65 °C and stirred for a further 16 h. A further colour change to yellow was observed. Volatiles were then removed under reduced pressure to afford [Cp*Ti{PhC(N^{i}Pr)$_2$}(μ-O)]$_2$ (**7**) and **21** as a brown oily solid. The resultant solid was extracted into cold diethyl ether (3 x 5 mL) cooled to -78 °C and the volatiles removed under reduced pressure. The resultant brown oil was then distilled (100°C, 8 x 10^{-2} mbar, 4.5 h) onto a dry ice/acetone cold finger affording **21** as a yellow oil. Yield: 0.190 g (71%). ^{1}H NMR (C_6D_6, 499.9 MHz, 293 K): δ 1.25 (9 H, s, NOCMe$_3$), 1.00 (9 H, s, NCMe$_3$) ppm. ^{13}C{^{1}H} NMR (C_6D_6, 125.7 MHz, 293 K): δ 143.6 (2 C, d, $^1J_{C\text{-}F}$ = 249.3 Hz, *o*-C_6F_5), 141.9 (1 C, d, $^1J_{C\text{-}F}$ = 253.8 Hz, *p*-C_6F_5), 139.8 (NCN or N<u>C</u>(Ar^{F5})N), 137.8 (2 C, d, $^1J_{C\text{-}F}$ = 251.1 Hz, *m*-C_6F_5), 133.0 (N<u>C</u>(Ar^{F5})N or NCN), 108.6 (1 C, t of d, $^2J_{C\text{-}F}$ = 20.1 Hz, $^3J_{C\text{-}F}$ = 3.9 Hz, *i*-C_6F_5), 80.6 (NO<u>C</u>Me$_3$), 58.3 (N<u>C</u>Me$_3$), 31.0 (NC<u>Me</u>$_3$), 27.4 (NOC<u>Me</u>$_3$) ppm. ^{19}F{^{1}H} NMR (C_6D_6, 282.1 MHz, 293 K): δ -138.2 (2 H, app. d., ^3J = 13.0 Hz, *o*-C_6F_5), -152.7 (1 H, t, ^3J = 21.7 Hz, *p*-C_6F_5), -161.9 (2 H, m, *m*-C_6F_5) ppm. IR (NaCl plates, thin film, cm^{-1}): 2977 (m), 2933 (w), 2872 (w), 2141 (s), 1653 (m), 1594 (br, m), 1521 (s), 1499 (s), 1457 (m), 1437 (m), 1389 (w), 1366 (m), 1317 (m), 1261 (w), 1238 (m), 1204 (s), 1173 (m), 1116 (w), 1103 (w), 1088 (m), 1071 (w), 1034 (w), 991 (s), 905 (m), 880 (m), 837 (w), 795 (w), 745 (w), 727 (w), 692 (w), 668 (w), 636 (w), 586 (w), 567 (w). FI-HRMS: *m/z* found (calcd. for $C_{16}H_{18}F_5N_3O$, $[M]^+$) 363.1380 (363.1370).

Cp*Ti{PhC(N^{i}Pr)$_2$}{N(C{Ar^{F5}}NO^{t}Bu)C(Ph)(H)O} (22a). To a solution of Cp*Ti{PhC(N^{i}Pr)$_2$}{NC(Ar^{F5})NO^{t}Bu} (**10**, 0.422 g, 0.634 mmol) in diethyl ether (5 mL) was added PhC(O)H (64.4 μL, 0.634 mmol) all at RT. An immediate colour change from lime green to brown was observed and the solution left to stir for 15 min. Volatiles were then removed under reduced pressure to afford **22a** as a brown powder which was dried *in vacuo*. Yield: 0.403 g (82%). Diffraction-quality crystals were grown from a saturated hexane solution at 4 °C. ^{1}H NMR (C_6D_6, 299.9 MHz, 293 K): δ 7.47 (1 H, d, ^3J = 7.2 Hz, o_a-$C_6H_5CN_2$), 7.22 (1 H, d, ^3J = 6.9 Hz, o_b-$C_6H_5CN_2$), 7.11 (3 H, m, overlapping *m*-$C_6H_5CN_2$ and *p*-C_6H_5), 6.93 (5 H, m, overlapping *p*-$C_6H_5CN_2$, *o*-C_6H_5

and *m*-C_6H_5), 5.99 (1 H, d, $J_{H\text{-}F}$ = 2.1 Hz, PhC(H)), 4.50 (1 H, app. sept., ^3J = 6.6 Hz, NCH_aMeMe), 3.44 (1 H, app. sept., ^3J = 6.6 Hz, NCH_bMeMe), 2.28 (15 H, s, C_5Me_5), 1.32 (3 H, d, ^3J = 6.6 Hz, NCH_aMeMe), 1.27 (9 H, s, NOCMe_3), 1.19 (3 H, d, ^3J = 6.9 Hz, NCH_aMeMe), 0.90 (3 H, d, ^3J = 6.9 Hz, NCH_bMeMe), 0.83 (3 H, d, ^3J = 6.6 Hz, NCH_bMeMe) ppm. $^{13}C\{^1H\}$ NMR (C_6D_6, 75.4 MHz, 293 K): δ 167.9 (PhCN_2), 148.7 (NC(Ar^{F5})NO^{t}Bu), 145.6 (*i*-C_6H_5), 135.6 (*i*-$C_6H_5CN_2$), 129.7 (*o*$_a$-$C_6H_5CN_2$), 128.9 (*p*-C_6H_5), 128.5 (*o*$_b$-$C_6H_5CN_2$), 127.9 (*m*-$C_6H_5CN_2$), 127.8 (*m*-C_6H_5), 127.7 (overlapping with solvent *p*-$C_6H_5CN_2$), 127.5 (C_5Me_5), 126.9 (*o*-C_6H_5), 112.6 (1 C, m, *i*-C_6F_5), 83.4 (1 C, d, $J_{C\text{-}F}$ = 1.2 Hz, PhC(H)), 76.9 (NOCMe_3), 49.9 (NCH_bMeMe), 48.9 (NCH_aMeMe), 28.2 (NOCMe_3), 25.7 (NCH_bMeMe), 25.4 (NCH_aMeMe), 24.8 (NCH_aMeMe), 24.6 (NCH_bMeMe), 12.4 (C_5Me_5) ppm. ^{13}C NMR (HMQC ^{19}F-observed, C_6D_6, 282.1 MHz, 293 K): δ 142.5 (*o*$_a$-C_6F_5), 141.9 (*o*$_b$-C_6F_5), 140.7 (*p*-C_6F_5), 137.3 (*m*$_a$-C_6F_5), 137.2 (*m*$_b$-C_6F_5) ppm. $^{19}F\{^1H\}$ NMR (C_6D_6, 282.1 MHz, 293 K): δ -134.8 (1 F, m, *o*$_a$-C_6F_5), -141.7 (1 F, m, *o*$_b$-C_6F_5), -156.6 (1 F, m, *p*-C_6F_5), -164.1 (1 F, m, *m*$_a$-C_6F_5), -164.8 (1 F, m, *m*$_b$-C_6F_5) ppm. Note: subscripts ″a″ and ″b″ refer to the inequivalent Ph and Ar^{F5} environments and ^{i}Pr groups. IR (NaCl plates, Nujol mull, cm^{-1}): 1653 (w), 1550 (m), 1519 (m), 1495 (s), 1363 (m), 1358 (m), 1346 (m), 1289 (w), 1267 (w), 1260 (w), 1230 (w), 1221 (w), 1196 (m), 1169 (w), 1151 (w), 1133 (w), 1112 (m), 1085 (w), 1059 (m), 1021 (m), 994 (m), 987 (m), 959 (m), 922 (w), 905 (w), 893 (w), 795 (w), 781 (w), 730 (w), 721 (w), 711 (w), 704 (m), 696 (w), 642 (m), 615 (w), 590 (w), 576 (w), 537 (w). Anal. found (calcd. for $C_{41}H_{49}F_5N_4O_2Ti$): C, 63.60 (63.73); H, 6.28 (6.39); N, 7.18 (7.25) %.

Cp*Ti{PhC(N^{i}Pr)$_2$}{N(C{Ar^{F5}}NO^{t}Bu)C(Tol)(H)O} (22b). To a solution of Cp*Ti{PhC(N^{i}Pr)$_2$}{NC(Ar^{F5})NO^{t}Bu} (**10**, 0.422 g, 0.634 mmol) in benzene (5 mL) was added *p*-TolC(O)H (74.6 μL, 0.634 mmol) all at RT. An immediate colour change from lime green to brown was observed and the solution left to stir for 30 min. Volatiles were then removed under reduced pressure to afford **22b** as a brown powder which was dried *in vacuo*. Yield: 0.490 g (98%). ^1H NMR (C_6D_6, 499.9 MHz, 293 K): δ 7.52 (1 H, d, ^3J = 7.5 Hz, *o*$_a$-$C_6H_5CN_2$), 7.23 (1 H, d, ^3J = 7.5 Hz, *o*$_b$-$C_6H_5CN_2$), 7.15-7.05 (3 H, m, overlapping *m*-$C_6H_5CN_2$ and *p*-$C_6H_5CN_2$), 6.90 (2 H, d, ^3J = 7.5 Hz, *o*-C_6H_4Me), 6.79 (2 H, d, ^3J = 7.5 Hz, *m*-C_6H_4Me), 5.99 (1 H, d, $J_{H\text{-}F}$ = 1.5 Hz, ArC(H)), 4.52 (1 H, sept., ^3J = 7.0 Hz, NCH_aMeMe), 3.48 (1 H, sept., ^3J = 6.5 Hz, NCH_bMeMe), 2.29 (15 H, s, C_5Me_5), 2.00 (3 H, s, C_6H_4Me) 1.34 (3 H, d, ^3J = 7.0 Hz, NCH_aMeMe), 1.27 (9

H, s, NOCMe$_3$), 1.20 (3 H, d, ^3J = 7.0 Hz, NCH$_a$MeMe), 0.95 (3 H, d, ^3J = 6.5 Hz, NCH$_b$MeMe), 0.87 (3 H, d, ^3J = 7.0 Hz, NCH$_b$MeMe) ppm. ^{13}C{^{1}H} NMR (C$_6$D$_6$, 125.7 MHz, 293 K): δ 167.9 (PhCN$_2$), 148.8 (NC(Ar^{F5})NO^{t}Bu), 143.0 (1 C, d, $^1J_{C\text{-}F}$ = 239.5 Hz, *o*-C$_6$F$_5$), 142.3 (1 C, d, $^1J_{C\text{-}F}$ = 240.8 Hz, *o*-C$_6$F$_5$), 142.7 (*i*-C$_6$H$_5$), 141.0 (1 C, d, $^1J_{C\text{-}F}$ = 250.8 Hz, *p*-C$_6$F$_5$), 137.8 (1 C, d, $^1J_{C\text{-}F}$ = 249.5 Hz, *m*-C$_6$F$_5$), 137.7 (1 C, d, $^1J_{C\text{-}F}$ = 248.3 Hz, *m*-C$_6$F$_5$), 137.3 (*p*-C$_6$H$_4$Me), 135.7 (*i*-C$_6$H$_5$CN$_2$), 129.7 (*o$_b$*-C$_6$H$_5$CN$_2$), 128.9 (*m*-C$_6$H$_5$CN$_2$), 128.6 (*o$_a$*-C$_6$H$_5$CN$_2$), 128.4 (*m*-C$_6$H$_4$Me), 128.1 (overlapping with solvent *p*-C$_6$H$_5$CN$_2$), 127.4 (C$_5$Me$_5$), 126.9 (*o*-C$_6$H$_4$Me), 112.7 (1 C, app. t, ^2J = 21.9 Hz, *i*-C$_6$F$_5$), 83.3 (ArC(H)), 76.9 (NOCMe$_3$), 49.9 (NCH$_b$MeMe), 48.9 (NCH$_a$MeMe), 28.2 (NOCMe$_3$), 25.8 (NCH$_b$MeMe), 25.4 (NCH$_a$MeMe), 24.8 (NCH$_a$MeMe), 24.6 (NCH$_b$MeMe), 21.0 (C$_6$H$_4$Me), 12.4 (C$_5$Me$_5$) ppm. ^{19}F{^{1}H} NMR (C$_6$D$_6$, 282.1 MHz, 293 K): δ -134.6 (1 F, app. d, ^3J = 22.6 Hz, *o*$_a$-C$_6$F$_5$), -141.9 (1 F, m, *o*$_b$-C$_6$F$_5$), -156.9 (1 F, app. t, ^3J = 22.6 Hz, *p*-C$_6$F$_5$), -164.3 (1 F, m, *m*$_a$-C$_6$F$_5$), -165.2 (1 F, m, *m*$_b$-C$_6$F$_5$) ppm. Note: subscripts ″a″ and ″b″ refer to the inequivalent Ph and Ar^{F5} environments and ^{i}Pr groups. IR (NaCl plates, Nujol mull, cm^{-1}): 1652 (w), 1551 (m), 1516 (s), 1497 (s), 1428 (m), 1363 (s), 1346 (m), 1288 (w), 1256 (w), 1223 (m), 1194 (m), 1169 (w), 1149 (w), 1123 (w), 1108 (m), 1070 (m), 1044 (w), 1021 (m), 987 (m), 947 (m), 910 (m), 890 (w), 838 (w), 818 (w), 804 (w), 778 (w), 767 (w), 730 (w), 704 (m), 684 (m), 639 (w), 624 (m), 606 (m). Anal. found (calcd. for C$_{42}$H$_{51}$F$_5$N$_4$O$_2$Ti): C, 64.23 (64.12); H, 6.64 (6.53); N, 6.97 (7.12) %.

Cp*Ti{PhC(N^{i}Pr)$_2$}{N(C{Ar^{F5}}NO^{t}Bu)C(4-C$_6$H$_4$^{t}Bu)(H)O} (22c). To a solution of Cp*Ti{PhC(N^{i}Pr)$_2$}{NC(Ar^{F5})NO^{t}Bu} (**10**, 0.422 g, 0.634 mmol) in diethyl ether (5 mL) was added (4-C$_6$H$_4$^{t}Bu)C(O)H (106 μL, 0.634 mmol) all at RT. An immediate colour change from lime green to brown was observed and the solution left to stir for 20 min. Volatiles were then removed under reduced pressure to afford **22c** as a brown powder which was dried *in vacuo*. Yield: 0.510 g (97%). ^{1}H NMR (C$_6$D$_6$, 299.9 MHz, 293 K): δ 7.58 (1 H, d, ^3J = 7.2 Hz, *o$_a$*-C$_6$H$_5$CN$_2$), 7.23 (1 H, d, ^3J = 6.9 Hz, *o$_b$*-C$_6$H$_5$CN$_2$), 7.15-6.99 (7 H, m, overlapping *m*-C$_6$H$_5$CN$_2$, *p*-C$_6$H$_5$CN$_2$, *o*-C$_6$H$_4$^{t}Bu and *m*-C$_6$H$_4$^{t}Bu), 6.04 (1 H, d, $J_{H\text{-}F}$ = 2.4 Hz, ArC(H)), 4.53 (1 H, app. sept., ^3J = 6.9 Hz, NCH$_a$MeMe), 3.48 (1 H, app. sept., ^3J = 6.9 Hz, NCH$_b$MeMe), 2.29 (15 H, s, C$_5$Me$_5$), 1.36 (3 H, d, ^3J = 6.6 Hz, NCH$_a$MeMe), 1.28 (9 H, s, NOCMe$_3$), 1.20 (3 H, d, ^3J = 6.9 Hz, NCH$_a$MeMe), 1.15 (9H, s, CMe$_3$), 0.96 (3 H, d, ^3J = 6.9 Hz, NCH$_b$MeMe), 0.87 (3 H, d, ^3J = 6.6 Hz, NCH$_b$MeMe) ppm. ^{13}C{^{1}H} NMR (C$_6$D$_6$, 75.4 MHz, 293 K): δ 167.9

(Ph<u>C</u>N_2), 150.8 (*p*-$C_6H_4{}^tBu$), 148.8 (N<u>C</u>(Ar^{F_5})NO^tBu), 142.5 (*i*-$C_6H_4{}^tBu$), 135.6 (*i*-$C_6H_5CN_2$), 129.7 (o_b-$C_6H_5CN_2$), 128.9 (*p*-$C_6H_5CN_2$), 128.6 (o_a-$C_6H_5CN_2$), 127.9 (*m*-$C_6H_5CN_2$), 127.4 (<u>C</u>$_5Me_5$), 126.8 (*o*-$C_6H_4{}^tBu$), 124.6 (*m*-$C_6H_4{}^tBu$), 83.2 (1 C, d, $J_{C\text{-}F}$ = 1.3 Hz, Ar<u>C</u>(H)), 76.9 (NO<u>C</u>Me_3), 49.9 (N<u>C</u>H_bMeMe), 48.9 (N<u>C</u>H_aMeMe), 34.5 (<u>C</u>Me_3), 31.3 (C<u>Me</u>$_3$), 28.2 (NOC<u>Me</u>$_3$), 25.8 (NCH$_b$Me<u>Me</u>), 25.4 (NCH$_a$Me<u>Me</u>), 24.9 (NCH$_a$<u>Me</u>Me), 24.6 (NCH$_b$<u>Me</u>Me), 12.4 (C$_5$<u>Me</u>$_5$) ppm. Resonances attributed to <u>C</u>$_6F_5$ could not be identified. $^{19}F\{^1H\}$ NMR (C_6D_6, 282.1 MHz, 293 K): δ -134.7 (1 F, m, o_a-C_6F_5), -141.8 (1 F, m, o_b-C_6F_5), -157.0 (1 F, td, ^3J = 21.0 Hz, ^4J = 1.97 Hz, *p*-C_6F_5), -164.4 (2 F, m, overlapping m_b-C_6F_5 and m_a-C_6F_5) ppm. Note: subscripts ″a″ and ″b″ refer to the inequivalent Ph and Ar^{F_5} environments and ^{i}Pr groups. IR (NaCl plates, Nujol mull, cm^{-1}): 1655 (w), 1641 (w), 1609 (w), 1553 (m), 1517 (m), 1500 (s), 1374 (s), 1347 (m), 1289 (w), 1266 (w), 1219 (w), 1198 (w), 1148 (w), 1108 (m), 1070 (w), 1020 (m), 989 (m), 955 (m), 915 (w), 890 (w), 834 (w), 784 (w), 729 (w), 708 (w), 678 (w), 616 (w), 600 (w). Anal. found (calcd. for $C_{45}H_{57}F_5N_4O_2Ti$): C, 65.06 (65.21); H, 6.87 (6.93); N, 6.89 (6.76) %.

Cp*Ti{PhC(N^{i}Pr)$_2$}{N(C{Ar^{F_5}}NO^{t}Bu)C(4-C$_6$H$_4$OMe)(H)O} (22d). To a solution of Cp*Ti{PhC(N^{i}Pr)$_2$}{NC(Ar^{F_5})NO^{t}Bu} (**10**, 0.422 g, 0.634 mmol) in diethyl ether (5 mL) was added (4-C_6H_4OMe)C(O)H (76.9 μL, 0.634 mmol) all at RT. An immediate colour change from lime green to brown was observed and the solution left to stir for 15 min. Volatiles were then removed under reduced pressure to afford **22d** as a brown powder which was dried *in vacuo*. Yield: 0.506 g (99%). ^1H NMR (C_6D_6, 499.9 MHz, 293 K): δ 7.48 (1 H, m, o_a-$C_6H_5CN_2$), 7.22 (1 H, m, o_b-$C_6H_5CN_2$), 7.14-7.03 (3 H, m, overlapping *m*-$C_6H_5CN_2$ and *p*-$C_6H_5CN_2$), 6.94 (2 H, d, ^3J = 8.4 Hz, *o*-C_6H_4OMe), 6.61 (2 H, d, ^3J = 8.7 Hz, *m*-C_6H_4OMe), 6.02 (1 H, d, $J_{H\text{-}F}$ = 2.0 Hz, ArC(<u>H</u>)), 4.52 (1 H, app. sept., ^3J = 6.9 Hz, NC<u>H</u>$_a$MeMe), 3.48 (1 H, app. sept., ^3J = 6.9 Hz, NC<u>H</u>$_b$MeMe), 3.21 (3 H, s, OMe), 2.30 (15 H, s, C_5Me_5), 1.34 (3 H, d, ^3J = 6.0 Hz, NCH$_a$<u>Me</u>Me), 1.28 (9 H, s, NOCMe_3), 1.19 (3 H, d, ^3J = 6.9 Hz, NCH$_a$Me<u>Me</u>), 0.97 (3 H, d, ^3J = 6.6 Hz, NCH$_b$<u>Me</u>Me), 0.88 (3 H, d, ^3J = 6.6 Hz, NCH$_b$Me<u>Me</u>) ppm. $^{13}C\{^1H\}$ NMR (C_6D_6, 125.7 MHz, 293 K): δ 167.9 (Ph<u>C</u>N_2), 159.8 (*p*-C_6H_5OMe), 148.8 (N<u>C</u>(Ar^{F_5})NO^tBu), 143.0 (1 C, d, $^1J_{C\text{-}F}$ = 251.4 Hz, *o*-C_6F_5), 142.3 (1 C, d, $^1J_{C\text{-}F}$ = 245.4 Hz, *o*-C_6F_5), 140.9 (1 C, d, $^1J_{C\text{-}F}$ = 245.3 Hz, *p*-C_6F_5), 137.8 (1 C, d, $^1J_{C\text{-}F}$ = 245.5 Hz, *m*-C_6F_5), 137.7 (*i*-C_6H_4OMe), 137.7 (1 C, d, $^1J_{C\text{-}F}$ = 249.8 Hz, *m*-C_6F_5), 135.6 (*i*-$C_6H_5CN_2$), 129.6 (o_b-$C_6H_5CN_2$), 128.9 (*m*-$C_6H_5CN_2$), 128.6 (o_a-$C_6H_5CN_2$), 128.06 (overlapping with solvent

p-$C_6H_5CN_2$ and *o*-C_6H_4OMe), 127.4 ($\underline{C}_5Me_5$), 113.3 (*m*-C_6H_4OMe), 112.8 (1 C, app. t, ^2J = 20.6 Hz, *i*-C_6F_5), 83.1 (Ar$\underline{C}$(H)), 76.9 (NO$\underline{C}Me_3$), 54.9 (OMe), 49.9 (N$\underline{C}H_bMeMe$), 48.9 (N$\underline{C}H_aMeMe$), 28.2 (NOC$\underline{Me}_3$), 25.8 (NCH$_b$Me$\underline{Me}$), 25.4 (NCH$_a$Me$\underline{Me}$), 24.9 (NCH$_a\underline{Me}$Me), 24.6 (NCH$_b\underline{Me}$Me), 12.4 ($C_5\underline{Me}_5$) ppm. $^{19}F\{^1H\}$ NMR (C_6D_6, 282.1 MHz, 293 K): δ -134.6 (1 F, m, o_a-C_6F_5), -141.8 (1 F, m, o_b-C_6F_5), -156.8 (1 F, t of d, ^3J =21.2 Hz, ^4J =1.7 Hz, *p*-C_6F_5), -164.3 (1 F, m, m_a-C_6F_5), -165.0 (1 F, m, m_b-C_6F_5) ppm. Note: subscripts ″a″ and ″b″ refer to the inequivalent Ph and Ar^{F_5} environments and ^{i}Pr groups. IR (NaCl plates, Nujol mull, cm^{-1}): 1655 (w), 1641 (w), 1609 (w), 1584 (w), 1544 (m), 1519 (m), 1511 (m), 1496 (s), 1429 (m), 1362 (m), 1281 (w), 1255 (m), 1223 (w), 1196 (m), 1180 (w), 1167 (m), 1150 (w), 1113 (m), 1069 (m),1031 (m), 988 (m), 960 (m), 933 (w), 909 (w), 894 (w), 829 (w), 794 (w), 781 (w), 728 (w), 706 (w),687 (w), 636 (w), 624 (m), 604 (m). Anal. found (calcd. for $C_{42}H_{51}F_5N_4O_3Ti$): C, 62.69 (62.84); H, 6.28 (6.40); N, 7.11 (6.98) %.

Cp*Ti{PhC(N^{i}Pr)$_2$}{N(C{Ar^{F_5}}NO^{t}Bu)C(4-C$_6$H$_4$NMe$_2$)(H)O} (22e). To a solution of Cp*Ti{PhC(N^{i}Pr)$_2$}{NC(Ar^{F_5})NO^{t}Bu} (**10**, 0.493 g, 0.739 mmol) in benzene (5 mL) was added (4-$C_6H_4ONMe_2$)C(O)H (0.110 g, 0.739 mmol) in benzene (5 mL) all at RT. An immediate colour change from lime green to brown was observed and the solution left to stir for 15 min. Volatiles were then removed under reduced pressure to afford **22e** as a brown powder which was dried *in vacuo*. Yield: 0.595 g (99%). ^1H NMR (C_6D_6, 499.9 MHz, 293 K): δ 7.61 (1 H, d, ^3J = 7.5 Hz, o_a-$C_6H_5CN_2$), 7.25 (1 H, d, ^3J = 7.0 Hz, o_b-$C_6H_5CN_2$), 7.15-7.04 (3 H, m, overlapping *m*-$C_6H_5CN_2$ and *p*-$C_6H_5CN_2$), 6.97 (2 H, d, ^3J = 8.5 Hz, *o*-$C_6H_4NMe_2$), 6.41 (2 H, d, ^3J = 9.0 Hz, *m*-$C_6H_4NMe_2$), 6.04 (1 H, d, $J_{H\text{-}F}$ = 2.0 Hz, ArC($\underline{H}$)), 4.56 (1 H, app. sept., ^3J =7.0 Hz, NC$\underline{H}_aMeMe$), 3.54 (1 H, app. sept., ^3J = 7.0 Hz, NC$\underline{H}_bMeMe$), 2.42 (6 H, s, NMe_2), 2.31 (15 H, s, C_5Me_5), 1.39 (3 H, d, ^3J = 6.5 Hz, NCH$_a\underline{Me}$Me), 1.29 (9 H, s, NOCMe_3), 1.22 (3 H, d, ^3J = 7.0 Hz, NCH$_a$Me$\underline{Me}$), 1.02 (3 H, d, ^3J = 7.0 Hz, NCH$_b\underline{Me}$Me), 0.93 (3 H, d, ^3J = 6.5 Hz, NCH$_b$Me$\underline{Me}$) ppm. $^{13}C\{^1H\}$ NMR (C_6D_6, 125.7 MHz, 293 K): δ 167.9 (Ph$\underline{C}N_2$), 150.6 (*p*-$C_6H_4NMe_2$), 148.9 (N$\underline{C}$(Ar^{F_5})NO^{t}Bu), 143.0 (1 C, d, $^1J_{C\text{-}F}$ = 248.6 Hz, *o*-C_6F_5), 142.3 (1 C, d, $^1J_{C\text{-}F}$ = 240.1 Hz, *o*-C_6F_5), 140.7 (1 C, d, $^1J_{C\text{-}F}$ = 248.7 Hz, *p*-C_6F_5), 137.9 (1 C, d, $^1J_{C\text{-}F}$ = 249.0 Hz, *m*-C_6F_5), 137.7 (1 C, d, $^1J_{C\text{-}F}$ = 249.0 Hz, *m*-C_6F_5), 135.9 (*i*-$C_6H_5CN_2$), 133.1 (*o*-$C_6H_4NMe_2$), 128.9, 128.6 (*p*-$C_6H_5CN_2$ and *m*-$C_6H_5CN_2$), 128.7 (o_b-$C_6H_5CN_2$), 129.8 (o_b-$C_6H_5CN_2$), 127.2 (C_5Me_5), 122.7 (*i*-$C_6H_4NMe_2$), 113.1 (1 C, app. t, ^2J = 22.6 Hz, *i*-C_6F_5), 112.0 (*m*-$C_6H_4NMe_2$), 83.4 (Ar$\underline{C}$(H)), 76.8 (NO$\underline{C}Me_3$),

49.9 (N<u>C</u>H$_b$MeMe), 48.9 (N<u>C</u>H$_a$MeMe), 40.4 (NMe$_2$), 28.2 (NOC<u>Me</u>$_3$), 25.8 (NCH$_b$Me<u>Me</u>), 25.4 (NCH$_a$Me<u>Me</u>), 25.0 (NCH$_a$<u>Me</u>Me), 24.7 (NCH$_b$<u>Me</u>Me), 12.4 (C$_5$<u>Me</u>$_5$) ppm. ^{19}F{^{1}H} NMR (C$_6$D$_6$, 282.1 MHz, 293 K): δ -134.1 (1 F, app. d, ^3J = 24.4 Hz, *o*$_a$-C$_6$F$_5$), -141.9 (1 F, app. d, ^3J = 25.8, *o*$_b$-C$_6$F$_5$), -157.3 (1 F, t of t, ^3J = 21.2 Hz, ^4J = 1.7 Hz, *p*-C$_6$F$_5$), -164.7 (1 F, m, *m*$_a$-C$_6$F$_5$), -165.3 (1 F, m, *m*$_b$-C$_6$F$_5$) ppm. Note: subscripts ″a″ and ″b″ refer to the inequivalent Ph and Ar^{F5} environments and ^{i}Pr groups. IR (NaCl plates, Nujol mull, cm^{-1}): 1654 (w), 1614 (w), 1597 (m), 1554 (w), 1520 (m), 1497 (s), 1375 (m), 1346 (m), 1320 (w), 1282 (w), 1260 (w), 1219 (w), 1178 (m), 1167 (w), 1148 (w), 1108 (w), 1069 (w), 1021 (w), 987 (m), 952 (w), 928 (w), 908 (w), 893 (w), 819 (w), 811 (w), 787 (w), 726 (w), 711 (w), 682 (w), 637 (w), 622 (m), 600 (m). Anal. found (calcd. for C$_{43}$H$_{54}$F$_5$N$_5$O$_2$Ti): C, 63.26 (63.31); H, 6.74 (6.67); N, 8.39 (8.58) %.

Cp*Ti{PhC(N^{i}Pr)$_2$}{N(C{Ar^{F5}}NO^{t}Bu)C(4-C$_6$H$_4$CF$_3$)(H)O} (22f). To a solution of Cp*Ti{PhC(N^{i}Pr)$_2$}{NC(Ar^{F5})NO^{t}Bu} (**10**, 0.422 g, 0.634 mmol) in benzene (5 mL) was added (4-C$_6$H$_4$CF$_3$)C(O)H (86.5 μL, 0.634 mmol) all at RT. An immediate colour change from lime green to brown was observed and the solution left to stir for 30 min. Volatiles were then removed under reduced pressure to afford **22f** as a brown powder which was dried *in vacuo*. Yield: 0.525 g (99%). ^{1}H NMR (C$_6$D$_6$, 499.9 MHz, 293 K): δ 7.32 (1 H, br. d, *o*$_a$-C$_6$H$_5$CN$_2$), 7.24 (1 H, d, ^3J = 8.0 Hz, *m*-C$_6$H$_4$CF$_3$), 7.19 (1 H, br. d, *o*$_b$-C$_6$H$_5$CN$_2$), 7.11-7.04 (3 H, m, overlapping *m*-C$_6$H$_5$CN$_2$ and *p*-C$_6$H$_5$CN$_2$), 6.93 (2 H, d, ^3J = 8.0 Hz, *o*-C$_6$H$_4$CF$_3$), 5.94 (1 H, d, $J_{H\text{-}F}$ = 1.5 Hz, ArC(<u>H</u>)), 4.46 (1 H, app. sept., ^3J = 7.0 Hz, NC<u>H</u>$_a$MeMe), 3.39 (1 H, app. sept., ^3J = 6.5 Hz, NC<u>H</u>$_b$MeMe), 2.25 (15 H, s, C$_5$Me$_5$), 1.28 (3 H, d, ^3J = 6.5 Hz, NCH$_a$<u>Me</u>Me), 1.25 (9 H, s, NOCMe$_3$), 1.16 (3 H, d, ^3J = 7.0 Hz, NCH$_a$Me<u>Me</u>), 0.86 (3 H, d, ^3J = 7.0 Hz, NCH$_b$<u>Me</u>Me), 0.80 (3 H, d, ^3J = 6.5 Hz, NCH$_b$Me<u>Me</u>) ppm. ^{13}C{^{1}H} NMR (C$_6$D$_6$, 125.7 MHz, 293 K): δ 168.0 (Ph<u>C</u>N$_2$), 149.8 (*i*-C$_6$H$_4$CF$_3$), 148.4 (N<u>C</u>(Ar^{F5})NO^{t}Bu), 142.8 (1 C, d, $^1J_{C\text{-}F}$ = 248.3 Hz, *o*-C$_6$F$_5$), 142.3 (1 C, d, $^1J_{C\text{-}F}$ = 243.3 Hz, *o*-C$_6$F$_5$), 141.2 (1 C, d, $^1J_{C\text{-}F}$ = 252.1 Hz, *p*-C$_6$F$_5$), 137.7 (1 C, d, $^1J_{C\text{-}F}$ = 250.8 Hz, *m*-C$_6$F$_5$), 137.6 (1 C, d, $^1J_{C\text{-}F}$ = 252.1 Hz, *m*-C$_6$F$_5$), 135.1 (*i*-C$_6$H$_5$CN$_2$), 130.0 (1 C, q, $^1J_{C\text{-}F}$ = 31.4, 4-C$_6$H$_4$<u>C</u>F$_3$), 129.5 (*p*-C$_6$H$_4$CF$_3$), 129.1 (*o*$_b$-C$_6$H$_5$CN$_2$), 128.4 (*m*$_a$-C$_6$H$_5$CN$_2$), 128.2 (*p*-C$_6$H$_5$CN$_2$), 128.0 (*m*$_b$-C$_6$H$_5$CN$_2$), 128.0 (*o*$_a$-C$_6$H$_5$CN$_2$), 127.3 (*o*-C$_6$H$_4$CF$_3$), 127.3 (C$_5$Me$_5$), 124.7 (1 C, q, ^4J = 3.8 Hz, *m*-C$_6$H$_4$CF$_3$) 112.4 (1 C, app. t, ^2J = 21.3 Hz, *i*-C$_6$F$_5$), 82.8 (Ar<u>C</u>(H)), 77.1 (NO<u>C</u>Me$_3$), 49.9 (N<u>C</u>H$_b$MeMe), 49.0 (N<u>C</u>H$_a$MeMe), 28.1 (NOC<u>Me</u>$_3$), 25.7 (NCH$_b$Me<u>Me</u>), 25.3

(NCH_aMeMe), 24.9 (NCH_aMeMe), 24.5 (NCH_bMeMe), 12.4 (C_5Me_5) ppm. $^{19}F\{^1H\}$ NMR (C_6D_6, 282.1 MHz, 293 K): δ -62.2 (3 F, s, CF_3), -135.0 (1 F, app. d, ^3J = 25.4 Hz, o_a-C_6F_5), -141.7 (1 F, app. d, ^3J = 25.4, o_b-C_6F_5), -155.5 (1 F, app. t, ^3J = 22.6 Hz, *p*-C_6F_5), -163.4 (1 F, m, m_a-C_6F_5), -164.3 (1 F, m, m_b-C_6F_5) ppm. Note: subscripts ″a″ and ″b″ refer to the inequivalent Ph and Ar^{F5} environments and ^{i}Pr groups. IR (NaCl plates, Nujol mull, cm^{-1}): 1651 (w), 1619 (w), 1551(m), 1517 (m), 1494 (m), 1425 (m), 1367 (s), 1345 (m), 1330 (s), 1290 (w), 1258 (w), 1222 (w), 1195 (w), 1171 (m), 1122 (m), 1106 (m), 1066 (m), 1044 (w), 1018 (w),1003 (m), 989 (m), 951 (w), 917 (w), 891 (w), 841 (w), 804 (w), 779 (w), 762 (w),731 (w), 706 (w), 692 (w), 661 (w), 619 (w), 606 (w), 595(m), 579 (m). Anal. found (calcd. for $C_{42}H_{48}F_8N_4O_2Ti$): C, 59.97 (60.00); H, 5.85 (5.75); N, 6.62 (6.66) %.

NMR tube scale reaction of Cp*Ti{PhC(N^{i}Pr)$_2$}{N(C{Ar^{F5}}NO^{t}Bu)C(Ph)(H)O} (22a) with Cp*Ti{PhC(N^{i}Pr)$_2$}(NO^{t}Bu) (3). To a solution of Cp*Ti{PhC(N^{i}Pr)$_2$}{N(C{Ar^{F5}}NO^{t}Bu)C(Ph)(H)O} (**22a,** 16.3 mg, 0.0211 mmol) in C_6D_6 (0.3 mL) in an NMR tube equipped with a J. Young Teflon valve was added Cp*Ti{PhC(N^{i}Pr)$_2$}(NO^{t}Bu) (**3**, 10.0 mg, 0.0211 mmol) in C_6D_6 (0.3 mL) at RT. A colour change from brown/green to yellow/green was observed. The reaction was monitored by ^1H and ^{19}F NMR spectroscopy. After 20 h Cp*Ti{PhC(N^{i}Pr)$_2$}{NC(Ar^{F5})NO^{t}Bu} (**10**), [Cp*Ti{PhC(N^{i}Pr)$_2$}(μ-O)]$_2$ (**7**) and PhC(NO^{t}Bu)H (**9a**) were observed in quantitative yield.

Equilibrium constants. A total of 0.5 mL of C_6D_6 was used in each experiment. The general procedure is as follows. To a solution of Cp*Ti{PhC(N^{i}Pr)$_2$}{N(C{Ar^{F5}}NO^{t}Bu)C(Ph)(H)O} (**22a**, 10.0 mg, 0.0129 mmol) in C_6D_6 in an NMR tube equipped with a J. Young Teflon valve was added ArC(O)H (0.0129 mmol), in C_6D_6 where necessary, all at RT. The reaction was monitored by ^1H (relaxtion delay = 100 s) and ^{19}F NMR spectroscopy. The ratios of reagents and products were calculated by measuring the integrals of the free and bound ArC<u>H</u> hydrogens giving the required equilibrium constants (in the case of 4-C_6H_4Me and 4-C_6H_4OMe it was necessary to integrate the methyl groups of the *iso*-propyl substituents instead).

PhC{NC(Ar^{F5})NO^{t}Bu}H (23a). To a solution of Cp*Ti{PhC(N^{i}Pr)$_2$}{NC(Ar^{F5})NO^{t}Bu} (**10**, 0.301 g, 0.452 mmol) in benzene (5 mL) was added PhC(O)H (45.9 μL, 0.452 mmol) all at RT. An immediate colour change from lime green to brown was observed and the solution left to stir for 15 min before being heated to 70 °C and stirred for a further 19 h. A further colour change to yellow was observed. Volatiles were then removed under reduced pressure to afford [Cp*Ti{PhC(N^{i}Pr)$_2$}(μ-O)]$_2$ (**7**) and **23a** as a yellow/brown oily solid. The resultant solid was sublimed (80 °C, 8 x 10^{-2} mbar, 2 h) onto a dry ice/acetone cold finger affording **23a** as a white solid. Yield: 0.104 g (62%). ^{1}H NMR (C_6D_6, 499.9 MHz, 293 K): δ 8.50 (1 H, s, PhC(N)<u>H</u>), 7.69 (2 H, m, *o*-C_6H_5), 7.05-6.97 (3 H, m, overlapping *m*-C_6H_5 and *p*-C_6H_5), 1.30 (9 H, s, NOCMe$_3$). ^{13}C{^{1}H} NMR (C_6D_6, 125.7 MHz, 293 K): δ 162.0 (Ph<u>C</u>(N)H), 149.2 (N<u>C</u>(Ar^{F5})NO^{t}Bu), 143.9 (2 C, d, $^1J_{C\text{-}F}$ = 251.3 Hz, *o*-C_6F_5), 141.9 (1 C, d overlapping with *o*-C_6F_5, $^1J_{C\text{-}F}$ = 253.8 Hz, *p*-C_6F_5), 138.0 (2 C, d, $^1J_{C\text{-}F}$ = 252.5 Hz, *m*-C_6F_5), 135.6 (*i*-C_6H_5), 132.5 (*p*-C_6H_5), 129.9 (*o*-C_6H_5), 129.0 (*m*-C_6H_5), 108.0 (1 C, t of d, $^2J_{C\text{-}F}$ = 20.0 Hz, $^3J_{C\text{-}F}$ = 3.8 Hz, *i*-C_6F_5), 81.2 (NO<u>C</u>Me$_3$), 27.5 (NOC<u>Me</u>$_3$) ppm. ^{19}F{^{1}H} NMR (C_6D_6, 282.1 MHz, 293 K): δ -138.2 (2 F, m, *o*-C_6F_5), -152.7 (1 F, t of t, ^3J = 21.2 Hz, ^4J = 2.3 Hz, *p*-C_6F_5), -161.8 (2 F, m, *m*-C_6F_5) ppm. IR (NaCl plates, Nujol mull, cm^{-1}): 1657 (m), 1623 (m), 1602 (w), 1592 (w), 1579 (m), 1520 (s), 1497 (s), 1454 (m), 1434 (m), 1364 (m), 1323 (w), 1313 (w), 1296 (w), 1261 (w), 1243 (w), 1205 (m), 1187 (m), 1101 (m), 1073 (w), 998 (m), 985 (s), 970 (s), 905 (m), 892 (w), 858 (m), 798 (w), 766 (m), 707 (m), 695 (m), 668 (w), 615 (w), 597 (m), 582 (m). ESI$^+$-HRMS: *m/z* found (calcd. for $C_{18}H_{15}F_5N_2NaO$, [*M* + Na]$^+$) 393.0989 (393.0997). UV-vis: λ_{max}(*n*-hexanes) 271 nm (ε = 3.0 x 10^4 mol^{-1} dm^3 cm^{-1}); λ_{max}(MeOH) 284 nm (ε = 2.4 x 10^4 mol^{-1} dm^3 cm^{-1}).

TolC{NC(Ar^{F5})NO^{t}Bu}H (23b). A solution of Cp*Ti{PhC(N^{i}Pr)$_2$}N(C{Ar^{F5}}NO^{t}Bu)C(Tol)(H)O} (**22b**, 0.468 g, 0.595 mmol) in benzene (5 mL) was heated to 65 °C for 17 h. A colour change from brown to yellow was observed. Volatiles were then removed under reduced pressure to afford [Cp*Ti{PhC(N^{i}Pr)$_2$}(μ-O)]$_2$ (**7**) and **23b** as a yellow/brown oily solid. The resultant solid was sublimed (80-110 °C, 8 x 10^{-2} mbar, 3.5 h) onto a dry ice/acetone cold finger affording **23b** as a cream solid. Yield: 0.150 g (66%). ^{1}H NMR (C_6D_6, 499.9 MHz, 293 K): δ 8.54 (1 H, s, ArC(N)<u>H</u>), 7.66 (2 H, d, ^3J = 8.0 Hz, *o*-C_6H_4Me), 6.82 (2 H, d, ^3J = 8.0 Hz, *m*-C_6H_4Me), 1.94 (3 H, s, C_6H_4<u>Me</u>) 1.31 (9 H, s, NOCMe$_3$). ^{13}C{^{1}H} NMR

(C_6D_6, 125.7 MHz, 293 K): δ 161.9 (Tol<u>C</u>(N)H), 149.4 (N<u>C</u>(Ar^{F_5})NO^{t}Bu), 143.8 (2 C, d, $^1J_{C\text{-}F}$ = 252.0 Hz, *o*-C_6F_5), 141.9 (1 C, d overlapping with *o*-C_6F_5, $^1J_{C\text{-}F}$ = 267.2 Hz, *p*-C_6F_5), 138.0 (2 C, d, $^1J_{C\text{-}F}$ = 251.7 Hz, *m*-C_6F_5), 133.2 (*i*-C_6H_4Me), 130.0 (*m*-C_6H_4Me), 129.8 (*o*-C_6H_4Me), 108.2 (1 C, t of d, $^2J_{C\text{-}F}$ = 20.8 Hz, $^3J_{C\text{-}F}$ = 3.5 Hz, *i*-C_6F_5), 81.03 (NO<u>C</u>Me_3), 27.5 (NOC<u>Me</u>$_3$), 21.5 (C_6H_4<u>Me</u>) ppm. $^{19}F\{^1H\}$ NMR (C_6D_6, 282.1 MHz, 293 K): δ -138.3 (2 F, m, *o*-C_6F_5), -152.9 (1 F, t of t, ^3J = 21.4 Hz, ^4J = 2.5 Hz, *p*-C_6F_5), -161.9 (2 F, m, *m*-C_6F_5) ppm. IR (NaCl plates, Nujol mull, cm^{-1}): 1652 (w), 1614 (m), 1603 (s), 1567 (m), 1519 (m), 1496 (s), 1424 (w), 1365 (m), 1318 (w), 1305 (w), 1262 (w), 1244 (w), 1204 (m), 1172 (m), 1099 (m), 1034 (w), 1015 (m), 993 (s), 972 (s), 947 (w), 910 (w), 897 (w), 865 (w), 842 (w), 815 (m), 795 (w), 767 (w), 713 (w), 702 (w), 687 (w), 668 (w). ESI$^+$-HRMS: *m/z* found (calcd. for $C_{19}H_{17}F_5N_2NaO$, $[M + Na]^+$) 407.1143 (407.1153). UV-vis: λ_{max}(*n*-hexanes) 275 nm (ε = 5.4 x 10^4 mol^{-1} dm^3 cm^{-1}).

(4-C_6H_4^{t}Bu)C{NC(Ar^{F_5})NO^{t}Bu}H (23c). A solution of Cp*Ti{PhC(N^{i}Pr)$_2$}{N(C{Ar^{F_5}}NO^{t}Bu)C(4-C_6H_4^{t}Bu)(H)O} (**22c**, 0.412 g, 0.497 mmol) in benzene (5 mL) was heated to 65 °C for 17 h. A colour change from brown to yellow was observed. Volatiles were then removed under reduced pressure to afford [Cp*Ti{PhC(N^{i}Pr)$_2$}(μ-O)]$_2$ (**7**) and **23c** as a yellow/brown oily solid. The resultant solid was sublimed (80-100 °C, 8 x 10^{-2} mbar, 4.5 h) onto a dry ice/acetone cold finger affording **23c** as a cream solid. Yield: 0.194 g (92%). ^1H NMR (C_6D_6, 299.9 MHz, 293 K): δ 8.61 (1 H, s, ArC(N)<u>H</u>), 7.76 (2 H, d, ^3J = 8.4 Hz, *o*-C_6H_4^{t}Bu), 7.16 (2 H, d, ^3J = 8.4 Hz, *m*-C_6H_4^{t}Bu), 1.32 (9 H, s, NOCMe_3), 1.09 (9 H, s, C_6H_4^{t}<u>Bu</u>). $^{13}C\{^1H\}$ NMR (C_6D_6, 75.4 MHz, 293 K): δ 161.9 (Ar<u>C</u>(N)H), 156.3 (*p*-C_6H_4^{t}Bu), 149.4 (N<u>C</u>(Ar^{F_5})NO^{t}Bu), 143.9 (2 C, d, $^1J_{C\text{-}F}$ = 254.6 Hz, *o*-C_6F_5), 141.9 (1 C, d, $^1J_{C\text{-}F}$ = 254.2 Hz, *p*-C_6F_5), 138.0 (2 C, d, $^1J_{C\text{-}F}$ = 253.6 Hz, *m*-C_6F_5), 133.2 (*i*-C_6H_4^{t}Bu), 130.0 (*o*-C_6H_4^{t}Bu), 126.1 (*m*-C_6H_4^{t}Bu), 108.2 (1 C, m, *i*-C_6F_5), 81.0 (NO<u>C</u>Me_3), 35.0 (<u>C</u>Me_3), 31.0 (C<u>Me</u>$_3$) 27.5 (NOC<u>Me</u>$_3$) ppm. $^{19}F\{^1H\}$ NMR (C_6D_6, 282.1 MHz, 293 K): δ -138.3 (2 F, m, *o*-C_6F_5), -152.8 (1 F, t of t, ^3J = 21.4 Hz, ^4J = 2.3 Hz, *p*-C_6F_5), -161.9 (2 F, m, *m*-C_6F_5) ppm. IR (NaCl plates, Nujol mull, cm^{-1}): 1730 (w), 1710 (w), 1654 (w), 1639 (w), 1619 (m), 1608 (m), 1570 (w), 1551 (w), 1519 (s), 1498 (s), 1416 (w), 1367 (m), 1322 (m), 1312 (w), 1298 (w), 1270 (w), 1223 (m), 1187 (m), 1118 (w), 1098 (m), 1036 (w), 1000 (s), 907 (w), 894 (m), 874 (w), 839 (w), 828 (w), 799 (w), 725 (w), 702 (w),

664 (w), 633 (w). ESI$^+$-HRMS: *m/z* found (calcd. for $C_{22}H_{23}F_5N_2NaO$, [*M* + Na]$^+$) 449.1613 (449.1623). UV-vis: λ_{max}(*n*-hexanes) 275 nm (ε = 3.7 x 10^4 mol^{-1} dm^3 cm^{-1}).

(4-C$_6$H$_4$OMe)C{NC(Ar^{F5})NO^{t}Bu}H (23d). A solution of Cp*Ti{PhC(N^{i}Pr)$_2$}-{N(C{Ar^{F5}}NO^{t}Bu)C(4-C$_6$H$_4$OMe)(H)O} (**22d**, 0.407 g, 0.508 mmol) in benzene (5 mL) was heated to 65 °C for 17 h. A colour change from brown to yellow was observed. Volatiles were then removed under reduced pressure to afford [Cp*Ti{PhC(N^{i}Pr)$_2$}(μ-O)]$_2$ (**7**) and **23d** as a yellow/brown oily solid. The resultant solid was sublimed (80-110 °C, 8 x 10^{-2} mbar, 5.5 h) onto a dry ice/acetone cold finger affording **23d** as a cream solid. Yield: 0.189 g (93%). ^{1}H NMR (C$_6$D$_6$, 299.9 MHz, 293 K): δ 8.54 (1 H, s, ArC(N)H), 7.69 (2 H, d, ^3J = 8.7 Hz, *o*-C$_6$H$_4$OMe), 6.58 (2 H, d, ^3J = 8.7 Hz, *m*-C$_6$H$_4$OMe), 3.12 (3 H, s, OMe), 1.32 (9 H, s, NOCMe$_3$) ppm. ^{13}C{^{1}H} NMR (C$_6$D$_6$, 75.4 MHz, 293 K): δ 163.6 (ArC(N)H), 161.2 (*p*-C$_6$H$_4$OMe), 149.5 (NC(Ar^{F5})NO^{t}Bu), 143.8 (2 C, d, $^1J_{C\text{-}F}$ = 249.4 Hz, *o*-C$_6$F$_5$), 141.8 (1 C, d, $^1J_{C\text{-}F}$ = 254.2 Hz, *p*-C$_6$F$_5$), 138.0 (2 C, d, $^1J_{C\text{-}F}$ = 253.4 Hz, *m*-C$_6$F$_5$), 131.9 (*o*-C$_6$H$_4$OMe), 128.6 (*i*-C$_6$H$_4$OMe), 114.6 (*m*-C$_6$H$_4$OMe), 108.4 (1 C, m, *i*-C$_6$F$_5$), 80.9 (NOCMe$_3$), 54.9 (OMe), 27.5 (NOCMe$_3$) ppm. ^{19}F{^{1}H} NMR (C$_6$D$_6$, 282.1 MHz, 293 K): δ -138.4 (2 F, m, *o*-C$_6$F$_5$), -153.1 (1 F, t of t, ^3J = 21.2 Hz, ^4J = 2.3 Hz, *p*-C$_6$F$_5$), -162.0 (2 F, m, *m*-C$_6$F$_5$) ppm. IR (thin film, cm^{-1}): 2977 (m), 2935 (m), 2841 (w), 1683 (w), 1653 (m), 1603 (s), 1573 (m), 1514 (s), 1497 (s), 1466 (m), 1443 (m), 1424 (m), 1389 (m), 1366 (m), 1311 (m), 1259 (s), 1208 (m), 1185 (m), 1166 (s), 1111 (m), 1097 (m), 1033 (m), 994 (s), 907 (m), 892 (m), 869 (m), 835 (m), 803 (w), 769 (w), 704 (w), 685 (w), 669 (w), 609 (w), 579 (w). ESI$^+$-HRMS: *m/z* found (calcd. for $C_{19}H_{17}F_5N_2NaO_2$, [*M* + Na]$^+$) 423.1100 (423.1102). UV-vis: λ_{max}(*n*-hexanes) 281 nm (ε = 5.8 x 10^4 mol^{-1} dm^3 cm^{-1}).

(4-C$_6$H$_4$NMe$_2$)C{NC(Ar^{F5})NO^{t}Bu}H (23e). A solution of Cp*Ti{PhC(N^{i}Pr)$_2$}-{N(C{Ar^{F5}}NO^{t}Bu)C(4-NC$_6$H$_4$NMe$_2$)(H)O} (**22e**, 0.484 g 0.594 mmol) in benzene (5 mL) was heated to 65 °C for 17 h. A colour change from brown to yellow was observed. Volatiles were then removed under reduced pressure to afford [Cp*Ti{PhC(N^{i}Pr)$_2$}(μ-O)]$_2$ (**7**) and **23e** as a yellow/brown oily solid. The resultant solid was sublimed (80-110 °C, 8 x 10^{-2} mbar, 3 h) onto a dry ice/acetone cold finger affording **23e** as an orange solid. Yield: 0.163 g (66%). Diffraction-quality crystals were grown from the slow evaporation of a pentane solution at RT. ^{1}H NMR (C$_6$D$_6$, 499.9 MHz, 293 K): δ 8.66 (1 H, s, ArC(N)H), 7.82 (2 H, d, ^3J = 8.5 Hz, *o*-C$_6$H$_4$NMe$_2$), 6.28 (2 H, d, ^3J = 9.5 Hz, *m*-C$_6$H$_4$NMe$_2$), 2.26 (6 H, s, C$_6$H$_4$NMe$_2$) 1.34 (9 H, s, NOCMe$_3$). ^{13}C{^{1}H} NMR (C$_6$D$_6$,

125.7 MHz, 293 K): δ 161.4 (Ar<u>C</u>(N)H), 153.3 (*p*-$C_6H_4NMe_2$), 149.4 (N<u>C</u>(Ar^{F_5})NO^{t}Bu), 143.9 (2 C, d, $^1J_{C\text{-}F}$ = 248.7 Hz, *o*-C_6F_5), 141.7 (1 C, d, $^1J_{C\text{-}F}$ = 253.2 Hz, *p*-C_6F_5), 138.0 (2 C, d, $^1J_{C\text{-}F}$ = 251.1 Hz, *m*-C_6F_5), 131.9 (*o*-$C_6H_4NMe_2$), 123.9 (*i*-$C_6H_4NMe_2$), 111.8 (*m*-$C_6H_4NMe_2$), 109.2 (1 C, t of d, $^2J_{C\text{-}F}$ = 21.1 Hz, $^3J_{C\text{-}F}$ = 3.4 Hz, *i*-C_6F_5), 80.4 (NO<u>C</u>Me_3), 39.4 (NMe_2), 27.6 (NOC<u>Me</u>$_3$) ppm. $^{19}F\{^1H\}$ NMR (C_6D_6, 282.1 MHz, 293 K): δ -138.5 (2 F, m, *o*-C_6F_5), -153.8 (1 F, t of t, ^3J = 21.4 Hz, ^4J = 2.0 Hz, *p*-C_6F_5), -162.3 (2 F, m, *m*-C_6F_5) ppm. IR (NaCl plates, Nujol mull, cm^{-1}): 1653 (w), 1613 (m), 1595 (s), 1537 (m), 1520 (s), 1496 (s), 1312 (m), 1261 (w), 1225 (m), 1176 (s), 1128 (w), 1097 (m), 1035 (w), 989 (s), 894 (w), 873 (w), 820 (m), 730 (w), 668 (w). ESI$^+$-HRMS: *m/z* found (calcd. for $C_{20}H_{20}F_5N_3NaO$, $[M + Na]^+$) 436.1407 (436.1419). UV-vis: λ_{max}(*n*-hexanes) 360 nm (ε = 5.3 x 10^4 mol^{-1} dm^3 cm^{-1}); λ_{max}(MeOH) 383 nm (ε = 5.7 x 10^4 mol^{-1} dm^3 cm^{-1}).

(4-$C_6H_4CF_3$)C{NC(Ar^{F_5})NO^{t}Bu}H (23f). A solution of Cp*Ti{PhC(N^{i}Pr)$_2$}{N(C{Ar^{F_5}}NO^{t}Bu)C(4-$C_6H_4CF_3$)(H)O} (**22f**) (0.503 mg, 0.598 mmol) in benzene (5 mL) was heated to 65 °C for 18 h. A colour change from brown to yellow was observed. Volatiles were then removed under reduced pressure to afford [Cp*Ti{PhC(N^{i}Pr)$_2$}(μ-O)]$_2$ (**7**) and **23f** as a yellow/brown oily solid. The resultant solid was distilled (80-110 °C, 8 x 10^{-2} mbar, 3 h) onto a dry ice/acetone cold finger affording **23f** as a yellow oil. Yield: 0.235 g (90%). ^1H NMR (C_6D_6, 499.9 MHz, 293 K): δ 8.30 (1 H, s, ArC(N)<u>H</u>), 7.45 (2 H, d, ^3J = 8.0 Hz, *o*-$C_6H_4CF_3$), 7.18 (2 H, d, ^3J = 8.5 Hz, *m*-C_6H_4Me), 1.30 (9 H, s, NOCMe_3). $^{13}C\{^1H\}$ NMR (C_6D_6, 125.7 MHz, 293 K): δ 160.3 (Ar<u>C</u>(N)H), 148.8 (N<u>C</u>(Ar^{F_5})NO^{t}Bu), 143.8 (2 C, d, $^1J_{C\text{-}F}$ = 249.7 Hz, *o*-C_6F_5), 142.1 (1 C, d, $^1J_{C\text{-}F}$ = 254.8 Hz, *p*-C_6F_5), 138.0 (2 C, d, $^1J_{C\text{-}F}$ = 248.4 Hz, *m*-C_6F_5), 138.3 (*i*-$C_6H_4CF_3$), 133.6 (1 C, q, $^1J_{C\text{-}F}$ = 32.4 Hz, *p*-$C_6H_4CF_3$), 129.9 (*o*- $C_6H_4CF_3$), 125.8 (1 C, q, $^4J_{C\text{-}F}$ = 3.1 Hz *m*-$C_6H_4CF_3$), 107.5 (1 C, t of d, $^2J_{C\text{-}F}$ = 20.7 Hz, $^3J_{C\text{-}F}$ = 3.5 Hz, *i*-C_6F_5), 81.6 (NO<u>C</u>Me_3), 27.4 (NOC<u>Me</u>$_3$) ppm. $^{19}F\{^1H\}$ NMR (C_6D_6, 282.1 MHz, 293 K): δ -62.8 (3 F, s, CF_3), -138.1 (2 F, app. d, ^3J = 26.4 Hz, *o*-C_6F_5), -151.9 (1 F, t of t, ^3J = 21.4 Hz, ^4J = 2.5 Hz, *p*-C_6F_5), -161.4 (2 F, m, *m*-C_6F_5) ppm. IR (thin film, cm^{-1}): 2979 (m), 2933 (w), 1713 (w), 1652 (m), 1622 (m), 1601 (w), 1579 (w), 1520 (s), 1498 (s), 1454 (m), 1427 (w), 1416 (w), 1389 (w), 1366 (m), 1323 (s), 1311 (m), 1262 (w), 1246 (w), 1205 (m), 1173 (m), 1134 (m), 1109 (m), 1098 (m), 1066 (m), 1036 (m), 994 (s), 928 (w), 910 (m), 891 (m), 865 (w), 841 (m), 784 (w), 761 (w), 744 (w), 706

(w), 669 (w). FI-HRMS: *m/z* found (calcd. for $C_{19}H_{14}F_8N_2O$, $[M]^+$) 438.0984 (438.0978). UV-vis: λ_{max}(*n*-hexanes) 274 nm ($\varepsilon = 1.4 \times 10^4$ mol^{-1} dm^3 cm^{-1}).

Kinetic measurements. The general procedure is as follows. Cp*Ti{PhC(N^{i}Pr)$_2$}{N(C{Ar^{F5}}NO^{t}Bu)C(Ar)(H)O} (**22a**-**22f**, 0.0129 mmol) was dissolved in C_6D_6 (0.6 mL) and transferred to a NMR tube equipped with a J. Young Teflon valve. The NMR probe was warmed to 70 °C and the sample added before being locked and shimmed. After allowing the sample to thermally equilibrate (*ca*. 10 min), the shimming was checked and an array set up recording a spectrum of 4 scans every 120 s. The ratios of the species were calculated by measuring the integrals of the ArC<u>H</u> protons. First order rate contants were obtained from linear plots of ln([**22a**-**22f**]$_t$/[**22a**-**22f**]$_0$) *vs.* time.

NMR tube scale reaction of Cp*Ti{PhC(N^{i}Pr)$_2$}{NC(Ar^{F5})NO^{t}Bu} (10) with PhC(O)H and (4-C$_6$H$_4$NMe$_2$)C(O)H (1:1 ratio). To a solution of Cp*Ti{PhC(N^{i}Pr)$_2$}{NC(Ar^{F5})NO^{t}Bu} (**10**, 21.1 mg, 0.0317 mmol) in C_6D_6 (0.3 mL) in an NMR tube equipped with a J. Young Teflon valve was added a pre-mixed solution of PhC(O)H (3.22 μL, 0.0317 mmol) and (4-$C_6H_4NMe_2$)C(O)H (4.73 mg, 0.0317 mmol) in C_6D_6 (0.3 mL) at RT. A colour change from lime green to brown was observed. After 1 h 45 min at RT, the solution was heated to 65 °C. After 20.5 h PhC{NC(Ar^{F5})NO^{t}Bu}H (**23a**) and (4-$C_6H_4NMe_2$)C{NC(Ar^{F5})NO^{t}Bu}H (**23e**) were observed, alongside [Cp*Ti{PhC(N^{i}Pr)$_2$}(μ-O)]$_2$ (**7**), in the ^{1}H NMR spectrum in a 64:36 ratio, respectively.

NMR tube scale synthesis of Cp*Ti{PhC(N^{i}Pr)$_2$}{NC(Ar^{F5})NO^{t}Bu}{OC(NMe$_2$)H} (24). To a solution of Cp*Ti{PhC(N^{i}Pr)$_2$}{N(C{Ar^{F5}}NO^{t}Bu)} (**10**, 17.0 mg, 0.0256 mmol) in C_6D_6 (0.3 mL) in an NMR tube equipped with a J. Young Teflon valve was added Me$_2$NC(O)H (1.87 mg, 0.0256 mmol) in C_6D_6 (0.3 mL) at RT. A colour change from lime green to red/brown was observed. The reaction was monitored by ^{1}H and ^{19}F NMR spectroscopy. Within 5 min **24** was observed alongside Me$_2$NC{NC(Ar^{F5})NO^{t}Bu}H (**25**) and [Cp*Ti{PhC(N^{i}Pr)$_2$}(μ-O)]$_2$ (**7**) in 92:8 ratio. **24** was characterised by ^{1}H and ^{19}F NMR spectroscopy. ^{1}H NMR (C_6D_6, 299.9 MHz, 293 K): δ 7.92 (1 H, br s, Me$_2$NC(<u>H</u>)), 7.32 (1 H, d, ^3J = 8.1 Hz, *o$_a$*-C_6H_5), 7.21-6.98 (4 H, m, *o$_b$*-C_6H_5, *m*-C_6H_5 and *p*-C_6H_5), 3.40 (2 H, sept., ^3J = 6.6 Hz, NC<u>H</u>MeMe), 2.36 (3 H, s, N<u>Me</u>Me), 2.22 (15 H, s, C_5Me_5), 1.95 (3 H, s, NMe<u>Me</u>), 1.40 (9 H, s, NOCMe$_3$), 0.86

(6 H, d, ^{3}J = 6.6 Hz, NCH<u>Me</u>Me), 0.81 (6 H, d, ^{3}J = 6.6 Hz, NCHMe<u>Me</u>) ppm. $^{19}F\{^{1}H\}$ NMR (C_6D_6, 282.1 MHz, 293 K): δ -140.0 (2 F, m, *o*-C_6F_5), -158.2 (1 F, t, ^{3}J = 21.2 Hz, *p*-C_6F_5), -164.0 (2 F, m, *m*-C_6F_5) ppm. Note: subscripts ″a″ and ″b″ refer to the inequivalent Ph environments.

$Me_2NC\{NC(Ar^{F_5})NO^tBu\}H$ (25). To a solution of $Cp^*Ti\{PhC(N^iPr)_2\}\{NC(Ar^{F_5})NO^tBu\}$ (**10**, 0.351 g, 0.528 mmol) in benzene (5 mL) was added $HC(O)NMe_2$ (40.9 μL, 0.528 mmol) all at RT. An immediate colour change from lime green to red/brown and then to yellow was observed and the solution left to stir for 3 h. The solution was then filtered and the volatiles were removed under reduced pressure to afford $[Cp^*Ti\{PhC(N^iPr)_2\}(\mu\text{-}O)]_2$ (**7**) and **25** as a yellow/brown oily solid. The resultant solid was sublimed (80 °C, 8 x 10^{-2} mbar, 3 h) onto a dry ice/acetone cold finger affording **25** as a white solid. Yield: 0.114 g (64%). Diffraction-quality crystals were grown from the slow evaporation of a pentane solution at RT. ^{1}H NMR (C_6D_6, 499.9 MHz, 293 K): δ 7.79 (1 H, s, <u>H</u>C(N)NMe_2), 2.42 (3 H, s, HC(N)N<u>Me</u>Me), 1.90 (3 H, s, HC(N)NMe<u>Me</u>), 1.37 (9 H, s, $NOCMe_3$) ppm.$^{13}C\{^{1}H\}$ NMR (C_6D_6, 125.7 MHz, 293 K): δ 152.8 (H<u>C</u>(N)NMe_2), 148.8 (N<u>C</u>(Ar^{F_5})N), 143.9 (2 C, d, $^{1}J_{C\text{-}F}$ = 247.5 Hz, *o*-C_6F_5), 141.2 (1 C, d, $^{1}J_{C\text{-}F}$ = 255.0 Hz, *p*-C_6F_5), 137.9 (2 C, d, $^{1}J_{C\text{-}F}$ = 250.0 Hz, *m*-C_6F_5), 112.1 (1 C, t of d, $^{2}J_{C\text{-}F}$ = 20.0 Hz, $^{3}J_{C\text{-}F}$ = 3.8 Hz, *i*-C_6F_5), 78.8 (NO<u>C</u>Me_3), 39.2 (HC(N)NMe<u>Me</u>), 33.9 (HC(N)N<u>Me</u>Me), 27.7 (NOC<u>Me</u>$_3$) ppm. $^{19}F\{^{1}H\}$ NMR (C_6D_6, 282.1 MHz, 293 K): δ -140.2 (2 F, m, *o*-C_6F_5), -155.8 (1 F, t of t, ^{3}J = 21.2 Hz, ^{4}J = 1.41 Hz, *p*-C_6F_5), -163.3 (2 F, m, *m*-C_6F_5) ppm. IR (NaCl plates, Nujol mull, cm^{-1}): 1626 (s), 1565 (m), 1520 (m), 1497 (s), 1441 (m), 1419 (m), 1410 (w), 1397 (w), 1364 (s), 1317 (w), 1256 (w), 1232 (w), 1191 (m), 1113 (s), 1095 (m), 1064 (w), 1036 (w), 995 (s), 985 (m), 960 (m), 927 (w), 910 (m), 900 (w), 866 (w), 800 (w), 700 (m), 681 (w), 610 (w), 581 (w). ESI^{+}-HRMS: *m/z* found (calcd. for $C_{14}H_{16}F_5N_3NaO$, $[M + Na]^{+}$) 360.1102 (360.1106).

NMR tube scale reaction of Cp*Ti{PhC(N^{i}Pr)$_2$}(NO^{t}Bu) (3) with PhC(O)H and ^{t}BuNCO (1:1 ratio). To a solution of Cp*Ti{PhC(N^{i}Pr)$_2$}(NO^{t}Bu) (**3**, 10.0 mg, 0.0211 mmol) in C_6D_6 (0.3 mL) in an NMR tube equipped with a J. Young Teflon valve was added a pre-mixed solution of PhC(O)H (2.15 μL, 0.0211 mmol) and ^{t}BuNCO (2.41 μL, 0.0211 mmol) in C_6D_6 (0.3 mL) at RT. A color change from lime green to yellow was observed. The reaction was monitored by ^{1}H and ^{19}F NMR spectroscopy and within 5 min [Cp*Ti{PhC(N^{i}Pr)$_2$}(μ-O)]$_2$ (**7**) and PhC(NO^{t}Bu)H (**9a**) were formed in quantitative yield.

NMR tube scale reaction of Cp*Ti{PhC(N^{i}Pr)$_2$}{NC(Ar^{F5})NO^{t}Bu} (10) with PhC(O)H and ^{t}BuNCO (1:1 ratio). To a solution of Cp*Ti{PhC(N^{i}Pr)$_2$}{NC(Ar^{F5})NO^{t}Bu} (**10**, 14.8 mg, 0.0222 mmol) in C_6D_6 (0.3 mL) in an NMR tube equipped with a J. Young Teflon valve was added a pre-mixed solution of PhC(O)H (2.48 μL, 0.0244 mmol) and ^{t}BuNCO (2.79 μL, 0.0244 μmol) in C_6D_6 (0.3 mL) at RT. A color change from lime green to brown was observed. The reaction was monitored by ^{1}H and ^{19}F NMR spectroscopy and after 5 min Cp*Ti{PhC(N^{i}Pr)$_2$}{N(C{Ar^{F5}}NO^{t}Bu)C(Ph)(H)O} (**22a**) was formed in quantitative yield.

NMR tube scale reaction of Cp*Ti{PhC(N^{i}Pr)$_2$}{N(C{Ar^{F5}}NO^{t}Bu)C(N^{t}Bu)O} (20) with PhC(O)H. To a solution of Cp*Ti{PhC(N^{i}Pr)$_2$}{N(C{Ar^{F5}}NO^{t}Bu)C(N^{t}Bu)O} (**20**, 20.0 mg, 0.0261 mmol) in C_6D_6 (0.6 mL) in an NMR tube equipped with a J. Young Teflon valve was added PhC(O)H (2.65 μL, 0.0261 mmol) at RT. A color change from lime green to red/orange was observed. The reaction was monitored by ^{1}H and ^{19}F NMR spectroscopy and after 35 min showed formation of **27** (unidentified) in quantitative yield. ^{1}H NMR (C_6D_6, 399.9 MHz, 293 K): δ 8.00 (2 H, d, ^3J = 7.6 Hz, aryl), 7.79 (1 H, d, ^3J = 7.6 Hz, aryl), 7.39 (2 H, t, ^3J = 7.6 Hz, aryl), 7.25-7.08 (5 H, m, aryl), 3.55 (2 H, m, overlapping NC$\underline{H}_a$MeMe and NC$\underline{H}_b$MeMe), 1.89 (15, s, C_5Me_5), 1.41 (9 H, s, NOCMe$_3$), 1.23 (3 H, d, ^3J = 6.4 Hz, NCH$\underline{MeMe}$), 1.06 (9 H, s, NCMe$_3$), 1.04 (3 H, d, ^3J = 6.8 Hz, NCH$\underline{MeMe}$), 0.90 (3 H, d, ^3J = 6.4 Hz, NCH$\underline{MeMe}$), 0.66 (3 H, d, ^3J = 6.8 Hz, NCH$\underline{MeMe}$) ppm. ^{19}F{^{1}H} NMR (C_6D_6, 376.4 MHz, 293 K): δ -128.0 (1 F, d, ^3J = 23.7 Hz, *o*-C_6F_5), -140.5 (1 F, d, ^3J = 25.6 Hz, *o*-C_6F_5), -157.5 (1 F, t, ^3J = 21.1 Hz, *p*-C_6F_5), -165.5 (1 F, m, *m*-C_6F_5), -165.7 (1 F, m, *m*-C_6F_5) ppm. Note: general assigments by analogy to data and assigments for similar compounds.

NMR tube scale reaction of Cp*Ti{PhC(N^{i}Pr)$_2$}{NC(Ar^{F5})NO^{t}Bu} (10) with Me$_2$NC(O)H and ^{t}BuNCO (1:1 ratio). To a solution of Cp*Ti{PhC(N^{i}Pr)$_2$}{NC(Ar^{F5})NO^{t}Bu} (**10**, 14.1 mg, 0.0211 mmol) in C_6D_6 (0.3 mL) in an NMR tube equipped with a J. Young Teflon valve was added a pre-mixed solution of $Me_2NC(O)H$ (1.64 μL, 0.0211 mmol) and ^{t}BuNCO (2.41 μL, 0.0211 mmol) in C_6D_6 (0.3 mL) at RT. A color change from lime green to red/brown to yellow was observed. The reaction was monitored by ^{1}H and ^{19}F NMR spectroscopy. Cp*Ti{PhC(N^{i}Pr)$_2$}{NC(Ar^{F5})NO^{t}Bu}{OC(NMe$_2$)(H)} (**24**, 52%) and Cp*Ti{PhC(N^{i}Pr)$_2$}{N(C{Ar^{F5}}NO^{t}Bu)C(N^{t}Bu)O} (**18**, 7%) was formed alongside [Cp*Ti{PhC(N^{i}Pr)$_2$}(μ-O)]$_2$ (**7**, 15%) and Me$_2$NC{NC(Ar^{F5})NO^{t}Bu}H (**25**, 26%) after 10 min.

NMR tube scale reaction of Cp*Ti{PhC(N^{i}Pr)$_2$}{NC(Ar^{F5})NO^{t}Bu} (10) with Me$_2$NC(O)H and PhC(O)H (1:1 ratio). To a solution of Cp*Ti{PhC(N^{i}Pr)$_2$}{NC(Ar^{F5})NO^{t}Bu} (**10**, 21.1 mg, 0.0317 mmol) in C_6D_6 (0.3 mL) in an NMR tube equipped with a J. Young Teflon valve was added a pre-mixed solution of $Me_2NC(O)H$ (2.45 μL, 0.0317 mmol) and PhC(O)H (3.22 μL, 0.0317 mmol) in C_6D_6 (0.3 mL) at RT. A color change from lime green to red/brown to yellow was observed. The reaction was monitored by ^{1}H and ^{19}F NMR spectroscopy and within 15 min Cp*Ti{PhC(N^{i}Pr)$_2$}{N(C{Ar^{F5}}NO^{t}Bu)C(Ph)(H)O} (**22a**) was formed in quantitative yield.

Cp*Ti{PhC(N^{i}Pr)$_2$}{NC(Ar^{F5})NO^{t}Bu}(CN^{t}Bu) (28). To a solution of Cp*Ti{PhC(N^{i}Pr)$_2$}{NC(Ar^{F5})NO^{t}Bu} (**10**, 0.422 g, 0.634 mmol) in diethyl ether (5 mL) was added ^{t}BuNC (71.7 μL, 0.634 mmol) all at RT. A colour change from lime green to orange was observed and the solution left to stir for 15 min. Volatiles were then removed under reduced pressure to afford **28** as an orange powder. The resultant orange solid was re-crystallised from a saturated pentane (5 mL) solution at -30 °C, filtered and dried *in vacuo*. Yield: 0.292 g (61%). Diffraction-quality crystals were grown from a saturated pentane solution at -30 °C. ^{1}H NMR (toluene-d_8, 299.9 MHz, 208 K): δ 7.14-6.89 (5 H, m, overlapping *o*-C_6H_5, *m*-C_6H_5 and *p*-C_6H_5), 3.31 (1 H, app. sept., ^3J = 6.3 Hz, NC$\underline{H}_a$MeMe), 3.17 (1 H, app. sept., ^3J = 6.3 Hz, NC$\underline{H}_b$MeMe), 2.30 (15 H, s, C_5Me_5), 1.52 (9 H, s, NOCMe_3), 1.07 (6 H, d, overlapping NCH$_a$$\underline{Me}$Me and NCH$_b$$\underline{Me}$Me), 1.04 (9 H, s, NC$Me_3$), 0.96 (3 H, d, ^3J = 6.3 Hz, NCH$_a$Me$\underline{Me}$), 0.91 (3 H, d, ^3J = 6.3 Hz, NCH$_b$Me$\underline{Me}$) ppm. ^{13}C{^{1}H} NMR (toluene-d_8, 75.4 MHz, 208 K): δ

172.3 (Ph<u>C</u>N_2), 153.8 (Ti<u>C</u>N^{t}Bu), 149.4 (N<u>C</u>(Ar^{F_5})N), 135.1 (*i*-C_6H_5), 129.1-127.0 (overlapping with solvent, *p*-C_6H_5, *m*-C_6H_5 and *o*-C_6H_5), 118.3 (<u>C</u>$_5$Me$_5$), 114.1 (1 C, t, $^2J_{C\text{-}F}$ = 23.0 Hz, *i*-C_6F_5), 77.4 (NO<u>C</u>Me$_3$), 55.9 (<u>C</u>NMe$_3$), 49.3 (N<u>C</u>H$_b$MeMe), 48.8 (N<u>C</u>H$_a$MeMe), 29.1 (CN<u>Me</u>$_3$), 27.9 (NOC<u>Me</u>$_3$), 26.3 (NCH$_b$Me<u>Me</u>), 25.7 (NCH$_a$Me<u>Me</u>), 25.2, 24.9 (NCH$_a$<u>Me</u>Me and NCH$_b$<u>Me</u>Me), 12.7 (C$_5$<u>Me</u>$_5$) ppm.^{13}C NMR (HMQC ^{19}F-observed, toluene-d_8, 282.1 MHz, 208 K): δ 143.2 (*o*$_b$-C_6F_5), 142.9 (*o*$_a$-C_6F_5), 139.9 (*p*-C_6F_5), 137.5 (*m*$_a$-C_6F_5), 137.2 (*m*$_b$-C_6F_5) ppm.^{19}F{^{1}H} NMR (toluene-d_8, 282.1 MHz, 208 K): δ -138.5 (1 F, m, *o*$_a$-C_6F_5), -141.4 (1 F, m, *o*$_b$-C_6F_5), -158.1 (1 F, t, ^3J = 21.4 Hz, *p*-C_6F_5), -163.8 (1 F, m, *m*$_b$-C_6F_5), -164.1 (1 F, m, *m*$_a$-C_6F_5) ppm. Note: subscripts ″a″ and ″b″ refer to the inequivalent Ar^{F_5} environments and ^{i}Pr groups. IR (NaCl plates, Nujol mull, cm^{-1}): 2186 (s), 1648 (m), 1576 (w), 1519 (s), 1499 (s), 1486 (s), 1368 (s), 1357 (s), 1336 (s), 1309 (m), 1292 (m), 1257 (m), 1239 (w), 1231 (w), 1194 (s), 1169 (m), 1133 (m), 1106 (m), 1075 (w), 1030 (m), 1008 (m), 990 (s), 981 (s), 973 (s), 937 (s), 917 (m), 892 (m), 860 (w), 810 (w), 792 (w), 781 (m), 739 (w), 719 (m), 706 (m), 670 (m), 607 (m), 595 (w), 580 (m). EI-MS: *m/z* = 666 [*M*-^{t}BuNC]$^+$ (70%). Anal. found (calcd. for $C_{39}H_{52}F_5N_5OTi$): C, 62.57 (62.48); H, 7.13 (6.99); N, 9.24 (9.34) %.

NMR tube scale synthesis of Cp*Ti{PhC(N^{i}Pr)$_2$}{NC(Ar^{F_5})NO^{t}Bu}(CNXyl) (29). To a solution of Cp*Ti{PhC(N^{i}Pr)$_2$}{NC(Ar^{F_5})NO^{t}Bu} (**10**, 14.1 mg, 0.0211 mmol) in toluene-d_8 (0.3 mL) in an NMR tube equipped with a J. Young Teflon valve was added XylNC (2.77 mg, 0.0211 mmol) in toluene-d_8 (0.3 mL) at RT. A colour change from lime green to orange/red was observed. The reaction was monitored by ^{1}H and ^{19}F NMR spectroscopy and within 5 min **29** was formed in quantitative yield. **29** was characterised by ^{1}H and ^{19}F NMR spectroscopy. ^{1}H NMR (toluene-d_8, 299.9 MHz, 203 K): δ 7.18 (1 H, d, *o*$_a$-C_6H_5 overlapping with solvent), 6.99 (4 H, m, overlapping *o*$_b$-C_6H_5, *m*-C_6H_5 and *p*-C_6H_5), 6.75 (1 H, t, ^3J = 7.5 Hz, *p*-C$_6$<u>H</u>$_3$Me$_2$), 6.55 (2 H, d, ^3J = 7.8 Hz, *m*-C$_6$<u>H</u>$_3$Me$_2$), 3.33 (1 H, app. sept., ^3J = 6.3 Hz, NC<u>H</u>$_a$MeMe), 3.19 (1 H, app. sept., ^3J = 6.3 Hz, NC<u>H</u>$_b$MeMe), 2.48 (6 H, s, C$_6$H$_3$<u>Me</u>$_2$), 2.35 (15 H, s, C$_5$Me$_5$), 1.41 (9 H, s, NOCMe$_3$), 1.11 (3 H, br. d., ^3J = 6.0 Hz, NCH$_a$<u>Me</u>Me), 0.94 (6 H, m, overlapping NCH$_a$Me<u>Me</u> and NCH$_b$<u>Me</u>Me), 0.88 (3 H, d, ^3J = 6.3 Hz, NCH$_b$Me<u>Me</u>) ppm. ^{19}F{^{1}H} NMR (toluene-d_8, 282.1 MHz, 203K): δ -137.5 (1 F, m, *o*$_a$-C_6F_5), -140.4 (1 F, m, *o*$_b$-C_6F_5), -157.4 (1 F, t, ^3J = 22.6 Hz, *p*-C_6H_5), -163.6 (2 F, m, *m*-C_6F_5) ppm.

Note: subscripts ″a″ and ″b″ refer to the inequivalent Ph and Ar^{F_5} environments and ^{i}Pr groups.

Cp*Ti{PhC(N^{i}Pr)$_2$}{NC(NO^{t}Bu)C$_6$F$_4$N(C$_6$H$_3$Me$_2$)C}(F) (30). To a solution of Cp*Ti{PhC(N^{i}Pr)$_2$}{NC(Ar^{F_5})NO^{t}Bu} (**10**, 0.493 g, 0.739 mmol) in diethyl ether (2 mL) was added XylNC (97.0 mg, 0.739 mmol) in diethyl ether (2 mL) all at RT. A colour change from lime green to red/orange was observed and the solution left to stir for 16 h. Volatiles were then removed under reduced pressure to afford **30** as an orange powder which was dried *in vacuo*. Yield: 0.501 g (85%). Diffraction-quality crystals were grown from a saturated *n*-hexanes solution at -4°C. ^{1}H NMR (toluene-d_8, 299.9 MHz, 253 K): δ 7.12-6.87 (7 H, m, overlapping o_a-C$_6$H$_5$, *m*-C$_6$H$_5$, *p*-C$_6$H$_5$, *m*-C$_6$H$_3$Me$_2$ and *p*-C$_6$H$_3$Me$_2$), 6.07 (1 H, d, ^{3}J = 7.5 Hz, o_b-C$_6$H$_5$), 3.69 (1 H, app. sept., ^{3}J = 6.6 Hz, NC<u>H</u>$_a$MeMe), 3.14 (1 H, app. sept., ^{3}J = 6.6 Hz, NC<u>H</u>$_b$MeMe), 2.46 (3 H, s, 2,6-C$_6$H$_3$<u>Me</u>$_a$Me$_b$), 2.36 (15 H, s, C$_5$Me$_5$), 1.98 (3 H, s, 2,6-C$_6$H$_3$Me$_a$<u>Me</u>$_b$), 1.48 (9 H, s, NOCMe$_3$), 1.05 (3 H, d, ^{3}J = 6.3 Hz, NCH$_a$<u>Me</u>Me), 1.00 (3 H, d, ^{3}J = 6.6 Hz NCH$_a$Me<u>Me</u>), 0.88 (3 H, d, ^{3}J = 6.9 Hz, NCH$_b$<u>Me</u>Me), 0.68 (3 H, d, ^{3}J = 6.6 Hz, NCH$_b$Me<u>Me</u>) ppm. ^{13}C{^{1}H} NMR (toluene-d_8, 75.4 MHz, 253 K): δ 216.7 (Ti-NC), 170.4 (Ph<u>C</u>N$_2$), 141.7 (1 C, d, *J* = 3.1 Hz, *i*-C$_6$H$_3$Me$_2$), 139.6 (br. s, N<u>C</u>(Ar^{F_5})N), 138.8 (1 C, d, *J* = 4.2 Hz, o_a-C$_6$H$_3$Me$_2$), 136.1 (*i*-C$_6$H$_5$), 135.2 (1 C, d, *J* = 4.1 Hz, o_b-C$_6$H$_3$Me$_2$), 129.6 (m_a-C$_6$H$_3$Me$_2$), 129.1-127.3 (overlapping with toluene-d_8, o_a–C$_6$H$_5$, o_b-C$_6$H$_5$, *m*-C$_6$H$_5$, *p*-C$_6$H$_5$ and *p*-C$_6$H$_3$Me$_2$), 127.7 (m_b-C$_6$H$_3$Me$_2$), 126.4 (<u>C</u>$_5$Me$_5$), 103.0 (1 C, dd, $^{2}J_{C\text{-}F}$ = 18.7 Hz, $^{3}J_{C\text{-}F}$ = 3.2 Hz, Ti{NC(NO^{t}Bu)<u>C</u>}), 79.6 (NO<u>C</u>Me$_3$), 49.4 (N<u>C</u>H$_a$MeMe), 48.7 (N<u>C</u>H$_b$MeMe), 27.7 (overlapping NOC<u>Me</u>$_3$ and NCH$_a$<u>Me</u>Me), 25.2 (NCH$_a$Me<u>Me</u>), 25.0 (NCH$_b$Me<u>Me</u>), 25.0 (NCH$_b$<u>Me</u>Me), 19.0 (1 C, br d, 2,6-C$_6$H$_3$<u>Me</u>$_a$Me$_b$), 18.2 (2,6-C$_6$H$_3$Me$_a$<u>Me</u>$_b$) 12.7 (C$_5$<u>Me</u>$_5$) ppm. The resonance attributed to Ti{<u>C</u>N(Xyl)} could not be observed. ^{13}C NMR (HMQC ^{19}F-observed, toluene-d_8, 282.1 MHz, 253 K): δ 144.2 (inner$_1$-C$_6$F$_4$N), 142.5 (inner$_2$-C$_6$F$_4$N), 137.6 (outer$_4$-C$_6$F$_4$N), 135.9 (outer$_3$-C$_6$F$_4$N) ppm. ^{19}F{^{1}H} NMR (toluene-d_8, 282.1 MHz, 253 K): δ -101.8 (1 F, br. s, Ti-F), -118.7 (1 F, dt, *J* = 24.8 Hz, *J* = 8.7 Hz, inner$_1$-C$_6$F$_4$N), -152.4 (1 F, td, *J* = 22.0, *J* = 7.6 Hz, inner$_2$-C$_6$F$_4$N), -155.2 (1 F, dd, *J* = 22.3, *J* = 22.0, outer$_3$-C$_6$F$_4$N), -162.7 (1 F, dd, *J* = 21.7, *J* = 21.7 Hz, outer$_4$-C$_6$F$_4$N) ppm. Note: subscripts ″a″ and ″b″ refer to the inequivalent Ph and 2,6-C$_6$H$_3$<u>Me</u>$_2$ environments and ^{i}Pr groups. IR (NaCl plates, Nujol mull, cm^{-1}): 2118 (w), 1638 (w), 1586 (w), 1511 (s), 1488 (s), 1366 (s), 1340 (m), 1328 (m), 1276 (w), 1258 (m), 1231 (w), 1218 (m), 1199 (m), 1190 (m),

1166 (w), 1146 (m), 1121 (w), 1100 (m), 1090 (m), 1038 (m), 1018 (m), 981 (s), 919 (w), 908 (m), 887 (m), 804 (w), 787 (w), 771 (m), 722 (w), 711 (m), 547 (w). EI-MS: *m/z* (calcd. for $[C_{43}H_{52}F_5N_5OTi]^+$): 797.3562 (797.3576) (2%). Anal. found (calcd. for $C_{43}H_{52}F_5N_5OTi$): C, 64.86 (64.74); H, 6.45 (6.57); N, 8.81 (8.78) %.

NMR tube scale synthesis of Cp*Ti{PhC(N^{i}Pr)$_2$}{NC(Ar^{F_2})NO^{t}Bu}(CNXyl) (31). To a solution of Cp*Ti{PhC(N^{i}Pr)$_2$}{NC(Ar^{F_2})NO^{t}Bu} (**11**, 56.3 mg, 0.0845 mmol) in toluene-d_8 (0.3 mL) in an NMR tube equipped with a J. Young Teflon valve was added XylNC (11.1 mg, 0.0845 mmol) in toluene-d_8 (0.3 mL) at RT. A colour change from lime green to orange/red was observed. The reaction was monitored by ^{1}H and ^{19}F NMR spectroscopy and within 30 min Cp*Ti{PhC(N^{i}Pr)$_2$}{NC(Ar^{F_2})NO^{t}Bu}(CNXyl) (**31**) was formed in quantitative yield. **31** was characterised by ^{1}H, ^{13}C and ^{19}F NMR spectroscopy. ^{1}H NMR (toluene-d_8, 299.9 MHz, 213 K): δ 7.07-6.98 (5 H, m, overlapping *o*-C_6H_5, *m*-C_6H_5 and *p*-C_6H_5), 6.76 (1 H, br. t, *p*-$C_6H_3Me_2$), 6.62 (2 H, br. d, *m*-$C_6H_3Me_2$), 6.58-6.47 (3 H, m, overlapping *m*-$C_6H_3F_2$ and *p*-$C_6H_3F_2$), 3.41 (1 H, m, NC$\underline{H}_a$MeMe), 3.30 (1 H, m, NC$\underline{H}_b$MeMe), 2.57 (6 H, s, $C_6H_3\underline{Me}_2$), 2.41 (15 H, s, C_5Me_5), 1.41 (9 H, s, NOCMe_3), 1.21-1.14 (6 H, br. m, overlapping NCH$_a\underline{Me}$Me and NCH$_b\underline{Me}$Me), 1.00-0.93 (6 H, br. dd, overlapping NCH$_a$Me$\underline{Me}$ and NCH$_b$Me$\underline{Me}$) ppm. ^{13}C{^{1}H} NMR (toluene-d_8, 75.4 MHz, 213 K): δ 171.8 (Ph$\underline{C}N_2$), 169.9 ($C_6H_3Me_2N\underline{C}$), 159.8 (1 C, dd, $^1J_{C\text{-}F}$ = 247.2 Hz, $^3J_{C\text{-}F}$ = 9.3 Hz, *o*$_b$-$C_6F_2H_3$), 159.5 (1 C, dd, $^1J_{C\text{-}F}$ = 248.7 Hz, $^3J_{C\text{-}F}$ = 9.3 Hz, *o*$_a$-$C_6F_2H_3$), 153.5 (N$\underline{C}$($C_6F_2H_3$)N), 135.6 (*i*-$C_6H_3Me_2$), 135.5 (*i*-C_6H_5), 129.1-127.5 (overlapping with toluene-d_8, *o*-C_6H_5, *m*-C_6H_5, *p*-C_6H_5, *o*-$C_6H_3Me_2$, *m*-$C_6H_3Me_2$ and *p*-$C_6F_2H_3$), 126.3 (*p*-$C_6H_3Me_2$), 118.2 ($\underline{C}_5Me_5$), 115.9 (1 C, app. t, $^2J_{C\text{-}F}$ = 23.6 Hz, *i*-$C_6F_2H_3$), 110.9 (2 C, m, *m*-$C_6F_2H_3$), 76.7 (NO$\underline{C}Me_3$), 49.4, 49.0 (N$\underline{C}$H$_a$MeMe and N$\underline{C}$H$_b$MeMe), 27.8 (NOC$\underline{Me}_3$), 26.7 (NCH$_a\underline{Me}$Me or NCH$_b\underline{Me}$Me), 25.8 (NCH$_a$Me$\underline{Me}$ or NCH$_b$Me$\underline{Me}$), 25.7 (NCH$_b\underline{Me}$Me or NCH$_a\underline{Me}$Me), 25.0 (NCH$_b$Me$\underline{Me}$ or NCH$_a$Me$\underline{Me}$), 19.5 ($C_6H_3\underline{Me}_2$), 12.9 ($C_5\underline{Me}_5$) ppm.^{19}F{^{1}H} NMR (toluene-d_8, 282.1 MHz, 213 K): δ -109.3 (1 F, br. s, *o*$_a$-$C_6F_2H_3$), -111.6 (1 F, m, *o*$_b$-$C_6F_2H_3$) ppm. Note: subscripts ″a″ and ″b″ refer to the inequivalent 2,6-$C_6H_3\underline{Me}_2$ environments and ^{i}Pr groups.

NMR tube scale synthesis of Cp*Ti{PhC(N^{i}Pr)$_2$}{NC(NO^{t}Bu)C$_6$FH$_3$N(Xyl)C}(F) (32). To a solution of Cp*Ti{PhC(N^{i}Pr)$_2$}{N(C{Ar^{F_2}}NO^{t}Bu)} (**11**, 12.9 mg, 0.0211 mmol) in C_6D_6 (0.3 mL) in an NMR tube equipped with a J. Young Teflon valve was added XylNC (2.77 mg, 0.0211 mmol) in C_6D_6 (0.3 mL) at RT. A colour change from lime green to orange was observed. The reaction was monitored by ^{1}H and ^{19}F NMR spectroscopy. Cp*Ti{PhC(N^{i}Pr)$_2$}{NC(NO^{t}Bu)C$_6$FH$_3$N(Xyl)C}(F) (**32**) formed in 70% yield after 5 d. **32** was characterised by ^{1}H and ^{19}F NMR spectroscopy. ^{1}H NMR (C_6D_6, 299.9 MHz, 293 K): δ 7.09-6.51 (10 H, m, overlapping aryl protons), 5.93 (1 H, d, ^{3}J = 8.1 Hz, o_b-C_6H_5), 3.74 (1 H, app. sept., ^{3}J = 6.9 Hz, NC<u>H</u>MeMe), 3.22 (1 H, app. sept., ^{3}J = 6.6 Hz, NC<u>H</u>MeMe), 2.32 (3 H, s, 2,6-C_6H_3<u>Me</u>$_a$Me$_b$), 2.38 (15 H, s, C_5Me_5), 1.93 (3 H, s, 2,6-C_6H_3Me$_a$<u>Me</u>$_b$), 1.54 (9 H, s, NOCMe$_3$), 1.07 (6 H, t, ^{3}J = 6.3 Hz, overlapping NCH<u>Me</u>Me and NCH<u>Me</u>Me), 0.87 (3 H, br d, ^{3}J = 7.5 Hz, NCH<u>Me</u>Me), 0.74 (3 H, d, ^{3}J = 6.6 Hz, NCHMe<u>Me</u>) ppm. ^{19}F{^{1}H} NMR (C_6D_6, 282.1 MHz, 293 K): δ – 90.9 (1 F, m, C_6H_3F), -104.5 (1 F, s, TiF) ppm. Note: subscripts ″a″ and ″b″ refer to the inequivalent Ph and 2,6-C_6H_3<u>Me</u>$_2$ environments.

NMR tube scale synthesis of Cp*Ti{PhC(N^{i}Pr)$_2$}{N(B{Ar^{F_5}}$_3$)C(Ar^{F_5})N(O^{t}Bu)} (33). To a solution of Cp*Ti{PhC(N^{i}Pr)$_2$}{N(C{Ar^{F_5}}NO^{t}Bu)} (**10**, 14.1 mg, 0.0211 mmol) in C_6D_6 (0.3 mL) in an NMR tube equipped with a J. Young Teflon valve was added B(Ar^{F_5})$_3$ (12.5 mg, 0.0422 mmol) in C_6D_6 (0.3 mL) at RT. The reaction was monitored by ^{1}H, ^{19}F and ^{11}B NMR spectroscopy. After *ca.* 7 h Cp*Ti{PhC(N^{i}Pr)$_2$}{N(B{Ar^{F_5}}$_3$)C(Ar^{F_5})N(O^{t}Bu)} (**33**) was formed alongside Cp*Ti{PhC(N^{i}Pr)$_2$}{ON(B{Ar^{F_5}}$_3$)C(Ar^{F_5})N(H)(B{Ar^{F_5}}$_3$)} (**34**) in a 86:14 ratio. **33** was characterised by ^{1}H, ^{19}F and ^{11}B NMR spectroscopy. ^{1}H NMR (C_6D_6, 299.9 MHz, 293 K): δ 7.40 (1 H, d, ^{3}J = 7.8 Hz, o_a-C_6H_5), 7.12-6.91 (4 H, m, o_a-C_6H_5, m-C_6H_5 and p-C_6H_5), 3.38 (2 H, sept., ^{3}J = 6.6 Hz, NC<u>H</u>MeMe), 2.19 (15 H, s, C_5Me_5), 1.46 (9 H, s, NOCMe$_3$), 0.80 (6 H, d, ^{3}J = 6.6 Hz, NCH<u>Me</u>Me), 0.76 (6 H, d, ^{3}J = 6.3 Hz, NCHMe<u>Me</u>) ppm. ^{19}F{^{1}H} NMR (C_6D_6, 282.1 MHz, 293 K): δ -126.7 (m), -130.6 (6 F, br s, B(Ar^{F_5})$_3$), -132.2 (m), -142.2 (3 F, m, B(Ar^{F_5})$_3$), -145.6 (br s), -154.6 (m), -158.4 (t), -160.8 (6 F, br s, B(Ar^{F_5})$_3$), -163.9 (m) ppm. ^{11}B NMR (C_6D_6, 96.2 MHz, 293 K): δ -7 (B(Ar^{F_5})$_3$) ppm. Note: subscripts ″a″ and ″b″ refer to the inequivalent Ph environments.

Cp*Ti{PhC(N^{i}Pr)$_2$}{ON(B{Ar^{F5}}$_3$)C(Ar^{F5})N(H)(B{Ar^{F5}}$_3$)} (34). To a solution of Cp*Ti{PhC(N^{i}Pr)$_2$}{NC(Ar^{F5})NO^{t}Bu} (**10**, 0.282 g, 0.422 mmol) in benzene (5 mL) was added a solution of B(Ar^{F5})$_3$ (0.250 g, 0.845 mmol) in benzene (5 mL) all at RT. A colour change from lime green to dark green was observed and the solution heated to 70 °C and left to stir for 4 d. Volatiles were then removed under reduced pressure to afford **34** as a dark green oily solid. The resultant green solid was washed with pentane (3 x 5 ml, RT), filtered and dried *in vacuo*. Yield: 0.362 g (76%). The resultant green powder was subsequently washed with diethyl ether (1 x 5 mL, RT), filtered and dried *in vacuo* to give an analytically pure sample. Yield: 0.124 g (26%). ^{1}H NMR (CD_2Cl_2, 499.9 MHz, 293 K): δ 7.52-7.47 (4 H, m, overlapping *o*$_a$-C_6H_5, *m*-C_6H_5 and *p*-C_6H_5), 7.33 (1 H, m, *o*$_b$-C_6H_5), 6.67 (1 H, s, NH), 3.46 (2 H, 2 x app. sept., ^{3}J = 6.5 Hz, overlapping NC$\underline{H}_a$MeMe and NC$\underline{H}_b$MeMe), 2.02 (15 H, s, C_5Me_5), 0.98 (3 H, d, ^{3}J = 6.5 Hz, NCH$_a$$\underline{Me}$Me), 0.93 (3 H, d, ^{3}J = 7.0 Hz, NCH$_a$Me$\underline{Me}$), 0.83 (3 H, d, ^{3}J = 6.5 Hz, NCH$_b$$\underline{Me}$Me), 0.82 (3 H, d, ^{3}J = 7.0 Hz, NCH$_b$Me$\underline{Me}$) ppm. ^{13}C{^{1}H} NMR (CD_2Cl_2, 125.7 MHz, 293 K): δ 167.1 (Ph$\underline{C}$N$_2$), 153.0 (N$\underline{C}$(Ar^{F5})N), 148.9 (2 C, br. d, $^{1}J_{C\text{-}F}$ = 235.0 Hz, *o*-C_6F_5), 145.7 (2 C, d, $^{1}J_{C\text{-}F}$ = 245.9 Hz, *o*-C_6F_5), 144.5 (1 C, d, $^{1}J_{C\text{-}F}$ = 251.2 Hz, *p*-C_6F_5), 143.1 (2 C, d, $^{1}J_{C\text{-}F}$ = 257.1 Hz, *m*-C_6F_5), 139.9 (1 C, d, $^{1}J_{C\text{-}F}$ = 248.0 Hz, *p*-C_6F_5), 137.2 (2 C, d, $^{1}J_{C\text{-}F}$ = 246.8 Hz, *m*-C_6F_5), 132.4 (*i*-C_6H_5), 131.1 ($\underline{C}_5Me_5$), 129.9, 129.1, 129.0, 128.9 (*o*$_a$-C_6H_5, *o*$_b$-C_6H_5, *m*-C_6H_5 and *p*-C_6H_5), 128.5 (1 C, br. s, *i*-C_6F_5), 108.9 (1 C, app. t, $^{2}J_{C\text{-}F}$ = 19.6 Hz, *i*-C_6F_5), 52.1 (N$\underline{C}$H$_a$MeMe), 51.1 (N$\underline{C}$H$_b$MeMe), 26.1 (NCH$_b$$\underline{Me}$Me), 25.4 (NCH$_a$$\underline{Me}$Me), 25.4 (NCH$_aMe\underline{Me}$), 24.2 (NCH$_bMe\underline{Me}$), 13.1 ($C_5\underline{Me}_5$) ppm. ^{19}F{^{1}H} NMR (CD_2Cl_2, 282.1 MHz, 293 K): δ -132.5 (br. s), -133.2 (2 F, br. s, *o*-C_6F_5), -134.2 (br. s), -135.7 (2 F, br. m, *o*-C_6F_5), -135.8 (br. m), -136.6 (br. s), 150.1 (1 F, t of t, ^{3}J = 20.6, ^{4}J = 3.7 Hz, *p*-C_6F_5), - 158.1 (br. s), -160.7 (br. s), -161.5 (1 F, t of d, ^{3}J = 21.6, ^{4}J = 8.2 Hz, *m*-C_6F_5), -162.5 (1 F, t of d, ^{3}J = 21.6, ^{4}J = 7.3 Hz, *m*-C_6F_5), -166.0 (br. m, *m*-C_6F_5), 166.8 (br. s) ppm. ^{11}B NMR (CD_2Cl_2, 96.2 MHz, 293 K): δ -7.1 (B(Ar^{F5})$_3$) ppm. ^{1}H NMR (CD_2Cl_2, 299.9 MHz, 213 K): δ 7.46 (4 H, br. s, overlapping *o*$_a$-C_6H_5, *m*-C_6H_5 and *p*-C_6H_5), 7.30 (1 H, br. m, *o*$_b$-C_6H_5), 6.65 (1 H, s, NH), 3.35 (2 H, 2 x br. m, overlapping NC$\underline{H}_a$MeMe and NC$\underline{H}_b$MeMe), 1.90 (15 H, s, C_5Me_5), 0.91 (3 H, br. d, NCH$_a$$\underline{Me}$Me), 0.84 (3 H, d, ^{3}J = 7.0 Hz, NCH$_a$Me$\underline{Me}$), 0.73 (6 H, br m, overlapping NCH$_b$$\underline{Me}$Me and NCH$_bMe\underline{Me}$) ppm. ^{19}F{^{1}H} NMR (CD_2Cl_2, 282.1 MHz, 213 K): δ -121.5 (br. s), -126.2 (br, t), -126.8 (br, t), -131.6 (br. t), -132.6 (br. m), -132.9 (br. d), -133.7 (br. m), -134.3 (br. d), -135.9 (br. d), -139.6 (br. s), -149.4 (1 F, t, ^{3}J = 21.2, *p*$_1$-C_6F_5), -156.9 (1 F, t, ^{3}J = 21.7,

p_2-C_6F_5), -159.8 (1 F, t, ^3J = 21.4, p_3-C_6F_5), -160.5 (1 F, t, ^3J = 21.4, p_4-C_6F_5), -161.4 (1 F, app. t, m_{1a}-C_6F_5), -161.8 (1 F, app. t, m_{1b}-C_6F_5), -162.8 (1 F, app. t, m_{2a}-C_6F_5), -165.0 (1 F, app. t, m_{4a}-C_6F_5), -166.1 (1 F, app. t, m_{3a}-C_6F_5), -166.3 (1 F, app. t, m_{4b}-C_6F_5), -166.6 (1 F, app. t, m_{2b}-C_6F_5), -167.0 (1 F, app. t, m_{3b}-C_6F_5) ppm. At this temperature the resonance attributed to $B(Ar^{F_5})_3$ in the ^{11}B NMR spectrum could not be identified. Note: subscript letters and numbers refer to the inequivalent Ph and Ar^{F_5} environments and ^{i}Pr groups. IR (NaCl plates, Nujol mull, cm^{-1}): 3393 (w), 1642 (m), 1517 (s), 1504 (m), 1406 (m), 1334 (m), 1278 (w), 1261 (w), 1221 (w), 1096 (m), 1018 (m), 1000 (m), 979 (m), 864 (w), 812 (m), 782 (m), 766 (w), 749 (w), 707 (w), 695 (w), 687 (w), 679 (w), 659 (w), 615 (m), 596 (m). EI-MS: *m/z* = 610 $[Cp^*Ti\{PhC(N^iPr)_2\}\{ONC(Ar^{F_5})N(H)\}, M - 2B(Ar^{F_5})_3]^+$ (5%). Anal. found (calcd. for $C_{66}H_{35}B_2F_{35}N_4OTi$): C, 48.59 (48.50); H, 2.23 (2.16); N, 3.48 (3.43) %.

5.6 X-ray data collection and processing parameters for Chapter Three

Crystal structure determinations for $Cp^*Ti\{PhC(N^iPr)_2\}(NO^tBu)$ (3), $Cp^*Ti\{PhC(N^iPr)_2\}\{OC(NO^tBu)N(Tol)C(NTol)O\}$ (6), $[Cp^*Ti\{PhC(N^iPr)_2\}(\mu\text{-}O)]_2$ (7), $PhC(NO^tBu)Ph$ (9c), $Cp^*Ti\{PhC(N^iPr)_2\}\{NC(Ar^{F_5})NO^tBu\}$ (10), $Cp^*Ti\{PhC(N^iPr)_2\}\{NC(Ar^{F_5})NC(Ar^{F_5})N(C\{Ar^{F_5}\}NO^tBu)\}$ (13), $[PhC(N^iPrH)_2][BPh_4]$ (15-BPh_4) and $Cp^*Ti\{PhC(N^iPr)_2\}\{\eta^2\text{-}ON(H)B(Ar^{F_5})_3\}$ (17). Crystal data collection and processing parameters are given in Table 5.1. Crystals were mounted on glass fibers using perfluoropolyether oil and cooled rapidly in a stream of cold N_2 using an Oxford Cryosystems Cryostream unit. Diffraction data were measured using either an Enraf-Nonius KappaCCD or Agilent Technologies Supernova diffractometer using Mo-K_α or Cu-K_α radiation, respectively. As appropriate, absorption and decay corrections were applied to the data and equivalent reflections merged.[17, 18] The structures were solved with SIR92[19] or Superflip,[20] and further refinements and all other crystallographic calculations were performed using the CRYSTALS program suite.[21] Other details of the structure solution and refinements are given in the Supporting Information (CIF data – see CD Appendix). A full listing of atomic coordinates, bond lengths and angles and displacement parameters for all the structures have been deposited at the Cambridge Crystallographic Data Centre. See Notice to Authors, Issue No. 1.

Table 5.1. X-ray data collection and processing parameters for Cp*Ti{PhC(N^iPr)$_2$}(NO^tBu) (**3**), Cp*Ti{PhC(N^iPr)$_2$}{OC(NO^tBu)N(Tol)C(NTol)O} (**6**), Cp*Ti{PhC(N^iPr)$_2$}(μ-O)]$_2$ (**7**), PhC(NO^tBu)Ph (**9c**), [Cp*Ti{PhC(N^iPr)$_2$}{NC(Ar^{F5})NO^tBu} (**10**), Cp*Ti{PhC(N^iPr)$_2$}{NC(Ar^{F5})NC(Ar^{F5})N(C{Ar^{F5}}NO^tBu)} (**13**), [PhC(N^iPrH)$_2$][BPh_4] (**15-BPh_4**) and Cp*Ti{PhC(N^iPr)$_2$}{η^2-ON(H)B(Ar^{F5})$_3$} (**17**).

compound	**3**	**6**	**7**	**9c**	**10**
empirical formula	$C_{27}H_{43}N_3OTi$	$C_{43}H_{57}N_5O_3Ti$	$C_{46}H_{68}N_4O_2Ti_2$	$C_{17}H_{19}NO$	$C_{34}H_{43}F_5N_4OTi$
fw	473.51	739.86	804.87	253.34	666.63
temp / K	150	150	150	150	150
wavelength / Å	0.71073	1.54184	0.71073	1.54184	0.71073
space group	$P\,2_12_12_1$	$P\,\bar{1}$	$P\,2_1/c$	$P\,2_12_12_1$	$P\,\bar{1}$
a / Å	16.6135(2)	10.8924(4)	32.0878(2)	8.46178(11)	10.6906(10)
b / Å	17.1813(2)	11.4025(4)	10.8165(1)	10.87960(15)	11.8098(11)
c / Å	19.3943(2)	18.6552(6)	26.5749(1)	15.6091(2)	13.8987(15)
α / deg	90	72.928(3)	90	90	96.244(4)
β / deg	90	79.432(3)	110.7542(3)	90	93.745(4)
γ / deg	90	68.018(3)	90	90	98.297(5)
V / Å^3	5535.94(11)	2046.79(13)	8625.03(10)	1436.99(3)	1720.2(3)
Z	8	2	8	4	2
d (calcd) / Mg.m^{-3}	1.136	1.200	1.240	1.171	1.287
abs coeff / mm^{-1}	0.331	2.109	0.411	0.562	0.308
R indices: R_1 =	0.0459[a]	0.0388[a]	0.0468[a]	0.0298[a]	0.0836[b]
R_w =	0.0520[a]	0.0431[a]	0.0564[a]	0.0322[a]	0.0732[b]

Table 5.1. (Cont.)

compound	**13**	**15-BPh_4**	**17·C_6H_6**
empirical formula	$C_{48}H_{43}F_{15}N_6OTi$	$C_{37}H_{41}BN_2$	$C_{41}H_{35}BF_{15}N_3OTi·C_6H_6$
fw	1052.78	524.56	1007.54
temp / K	150	150	150
wavelength / Å	0.71073	1.54180	1.54180
space group	P $2_1/n$	$P\ \bar{1}$	$P\ 2_1/c$
a / Å	12.62440(10)	9.7572(8)	13.2439(2)
b / Å	18.3472(2)	10.1086(7)	13.8026(3)
c / Å	20.5455(2)	16.5470(11)	24.0023(3)
α / deg	90	98.985(6)	90
β / deg	97.6073(4)	105.885(6)	97.7434(15)
γ / deg	90	95.944(6)	90
V / $Å^3$	4716.91(8)	1532.0(2)	4347.59(13)
Z	4	2	4
d (calcd) / $Mg.m^{-3}$	1.482	1.137	1.539
abs coeff / mm^{-1}	0.285	0.488	2.621
R indices: R_1 =	0.0340[a]	0.0581[b]	0.0324[a]
R_w =	0.0430[a]	0.0284[b]	0.0298[a]

[a] $R_1 = \Sigma||F_o|-|F_c|| / \Sigma|F_o|$; $R_w = \sqrt{\{\Sigma w(|F_o|-|F_c|)^2 / \Sigma w|F_o|^2\}}$ for data with $I > 3\sigma(I)$.
[b] $R_1 = \Sigma||F_o|-|F_c|| / \Sigma|F_o|$; $R_w = \sqrt{\{\Sigma w(|F_o|-|F_c|)^2 / \Sigma w|F_o|^2\}}$ for data with $I > 2\sigma(I)$.

5.7 X-ray data collection and processing parameters for Chapter Four

Crystal structure determinations for Cp*Ti{PhCN(^{i}Pr)$_2$}{NC(Ar^{F5})NO^{t}Bu)C(Ph)(H)O} (22a), (4-C$_6$H$_4$NMe$_2$)C{NC(Ar^{F5})NO^{t}Bu}H (23e), HC{NC(Ar^{F5})NO^{t}Bu}NMe$_2$ (25) Cp*Ti{PhC(N^{i}Pr)$_2$}{NC(Ar^{F5})NO^{t}Bu}(^{t}BuNC) (28), Cp*Ti{PhC(N^{i}Pr)$_2$}-{NC(NO^{t}Bu)C$_6$F$_4$N(C$_6$H$_3$Me$_2$)C}(F) (30). Crystal data collection and processing parameters are given in Table 5.2. Crystals were mounted on glass fibers using perfluoropolyether oil and cooled rapidly in a stream of cold N_2 using an Oxford Cryosystems Cryostream unit. Diffraction data were measured using either an Enraf-Nonius KappaCCD or Agilent Technologies Supernova diffractometer using Mo-K_α or Cu-K_α radiation, respectively. As appropriate, absorption and decay corrections were applied to the data and equivalent reflections merged.[17, 18] The structures were solved with SIR92[19] or Superflip,[20] and further refinements and all other crystallographic calculations were performed using the CRYSTALS program suite.[21] Other details of the structure solution and refinements are given in the Supporting Information (CIF data – see CD Appendix). A full listing of atomic coordinates, bond lengths and angles and displacement parameters for all the structures have been deposited at the Cambridge Crystallographic Data Centre. See Notice to Authors, Issue No. 1.

Table 5.2. X-ray data collection and processing parameters for Cp*Ti{PhCN(^{i}Pr)$_2$}{NC(Ar^{F5})NO^{t}Bu)C(Ph)(H)O} (**22a**), (4-C$_6$H$_4$NMe$_2$)C{NC(Ar^{F5})NO^{t}Bu}H (**23e**), HC{NC(Ar^{F5})NO^{t}Bu}NMe$_2$ (**25**) Cp*Ti{PhC(N^{i}Pr)$_2$}{NC(Ar^{F5})NO^{t}Bu}(^{t}BuNC) (**28**), Cp*Ti{PhC(N^{i}Pr)$_2$}{NC(NO^{t}Bu)C$_6$F$_4$N(C$_6$H$_3$Me$_2$)C}(F) (**30**).

compound	**22a**	**23e**	**25**	**28**	**30**
empirical formula	$C_{41}H_{49}F_5N_4O_2Ti$	$C_{20}H_{20}F_5N_3O_1$	$C_{14}H_{16}F_5N_3O_1$	$C_{39}H_{52}F_5N_5OTi$	$C_{43}H_{52}F_5N_5OTi$
fw	772.76	413.39	337.29	749.76	797.81
temp / K	150	150	150	150	150
wavelength / Å	1.54184	0.71073	0.71073	0.71073	0.71073
space group	*P* 2$_1$/n	*C* 2/c	*P* -1	*P*ccn	*P* 2$_1$/n
a / Å	13.70323(18)	35.1540(4)	8.3723(2)	19.0947(1)	14.0552(2)
b / Å	19.9090(3)	7.9437(9)	8.6069(2)	33.5176(2)	15.1126(2)
c / Å	15.2216(2)	14.4166(7)	12.1306(2)	12.3937(1)	21.0286(4)
α / deg	90	90	98.3332(11)	90	90
β / deg	107.8248(15)	92.337(3)	110.0682(12)	90	95.6103(6)
γ / deg	90	90	102.2578(9)	90	90
V / Å^3	3953.38(10)	4022.5(5)	779.42(3)	7932.07(9)	4445.30(12)
Z	4	8	2	8	4
d (calcd) / Mg·m^{-3}	1.298	1.365	1.437	1.256	1.192
abs coeff / mm^{-1}	2.368	0.118	0.133	0.275	0.250
R indices: R_1 =	0.0478[a]	0.0614[b]	0.0353[a]	0.0410[a]	0.0545[a]
R_w =	0.0551[a]	0.0425[b]	0.0367[a]	0.0404[a]	0.0606[a]

[a] $R_1 = \Sigma||F_o|-|F_c|| / \Sigma|F_o|$; $R_w = \sqrt{\{\Sigma w(|F_o|-|F_c|)^2 / \Sigma w|F_o|^2\}}$ for data with I $> 3\sigma$(I).

[b] $R_1 = \Sigma||F_o|-|F_c|| / \Sigma|F_o|$; $R_w = \sqrt{\{\Sigma w(|F_o|-|F_c|)^2 / \Sigma w|F_o|^2\}}$ for data with I $> 2\sigma$(I).

5.8 References

1. A. B. Pangborn, M. A. Giardello, R. H. Grubbs, R. K. Rosen and F. J. Timmers, *Organometallics*, 1996, **15**, 1518.
2. J. D. Selby, C. D. Manley, A. D. Schwarz, E. Clot and P. Mountford, *Organometallics*, 2008, **27**, 6479.
3. A. D. Schofield, A. Nova, J. D. Selby, C. D. Manley, A. D. Schwarz, E. Clot and P. Mountford, *J. Am. Chem. Soc.*, 2010, **132**, 10484.
4. A. E. Guiducci, C. L. Boyd and P. Mountford, *Organometallics*, 2006, **25**, 1167.
5. S. C. Dunn, P. Mountford and D. A. Robson, *J. Chem. Soc., Dalton Trans.*, 1997, 293.
6. S. G. Davies, C. J. Goodwin, D. Hepworth, P. M. Roberts and J. E. Thomson, *J. Org. Chem.*, 2010, **75**, 1214.
7. M. P. Coles, D. C. Swenson, R. F. Jordan and V. G. Young, *Organometallics*, 1997, **16**, 5183.
8. H. M. Weiss, K. M. Touchette, S. Angell and J. Khan, *Org. Bio. Chem.*, 2003, **1**, 2152.
9. Y. Zhang and J. Wen, *J. Fluorine Chem.*, 1990, **47**, 533.
10. T. Nishikawa, A. Ino and M. Isobe, *Tetrahedron*, 1994, **50**, 1449.
11. D. Robert, M. Kondracka and J. Okuda, *Dalton Trans.*, 2008, 2667.
12. H. Takahashi, T. Fukami, H. Kojima, T. Yamakawa, H. Takahashi, T. Sakamoto, T. Nishimura, M. Nakamura, T. Yosizumi, K. Niiyama, N. Ohtake and T. Hayama, *Tetrahedron*, 2005, **61**, 3473.
13. A. Xia, H. M. El-Kaderi, M. J. Heeg and C. H. Winter, *J. Organomet. Chem.*, 2003, **682**, 224.
14. J. Richter, J. Feiling, H.-G. Schmidt, M. Noltemeyer, W. Brueser and F. T. Edelmann, *Z. Anorg. Allg. Chem.*, 2004, **630**, 1269.
15. E. Buehler, *J. Org. Chem.*, 1967, **32**, 261.
16. L. H. J. P. De and C.-K. Tsai, *J. Org. Chem.*, 2004, **69**, 3057.
17. Z. Otwinowski and W. Minor, *Processing of X-ray Diffraction Data Collected in Oscillation Mode*, Academic press, New York, 1997.
18. Agilent Technologies, Oxford, 2011.
19. A. Altomare, G. Cascarano, G. Giacovazzo, A. Guagliardi, M. C. Burla, G. Polidori and M. Camalli, *J. Appl. Crystallogr.*, 1994, **27**, 435.

20. L. Palatinus and G. Chapuis, *J. Appl. Cryst.*, 2007, **40**, 786.
21. P. W. Betteridge, J. R. Cooper, R. I. Cooper, K. Prout and D. J. Watkin, *J. Appl. Cryst.*, 2003, **36**, 1487.

Appendix

A.1 Isosurfaces and energies of the HOMO, HOMO-1 and HOMO-2 of CpTi{MeC(NMe)$_2$}(NR)

1Q_Me

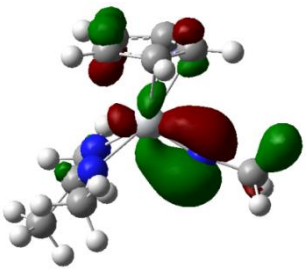

HOMO-1 = -5.47eV

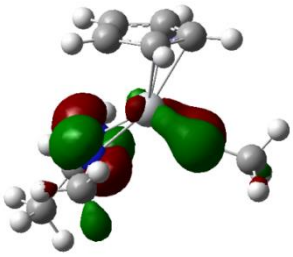

HOMO = -5.28eV

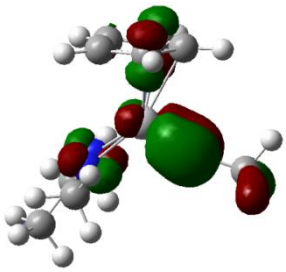

HOMO-2 = -5.93eV

1Q_Ph

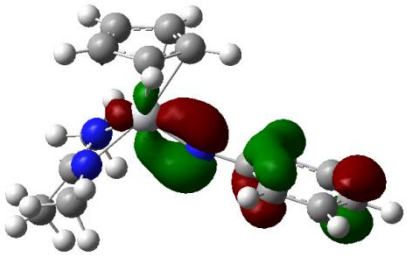

HOMO = -4.98eV

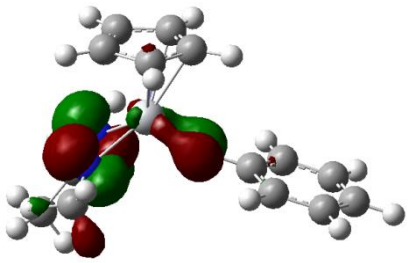

HOMO-1 = -5.58eV

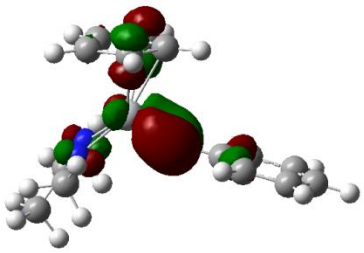

HOMO-2 = -6.28eV

Figure A1. (a) Model compounds CpTi{MeC(NMe)$_2$}(NR) (R = Me (**1Q_Me**) and Ph (**1Q _Ph**)) studied by DFT previously.[1] Associated isosurfaces and energies of the HOMO, HOMO-1 and HOMO-2.

1Q_NMe$_2$

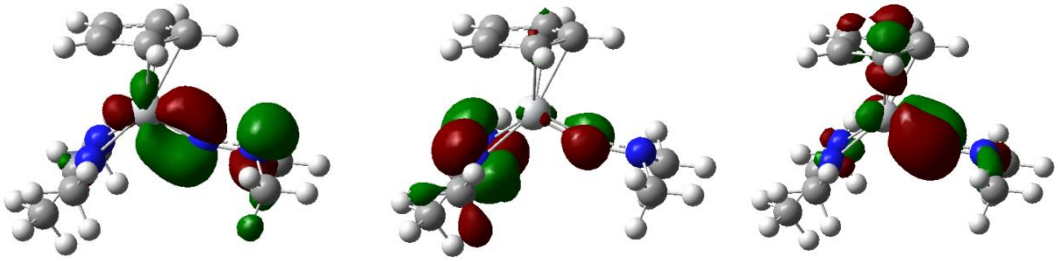

HOMO = -4.30eV | HOMO-1 = -5.25eV | HOMO-2 = -6.09eV

1Q_NPh$_2$

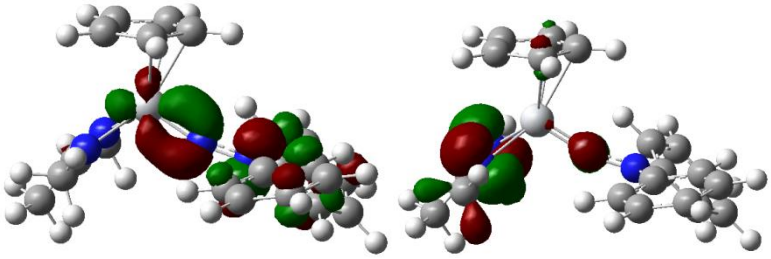

HOMO = -4.24eV | HOMO-1 = -5.50eV

Combination of orbitals

1Q_OMe

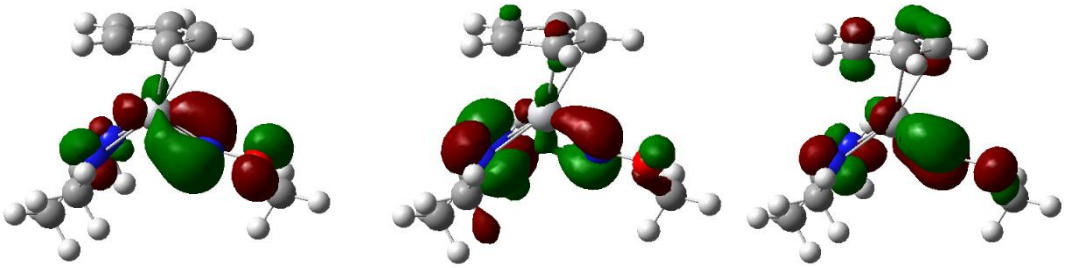

HOMO = -4.92eV | HOMO-1 = -5.39eV | HOMO-2 = -5.93eV

Figure A1. (b) Model compounds CpTi{MeC(NMe)$_2$}(NR) (R = NMe$_2$ (**1Q_NMe$_2$**), NPh$_2$ (**1Q_NPh$_2$**) or OMe (**1Q_OMe**)) studied by DFT. Associated isosurfaces and energies of the HOMO, HOMO-1 and HOMO-2. The models **1Q_NMe$_2$** and **1Q_NPh$_2$** have been reported previously.[1]

A.2 Isosurfaces and energies of the HOMOs and LUMOs of (4-C_6H_4X)C{NC(Ar^{F5})NO^{t}Bu}H (23a-23f)

23a

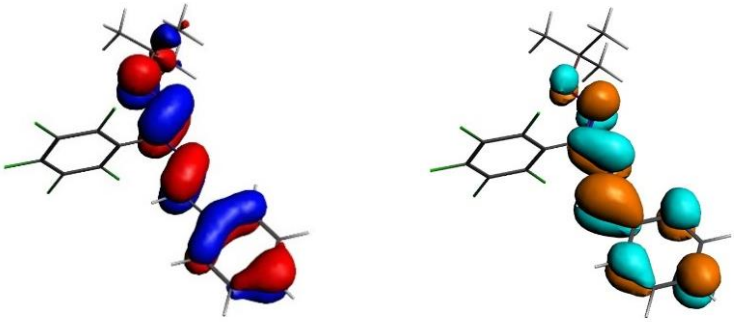

HOMO = 5.71 eV LUMO = -3.07 eV

23b

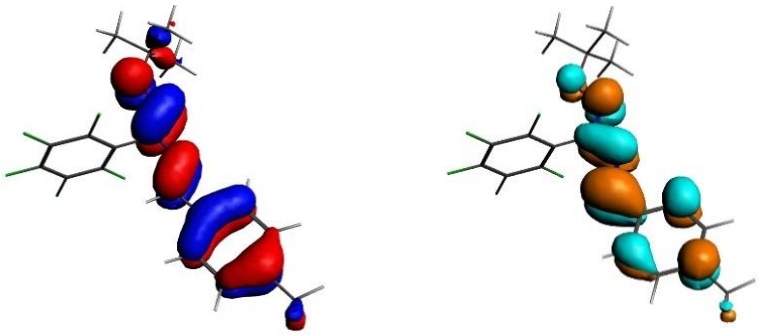

HOMO = -5.57 eV LUMO = -2.97 eV

23c

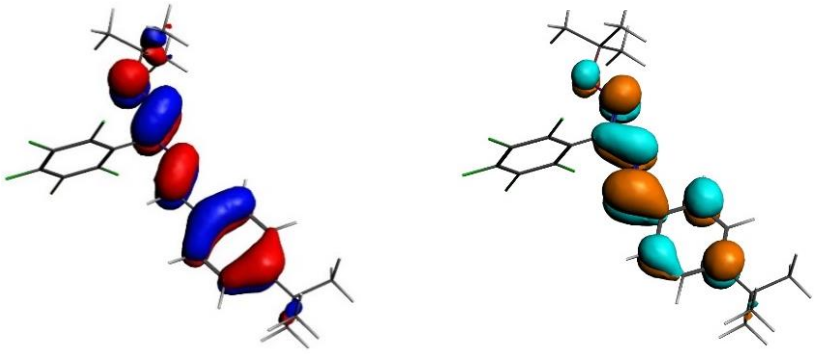

HOMO = -5.54 eV LUMO = -2.94 eV

Figure A2. (a) Isosurfaces and energies of the HOMOs and LUMOs of (4-C_6H_4X)C{NC(Ar^{F5})NO^{t}Bu}H (X = H (**23a**), Me (**23b**) or ^{t}Bu (**23c**))

23d

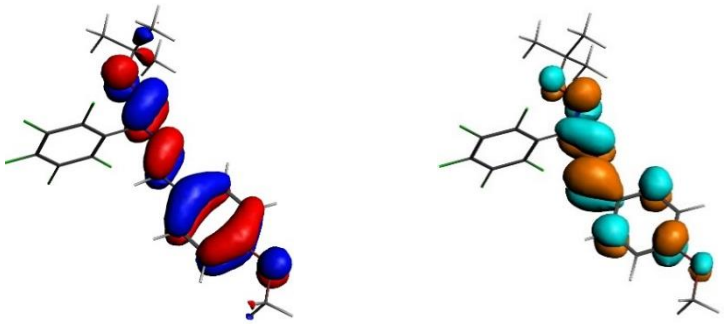

HOMO = -5.36 eV LUMO = -2.83 eV

23e

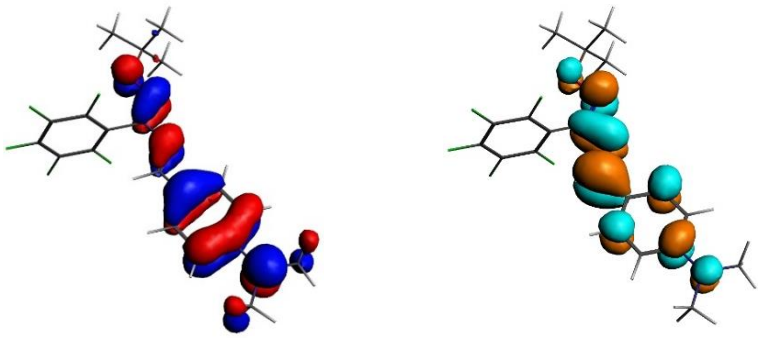

HOMO = -4.84 eV LUMO = -2.56 eV

23f

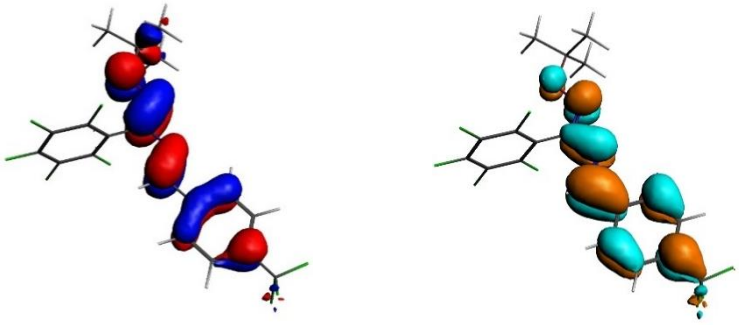

HOMO = -6.04 eV LUMO = -3.49 eV

Figure A2. (b) Isosurfaces and energies of the HOMOs and LUMOs of (4-C_6H_4X)C{NC(Ar^{F5})NO^tBu}H (X = OMe (**23d**), NMe_2 (**23e**) or CF_3 (**23f**)).

A.3 References

1. P. J. Tiong, A. Nova, L. R. Groom, A. D. Schwarz, J. D. Selby, A. D. Schofield, E. Clot and P. Mountford, *Organometallics*, 2011, **30**, 1182.